EXPERIMENTAL AND CLINICAL APPROACHES IN THE PURSUIT OF NOVEL THERAPEUTIC STRATEGIES FOR PERINATAL BRAIN INJURY AND ITS NEUROLOGICAL SEQUELAE

EDITED BY: Changlian Zhu, Chao Chen and Claire Thornton
PUBLISHED IN: Frontiers in Cellular Neuroscience, Frontiers in Neurology and Frontiers in Pediatrics

frontiers Research Topics

frontiers

ISSN 1664-8714
ISBN 978-2-88971-802-3
DOI 10.3389/978-2-88971-802-3

About Frontiers

Frontiers is more than just an open-access publisher of scholarly articles: it is a pioneering approach to the world of academia, radically improving the way scholarly research is managed. The grand vision of Frontiers is a world where all people have an equal opportunity to seek, share and generate knowledge. Frontiers provides immediate and permanent online open access to all its publications, but this alone is not enough to realize our grand goals.

Frontiers Journal Series

The Frontiers Journal Series is a multi-tier and interdisciplinary set of open-access, online journals, promising a paradigm shift from the current review, selection and dissemination processes in academic publishing. All Frontiers journals are driven by researchers for researchers; therefore, they constitute a service to the scholarly community. At the same time, the Frontiers Journal Series operates on a revolutionary invention, the tiered publishing system, initially addressing specific communities of scholars, and gradually climbing up to broader public understanding, thus serving the interests of the lay society, too.

Dedication to Quality

Each Frontiers article is a landmark of the highest quality, thanks to genuinely collaborative interactions between authors and review editors, who include some of the world's best academicians. Research must be certified by peers before entering a stream of knowledge that may eventually reach the public - and shape society; therefore, Frontiers only applies the most rigorous and unbiased reviews.
Frontiers revolutionizes research publishing by freely delivering the most outstanding research, evaluated with no bias from both the academic and social point of view. By applying the most advanced information technologies, Frontiers is catapulting scholarly publishing into a new generation.

What are Frontiers Research Topics?

Frontiers Research Topics are very popular trademarks of the Frontiers Journals Series: they are collections of at least ten articles, all centered on a particular subject. With their unique mix of varied contributions from Original Research to Review Articles, Frontiers Research Topics unify the most influential researchers, the latest key findings and historical advances in a hot research area! Find out more on how to host your own Frontiers Research Topic or contribute to one as an author by contacting the Frontiers Editorial Office: frontiersin.org/about/contact

EXPERIMENTAL AND CLINICAL APPROACHES IN THE PURSUIT OF NOVEL THERAPEUTIC STRATEGIES FOR PERINATAL BRAIN INJURY AND ITS NEUROLOGICAL SEQUELAE

Topic Editors:
Changlian Zhu, Third Affiliated Hospital of Zhengzhou University, China
Chao Chen, Fudan University, China
Claire Thornton, Royal Veterinary College (RVC), United Kingdom

Citation: Zhu, C., Chen, C., Thornton, C., eds. (2021). Experimental and Clinical Approaches in the Pursuit of Novel Therapeutic Strategies for Perinatal Brain Injury and its Neurological Sequelae. Lausanne: Frontiers Media SA.
doi: 10.3389/978-2-88971-802-3

Table of Contents

frontiers in Cellular Neuroscience

EDITORIAL
published: 11 October 2021
doi: 10.3389/fncel.2021.762111

Editorial: Experimental and Clinical Approaches in the Pursuit of Novel Therapeutic Strategies for Perinatal Brain Injury and Its Neurological Sequelae

Changlian Zhu[1,2]*, *Chao Chen*[3] *and Claire Thornton*[4]

[1] *Henan Key Laboratory of Child Brain Injury and Henan Pediatric Clinical Research Center, Institute of Neuroscience and Third Affiliated Hospital of Zhengzhou University, Zhengzhou, China,* [2] *Center for Brain Repair and Rehabilitation, Institute of Neuroscience and Physiology, Sahlgrenska Academy, University of Gothenburg, Gothenburg, Sweden,* [3] *Department of Neonatology, Children's Hospital of Fudan University, Shanghai, China,* [4] *Department of Comparative Biomedical Sciences, Royal Veterinary College, London, United Kingdom*

Keywords: perinatal brain injury, white matter injury, neuroprotection, cerebral palsy, autism, intellectual disability, cell death, preterm birth

Editorial on the Research Topic

Experimental and Clinical Approaches in the Pursuit of Novel Therapeutic Strategies for Perinatal Brain Injury and Its Neurological Sequelae

OPEN ACCESS

Edited and reviewed by:
Dirk M. Hermann, University of Duisburg-Essen, Germany

***Correspondence:**
Changlian Zhu
changlian.zhu@neuro.gu.se; zhuc@zzu.edu.cn

Specialty section:
This article was submitted to Cellular Neuropathology, a section of the journal Frontiers in Cellular Neuroscience

Received: *21 August 2021*
Accepted: *22 September 2021*
Published: *11 October 2021*

Citation:
Zhu C, Chen C and Thornton C (2021) Editorial: Experimental and Clinical Approaches in the Pursuit of Novel Therapeutic Strategies for Perinatal Brain Injury and Its Neurological Sequelae. Front. Cell. Neurosci. 15:762111. doi: 10.3389/fncel.2021.762111

Brain injuries during the perinatal period—resulting from encephalopathy-related asphyxia, prematurity, fetal growth restriction, antenatal toxicity exposure, neonatal stroke, systemic infections, and metabolic abnormalities—are a significant cause of adverse neurodevelopmental outcomes, and such injuries occur at different times during the perinatal period and in different clinical settings (Leaw et al., 2017). Perinatal brain injury causes developmental impairment and permanent neurological deficits such as cerebral palsy, autism, and intellectual disability in children, and these are major burdens to those afflicted, their families, and society as a whole. The progression of perinatal brain injury depends on the balance between persistent injury and the repair response, which can be modulated by external therapy (Nair et al., 2021; Song et al., 2021). Interventions against brain injury using hypothermia or recombinant human erythropoietin during the neonatal period have shown promising results in reducing the prevalence of cerebral palsy and other neurological sequelae such as autism, intellectual disability, and retinopathy of prematurity (Shankaran et al., 2012; Song et al., 2016). However, these interventions are not successful in all cases, especially in very preterm infants, and the current therapy for preterm brain injury is still mainly supportive (Juul et al., 2020). Therefore, there is a pressing need for a better understanding of the mechanisms of perinatal brain injury in order to develop strategies for conducting comparative and translational studies on how to reduce brain injuries and how to promote injury repair and improve neurological outcomes in both term and preterm infants.

This Research Topic is dedicated to understanding the influence of perinatal brain injuries on neurological complications, specifically the insult-induced cell death and inflammation signaling pathways. From this wider understanding, novel experimental intervention strategies could be hypothesized and developed. This Research Topic comprises 16 articles representing the work of 131 authors, including 7 animal studies, 3 clinical studies, 5 reviews, and 1 meta-analysis. Of the 7 animal studies, the majority used rodents, and 1 study used fetal sheep. Hypoxic-ischemic

brain injury was the most frequently used experimental model (3 articles) in this Research Topic collection. Other models included fetal growth restriction (FGR) (2 articles), germinal matrix hemorrhage (1 article), and perinatal toxicity exposure (1 article).

Hypoxic ischemic encephalopathy is a subtype of perinatal brain injury and is one of the major contributors to global neonatal morbidity and mortality. Brain injury resulting from birth asphyxia-related hypoxia-ischemia (HI) is associated with the development of cerebral palsy and cognitive deficits in those who survive such injuries (Zhang et al., 2020). HI induces neuronal cell death (Thornton et al., 2017) that persists for a long period and is related to inflammation and epigenetic dysregulation (Ma and Zhang, 2015; Albertsson et al., 2018). Recently, drugs used for the treatment of type 2 diabetes were found to have neuroprotective properties and therapeutic efficacy against neurological sequelae in an HI model, thus showing promising clinical translation potential (Rocha-Ferreira et al., 2018). Poupon-Bejuit et al. summarize recent findings on the use of diabetes drugs for the treatment of neonatal HI brain injury and indicate that diabetes drugs might be considered for clinical translation as a potential treatment. Epigenetic regulation plays an essential role during development, and perinatal insult-induced brain injury and subsequent pathological processes have been associated with lasting disruptions to the epigenetic control of gene expression contributing to neurological dysfunction. Bustelo et al. reviewed the current understanding of epigenetic mechanisms in perinatal HI brain injury and the potential clinical implications in terms of prognostic evaluation and therapeutic interventions. However, knowledge on the role of epigenetics in HI is still very limited and more efforts are needed for continued explorations in this area. Inflammation has been suggested to be a major etiological factor in perinatal brain injury (Hagberg et al., 2015), and innate lymphoid cells have been shown to play an important role in neuroinflammation (Nazmi et al., 2018). Zelco et al. investigated whether type 2 innate lymphoid cells contribute to the development of preterm brain injury in a mouse HI model. They found that even though innate lymphoid cells accumulate in the injured brain hemisphere, type 2 innate lymphoid cells do not contribute to the development of brain injury in the mouse model of preterm brain injury. High-mobility group box 1 (HMGB1) promotes neurite outgrowth and thus promotes brain development under physiological conditions. However, under pathological conditions, HMGB1 can act as a pro-inflammatory factor and can promote brain damage. Sun et al. studied the role of HMGB1 in neonatal rat HI-induced brain injury and found that it can lead to an imbalance in microglial polarization, suggesting that HMGB1 might be used as a therapeutic target against neonatal HI brain injury. To test whether perinatal HI results in deficits in complex cognitive and executive function, Maxwell et al. used a touchscreen platform to assess cognitive function in mice at postnatal day (P)70 (adulthood) following neonatal HI administered at P10 and showed that HI insult in the neonatal period is sufficient to cause long-lasting impairments in cognition and learning processes.

Preterm intraventricular hemorrhage (IVH) occurs in nearly half of infants born at <26 weeks' gestation, and 50–75% of survivors of IVH develop neurological disabilities. Moreover, around 25% of non-disabled survivors develop psychiatric disorders and problems with executive function (Luu et al., 2009; Stoll et al., 2015). Currently, no widely accepted effective prevention or treatment is available for preterm IVH, although recent studies have shown promising results. A previous clinical study showed that postnatal insulin-like growth factor-1 replacement might be a potential treatment for reducing comorbidities of prematurity (Ley et al., 2019). Following that study, Horsch et al. performed further *post-hoc* analyses to evaluate the effect of the replacement therapy on the incidence of brain injury in extremely preterm infants. They found that the potential protective effect of insulin-like growth factor-1 replacement on the occurrence of IVH was most pronounced in infants with no evidence of IVH at the start of treatment. To investigate the mechanisms and therapeutic strategies for IVH, Jinnai et al. established an intracranial collagenase injection model in P5 rats, which developed moderate brain injury affecting both the gray and white matter. These animals developed hyperactivity and showed reduced anxiety in the juvenile stage, which are relevant observations for mimicking IVH in preterm human infants. Post-hemorrhagic ventricular dilatation is a significant cause of death and disability, but few therapeutic options have so far been tested and new therapies are urgently needed for these infants. Mahoney et al. carried out a meta-analysis of 10 trials and concluded that drainage irrigation and fibrinolytic therapy appear to be the most likely candidates for improving outcomes after IVH.

FGR is a common complication of pregnancy often associated with neurological impairments, and there are currently no treatments for FGR. Kitase et al. established a novel FGR rat model that gradually restricted uterine/placental blood flow, which resulted in a 20% reduction in body weight among the offspring. They further investigated the potential of stem cell therapy for reversing the neurological impairment induced by FGR and found that intravenous administration of umbilical cord-derived mesenchymal stromal cells led to a significant amelioration of the reduced number of neurons and impaired behaviors induced by FGR. Glucocorticoids have been used prenatally to prevent complications in preterm infants, and Sutherland et al. investigated whether antenatal betamethasone altered brain development in a sheep model of FGR. They found that betamethasone administration resulted in independent subtle adverse effects on white matter development, which indicated that antenatal glucocorticoids should be administered with caution. The impact of toxic chemical exposure during the perinatal period on brain development has also attracted much attention. Newville et al. report that perinatal opioid (methadone) exposure exaggerated the peripheral immune responses and exacerbated inflammatory signaling, which in part contributed to neurological injury. Treatments to reduce inflammation could rescue the poor neural outcomes as a result of perinatal opioid exposure. Prenatal alcohol exposure is associated with different physical, behavioral, cognitive, and neurological impairments, and Almeida et al. summarize the current animal models of fetal alcohol spectrum disorders, including phenotypic features and neurodevelopmental deficits

as well as the methodologies used to evaluate behavioral and anatomical alterations produced by prenatal alcohol exposure in rodents.

Perinatal brain injury-related neurological sequelae studies are also included in this collection. Wang et al. report that brainstem auditory evoked potentials at the age of 6 months can predict developmental delays in cognitive and motor skills, and thus they propose that the assessment of brainstem auditory evoked potentials may be used as a potential indicator for neurodevelopment. Xie et al. carried out a meta-analysis of expression datasets and identified a set of preeclampsia-driven molecular triggers that shift the developing brain toward a risk of autism spectrum disorders, and Yang et al. evaluated the effectiveness and safety of a clonidine adhesive patch for children with tic disorders in a real-world setting. O'Dea et al. summarize non-neurological organ dysfunction, which not only has a negative effect on the long-term outcome of neonatal brain injury, but may also influence the efficacy of treatments in the acute phase. Further evidence-based research is needed in order to optimize the management of brain injury, prevent further organ dysfunction, and reduce neurodevelopmental impairment.

In summary, this Research Topic has gathered contributions from the groups working in the field of perinatal brain injury and neurological sequelae, with an emphasis on perinatal etiologies of neonatal brain injury. Insight into the mechanisms that underlie the onset and progression of neonatal brain injury might help to identify new avenues for therapeutic intervention. We firmly believe that this is a significant period for research on all aspects of perinatal brain injuries and better preventions and treatments for these injuries will be forthcoming in the very near future.

AUTHOR CONTRIBUTIONS

CZ, CC, and CT wrote the manuscript, acted as editors to this Research Topic, and selected the articles described therein. All authors contributed to the article and approved the submitted version.

FUNDING

Research in the authors' laboratories was supported by the National Natural Science Foundation of China (31761133015, U1704281, CZ), the Swedish Research Council (2018-02667, CZ), Action Medical Research (GN2796, CT), and the Medical Research Council (MR/T014725, CT).

REFERENCES

Albertsson, A. M., Zhang, X., Vontell, R., Bi, D., Bronson, R. T., Supramaniam, V., et al. (2018). gammadelta T cells contribute to injury in the developing brain. *Am. J. Pathol.* 188, 757–767. doi: 10.1016/j.ajpath.2017.11.012

Hagberg, H., Mallard, C., Ferriero, D. M., Vannucci, S. J., Levison, S. W., Vexler, Z. S., et al. (2015). The role of inflammation in perinatal brain injury. *Nat. Rev. Neurol.* 11, 192–208. doi: 10.1038/nrneurol.2015.13

Juul, S. E., Comstock, B. A., Wadhawan, R., Mayock, D. E., Courtney, S. E., Robinson, T., et al. (2020). A randomized trial of erythropoietin for neuroprotection in preterm infants. *N. Engl. J. Med.* 382, 233–243. doi: 10.1056/NEJMoa1907423

Leaw, B., Nair, S., Lim, R., Thornton, C., Mallard, C., and Hagberg, H. (2017). Mitochondria, bioenergetics and excitotoxicity: new therapeutic targets in perinatal brain injury. *Front. Cell. Neurosci.* 11:199. doi: 10.3389/fncel.2017.00199

Ley, D., Hallberg, B., Hansen-Pupp, I., Dani, C., Ramenghi, L. A., Marlow, N., et al. (2019). rhIGF-1/rhIGFBP-3 in preterm infants: a phase 2 randomized controlled trial. *J. Pediatr.* 206, 56–65 e58. doi: 10.1016/j.jpeds.2018.10.033

Luu, T. M., Ment, L. R., Schneider, K. C., Katz, K. H., Allan, W. C., and Vohr, B. R. (2009). Lasting effects of preterm birth and neonatal brain hemorrhage at 12 years of age. *Pediatrics* 123, 1037–1044. doi: 10.1542/peds.2008-1162

Ma, Q., and Zhang, L. (2015). Epigenetic programming of hypoxic-ischemic encephalopathy in response to fetal hypoxia. *Prog. Neurobiol.* 124, 28–48. doi: 10.1016/j.pneurobio.2014.11.001

Nair, S., Rocha-Ferreira, E., Fleiss, B., Nijboer, C. H., Gressens, P., Mallard, C., et al. (2021). Neuroprotection offered by mesenchymal stem cells in perinatal brain injury: role of mitochondria, inflammation, and reactive oxygen species. *J. Neurochem.* 158, 59–73. doi: 10.1111/jnc.15267

Nazmi, A., Albertsson, A. M., Rocha-Ferreira, E., Zhang, X., Vontell, R., Zelco, A., et al. (2018). Lymphocytes contribute to the pathophysiology of neonatal brain injury. *Front. Neurol.* 9:159. doi: 10.3389/fneur.2018.00159

Rocha-Ferreira, E., Poupon, L., Zelco, A., Leverin, A. L., Nair, S., Jonsdotter, A., et al. (2018). Neuroprotective exendin-4 enhances hypothermia therapy in a model of hypoxic-ischaemic encephalopathy. *Brain* 141, 2925–2942. doi: 10.1093/brain/awy220

Shankaran, S., Pappas, A., McDonald, S. A., Vohr, B. R., Hintz, S. R., Yolton, K., et al. (2012). Childhood outcomes after hypothermia for neonatal encephalopathy. *N. Engl. J. Med.* 366, 2085–2092. doi: 10.1056/NEJMoa1112066

Song, J., Sun, H., Xu, F., Kang, W., Gao, L., Guo, J., et al. (2016). Recombinant human erythropoietin improves neurological outcomes in very preterm infants. *Ann. Neurol.* 80, 24–34. doi: 10.1002/ana.24677

Song, J., Wang, Y., Xu, F., Sun, H., Zhang, X., Xia, L., et al. (2021). Erythropoietin improves poor outcomes in preterm infants with intraventricular hemorrhage. *CNS Drugs* 35, 681–690. doi: 10.1007/s40263-021-00817-w

Stoll, B. J., Hansen, N. I., Bell, E. F., Walsh, M. C., Carlo, W. A., Shankaran, S., et al. (2015). Trends in care practices, morbidity, and mortality of extremely preterm neonates, 1993-2012. *JAMA* 314, 1039–1051. doi: 10.1001/jama.2015.10244

Thornton, C., Leaw, B., Mallard, C., Nair, S., Jinnai, M., and Hagberg, H. (2017). Cell death in the developing brain after hypoxia-ischemia. *Front. Cell. Neurosci.* 11:248. doi: 10.3389/fncel.2017.00248

Zhang, S., Li, B., Zhang, X., Zhu, C., and Wang, X. (2020). Birth asphyxia is associated with increased risk of cerebral palsy: a meta-analysis. *Front. Neurol.* 11:704. doi: 10.3389/fneur.2020.00704

Conflict of Interest: The authors declare that the research was conducted in the absence of any commercial or financial relationships that could be construed as a potential conflict of interest.

Publisher's Note: All claims expressed in this article are solely those of the authors and do not necessarily represent those of their affiliated organizations, or those of the publisher, the editors and the reviewers. Any product that may be evaluated in this article, or claim that may be made by its manufacturer, is not guaranteed or endorsed by the publisher.

frontiers in Cellular Neuroscience

ORIGINAL RESEARCH
published: 11 December 2019
doi: 10.3389/fncel.2019.00506

High-Mobility Group Box 1 Contributes to Cerebral Cortex Injury in a Neonatal Hypoxic-Ischemic Rat Model by Regulating the Phenotypic Polarization of Microglia

Yanyan Sun[1], Mingyan Hei[2], Zhihui Fang[3], Zhen Tang[1], Bo Wang[2] and Na Hu[1]*

[1] Department of Pediatrics, The Third Xiangya Hospital of Central South University, Changsha, China, [2] Neonatal Center, Beijing Children's Hospital, Capital Medical University, Beijing, China, [3] Department of Nuclear Medicine, The Second Xiangya Hospital of Central South University, Changsha, China

OPEN ACCESS

Edited by:
Changlian Zhu,
Third Affiliated Hospital of Zhengzhou University, China

Reviewed by:
Yoshiaki Sato,
Nagoya University Hospital, Japan
Xiangning Jiang,
University of California, San Francisco, United States

***Correspondence:**
Mingyan Hei
heimingyan@bch.com.cn

Specialty section:
This article was submitted to Cellular Neuropathology, a section of the journal Frontiers in Cellular Neuroscience

Received: *16 August 2019*
Accepted: *28 October 2019*
Published: *11 December 2019*

Citation:
Sun Y, Hei M, Fang Z, Tang Z, Wang B and Hu N (2019) High-Mobility Group Box 1 Contributes to Cerebral Cortex Injury in a Neonatal Hypoxic-Ischemic Rat Model by Regulating the Phenotypic Polarization of Microglia. Front. Cell. Neurosci. 13:506. doi: 10.3389/fncel.2019.00506

Neonatal hypoxic-ischemic (HI) encephalopathy is a severe disease for which there is currently no curative treatment. Recent evidence suggests that high-mobility group box 1 (HMGB1) protein can promote neuroinflammation after stroke in adult rodents, but its role in perinatal hypoxic-ischemic brain damage (HIBD) remains largely uninvestigated. In the present work, the potential role of HMGB1 in the pathogenesis of HIBD was explored. A HIBD model was established in postpartum day 7 rat pups. HMGB1 expression, the cellular distribution of HMGB1, and microglial activation were all evaluated. Glycyrrhizin (GL), an inhibitor of HMGB1, was used to investigate whether the inhibition of HMGB1 modulated microglial M1/M2 polarization or attenuated brain damage after HI. HAPI microglial cells and primary neurons were cultured *in vitro* and an oxygen-glucose deprivation model was established to evaluate the effects of different microglial-conditioned media on neurons using GL and recombinant HMGB1. Results showed that the expression of HMGB1 was increased in both the ipsilateral cortex and peripheral blood 72 h after HI. Immunofluorescence analyses showed that HMGB1 in the cortex was primarily expressed in neurons. This increase in cortical HMGB1 expression 72 h after HI was characterized by increased co-expression with microglia, rather than neurons or astrocytes. The expression of both M1 and M2 microglia was upregulated 72 h after HI. The administration of GL significantly suppressed M1 microglial polarization and promoted M2 microglial polarization. Meanwhile, GL pretreatment significantly alleviated brain edema and cerebral infarction. *In vitro* experimentation showed that HMGB1-induced M1-conditioned media aggravated neuronal damage, but this effect was neutralized by GL. These findings suggest that HMGB1 may result in an imbalance of M1/M2 microglial polarization in the cortex and thus cause neuronal injury. Pharmacological blockade of HMGB1 signaling may attenuate this imbalanced polarization of microglia and thus could be used as a therapeutic strategy against brain injury in HIBD.

Keywords: hypoxic-ischemic (HI), HMGB1, microglia, polarization, cerebral cortex injury, neonatal

INTRODUCTION

Although neonatal resuscitation has been strongly promoted in recent years, moderate to severe hypoxic-ischemic brain damage (HIBD) still occurs after asphyxia (Barkhuizen et al., 2017). The pathogenesis of HIBD is complex, and there currently exists no effective treatment except for hypothermia. Even with timely hypothermia, more than 40% of neonates who experience severe asphyxia in the perinatal period still exhibit adverse outcomes, or even die as a result (Wu et al., 2016).

The expression of pro-inflammatory factors is higher in the developing brain than in the mature brain (Kaur et al., 2017). Given that HIBD is a pathological condition of the developing brain, it is hypothesized that inflammation, primarily mediated by microglia, may play an important role in HIBD after perinatal asphyxia. Microglia-related neuroinflammation is reported to be associated with the release of cytokines and additional inflammatory mediators, leading to secondary neuronal injury (Umekawa et al., 2015). Microglia can be classified into two main forms: M1-type (pro-inflammatory) and M2-type (anti-inflammatory) (Colton, 2009). M1 microglia promote neuronal death by expressing pro-inflammatory mediators, such as interleukin-6 (IL-6), tumor necrosis factor-α (TNF-α), and inducible nitric oxide synthase (iNOS). In contrast, M2 microglia promote tissue repair and support neuronal survival through the secretion of anti-inflammatory cytokines such as transforming growth factor-β (TGF-β), interleukin-10 (IL-10), and arginase-1 (Olah et al., 2011; Patel et al., 2013). Normally, there exists a careful balance of pro-inflammatory M1 and anti-inflammatory M2 microglia (Jin et al., 2019). Both *in vitro* and *in vivo* experiments have proved that correction of a polarization imbalance of M1/M2 microglia can inhibit the release of pro-inflammatory cytokines and decrease neurotoxicity (Weinstein et al., 2010; Xia et al., 2015; Zhou et al., 2019). *In vivo* studies have reported an imbalance of microglial M1/M2 polarization after hypoxic-ischemic (HI) exposure (Weinstein et al., 2010; Bhalala et al., 2014). However, the exact mechanism underlying this M1/M2 microglia imbalance after HI in neonatal models remains unclear.

High-mobility group box 1 (HMGB1) is a chromatin-associated protein widely expressed in the nuclei of brain cells, which, under physiological conditions, promotes neurite outgrowth and thus brain development (Merenmies et al., 1991; Guazzi et al., 2003; Liu et al., 2010). Under pathological conditions, HMGB1 can act as a pro-inflammatory factor, promoting brain damage (Wang et al., 1999; Zhang et al., 2011; Andersson et al., 2018). Studies have demonstrated that HMGB1 is involved in the pathogenesis of ischemic stroke in adult rodents, activating microglia and promoting neuroinflammation (Ye et al., 2019). In immature animal models, it was reported that HMGB1 translocated from nuclear to cytosolic compartments after HI (Zhang et al., 2016), and the translocation of HMGB1 was primarily in neurons along with release from apoptotic cells (Chen et al., 2019). This translocation may enable the action of HMGB1 as a proinflammatory cytokine that contributes to HI injury in the developing brain (Zhang et al., 2016). Unfortunately, the above studies mainly explored the cellular localization changes of HMGB1 after HI, further mechanism by which HMGB1 aggravates brain injury in HIBD is still unclear.

The objective of the present study was to explore whether HMGB1 played an important role in regulating the phenotypic balance of M1/M2 microglia in the cortex of neonatal SD rats after HI exposure, and whether the HMGB1 inhibitor, glycyrrhizin (GL), could modulate microglial M1/M2 polarization after HI *in vivo* and *in vitro*. We found that HMGB1 was upregulated in microglia after HI. Furthermore, HMGB1 was able to regulate the M1/M2 phenotypic polarization of microglia, leading to cortical injury.

MATERIALS AND METHODS

Animals and Ethical Permission

All experiments were performed in accordance with the guidelines for experimental animal use of Central South University. The protocol was approved by the ethics committee of the Third Xiangya Hospital of Central South University (No. 2016-S006). Perinatal Sprague-Dawley (SD) rats were purchased from Central South University (China). All rats were housed in a 12-h light/dark cycled facility with free access to food and water.

HIBD Animal Model and Drug Administration

The Rice and Vannucci HIBD model was induced with minor modifications in postpartum day 7 (P7) rat pups of both genders. In brief, rat pups were anesthetized with isoflurane and the left common carotid artery was permanently ligated with 5–0 silk sutures. Pups were returned to the dam for a 2 h recovery before initiation of a 2 h hypoxia exposure (37°C, 8% O_2/92% N_2). The sham-operation control animals were given only a small incision on the left side of the neck and the left common carotid artery was isolated without artery ligation or hypoxia treatment.

SD rat pups were randomly divided into three groups: sham + PBS, HI + PBS, and HI + GL. In the HI + GL group, GL was administered 1 h before artery ligation (20 mg/kg, i.p.). In the other two groups, an equal volume of 0.01M PBS was administered.

Primary Neuron Cultures and Microglial-Conditioned Media Treatment

Cells from the microglia-like cell line HAPI (highly aggressive proliferating cell type) were seeded into 6-well plates at 1×10^5/mL and incubated overnight in high-glucose Dulbecco's Modified Eagle Medium (DMEM) containing 10% fetal bovine serum (FBS). Then, an oxygen-glucose deprivation (OGD) model was established to mimic the *in vivo* HI process. HAPI cells were divided into the following three groups: OGD + PBS, OGD + GL, and OGD + r-HMGB1. In brief, PBS (0.01M), GL (55 μM), and recombinant HMGB1 (r-HMGB1, 10 ng/mL) were added to the respective cell groups for 2 h. The cells' medium was then replaced with glucose-free Earle's balanced salt solution, and they were placed in an oxygen- deprived incubator

(93% N_2/5% CO_2/2% O_2) at 37°C for 12 h. Finally, the culture supernatant was collected, one part was used for an ELISA, and the other was used as a conditioned medium (CM) for primary neurons.

Primary cortical neurons were obtained from P1 rat pups. In brief, the cortices of P1 rats were isolated, digested by trypsin, and filtered using a 50 μm sterile nylon filter. Cells were then placed in 24-well plates pre-coated with poly-L-lysine in a neurobasal medium with 10% FBS and B27 supplement. The cells were placed in an incubator (37°C, 5% CO_2) to differentiate for 7 days. At this point, the neuronal medium was removed and substituted with the aforementioned CM from HAPI microglial cells. To analyze the effects of CM on cell viability, neurons were cultured with this microglial CM for 24 h.

Cell Viability and Neurite Length Measurement

Primary cortical neurons were seeded in 96-well plates at a density of 5×10^3 cells/well. After culturing with microglial CM for 24 h, a cell viability assay was performed using a cell-counting kit (CCK-8; Beyotime, China). The optical density was read at a wave length of 450nm using an EnVision Xcite microplate reader (PerkinElmer, United States). Cell viability was calculated using the following formula:

$$Cell\ viability\ (\%) = \frac{optical\ density\ of\ treated\ group}{optical\ density\ of\ control\ group} \times 100$$

For neurite length measurement, three digital images were taken per well after microtubule-associated protein 2 (MAP-2) and 4′, 6′- diamidino-2-phenylindole (DAPI) immunostaining. Using the plugins NeuronJ and ImageScience, Image J software was then used to calculate the average neurite length of MAP-2- positive neurons in every image following the instructions provided.

Western Blotting

Western blotting was used to assess the expression of HMGB1, ionized calcium-binding adaptor molecule 1 (Iba-1), and β-actin in the cortex. Briefly, frozen cortex samples were completely homogenized in lysis buffer containing Phenylmethanesulfonyl fluoride (PMSF, Beyotime, China, ST505) and Radio Immunoprecipitation Assay (RIPA, Beyotime, China, P0013B) and centrifuged at 12,000 rpm for 15 min at 4°C. The supernatant was collected and contained the total protein extracted from the tissue. The quantity of protein in the samples was determined using a BCA protein assay kit (Beyotime, China), according to the manufacturer's instructions. Samples (30 μg per lane) were separated by 12% sodium dodecyl sulfate polyacrylamide gel electrophoresis (SDS-PAGE) and transferred to polyvinylidene fluoride (PVDF) membranes. Membranes were blocked with 5% defatted milk for 2 h at room temperature (temperature of 20–25°C) and, then incubated overnight at 4°C with primary antibodies: rabbit anti-HMGB1 (1:1000 dilution, Abcam, ab18256), rabbit anti-Iba1 (1:100 dilution, Abcam, ab178847), and rabbit anti-β-actin (1:2000 dilution, Proteintech, 14395-1-AP). After three washes in PBST (0.01M PBS containing 0.1% Tween-20), the membranes were incubated with secondary antibodies (goat anti-rabbit IgG, IRDye® 800CW Conjugated, 1:5000 dilution) at room temperature for 2 h. Finally, visualization of the blotted protein bands was accomplished using an infrared laser imaging system (Odyssey CLx, LI-COR, United States) and was quantified by densitometry. The relative expression levels of protein were normalized by the ratio of target protein (HMGB1 and Iba-1) to β-actin.

Enzyme-Linked Immunosorbent Assay (ELISA)

Under anesthesia, whole blood samples were collected from the left ventricles of the rats before transcardial perfusion. Subsequently, samples were centrifuged at 3000 rpm for 10 min at room temperature. The supernatants were collected and frozen at −80°C for further analyses. Before analysis, the samples were centrifuged again, and the supernatant was used for the ELISA assay. HMGB1 concentration was determined using an HMGB1 ELISA kit (Chondrex, United States, 6160), following the manufacturer's protocol.

For the *in vitro* experiment, the culture supernatant from HAPI microglia was collected for the ELISA. The concentrations of TNF-α, IL-1β, and IL-10 were determined using the following ELISA kits: TNF-α (Thermo Fisher, United States, 88-7340-22), IL-1β (R&D Systems, United States, DY501-05), and IL-10 (Abcam, United States, ab218796). All measurements were performed following the manufacturers' protocols.

Immunofluorescence Staining

Animals were anesthetized and, transcardially perfused with 0.01M PBS and 4% paraformaldehyde (PFA). The brains were then removed and post-fixed in 4% PFA immediately. After dehydration with a sucrose gradient, 20 serial coronal sections were cut across the middle of hemisphere. Sections were then washed three times with 0.01M PBS, blocked with 5% bovine serum albumin (BSA), and used for active HMGB1, Iba1, neuronal nuclei (NeuN), glial fibrillary acidic protein (GFAP), CD86, and CD206 staining. The sections were then incubated overnight at 4°C with the following primary antibodies: rabbit anti-Iba1 (1:100 dilution, Abcam, ab178847), rabbit anti-NeuN (1:300 dilution, Abcam, ab177487), mouse anti-HMGB1 (1:500 dilution, Gene Tex, GT348), mouse anti-GFAP (1:300 dilution, Cell Signaling, 3670T), rabbit anti-HMGB1 (1:1000 dilution, Abcam, ab18256), rabbit anti-CD86 (1:200 dilution, Proteintech, 13395-1-AP), rabbit anti-CD206 (1:500 dilution, Abcam, ab125028), and mouse anti- Iba1 (1:500 dilution, Abcam, ab15690). After three washes in 0.01M PBS, the sections were incubated with Cy3-conjugated goat anti-rabbit IgG (1:2000 dilution, Boster Biological Technology, BA1032) or FITC-conjugated goat anti-mouse IgG (1:2000 dilution, Boster Biological Technology, BA1101) for 1 h at room temperature. After three washes in 0.01M PBS, these were then covered with diamidino-2-phenylindole (DAPI, 1:1000, Beyotime, C1002) for 5 min. For each staining, five non-overlapping digital microscopic images of cortical areas were randomly captured

using a fluorescence microscope (IX71, OLYMPUS, Japan). The number of positive cells was determined using Image-Pro Plus 6.0 (Media Cybernetics, United States).

The cultured cortical neurons were fixed with 4% PFA for 24 h after culturing in microglial-CM. They were then incubated with rabbit anti-MAP2 antibodies (1:200 dilution, Proteintech, 17490-1-AP) overnight at 4°C. After three washes in 0.01M PBS, they were incubated with Cy3-conjugated goat anti-rabbit IgG (1:2000 dilution, Boster Biological Technology, BA1032) and then covered with DAPI. Digital microscopic images were taken using the aforementioned IX71 fluorescence microscope.

Reverse Transcription and qRT-PCR

Under deep anesthesia, the brains of the rats were removed and the cerebral cortex was rapidly separated and snap-frozen in liquid nitrogen. Total RNA was isolated using TRIzol reagent (Invitrogen, United States). The first-strand cDNA was synthesized using the Reverse Transcription System (Toyobo, Osaka, Japan), according to the manufacturer's protocol. The relative expression level of mRNA was then assessed using the SYBR Green Real-time PCR Master Mix Kit (Toyobo, Osaka, Japan) and quantified using the Mastercycler® ep realplex qRT-PCR system (Eppendorf, Germany) with glyceraldehyde 3-phosphate dehydrogenase (GAPDH) as the reference gene. All primers used in the qRT-PCR reactions were purchased from Sangon Biotech (China). The sequences of the primer pairs are described as follows: TNF-α (forward: 5′-GCA TGA TCC GAG ATG TGG AAC TGG-3′; reverse: 5′-CGC CAC GAG CAG GAA TGA GAA G-3′); IL-6 (forward: 5′-AGG AGT GGC TAA GGA CCA AGA CC-3′; reverse: 5′-TGC CGA GTA GAC CTC ATA GTG ACC-3′); IL-1β (forward: 5′-ATC TCA CAG CAT CTC GAC AAG-3′; reverse: 5′-CAC ACT AGC AGG TCG TCA TCC-3′); iNOS (forward: 5′-AGA TCC CGA AAC GCT ACA CTT-3′; reverse: 5′-TGC GGC TGG ACT TCT CAC TC-3′); arginase-1 (forward: 5′-ACA TCA ACA CTC CGC TGA CAA CC-3′; reverse: 5′-GCC GAT GTA CAC GAT GTC CTT GG-3′); TGF-β (forward: 5′-GGC ACC ATC CAT GAC ATG AAC CG-3′; reverse: 5′-GCC GTA CAC AGC AGT TCT CTG-3′); IL-4 (forward: 5′-CAA GGA ACA CCA CGG AGA ACG AG-3′; reverse: 5′-CTT CAA GCA CGG AGG TAC ATC ACG-3′); GAPDH (forward: 5′-GAC ATG CCG CCT GGA GAA AC-3′; reverse: 5′-AGC CCA GGA TGC CCT TTA GT-3′). The relative expression of mRNA was calculated using the $2^{-\Delta\Delta Ct}$ method.

Infarct Ratio Calculation

The rat brains were rapidly removed 3 days post-HI and frozen in a freezer at −20°C for 20 min. They were then taken out and four 1.5 mm thick sections were sliced. These sections were placed in 2% TTC staining solution, and incubated at 37°C for 20 min in the dark. Finally, the stained brain slices were placed on a drape for photographing. The aforementioned Image-Pro Plus 6.0 software was used to calculate the volume of each section. The following formula was used to calculate infarct ratio:

$$Ratio\ of\ infarct = \frac{infarct\ volume}{total\ section\ volume} \times 100$$

Brain Water Content

Rats were sacrificed under anesthesia24 h after HI. The brains were bisected to generate two hemispheres (ipsilateral and contralateral to the injury) which were then immediately weighed (wet weight). The hemispheres were then put in an oven (105°C)

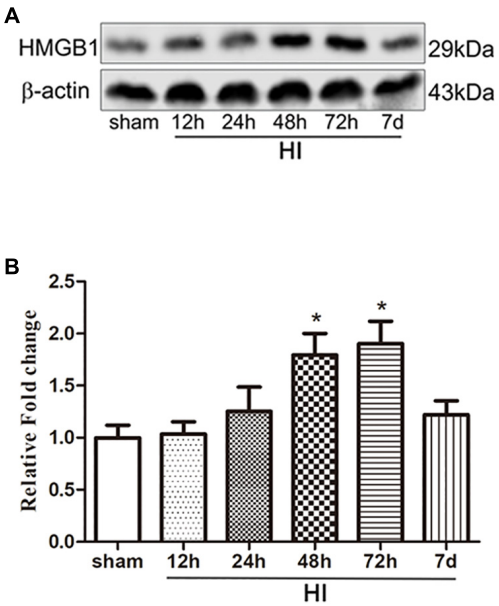

FIGURE 1 | Expression of HMGB1 in the cerebral cortex after HI. **(A)** Western blot bands of HMGB1 expression in the cerebral cortex of P7 SD rats at different time points from 12 h to 7 days after HI. **(B)** Quantitative analyses of the western blot bands (relative OD value) at different time points from 12 h to 7 days after HI, comparing to the sham group (n = 5 for each group). The expression of HMGB1 dramatically increased 24 h after HI and peaked 72 h after HI. Bars represent the mean ± SEM. *P < 0.05 compared to the sham group.

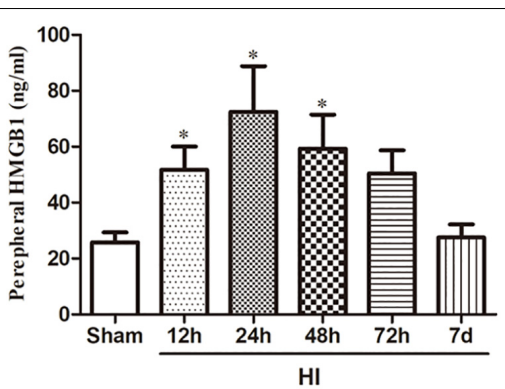

FIGURE 2 | Expression of HMGB1 in serum after HI. HMGB1 level in the peripheral blood detected by ELISA was increased significantly 12, 24, and 48 h after HI exposure with a peak level 24 h after HI comparing to the sham group (n = 10 for each group except n = 9 for the 12 and 24 h group). The serum level of HMGB1 7 days after HI was decreased to a similar level of the sham group. Bars represent the mean ± SEM. *P < 0.05 compared to the sham group.

for 48 h and weighed again (dry weight). The following formula was used to calculate brain water content:

$$Brain\ water\ content\ (\%) = \left[\frac{wet\ weight - dry\ weight}{wet\ weight}\right] \times 100$$

Statistical Analysis

All data are shown as means ± SEM. Data from the different experimental groups were analyzed using one-way ANOVA and the Tukey test for *post hoc* comparisons. Statistical Package for the Social Sciences 19.0 (SPSS, IBM, United States) and GraphPad Prism 5.0 (GraphPad, San Diego, CA, United States) were used for this statistical analysis. A p-value < 0.05 was considered statistically significant.

RESULTS

HMGB1 Was Upregulated in Both the Cerebral Cortex and Serum After HI

To investigate the effect of HI on HMGB1, we examined the expression of HMGB1 in the ipsilateral cerebral cortex and peripheral blood by western blotting and ELISA, respectively. Western blot analysis revealed that the expression of HMGB1 was increased in the ipsilateral cerebral cortex 48 h after HI, peaked 72 h after HI, and subsequently decreased to baseline level compared to the sham group (both $p < 0.05$) (**Figures 1A,B**). ELISA results revealed that the expression of HMGB1 was rapidly up-regulated in serum after HI, peaking at 24 h and gradually returning to a normal level (51.72 ± 8.32, 72.43 ± 16.38,

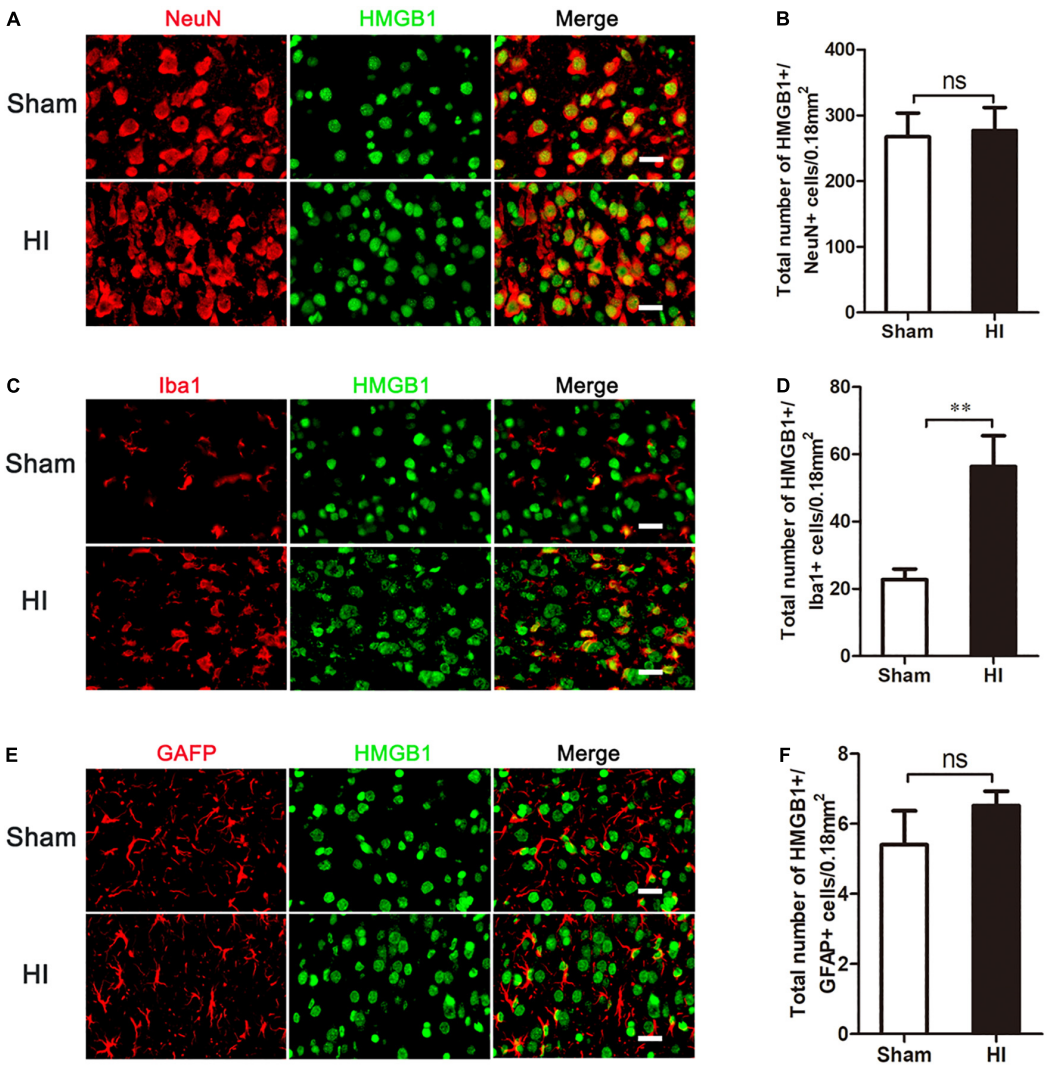

FIGURE 3 | Co-expression of HMGB1 and neural cells in the cerebral cortex after HI. **(A,C,E)** Double immunofluorescent labeling for HMGB1 with NeuN **(A)**, Iba-1 **(C)** and GFAP **(E)** in the cerebral cortex 72 h after HI. Scale bars = 20 μm. NeuN, Iba-1 and GFAP positive cells are red, HMGB1 positive cells are green and merged cells are yellow. **(B,D,F)** Statistical results of NeuN+/HMGB1+, Iba-1+/HMGB1+ and GFAP+/HMGB1+ cell numbers in 0.18 mm^2 area (n = 6 for each group). Iba-1+/HMGB1+ cell numbers significantly increased after HI. There were no significant changes in NeuN+/HMGB1+ and GFAP+/HMGB1+ cell numbers after HI compared to the sham group. Bars represent the mean ± SEM. $^{**}P < 0.01$, ns, no significance compared to the sham group.

59.32 ± 12.18 vs. 25.78 ± 3.58 ng/mL at 12, 24, 48 h post-HI compared to sham group respectively; all $p < 0.05$) (**Figure 2**).

Cortical HMGB1 Expression Was Increased in Microglia, but Not in Neurons or Astrocytes

As HMGB1 is widely expressed in the brain, we then explored in which type of cells HMGB1 was up-regulated. Double-labeled immunofluorescence of HMGB1 was performed in neurons, microglia, and astrocytes. In the sham group, cortical HMGB1 was primarily expressed in neurons (NeuN+/HMGB1+) (267.40 ± 36.04/0.18 mm^2), with low expression in microglia (Iba1+/HMGB1+) (22.72 ± 3.17/0.18 mm^2) and astrocytes (GFAP+/HMGB1+) (5.40 ± 0.97/0.18 mm^2) (**Figures 3A,C,E**). However, 72 h after HI, HMGB1 was increased in microglia [56.36 ± 9.13/0.18 mm^2 (HI) vs. 22.72 ± 3.17/0.18 mm^2 (Sham), $p < 0.01$], but not in neurons [267.40 ± 36.04/0.18 mm^2 (HI) vs. 276.90 ± 34.98/0.18 mm^2 (Sham), $p > 0.05$] or astrocytes [(5.40 ± 0.97/0.18 mm^2 (HI) vs. 6.52 ± 0.41/0.18 mm^2 (Sham), $p > 0.05$] (**Figures 3B,D,F**).

Microglial Activation Occurred in the Cerebral Cortex After HI

Previous studies have shown that microglia are activated in the pathophysiology of HIBD (Ferrazzano et al., 2013; Cengiz et al., 2019), and HMGB1, a pro-inflammatory factor, is upregulated in these activated microglia. Therefore, we explored whether microglial activation was induced in the cerebral cortex after HI. Immunofluorescence (**Figures 4A,B**) and western blot (**Figures 4C,D**) experiments showed that 72 h after HI injury, the expression of Iba-1, a marker of microglia, was significantly higher in the HI group than in the sham group ($p < 0.01$ and, $p < 0.05$, respectively). Meanwhile, microglial morphology changed from branch to amoeba-like after HI exposure. These changes demonstrated that cortical microglia were activated 72 h after HI.

HMGB1 Inhibition Altered M1/M2 Microglial Polarization and Cytokine Transcription

Having observed microglial activation, we further analyzed the M1/M2 polarization of microglia in the cerebral cortex and investigated if this was affected by GL, a specific inhibitor of HMGB1. We first used western blotting to detect whether the expression of HMGB1 in the cerebral cortex could be inhibited by GL pretreatment (**Figures 5A,B**). It was showed that GL could effectively attenuate the expression of HMGB1 in the cerebral cortex 72 h after HI. Then Iba1+/CD86+ and Iba1+/CD206+ co-staining were used to identify M1 and M2 phenotypes, respectively (**Figures 6A–D**). The results showed

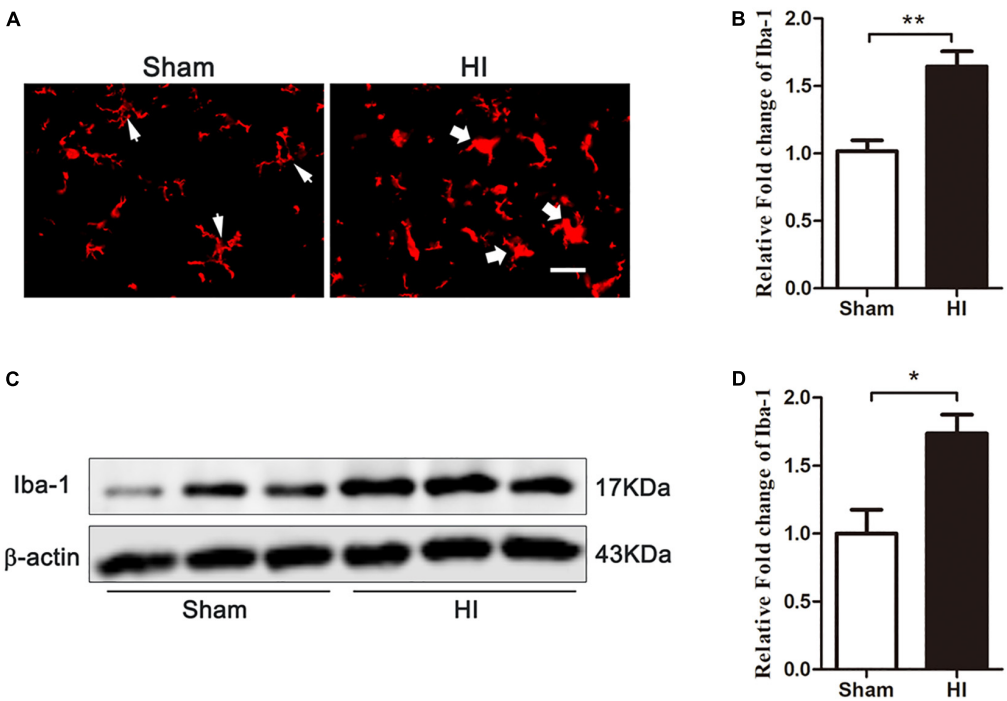

FIGURE 4 | Expression of microglia in the cerebral cortex after HI. **(A)** Immunofluorescent labeling of microglia (Iba-1) in the cerebral cortex 72 h after HI. The morphology of microglia changed from branch in sham group (white narrow arrows) to ameba-like in HI group (white wide arrows) after HI exposure. Scale bar = 20 μm. **(B)** Quantitative analyses of Iba-1 fluorescence intensity (relative OD value) showed that there was an increased expression of Iba-1 ($n = 6$ for each group). **(C)** The expression of Iba-1 in the cerebral cortex detected by western blot 72 h after HI. **(D)** Quantitative analyses of the western blot bands (relative OD value) revealed that there was a significantly increase in the expression of Iba-1 ($n = 6$ for each group). Bars represent the mean ± SEM. *$P < 0.05$ compared to the sham group, **$P < 0.01$ compared to the sham group.

that the expression of both M1 and M2 phenotypes was significantly increased 72 h after HI [37.00 ± 6.29 cells/0.18mm^2 (Sham + PBS) vs. 126.60 ± 23.74 cells/0.18mm^2 (HI + PBS); 23.60 ± 6.94 cells/0.18mm^2 (Sham + PBS) vs. 61.20 ± 8.12 cells/0.18mm^2 (HI + PBS), $p < 0.01$ and $p < 0.05$, respectively]. When rats were pretreated with GL, the number of M1 microglia (Iba1+/CD86+ cells) significantly reduced [126.60 ± 23.74 cells/0.18 mm^2 (HI + PBS) vs. 56.80 ± 9.12 cells/0.18 mm^2 (HI + GL), $p < 0.05$] (**Figures 6A,B**), while the number of M2 microglia (Iba1+/CD206+ cells) significantly increased [61.20 ± 8.12 cells/0.18 mm^2 (HI + PBS) vs. 127.60 ± 20.60 cells/0.18 mm^2 (HI + GL), $p < 0.05$] (**Figures 6C,D**).

We then detected the mRNA expression of M1 and M2 inflammatory factors using qRT-PCR. Results showed that the mRNA expression of M1 and M2 functional cytokines was significantly increased in the HI + PBS compared to the sham + PBS group 72 h after HI ($p < 0.05$, **Figures 7A,B**). The mRNA expression of M1 functional cytokines (iNOS, TNF-α, and IL-1β) was significantly decreased in the HI + GL group compared to the HI + PBS group (all $p < 0.05$, **Figure 7A**). In contrast, the mRNA expression of M2 functional cytokines (arginase1, IL-4, and TGF-β) was significantly increased in the HI + GL group compared to the HI + PBS group (all $p < 0.05$ except for arginase1, **Figure 7B**).

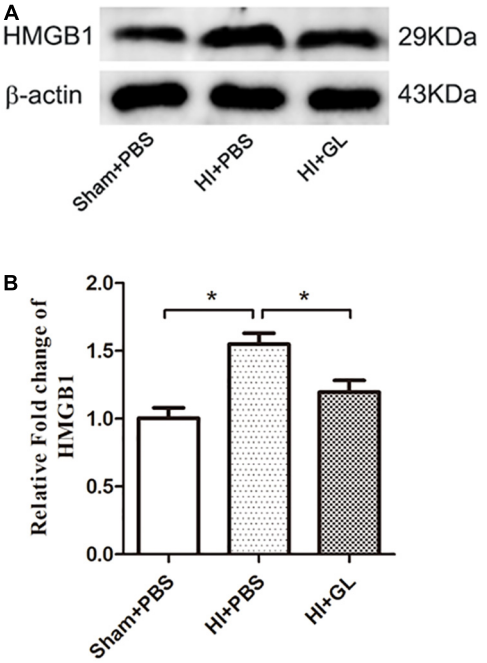

FIGURE 5 | Effect of GL on the expression of HMGB1 in the cerebral cortex after HI. **(A)** Western blot bands of HMGB1 expression in the cerebral cortex 72 h after HI. **(B)** Quantitative analyses of the western blot bands (relative OD value) showed that GL effectively inhibited the expression of HMGB1 in the cerebral cortex 72 h after HI ($n = 5$ for each group). Bars represent the mean ± SEM. *$P < 0.05$.

HMGB1 Aggravated Microglial-Induced Neurotoxicity *in vitro*

To further elucidate the effect of HMGB1 on microglial phenotype, an OGD model of HAPI microglial cells was established *in vitro*. The effects of r-HMGB1 and its inhibitor GL, on the phenotypic changes of HAPI microglial cells were examined (**Figure 8A**). ELISA analysis showed that GL significantly reduced the expression of the M1-associated inflammatory cytokines TNF-α [66.44 ± 4.84 pg/mL (OGD + PBS) vs. 35.08 ± 2.94 pg/mL (OGD + GL), $p < 0.05$] and IL-1β [113.00 ± 2.99 pg/mL (OGD + PBS) vs. 62.21 ± 2.85 pg/mL (OGD + GL), $p < 0.05$], and significantly increased the expression of the M2-associated inflammatory cytokine IL-10 [97.89 ± 3.08 pg/mL (OGD + PBS) vs. 221.90 ± 5.43 pg/mL (OGD + GL), $p < 0.05$]. In contrast, r-HMGB1 significantly increased the expression of TNF-α [66.44 ± 4.84 pg/mL (OGD + PBS) vs. 119.00 ± 2.70 pg/mL (OGD + r-HMGB1), $p < 0.05$] and IL-1β [113.00 ± 2.99 pg/mL (OGD + PBS) vs. 173.60 ± 2.77 pg/mL (OGD + r-HMGB1), $p < 0.05$], and significantly reduced the expression of IL-10 [97.89 ± 3.08 pg/mL (OGD + PBS) vs. 49.37 ± 3.98 pg/mL (OGD + GL), $p < 0.05$]. These results indicated that under OGD conditions, HMGB1 promoted the polarization of microglia to a M1-like phenotype. In contrast, inhibition of HMGB1 promoted the polarization of microglia to a M2-like phenotype.

Next, the effect of different CM from HAPI microglial cells on neurons was examined (**Figures 8B–D**). We defined CM from M1 and M2-like phenotypes, as M1-CM and M2-CM, respectively. We first used MAP2 as a marker to explore the effects of different CMs on the length of nerve dendrites using an immunofluorescence assay. It was noted that the mean neurite length of MAP2-positive cells significantly decreased in the presence of M1-CM. In contrast, the mean neurite length of MAP2-positive cells significantly increased in the presence of M2-CM (**Figures 8B,C**). The survival of cortical neurons was then evaluated using a CCK-8 assay. This showed that M1-CM from the OGD+ r-HMGB1 group significantly reduced the cell viability of the primary cortical neurons, while M2-CM from the OGD + GL group significantly increased the cell viability of the primary cortical neurons, compared to the OGD + PBS control group (**Figure 8D**). These results suggested that HMGB1 could aggravate microglial-induced neurotoxicity in OGD conditions.

HMGB1 Inhibition Alleviated HI-Induced Brain Injury

As HMGB1 induced microglial polarization to an M1 phenotype, leading to increased neurotoxicity, we then explored whether inhibition of HMGB1 could attenuate HI-induced brain damage using edema assessment and cerebral infarction detection (**Figures 9A–D**). As shown in **Figure 9A**, the ipsilateral side of the brain was visibly edematous 72 h after HI insult. Pretreatment with GL alleviated this edema and morphological damage in the HI group. As shown in **Figure 9B**, the water content of the ipsilateral hemispheres was significantly increased in the HI group compared to the sham group. The inhibition of HMGB1 significantly alleviated the water content of the ipsilateral hemispheres in the HI group ($p < 0.05$). TTC staining

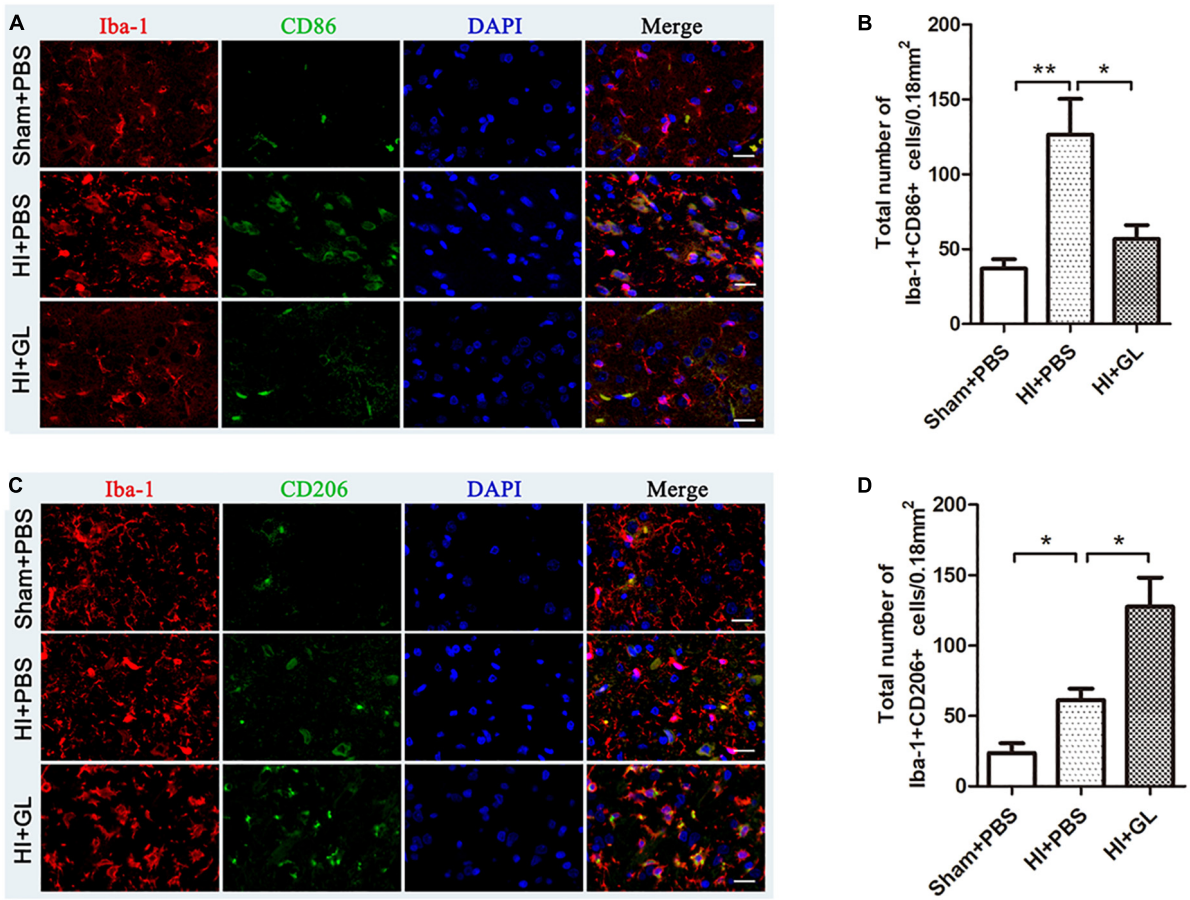

FIGURE 6 | Effect of GL on M1 and M2 phenotypes of microglia in the cerebral cortex after HI. **(A)** Immunofluorescent labeling of M1 phenotype (Iba-1+/CD86+) in the cerebral cortex 72 h after HI. Scale bars = 20 μm, Iba-1 positive cells are red, CD86 positive cells are green, DAPI-stained nuclei are blue and merged cells are yellow. **(B)** The statistical results of Iba-1+/CD86+ cell numbers in 0.18 mm^2 area. The expression of M1 phenotype significantly increased after HI. While it had a decrease in HI + GL group compared to HI + PBS group. **(C)** Immunofluorescent labeling of M2 phenotype (Iba-1+/CD206+) in the cerebral cortex 72 h after HI. Scale bars = 20 μm, Iba-1 positive cells are red, CD206 positive cells are green, DAPI-stained nuclei are blue and merged cells are yellow. **(D)** The statistical results of Iba-1+/CD206+ cell numbers in 0.18 mm^2 area. The expression of M2 phenotype significantly increased after HI and it had an increase in HI + GL group compared to HI + PBS group. $N = 6$ for each group, bars represent the mean ± SEM. $^*P < 0.05$, $^{**}P < 0.01$.

showed that HI insult substantially increased ipsilateral infarct size, which was reversed by pretreatment with HMGB1 inhibition ($p < 0.05$, **Figures 9C,D**). These results suggested that the inhibition of HMGB1 could alleviate HI-induced brain damage.

DISCUSSION

The present study investigated whether HMGB1 has a role in the pathogenesis of neonatal rat HIBD, focusing on the polarization of microglia. It was found that HMGB1 led to an imbalance in M1/M2 microglial polarization in the cortex, thus aggravating brain damage. This was alleviated by inhibiting HMGB1 with GL in HIBD.

HMGB1, a damage-associated protein, mediates neuroinflammation and brain damage in many neurological diseases including ischemic stroke (Angelopoulou et al., 2018; Paudel et al., 2018; Ye et al., 2019). Previous studies demonstrated that HMGB1 increased early at 3 h in serum and decreased in cerebral cortex after HI (Chen et al., 2019). Similarly, we found that HMGB1 was upregulated in peripheral blood after HI insult. But in our study, ipsilateral cortical HMGB1 also increased and serum HMGB1 increased 12 h after HI, inconsistent with the aforementioned results. These different results may be due to the different temperatures and different severity of injury after suffering from HI. It is suggested that pathological change and cerebral metabolic rate are different under different temperatures, and different temperatures can even affect clinical efficacy in hypothermia-treated HIE (Kim et al., 2014). And due to individual variation in animals, different severity of brain injury may occur, which could also lead to the discrepancy above.

Besides the serum and cortical upregulation of HMGB1, we also found that the expression of HMGB1 increased in peripheral blood much earlier than in the brain. There are two potential mechanisms underlying this experimental phenomenon. One possibility is that the early increase of peripheral HMGB1

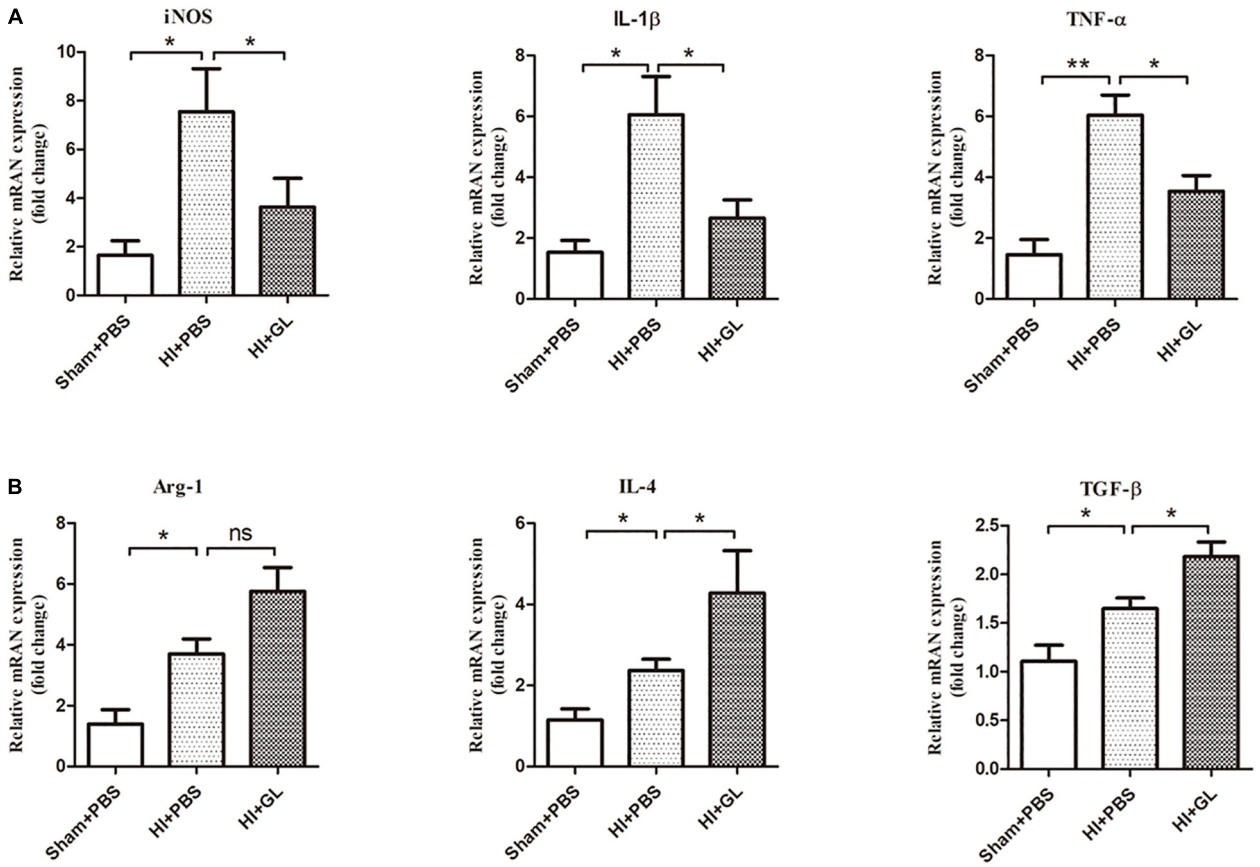

FIGURE 7 | Effect of GL on M1 and M2 functional cytokines in the cerebral cortex after HI. **(A)** The mRNA levels of M1 functional cytokines (iNOS, IL-1β, and TNF-α) were detected using qRT-PCR 72 h after HI. Results showed that the mRNA expression of M1 functional cytokines all increased after HI. While there was a significant decrease in HI + GL group compared to HI + PBS group. **(B)** The mRNA levels of M2 functional cytokines (Arg-1, IL-4, and TGF-β) were detected using qRT-PCR 72h after HI. Results showed that the expression of M2 functional cytokines all increased after HI and there was a higher level in HI + GL group compared to HI + PBS group. $N = 6$ for each group, bars represent the mean ± SEM, $^{*}P < 0.05$, $^{**}P < 0.01$, ns, no significance.

comes from brain tissue damage. As a typical damage-associated protein, HMGB1 could be released from damaged or necrotic brain tissue after HI insult, directing blood-brain barrier (BBB) breakdown and entering peripheral blood immediately, leading to a rapid increase of peripheral HMGB1 (Faraco et al., 2007; Ye et al., 2019). In addition, stimulation such as surgery and HI insult may have induced the release of HMGB1 from peripheral organs, causing peripheral HMGB1 to increase rapidly (Jellema et al., 2013; Terrando et al., 2016). The increased peripheral HMGB1 could in turn damage BBB and enter the brain, along with HMGB1 from the damaged brain tissue to lead to an increase of cerebral HMGB1. Our previous study showed that serum HMGB1 levels were significantly elevated in persistent pulmonary hypertension of the newborn (PPHN) and decreased dramatically after PPHN resolution (Tang et al., 2019). A meta-analysis by Le et al. (2018) demonstrated that circulating blood HMGB1 levels increased in ischemic stroke, with a higher HMGB1 level indicating a more serious condition. The rapid rise observed in peripheral HMGB1 after HI suggested that HMGB1 is sensitive to HI insult, and may potentially be useful as a biomarker in the early stage of HIBD.

In our study, we found that HMGB1 was widely expressed in the neurons of neonatal rat brains. However, the upregulation of HMGB1 after HI was characterized by an increased expression in microglia, but not in neurons or astrocytes. Several studies have demonstrated that HMGB1 can be transferred from the nucleus of the neuron to the cytoplasm or released extracellularly by stimulation such as brain ischemia (Qiu et al., 2008; Zhang et al., 2016; Chen et al., 2019) and subarachnoid hemorrhage (Sun et al., 2014). Under severe cerebral ischemic conditions, neuronal cells undergo apoptosis or necrosis by the induction of a number of pathways (Thal et al., 2011). As a result, HMGB1 could be released from necrotic neurons and interact with microglia as an extracellular cytokine (Frasch and Nygard, 2017). Based on the above research, it is therefore likely that HMGB1 was transferred extracellularly from neuronal nuclei or released from necrotic neurons after HI insult. This neuronal HMGB1 could then serve as an extracellular factor, binding to microglia and, resulting in the increase of HMGB1+/Iba1+ cells. As a group of innate immune cells in the central nervous system, it is known that microglial-mediated neuroinflammation plays an important role in the pathogenesis of many neurological

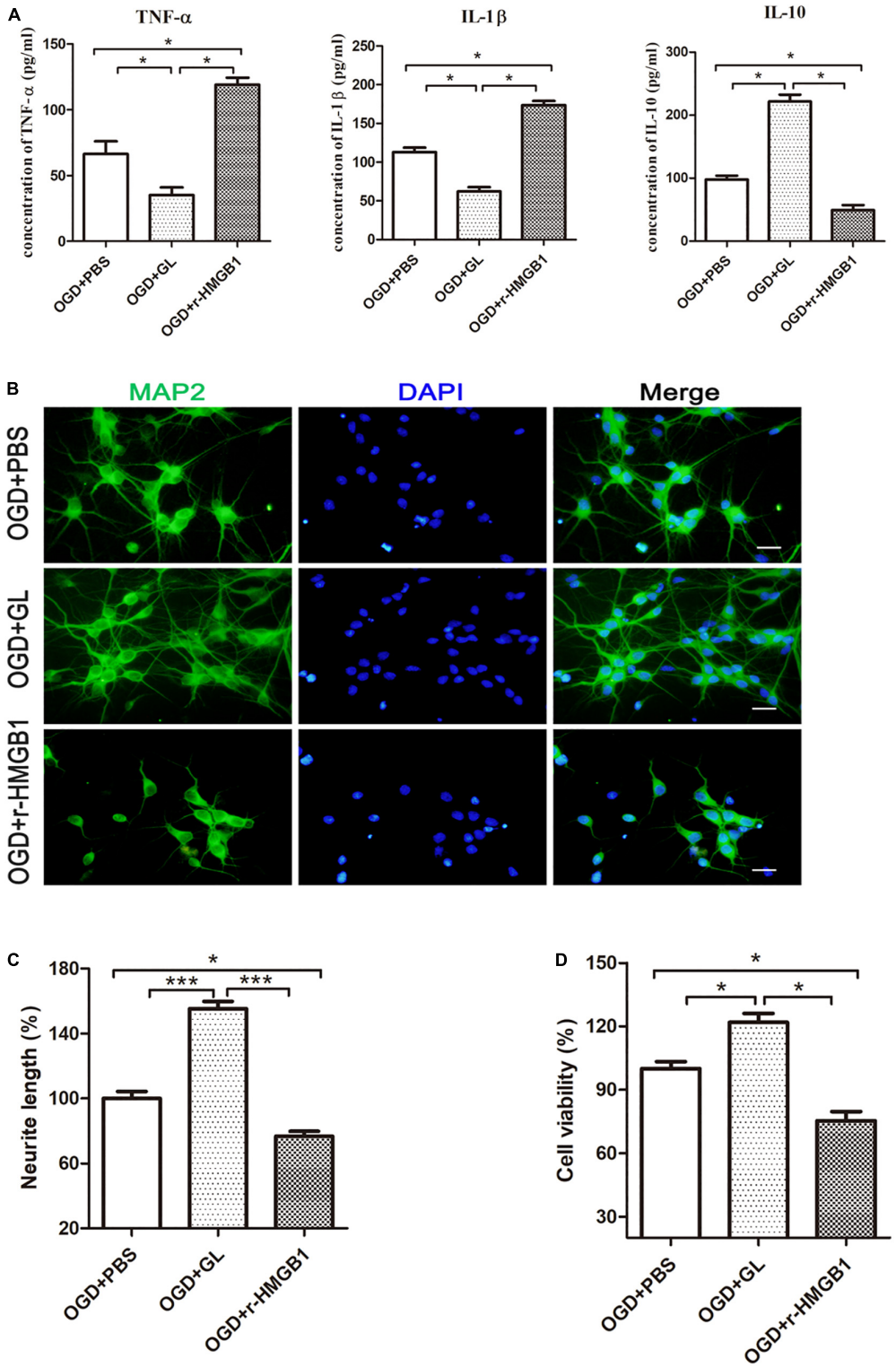

FIGURE 8 | Effect of HMGB1 on microglia-induced neurotoxicity *in vitro*. **(A)** HAPI microglia was pretreated with r-HMGB1 or GL and then undergoing OGD for 24 h. The expression of TNF-α, IL-1β and IL-10 in culture supernatant was measured by ELISA (n = 4 wells per group). **(B)** Immunofluorescent staining of primary cortical neurons (MAP2, green) with DAPI (blue) 48 h after incubation with different CM from HAPI microglial medium. Scale bars = 20 μm. **(C)** Quantitative analyses of relative neurite length of primary neurons after immunofluorescent staining using ImageJ. N = 4 wells for each group, 3 digital microscopic images for each well. **(D)** Cell viability of primary neurons 48 h after incubation with different CM from HAPI microglial medium using CCK8 method (n = 4 wells for each group). Bars represent the mean ± SEM, $^{*}P < 0.05$, $^{***}P < 0.001$.

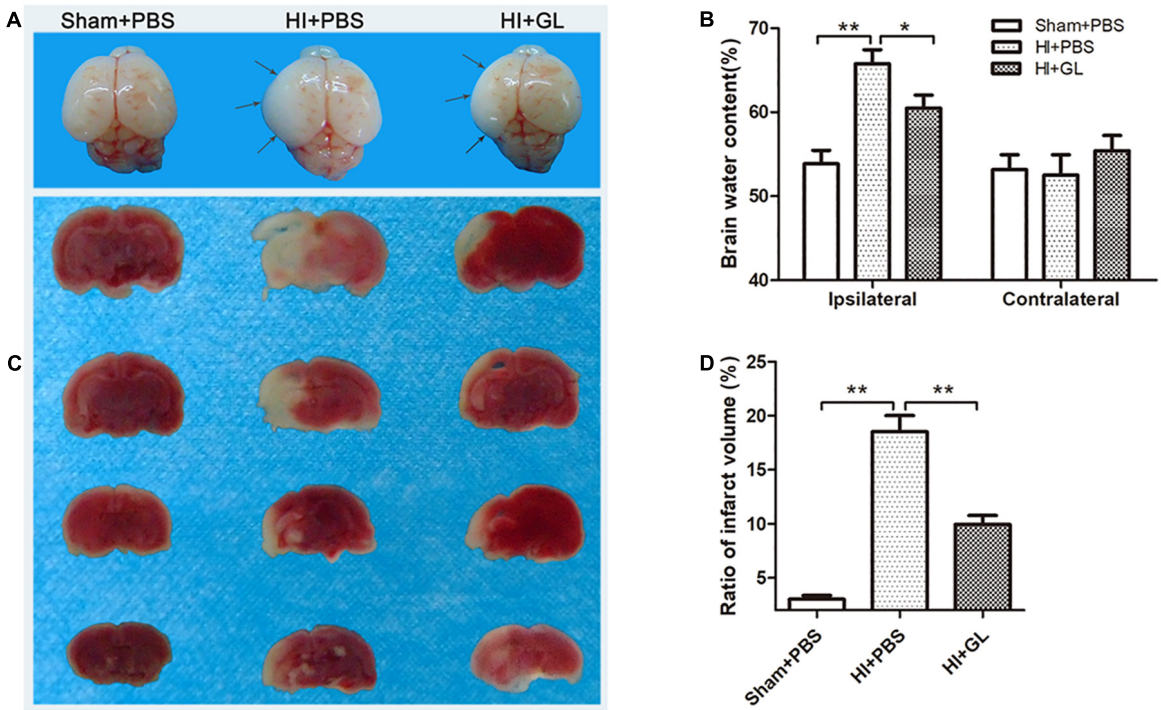

FIGURE 9 | Effect of GL treatment on HI-induced brain injury. **(A)** Whole brain photos showing cerebral edema 24 h after HI. Gray arrows indicate sites of significant edema. Cerebral edema area in HI + GL group was smaller than HI + PBS group. **(B)** The brain water content measurement showed that the ipsilateral brain water content in HI + GL group was significantly lower compared to the HI + PBS group (n = 6 for each group). **(C)** TTC staining of all treatment groups 72 h after HI. Normal tissues were red or pink, while infract tissues were white. The white area in HI + GL group was smaller than HI + PBS group. **(D)** Statistical results showed that the ratio of infract volume in HI + GL group was significantly lower compared to HI + PBS group (n = 5 for each group). Bars represent the mean ± SEM, $^{*}P < 0.05$, $^{**}P < 0.01$.

diseases, including HIBD (Fonken et al., 2016; Zhang et al., 2016; Kigerl et al., 2018). As an important inflammatory factor, the binding of HMGB1 to microglia could further promote this neuroinflammation (Sun et al., 2018), in turn triggering an inflammation cascade response and, aggravating brain damage. Further, the *in vitro* experiments in our study showed that HMGB1 increased the neurotoxicity of neurons under the condition of OGD (**Figure 8**). It is implied that the increase of HMGB1+/Iba1+ cells may result in a decrease of HMGB1+/NeuN+ cells. However, we did not find a decrease in the number of HMGB1+/NeuN+ cells 72 h after HI. Due to the sustained neuroinflammation, there is a great possibility that the number of HMGB1+/NeuN+ cells will decrease after 72 h post HI. Thus, inhibition of HMGB1 expression may help to reduce neuroinflammation.

Studies have shown that microglia can be activated after HI stimulation (Ohsawa and Kohsaka, 2011; Serdar et al., 2019). In our study, HI insult resulted in an increased expression of Iba-1 and a change in microglial morphology from branch to ameba-like. These results indicated that cortical microglia were activated after HI, consistent with previous research (Harry, 2013; Cengiz et al., 2019). Microglia can be differentiated into different subtypes after activation. The two main subtypes are M1 and M2 microglia, characterized by pro-inflammatory (neurotoxic) and anti- inflammatory (neuroprotective) phenotypes, respectively (Olah et al., 2011; Patel et al., 2013). In this study, the HMGB1 inhibitor GL was used to investigate the effect of HMGB1 on the M1/M2 polarization of microglia during the pathogenesis of HIBD. The results showed that the expression of both M1 and M2 microglia was significantly increased 72 h after HI. Inhibition of HMGB1 by GL reduced the expression of the M1 phenotype and promoted the expression of the M2 phenotype, indicating that HMGB1 was involved in the imbalance of M1/M2 microglial polarization in HIBD.

In addition, an *in vitro* experiment was conducted to mimic the HI process *in vivo*. We investigated the polarization state of microglia and the effect of microglia on HMGB1 expression in neurons during the process of OGD. We found that HMGB1 promoted the polarization of microglia to an M1 phenotype, enhancing the expression of pro-inflammatory factors such as TNF-α and IL-1β, and resulting in a decrease in neuronal activity and dendritic length. However, the above phenomenon could be neutralized by inhibiting HMGB1 with GL. We conducted further animal experiments and found that HMGB1 inhibition could reduce brain edema and cerebral infarction area after HI. The above effects of HMGB1 are similar to those reported by Gao et al. (2018) and Sun et al. (2018). Taken together, these findings suggest that HMGB1 may cause neuroinflammation and neuronal damage by inducing an imbalance of M1/M2 microglial polarization, leading to brain damage.

There exists a number of limitations of our study. As different pathological changes occur at different time points after HI (Park et al., 2018), the window of time during which post-HI treatment is administered has a significant impact on prognosis. Unfortunately, in our study, GL was only administered as a pre-treatment before HI and not at different time points after HI. In addition, this study did not explore the underlying mechanisms and specific pathways by which HMGB1 regulates the M1/M2 polarization of microglia. Finally, this study only examined the acute phase of HI (0–72 h), whereas it is known that, perinatal HI has a long-term effect on the development of the nervous system in children (Papazian, 2018; Sanches et al., 2019). This study did not investigate the effects of HMGB1 on the development of the brain in the late phase of HI. The aforementioned points therefore need to be addressed in further research.

CONCLUSION

Our findings suggest that HMGB1 may lead to an imbalance of M1/M2 microglial polarization in the cortex and thus neuronal injury. Such findings suggest that pharmacological blockade of HMGB1 signaling may attenuate this imbalanced polarization of microglia and thus could be used as a therapeutic strategy against brain injury in HIBD.

DATA AVAILABILITY STATEMENT

The raw data supporting the conclusions of this article will be made available by the authors, without undue reservation, to any qualified researcher.

ETHICS STATEMENT

All experiments were performed in accordance with the guidelines for experimental animal use of Central South University. The protocol was approved by the Ethics Committee of the Third Xiangya Hospital of Central South University (No. 2016-S006).

AUTHOR CONTRIBUTIONS

YS, ZF, and ZT performed the experiments, analyzed the data, and wrote the manuscript. NH and BW performed the experiments and analyzed the data. YS and MH designed the study and revised the manuscript. All of the authors read and approved the final manuscript.

FUNDING

This study was supported by the National Natural Science Foundation of China (81671505) and the Natural Scientific Foundation of Beijing (7192061).

ACKNOWLEDGMENTS

We would like to thank Editage (www.editage.com) for English language editing. We sincerely thank the staff in the central lab of the Third Xiangya Hospital of Central South University for their wonderful support in this study.

REFERENCES

Andersson, U., Yang, H., and Harris, H. (2018). High-mobility group box 1 protein (HMGB1) operates as an alarmin outside as well as inside cells. *Semin. Immunol.* 38, 40–48. doi: 10.1016/j.smim.2018.02.011

Angelopoulou, E., Piperi, C., and Papavassiliou, A. G. (2018). High-mobility group box 1 in Parkinson's disease: from pathogenesis to therapeutic approaches. *J. Neurochem.* 146, 211–218. doi: 10.1111/jnc.14450

Barkhuizen, M., van den Hove, D. L., Vles, J. S., Steinbusch, H. W., Kramer, B. W., and Gavilanes, A. W. (2017). 25 years of research on global asphyxia in the immature rat brain. *Neurosci. Biobehav. Rev.* 75, 166–182. doi: 10.1016/j.neubiorev.2017.01.042

Bhalala, U. S., Koehler, R. C., and Kannan, S. (2014). Neuroinflammation and neuroimmune dysregulation after acute hypoxic-ischemic injury of developing brain. *Front, Pediatr.* 2:144. doi: 10.3389/fped.2014.00144

Cengiz, P., Zafer, D., Chandrashekhar, J. H., Chanana, V., Bogost, J., Waldman, A., et al. (2019). Developmental differences in microglia morphology and gene expression during normal brain development and in response to hypoxia-ischemia. *Neurochem. Int.* 127, 137–147. doi: 10.1016/j.neuint.2018.12.016

Chen, X., Zhang, J., Kim, B., Jaitpal, S., and Meng, S. S. (2019). High-mobility group box-1 translocation and release after hypoxic ischemic brain injury in neonatal rats. *Exp. Neurol.* 311, 1–14. doi: 10.1016/j.expneurol.2018.09.007

Colton, C. A. (2009). Heterogeneity of microglial activation in the innate immune response in the brain. *J. Neuroimmune. Pharmacol.* 4, 399–418. doi: 10.1007/s11481-009-9164-4

Faraco, G., Fossati, S., Bianchi, M. E., Patrone, M., and Pedrazzi, M. (2007). High mobility group box 1 protein is released by neural cells upon different stresses and worsens ischemic neurodegeneration in vitro and in vivo. *J. Neurochem.* 103, 590–603. doi: 10.1111/j.1471-4159.2007.04788.x

Ferrazzano, P., Chanana, V., Uluc, K., Fidan, E., and Akture, E. (2013). Age-dependent microglial activation in immature brains after hypoxia-ischemia. *CNS Neurol. Disord. Drug Targets* 12, 338–349. doi: 10.2174/1871527311312030007

Fonken, L. K., Frank, M. G., Kitt, M. M., D'Angelo, H. M., and Norden, D. M. (2016). The alarmin HMGB1 mediates age-induced neuroinflammatory priming. *J. Neurosci.* 36, 7946–7956. doi: 10.1523/JNEUROSCI.1161-16.2016

Frasch, M. G., and Nygard, K. L. (2017). Location, location, location: appraising the pleiotropic function of HMGB1 in fetal brain. *J. Neuropathol. Exp. Neurol.* 76, 332–334. doi: 10.1093/jnen/nlx004

Gao, T., Chen, Z., Chen, H., Yuan, H., and Wang, Y. (2018). Inhibition of HMGB1 mediates neuroprotection of traumatic brain injury by modulating the microglia/macrophage polarization. *Biochem. Biophys. Res. Commun.* 497, 430–436. doi: 10.1016/j.bbrc.2018.02.102

Guazzi, S., Strangio, A., Franzi, A. T., and Bianchi, M. E. (2003). HMGB1, an architectural chromatin protein and extracellular signalling factor, has a spatially and temporally restricted expression pattern in mouse brain. *Gene. Expr. Patterns* 3, 29–33. doi: 10.1016/s1567-133x(02)00093-5

Harry, G. J. (2013). Microglia during development and aging. *Pharmacol. Ther.* 139, 313–326. doi: 10.1016/j.pharmthera.2013.04.013

Jellema, R. K., Lima, P. V., Zwanenburg, A., Ophelders, D. R., and De Munter, S. (2013). Cerebral inflammation and mobilization of the peripheral immune system following global hypoxia-ischemia in preterm sheep. *J. Neuroinflammation* 10:13. doi: 10.1186/1742-2094-10-13

Jin, X., Liu, M. Y., Zhang, D. F., Zhong, X., Du, K., Qian, P., et al. (2019). Natural products as a potential modulator of microglial polarization in

neurodegenerative diseases. *Pharmacol. Res.* 145:104253. doi: 10.1016/j.phrs.2019.104253

Kaur, C., Rathnasamy, G., and Ling, E. A. (2017). Biology of microglia in the developing brain. *J. Neuropathol. Exp. Neurol.* 76, 736–753. doi: 10.1093/jnen/nlx056

Kigerl, K. A., Lai, W., Wallace, L. M., Yang, H., and Popovich, P. G. (2018). High mobility group box-1 (HMGB1) is increased in injured mouse spinal cord and can elicit neurotoxic inflammation. *Brain Behav. Immun.* 72, 22–33. doi: 10.1016/j.bbi.2017.11.018

Kim, J. H., Yun, S. H., Jang, K. H., Park, J., and Han, H. S. (2014). Delayed and prolonged local brain hypothermia combined with decompressive craniectomy: a novel therapeutic strategy that modulates glial dynamics. *Exp. Neurobiol.* 23, 115–123. doi: 10.5607/en.2014.23.2.115

Le, K., Mo, S., Lu, X., Idriss, A. A., Yu, D., and Guo, Y. (2018). Association of circulating blood HMGB1 levels with ischemic stroke: a systematic review and meta-analysis. *Neurol. Res.* 40, 907–916. doi: 10.1080/01616412.2018.1497254

Liu, Y., Prasad, R., and Wilson, S. H. (2010). HMGB1: roles in base excision repair and related function. *Biochim. Biophys. Acta* 1799, 119–130. doi: 10.1016/j.bbagrm.2009.11.008

Merenmies, J., Pihlaskari, R., Laitinen, J., Wartiovaara, J., and Rauvala, H. (1991). 30-KDa heparin-binding protein of brain (amphoterin) involved in neurite outgrowth. Amino acid sequence and localization in the filopodia of the advancing plasma membrane. *J. Biol Chem.* 266, 16722–16729.

Ohsawa, K., and Kohsaka, S. (2011). Dynamic motility of microglia: purinergic modulation of microglial movement in the normal and pathological brain. *Glia* 59, 1793–1799. doi: 10.1002/glia.21238

Olah, M., Biber, K., Vinet, J., and Boddeke, H. W. (2011). Microglia phenotype diversity. *CNS Neurol. Disord. Drug Targets* 10, 108–118. doi: 10.2174/187152711794488575

Papazian, O. (2018). Neonatal hypoxic-ischemic encephalopathy. *Medicina* 78(Suppl. 2), 36–41.

Park, J. H., Noh, Y., Kim, S., Ahn, J. H., and Ohk, T. G. (2018). Time-course changes and new expressions of MIP-3 and its receptor, CCR6, in the gerbil hippocampal CA1 area following transient global cerebral ischemia. *Neurochem. Res.* 43, 2102–2110. doi: 10.1007/s11064-018-2632-6

Patel, A. R., Ritzel, R., McCullough, L. D., and Liu, F. (2013). Microglia and ischemic stroke: a double-edged sword. *Int. J. Physiol. Pathophysiol. Pharmacol.* 5, 73–90.

Paudel, Y. N., Shaikh, M. F., Chakraborti, A., Kumari, Y., and Aledo-Serrano, A. (2018). HMGB1: a common biomarker and potential target for TBI, neuroinflammation, epilepsy, and cognitive dysfunction. *Front. Neurosci.* 12:628. doi: 10.3389/fnins.2018.00628

Qiu, J., Nishimura, M., Wang, Y., Sims, J. R., and Qiu, S. (2008). Early release of HMGB-1 from neurons after the onset of brain ischemia. *J. Cereb. Blood Flow Metab* .28, 927–938. doi: 10.1038/sj.jcbfm.9600582

Sanches, E. F., van de Looij, Y., Toulotte, A., Sizonenko, S. V., and Lei, H. (2019). Mild neonatal brain Hypoxia-Ischemia in very immature rats causes Long-Term behavioral and cerebellar abnormalities at adulthood. *Front. Physiol.* 10:634. doi: 10.3389/fphys.2019.00634

Serdar, M., Kempe, K., Rizazad, M., Herz, J., and Bendix, I. (2019). Early pro-inflammatory microglia activation after inflammation-sensitized hypoxic-ischemic brain injury in neonatal rats. *Front. Cell Neurosci.* 13:237. doi: 10.3389/fncel.2019.00237

Sun, Q., Wu, W., Hu, Y. C., Li, H., and Zhang, D. (2014). Early release of high-mobility group box 1 (HMGB1) from neurons in experimental subarachnoid hemorrhage in vivo and in vitro. *J. Neuroinflammation* 11:106. doi: 10.1186/1742-2094-11-106

Sun, X., Zeng, H., Wang, Q., Yu, Q., and Wu, J. (2018). Glycyrrhizin ameliorates inflammatory pain by inhibiting microglial activation-mediated inflammatory response via blockage of the HMGB1-TLR4-NF-kB pathway. *Exp. Cell Res.* 369, 112–119. doi: 10.1016/j.yexcr.2018.05.012

Tang, Z., Jiang, M., Ou-Yang, Z., Wu, H., Dong, S., and Hei, M. (2019). High mobility group box 1 protein (HMGB1) as biomarker in hypoxia-induced persistent pulmonary hypertension of the newborn: a clinical and in vivo pilot study. *Int. J. Med. Sci.* 16, 1123–1131. doi: 10.7150/ijms.34344

Terrando, N., Yang, T., Wang, X., Fang, J., and Cao, M. (2016). Systemic HMGB1 neutralization prevents postoperative neurocognitive dysfunction in aged rats. *Front. Immunol.* 7:441. doi: 10.3389/fimmu.2016.00441

Thal, S. E., Zhu, C., Thal, S. C., Blomgren, K., and Plesnila, N. (2011). Role of apoptosis inducing factor (AIF) for hippocampal neuronal cell death following global cerebral ischemia in mice. *Neurosci. Lett.* 499, 1–3. doi: 10.1016/j.neulet.2011.05.016

Umekawa, T., Osman, A. M., Han, W., Ikeda, T., and Blomgren, K. (2015). Resident microglia, rather than blood-derived macrophages, contribute to the earlier and more pronounced inflammatory reaction in the immature compared with the adult hippocampus after hypoxia-ischemia. *Glia* 63, 2220–2230. doi: 10.1002/glia.22887

Wang, H., Bloom, O., Zhang, M., Vishnubhakat, J. M., and Ombrellino, M. (1999). HMG-1 as a late mediator of endotoxin lethality in mice. *Science* 285, 248–251. doi: 10.1126/science.285.5425.248

Weinstein, J. R., Koerner, I. P., and Moller, T. (2010). Microglia in ischemic brain injury. *Future Neurol.* 5, 227–246. doi: 10.2217/fnl.10.1

Wu, Y. W., Mathur, A. M., Chang, T., McKinstry, R. C., and Mulkey, S. B. (2016). High-Dose erythropoietin and hypothermia for Hypoxic-Ischemic encephalopathy: a phase II trial. *Pediatrics* 137:e20160191. doi: 10.1542/peds.2016-0191

Xia, C. Y., Zhang, S., Gao, Y., Wang, Z. Z., and Chen, N. H. (2015). Selective modulation of microglia polarization to M2 phenotype for stroke treatment. *Int. Immunopharmacol.* 25, 377–382. doi: 10.1016/j.intimp.2015.02.019

Ye, Y., Zeng, Z., Jin, T., Zhang, H., Xiong, X., and Gu, L. (2019). The role of high mobility group box 1 in ischemic stroke. *Front. Cell Neurosci.* 13:127. doi: 10.3389/fncel.2019.00127

Zhang, J., Klufas, D., Manalo, K., Adjepong, K., and Davidson, J. O. (2016). HMGB1 translocation after ischemia in the ovine fetal brain. *J. Neuropathol. Exp. Neurol.* 75, 527–538. doi: 10.1093/jnen/nlw030

Zhang, J., Takahashi, H. K., Liu, K., Wake, H., and Liu, R. (2011). Anti-high mobility group box-1 monoclonal antibody protects the blood-brain barrier from ischemia-induced disruption in rats. *Stroke* 42, 1420–1428. doi: 10.1161/STROKEAHA.110.598334

Zhou, X., Chu, X., Xin, D., Li, T., and Bai, X. (2019). L-Cysteine-Derived H2S promotes microglia m2 polarization via activation of the AMPK pathway in Hypoxia-Ischemic neonatal mice. *Front. Mol. Neurosci.* 12:58. doi: 10.3389/fnmol.2019.00058

Conflict of Interest: The authors declare that the research was conducted in the absence of any commercial or financial relationships that could be construed as a potential conflict of interest.

frontiers in Cellular Neuroscience

ORIGINAL RESEARCH
published: 30 April 2020
doi: 10.3389/fncel.2020.00100

Does Antenatal Betamethasone Alter White Matter Brain Development in Growth Restricted Fetal Sheep?

*Amy E. Sutherland[1], Tamara Yawno[1], Margie Castillo-Melendez[1], Beth J. Allison[1], Atul Malhotra[1,2], Graeme R. Polglase[1], Leo J. Cooper[1], Graham Jenkin[1] and Suzanne L. Miller[1]**

[1]Department of Obstetrics and Gynaecology, The Ritchie Centre, Hudson Institute of Medical Research, Monash University, Clayton, VIC, Australia, [2]Department of Paediatrics, Monash University, Clayton, VIC, Australia

Fetal growth restriction (FGR) is a common complication of pregnancy often associated with neurological impairments. Currently, there is no treatment for FGR, hence it is likely these babies will be delivered prematurely, thus being exposed to antenatal glucocorticoids. While there is no doubt that antenatal glucocorticoids reduce neonatal mortality and morbidities, their effects on the fetal brain, particularly in FGR babies, are less well recognized. We investigated the effects of both short- and long-term exposure to antenatal betamethasone treatment in both FGR and appropriately grown fetal sheep brains. Surgery was performed on pregnant Border-Leicester Merino crossbred ewes at 105–110 days gestation (term ∼150 days) to induce FGR by single umbilical artery ligation (SUAL) or sham surgery. Ewes were then treated with a clinical dose of betamethasone (11.4 mg intramuscularly) or saline at 113 and 114 days gestation. Animals were euthanized at 115 days (48 h following the initial betamethasone administration) or 125 days (10 days following the initial dose of betamethasone) and fetal brains collected for analysis. FGR fetuses were significantly smaller than controls (115 days: 1.68 ± 0.11 kg vs. 1.99 ± 0.11 kg, 125 days: 2.70 ± 0.15 kg vs. 3.31 ± 0.20 kg, $P < 0.001$) and betamethasone treatment reduced body weight in both control (115 days: 1.64 ± 0.10 kg, 125 days: 2.53 ± 0.10 kg) and FGR fetuses (115 days: 1.41 ± 0.10 kg, 125 days: 2.16 ± 0.17 kg, $P < 0.001$). Brain: body weight ratios were significantly increased with FGR ($P < 0.001$) and betamethasone treatment ($P = 0.002$). Within the fetal brain, FGR reduced CNPase-positive myelin staining in the subcortical white matter (SCWM; $P = 0.01$) and corpus callosum (CC; $P = 0.01$), increased GFAP staining in the SCWM ($P = 0.02$) and reduced the number of Olig2 cells in the periventricular white matter (PVWM; $P = 0.04$). Betamethasone treatment significantly increased CNPase staining in the external capsule (EC; $P = 0.02$), reduced GFAP staining in the CC ($P = 0.03$) and increased Olig2 staining in the SCWM ($P = 0.04$). Here we show that FGR has progressive adverse effects on the fetal brain, particularly within the white matter. Betamethasone exacerbated growth restriction in the FGR offspring, but betamethasone did not worsen white matter brain injury.

Keywords: fetal growth restriction, FGR, IUGR, glucocorticoids, brain injury, neuropathology, preterm

OPEN ACCESS

Edited by:
Changlian Zhu,
Third Affiliated Hospital of Zhengzhou University, China

Reviewed by:
Jorge Matias-Guiu,
Complutense University of Madrid, Spain
Lai Shuan Wang,
Fudan University, China

****Correspondence:***
Suzanne L. Miller
suzie.miller@monash.edu

Specialty section:
This article was submitted to Cellular Neuropathology, a section of the journal Frontiers in Cellular Neuroscience

Received: *10 January 2020*
Accepted: *01 April 2020*
Published: *30 April 2020*

Citation:
Sutherland AE, Yawno T, Castillo-Melendez M, Allison BJ, Malhotra A, Polglase GR, Cooper LJ, Jenkin G and Miller SL (2020) Does Antenatal Betamethasone Alter White Matter Brain Development in Growth Restricted Fetal Sheep? Front. Cell. Neurosci. 14:100. doi: 10.3389/fncel.2020.00100

INTRODUCTION

Fetal growth restriction (FGR) has many etiologies but most commonly occurs as a result of placental dysfunction, and is a major cause of perinatal mortality and, in survivors, morbidities related to pulmonary, cardiovascular and neurological structure and function (Malhotra et al., 2019). The presence of placental dysfunction is a defining feature of FGR (Gordijn et al., 2016), resulting in a reduction in the amount of oxygen and nutrients reaching the fetus, thus reducing fetal growth. As a result, the growth-restricted fetus is hypoxic, hypoglycaemic and hypercortisolemic (McMillen et al., 2001; Lipsett et al., 2006) and it is these states that are thought to contribute to the increased morbidities associated with FGR. The fetus mounts an adaptive response to chronic hypoxia (Giussani, 2016), which involves altered cardiovascular output to preferentially spare vital organ development in the brain and heart, called *brain sparing*. This term is however a misnomer and brain sparing does not guarantee normal development in the growth-restricted fetus (Miller et al., 2016). FGR is strongly associated with developmental deficits in brain structure and function, with long-term sequelae including reduced motor skills, memory and cognition, and altered neuropsychological behaviors (Miller et al., 2016). The most significant neurological problems are linked to the most severely affected growth-restricted infants who are born preterm (Schreuder et al., 2002; Baschat, 2014).

Infants at risk of preterm birth before 34 weeks gestation will be exposed to antenatal glucocorticoids *via* maternal administration to improve neonatal survival (Crowley, 2000). The beneficial effects of antenatal glucocorticoids—either betamethasone or dexamethasone—are well proven; a single course of antenatal glucocorticoids administered to at-risk pregnancies <34 weeks increases infant survival by 50% and decreases the rate of respiratory distress syndrome (RDS) by about the same degree (Crowley, 2000). Glucocorticoids promote lung maturation by increasing the production of surfactant, promoting lung structural maturation and enhancing the clearance of lung liquid (Liggins, 1994; Wallace et al., 1995). At the cellular level, endogenous and exogenous glucocorticoids mediate organ maturation *via* regulation of cell proliferation, differentiation, and apoptosis, and glucocorticoids are powerful mediators of vascular function (Fowden et al., 1998; Yang and Zhang, 2004; Michael and Papageorghiou, 2008). These cellular effects are critical in the lung to promote neonatal survival after preterm birth, but antenatal glucocorticoids also act on the developing brain. Exogenous glucocorticoids increase cerebral vascular resistance leading to decreased cerebral blood flow (Schwab et al., 2000; Miller et al., 2007) and impair cerebral oxygen delivery in a region-specific manner (Schwab et al., 2000). These changes in cerebral blood flow are associated with altered electrocortical activity, suggestive of dysfunctional complex neuronal activity and disturbed cerebral metabolism (Schwab et al., 2001). Dexamethasone, in particular, induces acute EEG hyperexcitability and sustained alterations in ovine fetal sleep patterns (Davidson et al., 2011). At the cellular level, synthetic glucocorticoids disrupt myelination within the brain of appropriately grown fetal sheep (Antonow-Schlorke et al., 2009), and reduce the neuronal number in fetal primates (Uno et al., 1990).

While multiple studies have examined the effects of antenatal glucocorticoids on the brain of appropriately grown (and otherwise healthy) fetuses, the effects of glucocorticoids on the developing FGR brain are less documented. In the absence of exogenous glucocorticoid exposure, we have shown significant neuropathology in growth-restricted fetal sheep and newborn lambs that includes white matter hypomyelination, axonal injury, neuroinflammation, increased cellular apoptosis, and altered vascularization (Miller et al., 2014; Castillo-Melendez et al., 2015; Alves de Alencar Rocha et al., 2017). The hemodynamic response of the FGR fetus is markedly different from that of the appropriately grown fetus (Schwab et al., 2000; Miller et al., 2007), mimicking differences seen between FGR and normally grown human fetuses (Wallace and Baker, 1999). The appropriately grown fetus responds to betamethasone with vasoconstriction, decreased cardiac output and decreased cerebral blood flow (Miller et al., 2009). In contrast, the FGR fetus responds with widespread systemic vasodilatation, increased cardiac output and increased blood flow to all major organs including the brain (Miller et al., 2009). Following betamethasone, cerebral blood flow in the FGR fetus shows a biphasic response, with an initial vasoconstriction followed by a prolonged increase in brain blood flow (Miller et al., 2007). This closely mimics what is seen clinically where betamethasone causes increased placental and cerebral blood flow in the FGR fetus (Wallace and Baker, 1999; Edwards et al., 2002), indicative of systemic vasodilatation. It remains unknown whether these differential hemodynamic responses in the FGR vs. appropriately grown fetus have an exacerbating effect on neuropathology.

Therefore, in the current study, we examined whether antenatal betamethasone induced brain injury in growth-restricted fetal sheep and if neuropathology was exacerbated in FGR compared to appropriately grown fetuses. We collected brains for histological analysis both immediately following glucocorticoid exposure and at 10 days following glucocorticoid administration to determine whether longer exposure to antenatal glucocorticoids would further impact neuropathology. We hypothesized that exposure to antenatal betamethasone would induce a greater degree of white matter brain injury in FGR fetuses compared to appropriately grown fetuses, and that this would remain evident 10 days later.

MATERIALS AND METHODS

Experimental procedures were approved by the Monash Medical Centre Animal Ethics Committee A (MMCA2010/23, MMCA2011/39), and complied with the National Health and Medical Research Council Australia Code of Practice for the Care and Use of Animals for Scientific Purposes.

Surgery was performed on 34 singleton- or twin-bearing Border-Leicester Merino crossbred ewes at 105–110 days gestation (term 150 days). Ewes in the 125-day cohort were given medroxyprogesterone acetate (MPA; 300 mg intramuscularly; i.m.; Pfizer, Australia) 1 day before surgery to prevent preterm labor in response to glucocorticoid exposure (Jenkin et al., 1985).

On the day of surgery, all ewes received an intravenous (i.v.) dose of ampicillin (Austrapen, 1g, CSL, Limited, Australia) before the induction of anesthesia with sodium thiopentone (Pentothal, 20 mg/kg, i.v.; Bomac Laboratories Limited, New Zealand). General anesthesia was maintained with 2.5% isoflurane (Isoflo, Abbott Private Limited, Australia) in oxygen and nitric oxide (70:30). Each fetus was exteriorized and the umbilical cord exposed before a small incision was made in the sheath surrounding the umbilical cord, approximately 3 cm from the fetal abdomen, to allow for single umbilical artery ligation (SUAL) to induce FGR. We have previously used this model to successfully induce FGR in sheep (Miller et al., 2007, 2012, 2014). Control fetuses had their cord manipulated but not ligated. All fetuses were implanted with a femoral artery catheter [inner diameter (ID) 0.8 mm, outer diameter (OD) 1.5 mm, Dural Plastics, Australia] and a catheter in the amniotic sac (ID 1.5 mm, OD 2.7 mm, Dural Plastics, Australia). Ewes received a jugular vein catheter (ID 1.5 mm, OD 2.7 mm, Dural Plastics, Australia) for the administration of antibiotics.

For 3 days following surgery, ampicillin was given to the ewe (500 mg i.v.) and into the fetal amniotic sac (500 mg into each amniotic catheter) and a daily fetal blood sample was taken for analysis of blood gas parameters (ABL700 blood gas analyzer, Radiometer, Denmark) to monitor fetal wellbeing. Ewes were then treated with a clinical dose of betamethasone (11.4 mg i.m.; Celestone Chronodose, Schering Plough, Australia) or an equal volume of saline at 113 and 114 days gestation. Fetal blood samples were collected throughout the experimental period to monitor fetal wellbeing. Animals were euthanized (sodium pentobarbitone; Lethabarb, Virbac, Australia) at either 115 days (24 h following the second betamethasone administration) or 125 days (11 days following the second dose of betamethasone). Fetal brains were removed, weighed and the two hemispheres cut sagitally before the right hemisphere was fixed in 4% paraformaldehyde and later processed for histological analysis and pieces of the left hemisphere snap-frozen and stored at −70°C for future studies.

Fetal brain sections were analyzed in duplicate using glial fibrillary acidic protein (GFAP; mouse anti-rabbit; diluted 1:400; Sigma–Aldrich, St. Louis, MO, USA), 2′,3′-cyclic-nucleotide 3′-phosphodiesterase (CNPase; mouse anti-human; diluted 1:300; Sigma–Aldrich, St. Louis, MO, USA), oligodendrocyte transcription factor 2 (Olig2; mouse anti-human; diluted 1:1,000; MerckMillipore, Australia) and myelin basic protein (MBP; rat monoclonal; diluted 1:100; MerckMillipore, Australia). Briefly, sections were dewaxed and rehydrated before antigen retrieval was carried out in citric acid buffer (0.1 M; Sigma-Aldrich, Australia). The sections were incubated overnight at 4°C with primary antibody followed by secondary antibody (MBP goat anti-rat; diluted 1;500; Vector Laboratories, Burlingame, CA, USA; GFAP, CNPase, Olig2 goat anti-mouse; diluted 1:200; Vector Laboratories, Burlingame, CA, USA) and streptavidin horseradish peroxidase (diluted 1:200; GE Healthcare, USA) before being visualized with diaminobenzidine (DAB; Thermo Fisher Scientific, Waltham, MA, USA). Negative controls that omitted the primary antibody were included in each run. The sections were viewed at 400× magnification (Olympus BX-41, Japan) with three fields of view used for each region from each section. Images were analyzed using ImageJ software (National Institutes of Health, USA).

Data are expressed as mean ± standard error of the mean (SEM) and analyzed by three-way analysis of variance (ANOVA) with fetal growth (control or FGR), maternal glucocorticoid treatment (vehicle or BM) and age (115 days or 125 days) as fixed variables (GraphPad Prism 8, GraphPad Software Inc., La Jolla, CA, USA). Fetal blood parameters were analyzed over time using a four-way repeated measures ANOVA (SigmaStat 12, Systat Software, USA). Where significant interactions were observed, differences between groups were isolated using a one-way ANOVA or mixed model with Tukey's multiple comparison test performed as required. Statistical significance was accepted when $P < 0.05$.

RESULTS

Fetal arterial blood samples were taken over the experimental period to monitor fetal wellbeing (**Table 1**). Baseline values were combined for all control and all FGR animals. The FGR groups (FGR and FGR+BM) were hypoxic compared to control animals (control and control+BM) at baseline recording (mean PaO_2 19.6 ± 0.8 mmHg vs. 23.0 ± 0.6 mmHg; $P < 0.001$). Following betamethasone, both partial pressure of oxygen (PaO_2) and oxygen saturation (SaO_2) were significantly reduced in the 115 days FGR+BM fetuses. There were no significant differences in oxygen levels in any other group (**Table 1**). FGR fetuses were hypoglycaemic at baseline when compared to control fetuses. Following each betamethasone administration, both control and FGR fetuses in both the 115 days and 125 days cohort had significantly higher glucose levels. This persisted at post mortem in the 115 days fetuses but had returned to baseline values by post mortem in the 125 days fetuses. Fetal lactate levels were also significantly increased in all fetuses exposed to betamethasone. FGR+BM fetuses had increased lactate levels at post mortem in the 115 days cohort (**Table 1**).

Fetal weights at the time of post mortem are shown in **Figure 1**. FGR fetuses weighed significantly less than controls ($P < 0.001$) while betamethasone treatment also significantly reduced fetal body weight ($P < 0.001$). FGR did not affect fetal brain weight ($P = 0.59$), but the brain:body weight ratios were increased in all FGR fetuses compared to controls ($P < 0.001$), indicative of brain sparing. Betamethasone reduced fetal brain weight ($P = 0.007$) and increased brain:body weight ratios ($P = 0.002$). Fetal age (115 days vs. 125 days) had a significant effect on weight parameters (**Figure 1**).

Within the fetal brain, the number of Olig2 positive oligodendrocyte lineage cells (**Figure 2**) was significantly reduced in FGR fetuses when compared to control in the periventricular white matter (PVWM; $P = 0.04$). Betamethasone treatment caused a significant decrease in oligodendrocyte lineage cells within the subcortical white matter (SCWM; $P = 0.04$). Oligodendrocyte cell counts were significantly increased in 125 days brains compared to 115 days brains in

TABLE 1 | Fetal characteristics and arterial blood parameters.

		Baseline		115 days				125 days			
		Control	FGR	Control	FGR	Control+BM	FGR+BM	Control	FGR	Control+BM	FGR+BM
Number (M/F)				9 (5/4)	9 (5/4)	8 (6/2)	8 (6/2)	9 (3/6)	7 (4/3)c	5 (2/3)	5 (1/4)
Gestational age at post mortem (d)				114.8 ± 0.7	114.8 ± 0.7	115.1 ± 0.8	115.1 ± 0.8	125.4 ± 0.5	125.9 ± 0.6	123.4 ± 0.2	124 ± 0.0
PaO_2 (mmHg)	Baseline	23.0 ± 0.6	**19.6 ± 0.8**$^{\#}$								
	BM1 +6 h			23.4 ± 0.9	20.5 ± 1.3	23.8 ± 1.2	20.8 ± 0.8	22.8 ± 1.1	21.5 ± 2.2	23.7 ± 0.7	20.2 ± 2.0
	BM2 +6 h			23.8 ± 1.2	22.1 ± 1.6	23.6 ± 1.9	**18.9 ± 1.2**$^{\#}$	23.3 ± 2.0	21.9 ± 2.9	23.6 ± 0.8	19.7 ± 0.9
	PM			21.0 ± 1.4	17.5 ± 1.6	23.7 ± 1.3	**16.4 ± 1.6**$^{\#}$	21.8 ± 2.5	19.2 ± 2.5	28.6 ± 0.0	17.3 ± 1.8
SaO_2 (%)	Baseline	63.6 ± 1.5	**52.4 ± 2.7**$^{\#}$								
	BM1 +6 h			61.7 ± 2.5	55.3 ± 3.4	61.7 ± 3.3	52.3 ± 2.2	63.7 ± 3.4	61.5 ± 6.8	70.5 ± 2.5	54.7 ± 6.3
	BM2 +6 h			63.0 ± 2.1	57.0 ± 4.1	61.3 ± 6.5	**46.3 ± 4.7**$^{\#}$	64.2 ± 7.3	58.1 ± 7.8	67.6 ± 1.1	52.3 ± 2.8
	PM			55.8 ± 4.3	47.6 ± 3.2	65.2 ± 3.5	**36.3 ± 6.6**$^{\#}$	65.2 ± 4.4	50.3 ± 8.9	76.6 ± 0.0	45.2 ± 5.2
Glucose (mmol/l)	Baseline	0.7 ± 0.0	**0.6 ± 0.0**$^{\#}$								
	BM1 +6 h			0.8 ± 0.1	0.7 ± 0.1	**1.9 ± 0.2**$^{*\#}$	**1.4 ± 0.1**$^{*\#}$	0.9 ± 0.1	0.7 ± 0.1	**1.8 ± 0.2**$^{*\#}$	**1.7 ± 0.2**$^{*\#}$
	BM2 +6 h			0.8 ± 0.1	0.7 ± 0.1	**2.4 ± 0.2**$^{*\#}$	**1.6 ± 0.2**$^{*\#}$	0.8 ± 0.1	0.6 ± 0.1	**1.9 ± 0.3**$^{*\#}$	**2.1 ± 0.3**$^{*\#}$
	PM			0.6 ± 0.1	0.5 ± 0.1	**1.6 ± 0.1**$^{*\#}$	**1.0 ± 0.1**$^{*\#}$	0.8 ± 0.1	0.8 ± 0.2	0.9 ± 0.0	0.6 ± 0.1
Lactate (mmol/l)	Baseline	1.1 ± 0.0	1.2 ± 0.0								
	BM1 +6 h			1.1 ± 0.1	1.4 ± 0.1	**2.6 ± 0.2**$^{*\#}$	**2.5 ± 0.2**$^{*\#}$	**1.4 ± 0.1***	1.5 ± 0.1	**2.4 ± 0.3**$^{*\#}$	**2.5 ± 0.2**$^{*\#}$
	BM2 +6 h			1.3 ± 0.1	1.5 ± 0.2	**2.5 ± 0.1**$^{*\#}$	**2.6 ± 0.2**$^{*\#}$	**1.5 ± 0.2***	1.7 ± 0.2	**2.8 ± 0.6**$^{*\#}$	**2.4 ± 0.3**$^{*\#}$
	PM			1.2 ± 0.1	1.7 ± 0.3	**2.2 ± 0.3***	**3.5 ± 0.6**$^{*\#}$	**1.6 ± 0.1***	3.1 ± 1.0*	0.6 ± 0.0	1.6 ± 0.1

Data are presented as mean ± SEM. Bold values indicate significant differences. $^{*}P < 0.05$, compared with baseline within the group. $^{\#}P < 0.05$, compared to same-age control at the same time.

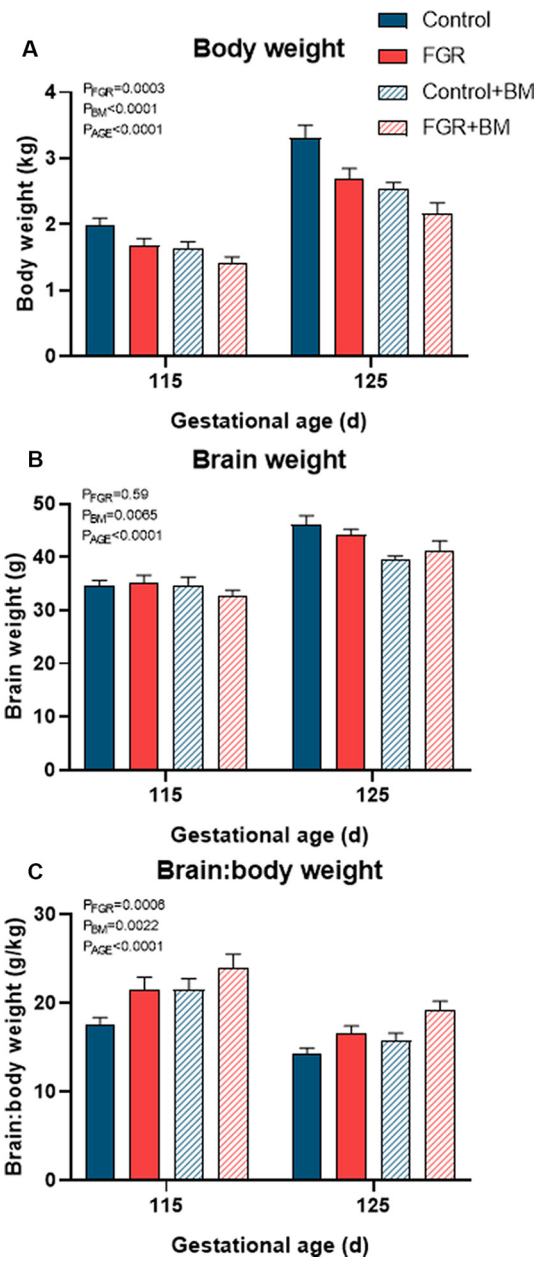

FIGURE 1 | Fetal weights at post mortem. Fetal body weight **(A)**, brain weight **(B)** and the brain: body weight ratio **(C)** at post mortem. Data are presented as mean ± SEM.

the SCWM ($P = 0.001$), corpus callosum (CC; $P < 0.001$) and PVWM ($P < 0.001$).

We utilized two staining markers of myelination density within the developing brain, CNPase, and MBP. There was significantly less CNPase-positive myelin in FGR fetuses compared to control within the SCWM ($P = 0.009$) and CC ($P = 0.01$; **Figure 3**). Betamethasone administration significantly increased CNPase-positive myelin staining in the external capsule (EC; $P = 0.02$) but did not alter staining in any other region examined. Overall, MBP density was not changed by FGR

or betamethasone administration (**Figure 4**). Over the 10 days of study, the degree of myelination was significantly increased from 115 days to 125 days gestation, as evidenced by increased density of staining for both CNPase and MBP (**Figures 3**, **4**). Interestingly, we observed that MBP-positive myelin density was increased >10-fold in the PVWM of control brains from 115 days to 125 days gestation, consistent with this period being critical for myelin production, however, within the FGR brains MBP-positive myelin density was increased ∼5-fold within the PVWM over the same period. Both CNPase and MBP staining appeared to be disorganized in FGR brains, with interrupted tracts present within the white matter.

We assessed GFAP immunoreactivity as a measure of astrogliosis within the fetal brain (**Figure 5**). Astrogliosis was evident within the SCWM in FGR brains ($P = 0.02$). Conversely, astrocyte staining intensity was significantly reduced following betamethasone administration within the CC ($P = 0.03$), contributed by a significant reduction in astrocytic staining within control brains between the control and control+BM 125 days cohort ($P = 0.04$).

DISCUSSION

We set out to examine whether a single course of antenatal betamethasone altered white matter brain development in fetal sheep that were either appropriately grown or compromised by FGR. We administered a course of 2 maternal injections of betamethasone separated by 24 h and assessed fetal cerebral white matter at 48 h post initial exposure to antenatal glucocorticoids (115 days gestation), or 10 days later (125 days gestation) in a separate cohort. Our results confirm that placental insufficiency and subsequent FGR adversely affects white matter brain development and, for the first time, we show that antenatal betamethasone does not exacerbate white matter deficits in FGR offspring. That is, a single course of betamethasone caused detrimental effects on fetal growth and brain development, but these were similar in appropriately grown and FGR fetuses. Within the developing brain, betamethasone exposure significantly reduced the number of oligodendrocyte lineage cells but promoted CNPase-positive myelin density in an area-specific manner within the cerebral white matter. Betamethasone demonstrated anti-inflammatory effects within control brains only, as evidenced by decreased astrocyte density within the CC. Reassuringly, our results do not support our hypothesis that antenatal glucocorticoids worsen white matter injury in FGR fetuses, but rather demonstrate that neuropathology associated with FGR is present antenatally and is principally caused by placental insufficiency.

A clinical course of antenatal betamethasone significantly reduced body weight in both appropriately grown and FGR fetuses (**Figure 1**). Unsurprisingly, the most severe growth restriction was observed in the FGR+BM cohort, weighing 35% less than control fetuses at 125 days gestation. Single and repeat courses of antenatal glucocorticoids reduce body weight in fetal sheep (Sloboda et al., 2000; Miller et al., 2007, 2012), with a dose-dependent effect (Ikegami et al., 1997). A large population-based Finnish study confirms that birth weight is significantly reduced in infants exposed to antenatal steroids in infants born preterm, near-term or at term (Rodriguez et al., 2019). This study did not stratify for infants with FGR, but noted that 44% of their glucocorticoid-exposed infants were born at term and therefore unnecessarily received steroids. A dose-dependent relationship on fetal growth is also present in human infants exposed to single and repeat courses of antenatal steroids (Murphy et al., 2012).

FGR was induced *via* a model of placental insufficiency that produced fetal hypoxia and hypoglycemia and resulted in reduced body weight of 15.6% at 115 days and 18% at 125 days compared to appropriately grown controls, and with apparent brain sparing. Despite brain sparing, white matter pathology was observed, with a decrease in total oligodendrocytes within the PVWM, and reduced myelin density (CNPase-positive) within the subcortical white matter and CC. The decrease in the oligodendrocyte pool within the PVWM is important, as injury to this brain region is highly associated with neurodevelopmental deficits (Volpe, 2009), and is a common imaging abnormality in growth-restricted infants (Padilla-Gomes et al., 2007). We observed sparse MBP-positive mature myelin staining at 115 days in the fetal sheep brain, but this was greatly increased by 125 days, confirming previous findings (Back et al., 2006; Antonow-Schlorke et al., 2009). Importantly, while control brains demonstrated a >10-fold increase in MBP-positive myelin density over this period, the FGR brains showed only a 5-fold increase in myelination, potentially contributed by the decrease observed in the oligodendrocyte pool. This significant myelination period between 115 days and 125 days gestation in the fetal sheep brain is approximately equivalent to white matter development in the human brain between 30–36 weeks (Back et al., 2006; Alves de Alencar Rocha et al., 2017), and this also corresponds to a high-risk period for preterm birth (and steroid exposure) in FGR infants (Lees et al., 2013). Our results also confirm that there are significant regional differences in the maturation of cerebral white matter and that third-trimester placental insufficiency adversely impacts white matter development. Reassuringly we did not find that antenatal glucocorticoids exacerbated white matter pathology in the FGR group, however, betamethasone did independently impact brain development in both appropriately grown controls and FGR fetuses.

The administration of betamethasone significantly reduced the number of oligodendrocyte lineage cells within the subcortical white matter in both control and FGR brains, with the lowest number of oligodendrocytes observed in the FGR+BM cohort. We did not observe any change to MBP-positive myelination with betamethasone exposure at either 115 days or 125 days. This is surprising in light of findings by Antonow-Schlorke and colleagues (Antonow-Schlorke et al., 2009) who demonstrated acute deficits in MBP-positive myelination with a single dose of betamethasone in sheep, but also showed no lasting deficits unless repeat steroids were administered. Similarly, a study in baboons shows that repeat courses of steroids have more profound adverse effects on the cerebral white matter than a single course (Shields et al., 2012). An

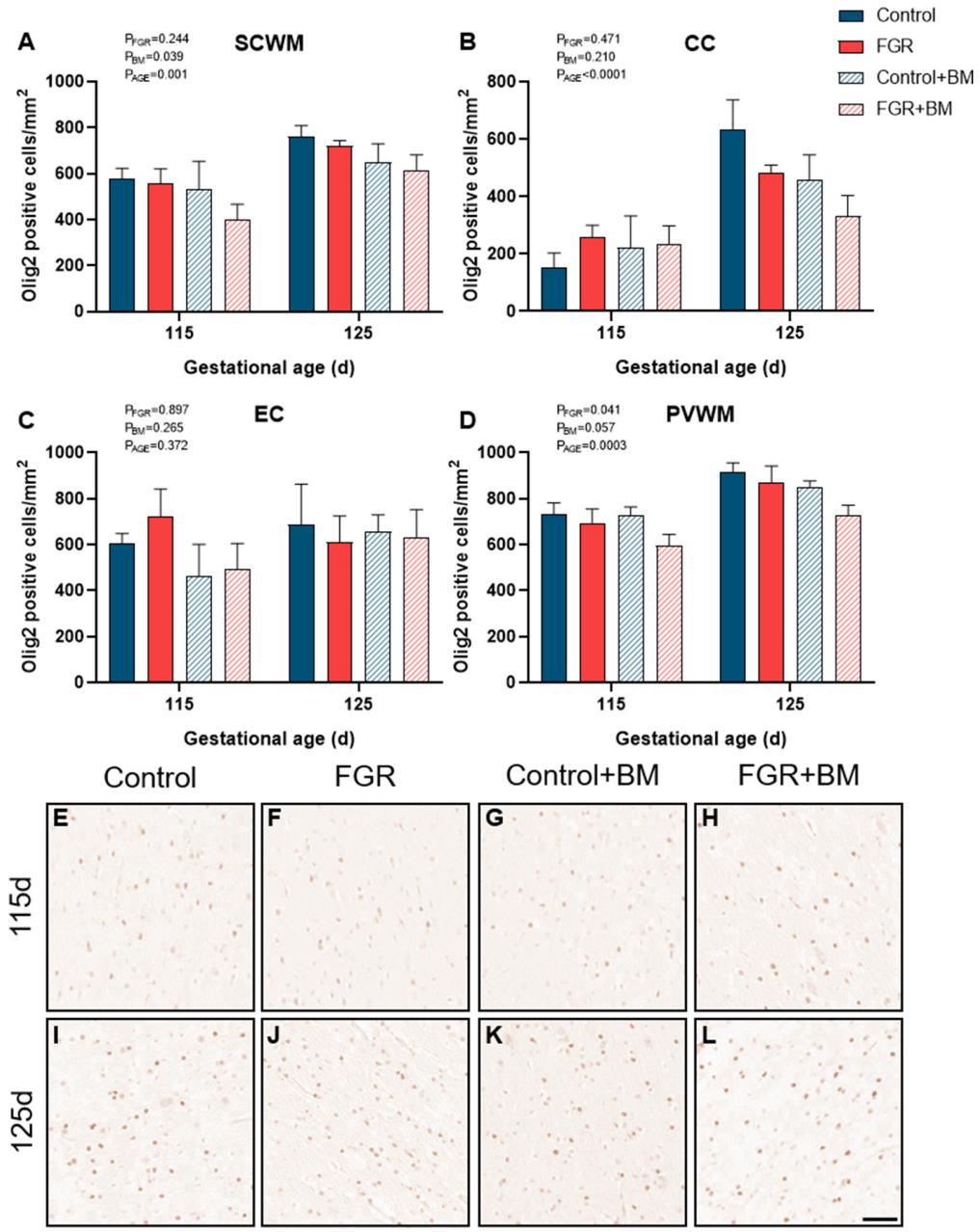

FIGURE 2 | Olig2 immunoreactivity. The number of Olig2 positive cells in the subcortical white matter (SCWM; **A**), corpus callosum (CC; **B**), external capsule (EC; **C**) and periventricular white matter (PVWM; **D**) and photomicrographs of the SCWM from 115 days control **(E)**, fetal growth restriction (FGR; **F**), control+BM **(G)**, FGR+BM **(H)** and 125 days control **(I)**, FGR **(J)**, control+BM **(K)** and FGR+BM **(L)** fetuses. Data are presented as mean ± SEM, scale bar = 50 μm.

unexpected finding was that betamethasone exposure induced a significant overall increase in CNPase-positive myelin density within the external capsule, and sub-analysis shows that this was contributed by an acute increase in myelination in the 115 days group (control and FGR). Glucocorticoids are potent mediators of cell maturation and differentiation, hence the use of synthetic glucocorticoids for fetal lung maturation before preterm birth (Bolt et al., 2001). Therefore it is conceivable that betamethasone might accelerate the process of myelination within the brain, and indeed, others have shown this to be the case (Raschke et al., 2008). This was, however, a transitory observation in the current study with no difference seen at 125 days gestation. Further, a noted benefit and mode of action of synthetic glucocorticoids is *via* anti-inflammatory effects within the immature lung (Bolt et al., 2001). In the current study, we also found that betamethasone demonstrated anti-inflammatory effects, although within control brains only, as evidenced by decreased astrocyte density within the CC.

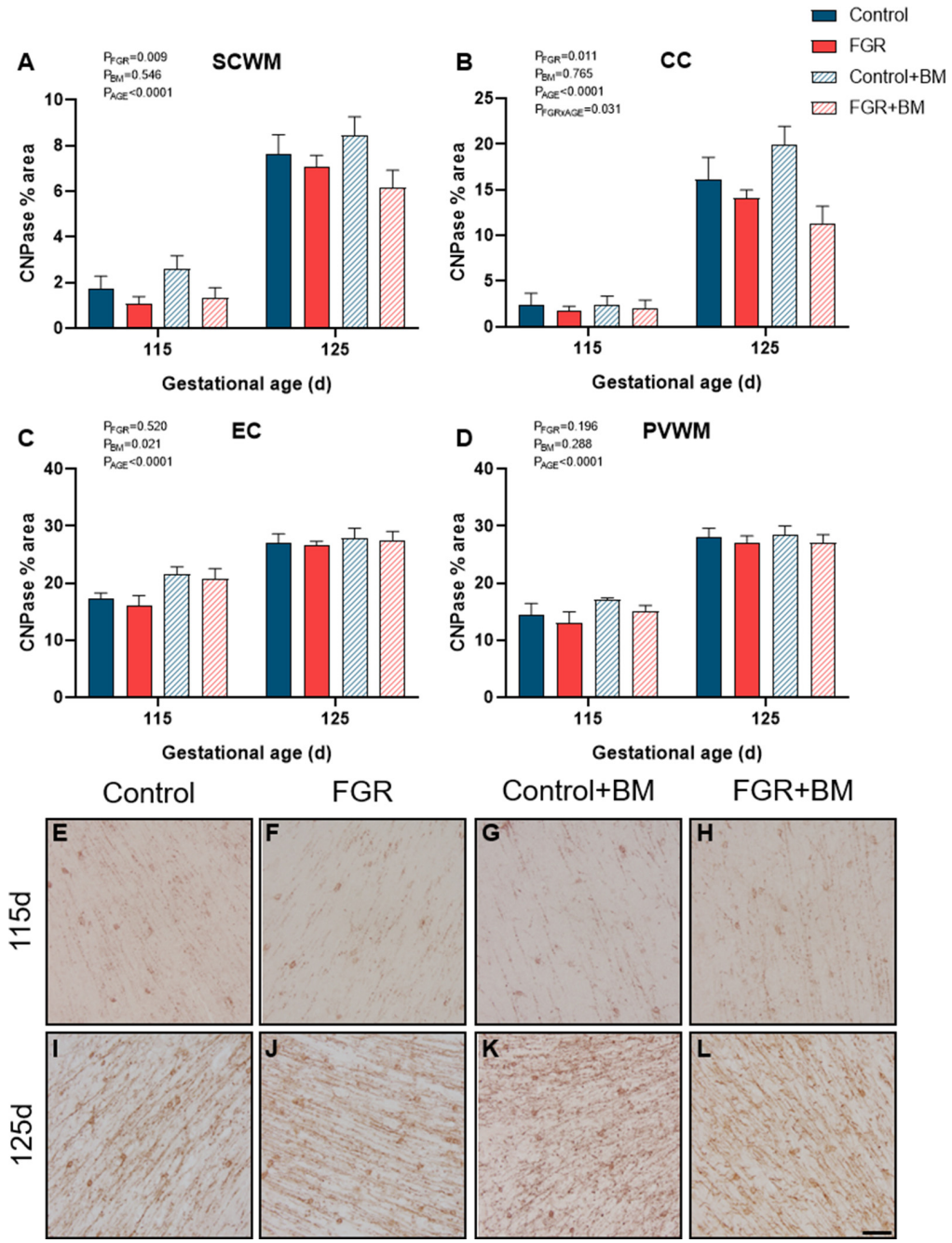

FIGURE 3 | CNPase immunoreactivity. The % area of CNPase positive staining in the SCWM **(A)**, CC **(B)**, EC **(C)** and PVWM **(D)** and photomicrographs of the SCWM from 115 days control **(E)**, FGR **(F)**, control+BM **(G)**, FGR+BM **(H)** and 125 days control **(I)**, FGR **(J)**, control+BM **(K)** and FGR+BM **(L)** fetuses. Data are presented as mean ± SEM, scale bar = 50 μm.

This result is in keeping with a previous study in guinea pigs showing that antenatal betamethasone decreased the density of astrocytes within the brain of appropriately grown, but not FGR, fetuses, with this effect only observed in males (McKendry et al., 2010). We did not have adequate numbers of males and females to undertake separate analysis of sex differences in the current study, but we have previously published data to show that antenatal betamethasone has differential effects on fetal growth and metabolism in males and females (Miller et al., 2012), and therefore further studies are encouraged to examine sex-specific effects. Taken together, the results obtained in this study, and other preclinical studies to date, strongly suggest that antenatal glucocorticoids have subtle but important modulatory effects on cerebral white matter

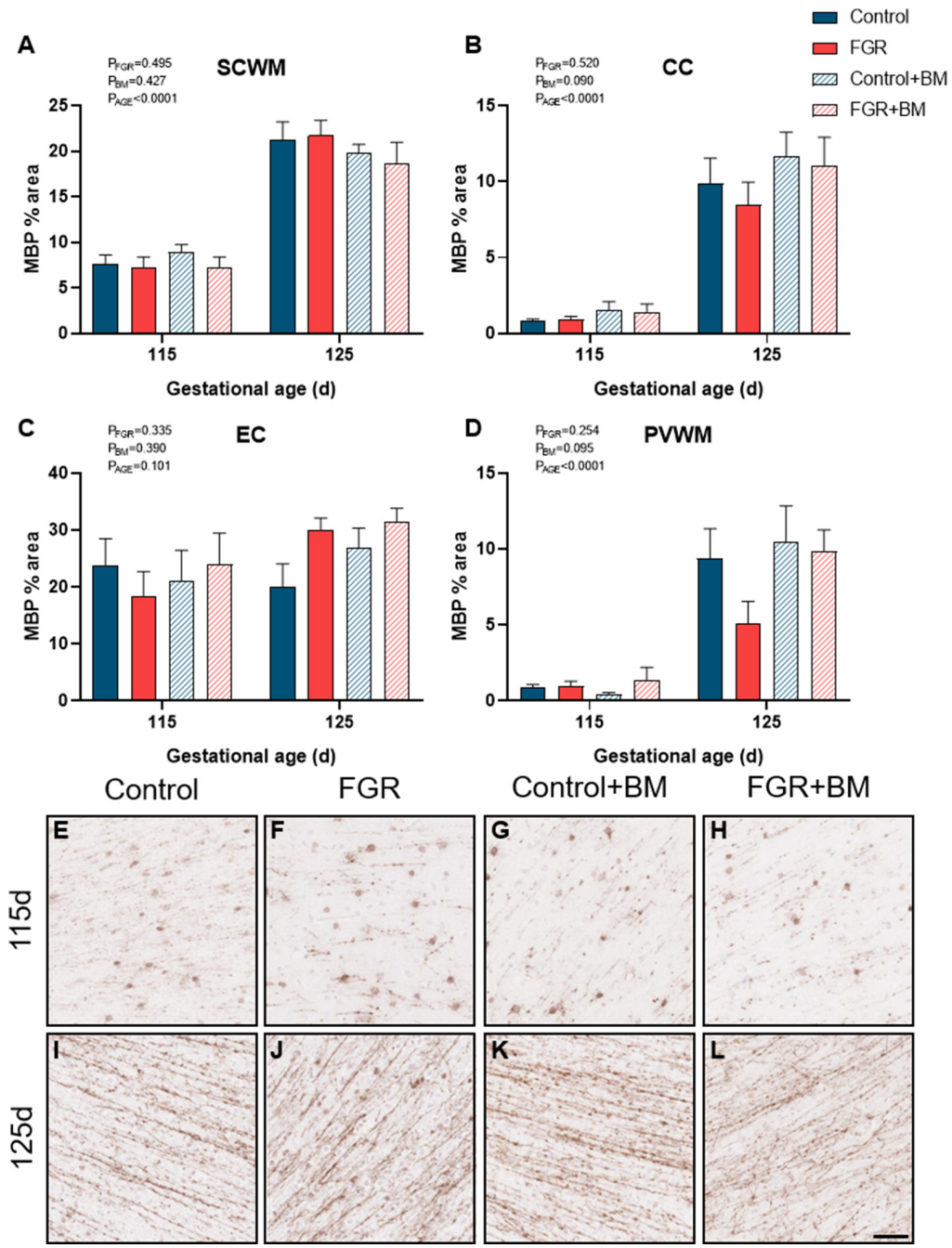

FIGURE 4 | MBP immunoreactivity. The % area of MBP positive staining in the SCWM **(A)**, CC **(B)**, EC **(C)** and PVWM **(D)** and photomicrographs of the SCWM from 115 days control **(E)**, FGR **(F)**, control+BM **(G)**, FGR+BM **(H)** and 125 days control **(I)**, FGR **(J)**, control+BM **(K)** and FGR+BM **(L)** fetuses. Data are presented as mean ± SEM, scale bar = 50 μm.

maturation that are region specific and appear dependent on the timing of steroid exposure, and the use of single or repeat doses (Antonow-Schlorke et al., 2009; Shields et al., 2012). It is not yet established whether myelination deficits are transient (delayed) or persist after birth. We did not set out to specifically examine mechanisms of glucocorticoid-induced alterations to white matter development, however, our results suggest that glucocorticoids alter oligodendrocyte maturation rather than directly affecting the myelin sheath.

Synthetic glucocorticoids are widely used during pregnancy but our results suggest that the actions of glucocorticoids are not specific to the immature lung, also mediating brain development. There is emerging clinical follow-up data to support this finding. The use of antenatal glucocorticoids is

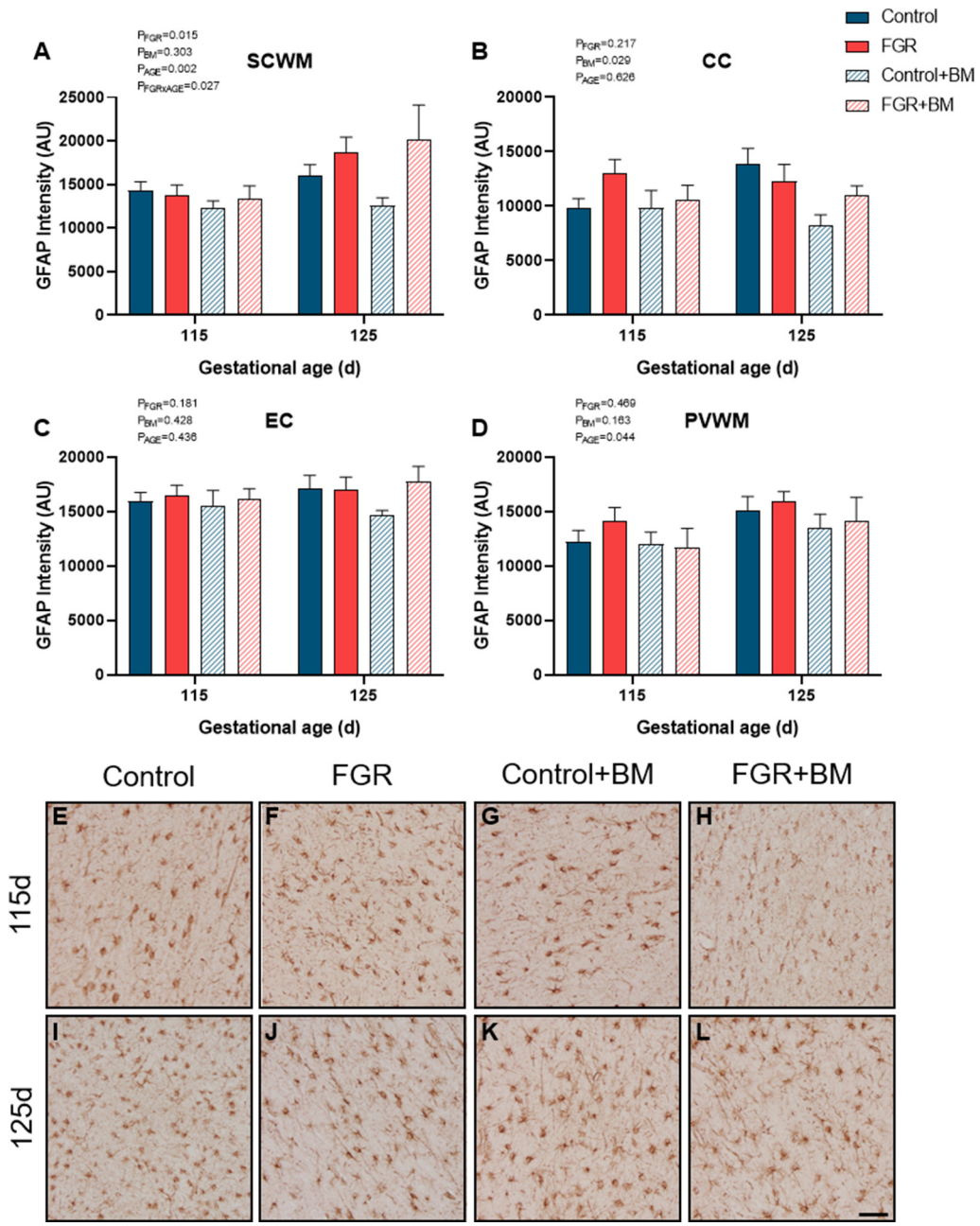

FIGURE 5 | GFAP immunoreactivity. The intensity of GFAP positive staining in the SCWM **(A)**, CC **(B)**, EC **(C)** and PVWM **(D)** and photomicrographs of the SCWM from 115 days control **(E)**, FGR **(F)**, control+BM **(G)**, FGR+BM **(H)** and 125 days control **(I)**, FGR **(J)**, control+BM **(K)** and FGR+BM **(L)** fetuses. Data are presented as mean ± SEM, scale bar = 50 μm.

linked to a significant increase in psychiatric disorders in school-age children that appears to persist in adolescence (Khalife et al., 2013). Furthermore, this effect can be isolated to glucocorticoids rather than preterm birth, since in a population of adolescents who were exposed to a single course of antenatal glucocorticoids but subsequently delivered at term, it was found that cognitive and behavioral control were significantly reduced (Ilg et al., 2018).

In the present study, we focused on cerebral white matter development, however, both FGR and synthetic glucocorticoids have other established actions on the immature brain. Of particular importance are potential effects on the cerebrovasculature given the strong vasoactive actions of glucocorticoids and the vulnerability of the neurovascular unit components in FGR lambs (Castillo-Melendez et al., 2015). Antenatal betamethasone has distinctly different actions

on cardiac output and cerebral blood flow redistribution in appropriately grown and FGR humans and sheep (Edwards et al., 2002; Miller et al., 2009), with FGR fetuses responding to betamethasone with significant vasodilation. A single course of antenatal steroids is also shown to induce cortical hyperactivity and markedly alters sleep architecture in appropriately grown fetal sheep (Davidson et al., 2011) but effects on growth-restricted fetuses have not yet been examined. In the current study, all fetuses remained *in utero* which is likely to be a relatively protective environment for brain development, and therefore future studies should re-create the clinical scenario in which many infants would be born preterm, soon after steroid exposure. Preterm birth and ventilation are linked with neuropathology in both appropriately grown and FGR infants (Barton et al., 2015; Malhotra et al., 2018).

Using two myelin protein markers at two timepoints in late gestation also provides us with information about the normal spatiotemporal profile of myelin production. CNPase accounts for approximately 5% of total myelin protein in the adult brain, whereas MBP is quantitatively greater than CNPase comprising ∼30% of total myelin (Trapp et al., 1988; Baumann and Pham-Dinh, 2001). Our results show regional differences in the developmental profile of myelin production. The external capsule was already well myelinated at 115 days gestation for both CNPase and MBP protein, and showed the least change over the following 10 days, suggesting relative maturity of this area. In contrast, very low levels of myelination were observed in the CC at 115 days using both markers, and both were increased to a similar degree in control brains at 125 days, but not in the FGR brains. In the subcortical white matter, MBP was more strongly evident than CNPase at an earlier age, with both proteins significantly upregulated between 115 and 125 days. Whereas in the PVWM the CNPase protein was present earlier and MBP was virtually absent, with MBP density showing a 10-fold increase over the 10 days. Myelination of the fetal brain occurs earlier and more rapidly in the fetal sheep brain than the human (Back et al., 2012), but these data confirm that antenatal compromise (e.g., FGR) or exposure to exogenous glucocorticoids during rapid myelination has region-specific adverse effects.

Here, we have shown that placental insufficiency and FGR disrupt cerebral white matter development that can already be detected at a time point in pregnancy when antenatal steroids might commonly be administered (115 days in fetal sheep, equivalent to ∼30 weeks of human gestation). In the absence of antenatal glucocorticoid exposure, FGR is associated with postnatal deficits in motor function, cognition, and behavior that are underpinned by altered brain structure (Miller et al., 2016). Betamethasone administration resulted in independent subtle adverse effects on white matter brain development in appropriately grown and FGR fetuses, but antenatal glucocorticoids did not exacerbate white matter pathology. This data shows that the administration of antenatal glucocorticoids should be targeted to the pregnancies of greatest risk for preterm birth because of the effects of glucocorticoids on the developing brain.

DATA AVAILABILITY STATEMENT

The datasets generated for this study are available on request to the corresponding author.

ETHICS STATEMENT

The animal study was reviewed and approved by Monash Medical Centre, Animal Ethics Committee A.

AUTHOR CONTRIBUTIONS

TY, MC-M, BA, GP, GJ, and SM contributed to the conception and design of the study. AS, TY, MC-M, BA, AM, GP, LC, GJ, and SM contributed to the acquisition, analysis, and interpretation of the data. AS and SM drafted the initial manuscript and all authors edited the manuscript for intellectual content and approved the final version for submission.

FUNDING

This work was funded by the Australian Research Council (ARC FT130100650), the Cerebral Palsy Alliance Australia (CDG313) and the Victorian Government's Operational Infrastructure Support Program.

ACKNOWLEDGMENTS

We wish to thank Ilias Nitsos, Jan Loose, Yen Pham, Dalibor Stanojkovic and Jamie Mihelakis for their technical assistance.

REFERENCES

Alves de Alencar Rocha, A. K., Allison, B. J., Yawno, T., Polglase, G. R., Sutherland, A. E., Malhotra, A., et al. (2017). Early- versus late-onset fetal growth restriction differentially affects the development of the fetal sheep brain. *Dev. Neurosci.* 39, 141–155. doi: 10.1159/000456542

Antonow-Schlorke, I., Helgert, A., Gey, C., Coksaygan, T., Schubert, H., Nathanielsz, P. W., et al. (2009). Adverse effects of antenatal glucocorticoids on cerebral myelination in sheep. *Obstet. Gynecol.* 113, 142–151. doi: 10.1097/aog.0b013e3181924d3b

Back, S. A., Riddle, A., Dean, J., and Hohimer, A. R. (2012). The instrumented fetal sheep as a model of cerebral white matter injury in the premature infant. *Neurotherapeutics* 9, 359–370. doi: 10.1007/s13311-012-0108-y

Back, S. A., Riddle, A., and Hohimer, A. R. (2006). Role of instrumented fetal sheep preparations in defining the pathogenesis of human periventricular white-matter injury. *J. Child Neurol.* 21, 582–589. doi: 10.1177/08830738060210070101

Barton, S. K., Tolcos, M., Miller, S. L., Roehr, C. C., Schmölzer, G. M., Davis, P. G., et al. (2015). Unraveling the links between the initiation of ventilation and brain injury in preterm infants. *Front. Pediatr.* 3:97. doi: 10.3389/fped.2015.00097

Baschat, A. A. (2014). Neurodevelopment after fetal growth restriction. *Fetal Diagn. Ther.* 36, 136–142. doi: 10.1159/000353631

Baumann, N., and Pham-Dinh, D. (2001). Biology of oligodendrocyte and myelin in the mammalian central nervous system. *Physiol. Rev.* 81, 871–927. doi: 10.1152/physrev.2001.81.2.871

Bolt, R. J., van Weissenbruch, M. M., Lafeber, H. N., and Delemarre-van de Waal, H. A. (2001). Glucocorticoids and lung development in the fetus and preterm infant. *Pediatr. Pulmonol.* 32, 76–91. doi: 10.1002/ppul.1092

Castillo-Melendez, M., Yawno, T., Allison, B. J., Jenkin, G., Wallace, E. M., and Miller, S. L. (2015). Cerebrovascular adaptations to chronic hypoxia in the growth restricted lamb. *Int. J. Dev. Neurosci.* 45, 55–65. doi: 10.1016/j.ijdevneu.2015.01.004

Crowley, P. (2000). Prophylactic corticosteroids for preterm birth. *Cochrane Database Syst. Rev.* 2:CD000065. doi: 10.1002/14651858.cd000065

Davidson, J. O., Quaedackers, J. S., George, S. A., Gunn, A. J., and Bennet, L. (2011). Maternal dexamethasone and EEG hyperactivity in preterm fetal sheep. *J. Physiol.* 589, 3823–3835. doi: 10.1113/jphysiol.2011.212043

Edwards, A., Baker, L. S., and Wallace, E. M. (2002). Changes in fetoplacental vessel flow velocity waveforms following maternal administration of betamethasone. *Ultrasound Obstet. Gynecol.* 20, 240–244. doi: 10.1046/j.1469-0705.2002.00782.x

Fowden, A. L., Li, J., and Forhead, A. J. (1998). Glucocrticoids and the preparation for life after birth: are there long-term consequences of the life insurance. *Proc. Nutr. Soc.* 57, 113–122. doi: 10.1079/pns19980017

Giussani, D. A. (2016). The fetal brain sparing response to hypoxia: physiological mechanisms. *J. Physiol.* 594, 1215–1230. doi: 10.1113/jp271099

Gordijn, S. J., Beune, I. M., Thilaganathan, B., Papageorghiou, A., Baschat, A. A., Baker, P. N., et al. (2016). Consensus definition of fetal growth restriction: a Delphi procedure. *Ultrasound Obstet. Gynecol.* 48, 333–339. doi: 10.1002/uog.15884

Ikegami, M., Jobe, A. H., Newnham, J., Polk, D. H., Willet, K. E., and Sly, P. (1997). Repetitive prenatal glucocorticoids improve lung function and decrease growth in preterm lambs. *Am. J. Respir. Crit. Care Med.* 156, 178–184. doi: 10.1164/ajrccm.156.1.9612036

Ilg, L., Klados, M., Alexander, N., Kirschbaum, C., and Li, S. C. (2018). Long-term impacts of prenatal synthetic glucocorticoids exposure on functional brain correlates of cognitive monitoring in adolescence. *Sci. Rep.* 8:7715. doi: 10.1038/s41598-018-26067-3

Jenkin, G., Jorgensen, G., Thorburn, G. D., Buster, J. E., and Nathanielsz, P. W. (1985). Induction of premature delivery in sheep following infusion of cortisol to the fetus. I. The effect of maternal administration of progestagens. *Can. J. Physiol. Pharmacol.* 63, 500–508. doi: 10.1139/y85-086

Khalife, N., Glover, V., Taanila, A., Ebeling, H., Järvelin, M. R., and Rodriguez, A. (2013). Prenatal glucocorticoid treatment and later mental health in children and adolescents. *PLoS One* 8:e81394. doi: 10.1371/journal.pone.0081394

Lees, C., Marlow, N., Arabin, B., Bilardo, C. M., Brezinka, C., Derks, J. B., et al. (2013). Perinatal morbidity and mortality in early-onset fetal growth restriction: cohort outcomes of the trial of randomized umbilical and fetal flow in Europe (TRUFFLE). *Ultrasound Obstet. Gynecol.* 42, 400–408. doi: 10.1002/uog.13190

Liggins, G. (1994). The role of cortisol in preparing the fetus for birth. *Reprod. Fertil. Dev.* 6, 141–150. doi: 10.1071/rd9940141

Lipsett, J., Tamblyn, M., Madigan, K., Roberts, P., Cool, J., Runciman, S., et al. (2006). Restricted fetal growth and lung development: a morphometric analysis of pulmonary structure. *Pediatr. Pulmonol.* 41, 1138–1145. doi: 10.1002/ppul.20480

Malhotra, A., Allison, B. J., Castillo-Melendez, M., Jenkin, G., Polglase, G. R., and Miller, S. L. (2019). Neonatal morbidities of fetal growth restriction: pathophysiology and impact. *Front. Endocrinol.* 10:55. doi: 10.3389/fendo.2019.00055

Malhotra, A., Castillo-Melendez, M., Allison, B. J., Sutherland, A. E., Nitsos, I., Pham, Y., et al. (2018). Neuropathology as a consequence of neonatal ventilation in premature growth-restricted lambs. *Am. J. Physiol. Regul. Integr. Comp. Physiol.* 315, R1183–R1194. doi: 10.1152/ajpregu.00171.2018

McKendry, A. A., Palliser, H. K., Yates, D. M., Walker, D. W., and Hirst, J. J. (2010). The effect of betamethasone treatment on neuroactive steroid synthesis in a foetal Guinea pig model of growth restriction. *J. Neuroendocrinol.* 22, 166–174. doi: 10.1111/j.1365-2826.2009.01949.x

McMillen, I. C., Adams, M., Ross, J., Coulter, C., Simonetta, G., Owens, J., et al. (2001). Fetal growth restriction: adaptations and consequences. *Reproduction* 122, 195–204. doi: 10.1530/reprod/122.2.195

Michael, A. E., and Papageorghiou, A. T. (2008). Potential significance of physiological and pharmacological glucocorticoids in early pregnancy. *Hum. Reprod. Update* 14, 497–517. doi: 10.1093/humupd/dmn021

Miller, S. L., Chai, M., Loose, J., Castillo-Meléndez, M., Walker, D. W., Jenkin, G., et al. (2007). The effects of maternal betamethasone administration on the intrauterine growth-restricted fetus. *Endocrinology* 148, 1288–1295. doi: 10.1210/en.2006-1058

Miller, S. L., Huppi, P. S., and Mallard, C. (2016). The consequences of fetal growth restriction on brain structure and neurodevelopmental outcome. *J. Physiol.* 594, 807–823. doi: 10.1113/jp271402

Miller, S. L., Supramaniam, V. G., Jenkin, G., Walker, D. W., and Wallace, E. M. (2009). Cardiovascular responses to maternal betamethasone administration in the intrauterine growth-restricted ovine fetus. *Am. J. Obstet. Gynecol.* 201, 613.e1–618.e8. doi: 10.1016/j.ajog.2009.07.028

Miller, S. L., Sutherland, A. E., Supramaniam, V. G., Walker, D. W., Jenkin, G., and Wallace, E. M. (2012). Antenatal glucocorticoids reduce growth in appropriately grown and growth-restricted ovine fetuses in a sex-specific manner. *Reprod. Fertil. Dev.* 24, 753–758. doi: 10.1071/rd11143

Miller, S. L., Yawno, T., Alers, N. O., Castillo-Melendez, M., Supramaniam, V. G., Vanzyl, N., et al. (2014). Antenatal antioxidant treatment with melatonin to decrease newborn neurodevelopmental deficits and brain injury caused by fetal growth restriction. *J. Pineal Res.* 56, 283–294. doi: 10.1111/jpi.12121

Murphy, K. E., Willan, A. R., Hannah, M. E., Ohlsson, A., Kelly, E. N., Matthews, S. G., et al. (2012). Effect of antenatal corticosteroids on fetal growth and gestational age at birth. *Obstet. Gynecol.* 119, 917–923. doi: 10.1097/AOG.0b013e31825189dc

Padilla-Gomes, N. F., Enriquez, G., Acosta-Rojas, R., Perapoch, J., Hernandez-Andrade, E., and Gratacos, E. (2007). Prevalence of neonatal ultrasound brain lesions in premature infants with and without intrauterine growth restriction. *Acta Paediatr.* 96, 1582–1587. doi: 10.1111/j.1651-2227.2007.00496.x

Raschke, C., Schmidt, S., Schwab, M., and Jirikowski, G. (2008). Effects of betamethasone treatment on central myelination in fetal sheep: an electron microscopical study. *Anat. Histol. Embryol.* 37, 95–100. doi: 10.1111/j.1439-0264.2007.00807.x

Rodriguez, A., Wang, Y., Ali Khan, A., Cartwright, R., Gissler, M., and Jarvelin, M. R. (2019). Antenatal corticosteroid therapy (ACT) and size at birth: a population-based analysis using the Finnish Medical Birth Register. *PLoS Med.* 16:e1002746. doi: 10.1371/journal.pmed.1002746

Schreuder, A. M., McDonnell, M., Gaffney, G., Johnson, A., and Hope, P. L. (2002). Outcome at school age following antenatal detection of absent or reversed end diastolic flow velocity in the umbilical artery. *J. Matern. Fetal Neonatal Med.* 86, F108–F114. doi: 10.1136/fn.86.2.f108

Schwab, M., Roedel, M., Anwar, M. A., Müller, T., Schubert, H., Buchwalder, L. F., et al. (2000). Effects of betamethasone administration to the fetal sheep in late gestation on fetal cerebral blood flow. *J. Physiol.* 528, 619–632. doi: 10.1111/j.1469-7793.2000.00619.x

Schwab, M., Schmidt, K., Roedel, M., Mueller, T., Schubert, H., Anwar, M. A., et al. (2001). Non-linear changes of electrocortical activity after antenatal betamethasone treatment in fetal sheep. *J. Physiol.* 531, 535–543. doi: 10.1111/j.1469-7793.2001.0535i.x

Shields, A., Thomson, M., Winter, V., Coalson, J., and Rees, S. (2012). Repeated courses of antenatal corticosteroids have adverse effects on aspects of brain development in naturally delivered baboon infants. *Pediatr. Res.* 71, 661–667. doi: 10.1038/pr.2012.18

Sloboda, D. M., Newnham, J. P., and Challis, J. R. (2000). Effects of repeated maternal betamethasone administration on growth and hypothalamic-pituitary-adrenal function of the ovine fetus at term. *J. Endocrinol.* 165, 79–91. doi: 10.1677/joe.0.1650079

Trapp, B. D., Bernier, L., Andrews, S. B., and Colman, D. R. (1988). Cellular and subcellular distribution of 2′,3′-cyclic nucleotide 3′-phosphodiesterase and its mRNA in the rat central nervous system. *J. Neurochem.* 51, 859–868. doi: 10.1111/j.1471-4159.1988.tb01822.x

Uno, H., Lohmiller, L., Thieme, C., Kemnitz, J. W., Engle, M. J., Roecker, E. B., et al. (1990). Brain damage induced by prenatal exposure to dexamethasone in fetal rhesus macaques. I. Hippocampus. *Dev. Brain Res.* 53, 157–167. doi: 10.1016/0165-3806(90)90002-g

Volpe, J. J. (2009). Brain injury in premature infants: a complex amalgam of destructive and developmental disturbances. *Lancet Neurol.* 8, 110–124. doi: 10.1016/s1474-4422(08)70294-1

Wallace, E. M., and Baker, L. S. (1999). Effect of antenatal betamethasone administration on placental vascular resistance. *Lancet* 353, 1404–1407. doi: 10.1016/s0140-6736(98)08229-4

Wallace, M. J., Hooper, S. B., and Harding, R. (1995). Effects of elevated fetal cortisol concentrations on the volume, secretion and reabsorption of lung liquid. *Am. J. Physiol.* 269, R881–R887. doi: 10.1152/ajpregu.1995.269.4.r881

Yang, S., and Zhang, L. (2004). Glucocorticoids and vascular reactivity. *Curr. Vasc. Pharmacol.* 2, 1–12. doi: 10.2174/1570161043476483

Conflict of Interest: The authors declare that the research was conducted in the absence of any commercial or financial relationships that could be construed as a potential conflict of interest.

frontiers in Cellular Neuroscience

MINI REVIEW
published: 06 May 2020
doi: 10.3389/fncel.2020.00112

Neuroprotective Effects of Diabetes Drugs for the Treatment of Neonatal Hypoxia-Ischemia Encephalopathy

*Laura Poupon-Bejuit[1], Eridan Rocha-Ferreira[2], Claire Thornton[3], Henrik Hagberg[2] and Ahad A. Rahim[1]**

[1] UCL School of Pharmacy, University College London, London, United Kingdom, [2] Centre for Perinatal Medicine and Health, Institute of Clinical Sciences, Sahlgrenska Academy, University of Gothenburg, Gothenburg, Sweden, [3] Department of Comparative Biomedical Sciences, Royal Veterinary College, London, United Kingdom

The perinatal period represents a time of great vulnerability for the developing brain. A variety of injuries can result in death or devastating injury causing profound neurocognitive deficits. Hypoxic-ischemic neonatal encephalopathy (HIE) remains the leading cause of brain injury in term infants during the perinatal period with limited options available to aid in recovery. It can result in long-term devastating consequences with neurologic complications varying from mild behavioral deficits to severe seizure, intellectual disability, and/or cerebral palsy in the newborn. Despite medical advances, the only viable option is therapeutic hypothermia which is classified as the gold standard but is not used, or may not be as effective in preterm cases, infection-associated cases or low resource settings. Therefore, alternatives or adjunct therapies are urgently needed. Ongoing research continues to advance our understanding of the mechanisms contributing to perinatal brain injury and identify new targets and treatments. Drugs used for the treatment of patients with type 2 diabetes mellitus (T2DM) have demonstrated neuroprotective properties and therapeutic efficacy from neurological sequelae following HIE insults in preclinical models, both alone, or in combination with induced hypothermia. In this short review, we have focused on recent findings on the use of diabetes drugs that provide a neuroprotective effect using *in vitro* and *in vivo* models of HIE that could be considered for clinical translation as a promising treatment.

Keywords: hypoxic-ischemic encephalopathy, perinatal brain injury, cerebral palsy, neuroprotection, hypothermia, diabetes

OPEN ACCESS

Edited by:
Chao Deng,
University of Wollongong, Australia

Reviewed by:
Sandra E. Juul,
University of Washington, United States
Hemmen Sabir,
University Hospital Bonn, Germany

***Correspondence:**
Ahad A. Rahim
a.rahim@ucl.ac.uk

Specialty section:
This article was submitted to Cellular Neuropathology, a section of the journal Frontiers in Cellular Neuroscience

Received: *14 February 2020*
Accepted: *08 April 2020*
Published: *06 May 2020*

Citation:
Poupon-Bejuit L, Rocha-Ferreira E, Thornton C, Hagberg H and Rahim AA (2020) Neuroprotective Effects of Diabetes Drugs for the Treatment of Neonatal Hypoxia-Ischemia Encephalopathy. Front. Cell. Neurosci. 14:112. doi: 10.3389/fncel.2020.00112

Abbreviations: AD, Alzheimer's disease; BBB, blood brain barrier; DPP-4, dipeptidyl peptidase-4; DMB, quinoxaline 6,7-dichloro-2-methylsulfonyl-3-N-tert-butylaminoquinoxaline; GLP1, glucagon-like peptide-1; GLP1-R, glucagon like peptide-1 receptor; HI, hypoxia-ischemia; HIE, hypoxic-ischemic encephalopathy; HBMVECs, primary human brain microvascular endothelial cells; MAPK, mitogen-activated protein kinase; MCAO, middle cerebral artery occlusion; ND, neurological disorder; NPCs, neural precursor cells; OGD, oxygen glucose deprivation; OGD/R, oxygen glucose deprivation reperfusion; OPCs, oligodendrocyte progenitor cells; PD, Parkinson's disease; PPAR-γ, peroxisome proliferator activated receptor-γ; ROS, reactive oxygen species; SUR, sulfonylurea; T2DM, type 2 diabetes mellitus; TH, therapeutic hypothermia; TBI, traumatic brain injury; TZD, thiazolidinedione

INTRODUCTION

Hypoxic-ischemic encephalopathy (HIE) is the most common neonatal encephalopathy accounting for up to 85% of cases (Volpe, 2012). It is caused by of an inadequate oxygen supply and blood flow resulting in a variety of clinical manifestations (Ferriero, 2004; Allen and Brandon, 2011; Hagberg et al., 2015). These include developmental delays, epilepsy, cerebral palsy, and death (Dilenge et al., 2001; Shankaran, 2012; Hagberg et al., 2016). One to six babies per 1,000 live births in high-income countries and approximately 20 infants per 1,000 live births in low- and middle-income countries die or develop a life-long brain condition. This accounts for approximately one million deaths annually (Lee et al., 2013; Pauliah et al., 2013; Wu et al., 2014).

Currently, the standard care for neonates with HIE is therapeutic hypothermia (TH), which is able to reduce overall neurodevelopmental disability and mortality (Jacobs et al., 2013; Azzopardi et al., 2014; Silveira and Procianoy, 2015; Rao et al., 2017). However, while TH is very promising, up to 55% of treated neonates are not protected and still develop life-long neurodisabilities, including cerebral palsy (Jacobs et al., 2013; Davidson et al., 2015). Therefore, there is a need to develop therapies that are either more effective than hypothermia, can be used in combination with hypothermia to enhance its therapeutic efficacy, or which can be used alone in lower resource environments.

Over the past decade, a growing number of pre-clinical and now clinical studies have provided evidence of drugs licensed for the treatment of diabetes as having protective effects on the brain (Athauda et al., 2017; Rotermund et al., 2018; Mousa and Ayoub, 2019). These effects have been proven in different neurological conditions such as Alzheimer's disease (AD) and Parkinson's Disease (PD), traumatic brain injury (TBI), stroke and epilepsy (**Figure 1**). Given the need to develop effective treatments for neonatal HIE, researchers have investigated these diabetes drugs to assess their therapeutic efficacy for this indication.

In this short review, we first describe the experimental and animal models of HIE that are used in preclinical studies to assess the therapeutic efficacy of candidate drugs (**Table 1**). We then highlight the studies that support the potential of commonly used diabetes medicines to ameliorate neurological damage from HIE. This includes recent data demonstrating that diabetes drugs can enhance the therapeutic effect of TH.

EXPERIMENTAL AND ANIMAL MODELS OF HIE

Hypoxic-ischemic encephalopathy is an evolving process that involves distinct phases leading to a delayed cell death, including primary injury, latent phase, secondary phase, and tertiary phase (Wyatt et al., 1989; Fleiss and Gressens, 2012; Davidson et al., 2015). Understanding the characteristics observed during the different phases leading to neonatal encephalopathy are key to the development of new therapeutics, when they can be used to ameliorate HIE and the multiple possible subsequent sequela. The timing of the events following hypoxia-ischemia (HI) and the therapeutic window in rodent models is well defined at ∼6 h correlating with initiation of the secondary phase of brain injury (Nair and Kumar, 2018). Therefore, there is a narrow window within the first few hours of birth during which a therapy should be initiated for optimal outcomes (Silveira and Procianoy, 2015; Martinello et al., 2017). Furthermore, if the drug is administered systemically, then it should be able to reach the brain quickly and cross the blood brain barrier (BBB).

The neuroprotective properties of diabetes drugs were first recognized by positive neurological effects in type 2 diabetes mellitus (T2DM) patients under treatment (Grant et al., 2011) and now in various studies for the treatment of different neurological conditions (Hussien et al., 2018; Rotermund et al., 2018; Erbil et al., 2019). A number of studies have demonstrated that diabetes drugs are indeed capable of entering the brain following systemic administrations and mediating a physiological response, e.g., metformin (Lv et al., 2012), sulfonylurea (SUR) (Simard et al., 2012), thiazolidine (Grommes et al., 2013), dipeptidyl peptidase-4 (DPP-4) inhibitors (Mousa and Ayoub, 2019), and glucagon-like peptide-1 receptor (GLP1-R) agonists (Hunter and Hölscher, 2012).

Accurate and reliable *in vitro* and *in vivo* models of HIE are of utmost importance in determining the mechanisms of damage and also evaluating the efficacy of potential treatments. The development of a variety of *in vitro* and *in vivo* models of HIE have facilitated this process.

Oxygen Glucose Deprivation

Oxygen glucose deprivation is widely used as a relatively convenient *in vitro* model for ischemia, stroke or HIE, showing similarities with the *in vivo* models of brain ischemia (Tasca et al., 2015). This primary neural cell or immortalized cell culture model has been used extensively to examine the cellular mechanisms mediating ischemia–reperfusion injury (Rousset et al., 2015; Gao et al., 2019). The OGD model is a simple process that firstly involves changes to the cell culture medium to exclude glucose. The cells are incubated in a hypoxic incubator with decreased O_2 and increased N_2 levels with a saturated humidity atmosphere at 37°C over a specific period of time. Thus, cultured cells subjected to hypoxia, fuel deprivation and then reoxygenation mimic the scenario of ischemia–reperfusion.

Hypoxia-Ischemia Surgery

The rodent model of neonatal HIE was first validated by Rice et al. (1981) and has since been extensively used to identify mechanisms of brain injury resulting from perinatal HI (Vannucci and Vannucci, 2005). It is also used to test potential therapeutic interventions. The HIE model is a two-step process and involves the ligation of one common carotid artery followed by exposure to a hypoxic environment before restoration to normal atmospheric conditions. Traditional models of HIE have utilized rodents at postnatal day 7–10 as being roughly equivalent to a near-term or term human infant based on electrophysiological, neurochemical, cardiovascular, and metabolic criteria of brain development (Hagberg et al., 1997; Semple et al., 2013). There are a wide variety of HI animal models used to investigate different aspects of HIE. Examples of this

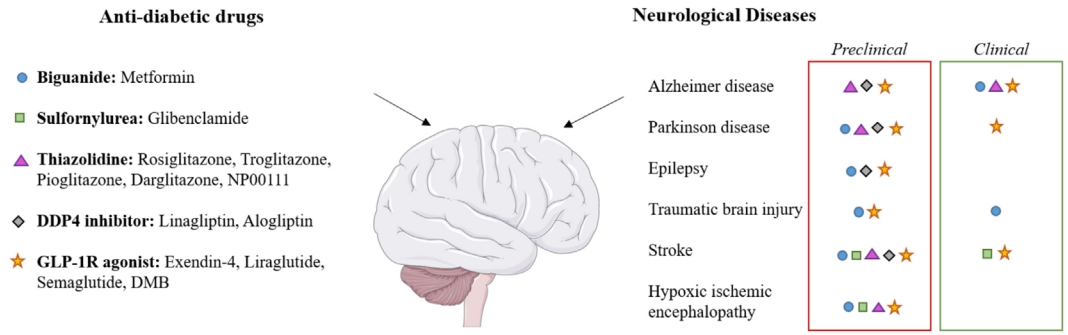

FIGURE 1 | Effects of diabetes drugs on various neurological diseases. The applied color code indicates whether the effect on the target disease has been observed in preclinical studies (red boxes) or in clinical studies (green boxes). Each class of drugs corresponds to a symbol which is indicated in neurological diseases for which clinical and/or preclinical studies has been performed. Brain image taken from the SMART Servier Medical Art Library (https://smart.servier.com).

include; rodents (Recker et al., 2009), rabbits (Derrick et al., 2004), term piglet (Rocha-Ferreira et al., 2016, 2017), preterm sheep (Nitsos et al., 2014), and non-human primates (Juul et al., 2007). To date, existing preclinical data using diabetes drugs as a treatment for HIE have only been performed on rodent models. Furthermore, rodents have limitations in simulating the range, accuracy, and physiology of clinical HI and the relevant systems neuropathology that contribute to the human brain injury pattern. Large animal models of perinatal HI can better replicate the conditions of human HIE (Koehler et al., 2018).Therefore, the availability of these larger animal models of HIE are an invaluable tool to evaluate the therapeutic efficacy of these candidate diabetes drugs prior to any clinical trials.

DIABETES DRUGS AND NEUROLOGICAL DISEASES

Pharmacologic therapy of T2DM has changed dramatically in the last 10 years, with new drugs and drug classes becoming available. Among the different categories of therapies for T2DM, metformin serves as the first line drug whereas other hypoglycaemic agents (SUR, thiazolidine, DPP4 inhibitor, incretin) are used as second line therapies, or in combination with metformin. Over the past three decades, numerous epidemiological studies have shown a clear association between T2DM and an increased risk of developing neurological disorders (NDs) such as AD (Li et al., 2015), PD (Khan et al., 2014), epilepsy/seizure (Yun and Xuefeng, 2013), and stroke (Putaala et al., 2011).

Various studies suggest a comorbid association between NDs and T2DM indicating that there could be shared underlying pathophysiological mechanisms. Using comparative analysis, several putative "shared pathways" have been indentified and demonstrated how the insulin signaling pathway is related to other significant ND pathways. These include the signaling pathways for neurotrophin (Tong et al., 2009; Karki et al., 2017), PI3K/AKT (Gabbouj et al., 2019), mTOR (Bryan and Bowman, 2017; Sun et al., 2019), and mitogen-activated protein kinase (MAPK) (Santiago and Potashkin, 2013; Karki et al., 2017) and how these pathways cross-talk with each other. Consequently, studies started to investigate T2DM treatments as neuroprotective strategies for different types of ND, including perinatal HIE.

Metformin

Metformin is a biguanide drug widely used since the 1960s for the treatment of patients with T2DM. It enhances insulin sensitivity, induces glycolysis, and suppresses gluconeogenesis in the liver (Martin-Montalvo et al., 2013). Pre-clinical studies have also reported the promising therapeutic effect of metformin against neurodegeneration in conditions such as PD (Patil et al., 2014), epilepsy (Yimer et al., 2019), and cerebral ischaemia/reperfusion injury (Ge et al., 2017; Leech et al., 2019). In addition to its neuroprotective effects, metformin has been shown to promote neurogenesis by enhancing neural precursor self-renewal, proliferation, and differentiation (Potts and Lim, 2012; Wang J. et al., 2012). Increased neurogenesis upon metformin treatment resulted in improved memory formation in multiple experimental models of brain injury (Jin et al., 2014; Liu et al., 2014; Dadwal et al., 2015; Ge et al., 2017; Qi et al., 2017). *In vitro* studies using the OGD model demonstrated that metformin improves neuronal viability and regulates programmed cell death in a caspase-independent manner, thereby reducing ischemic reperfusion injuries (Mielke et al., 2006; Meng et al., 2016; Gabryel and Liber, 2018; Mohammad Alizadeh et al., 2018). Metformin treatment remarkably attenuated brain infarct volumes, brain oedema and restored behavior deficits in a neonatal rat model of HI (Qi et al., 2017). It also induced activation of endogenous neural precursor cells (NPCs) (Dadwal et al., 2015). A rodent model of neonatal HI injury showed better neuroprotection induced by metformin in females following early injury relative to males. Indeed, metformin treatment in mice increased the NPC pool in both sexes in neonates but only in females at the adult stage. Consequently, long-term metformin treatment leads to cognitive improvements in females, but not males following early HI injury (Ruddy et al., 2019). The mechanism could be linked to the sex hormones (Ruddy et al., 2019) but further exploration of the mechanism underlying this effect is required. Of note, females have an

TABLE 1 | Evidence supporting the neuroprotective properties of diabetes drugs use in the context of treatments for hypoxia-ischemia encephalopathy.

Diabetes drug	Model	Species	Treatment	Effects	References
Biguanide	OGD	bEND.3 cells	Metformin	Inhibition of inflammatory signaling pathways	Liu et al., 2014
Biguanide	OGD	Rat cortical neurons	Metformin	Pre-treatment of neurons alleviated OGD/R-induced injury	Meng et al., 2016
Biguanide	OGD	Primary rat fetal-derived astrocytes	Metformin	Improve cell viability via reduction of apoptosis mechanisms	Gabryel and Liber, 2018
Biguanide	OGD	PC-12 cells	Metformin	Reduce cell death under OGD/R condition and attenuation of ROS generation	Mohammad Alizadeh et al., 2018
Biguanide	OGD	Primary cortical and hippocampal neurons	Metformin	Moderate improvement of cell viability	Mielke et al., 2006
TZD	OGD	Rat hippocampal slices	NP00111 Rosiglitazone	Protection against OGD by a mechanism related to phosphorylation of ERK1/2 via activation of PPARγ	Rosa et al., 2008
TZD	OGD	Primary cultured astrocytes	Pioglitazone	Protective effects with inhibition of pyroptosis mechanism induced by the OGD	Xia et al., 2018
DPP4	OGD	HBMVECs	Alogliptin	Protection against OGD and increasing of permeability in human brain vascular cells	Hao et al., 2019
Incretin GLP1-R agonist	OGD	Rat cortical neurons	Exendin-4	Protects neurons through PKA pathway	Wang M.-D. et al., 2012
Incretin GLP1-R agonist	OGD	Rat cortical neurons	Liraglutide	Neuroprotective action with reduction of apoptosis and ROS via activation of the PI3K/AKT and MAPK pathways	Zhu et al., 2016
Incretin GLP1-R agonist	OGD	Mouse cortical neurons	DMB	Neuroprotection with anti-apoptotic effects, mediated by activation of the GLP-1R through the cAMP-PKA-CREB signaling pathway	Zhang et al., 2016
Sulfonylurea	HI P10	Rat	Glibenclamide	No effects on severe HI model Improvement neurological functions in moderate HI model	Zhou et al., 2009
TZD	HI 8W	Ob/Ob mouse	Darglitazone	Reduction of the infarct size and neuroinflammation response	Kumari et al., 2010
Biguanide	HI P8	Mouse	Metformin	Activation of endogenous NPCs, promoting their migration and differentiation in the injured brain Restoration of sensory-motor function	Dadwal et al., 2015
Biguanide	HI P3	Rat	Metformin	Attenuation of cognitive impairments Induction of OPCs proliferation reducing myelination damage	Qi et al., 2017
Biguanide	HI P7	Rat	Metformin	Attenuation brain infarct and oedema Inhibition of neuronal apoptosis, and neuroinflammation + amelioration of the blood brain barrier breakdown	Fang et al., 2017
Biguanide	HI P8	Mouse	Metformin	Sex-dependent effects on proliferation but increases neurogenesis in both sexes; rescues cognitive deficits in adult females	Ruddy et al., 2019
Incretin GLP1-R agonist	HI P7/P10	Mouse	Exendin-4**	Neuroprotective effect alone or in combination with therapeutic hypothermia	Rocha-Ferreira et al., 2018
Incretin GLP1-R agonist	HI P7	Rat	Liraglutide	Inhibited apoptosis and promoted neuronal survival; PI3K/Akt pathway involved	Zeng et al., 2020

*In vitro model with OGD on different cell types and in vivo models with HI at different stage of age. **Only study using combination with hypothermia.*

advantage following neonatal hypoxia ischemia; larger cognitive deficits and less functional recovery have been observed in males despite a comparable neuropathology across sexes (Smith et al., 2014). The neuroprotective properties of metformin were associated with inhibition of neuronal apoptosis, suppression of neuroinflammation and amelioration of the blood-brain barrier breakdown via downregulation of the NFκB signaling pathway (Fang et al., 2017). Overall, these studies have highlighted this drug as a promising potential treatment in childhood brain injury models.

Sulfonylurea

Sulfonylurea agents are the second oral hypoglycaemic drugs after metformin and they remain an imperative tool for glucose control (Thulé and Umpierrez, 2014). Recent studies demonstrated that sulfonylurea receptor 1 (SUR1) is involved in brain injury in rodent models of stroke (Hussien et al., 2018). The SUR drugs glibenclamide and glimepiride have neuroprotective effects (Ortega et al., 2013; Wang et al., 2019) and ameliorate cerebral stroke, spinal cord injury, premature encephalopathy, and TBI (Tosun et al., 2013). The neuroprotective effect of SUR agents is not fully understood but glibenclamide blocks SUR1, a regulatory subunit of the microglial K_{ATP} channel. This channel is overexpressed in rodent models of stroke and the effect of blocking SUR1 could inhibit microglia activation which release inflammatory cytokines and initiate downstream signaling pathways, resulting in neuronal cell loss and necrosis (Ortega et al., 2013). Glibenclamide is clinically effective in preventing oedema and improving outcome after focal ischemia (Sheth et al., 2014); clinical studies are being conducted to evaluate its efficacy in acute cerebral embolism and severe cerebral edema (NCT03284463, NCT02864953). In a rat model of HI injury, glibenclamide improved several neurological parameters but failed to attenuate brain edema, infarct volume or brain tissue loss (Zhou et al., 2009). This may be attributed to the significant reduction in blood glucose induced by the dose of glibenclamide used, which may exacerbate the ischemic brain injury. More investigations need to be performed around the dose and its full potential as a treatment for childhood brain injury models.

Thiazolidine

Thiazolidinedione [also called glitazone or peroxisome proliferator activated receptor-γ (PPARγ) agonists] are a group of oral anti-diabetic drugs designed to treat patients with T2DM. They enhance insulin sensitivity and reduce serum glucose in diabetic patients, without significant alterations in serum glucose of non-diabetic animals or humans (Plutzky, 2003). Rosiglitazone, troglitazone, and pioglitazone suppressed the activation and infiltration of macrophages and reduced the infarct size after cerebral ischemia in a middle cerebral artery occlusion (MCAO) model by reducing levels of proinflammatory cytokines (Sundararajan et al., 2005; Culman et al., 2007; Xia et al., 2018). Moreover, PPARγ agonists such as NP00111, rosiglitazone and pioglitazone treatments could relieve OGD-induced hypoxia injury *in vitro* and exert neuroprotective effects (Rosa et al., 2008; Xia et al., 2018). The neuroprotective effect of TZD requires further investigation. However, data suggests activation of PPARγ mediates suppression of NF-κB signaling pathway, inhibiting apoptosis and reducing neuronal loss (Zhang et al., 2011). In the context of adult HI injury, TZD has shown therapeutic efficacy in Ob/Ob mice, a model for T2DM and obesity. This model was chosen for its high risk factor of stroke and increased risk of brain damage. Darglitazone treatment in this adult diabetic mouse resulted in significant neuroprotection associated with a complete restoration of the initial microglial response and reduction of the infarct brain size at 24 h of recovery (Kumari et al., 2010). No studies have yet been conducted in a neonatal HI model but the proven neuroprotective properties and potent anti-ischemic effects of this class of diabetes drug could be a promising option.

Incretin / GLP1-Receptor Agonists

Glucagon-like peptide-1-receptor agonists are used in combination with diet and exercise in the therapy of T2DM, either alone or in combination with other antidiabetic agents. GLP1-R agonists have been found to enter the brain following systemic administration (Hunter and Hölscher, 2012; Athauda et al., 2017) and have neuroprotective properties when assessed in various rodent models of neurological disease and damage such as AD (Xu et al., 2015; Cai et al., 2018), PD (Yun et al., 2018), epilepsy (Wen et al., 2019), TBI (Glotfelty et al., 2019), and stroke. As a result, a number of clinical trials are already underway for some of these molecules such as exendin-4 (NCT03456687, NCT02829502, NCT03287076), liraglutide (NCT02953665, NCT01469351, NCT01843075, NCT03948347) or semaglutide (NCT03659682) to assess benefits to AD, PD, or stroke patients. A PD trial is already completed and has reported that patients on exendin-4 show a statistically significant improvement in clinical motor and cognitive measures compared to the control group (Athauda et al., 2017). Numerous experimental studies also demonstrated the potential of glucagon-like peptide-1 (GLP1) and analog, such as liraglutide or semaglutide, to reduce acute ischaemic damage in the brain (Wang M.-D. et al., 2012; Zhu et al., 2016; Basalay et al., 2019; Yang et al., 2019). Exendin-4, liraglutide and quinoxaline 6,7-dichloro-2-methylsulfonyl-3-N-tert-butylaminoquinoxaline (DMB, an agonist and allosteric modulator of the GLP-1R) have been shown to increase neuron survival under OGD *in vitro* by reducing reactive oxygen species (ROS), apoptotic and necrotic mechanisms (Wang M.-D. et al., 2012; Zhang et al., 2016; Zhu et al., 2016). The potential that GLP1-R agonists have for treating perinatal HIE has been further strengthened in two recent studies demonstrating: (1) that exendin-4 has significant therapeutic efficacy in the mouse model of neonatal HIE (Rocha-Ferreira et al., 2018), (2) and that liraglutide exerts neuroprotection via the PI3k/Akt pathway (Zeng et al., 2020). The study by Rocha-Ferreira and colleagues demonstrated that systemic administration either directly after HI injury, or even 2 h later significantly reduced the size of the brain infarct, the inflammatory response and the oxidative stress. Exendin-4 treatment was able to work synergistically with hypothermia to further enhance therapeutic efficacy (Rocha-Ferreira et al., 2018).

DPP-4 Inhibitor

Also called gliptins, DPP-4 inhibitors are a class of glucose-lowering agents for the treatment of T2DM. Their actions are mediated indirectly through preservation of GLP-1 incretins that are mainly metabolized by the key enzyme DPP-4 (Andersen et al., 2018). Preclinical studies have shown that DPP-4 inhibitors have neuroprotective effects (Darsalia et al., 2019; Mousa and Ayoub, 2019) but unlike GLP-1 receptor agonists (incretins), the ability of DPP-4 inhibitors to cross the blood-brain barrier are still unclear (Chen et al., 2015). However, they could indirectly increase levels of active GLP-1 in the brain that crosses from the blood (Yang et al., 2013). Several kinds of gliptins have been shown to be effective in different experimental models of neurological diseases such as AD (Wiciński et al., 2018; Dong et al., 2019), PD, epilepsy and stroke (Darsalia et al., 2019; Mousa and Ayoub, 2019). In the MCAO model mimicking stroke, linagliptin and alogliptin reduced infarct volume and neurological deficits (Chiazza et al., 2018; Hao et al., 2019). In the same study, alogliptin protectsed against oxygen glucose deprivation reperfusion (OGD/R) and has a neurovascular protective effect increasing permeability in human brain vascular cells (Hao et al., 2019). No data exists in an experimental neonatal HIE model but DPP-4 enzyme activity is known to increase in the blood serum of term and preterm neonates with cerebral ischemia (Yakovleva et al., 2015). Because DPP-4 inhibitors have shown neuroprotective properties and increase levels of GLP-1 in the brain, this could suggest that they have potential for treating HIE.

SUMMARY

The neuroprotective properties of diabetes drugs were first recognized by improvements in the neuropathic aspects in T2DM patients under treatment (Grant et al., 2011). The role of insulin as a pro-survival neurotrophic factor, where its receptor is widely expressed in cognitive areas of the brain such as the hippocampus and in the dopaminergic system also helped to consolidate this hypothesis (Haas et al., 2016; Fiory et al., 2019). The emerging evidence has suggested a beneficial effect of diabetes drugs in the management of diabetic and non-diabetic NDs. Furthermore, data supporting their neuroprotective effects are supported by a growing number of preclinical studies in neurodegenerative disorders such as AD (Cai et al., 2018; Dong et al., 2019) and PD (Athauda and Foltynie, 2016; Ayoub et al., 2018). Importantly, therapeutic efficacy had also been demonstrated in a clinical trial in PD patients (Athauda et al., 2017). However, many developmental, functional, and injury time course differences exist between the neonatal and the adult brain (Ferriero, 2004). Drug delivery properties, dosage and use can also be complex to translate from a adult to neonatal setting.

Several proof-of-concept studies with different classes of diabetes drugs as a treatment in neonatal HIE have been identified with glibenclamide (Zhou et al., 2009), metformin (Dadwal et al., 2015; Fang et al., 2017; Qi et al., 2017) and exendin-4 (Rocha-Ferreira et al., 2018). These diabetes drugs act on a plethora of biological pathways (Rosa et al., 2008; Wang M.-D. et al., 2012; Zhang et al., 2016; Zhu et al., 2016) and the precise mechanisms of action of diabetes drugs for neuroprotection are still not fully understood. However, in the context of HIE several studies have demonstrated neuroprotective actions of the GLP1-R agonists (Kimura et al., 2009; Jiang et al., 2016; Zhao et al., 2018) and metformin (Khallaghi et al., 2016) through the PI3K/Akt signaling pathway. In cases of brain injury, diabetes drugs have shown to be able to help repair the brain by modulating cell death mechanisms (Mielke et al., 2006; Gabryel and Liber, 2018; Xia et al., 2018), reducing neuronal oxidative stress (Mohammad Alizadeh et al., 2018) and promoting growth of new neurons and cells (Dadwal et al., 2015; Qi et al., 2017).

In adults, diabetes drugs are generally well tolerated with a long track record in the clinic and demonstrable safety profiles. However, this requires to be established in new born babies. Therefore, the normal advantages of rapidly repurposing drugs at a lower cost than the drug development process (Ayoub et al., 2018; Mousa and Ayoub, 2019) may be diminished for application to HIE. Potential safety risks could be reduced since the administration of the drug would likely only be required during a short acute period following the HI insult over a 48 h period (Rocha-Ferreira et al., 2018). However, depending on the diabetes drug in question, an important consideration is the potential to induce a hypoglycaemic effects when perturbations in glucose metabolism (hypoglycaemia and hyperglycemia) are already common in newborn infants with HIE (Vannucci, 1992; Salhab et al., 2004; Basu et al., 2009). This issue of hypoglycaemia exacerbating brain injury has been highlighted in the previously mentioned pre-clinical study using glibenclamide (Zhou et al., 2009). Therefore, the evaluation of the safety of diabetes drugs must be conducted in preclinical neonatal models, including larger animals prior to clinical trials.

CONCLUSION

In conclusion, there is a growing body of evidence supporting the neuroprotective and anti-neuroinflammatory properties of specific diabetes drugs. Furthermore, the emerging proof of concept studies supporting their potential use as a treatment for HIE, either independently or in combination with hypothermia, is highly encouraging and warrants further investigation.

AUTHOR CONTRIBUTIONS

LP-B, ER-F, CT, HH, and AR drafted the manuscript.

FUNDING

LP-B, ER-F, CT, HH, and AR are funded by Action Medical Research (GN2485). AR is also funded by UK Medical Research Council Grants (MR/R025134/1, MR/R015325/1, MR/S009434/1, MR/N026101/1, and MR/S036784/1) and the Wellcome Trust Institutional Strategic Support Fund/UCL Therapeutic Acceleration Support (TAS) Fund (204841/Z/16/Z). ER-F is funded by the Hasselblad Foundation (2020–2021)

and the Åke Wibergs Foundation (M19-0660). HH is funded by governmental grants to Swedish University Hospital (ALF-GBG 432291), ERA-NET (Contract: 0755101), Swedish Medical Research Council (2019-01320), Brain Foundation (2015-0004), and EU (contract: 874721 Horizon 2020). CT is funded by UK Medical Research Council New Investigator Research Grant (MR/T014725/1), and by Action Medical Research (GN2796).

REFERENCES

Allen, K. A., and Brandon, D. H. (2011). Hypoxic ischemic encephalopathy: pathophysiology and experimental treatments. *Newborn Infant Nurs. Rev.* 11, 125–133. doi: 10.1053/j.nainr.2011.07.004

Andersen, E. S., Deacon, C. F., and Holst, J. J. (2018). Do we know the true mechanism of action of the DPP-4 inhibitors? *Diab. Obes. Metab.* 20, 34–41. doi: 10.1111/dom.13018

Athauda, D., and Foltynie, T. (2016). The glucagon-like peptide 1 (GLP) receptor as a therapeutic target in Parkinson's disease: mechanisms of action. *Drug Discov. Today* 21, 802–818. doi: 10.1016/j.drudis.2016.01.013

Athauda, D., Maclagan, K., Skene, S. S., Bajwa-Joseph, M., Letchford, D., Chowdhury, K., et al. (2017). Exenatide once weekly versus placebo in Parkinson's disease: a randomised, double-blind, placebo-controlled trial. *Lancet* 390, 1664–1675. doi: 10.1016/S0140-6736(17)31585-4

Ayoub, B. M., Mowaka, S., Safar, M. M., Ashoush, N., Arafa, M. G., Michel, H. E., et al. (2018). Repositioning of omarigliptin as a once-weekly intranasal Anti-parkinsonian agent. *Sci. Rep.* 8:8959. doi: 10.1038/s41598-018-27395-0

Azzopardi, D., Strohm, B., Marlow, N., Brocklehurst, P., Deierl, A., Eddama, O., et al. (2014). Effects of hypothermia for perinatal asphyxia on childhood outcomes. *N. Engl. J. Med.* 371, 140–149. doi: 10.1056/NEJMoa1315788

Basalay, M. V., Davidson, S. M., and Yellon, D. M. (2019). Neuroprotection in rats following ischaemia-reperfusion injury by GLP-1 analogues-liraglutide and semaglutide. *Cardiovasc. Drugs Ther.* 33, 661–667. doi: 10.1007/s10557-019-06915-8

Basu, P., Som, S., Choudhuri, N., and Das, H. (2009). Contribution of the blood glucose level in perinatal asphyxia. *Eur. J. Pediatr.* 168, 833–838. doi: 10.1007/s00431-008-0844-5

Bryan, M. R., and Bowman, A. B. (2017). Manganese and the insulin-IGF signaling network in Huntington's disease and other neurodegenerative disorders. *Adv. Neurobiol.* 18, 113–142. doi: 10.1007/978-3-319-60189-2_6

Cai, H.-Y., Yang, J.-T., Wang, Z.-J., Zhang, J., Yang, W., Wu, M.-N., et al. (2018). Lixisenatide reduces amyloid plaques, neurofibrillary tangles and neuroinflammation in an APP/PS1/tau mouse model of Alzheimer's disease. *Biochem. Biophys. Res. Commun.* 495, 1034–1040. doi: 10.1016/j.bbrc.2017.11.114

Chen, D.-Y., Wang, S.-H., Mao, C.-T., Tsai, M.-L., Lin, Y.-S., Su, F.-C., et al. (2015). Sitagliptin after ischemic stroke in type 2 diabetic patients: a nationwide cohort study. *Medicine (Baltimore)* 94, e1128. doi: 10.1097/MD.0000000000001128

Chiazza, F., Tammen, H., Pintana, H., Lietzau, G., Collino, M., Nyström, T., et al. (2018). The effect of DPP-4 inhibition to improve functional outcome after stroke is mediated by the SDF-1α/CXCR4 pathway. *Cardiovasc. Diabetol.* 17:60. doi: 10.1186/s12933-018-0702-3

Culman, J., Zhao, Y., Gohlke, P., and Herdegen, T. (2007). PPAR-gamma: therapeutic target for ischemic stroke. *Trends Pharmacol. Sci.* 28, 244–249. doi: 10.1016/j.tips.2007.03.004

Dadwal, P., Mahmud, N., Sinai, L., Azimi, A., Fatt, M., Wondisford, F. E., et al. (2015). Activating endogenous neural precursor cells using metformin leads to neural repair and functional recovery in a model of childhood brain injury. *Stem Cell Rep.* 5, 166–173. doi: 10.1016/j.stemcr.2015.06.011

Darsalia, V., Johansen, O. E., Lietzau, G., Nyström, T., Klein, T., and Patrone, C. (2019). Dipeptidyl peptidase-4 inhibitors for the potential treatment of brain disorders; a mini-review with special focus on linagliptin and stroke. *Front. Neurol.* 10:493. doi: 10.3389/fneur.2019.00493

Davidson, J. O., Wassink, G., van den Heuij, L. G., Bennet, L., and Gunn, A. J. (2015). Therapeutic hypothermia for neonatal hypoxic–ischemic encephalopathy–where to from here? *Front. Neurol.* 6:198. doi: 10.3389/fneur.2015.00198

Derrick, M., Luo, N. L., Bregman, J. C., Jilling, T., Ji, X., Fisher, K., et al. (2004). Preterm fetal hypoxia-ischemia causes hypertonia and motor deficits in the neonatal rabbit: a model for human cerebral palsy? *J. Neurosci.* 24, 24–34. doi: 10.1523/JNEUROSCI.2816-03.2004

Dilenge, M. E., Majnemer, A., and Shevell, M. I. (2001). Long-term developmental outcome of asphyxiated term neonates. *J. Child Neurol.* 16, 781–792. doi: 10.1177/088307380101601102 01

Dong, Q., Teng, S.-W., Wang, Y., Qin, F., Li, Y., Ai, L.-L., et al. (2019). Sitagliptin protects the cognition function of the Alzheimer's disease mice through activating glucagon-like peptide-1 and BDNF-TrkB signalings. *Neurosci. Lett.* 696, 184–190. doi: 10.1016/j.neulet.2018.12.041

Erbil, D., Eren, C. Y., Demirel, C., Küçüker, M. U., Solaroğlu, I., and Eser, H. Y. (2019). GLP-1's role in neuroprotection: a systematic review. *Brain Inj.* 33, 734–819. doi: 10.1080/02699052.2019.1587000

Fang, M., Jiang, H., Ye, L., Cai, C., Hu, Y., Pan, S., et al. (2017). Metformin treatment after the hypoxia-ischemia attenuates brain injury in newborn rats. *Oncotarget* 8, 75308–75325. doi: 10.18632/oncotarget.20779

Ferriero, D. M. (2004). Neonatal brain injury. *N. Engl. J. Med.* 351, 1985–1995. doi: 10.1056/NEJMra041996

Fiory, F., Perruolo, G., Cimmino, I., Cabaro, S., Pignalosa, F. C., Miele, C., et al. (2019). The relevance of insulin action in the dopaminergic system. *Front. Neurosci.* 13:868. doi: 10.3389/fnins.2019.00868

Fleiss, B., and Gressens, P. (2012). Tertiary mechanisms of brain damage: a new hope for treatment of cerebral palsy? *Lancet Neurol.* 11, 556–566. doi: 10.1016/S1474-4422(12)70058-3

Gabbouj, S., Ryhänen, S., Marttinen, M., Wittrahm, R., Takalo, M., Kemppainen, S., et al. (2019). Altered insulin signaling in Alzheimer's disease brain – special emphasis on PI3K-Akt pathway. *Front. Neurosci.* 13:629. doi: 10.3389/fnins.2019.00629

Gabryel, B., and Liber, S. (2018). Metformin limits apoptosis in primary rat cortical astrocytes subjected to oxygen and glucose deprivation. *Folia Neuropathol.* 56, 328–336. doi: 10.5114/fn.2018.80866

Gao, Y., Wang, Z., He, W., Ma, W., and Ni, X. (2019). Mild hypothermia protects neurons against oxygen glucose deprivation via poly (ADP-ribose) signaling. *J. Matern. Fetal Neonatal Med.* 32, 1633–1639. doi: 10.1080/14767058.2017.1413548

Ge, X.-H., Zhu, G.-J., Geng, D.-Q., Zhang, H.-Z., He, J.-M., Guo, A.-Z., et al. (2017). Metformin protects the brain against ischemia/reperfusion injury through PI3K/Akt1/JNK3 signaling pathways in rats. *Physiol. Behav.* 170, 115–123. doi: 10.1016/j.physbeh.2016.12.021

Glotfelty, E. J., Delgado, T., Tovar-Y-Romo, L. B., Luo, Y., Hoffer, B., Olson, L., et al. (2019). Incretin mimetics as rational candidates for the treatment of traumatic brain injury. *ACS Pharmacol. Transl. Sci.* 2, 66–91. doi: 10.1021/acsptsci.9b00003

Grant, P., Lipscomb, D., and Quin, J. (2011). Psychological and quality of life changes in patients using GLP-1 analogues. *J. Diab. Complicat.* 25, 244–246. doi: 10.1016/j.jdiacomp.2011.03.002

Grommes, C., Karlo, J. C., Caprariello, A., Blankenship, D., Dechant, A., and Landreth, G. E. (2013). The PPARγ agonist pioglitazone crosses the blood-brain barrier and reduces tumor growth in a human xenograft model. *Cancer Chemother. Pharmacol.* 71, 929–936. doi: 10.1007/s00280-013-2084-2

Haas, C. B., Kalinine, E., Zimmer, E. R., Hansel, G., Brochier, A. W., Oses, J. P., et al. (2016). Brain insulin administration triggers distinct cognitive and neurotrophic responses in young and aged rats. *Mol. Neurobiol.* 53, 5807–5817. doi: 10.1007/s12035-015-9494-6

Hagberg, H., Bona, E., Gilland, E., and Puka-Sundvall, M. (1997). Hypoxia-ischaemia model in the 7-day-old rat: possibilities and shortcomings. *Acta Paediatr. Suppl.* 86, 85–88.

Hagberg, H., David Edwards, A., and Groenendaal, F. (2016). Perinatal brain damage: the term infant. *Neurobiol. Dis.* 92, 102–112. doi: 10.1016/j.nbd.2015.09.011

Hagberg, H., Mallard, C., Ferriero, D. M., Vannucci, S. J., Levison, S. W., Vexler, Z. S., et al. (2015). The role of inflammation in perinatal brain injury. *Nat. Rev. Neurol.* 11, 192–208. doi: 10.1038/nrneurol.2015.13

Hao, F., Han, X., Wang, X., Zhao, Z., Guo, A., Lu, X., et al. (2019). The neurovascular protective effect of alogliptin in murine MCAO model and brain endothelial cells. *Biomed. Pharmacother.* 109, 181–187. doi: 10.1016/j.biopha.2018.10.064

Hunter, K., and Hölscher, C. (2012). Drugs developed to treat diabetes, liraglutide and lixisenatide, cross the blood brain barrier and enhance neurogenesis. *BMC Neurosci.* 13:33. doi: 10.1186/1471-2202-13-33

Hussien, N. R., Al-Naimi, M. S., Rasheed, H. A., Al-Kuraishy, H. M., and Al-Gareeb, A. I. (2018). Sulfonylurea and neuroprotection: the bright side of the moon. *J. Adv. Pharm. Technol. Res.* 9, 120–123. doi: 10.4103/japtr.JAPTR_317_18

Jacobs, S. E., Berg, M., Hunt, R., Tarnow-Mordi, W. O., Inder, T. E., and Davis, P. G. (2013). Cooling for newborns with hypoxic ischaemic encephalopathy. *Cochrane Database Syst. Rev.* 2013:CD003311. doi: 10.1002/14651858

Jiang, Y.-Q., Chang, G.-L., Wang, Y., Zhang, D.-Y., Cao, L., and Liu, J. (2016). Geniposide prevents hypoxia/reoxygenation-induced apoptosis in H9c2 cells: improvement of mitochondrial dysfunction and activation of GLP-1R and the PI3K/AKT signaling pathway. *Cell. Physiol. Biochem.* 39, 407–421. doi: 10.1159/000445634

Jin, Q., Cheng, J., Liu, Y., Wu, J., Wang, X., Wei, S., et al. (2014). Improvement of functional recovery by chronic metformin treatment is associated with enhanced alternative activation of microglia/macrophages and increased angiogenesis and neurogenesis following experimental stroke. *Brain Behav. Immun.* 40, 131–142. doi: 10.1016/j.bbi.2014.03.003

Juul, S. E., Aylward, E., Richards, T., McPherson, R. J., Kuratani, J., and Burbacher, T. M. (2007). Prenatal cord clamping in newborn *Macaca nemestrina*: a model of perinatal asphyxia. *Dev. Neurosci.* 29, 311–320. doi: 10.1159/000105472

Karki, R., Kodamullil, A. T., and Hofmann-Apitius, M. (2017). Comorbidity analysis between Alzheimer's disease and type 2 diabetes mellitus (T2DM) based on shared pathways and the role of T2DM drugs. *J. Alzheimers Dis.* 60, 721–731. doi: 10.3233/JAD-170440

Khallaghi, B., Safarian, F., Nasoohi, S., Ahmadiani, A., and Dargahi, L. (2016). Metformin-induced protection against oxidative stress is associated with AKT/mTOR restoration in PC12 cells. *Life Sci.* 148, 286–292. doi: 10.1016/j.lfs.2016.02.024

Khan, N. M., Ahmad, A., Tiwari, R. K., Kamal, M. A., Mushtaq, G., and Ashraf, G. M. (2014). Current challenges to overcome in the management of type 2 diabetes mellitus and associated neurological disorders. *CNS Neurol. Disord. Drug Targets* 13, 1440–1457. doi: 10.2174/1871527313666141023160448

Kimura, R., Okouchi, M., Fujioka, H., Ichiyanagi, A., Ryuge, F., Mizuno, T., et al. (2009). Glucagon-like peptide-1 (GLP-1) protects against methylglyoxal-induced PC12 cell apoptosis through the PI3K/Akt/mTOR/GCLc/redox signaling pathway. *Neuroscience* 162, 1212–1219. doi: 10.1016/j.neuroscience.2009.05.025

Koehler, R. C., Yang, Z.-J., Lee, J. K., and Martin, L. J. (2018). Perinatal hypoxic-ischemic brain injury in large animal models: relevance to human neonatal encephalopathy. *J. Cereb. Blood Flow Metab.* 38, 2092–2111. doi: 10.1177/0271678X18797328

Kumari, R., Willing, L. B., Patel, S. D., Krady, J. K., Zavadoski, W. J., Gibbs, E. M., et al. (2010). The PPAR-γ agonist, darglitazone, restores acute inflammatory responses to cerebral hypoxia–ischemia in the diabetic ob/ob mouse. *J. Cereb. Blood Flow Metab.* 30, 352–360. doi: 10.1038/jcbfm.2009.221

Lee, A. C. C., Kozuki, N., Blencowe, H., Vos, T., Bahalim, A., Darmstadt, G. L., et al. (2013). Intrapartum-related neonatal encephalopathy incidence and impairment at regional and global levels for 2010 with trends from 1990. *Pediatr. Res.* 74(Suppl. 1), 50–72. doi: 10.1038/pr.2013.206

Leech, T., Chattipakorn, N., and Chattipakorn, S. C. (2019). The beneficial roles of metformin on the brain with cerebral ischaemia/reperfusion injury. *Pharmacol. Res.* 146:104261. doi: 10.1016/j.phrs.2019.104261

Li, X., Song, D., and Leng, S. X. (2015). Link between type 2 diabetes and Alzheimer's disease: from epidemiology to mechanism and treatment. *Clin. Interv. Aging* 10, 549–560. doi: 10.2147/CIA.S74042

Liu, Y., Tang, G., Li, Y., Wang, Y., Chen, X., Gu, X., et al. (2014). Metformin attenuates blood-brain barrier disruption in mice following middle cerebral artery occlusion. *J. Neuroinflamm.* 11:177. doi: 10.1186/s12974-014-0177-4

Lv, W.-S., Wen, J.-P., Li, L., Sun, R.-X., Wang, J., Xian, Y.-X., et al. (2012). The effect of metformin on food intake and its potential role in hypothalamic regulation in obese diabetic rats. *Brain Res.* 1444, 11–19. doi: 10.1016/j.brainres.2012.01.028

Martinello, K., Hart, A. R., Yap, S., Mitra, S., and Robertson, N. J. (2017). Management and investigation of neonatal encephalopathy: 2017 update. *Arch. Dis. Child. Fetal Neonatal Ed.* 102, F346–F358. doi: 10.1136/archdischild-2015-309639

Martin-Montalvo, A., Mercken, E. M., Mitchell, S. J., Palacios, H. H., Mote, P. L., Scheibye-Knudsen, M., et al. (2013). Metformin improves healthspan and lifespan in mice. *Nat. Commun.* 4:2192. doi: 10.1038/ncomms3192

Meng, X., Chu, G., Yang, Z., Qiu, P., Hu, Y., Chen, X., et al. (2016). Metformin protects neurons against oxygen-glucose deprivation/reoxygenation -induced injury by down-regulating MAD2B. *Cell. Physiol. Biochem.* 40, 477–485. doi: 10.1159/000452562

Mielke, J. G., Taghibiglou, C., and Wang, Y. T. (2006). Endogenous insulin signaling protects cultured neurons from oxygen–glucose deprivation-induced cell death. *Neuroscience* 143, 165–173. doi: 10.1016/j.neuroscience.2006.07.055

Mohammad Alizadeh, E., Mahdavi, M., Jenani Fard, F., Chamani, S., Farajdokht, F., and Karimi, P. (2018). Metformin protects PC12 cells against oxygen-glucose deprivation/reperfusion injury. *Toxicol. Mech. Methods* 28, 622–629. doi: 10.1080/15376516.2018.1486495

Mousa, S. A., and Ayoub, B. M. (2019). Repositioning of dipeptidyl peptidase-4 inhibitors and glucagon like peptide-1 agonists as potential neuroprotective agents. *Neural Regen. Res.* 14, 745–748. doi: 10.4103/1673-5374.249217

Nair, J., and Kumar, V. H. S. (2018). Current and emerging therapies in the management of hypoxic ischemic encephalopathy in neonates. *Children (Basel)* 5:E99. doi: 10.3390/children5070099

Nitsos, I., Newnham, J. P., Rees, S. M., Harding, R., and Moss, T. J. M. (2014). The impact of chronic intrauterine inflammation on the physiologic and neurodevelopmental consequences of intermittent umbilical cord occlusion in fetal sheep. *Reprod. Sci.* 21, 658–670. doi: 10.1177/1933719111399928

Ortega, F. J., Jolkkonen, J., Mahy, N., and Rodríguez, M. J. (2013). Glibenclamide enhances neurogenesis and improves long-term functional recovery after transient focal cerebral ischemia. *J. Cereb. Blood Flow Metab.* 33, 356–364. doi: 10.1038/jcbfm.2012.166

Patil, S. P., Jain, P. D., Ghumatkar, P. J., Tambe, R., and Sathaye, S. (2014). Neuroprotective effect of metformin in MPTP-induced Parkinson's disease in mice. *Neuroscience* 277, 747–754. doi: 10.1016/j.neuroscience.2014.07.046

Pauliah, S. S., Shankaran, S., Wade, A., Cady, E. B., and Thayyil, S. (2013). Therapeutic hypothermia for neonatal encephalopathy in low- and middle-income countries: a systematic review and meta-analysis. *PLoS One* 8:e58834. doi: 10.1371/journal.pone.0058834

Plutzky, J. (2003). The potential role of peroxisome proliferator–activated receptors on inflammation in type 2 diabetes mellitus and atherosclerosis. *Am. J. Cardiol.* 92, 34–41. doi: 10.1016/S0002-9149(03)00614-3

Potts, M. B., and Lim, D. A. (2012). An old drug for new ideas: metformin promotes adult neurogenesis and spatial memory formation. *Cell Stem Cell* 11, 5–6. doi: 10.1016/j.stem.2012.06.003

Putaala, J., Liebkind, R., Gordin, D., Thorn, L. M., Haapaniemi, E., Forsblom, C., et al. (2011). Diabetes mellitus and ischemic stroke in the young: clinical features and long-term prognosis. *Neurology* 76, 1831–1837. doi: 10.1212/WNL.0b013e31821cccc2

Qi, B., Hu, L., Zhu, L., Shang, L., Sheng, L., Wang, X., et al. (2017). Metformin attenuates cognitive impairments in hypoxia–ischemia neonatal rats via improving remyelination. *Cell Mol. Neurobiol.* 37, 1269–1278. doi: 10.1007/s10571-016-0459-8

Rao, R., Trivedi, S., Vesoulis, Z., Liao, S. M., Smyser, C. D., and Mathur, A. M. (2017). Safety and short-term outcomes of therapeutic hypothermia in preterm neonates 34-35 weeks gestational age with hypoxic-ischemic encephalopathy. *J. Pediatr.* 183, 37–42. doi: 10.1016/j.jpeds.2016.11.019

Recker, R., Adami, A., Tone, B., Tian, H. R., Lalas, S., Hartman, R. E., et al. (2009). Rodent neonatal bilateral carotid artery occlusion with hypoxia mimics human hypoxic-ischemic injury. *J. Cereb. Blood Flow Metab.* 29, 1305–1316. doi: 10.1038/jcbfm.2009.56

Rice, J. E., Vannucci, R. C., and Brierley, J. B. (1981). The influence of immaturity on hypoxic-ischemic brain damage in the rat. *Ann. Neurol.* 9, 131–141. doi: 10.1002/ana.410090206

Rocha-Ferreira, E., Kelen, D., Faulkner, S., Broad, K. D., Chandrasekaran, M., Kerenyi, Á, et al. (2017). Systemic pro-inflammatory cytokine status following therapeutic hypothermia in a piglet hypoxia-ischemia model. *J. Neuroinflamm.* 14:44. doi: 10.1186/s12974-017-0821-x

Rocha-Ferreira, E., Poupon, L., Zelco, A., Leverin, A.-L., Nair, S., Jonsdotter, A., et al. (2018). Neuroprotective exendin-4 enhances hypothermia therapy in a model of hypoxic-ischaemic encephalopathy. *Brain* 141, 2925–2942. doi: 10.1093/brain/awy220

Rocha-Ferreira, E., Rudge, B., Hughes, M. P., Rahim, A. A., Hristova, M., and Robertson, N. J. (2016). Immediate remote ischemic postconditioning reduces brain nitrotyrosine formation in a piglet asphyxia model. *Oxid. Med. Cell Longev.* 2016:5763743. doi: 10.1155/2016/5763743

Rosa, A. O., Egea, J., Martínez, A., García, A. G., and López, M. G. (2008). Neuroprotective effect of the new thiadiazolidinone NP00111 against oxygen-glucose deprivation in rat hippocampal slices: implication of ERK1/2 and PPARgamma receptors. *Exp. Neurol.* 212, 93–99. doi: 10.1016/j.expneurol.2008.03.008

Rotermund, C., Machetanz, G., and Fitzgerald, J. C. (2018). The therapeutic potential of metformin in neurodegenerative diseases. *Front. Endocrinol. (Lausanne)* 9:400. doi: 10.3389/fendo.2018.00400

Rousset, C. I., Leiper, F. C., Kichev, A., Gressens, P., Carling, D., Hagberg, H., et al. (2015). A dual role for AMP-activated protein kinase (AMPK) during neonatal hypoxic-ischaemic brain injury in mice. *J. Neurochem.* 133, 242–252. doi: 10.1111/jnc.13034

Ruddy, R. M., Adams, K. V., and Morshead, C. M. (2019). Age- and sex-dependent effects of metformin on neural precursor cells and cognitive recovery in a model of neonatal stroke. *Sci. Adv.* 5:eaax1912. doi: 10.1126/sciadv.aax1912

Salhab, W. A., Wyckoff, M. H., Laptook, A. R., and Perlman, J. M. (2004). Initial hypoglycemia and neonatal brain injury in term infants with severe fetal acidemia. *Pediatrics* 114, 361–366. doi: 10.1542/peds.114.2.361

Santiago, J. A., and Potashkin, J. A. (2013). Shared dysregulated pathways lead to Parkinson's disease and diabetes. *Trends Mol. Med.* 19, 176–186. doi: 10.1016/j.molmed.2013.01.002

Semple, B. D., Blomgren, K., Gimlin, K., Ferriero, D. M., and Noble-Haeusslein, L. J. (2013). Brain development in rodents and humans: identifying benchmarks of maturation and vulnerability to injury across species. *Prog. Neurobiol.* 106–107, 1–16. doi: 10.1016/j.pneurobio.2013.04.001

Shankaran, S. (2012). Hypoxic-ischemic encephalopathy and novel strategies for neuroprotection. *Clin. Perinatol.* 39, 919–929. doi: 10.1016/j.clp.2012.09.008

Sheth, K. N., Kimberly, W. T., Elm, J. J., Kent, T. A., Mandava, P., Yoo, A. J., et al. (2014). Pilot study of intravenous glyburide in patients with a large ischemic stroke. *Stroke* 45, 281–283. doi: 10.1161/STROKEAHA.113.003352

Silveira, R. C., and Procianoy, R. S. (2015). Hypothermia therapy for newborns with hypoxic ischemic encephalopathy. *J. Pediatr. (Rio J)* 91, S78–S83. doi: 10.1016/j.jped.2015.07.004

Simard, J. M., Woo, S. K., Schwartzbauer, G. T., and Gerzanich, V. (2012). Sulfonylurea receptor 1 in central nervous system injury: a focused review. *J. Cereb. Blood Flow Metab.* 32, 1699–1717. doi: 10.1038/jcbfm.2012.91

Smith, A. L., Alexander, M., Rosenkrantz, T. S., Sadek, M. L., and Fitch, R. H. (2014). Sex differences in behavioral outcome following neonatal hypoxia ischemia: insights from a clinical meta-analysis and a rodent model of induced hypoxic ischemic brain injury. *Exp. Neurol.* 254, 54–67. doi: 10.1016/j.expneurol.2014.01.003

Sun, Q., Wei, L.-L., Zhang, M., Li, T.-X., Yang, C., Deng, S.-P., et al. (2019). Rapamycin inhibits activation of AMPK-mTOR signaling pathway-induced Alzheimer's disease lesion in hippocampus of rats with type 2 diabetes mellitus. *Int. J. Neurosci.* 129, 179–188. doi: 10.1080/00207454.2018.1491571

Sundararajan, S., Gamboa, J. L., Victor, N. A., Wanderi, E. W., Lust, W. D., and Landreth, G. E. (2005). Peroxisome proliferator-activated receptor-γ ligands reduce inflammation and infarction size in transient focal ischemia. *Neuroscience* 130, 685–696. doi: 10.1016/j.neuroscience.2004.10.021

Tasca, C. I., Dal-Cim, T., and Cimarosti, H. (2015). In vitro oxygen-glucose deprivation to study ischemic cell death. *Methods Mol. Biol.* 1254, 197–210. doi: 10.1007/978-1-4939-2152-2_15

Thulé, P. M., and Umpierrez, G. (2014). Sulfonylureas: a new look at old therapy. *Curr. Diab. Rep.* 14:473. doi: 10.1007/s11892-014-0473-5

Tong, M., Dong, M., and de la Monte, S. M. (2009). Brain insulin-like growth factor and neurotrophin resistance in Parkinson's disease and dementia with Lewy bodies: potential role of manganese neurotoxicity. *J. Alzheimers Dis.* 16, 585–599. doi: 10.3233/JAD-2009-0995

Tosun, C., Koltz, M. T., Kurland, D. B., Ijaz, H., Gurakar, M., Schwartzbauer, G., et al. (2013). The protective effect of glibenclamide in a model of hemorrhagic encephalopathy of prematurity. *Brain Sci.* 3, 215–238. doi: 10.3390/brainsci3010215

Vannucci, R. C. (1992). Cerebral carbohydrate and energy metabolism in perinatal hypoxic-ischemic brain damage. *Brain Pathol.* 2, 229–234. doi: 10.1111/j.1750-3639.1992.tb00696.x

Vannucci, R. C., and Vannucci, S. J. (2005). Perinatal hypoxic-ischemic brain damage: evolution of an animal model. *Dev. Neurosci.* 27, 81–86. doi: 10.1159/000085978

Volpe, J. J. (2012). Neonatal encephalopathy: an inadequate term for hypoxic-ischemic encephalopathy. *Ann. Neurol.* 72, 156–166. doi: 10.1002/ana.23647

Wang, J., Gallagher, D., DeVito, L. M., Cancino, G. I., Tsui, D., He, L., et al. (2012). Metformin activates an atypical PKC-CBP pathway to promote neurogenesis and enhance spatial memory formation. *Cell Stem Cell* 11, 23–35. doi: 10.1016/j.stem.2012.03.016

Wang, M.-D., Huang, Y., Zhang, G.-P., Mao, L., Xia, Y.-P., Mei, Y.-W., et al. (2012). Exendin-4 improved rat cortical neuron survival under oxygen/glucose deprivation through PKA pathway. *Neuroscience* 226, 388–396. doi: 10.1016/j.neuroscience.2012.09.025

Wang, X., Chang, Y., He, Y., Lyu, C., Li, H., Zhu, J., et al. (2019). Glimepiride and glibenclamide have comparable efficacy in treating acute ischemic stroke in mice. *Neuropharmacology* 162, 107845. doi: 10.1016/j.neuropharm.2019.107845

Wen, Y., Wu, K., Xie, Y., Dan, W., Zhan, Y., and Shi, Q. (2019). Inhibitory effects of glucagon-like peptide-1 receptor on epilepsy. *Biochem. Biophys. Res. Commun.* 511, 79–86. doi: 10.1016/j.bbrc.2019.02.028

Wiciński, M., Wódkiewicz, E., Słupski, M., Walczak, M., Socha, M., Malinowski, B., et al. (2018). Neuroprotective activity of sitagliptin via reduction of neuroinflammation beyond the incretin effect: focus on Alzheimer's disease. *Biomed. Res. Int.* 2018:6091014. doi: 10.1155/2018/6091014

Wu, T.-W., McLean, C., Friedlich, P., Wisnowski, J., Grimm, J., Panigrahy, A., et al. (2014). Brain temperature in neonates with hypoxic-ischemic encephalopathy during therapeutic hypothermia. *J. Pediatr.* 165, 1129–1134. doi: 10.1016/j.jpeds.2014.07.022

Wyatt, J. S., Edwards, A. D., Azzopardi, D., and Reynolds, E. O. (1989). Magnetic resonance and near infrared spectroscopy for investigation of perinatal hypoxic-ischaemic brain injury. *Arch. Dis. Child.* 64, 953–963.

Xia, P., Pan, Y., Zhang, F., Wang, N., Wang, E., Guo, Q., et al. (2018). Pioglitazone confers neuroprotection against ischemia-induced pyroptosis due to its inhibitory effects on HMGB-1/RAGE and Rac1/ROS pathway by activating PPAR-?. *CPB* 45, 2351–2368. doi: 10.1159/000488183

Xu, W., Yang, Y., Yuan, G., Zhu, W., Ma, D., and Hu, S. (2015). Exendin-4, a glucagon-like peptide-1 receptor agonist, reduces Alzheimer disease-associated tau hyperphosphorylation in the hippocampus of rats with type 2 diabetes. *J. Investig. Med.* 63, 267–272. doi: 10.1097/JIM.0000000000000129

Yakovleva, A. A., Zolotov, N. N., Sokolov, O. Y., Kost, N. V., Kolyasnikova, K. N., and Micheeva, I. G. (2015). Dipeptidylpeptidase 4 (DPP4, CD26) activity in the blood serum of term and preterm neonates with cerebral ischemia. *Neuropeptides* 52, 113–117. doi: 10.1016/j.npep.2015.05.001

Yang, D., Nakajo, Y., Iihara, K., Kataoka, H., and Yanamoto, H. (2013). Alogliptin, a dipeptidylpeptidase-4 inhibitor, for patients with diabetes mellitus type 2, induces tolerance to focal cerebral ischemia in non-diabetic, normal mice. *Brain Res.* 1517, 104–113. doi: 10.1016/j.brainres.2013.04.015

Yang, X., Feng, P., Zhang, X., Li, D., Wang, R., Ji, C., et al. (2019). The diabetes drug semaglutide reduces infarct size, inflammation, and apoptosis, and normalizes neurogenesis in a rat model of stroke. *Neuropharmacology* 158:107748. doi: 10.1016/j.neuropharm.2019.107748

Yimer, E. M., Surur, A., Wondafrash, D. Z., and Gebre, A. K. (2019). The effect of metformin in experimentally induced animal models of epileptic seizure. *Behav. Neurol.* 2019:6234758. doi: 10.1155/2019/6234758

Yun, C., and Xuefeng, W. (2013). Association between seizures and diabetes mellitus: a comprehensive review of literature. *Curr. Diab. Rev.* 9, 350–354. doi: 10.2174/15733998113099990060

Yun, S. P., Kam, T.-I., Panicker, N., Kim, S., Oh, Y., Park, J.-S., et al. (2018). Block of A1 astrocyte conversion by microglia is neuroprotective in models of Parkinson's disease. *Nat. Med.* 24, 931–938. doi: 10.1038/s41591-018-0051-5

Zeng, S., Bai, J., Jiang, H., Zhu, J., Fu, C., He, M., et al. (2020). Treatment with liraglutide exerts neuroprotection after hypoxic–ischemic brain injury in neonatal rats via the PI3K/AKT/GSK3β pathway. *Front. Cell. Neurosci.* 13:585. doi: 10.3389/fncel.2019.00585

Zhang, H., Liu, Y., Guan, S., Qu, D., Wang, L., Wang, X., et al. (2016). An orally active allosteric GLP-1 receptor agonist is neuroprotective in cellular and rodent models of stroke. *PLoS One* 11:e0148827. doi: 10.1371/journal.pone.0148827

Zhang, H.-L., Xu, M., Wei, C., Qin, A.-P., Liu, C.-F., Hong, L.-Z., et al. (2011). Neuroprotective effects of pioglitazone in a rat model of permanent focal cerebral ischemia are associated with peroxisome proliferator-activated receptor gamma-mediated suppression of nuclear factor-κB signaling pathway. *Neuroscience* 176, 381–395. doi: 10.1016/j.neuroscience.2010.12.029

Zhao, Y., Li, H., Fang, F., Qin, T., Xiao, W., Wang, Z., et al. (2018). Geniposide improves repeated restraint stress-induced depression-like behavior in mice by ameliorating neuronal apoptosis via regulating GLP-1R/AKT signaling pathway. *Neurosci. Lett.* 676, 19–26. doi: 10.1016/j.neulet.2018.04.010

Zhou, Y., Fathali, N., Lekic, T., Tang, J., and Zhang, J. H. (2009). Glibenclamide improves neurological function in neonatal hypoxia-ischemia in rats. *Brain Res.* 1270, 131–139. doi: 10.1016/j.brainres.2009.03.010

Zhu, H., Zhang, Y., Shi, Z., Lu, D., Li, T., Ding, Y., et al. (2016). The neuroprotection of liraglutide against ischaemia-induced apoptosis through the activation of the PI3K/AKT and MAPK pathways. *Sci. Rep.* 6:26859. doi: 10.1038/srep26859

Conflict of Interest: The authors declare that the research was conducted in the absence of any commercial or financial relationships that could be construed as a potential conflict of interest.

frontiers in Neurology

ORIGINAL RESEARCH
published: 08 May 2020
doi: 10.3389/fneur.2020.00361

Effectiveness and Safety of a Clonidine Adhesive Patch for Children With Tic Disorders: Study in a Real-World Practice

Chunsong Yang[1,2†], BingYao Kang[3†], Dan Yu[4], Li Zhao[2] and Lingli Zhang[1*]*

[1] Department of Pharmacy, Evidence-Based Pharmacy Center, West China Second Hospital, Sichuan University, Key Laboratory of Birth Defects and Related Diseases of Women and Children (Sichuan University), Ministry of Education, Chengdu, China, [2] Department of Health Policy and Management, West China School of Public Health, and West China Fourth Hospital, Sichuan University, Chengdu, China, [3] Department of Pediatric Clinic, West China Second Hospital, Sichuan University, Chengdu, China, [4] Department of Children's Genetic Endocrinology and Metabolism, West China Second Hospital, Sichuan University, Key Laboratory of Birth Defects and Related Diseases of Women and Children (Sichuan University), Ministry of Education, Chengdu, China

OPEN ACCESS

Edited by:
Changlian Zhu,
Third Affiliated Hospital of Zhengzhou University, China

Reviewed by:
Giovanni Messina,
University of Foggia, Italy
Emily Ricketts,
University of California, Los Angeles, United States

***Correspondence:**
Li Zhao
zhaoli@scu.edu.cn
Lingli Zhang
zhlingli@sina.com

[†]These authors have contributed equally to this work

Specialty section:
This article was submitted to Pediatric Neurology, a section of the journal Frontiers in Neurology

Received: *07 November 2019*
Accepted: *14 April 2020*
Published: *08 May 2020*

Citation:
Yang C, Kang B, Yu D, Zhao L and Zhang L (2020) Effectiveness and Safety of a Clonidine Adhesive Patch for Children With Tic Disorders: Study in a Real-World Practice. Front. Neurol. 11:361. doi: 10.3389/fneur.2020.00361

Background: Real-world evidence includes data from retrospective/prospective observational studies and observational registries, and provides insights beyond those addressed by randomized controlled trials. This study aimed to evaluate the effectiveness and safety of a clonidine adhesive patch (CAP) for children with tic disorder (TD) in a real-world setting (RWS).

Methods: This was an open-label, non-interventional, post-marketing, observational study in a RWS. Children diagnosed with TDs were enrolled from a pediatric neurology clinic in China, and the change in tic symptom severity following 6 weeks pharmacologic treatments was investigated using Yale Global Tic Severity Scale (YGTSS) during visits at weeks 0, 4, 8, and 12.

Results: Of 150 patients, 76% (114/150) were male (age range, 3.03–14.24 years; mean, 8.11 ± 2.48 years). Patients were divided into three groups: tiapride ($n = 94$), CAP ($n = 14$), and CAP + tiapride ($n = 42$). The mean YGTSS improved 11.02, 15.14, 11.13 points from baseline to posttreatment for tiapride, CAP, and CAP + tiapride, respectively, but variance analysis showed there was no significant difference in YGTSS related to different pharmacologic intervention during subsequent visits at weeks 4, 8, and 12. Repeated measure analysis showed there was no significant difference between different medication types for reducing the YGTSS score ($F = 0.553$, $P = 0.576$). No serious adverse events (AEs) occurred, and there was no significant difference in the prevalence of AEs between the three groups.

Conclusion: The CAP is effective and safe for TD management in a RWS, because of the limitation of sample size and the period of follow up, observational studies with longer-term outcomes, and larger sample size are needed.

Keywords: effectiveness, safety, clonidine adhesive patch, tic disorders, real-world study

INTRODUCTION

Tic disorders (TDs) have been conceptualized as hyperkinetic-movement disorders and chronic neuropsychiatric disorder with childhood onset. TDs are characterized by multiple motor and one or more phonic tics; males are three-times more likely to suffer from TDs than females (1, 2). There are three types of TDs: transient tic disorder (TTD), chronic tic disorder (CTD), and Tourette syndrome (TS). One meta-analysis showed the worldwide prevalence of TTD to be 2.99%, followed by CTD (1.61%), and TS (0.77%) (3). In China, the combined prevalence of TDs has been reported to be 6.1%. One meta-analysis stated the prevalence of TTD, CTD, and TS in China to be 1.7, 1.2, and 0.3%, respectively (4). Despite the core symptom being tics, co-occurring psychiatric disorders are common in children suffering from TDs, such as attention deficit and hyperactivity disorder (ADHD), obsessive-compulsive disorder (OCD), and anxiety disorder (5–7).

Pharmacologic treatment is the main therapy for the management of tics and comorbidities (8, 9). Several randomized controlled trials (RCTs) have shown that clonidine can reduce some of the tics and other behavioral symptoms associated with TDs, and that clonidine is safe to use (10–12). In 2016, a systematic review by Wang and colleagues encompassing six RCTs (1,145 participants) evaluated the effectiveness of a clonidine adhesive patch (CAP) for TD treatment (13). They showed that the CAP may be as effective as haloperidol or tiapride for TDs, and that the prevalence of adverse events (AEs) of the CAP was low. Nevertheless, additional studies are needed urgently to reevaluate the effectiveness and safety of the CAP.

RCTs are undertaken according to regulatory and scientific standards, so extrapolation of research results is limited. Hence, RCTs may not necessarily reflect what happens in real-world settings (14). Real-world evidence helps to improve decision-making in healthcare settings. Hence, this study aimed to evaluate the effectiveness and safety of CAP for children with tic disorder (TD) in a real-world setting (RWS).

MATERIALS AND METHODS

Study Design

This was an open-label, non-interventional, post-marketing, observational study to investigate the change in severity of tic symptoms in TD patients following different pharmacologic treatments in a real-world practice. The study was conducted from January to May 2019. The non-interventional, post-marketing nature of our study meant that registration in a clinical trial registry was not mandatory. Nevertheless, the study protocol was approved by the Office of Research Ethics Committees of West China Second Hospital (Chengdu, China).

Inclusion Criteria

The inclusion criteria were: (i) a clinically confirmed diagnosis of TD according to the *Diagnostic and Statistical Manual of Mental Disorders-IV-Text Revision*; (ii) age <18 years; (iii) provision of written informed consent.

Exclusion Criteria

The exclusion criteria were: (i) delays or problems with mental development (Wechsler intelligence-quotient score <70 points); (ii) cerebral palsy, neurodevelopmental delay, history of inherited metabolism, or poor development of motor language; (iii) non-provision of written informed consent. Voluntary written informed consent was provided by all caregivers or children aged >8 years.

Treatment

Assignment of patients to pharmacologic therapy was decided according to standard practice and medical indications assessed by the treating physician. Eligible patients were prescribed a drug dose by their treating physician depending on its effectiveness and toxicity and patient weight. This dosing regimen conformed to standard medical practices and the terms of local marketing authorization and reimbursement guidelines.

For CAPs, patients of weight 20–40 kg were given 1.0 mg/film; 40–60 kg were given 1.5 mg/film; >60 kg were given 2.0 mg/film. For tiapride, each child was started on 50 mg/day and the dose increased gradually to a maximum of 400 mg/day. The stable dose of medication was maintained for 6 weeks.

Assessments

Baseline data (age, sex, disorder duration, type of TD) were obtained by the treating physician, followed by assessments during subsequent visits at weeks 0, 4, 8, and 12. The primary outcome was measured by the Yale Global Tic Severity Scale (YGTSS). This consists of a separate rating of severity for motor and vocal tics along five discriminant dimensions (number, frequency, intensity, complexity, and interference) on a scale of 0–5 for each. Summation of these scores (i.e., 0–50) results in a total tic score (TTS). The tic impairment score (TIS), from zero to a maximum of 50 points, is based on the impact of the tic disorder on self-esteem, family life, social acceptance, and school performance. The TIS is added to the TTS to obtain the total YGTSS (YGTSS-T) score. The secondary outcome was AEs, which were assessed via an interview of self-report by participants or their caregivers during the follow-up. The study flow of screening the participants was shown in **Figure 1**.

Statistical Analyses

The intent-to-treat population (which comprised all patients who received the study drug and who had a baseline visit and at least one on-treatment post-baseline visit) was used to assess all effectiveness and safety variables. For the comparability of baseline variables with continuous variables, they are shown as the mean ± standard deviation. If data followed a normal distribution, one-way ANOVA was used. If data did not follow a normal distribution, they were analyzed by the Wilcoxon rank sum test. Categorical variables are shown as frequencies and percentages, and the chi-square test or Fisher's exact test were used as appropriate.

Repeated measure analysis of variance was used to test the difference of treatment effects for different drugs. First, we used the Mauchly sphericity test to ascertain if the measured

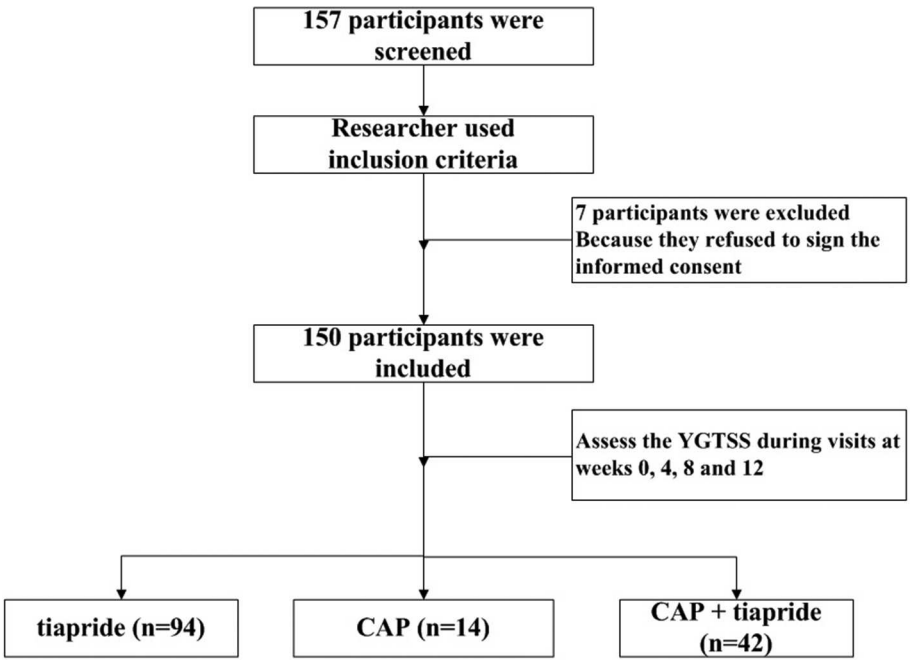

FIGURE 1 | The study flow of screening the participants.

data satisfied the test hypothesis. If not, the Greenhouse–Geisser correction was carried out. $P \leq 0.05$ was considered significant. We used SPSS v22 (IBM, Armonk, NY, USA) for statistical analyses.

RESULTS

Characteristics of Patients (Table 1)

Children diagnosed with TDs were enrolled from a pediatric neurology clinic at West China Second Hospital. Initially, 157 patients were recruited. Seven patients discontinued treatment because they refused to sign the informed consent, so 150 patients completed the study. Among these 150 children, 76% (114/150) were male, and ranged in age from 3.03 years to 14.24 (mean, 8.11 $\pm$ 2.48) years. These patients were divided into three intervention groups: tiapride ($n = 94$), CAP ($n = 14$), and CAP + tiapride ($n = 42$).

There was no significant difference between the three groups in terms of sex, disorder duration, type of TD, or baseline YGTSS score, but there was a significant difference in age, so we included age as a covariate in the statistical model for analyses.

Effectiveness of Different Pharmacologic Interventions

The YGTSS score was reduced at different times after pharmacologic intervention. For tiapride, the mean YGTSS improved 11.02 points from baseline to posttreatment (24.8 vs. 13.78). For CAP, the mean YGTSS improved 15.14 points from baseline to posttreatment (28.0 vs. 12.86). For CAP + tiapride, the mean YGTSS improved 11.13 points from baseline to posttreatment (27.64 vs. 16.31), but variance analysis showed there was no significant difference in YGTSS related to different pharmacologic intervention during subsequent visits at weeks 4, 8, and 12 (**Table 2**).

Repeated measure analysis also showed a significant difference for the YGTSS score for different medications at different follow-up times ($F = 18.949$, $P = 0.000$), but we found no interaction between the medication time and medication type ($F = 1.043$, $P = 0.389$) or between the medication time and age ($F = 2.384$, $P = 0.069$). A test of within-participant effects showed no significant difference between different medication types for reducing the YGTSS score ($F = 0.553$, $P = 0.576$).

Safety

We found that 10.6% (10/94) of patients reported AEs in the tiapride group (**Table 3**); the most common AEs were dizziness and abdominal pain. Also, 7.1% (1/14) of patients reported AEs in the CAP group; the most common AEs were rash. In addition, 23.1% (10/42) of patients reported AEs in the CAP + tiapride group; the most common AEs were dizziness, abdominal pain, and drowsiness. The chi-square test showed no significant difference in the prevalence of AEs between the three groups.

DISCUSSION

We used an observational study design to investigate the effectiveness and safety of different pharmacologic treatments in a real-world practice. We compared three pharmacologic interventions (tiapride, CAP, tiapride+ CAP) in 150 patients with TDs. We observed no significant difference between the

TABLE 1 | Demographics and baseline patient characteristic.

Group		Tiapride ($n = 94$)	Clonidine ($n = 14$)	Clonidine + tiapride ($n = 42$)	χ^2/F	*P*
Age		7.958 ± 2.499	6.965 ± 2.341	8.822 ± 2.338	3.507	0.033
Gender	Male	67	13	34	4.483	0.106
	Female	27	1	8		
Time of disorder (year)		1.555 ± 1.451	1.001 ± 1.138	1.750 ± 1.613	1.358	0.260
Type of TDs	TTD	36	9	15	3.969	0.410
	CTD	35	3	15		
	TS	23	2	12		
YGTSS score	Total scores	24.800 ± 7.003	28.00 ± 13.801	27.64 ± 10.727	1.898	0.154
	Motor tic	10.320 ± 3.303	10.640 ± 3.875	10.500 ± 3.624	0.078	0.925
	Vocal tic	3.970 ± 4.723	4.500 ± 5.095	5.480 ± 5.260	1.369	0.258
	Tic impairment score	10.530 ± 4.242	12.860 ± 8.254	11.670 ± 5.372	1.706	0.185

TABLE 2 | YGTSS scores for different treatment times in three groups.

	Baseline	4 weeks	8 weeks	12 weeks
Tiapride	24.800 ± 7.003	21.050 ± 9.141	18.300 ± 9.562	13.780 ± 11.577
Clonidine	28.00 ± 13.801	17.860 ± 10.037	16.360 ± 12.768	12.860 ± 12.805
Clonidine + tiapride	27.64 ± 10.727	23.140 ± 12.233	20.710 ± 13.349	16.310 ± 14.338
F	1.89	1.517	1.071	0.712
P	0.154	0.223	0.345	0.492

TABLE 3 | Reported side effects during follow up period.

	Tiapride	Clonidine	Clonidine + tiapride
Dizzy	3	0	4
Abdominal pain	2	0	2
Drowsiness	1	0	2
Insomnia	1	0	0
Nausea/vomit	1	0	0
Loss of appetite	1	0	0
Rash	1	1	0
Mental distress	0	0	2
Total	10	1	10

medication groups in terms of reducing the YGTSS score after 8 weeks of treatment. In general, tiapride and the CAP were well-tolerated, and elicited few AEs.

Clonidine use is strongly recommended in Canadian guidelines, and it is regarded as first-line treatment in Chinese clinical guidelines, for TDs (15, 16). However, European guidelines recommend clonidine as second-line treatment for TDs (antipsychotic agents are first-line treatment) (17). Clonidine is seldom chosen to treat TDs in Japan (but clonidine is the only α2 adrenergic receptor agonist used to treat hypertension in Japan) (18). North American guidelines recommend α2 adrenergic agonists for the treatment of tics if the benefits of treatment outweigh the risks (with evidence level B), but physicians should monitor common side effects, such as sedation, heart rate, and blood pressure (level-A evidence) (19). Hence, the safety of the medication is an important concern for long-term treatment of TDs. We did not find serious AEs in TD treatment in a real-world practice during a short follow-up period, but common side effects must be monitored.

No clinical guidelines have mentioned CAP use, and there may be two reasons for this. First, formulations applied as an adhesive patch are not used widely. Nevertheless, a CAP releases clonidine at a relatively invariable rate for 1 week without trough or peak changes in plasma concentrations, so it is a very convenient treatment. Second, adhesive patches are relatively expensive, but the convenience of treatment may improve the quality of life of patients with TDs. Hence, cost–benefit analyses should be carried out. Therefore, future research should be considered from these two perspectives.

Our findings are similar to the study conducted by Joo and Kim (20), they assessed the effectiveness and safety of clonidine extended release (ER) treatment in Korean youth with ADHD and/or TS and included 29 children treated with clonidine ER, the result showed significant decreases in the CGI-S scores for both ADHD and tic symptoms were noted over 12 weeks, and life-threatening adverse effects were not observed.

Our study had three main limitations. First, included patients were from a single center, so a selection bias was evident. Nevertheless, the West China Second Hospital is the largest hospital in western China, so the research results carry a certain representativeness. Second, the observational, non-interventional design of our study may have introduced some bias toward overestimation of the treatment effect.

Nevertheless, our study provides important insights into the real-world management of TDs. Finally, an observational study may underestimate AEs because adverse events were only assessed via an interview of self-report by participants or their caregivers, sometimes they may ignore reporting adverse reactions. Further studies are needed to overcome the shortcomings mentioned above.

CONCLUSIONS

The CAP is effective and safe for TD management in a RWS, because of the limitation of sample size and the period of follow up, observational studies with longer-term outcomes and larger sample size are needed.

DATA AVAILABILITY STATEMENT

The raw data supporting the conclusions of this article will be made available by the authors, without undue reservation, to any qualified researcher.

ETHICS STATEMENT

The studies involving human participants were reviewed and approved by the Office of Research Ethics Committees of West China Second Hospital. Written informed consent to participate in this study was provided by the participants' legal guardian/next of kin. Written informed consent was obtained from the individual(s), and minor(s)' legal guardian/next of kin, for the publication of any potentially identifiable images or data included in this article.

AUTHOR CONTRIBUTIONS

CY designed the review, collected data, carried out analysis and interpretation of the data, and wrote the review. BK and DY designed the review, collected data, checked the data, and wrote the review. LZhao and LZhan designed the review, commented on drafts for previous version.

FUNDING

This study was funded by Sichuan Health and Wellness Committee: Evidence-based construction of clinical drug route for children with tic disorder (18PJ528). The sponsor had no role in the study design, writing of the manuscript, or decision to submit this or future manuscripts for publication.

ACKNOWLEDGMENTS

We also thank Rachel James, Ph.D. from Liwen Bianji, Edanz Group China (www.liwenbianji.cn/ac), for editing the English text of a draft of this manuscript.

REFERENCES

1. Sanger TD, Chen D, Fehlings DL, Hallett M, Lang AE, Mink JW, et al. Definition and classification of hyperkinetic movements in childhood. *Mov Disord.* (2010) 25:1538–49. doi: 10.1002/mds.23088
2. Robertson MM. The gilles de la tourette syndrome: the current status. *Arch Dis Child.* (2012) 97:166–75. doi: 10.1136/archdischild-2011-300585
3. Knight T, Steeves T, Day L, Lowerison M, Jette N, Pringsheim T. Prevalence of tic disorders: a systematic review and meta-analysis. *Pediatr Neurol.* (2012) 47:77–90. doi: 10.1016/j.pediatrneurol.2012.05.002
4. Yang C, Zhang L, Zhu P, Zhu C, Guo Q. The prevalence of tic disorders for children in China:a systematic review and meta-analysis. *Medicine.* (2016) 95:e4354. doi: 10.1097/MD.0000000000004354
5. Yang C, Cheng X, Zhang Q, Yu D, Li J, Zhang L. Interventions for tic disorders: an updated overview of systematic reviews and meta analyses. *Psychiatry Res.* (2020) 287:112905. doi: 10.1016/j.psychres.2020.112905
6. Robertson MM. A personal 35 year perspective on gilles de la tourette syndrome: assessment, investigations, and management. *Lancet Psychiatry.* (2015) 2:88–104. doi: 10.1016/S2215-0366(14)00133-3
7. Freeman RD, Fast DK, Burd L, Kerbeshian J, Robertson MM, Sandor P. An international perspective on Tourette syndrome: selected findings from 3,500 individuals in 22 countries. *Dev Med Child Neurol.* (2000) 42:436–47. doi: 10.1017/S0012162200000839
8. Ganos C, Martino D, Pringsheim T. Tics in the pediatric population: pragmatic management. *Mov Disord Clin Pract.* (2017) 4:160–72. doi: 10.1002/mdc3.12428
9. Hollis C, Pennant M, Cuenca J, Glazebrook C, Kendall T, Whittington C, et al. Clinical effectiveness and patient perspectives of different treatment strategies for tics in children and adolescents with Tourette syndrome: a systematic review and qualitative analysis. *Health Technol Assess.* (2016) 20:1–450. doi: 10.3310/hta20040
10. Goetz CG, Tanner CM, Wilson RS, Carroll VS, Como PG, Shannon KM. Clonidine and Gilles de la Tourette's syndrome: double-blind study using objective rating methods. *Ann Neurol.* (1987) 21:307–10. doi: 10.1002/ana.410210313
11. Leckman JF, Hardin MT, Riddle MA, Stevenson J, Ort SI, Cohen DJ. Clonidine treatment of Gilles de la Tourette's syndrome. *Arch Gen Psychiatry.* (1991) 48:324–8. doi: 10.1001/archpsyc.1991.01810280040006
12. Du YS, Li HF, Vance A, Zhong YQ, Jiao FY, Wang HM, et al. Randomized double-blind multicentre placebo-controlled clinical trial of the clonidine adhesive patch for the treatment of tic disorders. *Aust N Z J Psychiatry.* (2008) 42:807–13. doi: 10.1080/00048670802277222
13. Wang S, Wei YZ, Yang J, Zhou Y, Zheng Y. Clonidine adhesive patch for the treatment of tic disorders: a systematic review meta-analysis. *Eur J Paediatr Neurol.* (2017) 21:614–20. doi: 10.1016/j.ejpn.2017.03.003
14. Schwartz D, Lellouch J. Explanatory and pragmatic attitudes in therapeutic trials. *J Clin Epidemiol.* (2009) 62:499–505. doi: 10.1016/j.jclinepi.2009.01.012
15. Pringsheim T, Doja A, Gorman D, McKinlay D, Day L, Billinghurst L, et al. Canadian guidelines for the evidence-based treatment of tic disorders: pharmacotherapy. *Can J Psychiatry.* (2012) 57:133–43. doi: 10.1177/070674371205700302
16. The Branch of Neurology of Chinese Medical Association. The guideline of the diagnosis and treatment for tic disorders in children. *J Clin J Appl Clin Pediatr.* (2017) 32:1137–40. doi: 10.3760/cma.j.issn.2095-428X
17. Roessner V, Plessen KJ, Rothenberger A, Ludolph AG, Rizzo R, Skov L, et al. European clinical guidelines for Tourette syndrome and other tic disorders. part II: pharmacological treatment. *Eur Child Adolesc Psychiatry.* (2011) 20:173–96. doi: 10.1007/s00787-011-0163-7

18. Hamamoto Y, Fujio M, Nonaka M, Matsuda N, Kono T, Kano Y. Expert consensus on pharmacotherapy for tic disorders in Japan. *Brain Dev*. (2019) 41:501–6. doi: 10.1016/j.braindev.2019.02.003
19. Pringsheim T, Okun MS, Müller-Vahl K, Martino D, Jankovic J, Cavanna AE, et al. Practice guideline recommendations summary: treatment of tics in people with Tourette syndrome and chronic tic disorders. *Neurology*. (2019) 92:896–906. doi: 10.1212/WNL.0000000000007466
20. Joo SW, Kim HW. Treatment of children and adolescents with attention deficit hyperactivity disorder and/or tourette's disorder with clonidine extended release. *Psychiatry Investig*. (2018) 15:90–3. doi: 10.4306/pi.2018.15.1.90

Conflict of Interest: The authors declare that the research was conducted in the absence of any commercial or financial relationships that could be construed as a potential conflict of interest.

frontiers in Pediatrics

REVIEW
published: 15 May 2020
doi: 10.3389/fped.2020.00239

Management of Multi Organ Dysfunction in Neonatal Encephalopathy

Mary O'Dea[1,2,3,4], *Deirdre Sweetman*[4,5], *Sonia Lomeli Bonifacio*[6], *Mohamed El-Dib*[7], *Topun Austin*[8] *and Eleanor J. Molloy*[1,2,3,4,5,9,10]*

[1] Discipline of Paediatrics, Trinity College, The University of Dublin, Dublin, Ireland, [2] Paediatric Research Laboratory, Trinity Translational Institute, St. James' Hospital, Dublin, Ireland, [3] Neonatology, Coombe Women and Infant's University Hospital, Dublin, Ireland, [4] National Children's Research Centre, Dublin, Ireland, [5] Paediatrics, National Maternity Hospital, Dublin, Ireland, [6] Department of Pediatrics, Stanford University School of Medicine, Stanford, CA, United States, [7] Brigham and Women's Hospital, Harvard Medical School, Boston, MA, United States, [8] Neonatal Intensive Care Unit, Cambridge University Hospitals NHS Foundation Trust, Cambridge, United Kingdom, [9] Neonatology, Children's Hospital Ireland (CHI) at Crumlin, Dublin, Ireland, [10] Paediatrics, CHI at Tallaght, Tallaght University Hospital, Dublin, Ireland

Neonatal Encephalopathy (NE) describes neonates with disturbed neurological function in the first post-natal days of life. NE is an overall term that does not specify the etiology of the encephalopathy although it often involves hypoxia-ischaemia. In NE, although neurological dysfunction is part of the injury and is most predictive of long-term outcome, these infants may also have multiorgan injury and compromise, which further contribute to neurological impairment and long-term morbidities. Therapeutic hypothermia (TH) is the standard of care for moderate to severe NE. Infants with NE may have co-existing immune, respiratory, endocrine, renal, hepatic, and cardiac dysfunction that require individualized management and can be impacted by TH. Non-neurological organ dysfunction not only has a negative effect on long term outcome but may also influence the efficacy of treatments in the acute phase. Post resuscitative care involves stabilization and decisions regarding TH and management of multi-organ dysfunction. This management includes detailed neurological assessment, cardio-respiratory stabilization, glycaemic and fluid control, sepsis evaluation and antibiotics, seizure identification, and monitoring and responding to biochemical and coagulation derangements. The emergence of new biomarkers of specific organ injury may have predictive value and improve the definition of organ injury and prognosis. Further evidence-based research is needed to optimize management of NE, prevent further organ dysfunction and reduce neurodevelopmental impairment.

Keywords: Neonatal Encephalopathy, Therapeutic hypothermia, brain injury, multi-organ dysfunction, neurodevelopmental outcome

OPEN ACCESS

Edited by:
Claire Thornton,
Royal Veterinary College (RVC),
United Kingdom

Reviewed by:
Jonathan Michael Davis,
Tufts University, United States
Tomoki Arichi,
King's College London,
United Kingdom

***Correspondence:**
Eleanor J. Molloy
Eleanor.molloy@tcd.ie

Specialty section:
This article was submitted to Neonatology, a section of the journal Frontiers in Pediatrics

Received: *17 August 2019*
Accepted: *20 April 2020*
Published: *15 May 2020*

Citation:
O'Dea M, Sweetman D, Bonifacio SL, El-Dib M, Austin T and Molloy EJ (2020) Management of Multi Organ Dysfunction in Neonatal Encephalopathy. Front. Pediatr. 8:239. doi: 10.3389/fped.2020.00239

INTRODUCTION

Neonatal encephalopathy (NE), is a clinically defined syndrome of disturbed neurologic function in the earliest post-natal days of life in an infant born at or beyond 35 weeks of gestation, manifested by a subnormal level of consciousness or seizures, and often accompanied by difficulty with initiating and maintaining respiration and depression of tone and reflexes (1). In up to 50% of cases of NE the exact underlying cause is unknown and is commonly a combination of factors (2). The terms

NE and hypoxic-ischaemic encephalopathy (HIE) are used interchangeably in the literature but as NE is all-encompassing and does not specify etiology, it is the term used in this review (3–5).

The neonatal period is the highest risk for brain injury during the lifespan. In 2010, the estimated global burden of NE was 1.15 million, with 96% of these infants being born in low and middle income countries (6). The global estimated incidence from a systematic review in 2010 is 8.5 per 1,000 live births, with an estimated incidence of 1–3 per 1,000 births in high income countries.

Therapeutic hypothermia (TH) is known to be neuroprotective by addressing the cascade of injurious events that follow a hypoxic-ischemic insult in NE. Randomized controlled trials demonstrated the safety and the efficacy of TH by demonstrating a reduction in death and major neuro-disability for infants with moderate to severe NE when their clinical history, laboratory criteria, and neurological exam meets agreed standardized criteria. Despite TH, the incidence of death or moderate/severe disability remains high at 48% (7). A systematic review including seven randomized controlled trials (RCT) with 1,214 neonates with NE undergoing TH concluded an overall mortality of 28%, with a range of 24–38% (7), with the following incidences of neurological impairment; cognitive impairment 24%, cerebral palsy 22%, epilepsy 19%, and cortical visual impairment 6%.

These high morbidity and mortality rates suggest that there is a need to improve outcomes by further optimizing TH candidate selection, improving timeliness of treatment initiation, increasing the use of brain monitoring for the identification and treatment of seizures, improving multi-organ management during TH, and identifying biomarkers to offer individualized adjunctive therapies during TH. There is no single gold standard diagnostic test to determine etiology, severity, or prognosis at present (8, 9).

Neurological dysfunction is only part of the spectrum of injury in NE following hypoxic ischemic insult, infants can have co-existing multi-organ dysfunction which contributes to subsequent morbidities and mortality. The pathophysiology underlying the brain injury in NE affects the immune, respiratory, endocrine, renal, hepatic, and cardiac functioning (10, 11). In addition, exposing these infants to TH has its own impact on multi-organ function. Optimisation of multi-organ monitoring and support during TH has the potential to prevent injury progression and enhance the neuroprotective effects of TH.

THERAPEUTIC HYPOTHERMIA

TH is the standard of care for moderate and severe NE. Major randomized clinical trials (RCT) have demonstrated a reduction in death and disability with TH (12). A Cochrane meta-analysis of these trials concluded that in infants over 35 weeks and <6 h of age with moderate or severe NE ($n = 638$), TH to 33.5–34.5°C for 72 h, reduced the mortality and disability at 18 months of age with a typical risk ratio (RR) of 0.75 with a number needed to treat (NNT) of 7 (12). The National Institute of Child Health and Human Development (NICHD) and Committee of the Fetus and Newborn of the American Academy of Pediatrics (AAP) subsequently published a framework to ensure the appropriate use of TH (13), and recommended that infants should meet inclusion criteria outlined in clinical trials as follows: gestational age >36 weeks; age <6 h; pH of ≤ 7.0 or a base deficit of ≥ 16 mmol/L in of umbilical cord blood or blood obtained during the first hour after birth; history of an acute perinatal event; 10 min Apgar score of <5 or assisted ventilation at birth and for 10+ min; neurologic examination demonstrating moderate to severe encephalopathy.

Evidence from animal studies suggest that earlier TH initiation increases neuroprotection (14). The Neonatal Resuscitation Programme (NRP) notes however that there is a paucity of evidence regarding commencement of hypothermia during resuscitation, as passive hypothermia without core temperature monitoring during resuscitation may result in overcooling with serious adverse effects (15). Thoresen et al., showed significantly improved motor development scores at 18 months when TH is initiated <3 h ($n = 35$) compared to >3 h of age ($n = 30$) (16). This suggests that once indicated, TH should be initiated immediately after resuscitation.

Two further RCT examined modifications from the original TH protocols. Laptook et al. (17) examined late initiation of TH in NE at between 6 and 24 h of age. The trial was a multicentre RCT ($n = 164$) comparing late initiation of TH with normothermia. Although there was no statistically significant difference in death and disability between groups, the authors used a pre-specified Bayesian analysis to demonstrate that there was an increased probability of reduction in death or disability with minimal adverse events in the TH group. Shankaran et al. (18) examined TH to a lower temperature of 32°C and/or for a longer duration of 120 h in a multi-center RCT. The trial was stopped at 50% ($n = 364$) of the planned recruitment due to a number of adverse events including anuria, arrhythmia, increased inhaled nitric oxide requirement and extra corporeal membrane oxygenation (ECMO) use, more days of oxygen and a higher incidence of bradycardia as well as trend toward increased mortality. There was no difference between treatment groups in the primary outcome of death or neuro-disability at 18–22 months of age.

The initial TH protocols included infants with moderate to severe NE. Despite recommendations from organizations like the AAP, there is evidence of therapeutic drift with TH being provided to neonates with mild NE. A national survey in the UK reported that 75% of centers offered TH to infants with mild NE (19). The Prospective Research on Infants with Mild Encephalopathy (PRIME) Study found that 52% of infants with mild NE had an abnormal early aEEG or seizures, abnormal brain MRI, or neurological exam at discharge (20). At follow up at a mean of 19 months, 16% of infants had a disability and 40% had Bayley III scores <85 (21). Murray et al. noted that children with mild NE, not treated with TH, had cognitive outcomes similar to that of children with moderate NE, who were treated with TH (22). A systematic review examining outcome of infants with mild NE found that 25% ($n = 341$) had abnormal neurodevelopment outcome (23). There is an ongoing phase two

RCT by Thayyil et al., Optimizing the duration of Cooling in Mild NE (COMET Study; NCT03409770), examining the feasibility and duration of TH in mild NE in the UK. Interpretation of research and smaller cohort studies of neonates with mild NE is limited by a lack of consistent definition of mild NE across study groups. Although a beneficial effect of TH in this population is plausible, to date this benefit has not been demonstrated in an RCT (24).

NEUROLOGICAL ASSESSMENT AND MONITORING

Neurological Assessment

A detailed neurological assessment is required to diagnose NE and ideally before the administration of sedating medications that may alter the neurological examination. The Modified Sarnat Examination (25) is used in the evaluation of neurological status for initiation of TH. This was used as entry criteria in the main TH RCTs (26) apart from the Total Body Hypothermia (TOBY) trial and the Cool Cap Study, both of which included amplitude integrated electroencephalogram (aEEG) as an entry criterion (27). The Sarnat Score assesses three stages of NE: mild (NE I), moderate (NE II), and severe (NE III) which were correlated with clinical outcome. The score is derived from a study of 21 infants with NE graded according to their level of encephalopathy and EEG findings over the first post-natal week of life. Sarnat et al. concluded that persistence of moderate encephalopathy for more than 7 post-natal days was associated with poor neurologic outcome or death (25). A systematic review of newborn assessment to predict neurological outcome including 12 studies concluded that the risk of neonatal death was 24-fold higher in Sarnat III than Sarnat II, and 171 times higher in Sarnat III than Sarnat I (28).

The Amiel-Tison Neurologic Assessment at Term (ATNAT) (29) was developed to provide a framework for observing the development of cortical control in infants at term and has been shown to predict the occurrence of cerebral palsy after birth asphyxia. Amess et al. examined term infants postnatally ($n = 28$) with NE with the ATNAT at 8 h and at 7 days. Both early and late neurological examinations were reliable indicators of a favorable outcome at 1 year, having negative predictive values of 100 and 91%, respectively (30). Murray et al., used the ATNAT serially over the first 3 days of post-natal life in 57 infants with NE, and found a significant correlation between ATNAT and neurological outcome at 2 years (31). A normal early assessment predicted a normal outcome, and a persistent neurological abnormality on day of life 3 was associated with neuro-disability. The risk was 100% in those with a severely abnormal ATNAT, and 41% in those with a moderately abnormal assessment.

The Thompson score is a clinical tool assessing central nervous system dysfunction in NE, based on the longitudinal clinical assessment of 9 signs, including tone, level of consciousness, seizures, posture, Moro, grasp, suck, respiratory function, and anterior fontanelle tension (32). Kothapali et al. showed that the Thompson score has a good short-term predictive capacity of morbidity and mortality ($n = 145$) (33). Mendler et al. showed a strong association between Thompson score and long-term, at a mean age of 53 months in infants with NE ($n = 36$) (34). Almost all surviving infants with a maximal Thompson score $\leq$10 had a normal IQ and almost all infants with an impaired IQ (<85) had a Thompson Score $\geq$11.

Prechtl's assessment of general movements assesses spontaneous motor activity and has proven sensitive in the prediction of cerebral palsy (35). General movements assesses for two distinct patterns of normal movements, writhing movements at 6–9 weeks post term, and fidgety movements at 6–20 weeks. Abnormal movements include poor repertoire, cramped-synchronized, and absent fidgety general movements. General movements were highly correlated to gray matter injury in infants with NE (36). All infants with severely abnormal general movements had gray matter injury and poor motor outcome. Infants with predominantly white matter, cortical lesions or mild basal ganglia or thalamic injury had normal or transiently abnormal general movements and normal or mild motor impairment. The ATNAT was compared to Prechtl's qualitative assessment of general movement in a group of 45 preterm infants with risk factors for brain injury and correlated better with neurodevelopmental outcome (37).

AMPLITUDE INTEGRATED EEG (AEEG) AND IDENTIFICATION AND MANAGEMENT OF NEONATAL SEIZURES

The incidence of seizures in NE is ∼50% (38). The presence of seizures increases the incidence of neurodevelopmental impairment. A cumulative seizure burden of 40 min increases neurodevelopmental impairment by nine-fold, independent of grade of encephalopathy and TH (39). TH reduces the seizure burden, especially in moderate NE (40). Seizures can be difficult to diagnose in neonates as ∼50% do not have obvious clinical signs (41, 42).

AMPLITUDE INTEGRATED EEG (AEEG)

Availability of continuous Electroencephalography (EEG) with real-time interpretation by trained staff is ideal but most NICUs use the modified form of amplitude integrated EEG (aEEG), a single or double lead EEG recording from two parietal electrodes. aEEG is useful to monitor baseline brain activity and to detect seizures (43). The combination of early neurological examination and aEEG, in comparison to each individually enhances the ability to identify infants with NE (44). Svenningsen et al. demonstrated that aEEG background activity over the first 6 h of post-natal life accurately predicted neurological outcome (45). The limitations of aEEG include limited short low voltage seizure detection (46) and inaccurate readings due to artifact compared to EEG. aEEG has been demonstrated to be less predictive of outcome at early time points in infants treated with TH compared to normothermia; infants with good outcome had normalized background pattern by 24 h when treated with normothermia and by 48 h when treated with hypothermia (47). Various aEEG training modalities are available such as from the

Total Body Hypothermia Register website (https://www.npeu.ox.ac.uk/downloads/files/toby/TOBY-CFM-Manual.pdf).

TREATMENT OF NEONATAL SEIZURES

The treatment of seizures in NE remains a therapeutic challenge (48). Phenobarbitone is used as first line agent (49), however its efficacy is limited. Phenobarbitone has been demonstrated to reduce both the amplitude and propagation of seizures (50) which may result in electroclinical uncoupling of seizures, which refers to electrographic seizure activity that is not clinically manifested and may make seizure detection more difficult on aEEG monitoring. There are concerns about adverse cognitive effects of phenobarbitone on the neonatal developing brain (51). Animal models have demonstrated that early phenobarbitone exposure causes adverse neurological outcomes later in life (52) and most of the pharmacological data on phenobarbitone is extrapolated from adult data (53). The "efficacy of intravenous levetiracetam in neonatal seizures" trial (NEOLEV2; NCT01720667) examined the efficacy of using levetiracetam first line in comparison to phenobarbitone for neonatal seizures from all causes. The primary outcome was to determine the efficacy of intravenous levetiracetam in terminating neonatal seizures (from all causes) when given as first line therapy compared to phenobarbitone. The provisional results demonstrated that phenobarbitone was more effective then levetiracetam with 80% remaining seizure free for 24 h compared to 28% (54). Sharpe et al. provided continuous monitoring for patients in the NEOLEV2 trial with real-time response to seizure detection. They reported that automatic seizure detection algorithm was useful but not accurate enough to replace human review and that placement of EEG monitors after hours was problematic (55). Levetiracetam pharmacokinetic studies in term neonates found a higher than expected renal clearance, that increased significantly over the first week of post-natal life requiring increased interval dosing (56).

Second line agents to treat neonatal seizures include phenytoin, levetiracetam, topiramate, lidocaine, and midazolam (57). Phenytoin was found to be 57% effective as a combination therapy with phenobarbitone to achieve seizure control in an RCT of neonates with seizures from all causes ($n = 59$) (53). Bumetanide was evaluated as a second line therapy for neonatal seizures via the NEMO (Treatment of Neonatal seizures with Medication Off-patent: evaluation of efficacy and safety of bumetanide) open label feasibility trial. The trial had safety concerns regarding ototoxicity and was stopped prematurely ($n = 14$) (58). Bumetanide did not show signs of clinical efficacy for the treatment of neonatal seizures in the 14 infants that were studied prior to the premature cessation.

A survey of 55 pediatric neurologists predominantly based in USA showed a high off label use of levetiracetam and topiramate as second line for neonatal seizures (3). No side effects in the levetiracetam group were reported in the survey and the treatment was reported as beneficial in over half of cases. There was no consensus on the dosage to use and a wide range of doses were reported (10–30 mg/kg). Midazolam has been shown to have a good response rate in seizure termination in a group of neonates with seizures refractory to phenobarbitone and phenytoin (59). A retrospective review of neonatal seizure management reported that lidocaine demonstrated effectiveness in 50% of neonatal seizures as second line therapy but caution is warranted in view of cardiac toxicity, with bradycardia reported in 3% of patients (60). These studies demonstrate that there is an urgent need for clinical trials to determine safe and effective treatment for neonatal seizures (61).

In summary, 50% of infants with NE have seizures, with phenobarbitone remaining the first line agent with demonstrated clinical efficacy but some overall safety concerns. A global working group of experts established a consensus for protocols for new RCTs in neonatal seizures using evidence based neonatal seizure treatment (62).

NEURO IMAGING

MRI is the gold standard technique to detect patterns of cerebral damage in NE and provides a reliable guide to prognosis (63). Cranial ultrasound (US) and Doppler sonography have useful adjuncts in early diagnostic imaging (64–66). Conventional MRI, with T1 and T2 weighted images, has been demonstrated to have good diagnostic ability to detect brain injury at the end of the first post-natal week of life. There are limitations to the predictive value of MRIs, a normal MRI does not guarantee a normal neurodevelopmental outcome. In one study 32% of infants who had a normal MRI brain in the neonatal period post TH had abnormal development at follow up (67).

The advancement of MR diffusion weighted imaging (DWI) (68) and magnetic resonance spectroscopy (MRS) means lesions may be visualized within the first few post-natal days.

The optimal timing of the MRI brain is important for clinical prognostication and potential redirection of care in the case of end of life decisions, with most cases of withdrawal of care occurring in the first three post-natal days of life (69).

High correlation of sequential conventional MRI and DWI on post-natal day 4 and during the second week was demonstrated in 15 patients with NE (70). 3 Tesla (T) MRI brain was performed in 12 infants with NE at four time points, on post-natal day 1, days 2–3, days 8–13, and at 1 month of age (71). All injuries were already visible on early MRI scans, the later MRIs did not show any new lesions, and in severe NE, DWI changes were subtle on post-natal day 1 and became more apparent on days 2–3. The image quality and diagnostic accuracy in comparison is better with 3T in comparison to a conventional 1.5 T MRI (72). 3T MRI has a good safety profile and is safe for the developing brain but is not universally available (73).

MRI changes in NE may commonly involve parasagittal watershed infarcts between anterior/middle cerebral artery and middle/posterior cerebral artery, with both cortical and subcortical involvement, and injury to metabolically active tissues such as the basal ganglia (BG), thalami, putamen, hippocampi, brainstem, and corticospinal tracts (74). Abnormalities in the signal of the posterior limb of the internal capsule (PLIC), BG and thalami have been demonstrated

to have the greatest predictive value of poor neurodevelopmental outcome, in particular for motor outcome (75, 76). Severe BG and thalami lesions predictive accuracy for severe motor impairment was 0.89 in one study, with abnormal PLIC signal intensity predicting the inability to walk independently by 2 years with a positive predictive value of 0.88 (77). In contrast, infants with white matter damage and no BG or thalamic injury had a good prognosis for independent walking by 2 years of age in infants with NE ($n = 270$) (78).

TH has demonstrated a reduction in BG, thalamic, white matter, and PLIC signal abnormalities (79). TH may be better at reducing the severity of BG and thalamic injury as these regions are selectively vulnerable to acute hypoxia-ischemia compared to parasagittal areas which are more associated with partial prolonged injury (80). The accuracy of MRI as a biomarker to predict outcome is not altered by TH (79).

Magnetic resonance spectroscopy (MRS) provides a non-invasive examination of biochemical brain biomarkers. The Magnetic Resonance Biomarkers in Neonatal Encephalopathy (MARBLE) Study (81) found that thalamic N-acetyl aspartate (NAA) concentration had the highest sensitivity (100%) and specificity (97%) to predict neurodevelopmental outcome at 2 years ($n = 223$). A meta-analysis on MR biomarkers identified MRS deep gray matter Lactate/NAA as the most accurate biomarker to predict neonatal outcome and commented that MRS scoring systems can increase prognostic objectivity (82).

Diffusion tensor MRI is more sensitive than conventional MRI to explore brain development and white matter fibers density and maturation (83), and can display early injury prior to T1 and T2 abnormalities being apparent (84). A systematic review by Dibble et al., of white matter tracts in NE, found three areas of altered diffusion commonly seen in NE were associated with adverse outcomes, the posterior limb of internal capsule and the genu and splenium of the corpus callosum (85). Gray matter diffusion changes in the BG and thalami post NE are associated with dyskinetic cerebral palsy (86). Weeke et al. included diffusion weighted changes in the corpus callosum in a new NE MRI brain scoring system correlating with outcome at 2 years (87). The limitation however of DWI is that the changes normalize within the first week (88).

In addition to conventional MRI techniques, there are further advanced research methods where the acquired data is amenable to derive specific measures through computational analysis and exploration of their ability to predict outcome. This includes diffusion MRI tractography to visualize white matter structure (89–91), and model based measures of tissue microstructure such as Neurite Orientation Dispersion and Density Imaging (NODDI) (92, 93) and diffusion tensor imaging (DTI) based parameters like apparent diffusion coefficient (ADC), radial diffusivity (RD) and fractional anisotropy (FA) (94). Other physiological parameters such as regional cerebral blood flow can be measured with Arterial Spin Labeling (ASL) (95).

Near-infrared spectroscopy (NIRS) is a tool to monitor regional cerebral oxygen saturation, via a calculation based on the absorption spectra of oxygenated and deoxygenated hemoglobin. The measurement of regional cerebral oxygen saturation represented mixed oxygenation of both arterial, venous and capillary readings (96). A systematic review of the use of NIRS in NE showed an association between impaired cerebral autoregulation and cardio-respiratory injury, abnormal MRI and long-term outcome (97).

NEUROCRITICAL CARE

Neurocritical care is an evolving field of tertiary intensive care units through collaboration of neonatologists, neurologists, nurse specialists, and allied health professionals who coordinate care for neurologically ill neonates and has improved outcome of babies with NE (98).

Neurocritical care provides consistency in diagnostic and management strategies focused on improved neurological outcomes. A retrospective review compared the MRI brains' of infants cared for in their normal NICU ($n = 109$) to those of infants cared for after their introduction of a neurocritical ICU ($n = 107$) (99) and demonstrated a reduction in abnormalities on MRI brain of infants cared for in the neuro NICU after adjusting for confounding factors (odds ratio 0.3, CI 0.15–0.57, $p < 0.001$). The changes implemented in that neuro NICU included the introduction of a new multi-disciplinary team, full EEG monitoring done for duration of hypothermia and rewarming, neuroprotection protocols, quality improvement practices, and implementation of a long-term follow-up program.

CARDIOVASCULAR

The spectrum of cardiovascular (CVS) dysfunction in NE ranges in severity and may be attributed to hypoxia or be secondary to ischemia, metabolic acidosis, and multiorgan injury (100). Myocardial contractility, cardiac output and blood pressure are all negatively impacted and co-existing pulmonary hypertension is common. CVS dysfunction may be evaluated from a number of modalities including vital signs, biochemical parameters, echocardiography, and other haemodynamic assessments.

TH affects haemodynamic functioning by causing bradycardia (101), peripheral vasoconstriction, and decreasing cardiac output (102). TH increases the QT_c interval (103) and increases the risk of cardiac arrhythmias (104). The initial TH RCTs were not adequately powered to examine cardiovascular benefit however creatinine-kinase muscle/brain (CK MB) and brain natriuretic peptide (BNP) decrease with TH suggesting a cardioprotective effect (105) and animal model studies have demonstrated an improvement in cardiac ischaemia (106).

Both troponin-T and troponin-I have been demonstrated to be sensitive markers of cardiac dysfunction in NE (100, 107). Gunes et al. measured serial troponin-T, creatinine Kinase (CK-MB), in 45 infants with NE (108). CK-MB levels were significantly higher in moderate and severe NE then in mild NE. Boo et al. found the sensitivity of serum troponin-T in detecting myocardial injury in NE presenting with heart failure was 72.7% and the specificity was 35.9% (109). Serial serum troponin levels during the first 48 h of post-natal life have been found to be significantly higher in infants with NE who died.

Hypotension is observed in up to 62% of patients and may cause secondary multiorgan ischaemic injury. There is no consensus on the ideal target mean systolic, diastolic nor pulse pressure during TH nor on the best pharmacologic agents to maintain it. Long term clinical outcomes of inotropic and chronotropic support lack evidence, with dopamine, dobutamine, and adrenaline commonly chosen demonstrating short term haemodynamic improvements in BP (110). Vasopressor use warrants caution due to potential pulmonary and systemic vasoconstriction (110). McNamara et al. recommended that inotropes administration be done on an individual patient basis depending on echocardiography (ECHO) and clinical status (111). Echo is the best diagnostic tool available to assess cardiovascular function and guide inotropic, chronotropic, and fluid management.

Medications used to treat systemic hypotension include dopamine, dobutamine, adrenaline and noradrenaline, depending on coexisting myocardial dysfunction. Adrenaline may be the most appropriate inotrope due to its' action on α_1, α_2, β_1, and β_2 receptors and its' favorable impact on pulmonary vascular resistance (PVR)/systemic vascular resistance (SVR) ratio (112). The action of dobutamine via α and β receptors decreasing SVR may have advantages as an inotrope in the context of persistent pulmonary hypertension of the newborn (PPHN) and myocardial dysfunction but has not been subject to controlled trials (113). Dopamine is predominantly a vasopressor and in neonatal animal studies has been shown to increase PVR and SVR (112), which has the potential to increase afterload, decrease left-to-right shunting, and compromise systemic oxygen delivery (113). Dopamine is the most widely studied and the most commonly prescribed inotrope in neonatology (114). Studies of developmental outcome favor dobutamine use over dopamine in the preterm population but there are no comparative RCTs in NE (115). McNamara et al. recommended dobutamine use in NE to improve cardiac contractility and heart rate. Milrinone has altered pharmacokinetics during TH affecting its clearance and caution needs to be used with noradrenaline administration as there is little evidence of benefit and it has not been subject to RCT for follow up data (111).

A sustained difference of >5–10% between continuous pre- and post- ductal saturation monitoring may indicate PPHN, which can be confirmed on echocardiography (116). Echocardiography helps to quantify the degree of PPHN and guides treatment including choice of inotropic support. The development of serial functional echocardiography in the NICU allows tracking of the dynamic changes occurring over the course of PPHN (113, 117).

The management of PPHN involves reducing the cardiac afterload and maintaining high preductal mean blood pressures (113, 118). Milrinone has been shown to improve oxygenation index in term neonates with severe PPHN without compromising systemic blood pressure (119). A Cochrane review (120) concluded that the efficacy and safety of milrinone in the treatment of PPHN are not known and recommended that use is restricted to RCTs. Milrinone metabolism is known to be decreased by TH and in an animal model study the inotropic effect was abolished at temperatures of between 31 and 34°C (121). Sildenafil is increasingly used in PPHN. A Cochrane review of sildenafil for PPHN found a significant reduction in mortality in the sildenafil group vs. the control group with a number needed to treat of three (122). The review concluded that sildenafil has significant benefits especially in resource-limited settings and recommended a large-scale randomized control trial comparing sildenafil to the currently used vasodilator inhaled Nitric Oxide (iNO). A Cochrane Review (123) of iNO for respiratory failure in near term or term infants found that iNO improved the outcome in hypoxaemic term infants by reducing the incidence of the combined endpoint of death or need for extra-corporeal membrane oxygenation (ECMO). Oxygenation improved in ∼50% of infants receiving iNO. Long-term follow up studies have found no increase in neurodevelopmental impairment with its use (124, 125).

In summary, cardiovascular dysfunction in NE can be negatively impacted by TH. Echo is the best tool to guide management and other physiological parameter thresholds have not been well-defined. Inotropic and chronotropic medications have altered pharmacokinetics during TH and the choice of agent is best guided by individual hemodynamics.

RESPIRATORY MANAGEMENT IN NE

The incidence of respiratory dysfunction in babies with NE varies from 23 to 86% (10, 11, 126, 127). The spectrum of injury ranges from transient oxygen requirement to severe persistent pulmonary hypertension (PPHN). The pathogenesis of pulmonary dysfunction is complex, although hypoxia is a major component via disruption of the normal physiological fall in pulmonary vascular resistance (113, 118, 128, 129).

The Neonatal Resuscitation Program® (NRP), 7th edition (130) and European Resuscitation Council Guidelines (131) advise on initial management and resuscitation for a non-vigorous term infant. The NRP recommends resuscitation using 21% fraction of inspired oxygen concentration and titrating the oxygen to maintain oxygen saturations within a standardized oxygen centile range depending on minutes of life. The exception to this is if a neonate requires cardiopulmonary resuscitation to titrate the fraction of oxygen to 100%. Neonates are at risk of hyperoxia when exposed to high oxygen concentration, after coming from a relatively hypoxic environment *in utero* and their free radical scavenger systems are underdeveloped (132). Infants with perinatal stress ($n = 609$) were enrolled in a multi-center RCT comparing resuscitation at 100% fraction of inspired oxygen to 21% (133). The infants with higher oxygen exposure had more oxidative stress but no differences were found in mortality or short-term morbidity. This study was limited by the fact that the infants who were resuscitated were relatively well, as all had oxygen saturations of over 90% at 2 min and <2% of them required supplementary oxygen after resuscitation. Expert opinion from this study recommended restoring normoxia as quickly as possible during resuscitation and that a properly powered RCT to establish correct fraction of inspired oxygen would need to recruit 7,000 neonates (134).

Respiratory support in NE aims to maintain a pH over 7.25 and a normal to high partial pressure of arterial carbon dioxide ($PaCO_2$ 5–7 kPa, 37.5–52.5 mmHg) (113, 135–137). Hypocarbia has detrimental effects on cerebral perfusion in an already compromised infant (138–143) and is associated with neurosensory hearing impairment and abnormal neurodevelopment (143, 144). Both isolated low $PaCO_2$ levels and cumulative $PaCO_2$ <4.6 kPa (35 mmHg) were associated with death and disability.

Hypothermia is known to decrease the partial pressure of oxygen and carbon dioxide whilst increasing the pH (142, 145–147). The temperature corrected blood gas values can be obtained by inputting the temperature to the blood gas analyser. Fraction of inspired oxygen, mean airway pressure, oxygenation index, and alveolar-arterial gradient decrease during induction of TH increase during rewarming. Minute ventilation increases with TH and decreases upon rewarming. The inspiratory time, respiratory rate, and positive end expiratory pressure are unaffected. Eicher reported a higher iNO requirement with TH, with 5/35 neonates requiring iNO compared to 1/30 managed at normothermia ($p < 0.01$) (148), however a Cochrane meta-analysis of four TH trials showed no significant effect of hypothermia on PPHN (26).

In summary TH impacts respiratory function in neonates and requires altered blood gas interpretation. Tight control of carbon dioxide and avoidance of hypoxia is essential. There is expert evidence on the use of iNO in PPHN however trials to evaluate the evidence of milrinone and sildenafil use are required.

RENAL MANAGEMENT IN NE

Renal dysfunction resulting in acute kidney injury (AKI) varies from 22 to 70% in NE (149). Selewski (150) reported that infants with NE and co-existing AKI had both a longer length of stay even after controlling for other confounders and an increased incidence of abnormal MRI brain (151). TH has not been associated with a reduction in AKI in NE (150).

The current Kidney Disease Improving Global Outcomes (152) (KDIGO) guidelines for AKI use a rise in creatinine as part of its definition. Creatinine is not an ideal biomarker of neonatal AKI as it peaks late, only rises when 50% of renal function is impaired, may reflect maternal creatinine level, and reflects kidney function rather than injury.

The optimal biomarker would diagnose AKI earlier so active management can be initiated. Cystatin C is a better indicator of glomerular filtration rate than creatinine and correlates with NE severity (153, 154). Neutrophil gelatinase- associated lipocalin (NGAL) correlates to severity of NE and can predict a later creatinine rise (155). Neonates with moderate to severe NE had significantly elevated urinary levels of cystatin-C, NGAL and lower epidermal growth factor in comparison to mildly affected infants (156).

Electrolyte abnormalities were seen in 50% of infants, with hyponatraemia, hypokalaemia, and hypocalcaemia being the most common (157). Renal profile, fluid balance, urine electrolytes, and acid-base balance need regularly monitoring. Urinary catheterisation may be necessary as morphine can cause urinary retention via anti-cholinergic effects.

Oliguria is common in NE. There is a significant risk of fluid retention and hyponatremia due to a poor capacity to produce urine. Fluid intake is frequently restricted in NE during TH due to concerns regarding cerebral oedema (158). A Cochrane review however found no RCT evidence to support this practice and recommended further studies (158). A subsequent RCT of infants with NE undergoing TH randomized infants to a restricted fluid intake of two thirds of normal ($n = 40$); at 40, 55, 65, and 80 mls per kilogram per day on post-natal days one to four of life, respectively, vs. normal fluid intake ($n = 40$); of 60, 80, 100, and 120 mls per kilogram per day, respectively, for the first four post-natal days of life. The fluid composition was 10% dextrose in the first 48 h of post-natal life with sodium and postassium added to the dextrose over the next 48 h. Restricted fluid did not reduce death or major neuro-disability at 6 months of age and was associated with a trend toward more hypoglycaemia (159). Hyponatraemia can result from kidney injury causing fluid retention, the syndrome of inappropriate anti diuretic hormone (SIADH), and tubular dysfunction. The Bartter and Schwartz (160) criteria define SIADH as hyponatremia (serum Na^+ <135 mmol/L) with a corresponding serum hypoosmolality (<280 mOsm/kg), and continued renal excretion of Na^+ (>40 mEq/L), in the absence of clinical evidence of volume and of other causes of hyponatremia. Water restriction is necessary to manage the SIADH safely (161).

During TH renal perfusion is reduced, pharmacokinetic parameters change, and therefore there is a reduction in renally excreted drugs. Nephrotoxic medications, such as acyclovir, aminoglycosides, non-steroidal anti-inflammatory drugs, and vancomycin administration are recommended at renal doses and require therapeutic monitoring. Cefotaxime can be substituted for gentamicin as it has similar coverage without nephrotoxicity (162). The PharmaCool study group demonstrated that morphine-6-glucuronide, the active metabolite of morphine, excretion was decreased during TH. They recommend a loading dose of 50 mg/kg of morphine followed by 5 mcg/kg/hour during TH but acknowledged that there is a large variability of plasma concentrations between patients so dosing may require alterations on an individual patient basis (163).

Renal replacement therapy for severe AKI refractory to medical therapy is not a frequently used therapy, but when indicated peritoneal dialysis is preferred over continuous renal replacement therapy (164). There is a lack of data with long term renal follow up of neonates from a renal perspective post AKI, despite the knowledge that AKI from all causes carries the risk of chronic kidney disease (CKD) with Mammen (165) et al. finding that 10.3% of children had CKD in the 1–3 years post AKI. Askenazi et al. (149) recommend the need for post AKI long term follow up on a three monthly basis with urinalysis and blood pressure measurement identify those children who will go on to develop chronic kidney disease.

To summarize, the definition of AKI is less suitable in neonatal AKI. Electrolyte disturbance and SIADH are common in NE and require monitoring. Morphine elimination is decreased by TH. There is no consensus on AKI management in NE nor

recommendation for long term follow up which is essential post AKI. The optimal fluid management was subject to a small RCT on whether to restrict fluids with no difference in outcome.

GASTROINTESTINAL, LIVER, AND NUTRITION

Enteral feeds were held in the initial TH RCTs, although the risk of necrotizing enterocolitis was similar in TH and neonates managed at normothermia. Some TH centers are now implementing trophic enteral feeds of expressed breast milk (166, 167). A pilot retrospective review of 17 neonates who received minimal enteral nutrition compared to no enteral feed during TH ($n = 17$) found the enteral feeding group was associated with a reduced length of stay and time to full feeds, and did not increase feeding complications nor systemic inflammation (168).

An important finding on the review of available evidence and literature is that no trials have examined the optimal type of fluids to be used. There are no recommendations on whether TPN or dextrose plus electrolytes is the optimal fluids. In anuric renal failure, losses (30 ml/kg/day) plus urine output replacement are recommended for infusion volume (169). There is no evidence to support the use of frusemide in fluid overload in NE.

Glycaemic control is critical in NE as glycogen stores are metabolized via anaerobic metabolism commonly resulting in hypoglycaemia. Initial hypoglycaemia and subsequent hyperglycaemia are associated with poor neurological outcome (170–175). Optimal timing and intervals of glucose monitoring is unknown, however, one evidenced based recommendation is to initiate glucose infusion rate (GIR) of 6–8 mg/kg/min, with 2 mg/kg/min increases in GIR if hypoglycaemia occurs (176). Glucose monitoring recommendation is every 30–60 min until the glucose is over 2.8 mmol/L (50 mg/dl) and subsequently every 4–6 h.

Shah et al. (10) defined hepatic involvement in NE as an elevated aspartate aminotransferase (AST) or alanine aminotransferase (ALT) to >100 IU/ during the first week after birth. Transaminitis, defined as 1.5 times the upper limit of normal was reported in 80% of babies with NE by Hankins et al. (126). They suggested that elevated lactate dehydrogenase, ALT and AST to 1.5 times the upper normal level indicates liver involvement in NE (177). Severity of NE is associated with higher ALT and AST (178). Abnormalities in markers of hepatic synthetic function such as albumin and prothrombin have not been shown to correlate with severity of NE (178, 179). Management of liver dysfunction in NE remains supportive in nature, with platelet, plasma, and albumin infusions as necessary and vitamin K administration. Caution is warranted with use of hepatotoxic medications (paracetamol, ampicillin, and gentamicin). Ensuring normalization of liver function testing in the neonatal periods avoids missing underlying metabolic disorders.

In summary, glycaemic control is critical and can contribute to neurological morbidities. There is a lack of evidence from RCTs regarding enteral nutrition during TH, and optimal fluid volume and type to be infused parenterally. Liver dysfunction requires monitoring alongside caution with hepatotoxic medications.

HEMATOLOGICAL ASSESSMENT AND MONITORING

NE is associated with elevated nucleated red blood cells, thrombocytopenia, and prolonged coagulation profile. Coagulopathy is caused by blood loss, hypoxia-ischaemia, and disseminated intravascular coagulation. The incidence of coagulopathy causing major or life threatening bleeding reported in the initial TH RCTs ranged from 3 to 12% (26). Coagulopathy was reported in 18% in the NICHD study, 19% in the Cool CAP study, and 40% in the TOBY study. There is limited data regarding recommended levels to currently transfuse neonates to overcome coagulopathic or anemic states (180). One study reported that 57% of NE infants required a blood product transfusion in the first 12 h (180).

Foreman et al. established a higher incidence of clinically significant bleeding in infants with NE with platelets below 130 $\times$ 10 ^{9}/L, fibrinogen under 1.5 g/L and international normalized ratio (INR) over 2 (181). Patel et al. define haemostatic dysfunction as prothrombin time (PT) $\geq$18 s, platelet count <100 $\times$ 10^9/L and/or fibrinogen <150 mg/dl (180). Hankins et al. (177) defined hematological injury as the development of early thrombocytopenia (<100 $\times$ 10^9 per liter) in the absence of other causes, or an increase in nucleated red blood cell count to $\geq$26 per 100 white blood cells. A number of guidelines recommend discontinuation of TH in the case of life threatening hemorrhage and ILCOR recommend platelet monitoring but do not specify intervals nor thresholds to intervene at (182).

TH is known to slow the production of enzymes involved in the coagulation cascade (183), but has not been demonstrated to cause an increase in any major hemorrhage (184). Severe hypoxia has been shown to decrease the platelet lifespan (185), whereas hyperoxia exposure has been demonstrated to worsen platelet aggregatory response (186). Protein C, protein S, and antithrombin III were increased in 100% of infants with NE demonstrating a potential to have an increase in thromboembolic events (187). Fetal thrombotic vasculopathy is a common finding on placental pathology in NE (188).

Neonatal stroke was implicated in 4.8% of cases of NE in one study (189). Neonatal stroke as the etiology of NE has been demonstrated to have a worse long term outcome (189, 190). The stroke may be venous or arterial in nature, and of hemorrhagic or ischemic origin. Arterial ischemic stroke previously is demonstrated to have a higher incidence in the literature, however it is more common preterm infants in comparison to term infants. Radiconi et al. hypothesized the incidence of cerebral sino-venous thrombosis is underrecognized in neonates undergoing TH (191). They found 27% of neonates had cerebral sinovenous thrombosis by performing MR venography post rewarming.

Antenatal fetal, maternal, and placental risk factors are all be implicated, including placental infarction, pre-eclampsia, maternal smoking, maternal chorioamnionitis, perinatal

asphyxia, resuscitation, low Apgar scores, fetal thrombophilia (for venous stroke), and congenital heart disease (192). Alongside TH if indicated in the case of stroke causing NE, the management involves treating underlying condition.

Leukocytosis has been shown to correlate to abnormal neurodevelopmental outcome (193, 194). Morkos reported that elevated neutrophil best predicted adverse neurological outcome at 1 year.

In summary, coagulopathy is common in NE at up to 40% and blood product transfusion requirement is common. Stroke may be implicated in the etiology of NE. TH impacts coagulopathy and may require discontinuation in event of life threatening hemorrhage.

INFECTION

Infection and inflammation are implicated in the etiology of NE (195). Maternal chorioamnionitis is a risk factor for NE, with up to one third of placentas in NE displaying histological chorioamnionitis (179). The Vermont Oxford Network reported that 24% of cases of NE have an associated antenatal inflammatory finding (2).

TH has not been associated with a higher incidence of culture positive sepsis (26). Robertson et al. postulated that the higher mortality in a pilot RCT in Uganda in infants receiving TH (33% died) compared to normothermia (7%), may have been related to a higher incidence of sepsis during TH, but the laboratory infrastructure was lacking to support this hypothesis (196). In animal model study TH appears to be protective in gram positive infection but not gram-negative sepsis (197). This has not been studied in controlled studies in human neonates.

Broad spectrum antibiotic therapy covering gram positive, negative, and anaerobes is common practice until sepsis has been excluded, with negative blood cultures and normal infection markers of white cell count and C-reactive protein (CRP). Caution with CRP interpretation is advised as the peak value is delayed by TH (198). Group B Streptococcal (GBS) sepsis was implicated in 0.58% of cases of NE from a systematic review (199). The NE mortality was higher in cases of GBS associated NE at 21% compared to NE mortality not complicated by GBS at 13.7%. The systematic review identified that infants with NE have a 10-fold higher risk of GBS in comparison to term infants without NE (199).

A small pilot study of 16 infants with NE screened extensively for neurotropic viruses, bacteria, and protozoa, by performing bacterial cultures in blood and cerebrospinal fluid (CSF) before antibiotic treatment, and viral CSF, polymerase chain reaction (PCR) for cytomegalovirus, herpes simplex 1 and 2, Epstein-Barr virus, enterovirus, and human parechovirus (200). One case of blood culture positive bacterial sepsis and four cases of clinical sepsis were diagnosed, with no PCR positive results.

Neonatal herpes simplex virus (HSV) central nervous system (CNS) infection may be associated with neonatal seizures and present as with similar signs to NE (201). Maternal primary infection of HSV during the third trimester or maternal mucocutaneous or genital lesions raises suspicion and warrants investigation and empiric treatment in the neonate. Mucocutaneous infection has an absence of clinical lesions in 20% of cases (202) and in 80% of neonatal HSV infection there are no known maternal risk factors (202). A rapid HSV Swab PCR testing and viral culture with the areas of skin swabbing to include the anus, conjunctivae, mouth, nasopharynx, and any suspected vesicles is advised with clinical suspicion (201). Renal function monitoring and adequate hydration are important in view of nephrotoxicity associated with acyclovir (203).

In summary, sepsis evaluation and broad spectrum antibiotics are routine in NE but there is no expert or evidence-based consensus on indication to sample cerebrospinal fluid (CSF) nor viral and bacterial PCR screening. The incidence of HSV and GBS is higher in NE.

SKIN

Regular full skin observation is suggested in view of the potential complications during TH such as subcutaneous fat necrosis, a benign condition characterized by inflammation and necrosis of subcutaneous fat, and cold panniculitis which is an acute nodular, erythematous eruption. In the TOBY RCT 1% of infants had subcutaneous fat necrosis (204) which can be complicated by hypercalcaemia and require hyperhydration and diuretic treatment (205). Sclerema neonatorum is a diffuse hardening of the subcutaneous tissue during TH that usually self resolves. The use of a gradient variable mode of temperature control has less adverse skin events than automatic servo-controlled mode (206).

In summary, daily skin examination for complications and calcium monitoring during TH is recommended.

INBORN ERRORS OF METABOLISM (IEM)

Many IEM present with NE due to early accumulation of toxic metabolites in the CNS including urea cycle defects, amino acid, and organic acid disorders. IEM of energy deficiency most commonly present in the first few hours and days of postnatal life, with NE, cardiorespiratory compromise and organomegaly, including galactosemia, some organic acidemias, urea cycle defects and fatty acid oxidation defects, whereas inborn errors of intermediate metabolism and substrate usually present later.

Persistent acidosis, hyperlactaemia, and refractory hypoglycaemia may indicate an IEM causing the encephalopathy. Congenital malformations, dysplasias, and dysmorphic features raise suspicion of inherited metabolic disorders in an infant with NE (207). Opisthotonus and myoclonic jerks may distinguish metabolic encephalopathies from other etiologies of NE (208). Full family history of metabolic disorders, sudden infant death, failure to thrive, specialized dietary requirement, developmental delay, and consanguinity may help with the diagnosis.

In the context where an IEM is suspected, Burton et al., recommend serum investigations of blood gas, electrolytes, glucose, ammonia, amino acids, and lactate as well as urinalysis for reducing substances, ketones, amino acids, and organic acids as first line investigations (209). Laboratory findings of lactic acidosis with normoglycaemia may indicate

TABLE 1 | Comparison of definitions of Multi-Organ Dysfunction in Neonatal Encephalopathy.

	Shah et al. (10)	Hankins et al. (177)	Martin-Ancel et al. (11)	Perlman et al. (213)	Alsina et al. (214)
Multi-Organ dysfunction in neonatal encephalopathy					
CVS	Hypotension treated with an inotrope for >24 h to maintain normal BP ECG evidence of transient myocardial ischaemia	Need for inotropic support beyond 2 h post birth Elevated CK-MB isoenzyme	Systolic and or diastolic BP <5th percentile for age and sex ECG abnormalities ECHO abnormalities	ECG or ECHO abnormalities (values > 2 SDs from the mean normal values)	Troponin >1 ug/L Need for vasoactive drugs
Hepatic	AST or ALT> 100 IU/l during week one	Elevation of AST, ALT, LDH to 1.5 x upper normal level	Not included	Not included	GOT or GPT >100 Prothrombin activity <60%
Renal	Anuria or oliguria for ≥24 h and a SCr >100 mmol/l Anuria/oliguria for >36 h Any SCr >125 mmol/l Serial SCr increasing postnatally	Elevation of SCr to ≥88.4 mmol/l Oliguria >24 h Persistent haematuria or proteinuria	Oliguria for > 24 h ≥2+ of proteinuria Azotaemia = BUN >7 mmol/l	Urea >7 mmol/l azotaemia SCr >90 mmol/l after post-natal D3 Oliguria (<1 ml/kg/hr) for >24 h	Creatinine >1 mg/dl Diuresis <0.99 ml/kg/h Need for replacement therapy
Neuro	Not included	Clinical evidence of NE EEG abnormalities Neuroimaging abnormalities	Abnormal Neurological exam EEG abnormalities Neuroimaging abnormalities	Abnormal neurological exam Cranial ultrasound abnormalities	Not included
Resp	Need for ventilatory support with 40% oxygen for at least the first 4 h after birth	Not included	Abnormal Silverman Score Need for 0_2 supplementation Need for Mechanical Ventilation	Requirement for intubation and Mechanical Ventilation > 48 h post birth	Need for resp support due to causes other than central apnoea or pharmacological effects
GI	Not included	Not included	Gastric residuals, vomiting, abdominal distension/tenderness, and GI bleeding	Evidence of NEC	Not included
Haem	Not included	Thrombocytopenia (<100 × 10^9/L) Increase in nRBCs to ≥26 per 100 WBCs	Not included	Not included	Leucocyte <4.5 or >30 mm^3 Platelet <149 APTT >45 s Platelet or FFP

Scoring systems by Shah, Hankins, Martin-Ancel, Perlman, and Alsina assess systems of Cardiovascular, Hepatic, Renal, Neurological, Gastrointestinal, and Hematological Dysfunction. CVS, cardiovascular; Neuro, neurological; resp, respiratory; GI, gastrointestinal; Haem, hematological; BP, Blood Pressure; AST, Aspartate Amino Transferase; ALT, Alanine Amino Transferase; SCr, Serum Creatinine; CK-MB, Creatinine Kinase Muscle-Brain-Type Isoenzyme; ECG, Electrocardiographic; ECHO, Echocardiographic; SDs, Standard Deviations; NE, Neonatal Encephalopathy; EEG, Electroencephalographic; BUN, Blood Urea Nitrogen; 0_2, Oxygen; GI, Gastrointestinal; MV, Mechanical Ventilation; NEC, Necrotising Enterocolitis; nRBCs, Nucleated Red Blood Cells; WBCs, White Blood Cell; Glutamic oxaloacetic transaminase (GOT) Glutamic pyruvic transaminase (GPT).

potential medium or long chain fatty acid disorder or glutaric aciduria T2, whereas lactic acidosis with hypoglycaemia may indicate an oxidative phosphorylation disorder. Ketosis with normoglycaemia differential include the organic acidurias, however an acquired metabolic disorder from sepsis and/or dehydration may present similarly (210). Moderately high ammonia levels may be seen in NE without an IEM disorder, with mean levels of 222 μg/dl in one review of infants with NE (211). Higher levels of ammonia is seen in both urea cycle defects are accompanied by respiratory alkalosis and no acidosis and in organic acidemias distinguished by an accompanied metabolic acidosis.

Management of IEM is dependent on the underlying etiology and is done in conjunction with metabolic specialist advice. The overall management includes prevention of accumulation of harmful substances by stopping enteral and parenteral nutrition and correction of metabolic abnormalities by normalizing glucose with IV dextrose, and aiming to normalize blood pH, and eliminate toxic metabolite accumulation (212).

In conclusion; IEM may present as NE, with distinguishing laboratory and or dysmorphic features. Prompt investigation and targeted management of the underlying IEM disorder is necessary. Acquired metabolic disorders secondary to other etiologies of NE may present with laboratory findings of high lactate levels, moderately high ammonia, and hypoglycaemia.

MULTI-ORGAN SCORING IN NE

In view of the multiorgan involvement on NE several groups have developed scoring systems to evaluate organ involvement (**Table 1**). Shah et al. described multi organ scoring dysfunction in infants with severe NE ($n = 144$) (10). They included renal, pulmonary, cardiovascular, and hepatic parameters. All infants had minimum of one end organ dysfunction. Renal, cardiovascular, pulmonary, and hepatic dysfunction were found to present in 70, 62, 86, and 85% of infants, respectively. They concluded that multi organ dysfunction may be included to support a diagnosis of NE, but that multi-organ dysfunction did not correlate with adverse neurodevelopmental outcomes or death.

Martin-Ancel et al. examined multi organ dysfunction in 72 infants with perinatal asphyxia (11) and found the following distribution: pulmonary (26%), cardiac (29%), gastrointestinal (29%), renal (15%), and respiratory (19%). They included infants from mild to severe NE but only 35% of their included infants required NICU admission, suggesting many of the included infants had milder NE. Apgar score was the only perinatal factor that correlated with the degree of multi- organ dysfunction in their review.

Hankins et al. reported liver injury in 80%, cardiac involvement in 78%, and renal injury in 72% in a prospective review ($n = 46$) (126). These scoring systems allow the evaluation of organ dysfunction but have not yet been assessed in conjunction with longer-term neurodevelopmental or multiorgan follow-up in childhood.

CONCLUSION

There has been significant progress over the past two decades in neuroprotective strategies and with the establishment of TH as the standard of care in NE. There remains a gap in the full understanding of the optimal management of the infants during TH, and evidenced based multi-organ support. Ongoing RCTs and systematic reviews to gather information to recommend evidence based best practices is essential to establish the most appropriate practices for management of neonatal seizures, fluid status, inotropic support, and respiratory support.

Establishing evidenced based guidelines for managing multi-organ dysfunction in NE during TH can reduce practice variation, optimize management, and contribute to better outcomes. New adjunctive therapies for NE efficacy may be dependent on the adequate functioning of specific end organs. Dysfunction of these end organs may negatively impact on the efficacy of new treatments and conversely new treatments may have possible adverse side effects on already impaired organ functioning. The introduction of specialized neurocritical care units shows promise in non-pharmacological advancements of management of NE.

Further biomarker development and validation is important to aid in diagnosis of organ injury and prediction of long term outcome, with the BEST (Biomarkers, EndpointS, and other Tools) and twenty first Century Cures Act, providing framework and supportive infrastructure for this (215). Development of an overall predictive model which includes multiorgan dysfunction as part of its criteria is vital to furthering our understanding of NE, and will help in the long-term follow up and care of survivors of NE.

AUTHOR CONTRIBUTIONS

MO'D: main writer of paper. DS: original idea for paper and table of multi organ dysfunction. EM: supervisor and advisor of paper and also devised and designed the review. SB, TA, and ME-B: experts in area and reviewed and provided advise on subsections.

FUNDING

This work was supported by National Children's Hospital Foundation, National Children's Research Centre, Ireland.

REFERENCES

1. Executive summary: Neonatal encephalopathy and neurologic outcome, second edition. Report of the American College of Obstetricians and Gynecologists' Task Force on Neonatal Encephalopathy. *Obstet Gynecol.* (2014) 123:896–901. doi: 10.1097/01.AOG.0000445580.65983.d2
2. Nelson KB, Bingham P, Edwards EM, Horbar JD, Kenny MJ, Inder T, et al. Antecedents of neonatal encephalopathy in the vermont oxford network encephalopathy registry. *Pediatrics.* (2012) 130:878–86. doi: 10.1542/peds.2012-0714
3. Molloy EJ, Bearer C. Neonatal encephalopathy versus hypoxic-ischemic encephalopathy. *Pediatr Res.* (2018) 84:574. doi: 10.1038/s41390-018-0169-7
4. Chalak L, Ferriero DM, Gressens P, Molloy E, Bearer C. A 20 years conundrum of neonatal encephalopathy and hypoxic ischemic encephalopathy: are we closer to a consensus guideline? *Pediatr Res.* (2019) 86:548–9. doi: 10.1038/s41390-019-0547-9
5. Dammann O, Ferriero D, Gressens P. Neonatal encephalopathy or hypoxic-ischemic encephalopathy? Appropriate terminology matters. *Pediatr Res.* (2011) 70:1–2. doi: 10.1203/PDR.0b013e318223f38d
6. Lee AC, Kozuki N, Blencowe H, Vos T, Bahalim A, Darmstadt GL, et al. Intrapartum-related neonatal encephalopathy incidence and impairment at regional and global levels for 2010 with trends from 1990. *Pediatr Res.* (2013) 74 (Suppl. 1):50–72. doi: 10.1038/pr.2013.206
7. Tagin MA, Woolcott CG, Vincer MJ, Whyte RK, Stinson DA. Hypothermia for neonatal hypoxic ischemic encephalopathy: an updated systematic review and meta-analysis. *Arch Pediatr Adolesc Med.* (2012) 166:558–66. doi: 10.1001/archpediatrics.2011.1772
8. Schendel D, Nelson KB, Blair E. Neonatal encephalopathy or hypoxic-ischemic encephalopathy? *Ann Neurol.* (2012) 72:984–5. doi: 10.1002/ana.23753
9. Aslam S, Strickland T, Molloy EJ. Neonatal encephalopathy: need for recognition of multiple etiologies for optimal management. *Front Pediatr.* (2019) 7:142. doi: 10.3389/fped.2019.00142
10. Shah P, Riphagen S, Beyene J, Perlman M. Multiorgan dysfunction in infants with post-asphyxial hypoxic-ischaemic encephalopathy. *Arch Dis Child Fetal Neonatal Ed.* (2004) 89:F152–5. doi: 10.1136/adc.2002.023093

11. Martin-Ancel A, Garcia-Alix A, Gaya F, Cabanas F, Burgueros M, Quero J. Multiple organ involvement in perinatal asphyxia. *J Pediatr.* (1995) 127:786–93. doi: 10.1016/S0022-3476(95)70174-5
12. Jacobs SE, Berg M, Hunt R, Tarnow-Mordi WO, Inder TE, Davis PG. Cooling for newborns with hypoxic ischaemic encephalopathy. *Cochrane Database Syst Rev*. (2013) 2013:Cd003311. doi: 10.1002/14651858.CD003311.pub3
13. Committee on F, Newborn, Papile LA, Baley JE, Benitz W, Cummings J, et al. Hypothermia and neonatal encephalopathy. *Pediatrics.* (2014) 133:1146–50. doi: 10.1542/peds.2014-0899
14. Gunn AJ, Thoresen M. Hypothermic neuroprotection. *NeuroRx.* (2006) 3:154–69. doi: 10.1016/j.nurx.2006.01.007
15. Manley BJ, Owen LS, Hooper SB, Jacobs SE, Cheong JLY, Doyle LW, et al. Towards evidence-based resuscitation of the newborn infant. *Lancet.* (2017) 389:1639–48. doi: 10.1016/S0140-6736(17)30547-0
16. Thoresen M, Tooley J, Liu X, Jary S, Fleming P, Luyt K, et al. Time is brain: starting therapeutic hypothermia within three hours after birth improves motor outcome in asphyxiated newborns. *Neonatology.* (2013) 104:228–33. doi: 10.1159/000353948
17. Laptook AR, Shankaran S, Tyson JE, Munoz B, Bell EF, Goldberg RN, et al. Effect of therapeutic hypothermia initiated after 6 hours of age on death or disability among newborns with hypoxic-ischemic encephalopathy: a randomized clinical trial. *JAMA*. (2017) 318:1550–60. doi: 10.1001/jama.2017.14972
18. Shankaran S, Laptook AR, Pappas A, McDonald SA, Das A, Tyson JE, et al. Effect of depth and duration of cooling on deaths in the NICU among neonates with hypoxic ischemic encephalopathy: a randomized clinical trial. *JAMA*. (2014) 312:2629–39. doi: 10.1001/jama.2014.16058
19. Oliveira V, Singhvi DP, Montaldo P, Lally PJ, Mendoza J, Manerkar S, et al. Therapeutic hypothermia in mild neonatal encephalopathy: a national survey of practice in the UK. *Arch Dis Child Fetal Neonatal Ed.* (2018) 103:F388–f90. doi: 10.1136/archdischild-2017-313320
20. Prempunpong C, Chalak LF, Garfinkle J, Shah B, Kalra V, Rollins N, et al. Prospective research on infants with mild encephalopathy: the PRIME study. *J Perinatol.* (2018) 38:80–5. doi: 10.1038/jp.2017.164
21. Chalak LF, Nguyen KA, Prempunpong C, Heyne R, Thayyil S, Shankaran S, et al. Prospective research in infants with mild encephalopathy identified in the first six hours of life: neurodevelopmental outcomes at 18-22 months. *Pediatr Res.* (2018) 84:861–8. doi: 10.1038/s41390-018-0174-x
22. Murray DM, O'Connor CM, Ryan CA, Korotchikova I, Boylan GB. Early EEG grade and outcome at 5 years after mild neonatal hypoxic ischemic encephalopathy. *Pediatrics.* (2016) 138:e20160659. doi: 10.1542/peds.2016-0659
23. Conway JM, Walsh BH, Boylan GB, Murray DM. Mild hypoxic ischaemic encephalopathy and long term neurodevelopmental outcome - a systematic review. *Early Hum Dev.* (2018) 120:80–7. doi: 10.1016/j.earlhumdev.2018.02.007
24. El-Dib M, Inder TE, Chalak LF, Massaro AN, Thoresen M, Gunn AJ. Should therapeutic hypothermia be offered to babies with mild neonatal encephalopathy in the first 6 h after birth? *Pediatr Res.* (2019) 85:442–8. doi: 10.1038/s41390-019-0291-1
25. Sarnat HB, Sarnat MS. Neonatal encephalopathy following fetal distress. a clinical and electroencephalographic study. *Arch Neurol.* (1976) 33:696–705. doi: 10.1001/archneur.1976.00500100030012
26. Jacobs S, Hunt R, Tarnow-Mordi W, Inder T, Davis P. Cooling for newborns with hypoxic ischaemic encephalopathy. *Cochrane Database Syst Rev*. (2007) 17:Cd003311. doi: 10.1002/14651858.CD003311.pub2
27. Azzopardi DV, Strohm B, Edwards AD, Dyet L, Halliday HL, Juszczak E, et al. Moderate hypothermia to treat perinatal asphyxial encephalopathy. *N Engl J Med.* (2009) 361:1349–58. doi: 10.1056/NEJMoa0900854
28. van de Riet JE, Vandenbussche FP, Le Cessie S, Keirse MJ. Newborn assessment and long-term adverse outcome: a systematic review. *Am J Obstet Gynecol.* (1999) 180:1024–9. doi: 10.1016/S0002-9378(99)70676-9
29. Gosselin J, Gahagan S, Amiel-Tison C. The amiel-tison neurological assessment at term: conceptual and methodological continuity in the course of follow-up. *Ment Retard Dev Disabil Res Rev.* (2005) 11:34–51. doi: 10.1002/mrdd.20049
30. Amess PN, Penrice J, Wylezinska M, Lorek A, Townsend J, Wyatt JS, et al. Early brain proton magnetic resonance spectroscopy and neonatal neurology related to neurodevelopmental outcome at 1 year in term infants after presumed hypoxic-ischaemic brain injury. *Dev Med Child Neurol.* (1999) 41:436–45. doi: 10.1017/S0012162299000973
31. Murray DM, Bala P, O'Connor CM, Ryan CA, Connolly S, Boylan GB. The predictive value of early neurological examination in neonatal hypoxic-ischaemic encephalopathy and neurodevelopmental outcome at 24 months. *Dev Med Child Neurol.* (2010) 52:e55–9. doi: 10.1111/j.1469-8749.2009.03550.x
32. Thompson CM, Puterman AS, Linley LL, Hann FM, van der Elst CW, Molteno CD, et al. The value of a scoring system for hypoxic ischaemic encephalopathy in predicting neurodevelopmental outcome. *Acta Paediatrica.* (1997) 86:757–61. doi: 10.1111/j.1651-2227.1997.tb08581.x
33. Bhagwani DK, Sharma M, Dolker S, Kothapalli S. To study the correlation of thompson scoring in predicting early neonatal outcome in post asphyxiated term neonates. *JCDR.* (2016) 10:Sc16-sc9. doi: 10.7860/JCDR/2016/22896.8882
34. Mendler MR, Mendler I, Hassan MA, Mayer B, Bode H, Hummler HD. Predictive value of thompson-score for long-term neurological and cognitive outcome in term newborns with perinatal asphyxia and hypoxic-ischemic encephalopathy undergoing controlled hypothermia treatment. *Neonatology.* (2018) 114:341–7. doi: 10.1159/000490721
35. Kwong AKL, Fitzgerald TL, Doyle LW, Cheong JLY, Spittle AJ. Predictive validity of spontaneous early infant movement for later cerebral palsy: a systematic review. *Dev Med Child Neurol.* (2018) 60:480–9. doi: 10.1111/dmcn.13697
36. Ferrari F, Todeschini A, Guidotti I, Martinez-Biarge M, Roversi MF, Berardi A, et al. General movements in full-term infants with perinatal asphyxia are related to Basal Ganglia and thalamic lesions. *J Pediatr.* (2011) 158:904–11. doi: 10.1016/j.jpeds.2010.11.037
37. Paro-Panjan D, Sustersic B, Neubauer D. Comparison of two methods of neurologic assessment in infants. *Pediatr Neurol.* (2005) 33:317–24. doi: 10.1016/j.pediatrneurol.2005.05.008
38. Lynch NE, Stevenson NJ, Livingstone V, Murphy BP, Rennie JM, Boylan GB. The temporal evolution of electrographic seizure burden in neonatal hypoxic ischemic encephalopathy. *Epilepsia.* (2012) 53:549–57. doi: 10.1111/j.1528-1167.2011.03401.x
39. Kharoshankaya L, Stevenson NJ, Livingstone V, Murray DM, Murphy BP, Ahearne CE, et al. Seizure burden and neurodevelopmental outcome in neonates with hypoxic-ischemic encephalopathy. *Dev Med Child Neurol.* (2016) 58:1242–8. doi: 10.1111/dmcn.13215
40. Low E, Boylan GB, Mathieson SR, Murray DM, Korotchikova I, Stevenson NJ, et al. Cooling and seizure burden in term neonates: an observational study. *Arch Dis Child Fetal Neonatal Ed.* (2012) 97:F267–72. doi: 10.1136/archdischild-2011-300716
41. Murray DM, Boylan GB, Ali I, Ryan CA, Murphy BP, Connolly S. Defining the gap between electrographic seizure burden, clinical expression and staff recognition of neonatal seizures. *Arch Dis Child Fetal Neonatal Ed.* (2008) 93:F187–91. doi: 10.1136/adc.2005.086314
42. Boylan GB, Stevenson NJ, Vanhatalo S. Monitoring neonatal seizures. *Semin Fetal Neonatal Med.* (2013) 18:202–8. doi: 10.1016/j.siny.2013.04.004
43. El-Dib M, Chang T, Tsuchida TN, Clancy RR. Amplitude-integrated electroencephalography in neonates. *Pediatr Neurol.* (2009) 41:315–26. doi: 10.1016/j.pediatrneurol.2009.05.002
44. Shalak LF, Laptook AR, Velaphi SC, Perlman JM. Amplitude-integrated electroencephalography coupled with an early neurologic examination enhances prediction of term infants at risk for persistent encephalopathy. *Pediatrics.* (2003) 111:351–7. doi: 10.1542/peds.111.2.351
45. Hellstrom-Westas L, Rosen I, Svenningsen NW. Predictive value of early continuous amplitude integrated EEG recordings on outcome after severe birth asphyxia in full term infants. *Arch Dis Child Fetal Neonatal Ed.* (1995) 72:F34–8. doi: 10.1136/fn.72.1.F34
46. Toet MC, van der Meij W, de Vries LS, Uiterwaal CS, van Huffelen KC. Comparison between simultaneously recorded amplitude integrated electroencephalogram (cerebral function monitor) and standard electroencephalogram in neonates. *Pediatrics.* (2002) 109:772–9. doi: 10.1542/peds.109.5.772
47. Thoresen M, Hellstrom-Westas L, Liu X, de Vries LS. Effect of hypothermia on amplitude-integrated electroencephalogram in infants

with asphyxia. *Pediatrics.* (2010) 126:e131–9. doi: 10.1542/peds.2009-2938
48. El-Dib M, Soul JS. The use of phenobarbital and other anti-seizure drugs in newborns. *Semin Fetal Neonatal Med.* (2017) 22:321–7. doi: 10.1016/j.siny.2017.07.008
49. Glass HC, Wirrell E. Controversies in neonatal seizure management. *J Child Neurol.* (2009) 24:591–9. doi: 10.1177/0883073808327832
50. Mathieson SR, Livingstone V, Low E, Pressler R, Rennie JM, Boylan GB. Phenobarbital reduces EEG amplitude and propagation of neonatal seizures but does not alter performance of automated seizure detection. *Clin Neurophysiol.* (2016) 127:3343–50. doi: 10.1016/j.clinph.2016.07.007
51. Vining EP, Mellitis ED, Dorsen MM, Cataldo MF, Quaskey SA, Spielberg SP, et al. Psychologic and behavioral effects of antiepileptic drugs in children: a double-blind comparison between phenobarbital and valproic acid. *Pediatrics.* (1987) 80:165–74.
52. Quinlan SMM, Rodriguez-Alvarez N, Molloy EJ, Madden SF, Boylan GB, Henshall DC, et al. Complex spectrum of phenobarbital effects in a mouse model of neonatal hypoxia-induced seizures. *Sci Rep.* (2018) 8:9986. doi: 10.1038/s41598-018-28044-2
53. Painter MJ, Scher MS, Stein AD, Armatti S, Wang Z, Gardiner JC, et al. Phenobarbital compared with phenytoin for the treatment of neonatal seizures. *N Engl J Med.* (1999) 341:485–9. doi: 10.1056/NEJM199908123410704
54. Haas R, Sharpe C, Rasmussen M, Harbert MJ, Kuperman R, Michelson D, et al. Efficacy of intravenous levetiracetam in neonatal seizures: NEOLEV2 - a multicenter, randomized, blinded, controlled phase IIb trial of the optimal dose, efficacy and safety of levetiracetam compared with phenobarbital in the first-line treatment of neonatal seizures. *PAS Abstract.* (2019). doi: 10.2139/ssrn.3405581
55. Sharpe C, Davis SL, Reiner GE, Lee LI, Gold JJ, Nespeca M, et al. Assessing the feasibility of providing a real-time response to seizures detected with continuous long-term neonatal electroencephalography monitoring. *J Clin Neurophysiol.* (2019) 36:9–13. doi: 10.1097/WNP.0000000000000525
56. Sharpe CM, Capparelli EV, Mower A, Farrell MJ, Soldin SJ, Haas RH. A seven-day study of the pharmacokinetics of intravenous levetiracetam in neonates: marked changes in pharmacokinetics occur during the first week of life. *Pediatr Res.* (2012) 72:43–9. doi: 10.1038/pr.2012.51
57. Glass HC, Kan J, Bonifacio SL, Ferriero DM. Neonatal seizures: treatment practices among term and preterm infants. *Pediatr Neurol.* (2012) 46:111–5. doi: 10.1016/j.pediatrneurol.2011.11.006
58. Pressler RM, Boylan GB, Marlow N, Blennow M, Chiron C, Cross JH, et al. Bumetanide for the treatment of seizures in newborn babies with hypoxic ischaemic encephalopathy (NEMO): an open-label, dose finding, and feasibility phase 1/2 trial. *Lancet Neurol.* (2015) 14:469–77. doi: 10.1016/S1474-4422(14)70303-5
59. Castro Conde JR, Hernandez Borges AA, Domenech Martinez E, Gonzalez Campo C, Perera Soler R. Midazolam in neonatal seizures with no response to phenobarbital. *Neurology.* (2005) 64:876–9. doi: 10.1212/01.WNL.0000152891.58694.71
60. Lundqvist M, Agren J, Hellstrom-Westas L, Flink R, Wickstrom R. Efficacy and safety of lidocaine for treatment of neonatal seizures. *Acta Paediatr.* (2013) 102:863–7. doi: 10.1111/apa.12311
61. Silverstein FS, Ferriero DM. Off-label use of antiepileptic drugs for the treatment of neonatal seizures. *Pediatr Neurol.* (2008) 39:77–9. doi: 10.1016/j.pediatrneurol.2008.04.008
62. Soul JS, Pressler R, Allen M, Boylan G, Rabe H, Portman R, et al. Recommendations for the design of therapeutic trials for neonatal seizures. *Pediatr Res.* (2019) 85:943–54. doi: 10.1038/s41390-018-0242-2
63. Rutherford M, Biarge MM, Allsop J, Counsell S, Cowan F. MRI of perinatal brain injury. *Pediatric Radiol.* (2010) 40:819–33. doi: 10.1007/s00247-010-1620-z
64. Daneman A, Epelman M, Blaser S, Jarrin JR. Imaging of the brain in full-term neonates: does sonography still play a role? *Pediatr Radiol.* (2006) 36:636–46. doi: 10.1007/s00247-006-0201-7
65. Radiological Society of North America. *85th Scientific Assembly and Annual Meeting.* Chicago, IL (1999). p. 101-491.
66. Benson JE, Bishop MR, Cohen HL. Intracranial neonatal neurosonography: an update. *Ultrasound Quart.* (2002) 18:89–114. doi: 10.1097/00013644-200206000-00003
67. Hayes BC, Ryan S, McGarvey C, Mulvany S, Doherty E, Grehan A, et al. Brain magnetic resonance imaging and outcome after hypoxic ischaemic encephalopathy. *J Matern Fetal Neonatal Med.* (2016) 29:777–82. doi: 10.3109/14767058.2015.1018167
68. Robertson RL, Ben-Sira L, Barnes PD, Mulkern RV, Robson CD, Maier SE, et al. MR line-scan diffusion-weighted imaging of term neonates with perinatal brain ischemia. *AJNR.* (1999) 20:1658–70.
69. Garcia-Alix A, Arnaez J, Cortes V, Girabent-Farres M, Arca G, Balaguer A. Neonatal hypoxic-ischaemic encephalopathy: most deaths followed end-of-life decisions within three days of birth. *Acta Paediatr.* (2013) 102:1137–43. doi: 10.1111/apa.12420
70. Agut T, Leon M, Rebollo M, Muchart J, Arca G, Garcia-Alix A. Early identification of brain injury in infants with hypoxic ischemic encephalopathy at high risk for severe impairments: accuracy of MRI performed in the first days of life. *BMC Pediatr.* (2014) 14:177. doi: 10.1186/1471-2431-14-177
71. Wintermark P, Hansen A, Soul J, Labrecque M, Robertson RL, Warfield SK. Early versus late MRI in asphyxiated newborns treated with hypothermia. *Arch Dis Childhood Fetal Neonatal Ed.* (2011) 96:F36–44. doi: 10.1136/adc.2010.184291
72. Wardlaw JM, Brindle W, Casado AM, Shuler K, Henderson M, Thomas B, et al. A systematic review of the utility of 1.5 versus 3 Tesla magnetic resonance brain imaging in clinical practice and research. *Eur Radiol.* (2012) 22:2295–303. doi: 10.1007/s00330-012-2500-8
73. Tocchio S, Kline-Fath B, Kanal E, Schmithorst VJ, Panigrahy A. MRI evaluation and safety in the developing brain. *Semin Perinatol.* (2015) 39:73–104. doi: 10.1053/j.semperi.2015.01.002
74. Bano S, Chaudhary V, Garga UC. Neonatal hypoxic-ischemic encephalopathy: a radiological review. *J Pediatr Neurosci.* (2017) 12:1–6. doi: 10.4103/1817-1745.205646
75. Cheong JL, Coleman L, Hunt RW, Lee KJ, Doyle LW, Inder TE, et al. Prognostic utility of magnetic resonance imaging in neonatal hypoxic-ischemic encephalopathy: substudy of a randomized trial. *Arch Pediatr Adolesc Med.* (2012) 166:634–40. doi: 10.1001/archpediatrics.2012.284
76. Shankaran S, McDonald SA, Laptook AR, Hintz SR, Barnes PD, Das A, et al. Neonatal magnetic resonance imaging pattern of brain injury as a biomarker of childhood outcomes following a trial of hypothermia for neonatal hypoxic-ischemic encephalopathy. *J Pediatr.* (2015) 167:987.
77. Martinez-Biarge M, Diez-Sebastian J, Kapellou O, Gindner D, Allsop JM, Rutherford MA, et al. Predicting motor outcome and death in term hypoxic-ischemic encephalopathy. *Neurology.* (2011) 76:2055–61. doi: 10.1212/WNL.0b013e31821f442d
78. Bregant T, Cowan RM, White F. Matter lesions in term infants with neonatal encephalopathy:correlation with later scans and neurodevelopmental outcome. *Early Hum Dev.* (2007) 83:128. doi: 10.1016/j.earlhumdev.2006.09.023
79. Rutherford M, Ramenghi LA, Edwards AD, Brocklehurst P, Halliday H, Levene M, et al. Assessment of brain tissue injury after moderate hypothermia in neonates with hypoxic-ischaemic encephalopathy: a nested substudy of a randomised controlled trial. *Lancet Neurol.* (2010) 9:39–45. doi: 10.1016/S1474-4422(09)70295-9
80. Bonifacio SL, Glass HC, Vanderpluym J, Agrawal AT, Xu D, Barkovich AJ, et al. Perinatal events and early magnetic resonance imaging in therapeutic hypothermia. *J Pediatrics.* (2011) 158:360–5. doi: 10.1016/j.jpeds.2010.09.003
81. Lally PJ, Pauliah S, Montaldo P, Chaban B, Oliveira V, Bainbridge A, et al. Magnetic Resonance Biomarkers in Neonatal Encephalopathy (MARBLE): a prospective multicountry study. *BMJ Open.* (2015) 5. doi: 10.1136/bmjopen-2015-008912
82. Thayyil S, Chandrasekaran M, Taylor A, Bainbridge A, Cady EB, Chong WK, et al. Cerebral magnetic resonance biomarkers in neonatal encephalopathy: a meta-analysis. *Pediatrics.* (2010) 125:e382–95. doi: 10.1542/peds.2009-1046
83. Neil J, Miller J, Mukherjee P, Huppi PS. Diffusion tensor imaging of normal and injured developing human brain - a technical review. *NMR Biomed.* (2002) 15:543–52. doi: 10.1002/nbm.784

84. Rutherford M, Counsell S, Allsop J, Boardman J, Kapellou O, Larkman D, et al. Diffusion-weighted magnetic resonance imaging in term perinatal brain injury: a comparison with site of lesion and time from birth. *Pediatrics.* (2004) 114:1004–14. doi: 10.1542/peds.2004-0222
85. Dibble M, O'Dea MI, Hurley T, Byrne A, Colleran G, Molloy EJ, et al. Diffusion tensor imaging in neonatal encephalopathy: a systematic review. *Arch Dis Child Fetal Neonatal Ed.* (2019). doi: 10.1136/archdischild-2019-318025. [Epub ahead of print].
86. de Vries LS, Groenendaal F. Patterns of neonatal hypoxic-ischaemic brain injury. *Neuroradiology.* (2010) 52:555–66. doi: 10.1007/s00234-010-0674-9
87. Weeke LC, Groenendaal F, Mudigonda K, Blennow M, Lequin MH, Meiners LC, et al. A novel magnetic resonance imaging score predicts neurodevelopmental outcome after perinatal asphyxia and therapeutic hypothermia. *J Pediatr.* (2018) 192:33–40.e2. doi: 10.1016/j.jpeds.2017.09.043
88. Groenendaal F, de Vries LS. Fifty years of brain imaging in neonatal encephalopathy following perinatal asphyxia. *Pediatr Res.* (2017) 81:150–5. doi: 10.1038/pr.2016.195
89. van Pul C, Buijs J, Vilanova A, Roos FG, Wijn PF. Infants with perinatal hypoxic ischemia: feasibility of fiber tracking at birth and 3 months. *Radiology.* (2006) 240:203–14. doi: 10.1148/radiol.2393041523
90. Massaro AN, Evangelou I, Fatemi A, Vezina G, McCarter R, Glass P, et al. White matter tract integrity and developmental outcome in newborn infants with hypoxic-ischemic encephalopathy treated with hypothermia. *Dev Med Child Neurol.* (2015) 57:441–8. doi: 10.1111/dmcn.12646
91. Porter EJ, Counsell SJ, Edwards AD, Allsop J, Azzopardi D. Tract-based spatial statistics of magnetic resonance images to assess disease and treatment effects in perinatal asphyxial encephalopathy. *Pediatr Res.* (2010) 68:205–9. doi: 10.1203/PDR.0b013e3181e9f1ba
92. Lally PZH, Pauliah S, Zhang H, Price DI, Balraj G, Brainbridge A, et al. Microstructural changes in neonatal encephalopathy revealed with the Neurite Orientation Dispersion and Density Imaging (NODDI) model. *Arch Dis Child.* (2014) 99(Suppl. 1):A14. doi: 10.1136/archdischild-2014-306576.38
93. Kansagra AP, Mabray MC, Ferriero DM, Barkovich AJ, Xu D, Hess CP. Microstructural maturation of white matter tracts in encephalopathic neonates. *Clin Imaging.* (2016) 40:1009–13. doi: 10.1016/j.clinimag.2016.05.009
94. Kushwah S, Kumar A, Verma A, Basu S, Kumar A. Comparison of fractional anisotropy and apparent diffusion coefficient among hypoxic ischemic encephalopathy stages 1, 2, and 3 and with nonasphyxiated newborns in 18 areas of brain. *Indian J Radiol Imaging.* (2017) 27:447–56. doi: 10.4103/ijri.IJRI_384_16
95. Proisy M, Corouge I, Legouhy A, Nicolas A, Charon V, Mazille N, et al. Changes in brain perfusion in successive arterial spin labeling MRI scans in neonates with hypoxic-ischemic encephalopathy. *NeuroImage Clin.* (2019) 24:101939. doi: 10.1016/j.nicl.2019.101939
96. Pellicer A, Bravo Mdel C. Near-infrared spectroscopy: a methodology-focused review. *Semin Fetal Neonatal Med.* (2011) 16:42–9. doi: 10.1016/j.siny.2010.05.003
97. Thewissen L, Caicedo A, Lemmers P, Van Bel F, Van Huffel S, Naulaers G. Measuring near-infrared spectroscopy derived cerebral autoregulation in neonates: from research tool toward bedside multimodal monitoring. *Front Pediatr.* (2018) 6:117. doi: 10.3389/fped.2018.00117
98. Glass HC, Bonifacio SL, Peloquin S, Shimotake T, Sehring S, Sun Y, et al. Neurocritical care for neonates. *Neurocrit Care.* (2010) 12:421–9. doi: 10.1007/s12028-009-9324-7
99. Roychoudhury S, Esser MJ, Buchhalter J, Bello-Espinosa L, Zein H, Howlett A, et al. Implementation of neonatal neurocritical care program improved short-term outcomes in neonates with moderate-to-severe hypoxic ischemic encephalopathy. *Pediatr Neurol.* (2019) 101, 64–70. doi: 10.1016/j.pediatrneurol.2019.02.023
100. Armstrong K, Franklin O, Sweetman D, Molloy EJ. Cardiovascular dysfunction in infants with neonatal encephalopathy. *Arch Dis Child.* (2012) 97:372–5. doi: 10.1136/adc.2011.214205
101. Wood T, Thoresen M. Physiological responses to hypothermia. *Semin Fetal Neonatal Med.* (2015) 20:87–96. doi: 10.1016/j.siny.2014.10.005
102. Gebauer CM, Knuepfer M, Robel-Tillig E, Pulzer F, Vogtmann C. Hemodynamics among neonates with hypoxic-ischemic encephalopathy during whole-body hypothermia and passive rewarming. *Pediatrics.* (2006) 117:843–50. doi: 10.1542/peds.2004-1587
103. Vega L, Boix H, Albert D, Delgado I, Castillo F. [Corrected QT interval during therapeutic hypothermia in hypoxic ischaemic encephalopathy]. *An Pediatr.* (2016) 85:312–7. doi: 10.1016/j.anpede.2016.10.001
104. Zhang W, Lu M, Zhang C, Zhang R, Ou X, Zhou J, et al. Therapeutic hypothermia increases the risk of cardiac arrhythmia for perinatal hypoxic ischaemic encephalopathy: a meta-analysis. *PLoS ONE.* (2017) 12:e0173006. doi: 10.1371/journal.pone.0173006
105. Vijlbrief DC, Benders M, Kemperman H, van Bel F, de Vries WB. Cardiac biomarkers as indicators of hemodynamic adaptation during postasphyxial hypothermia treatment. *Neonatology.* (2012) 102:243–8. doi: 10.1159/000339117
106. Liu X, Tooley J, Loberg EM, Suleiman MS, Thoresen M. Immediate hypothermia reduces cardiac troponin I after hypoxic-ischemic encephalopathy in newborn pigs. *Pediatr Res.* (2011) 70:352–6. doi: 10.1203/PDR.0b013e31822941ee
107. Sweetman D, Armstrong K, Murphy JFA, Molloy EJ. Cardiac biomarkers in neonatal hypoxic ischaemia. *Acta Paediatrica.* (2012) 101:338–43. doi: 10.1111/j.1651-2227.2011.02539.x
108. Gunes T, Ozturk MA, Koklu SM, Narin N, Koklu E. Troponin-T levels in perinatally asphyxiated infants during the first 15 days of life. *Acta Paediatr.* (2005) 94:1638–43. doi: 10.1080/08035250510041222
109. Boo NY, Hafidz H, Nawawi HM, Cheah FC, Fadzil YJ, Abdul-Aziz BB, et al. Comparison of serum cardiac troponin T and creatine kinase MB isoenzyme mass concentrations in asphyxiated term infants during the first 48 h of life. *J Paediatr Child Health.* (2005) 41:331–7. doi: 10.1111/j.1440-1754.2005.00626.x
110. Evans N. Which inotrope for which baby? *Arch Dis Child Fetal Neonatal Ed.* (2006) 91:F213–20. doi: 10.1136/adc.2005.071829
111. Giesinger RE, Bailey LJ, Deshpande P, McNamara PJ. Hypoxic-Ischemic encephalopathy and therapeutic hypothermia: the hemodynamic perspective. *J Pediatr.* (2017) 180:22–30. doi: 10.1016/j.jpeds.2016.09.009
112. Cheung PY, Barrington KJ. The effects of dopamine and epinephrine on hemodynamics and oxygen metabolism in hypoxic anesthetized piglets. *Crit Care.* (2001) 5:158–66. doi: 10.1186/cc1016
113. Lapointe A, Barrington KJ. Pulmonary hypertension and the asphyxiated newborn. *J Pediatr.* (2011) 158(Suppl. 2):e19–24. doi: 10.1016/j.jpeds.2010.11.008
114. Dempsey E, Rabe H. The use of cardiotonic drugs in neonates. *Clin Perinatol.* (2019) 46:273–90. doi: 10.1016/j.clp.2019.02.010
115. Osborn DA, Evans N, Kluckow M, Bowen JR, Rieger I. Low superior vena cava flow and effect of inotropes on neurodevelopment to 3 years in preterm infants. *Pediatrics.* (2007) 120:372–80. doi: 10.1542/peds.2006-3398
116. Nair J, Lakshminrusimha S. Update on pphn: mechanisms and treatment. *Semin Perinatol.* (2014) 38:78–91. doi: 10.1053/j.semperi.2013.11.004
117. Kluckow M. Functional echocardiography in assessment of the cardiovascular system in asphyxiated neonates. *J Pediatr.* (2011) 158(Suppl. 2):e13–8. doi: 10.1016/j.jpeds.2010.11.007
118. Konduri GG, Kim UO. Advances in the diagnosis and management of persistent pulmonary hypertension of the newborn. *Pediatr Clin North America.* (2009) 56:579–600. doi: 10.1016/j.pcl.2009.04.004
119. McNamara PJ, Laique F, Muang-In S, Whyte HE. Milrinone improves oxygenation in neonates with severe persistent pulmonary hypertension of the newborn. *J Crit Care.* (2006) 21:217–22. doi: 10.1016/j.jcrc.2006.01.001
120. Bassler D, Kreutzer K, McNamara P, Kirpalani H. Milrinone for persistent pulmonary hypertension of the newborn. *Cochrane Database Syst Rev.* (2010) 2010:Cd007802. doi: 10.1002/14651858.CD007802.pub2
121. Rieg AD, Schroth SC, Grottke O, Hein M, Ackermann D, Rossaint R, et al. Influence of temperature on the positive inotropic effect of levosimendan, dobutamine and milrinone. *Eur J Anaesthesiol.* (2009) 26:946–53. doi: 10.1097/EJA.0b013e328330e9a0
122. Kelly LE, Ohlsson A, Shah PS. Sildenafil for pulmonary hypertension in neonates. *The Cochrane Database Syst Rev.* (2017) 8:Cd005494. doi: 10.1002/14651858.CD005494.pub4

123. Barrington KJ, Finer N, Pennaforte T, Altit G. Nitric oxide for respiratory failure in infants born at or near term. *Cochrane Database Syst Rev.* (2017) 1:Cd000399. doi: 10.1002/14651858.CD000399.pub3
124. Rosenberg AA, Lee NR, Vaver KN, Werner D, Fashaw L, Hale K, et al. School-age outcomes of newborns treated for persistent pulmonary hypertension. *J Perinatol.* (2010) 30:127–34. doi: 10.1038/jp.2009.139
125. Lipkin PH, Davidson D, Spivak L, Straube R, Rhines J, Chang CT. Neurodevelopmental and medical outcomes of persistent pulmonary hypertension in term newborns treated with nitric oxide. *J Pediatr.* (2002) 140:306–10. doi: 10.1067/mpd.2002.122730
126. Hankins GD, Koen S, Gei AF, Lopez SM, Van Hook JW, Anderson GD. Neonatal organ system injury in acute birth asphyxia sufficient to result in neonatal encephalopathy. *Obstet Gynecol.* (2002) 99:688–91. doi: 10.1097/00006250-200205000-00004
127. Szakmar E, Jermendy A, El-Dib M. Respiratory management during therapeutic hypothermia for hypoxic-ischemic encephalopathy. *J Perinatol.* (2019) 39:763–73. doi: 10.1038/s41372-019-0349-2
128. Stayer SA, Liu Y. Pulmonary hypertension of the newborn. *Best Pract Res Clin Anaesthesiol.* (2010) 24:375–86. doi: 10.1016/j.bpa.2010.02.021
129. Dhillon R. The management of neonatal pulmonary hypertension. *Arch Disease Child Fetal Neonatal Ed.* (2012) 97:F223–8. doi: 10.1136/adc.2009.180091
130. American Academy of Pediatrics American Heart Association GMW, MD,FAAP Jeanette Zaichkin, RN,MN,NNP-BC. *Neonatal Resuscitation Guideline*. (2016). 7th addition.
131. "Jonathan Wylliea? Jos B, Charles Christoph Roehrde, Mario Rüdigerf, Daniele Trevisanutoc, Berndt Urlesbergerg,". European Resuscitation Council Guidelines. (2015).
132. Torres-Cuevas I, Parra-Llorca A, Sanchez-Illana A, Nunez-Ramiro A, Kuligowski J, Chafer-Pericas C, et al. Oxygen and oxidative stress in the perinatal period. *Redox Biol.* (2017) 12:674–81. doi: 10.1016/j.redox.2017.03.011
133. Vento M, Asensi M, Sastre J, Lloret A, Garcia-Sala F, Vina J. Oxidative stress in asphyxiated term infants resuscitated with 100% oxygen. *J Pediatr.* (2003) 142:240–6. doi: 10.1067/mpd.2003.91
134. Kattwinkel J. Evaluating resuscitation practices on the basis of evidence: the findings at first glance may seem illogical. *J Pediatr.* (2003) 142:221–2. doi: 10.1067/mpd.2003.147
135. Wung JT, James LS, Kilchevsky E, James E. Management of infants with severe respiratory failure and persistence of the fetal circulation, without hyperventilation. *Pediatrics.* (1985) 76:488–94.
136. Walsh-Sukys MC, Cornell DJ, Houston LN, Keszler M, Kanto WP Jr. Treatment of persistent pulmonary hypertension of the newborn without hyperventilation: an assessment of diffusion of innovation. *Pediatrics.* (1994) 94:303–6.
137. Sahni R, Wung JT, James LS. Controversies in management of persistent pulmonary hypertension of the newborn. *Pediatrics.* (1994) 94:307–9.
138. Abu-Osba YK. Treatment of persistent pulmonary hypertension of the newborn: update. *Arch Dis Child.* (1991) 66:74–7. doi: 10.1136/adc.66.1_Spec_No.74
139. Marron MJ, Crisafi MA, Driscoll JM Jr, Wung JT, Driscoll YT, et al. Hearing and neurodevelopmental outcome in survivors of persistent pulmonary hypertension of the newborn. *Pediatrics.* (1992) 90:392–6.
140. Kety SS, Schmidt CF. The effects of active and passive hyperventilation on cerebral blood flow, cerebral oxygen consumption, cardiac output, and blood pressure of normal young men. *J Clin Invest.* (1946) 25:107–19. doi: 10.1172/JCI101680
141. Kennealy JA, McLennan JE, Loudon RG, McLaurin RL. Hyperventilation-induced cerebral hypoxia. *Am Rev Resp Dis.* (1980) 122:407–12.
142. Pappas A, Shankaran S, Laptook AR, Langer JC, Bara R, Ehrenkranz RA, et al. Hypocarbia and adverse outcome in neonatal hypoxic-ischemic encephalopathy. *J Pediatr.* (2011) 158:752–8. doi: 10.1016/j.jpeds.2010.10.019
143. Ferrara B, Johnson DE, Chang PN, Thompson TR. Efficacy and neurologic outcome of profound hypocapneic alkalosis for the treatment of persistent pulmonary hypertension in infancy. *J Pediatr.* (1984) 105:457–61. doi: 10.1016/S0022-3476(84)80029-3
144. Graziani LJ, Baumgart S, Desai S, Stanley C, Gringlas M, Spitzer AR. Clinical antecedents of neurologic and audiologic abnormalities in survivors of neonatal extracorporeal membrane oxygenation. *J Child Neurol.* (1997) 12:415–22. doi: 10.1177/088307389701200702
145. Groenendaal F, De Vooght KM, van Bel F. Blood gas values during hypothermia in asphyxiated term neonates. *Pediatrics.* (2009) 123:170–2. doi: 10.1542/peds.2008-1955
146. Klinger G, Beyene J, Shah P, Perlman M. Do hyperoxaemia and hypocapnia add to the risk of brain injury after intrapartum asphyxia? *Arch Dis Child Fetal Neonatal Ed.* (2005) 90:F49–52. doi: 10.1136/adc.2003.048785
147. Bisson J, Younker J. Correcting arterial blood gases for temperature: (when) is it clinically significant? *Crit Care Nurse.* (2006) 11:232–8. doi: 10.1111/j.1478-5153.2006.00177.x
148. Eicher DJ, Wagner CL, Katikaneni LP, Hulsey TC, Bass WT, Kaufman DA, et al. Moderate hypothermia in neonatal encephalopathy: safety outcomes. *Pediatr Neurol.* (2005) 32:18–24. doi: 10.1016/j.pediatrneurol.2004.06.015
149. Askenazi DJ, Ambalavanan N, Goldstein SL. Acute kidney injury in critically ill newborns: what do we know? What do we need to learn? *Pediatr Nephrol.* (2009) 24:265–74. doi: 10.1007/s00467-008-1060-2
150. Selewski DT, Jordan BK, Askenazi DJ, Dechert RE, Sarkar S. Acute kidney injury in asphyxiated newborns treated with therapeutic hypothermia. *J Pediatr.* (2013) 162:725–9. doi: 10.1016/j.jpeds.2012.10.002
151. Sarkar S, Askenazi DJ, Jordan BK, Bhagat I, Bapuraj JR, Dechert RE, et al. Relationship between acute kidney injury and brain MRI findings in asphyxiated newborns after therapeutic hypothermia. *Pediatr Res.* (2014) 75:431–5. doi: 10.1038/pr.2013.230
152. Kidney Disease: Improving Global Outcomes (KDIGO) CKD-MBD Work Group. KDIGO clinical practice guideline for the diagnosis, evaluation, prevention, and treatment of Chronic Kidney Disease-Mineral and Bone Disorder (CKD-MBD). *Kidney Int Suppl.* (2009) S1–130. doi: 10.1038/ki.2009.188
153. Treiber M, Gorenjak M, Balon BP. Serum cystatin-c as a marker of acute kidney injury in the newborn after perinatal hypoxia/asphyxia. *Ther Apher Dial.* (2014) 18:57–67. doi: 10.1111/1744-9987.12054
154. Goldstein SL. Urinary NGAL to define AKI in asphyxiated infants. *Pediatr Nephrol.* (2015) 30:1047–9. doi: 10.1007/s00467-015-3046-1
155. Sweetman DU, Molloy EJ. Biomarkers of acute kidney injury in neonatal encephalopathy. *Eur J Pediatr.* (2013) 172:305–16. doi: 10.1007/s00431-012-1890-6
156. Sweetman DU, Onwuneme C, Watson WR, O'Neill A, Murphy JF, Molloy EJ. Renal function and novel urinary biomarkers in infants with neonatal encephalopathy. *Acta Paediatr.* (2016) 105:e513–e9. doi: 10.1111/apa.13555
157. Jacobs SE. Selective head cooling with mild systemic hypothermia after neonatal encephalopathy: Multicentre randomised trial. *J Pediatr.* (2005) 147:122–3. doi: 10.1016/j.jpeds.2005.04.047
158. Kecskes Z, Healy G, Jensen A. Fluid restriction for term infants with hypoxic-ischaemic encephalopathy following perinatal asphyxia. *Cochrane Database Syst Rev*. (2005) 2005:Cd004337. doi: 10.1002/14651858.CD004337.pub2
159. Tanigasalam V, Plakkal N, Vishnu Bhat B, Chinnakali P. Does fluid restriction improve outcomes in infants with hypoxic ischemic encephalopathy? A pilot randomized controlled trial. *J Perinatol.* (2018) 38:1512–7. doi: 10.1038/s41372-018-0223-7
160. Bartter FC, Schwartz WB. The syndrome of inappropriate secretion of antidiuretic hormone. *Am J Med.* (1967) 42:790–806. doi: 10.1016/0002-9343(67)90096-4
161. Modi N. Hyponatraemia in the newborn. *Arch Dis Child Fetal Neonatal Ed.* (1998) 78:F81–4. doi: 10.1136/fn.78.2.F81
162. Bergelson J, Zaoutis T, Shah SS. *Pediatric Infectious Diseases: The Requisites in Pediatrics*. Philadelphia, PA: Mosby (2008).
163. Favie LMA, Groenendaal F, van den Broek MPH, Rademaker CMA, de Haan TR, van Straaten HLM, et al. Pharmacokinetics of morphine in encephalopathic neonates treated with therapeutic hypothermia. *PLoS ONE.* (2019) 14:e0211910. doi: 10.1371/journal.pone.0211910
164. Yildiz N, Erguven M, Yildiz M, Ozdogan T, Turhan P. Acute peritoneal dialysis in neonates with acute kidney injury and hypernatremic dehydration. *Perit Dial Int.* (2013) 33:290–6. doi: 10.3747/pdi.2011.00211
165. Mammen C, Al Abbas A, Skippen P, Nadel H, Levine D, Collet JP, et al. Long-term risk of CKD in children surviving episodes of acute kidney injury in

the intensive care unit: a prospective cohort study. *Am J Kidney Dis.* (2012) 59:523–30. doi: 10.1053/j.ajkd.2011.10.048
166. Gluckman PD, Wyatt JS, Azzopardi D, Ballard R, Edwards AD, Ferriero DM, et al. Selective head cooling with mild systemic hypothermia after neonatal encephalopathy: multicentre randomised trial. *Lancet.* (2005) 365:663–70. doi: 10.1016/S0140-6736(05)70932-6
167. Shankaran S, Laptook AR, Ehrenkranz RA, Tyson JE, McDonald SA, Donovan EF, et al. Whole-body hypothermia for neonates with hypoxic-ischemic encephalopathy. *N Engl J Med.* (2005) 353:1574–84. doi: 10.1056/NEJMcps050929
168. Chang LL, Wynn JL, Pacella MJ, Rossignol CC, Banadera F, Alviedo N, et al. Enteral feeding as an adjunct to hypothermia in neonates with hypoxic-ischemic encephalopathy. *Neonatology.* (2018) 113:347–52. doi: 10.1159/000487848
169. Sweetman DU, Riordan M, Molloy EJ. Management of renal dysfunction following term perinatal hypoxia-ischaemia. *Acta Paediatr.* (2013) 102:233–41. doi: 10.1111/apa.12116
170. Nadeem M, Murray DM, Boylan GB, Dempsey EM, Ryan CA. Early blood glucose profile and neurodevelopmental outcome at two years in neonatal hypoxic-ischaemic encephalopathy. *BMC Pediatr.* (2011) 11:10. doi: 10.1186/1471-2431-11-10
171. Tam EW, Haeusslein LA, Bonifacio SL, Glass HC, Rogers EE, Jeremy RJ, et al. Hypoglycemia is associated with increased risk for brain injury and adverse neurodevelopmental outcome in neonates at risk for encephalopathy. *J Pediatr.* (2012) 161:88–93. doi: 10.1016/j.jpeds.2011.12.047
172. Kramer AH, Roberts DJ, Zygun DA. Optimal glycemic control in neurocritical care patients: a systematic review and meta-analysis. *Crit Care.* (2012) 16:R203. doi: 10.1186/cc11812
173. Wong DS, Poskitt KJ, Chau V, Miller SP, Roland E, Hill A, et al. Brain injury patterns in hypoglycemia in neonatal encephalopathy. *AJNR.* (2013) 34:1456–61. doi: 10.3174/ajnr.A3423
174. Spies EE, Lababidi SL, McBride MC. Early hyperglycemia is associated with poor gross motor outcome in asphyxiated term newborns. *Pediatr Neurol.* (2014) 50:586–90. doi: 10.1016/j.pediatrneurol.2014.01.043
175. Basu P, Som S, Choudhuri N, Das H. Contribution of the blood glucose level in perinatal asphyxia. *Eur J Pediatr.* (2009) 168:833–8. doi: 10.1007/s00431-008-0844-5
176. Kallem VR, Pandita A, Gupta G. Hypoglycemia: when to treat? *Clin Med Insights Pediatr.* (2017) 11:1179556517748913. doi: 10.1177/1179556517748913
177. Hankins GDV, Koen S, Gei AF, Lopez SM, Van Hook JW, Anderson GD. Neonatal organ system injury in acute birth asphyxia sufficient to result in neonatal encephalopathy. *Obstet Gynecol.* (2002) 99:688–91. doi: 10.1016/S0029-7844(02)01959-2
178. Choudhary M, Sharma D, Dabi D, Lamba M, Pandita A, Shastri S. Hepatic dysfunction in asphyxiated neonates: prospective case-controlled study. *Clin Med Insights Pediatr.* (2015) 9:1–6. doi: 10.4137/CMPed.S21426
179. Muniraman H, Gardner D, Skinner J, Paweletz A, Vayalakkad A, Chee YH, et al. Biomarkers of hepatic injury and function in neonatal hypoxic ischemic encephalopathy and with therapeutic hypothermia. *Eur J Pediatr.* (2017) 176:1295–303. doi: 10.1007/s00431-017-2956-2
180. Pakvasa MA, Winkler AM, Hamrick SE, Josephson CD, Patel RM. Observational study of haemostatic dysfunction and bleeding in neonates with hypoxic-ischaemic encephalopathy. *BMJ Open.* (2017) 7:e013787. doi: 10.1136/bmjopen-2016-013787
181. Forman KR, Diab Y, Wong EC, Baumgart S, Luban NL, Massaro AN. Coagulopathy in newborns with hypoxic ischemic encephalopathy (HIE) treated with therapeutic hypothermia: a retrospective case-control study. *BMC Pediatr.* (2014) 14:277. doi: 10.1186/1471-2431-14-277
182. Perlman JM, Davis P, Wyllie J, Kattwinkel J. Therapeutic hypothermia following intrapartum hypoxia-ischemia. an advisory statement from the Neonatal Task Force of the International Liaison Committee on Resuscitation. *Resuscitation.* (2010) 81:1459–61. doi: 10.1016/j.resuscitation.2010.07.006
183. Rohrer MJ, Natale AM. Effect of hypothermia on the coagulation cascade. *Crit. Care Med.* (1992) 20:1402–5. doi: 10.1097/00003246-199210000-00007
184. Shankaran S, Pappas A, Laptook AR, McDonald SA, Ehrenkranz RA, Tyson JE, et al. Outcomes of safety and effectiveness in a multicenter randomized, controlled trial of whole-body hypothermia for neonatal hypoxic-ischemic encephalopathy. *Pediatrics.* (2008) 122:e791–8. doi: 10.1542/peds.2008-0456
185. Castle V, Coates G, Mitchell LG, O'Brodovich H, Andrew M. The effect of hypoxia on platelet survival and site of sequestration in the newborn rabbit. *Thromb. Haemost.* (1988) 59:45–8. doi: 10.1055/s-0038-1642563
186. Cheung PY, Stevens JP, Haase E, Stang L, Bigam DL, Etches W, et al. Platelet dysfunction in asphyxiated newborn piglets resuscitated with 21% and 100% oxygen. *Pediatr Res.* (2006) 59:636–40. doi: 10.1203/01.pdr.0000214894.18097.c4
187. El Beshlawy A, Hussein HA, Abou-Elew HH, Abdel Kader MS. Study of protein C, protein S, and antithrombin III in hypoxic newborns. *Pediatr Crit Care Med.* (2004) 5:163–6. doi: 10.1097/01.PCC.0000113261.13338.C3
188. McDonald DG, Kelehan P, McMenamin JB, Gorman WA, Madden D, Tobbia IN, et al. Placental fetal thrombotic vasculopathy is associated with neonatal encephalopathy. *Hum. Pathol.* (2004) 35:875–80. doi: 10.1016/j.humpath.2004.02.014
189. Ramaswamy V, Miller SP, Barkovich AJ, Partridge JC, Ferriero DM. Perinatal stroke in term infants with neonatal encephalopathy. *Neurology.* (2004) 62:2088–91. doi: 10.1212/01.WNL.0000129909.77753.C4
190. Harbert MJ, Tam EW, Glass HC, Bonifacio SL, Haeusslein LA, Barkovich AJ, et al. Hypothermia is correlated with seizure absence in perinatal stroke. *J Child Neurol.* (2011) 26:1126–30. doi: 10.1177/0883073811408092
191. Radicioni M, Bini V, Chiarini P, Fantauzzi A, Leone F, Scattoni R, et al. Cerebral sinovenous thrombosis in the asphyxiated cooled infants: a prospective observational study. *Pediatr Neurol.* (2017) 66:63–8. doi: 10.1016/j.pediatrneurol.2016.09.006
192. Lehman LL, Rivkin MJ. Perinatal arterial ischemic stroke: presentation, risk factors, evaluation, and outcome. *Pediatr Neurol.* (2014) 51:760–8. doi: 10.1016/j.pediatrneurol.2014.07.031
193. Sweetman DLP, Molloy E. Poor motor outcome at 2 years of age is predicted by elevated leukocyte count in infants with perinatal asphyxia. *Arch Dis Child.* (2012) 97:A304. doi: 10.1136/archdischild-2012-302724.1060
194. Morkos AA, Hopper AO, Deming DD, Yellon SM, Wycliffe N, Ashwal S, et al. Elevated total peripheral leukocyte count may identify risk for neurological disability in asphyxiated term neonates. *J Perinatol.* (2007) 27:365–70. doi: 10.1038/sj.jp.7211750
195. Nelson KB, Leviton A. How much of neonatal encephalopathy is due to birth asphyxia? *Am J Dis Child.* (1991) 145:1325–31. doi: 10.1001/archpedi.1991.02160110117034
196. Robertson NJ, Nakakeeto M, Hagmann C, Cowan FM, Acolet D, Iwata O, et al. Therapeutic hypothermia for birth asphyxia in low-resource settings: a pilot randomised controlled trial. *Lancet.* (2008) 372:801–3. doi: 10.1016/S0140-6736(08)61329-X
197. Falck M, Osredkar D, Maes E, Flatebo T, Wood TR, Sabir H, et al. Hypothermic neuronal rescue from infection-sensitised hypoxic-ischaemic brain injury is pathogen dependent. *Dev Neurosci.* (2017) 39:238–47. doi: 10.1159/000455838
198. Shang Y, Mu L, Guo X, Li Y, Wang L, Yang W, et al. Clinical significance of interleukin-6, tumor necrosis factor-alpha and high-sensitivity C-reactive protein in neonates with hypoxic-ischemic encephalopathy. *Exp. Ther. Med.* (2014) 8:1259–62. doi: 10.3892/etm.2014.1869
199. Tann CJ, Martinello KA, Sadoo S, Lawn JE, Seale AC, Vega-Poblete M, et al. Neonatal encephalopathy with group B streptococcal disease worldwide: systematic review, investigator group datasets, and meta-analysis. *Clini Infect Dis.* (2017) 65(Suppl. 2):S173–89. doi: 10.1093/cid/cix662
200. Cilla A, Arnaez J, Suarez J, Megias G, Cabrerizo M, Garcia-Alix A. Perinatal infection and hypoxic-ischemic encephalopathy: a pilot study. *J Matern Fetal Neonatal Med.* (2016) 29:140–2. doi: 10.3109/14767058.2014.991303
201. Allen UD, Robinson JL. Prevention and management of neonatal herpes simplex virus infections. *Paediatr Child Health.* (2014) 19:201–12. doi: 10.1093/pch/19.4.201
202. Cherpes TL, Matthews DB, Maryak SA. Neonatal herpes simplex virus infection. *Clin Obstetr Gynecol.* (2012) 55:938–44. doi: 10.1097/GRF.0b013e31827146a7
203. Schreiber R, Wolpin J, Koren G. Determinants of aciclovir-induced nephrotoxicity in children. *Paediatr Drugs.* (2008) 10:135–9. doi: 10.2165/00148581-200810020-00008

204. Strohm B, Hobson A, Brocklehurst P, Edwards AD, Azzopardi D. Subcutaneous fat necrosis after moderate therapeutic hypothermia in neonates. *Pediatrics.* (2011) 128:e450–2. doi: 10.1542/peds.2010-3508
205. Samedi VM, Yusuf K, Yee W, Obaid H, Al Awad EH. Neonatal hypercalcemia secondary to subcutaneous fat necrosis successfully treated with pamidronate: a case series and literature review. *AJP Rep.* (2014) 4:e93–6. doi: 10.1055/s-0034-1395987
206. Filippi L, Catarzi S, Padrini L, Fiorini P, la Marca G, Guerrini R, et al. Strategies for reducing the incidence of skin complications in newborns treated with whole-body hypothermia. *J Matern Fetal Neonatal Med.* (2012) 25:2115–21. doi: 10.3109/14767058.2012.683898
207. Saudubray JM, Garcia-Cazorla A. Inborn errors of metabolism overview: pathophysiology, manifestations, evaluation, and management. *Pediatr Clin North Am.* (2018) 65:179–208. doi: 10.1016/j.pcl.2017.11.002
208. Lin CC. [EEG manifestations in metabolic encephalopathy]. *Acta Neurol Taiwanica.* (2005) 14:151–61.
209. Burton BK. Inborn errors of metabolism in infancy: a guide to diagnosis. *Pediatrics.* (1998) 102:E69. doi: 10.1542/peds.102.6.e69
210. Mary Rutherford ZP, Nicola J, Robertson I, Jane C. *MRI of the Neonatal Brain*. Available online at: http://www.mrineonatalbrain.com/
211. Khalessi N, Khosravi N, Mirjafari M, Afsharkhas L. Plasma ammonia levels in newborns with asphyxia. *Iran J Child Neurol.* (2016) 10:42–6.
212. Janet M Rennie GK. *A Manual of Neonatal Intensive Care* (2013).
213. Perlman JM, Tack ED, Martin T, Shackelford G, Amon E. Acute systemic organ injury in term infants after asphyxia. *Am J Dis Child.* (1989). 143:617–20. doi: 10.1001/archpedi.1989.02150170119037
214. Alsina M, Martin-Ancel A, Alarcon-Allen A, Arca G, Gaya F, Garcia-Alix A. The severity of hypoxic-ischemic encephalopathy correlates with multiple organ dysfunction in the hypothermia era. *Pediatr Crit Care Med.* (2017) 18:234–40. doi: 10.1097/PCC.0000000000001068
215. Group D-NBW. *FDA-NIH Biomarker Working Group*. BEST (Biomarkers, EndpointS, and other Tools)

Conflict of Interest: The authors declare that the research was conducted in the absence of any commercial or financial relationships that could be construed as a potential conflict of interest.

frontiers in Pediatrics

ORIGINAL RESEARCH
published: 05 June 2020
doi: 10.3389/fped.2020.00289

Neonatal Hypoxic-Ischemic Encephalopathy Yields Permanent Deficits in Learning Acquisition: A Preclinical Touchscreen Assessment

Jessie R. Maxwell[1,2], *Amber J. Zimmerman*[2], *Nathaniel Pavlik*[1], *Jessie C. Newville*[2], *Katherine Carlin*[3], *Shenandoah Robinson*[4], *Jonathan L. Brigman*[2], *Frances J. Northington*[3] *and Lauren L. Jantzie*[3,5,6]*

[1] Department of Pediatrics, University of New Mexico, Albuquerque, NM, United States, [2] Department of Neurosciences, University of New Mexico, Albuquerque, NM, United States, [3] Division of Neonatal-Perinatal Medicine, Department of Pediatrics, Johns Hopkins University School of Medicine, Baltimore, MD, United States, [4] Department of Neurosurgery, Johns Hopkins University School of Medicine, Baltimore, MD, United States, [5] Department of Neurology, Johns Hopkins University School of Medicine, Baltimore, MD, United States, [6] Department of Neurology, Kennedy Krieger Institute, Baltimore, MD, United States

OPEN ACCESS

Edited by:
Changlian Zhu,
Third Affiliated Hospital of Zhengzhou University, China

Reviewed by:
Ana A. Baburamani,
King's College London, United Kingdom
Jacques-Olivier Coq,
UMR7289 Institut de Neurosciences de la Timone (INT), France

***Correspondence:**
Lauren L. Jantzie
LJantzie@jhmi.edu

Specialty section:
This article was submitted to Neonatology, a section of the journal Frontiers in Pediatrics

Received: *10 January 2020*
Accepted: *07 May 2020*
Published: *05 June 2020*

Citation:
Maxwell JR, Zimmerman AJ, Pavlik N, Newville JC, Carlin K, Robinson S, Brigman JL, Northington FJ and Jantzie LL (2020) Neonatal Hypoxic-Ischemic Encephalopathy Yields Permanent Deficits in Learning Acquisition: A Preclinical Touchscreen Assessment. Front. Pediatr. 8:289. doi: 10.3389/fped.2020.00289

Neonatal hypoxic-ischemic encephalopathy (HIE) remains a common problem world-wide for infants born at term. The impact of HIE on long-term outcomes, especially into adulthood, is not well-described. To facilitate identification of biobehavioral biomarkers utilizing a translational platform, we sought to investigate the impact of HIE on executive function and cognitive outcomes into adulthood utilizing a murine model of HIE. HIE mice (unilateral common carotid artery occlusion to induce ischemia, followed by hypoxia with a FiO_2 of 0.08 for 45 min) and control mice were tested on discrimination and reversal touchscreen tasks (using their noses) shown to be sensitive to loss of basal ganglia or cortical function, respectively. We hypothesized that the HIE injury would result in deficits in reversal learning, revealing complex cognitive and executive functioning impairments. Following HIE, mice had a mild discrimination impairment as measured by incorrect responses but were able to learn the paradigm to similar levels as controls. During reversal, HIE mice required significantly more total trials, errors and correction trials across the paradigm. Analysis of specific stages showed that reversal impairments in HIE were driven by significant increases in all measured parameters during the late learning, striatal-mediated portion of the task. Together, these results support the concept that HIE occurring during the neonatal period results in abnormal neurodevelopment that persists into adulthood, which can impact efficient associated learning. Further, these data show that utilization of an established model of HIE coupled with touchscreen learning provides valuable information for screening therapeutic interventions that could mitigate these deficits to improve the long-term outcomes of this vulnerable population.

Keywords: biobehavioral biomarker, HIE, touchscreen, learning acquisition, cognitive flexibility, reversal learning

INTRODUCTION

Neonatal hypoxic-ischemic encephalopathy (HIE) occurs in as many as 6 infants per 1,000 live births (1–4). While there is likely an acute event occurring around delivery, the injury observed in HIE is likely a combination of acute on chronic injury (5). Recent placental studies have found that chronic fetal vascular malperfusion appears to be associated with neonatal HIE, leading to the hypothesis that impaired fetal blood flow may result in the infant being more susceptible to brain injury from altered cerebral blood flow in the setting of an acute event (5, 6).

Children with a history of HIE are at high risk of abnormal cognitive development. Unfortunately, more than half of infants have abnormal neurodevelopment following HIE (1, 7). Additionally, even those infants with mild HIE, previously thought to have normal outcomes, have been observed to have abnormal neurodevelopment with deficits apparent in childhood including lower cognitive composite scores (1, 8). While executive function is an umbrella term used to describe the processes necessary to achieve goal-directed behavior, multiple domain specific deficits have been reported after HIE in children. A recent analysis reports that 22% of children with moderate HIE and no cerebral palsy were found to attend special education, compared to all of the control group attending mainstream school (9). Thus, it is paramount that we further investigate the long-term deficits in cognition these children may have following this perinatal injury.

Characterizing the spectrum of brain injury and identifying biobehavioral biomarkers are critical to predict outcomes and advance novel therapeutic interventions for children with HIE. Brain magnetic resonance imaging (MRI) was used in a term infant population with neonatal encephalopathy, and found evidence of acute insult without evidence of established injury or atrophy in 69–80% of the infants imaged (10–12), supporting the concept that the brain injury is occurring around the time of delivery. Specific regions of the brain seem to be more susceptible to injury in the setting of HIE, and include cerebral cortex, basal ganglia, putamen, thalamus, and brainstem (13–15). Additionally, cerebral white matter is also often injured (15) as well as the hippocampus (16).

Animal models have been utilized to characterize the brain injury following HIE more specifically, with rigorous characterization of the pathophysiology occurring during the newborn period. The Rice-Vannucci model is currently accepted as the standard model of term HIE. Studies have described the injury that occurs following this model, including cellular injury from mitochondrial dysfunction and oxidative stress, injury to the hippocampus, caudate-putamen, cerebral cortex, and thalamus (17–20). Currently, data defining the specific pillars of cognition impacted in adulthood by HIE is a gap in knowledge. Therefore, we sought to test the hypothesis that HIE would yield deficits in complex cognitive and executive functioning using a translational touchscreen approach sensitive enough to detect changes in functional outcome across many models of perinatal brain injury. Specifically, we tested the effects of neonatal HIE on a touchscreen platform to assess cognitive function in adulthood and we examined whether pairwise visual discrimination learning and reversal, known to be mediated by separate regions of the brain (21), were sensitive to long-term injury following HIE. Utilizing a touchscreen platform that incorporates stimuli, learning rules and response actions that mimic those used in human cognitive assessments such as the Cambridge Automated Neuropsychological Test Automated Battery (CANTAB), we investigated a validated, translational measure of cognitive function following HIE (22–24). Discrimination and reversal learning are heavily dependent on orbitofrontal-striatal connections in both humans and rodents (25, 26). Reversal learning is a paradigm to assess cognitive flexibility in the setting of changing stimulus-outcome or response-outcome (26). Different stages of learning can be assessed by looking at specific times during the reversal paradigm, including early (<50% correct) and late (>50% correct). Thus, the utilization of this testing paradigm allows for insight into specific characterization of cognitive deficits observed followed HIE in a preclinical model. We predicted that mice subject to HIE would have cognitive deficits as adults, defined by deficits in reversal learning, specifically the learning or later portion, reflective of the structural brain injury extensively published in this model (13, 17–20, 27–32).

MATERIALS AND METHODS

Animals

All experimental procedures were approved by the Institutional Animal Care and Use Committee (IACUC) of the University of New Mexico. All animal studies were carried out with standards of care and housing in accordance with the National Institutes of Health Guide for the Care and Use of Laboratory Animals, US Department of Health and Human Services. C57BL/6 male ($n = 12$) and female mice ($n = 16$) were used for a total of 28 mice.

Neonatal Hypoxic Ischemic Brain Injury Model

To induce hypoxic-ischemic (HI) injury in a term-equivalent population, the Rice-Vannucci model was adapted for use in mice at postnatal day 10 (P10), as previously published (18, 29, 33–35). Briefly, mice were anesthetized with 3% isoflurane for induction and maintained with 1% isoflurane throughout the procedure and kept normothermic. The right common carotid artery was isolated and ligated via double suture to result in a permanent unilateral carotid ligation. The incision was closed with dermabond, and the mouse recovered for 1 h with their littermates. Mice with unilateral carotid ligation then underwent hypoxia for 45 min with an FiO_2 of 0.08 in a humidified, temperature-controlled hypoxia chamber (29, 36, 37). Sham mice were anesthetized, with carotid artery isolated but not ligated. They were not exposed to hypoxia. Each litter consisted of both HI and sham mice. Following completion of the experiment, mice matured with their dams until weaning at P21.

Touchscreen Cognitive Assessment

All operant behavior was conducted in a chamber measuring 21.6 × 17.8 × 12.7 cm (model # ENV-307W, Med Associates, St.

Albans, VT) housed within a sound- and light attenuating box (Med Associates, St. Albans, VT). A solid acrylic plate was used to cover the grid floor of the chamber to facilitate ambulation. A peristaltic pump delivered 30 μl of liquid strawberry milkshake (strawberry Nesquik mixed with skim milk) into a magazine as required. A house-light, tone generator and an ultra-sensitive lever was located on one end of the chamber, while a touch-sensitive screen (Conclusive Solutions, Sawbridgeworth, U.K.) was on the opposite side of the chamber covered by a black acrylic aperture plate, which creates two 7.5 × 7.5 cm touch areas separated by 1 cm and located at a height of 0.8 cm from the floor of the chamber. KLimbic Software Package v1.20.2 (Conclusive Solutions) controlled and recorded stimulus presentation and touches in the response windows.

Pretraining

Beginning at 8 weeks of age (∼P60 or adolescent human age equivalent), all mice were handled daily and were food-restricted to 85% of their free-feeding body weight. Food restriction ensures animals are properly motivated to obtain the reward during task performance and did not begin until all mice had reached 20 grams in weight. While HI mice were slightly smaller after HI surgery and through the second and third postnatal week consistent with the model, all mice reached the same weight prior to starting the food restriction. Operant training began once mice reached food-restricted weight at ∼10 weeks of age. Mice were first acclimated to the liquid reward by provision of ∼30 μl/mouse in the home cage for 3 days and then habituated to retrieving reward in the operant chamber. Mice were allowed 30 min to freely retrieve rewards available in the magazine. Mice retrieving at least 10 rewards within 30 min were moved to lever press training. Here, mice could only obtain reward by responding on an ultrasensitive lever within the chamber. Reward delivery was accompanied by the presentation of secondary reinforcers: a 2-sec, 65 dB auditory tone and illumination of a magazine light. For each trial, mice were required to collect the delivered reward (measured by magazine beam-break) before another reward was available via an active lever response. Mice were required to lever-press and collect 30 rewards in under 30 min before moving to acquisition testing.

Discrimination and Reversal

Pairwise discrimination and reversal was tested as previously described (38–41). Briefly, mice were first trained to discriminate 2 novel, approximately equally-luminescent stimuli, presented in the center of each window in a spatially pseudorandomized (left/right) manner, over 30-trial sessions (5-s inter-trial interval) using their nose (21, 42). The stimulus designated as correct was counterbalanced across mice and treatment. Responses at the correct stimulus window resulted in a 30 μl liquid reward, cued by a 1-s tone and illumination of the magazine. Responses at the incorrect stimulus window resulted in a forced timeout (10 s), signaled by illumination of the house-light. Correction trials following errors were presented with the correct stimulus presentation in the same window until a correct response was made. Discrimination criterion was ≥85% correct responding out of 30 trials, excluding correction trials, over 2 consecutive sessions. Reversal training began on the session after discrimination criterion was attained. Here, the designation of correct verses incorrect stimuli was reversed for each mouse. As for discrimination, there were 30-trial daily sessions until the mice reached a criterion of ≥85% correct responding (excluding correction trials) over 2 consecutive sessions. **Figure 1** summarizes the surgical procedure completed at P10, followed by recovery and pretraining on the touchscreen platform at 8 weeks of age. Visual discrimination was then completed, in which one stimulus was the correct response. Upon reaching criterion, reversal testing occurred in which the previously correct stimulus was now incorrect.

Statistical Analysis

For discrimination and reversal, the following dependent variables were analyzed: trials, errors, correction errors, reaction time (time from lever press initiation to screen touch) and magazine latency (time from screen touch to reward retrieval). In order to examine distinct phases of reversal (early perseverative and late learning) errors and correction errors for sessions where performance was below 50% and performance from 50% to criterion, were separately analyzed as previously described (25, 43). To analyze use of feedback for learning, correct and incorrect responses were further categorized based on previous trial outcome: correct responses were characterized as *win-stay* (following correct response) or *lose-shift* (following an error trial), while error trials were characterized as *perseverative* (following an error trial) or *regressive* (following correct response) as previously described (40). As assumptions for normality and equivalent variance were met, data were analyzed using unpaired *t*-tests followed by Bonferroni correction for multiple comparisons. Data is represented as mean ± standard error of the mean (SEM), with $p < 0.05$ designated as statistically significant.

RESULTS

Analysis of sex as a biological variable found no main effect of sex on any measure, and thus both sexes were combined by treatment for subsequent analysis [12 males (6 sham, 6 HIE) and 16 females (7 sham and 9 HIE) were used in total]. The average weights of the mice prior to food restriction was 20.01 grams ± 0.79. Examining pretraining, we found no significant differences between groups on any of the three stages (HIE: $n = 15$; Sham: $n = 13$). All mice in each group successfully completed visual discrimination to criterion. However, while the total number of trials during visual discrimination did not differ significantly between the HIE and sham groups ($t_{(26)} = 1.768$, $p = 0.09$; **Figure 2A**), the HIE group had significantly more incorrect responses compared to sham ($t_{(26)} = 2.304$, $p = 0.03$; **Figure 2B**). Additionally, no significant difference was noted in the number of correction trials during visual discrimination ($t_{(26)} = 1.540$, $p = 0.13$; **Figure 2C**). There was also no significant difference in the reaction time ($t_{(26)} = 1.204$, $p = 0.24$) or magazine latency ($t_{(26)} = 1.114$. $p = 0.28$) between the two groups during visual discrimination (**Figure 2D**), suggesting that alterations in learning were not

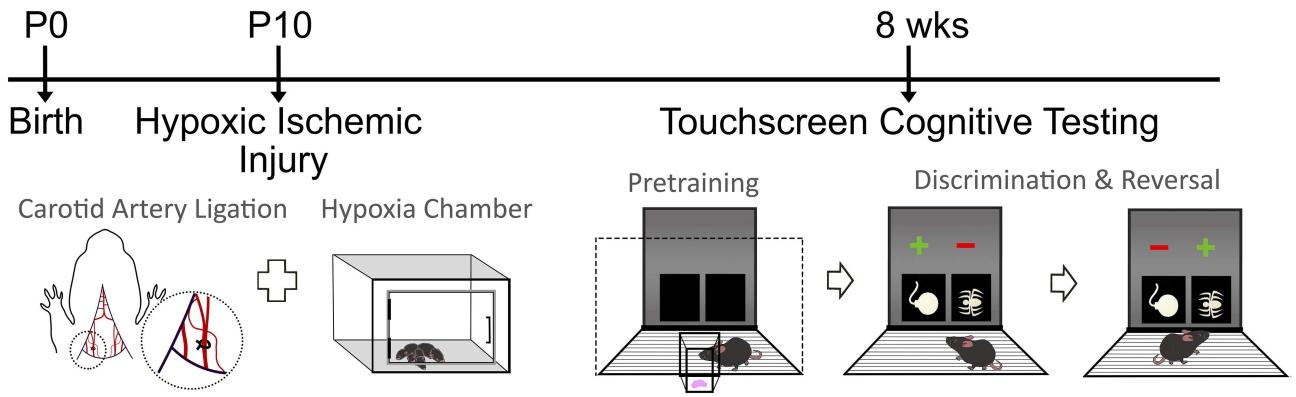

FIGURE 1 | Timeline of experimental design. Mice randomized to the HIE group underwent the carotid artery ligation and hypoxia chamber exposure at postnatal day 10 (P10). Following recovery, the touchscreen cognitive testing started with pretraining, followed by discrimination and reversal tasks in both sham and HIE groups. During pretraining, mice became familiar with the chamber and the food reward system. In discrimination, one symbol was the correct answer, which would result in a food reward if chosen. During reversal, the symbol that was previously correct became the incorrect response.

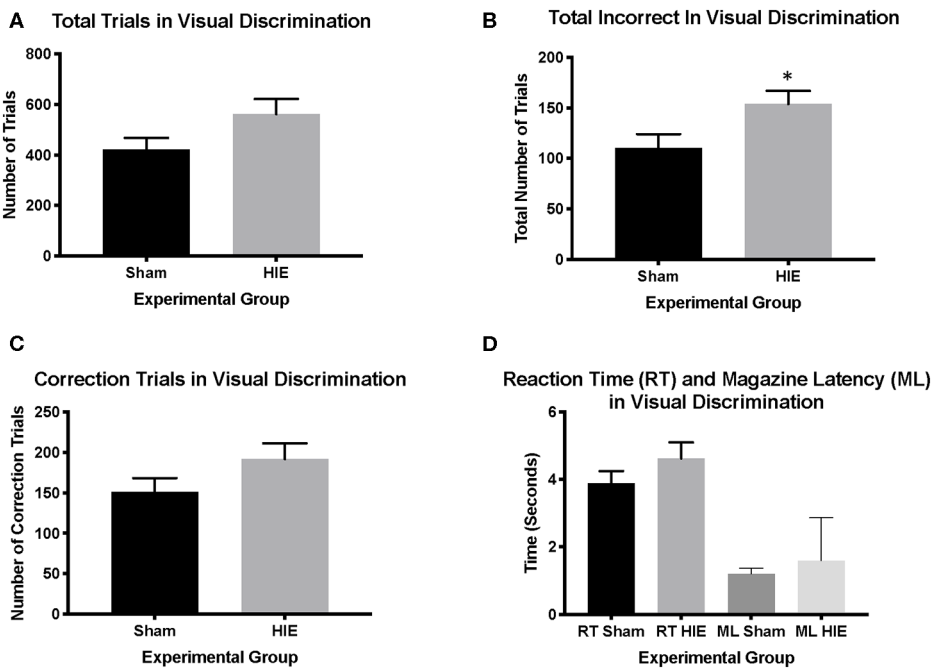

FIGURE 2 | Visual discrimination revealed more incorrect trials in the HIE group compared to sham. During visual discrimination, the total number of trials between the sham and the HIE group were not significantly different **(A)**. The HIE group did require significantly more incorrect trials to complete the visual discrimination component compared to sham **(B)**. Although the HIE group had more correction trials during visual discrimination, this was not significant **(C)**. There was no difference in either the reaction time or magazine latency between the two groups during visual discrimination **(D)** ($n = 13$–15, $^*p < 0.05$). Data is represented as mean ± standard error of the mean (SEM).

due to differences in motor behavior or motivation to work for reward.

Analysis of reversal performance revealed multiple significant differences between HIE and Sham control animals. HIE mice required significantly more total trials to complete the reversal compared to sham ($t_{(26)} = 2.196$, $p = 0.02$, **Figure 3A**). Similarly, HIE made significantly more errors ($t_{(26)} = 2.118$, $p = 0.04$, **Figure 3B**) and correction errors ($t_{(26)} = 2.494$, $p = 0.02$, **Figures 2**, **3C**) compared to sham control animals. Consistent with discrimination, HIE and sham did not differ significantly on either reaction time ($t_{(26)} = 0.911$, p=0.37) or magazine latency ($t_{(26)} = 0.722$, $p = 0.48$) across the reversal (**Figure 3D**). Analysis of reversal learning by stage revealed that HIE animals needed similar number of trials ($t_{(26)} = 1.948$, $p = 0.06$) and made similar numbers errors ($t_{(26)} = 0.978$, $p = 0.33$) and correction errors ($t_{(26)} = 1.384$, $p = 0.18$) during the early, perseverative,

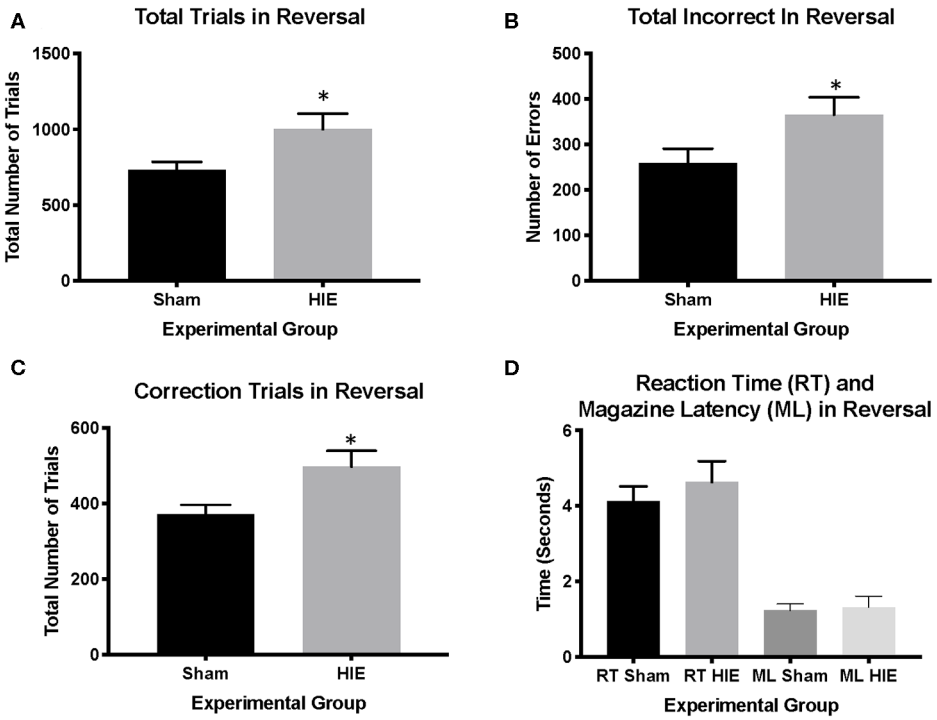

FIGURE 3 | HIE induces reversal learning Deficits. The HIE group required significantly more trials to complete reversal compared to the sham group **(A)**, as well as more incorrect responses during reversal **(B)**. Additionally, the HIE group completed significantly more correction trials compared to the sham group **(C)**. There was no difference in either the reaction time or magazine latency between the two groups during reversal **(D)** ($n = 13$–15, $^*p < 0.05$). Data is represented as mean ± standard error of the mean (SEM).

stage of reversal (**Figures 4A–C**). However, during the learning phase of reversal testing, the HIE group needed significantly more trials ($t_{(26)} = 2.374$, $p = 0.03$, **Figure 4D**), and made significantly more errors ($t_{(26)} = 3.021$, $p = 0.005$, **Figure 4E**) and required more correction trials ($t_{(26)} = 2.723$, $p = 0.01$; **Figure 4F**) vs. controls. While both the HIE and control group were able to complete the visual discrimination portion of the paradigm, the HIE group had more significant differences during the late, learning phase of reversal, a portion of testing sensitive to striatal-mediated functions.

DISCUSSION

While clinical studies have shown significant cognitive delays at 18 to 24 months of age following HIE as determined by lower mental developmental index scores and subnormal intelligence quotient scores at age 6 to 7, outcome studies beyond this time are extremely limited (44). Here, we investigated the long-term impact of HIE on learning and cognitive flexibility in adult mice following a neonatal HIE insult utilizing a translational touchscreen task. We found that HIE at term equivalent stage of development was sufficient to produce permanent deficits in learning, both in discrimination and late stage reversal learning. To date, this is the first report of deficits of cognition using a translational touchscreen platform and the first evidence establishing the long-term cognitive deficits that can occur following HIE in rodents. Prior studies in animals however have focused on sensory motor impairments and basic assessments of reflexes. For example, Y-maze testing and object location task after HIE, without and with therapeutic hypothermia, revealed a lower exploratory preference after HIE. The memory impairments were not altered by therapeutic hypothermia (33). In a different study, three developmental reflexes (righting, cliff aversion and geotaxis) were assessed 24 h after HIE in mice, and correlated with Morris Water Maze testing 8 weeks later (45). The Morris Water Maze testing of navigational learning and memory supported neurofunction deficits, leading the authors to conclude that sensorimotor reflex performance in the acute phase of HIE may have predictive values for long-term outcome (45). Given that these tests rely on aversive motivation, we chose to utilize the touchscreen testing platform which relies on positive motivation (food) as a means to test the hypothesis that HIE yield complex impairments in cognition and executive function that are specific to brain regions susceptible to injury. Additionally, touchscreen offers sophisticated, reproducible analysis of multiple pillars of behavior using a platform that directly corresponds to human testing (46–48).

Children with a history of HIE are at high risk of abnormal cognitive development. However, few studies have utilized animal models of HIE to examine the long-term impacts on cognitive function, with testing occurring into adulthood.

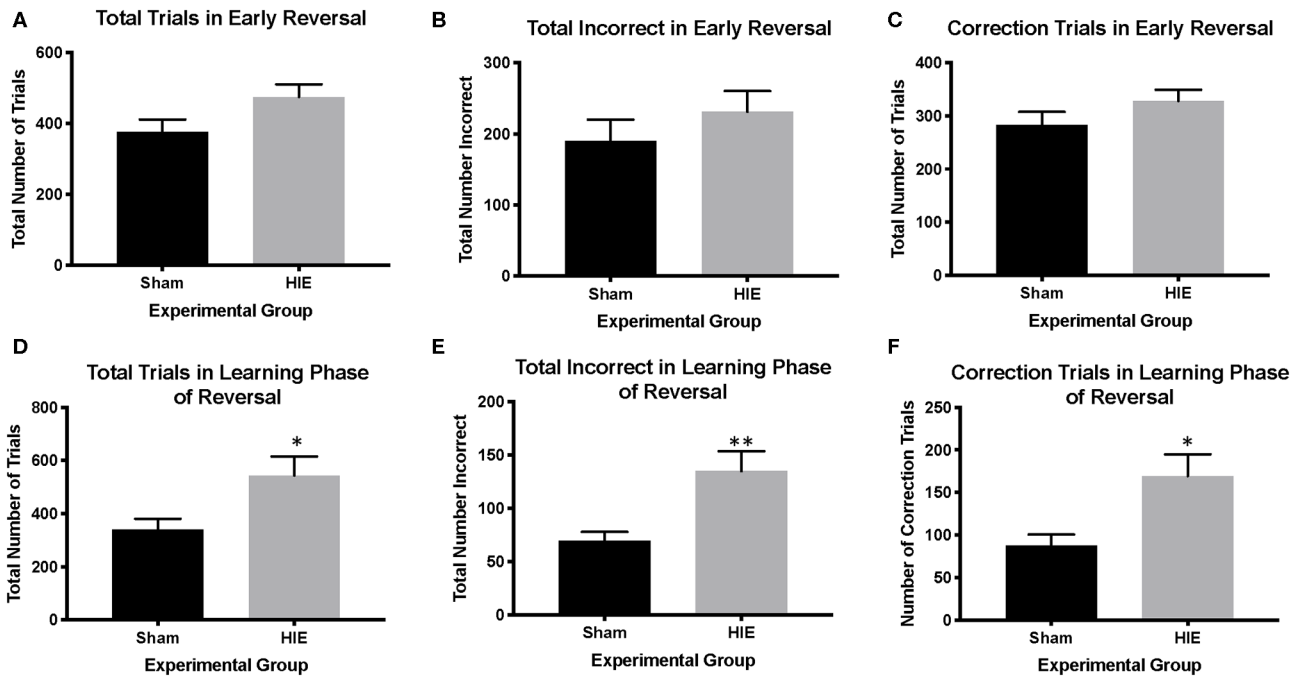

FIGURE 4 | HIE yields distinct early phase and learning phase reversal deficits. In the early phase of reversal, there were no significant differences between HIE and sham in the total trials completed, the total incorrect, and the number of correction trials **(A–C)**. However, in the learning phase of reversal, the HIE group had significantly more total trials **(D)**, more incorrect trials **(E)** and more correction trials **(F)** compared to sham ($n = 13$–15, $^{*}p < 0.05$, $^{**}p < 0.01$). Data is represented as mean ± standard error of the mean (SEM).

Notably, mice at the conclusion of touchscreen training are over 150 days old. Utilizing a touchscreen platform, we found multiple deficits in learning, both during an initial pairwise discrimination, and during late stage reversal, when animals learn the new response rule to a high degree of consistency. HIE did not globally impair response learning, as mice were able to learn initiation and response behaviors in the absence of a discrimination during pretraining at levels similar to control. During discrimination, HIE animals showed consistently lower performance on all measures, although they were only significantly worse than control as measured by first-presentation correction errors. Importantly, secondary latency measures, such as reaction time and the time to retrieve a reward, did not differ across groups, suggesting that HIE did not globally impair motor behavior, or motivation to work for food reward. While they did have more incorrect responses on their way to completing the discrimination task, all HIE mice were able to perform at a high criterion level, allowing us to test them on reversal learning.

During reversal, the HIE group demonstrated a global impairment as measured by number of trials, errors and correction errors across the entire paradigm. However, the impairment was not typified by a cortical-mediated loss of flexibility. Reversal learning, and particularly the early, perseverative phase, has consistently been shown to be mediated by the orbitofrontal cortex (OFC) across species (26, 49–52). In the current study, HIE did not significantly differ on any measure during the perseverative phase (39, 40, 53). Rather, analysis of learning stage revealed that the reversal impairment was driven by significant increases in trials, errors, and correction trials during the later stages of reversal, when performance has reached or exceeded chance levels. Together, the increase in incorrect responses during initial learning together with impaired late-stage reversal suggest an impairment in the acquisition of well-trained stimulus-response contingencies, which is mediated by subcortical structures such as the dorsal striatum (dS) (25, 39). The efficient balance of associative learning and behavioral flexibility is mediated by cortico-striatal-thalamic loops (54) and single unit recording and imaging studies have demonstrated that the striatum plays a critical role in the representation of reward-action relationships required to efficiently guide choices (25, 55, 56). Interestingly, the touchscreen results of impaired learning implicate the dorsal striatum, in alignment with evidence that human infants with term HIE are more likely to have injury to the basal ganglia on present on neuroimaging evaluation.

Our study provides evidence of a significant and selective deficits in associative learning in mice with HIE. Upon acquiring a pairwise visual discrimination, when the reinforcement contingencies of the learned association were reversed, HIE mice were significantly impaired compared to shams. This was due to deficient learning of the new association rather than impaired reversal *per se*. Both groups performed at equivalent levels during reversal sessions when performance was low and perseveration high (i.e., <50%), while HIE mice committed more trials and errors during sessions when performance was largely learning related (i.e., >50%). This deficit is in contrast to previously published touchscreen assessments in animal models of perinatal brain injury (38, 41, 57). Specifically, adult rats perinatal brain injury secondary to chorioamnionitis have a perseverative

phenotype and significant deficit in cognitive control defined by a reversal deficit (38). Similarly, adult rats suffering severe traumatic brain injury in infancy perseverate, lack cognitive flexibility and struggle to pass reversal learning criteria (41). The extensive white matter brain injury and orbitofrontocortical decoupling observed in both chorioamnionitis and traumatic brain injury may partially explain these findings. Interestingly, animals with perinatal exposure to methadone have a mixed phenotype of executive dysfunction with rats committing significantly more correction errors both during the perseverative phase and during the later learning phase compared to saline control animals (57). Together, these data indicate that adult rats exposed to perinatal methadone are impaired in both early and late reversal learning, consistent with global learning and executive control dysfunction (57) and widespread structural brain injury. In contrast to methadone exposure, prenatal alcohol exposure in mice results in behavioral inflexibility during early reversal testing, with persistent aberrant lateral orbital frontal cortex to dorsolateral striatum signaling (58). Taken together, these data indicate that the timing of injury (prenatal, perinatal or postnatal) has an impact on the type of cognitive deficits observed. While there are similarities in the injuries discussed such as inflammation, each injury results in a distinct behavioral phenotype. Notably, impaired performance as observed in HIE mice are not due to non-specific motivation or sensorimotor related performance as evidenced by normal scores on reaction response times and reward retrieval latency. Thus, although each injury model was different, the touchscreen platform is sensitive enough to detect distinct differences in cognitive domains following different types of perinatal brain injury.

Importantly, the impairments in learning during discrimination and reversal seen after HIE persist into adulthood. While more studies have reviewed outcomes of infants at a young age, few have observed this cohort into adolescence or adulthood (16). There has been greater recognition that HIE can have long-lasting impact on developmental trajectories, and studies have begun to assess the neurodevelopmental outcomes of children following HIE in the newborn period (9, 44, 59). Interestingly, children diagnosed with severe neonatal encephalopathy were found to be more than one grade behind the expected level for their age, with children diagnosed with moderate neonatal encephalopathy having difficulties in reading, spelling and mathematics (16). A recent prospective case-control study in the United Kingdom reported significantly lower mean full-scale IQ at 6–8 years of age after an HIE event, when compared to controls (59). Children with HIE also have significant differences in verbal comprehension, perceptual reasoning, working memory and processing speed (59). Similarly, a systematic review of five published studies reported a higher proportion of cognitive impairments at school age in children with a history of HIE, specifically in the area of executive functioning (9). The current results underline the idea that following infants diagnosed with neonatal encephalopathy is critically important, as they are at high risk of not only having difficulties at school age, but also into adulthood.

This study had limitations. While our data indicate significant differences in the HIE group, there is known variability of injury that occurs with the use of the Rice-Vannucci model (60). This variability can be beneficial, as it mimics the variation of injury observed in infants following HIE. Additionally, no environmental enrichment was used in the study, which could impact the neurodevelopmental outcomes (61, 62). Both sexes were utilized in this study, which adds to the generalizability of the results. The touchscreen platform is more robust and less vulnerable to environmental confounders than other modes of testing such as the Morris Water Maze. The rigor and reproducibility of the touchscreen testing, with the sensitivity of the measures obtained, allows for differences in performance from therapeutic interventions to be readily detected. Correlating outcomes on this touchscreen assessment of diverse pillars of cognition with pathology, lesion size, and multi-modal high-resolution neuroimaging could be investigated as a future direction. Finally, we did not include treatment within this study, such as hypothermia. Investigation the effect of hypothermia on the cognitive impairment reported here would be an essential element for future investigation as hypothermia is the only approved treatment for HIE in humans.

In sum, this is the first report that HIE in rodents is sufficient to cause long-lasting impairments in basal-ganglia mediated learning processes. This approach provides an important model platform for studies trialing adjunctive therapies to improve outcomes after HIE. Future studies should examine whether therapeutic hypothermia with additional therapies can mitigate the specific cognitive deficits that occur following HIE.

DATA AVAILABILITY STATEMENT

The datasets generated for this study are available on request to the corresponding author.

ETHICS STATEMENT

The animal study was reviewed and approved by Institutional Animal Care and Use Committee (IACUC) of the University of New Mexico.

AUTHOR CONTRIBUTIONS

LJ conceptualized the hypothesis, designed and supervised the experiments. JM, AZ, NP, JN, KC, and LJ performed the experiments. JM, SR, JB, FN and LJ interpreted the data. JM, AZ, SR, FN, and LJ wrote the manuscript. All authors contributed to manuscript revision and approved the final version.

FUNDING

This study was supported by generous funding from the National Institutes of Health R01HL139492 to LJ.

ACKNOWLEDGMENTS

The authors would like to acknowledge the contributions of Haikun Zhang and Tracylyn R. Yellowhair.

REFERENCES

1. Finder M, Boylan GB, Twomey D, Ahearne C, Murray DM, Hallberg B. Two-year neurodevelopmental outcomes after mild hypoxic ischemic encephalopathy in the era of therapeutic hypothermia. *JAMA Pediatr*. (2019) 174:48–55. doi: 10.1001/jamapediatrics.2019.4011
2. Goswami IR, Whyte H, Wintermark P, Mohammad K, Shivananda S, Louis D, et al. Characteristics and short-term outcomes of neonates with mild hypoxic-ischemic encephalopathy treated with hypothermia. *J Perinatol*. (2019) 40:275–83. doi: 10.1038/s41372-019-0551-2
3. Kurinczuk JJ, White-Koning M, Badawi N. Epidemiology of neonatal encephalopathy and hypoxic-ischaemic encephalopathy. *Early Hum Dev*. (2010) 86:329–38. doi: 10.1016/j.earlhumdev.2010.05.010
4. Shankaran S. Neonatal encephalopathy: treatment with hypothermia. *J Neurotrauma*. (2009) 26:437–43. doi: 10.1089/neu.2008.0678
5. Wu YW, Goodman AM, Chang T, Mulkey SB, Gonzalez FF, Mayock DE, et al. Placental pathology and neonatal brain MRI in a randomized trial of erythropoietin for hypoxic-ischemic encephalopathy. *Pediatr Res*. (2019) 87:1. doi: 10.1038/s41390-019-0493-6
6. Volpe JJ. Placental assessment provides insight into mechanisms and timing of neonatal hypoxic-ischemic encephalopathy. *J Neonatal Perinatal Med*. (2019) 12:113–6. doi: 10.3233/NPM-190270
7. Chiang MC, Lien R, Chu SM, Yang PH, Lin JJ, Hsu JF, et al. Serum lactate, brain magnetic resonance imaging and outcome of neonatal hypoxic ischemic encephalopathy after therapeutic hypothermia. *Pediatr Neonatol*. (2016) 57:35–40. doi: 10.1016/j.pedneo.2015.04.008
8. Lodygensky GA, Battin MR, Gunn AJ. Mild neonatal encephalopathy-how, when, and how much to treat?. *JAMA Pediatr*. (2018) 172:3–4. doi: 10.1001/jamapediatrics.2017.3044
9. Schreglmann M, Ground A, Vollmer B, Johnson MJ. Systematic review: long-term cognitive and behavioural outcomes of neonatal hypoxic-ischaemic encephalopathy in children without cerebral palsy. *Acta Paediatr*. (2019) 109:20–30. doi: 10.1111/apa.14821
10. Cabaj A, Bekiesinska-Figatowska M, Madzik J. MRI patterns of hypoxic-ischemic brain injury in preterm and full term infants - classical and less common MR findings. *Pol J Radiol*. (2012) 77:71–6. doi: 10.12659/PJR.883379
11. Cowan F, Rutherford M, Groenendaal F, Eken P, Mercuri E, Bydder GM, et al. Origin and timing of brain lesions in term infants with neonatal encephalopathy. *Lancet*. (2003) 361:736–42. doi: 10.1016/S0140-6736(03)12658-X
12. Krishnan P, Shroff M. Neuroimaging in neonatal hypoxic ischemic encephalopathy. *Indian J Pediatr*. (2016) 83:995–1002. doi: 10.1007/s12098-016-2042-1
13. Gerner GJ, Newman EI, Burton VJ, Roman B, Cristofalo EA, Leppert M, et al. Correlation between white matter injury identified by neonatal diffusion tensor imaging and neurodevelopmental outcomes following term neonatal asphyxia and therapeutic hypothermia: an exploratory pilot study. *J Child Neurol*. (2019) 34:556–66. doi: 10.1177/0883073819841717
14. Jisa KA, Clarey DD, Peeples ES. Magnetic resonance imaging findings of term and preterm hypoxic-ischemic encephalopathy: a review of relevant animal models and correlation to human imaging. *Open Neuroimag J*. (2018) 12:55–65. doi: 10.2174/1874440001812010055
15. Volpe JJ. Neonatal encephalopathy: an inadequate term for hypoxic-ischemic encephalopathy. *Ann Neurol*. (2012) 72:156–66. doi: 10.1002/ana.23647
16. van Handel M, Swaab H, de Vries LS, Jongmans MJ. Long-term cognitive and behavioral consequences of neonatal encephalopathy following perinatal asphyxia: a review. *Eur J Pediatr*. (2007) 166:645–54. doi: 10.1007/s00431-007-0437-8
17. Aggarwal M, Burnsed J, Martin LJ, Northington FJ, Zhang J. Imaging neurodegeneration in the mouse hippocampus after neonatal hypoxia-ischemia using oscillating gradient diffusion MRI. *Magn Reson Med*. (2014) 72:829–40. doi: 10.1002/mrm.24956
18. Fang J, Chavez-Valdez R, Flock DL, Avaritt O, Saraswati M, Robertson C, et al. An inhibitor of the mitochondrial permeability transition pore lacks therapeutic efficacy following neonatal hypoxia ischemia in mice. *Neuroscience*. (2019) 406:202–11. doi: 10.1016/j.neuroscience.2019.02.030
19. Stone BS, Zhang J, Mack DW, Mori S, Martin LJ, Northington FJ. Delayed neural network degeneration after neonatal hypoxia-ischemia. *Ann Neurol*. (2008) 64:535–46. doi: 10.1002/ana.21517
20. Tsuji S, Di Martino E, Mukai T, Tsuji S, Murakami T, Harris RA, et al. Aggravated brain injury after neonatal hypoxic ischemia in microglia-depleted mice. *J Neuroinflammation*. (2020) 17:111. doi: 10.1186/s12974-020-01792-7
21. Horner AE, Heath CJ, Hvoslef-Eide M, Kent BA, Kim CH, Nilsson SR, et al. The touchscreen operant platform for testing learning and memory in rats and mice. *Nat Protoc*. (2013) 8:1961–84. doi: 10.1038/nprot.2013.122
22. MacQueen DA, Minassian A, Kenton JA, Geyer MA, Perry W, Brigman JL, et al. Amphetamine improves mouse and human attention in the 5-choice continuous performance test. *Neuropharmacology*. (2018) 138:87–96. doi: 10.1016/j.neuropharm.2018.05.034
23. Nithianantharajah J, Grant SG. Cognitive components in mice and humans: combining genetics and touchscreens for medical translation. *Neurobiol Learn Mem*. (2013) 105:13–9. doi: 10.1016/j.nlm.2013.06.006
24. Nithianantharajah J, McKechanie AG, Stewart TJ, Johnstone M, Blackwood DH, St Clair D, et al. Bridging the translational divide: identical cognitive touchscreen testing in mice and humans carrying mutations in a disease-relevant homologous gene. *Sci Rep*. (2015) 5:14613. doi: 10.1038/srep14613
25. Brigman JL, Daut RA, Wright T, Gunduz-Cinar O, Graybeal C, Davis MI, et al. GluN2B in corticostriatal circuits governs choice learning and choice shifting. *Nat Neurosci*. (2013) 16:1101–10. doi: 10.1038/nn.3457
26. Izquierdo A, Brigman JL, Radke AK, Rudebeck PH, Holmes A. The neural basis of reversal learning: an updated perspective. *Neuroscience*. (2017) 345:12–26. doi: 10.1016/j.neuroscience.2016.03.021
27. Carrasco M, Perin J, Jennings JM, Parkinson C, Gilmore MM, Chavez-Valdez R, et al. Cerebral autoregulation and conventional and diffusion tensor imaging magnetic resonance imaging in neonatal hypoxic-ischemic encephalopathy. *Pediatr Neurol*. (2018) 82:36–43. doi: 10.1016/j.pediatrneurol.2018.02.004
28. McNally MA, Chavez-Valdez R, Felling RJ, Flock DL, Northington FJ, Stafstrom CE. Seizure susceptibility correlates with brain injury in male mice treated with hypothermia after neonatal hypoxia-ischemia. *Dev Neurosci*. (2019) 69:1–10. doi: 10.1159/000496468
29. Northington FJ, Chavez-Valdez R, Martin LJ. Neuronal cell death in neonatal hypoxia-ischemia. *Ann Neurol*. (2011) 69:743–58. doi: 10.1002/ana.22419
30. Salas J, Reddy N, Orru E, Carson KA, Chavez-Valdez R, Burton VJ, et al. The role of diffusion tensor imaging in detecting hippocampal injury following neonatal hypoxic-ischemic encephalopathy. *J Neuroimaging*. (2019) 29:252–9. doi: 10.1111/jon.12572
31. Salas J, Tekes A, Hwang M, Northington FJ, Huisman T. Head ultrasound in neonatal hypoxic-ischemic injury and its mimickers for clinicians: a review of the patterns of injury and the evolution of findings over time. *Neonatology*. (2018) 114:185–97. doi: 10.1159/000487913
32. Wu D, Martin LJ, Northington FJ, Zhang J. Oscillating-gradient diffusion magnetic resonance imaging detects acute subcellular structural changes in the mouse forebrain after neonatal hypoxia-ischemia. *J Cereb Blood Flow Metab*. (2019) 39:1336–48. doi: 10.1177/0271678X18759859
33. Diaz J, Abiola S, Kim N, Avaritt O, Flock D, Yu J, et al. Therapeutic hypothermia provides variable protection against behavioral deficits after neonatal hypoxia-ischemia: a potential role for brain-derived neurotrophic factor. *Dev Neurosci*. (2017) 39:257–72. doi: 10.1159/000454949
34. Rice JE, Vannucci RC, Brierley JB. The influence of immaturity on hypoxic-ischemic brain damage in the rat. *Ann Neurol*. (1981) 9:131–41. doi: 10.1002/ana.410090206
35. Vannucci RC, Vannucci SJ. Perinatal hypoxic-ischemic brain damage: evolution of an animal model. *Dev Neurosci*. (2005) 27:81–6. doi: 10.1159/000085978
36. Jantzie LL, Talos DM, Selip DB, An L, Jackson MC, Folkerth RD, et al. Developmental regulation of group I metabotropic glutamate receptors in the premature brain and their protective role in a rodent model of periventricular leukomalacia. *Neuron Glia Biol*. (2010) 6:277–88. doi: 10.1017/S1740925X11000111
37. Jantzie LL, Todd KG. Doxycycline inhibits proinflammatory cytokines but not acute cerebral cytogenesis after hypoxia-ischemia in neonatal rats. *J Psychiatry Neurosci*. (2010) 35:20–32. doi: 10.1503/jpn.090061

38. Jantzie LL, Oppong AY, Conteh FS, Yellowhair TR, Kim J, Fink G, et al. Repetitive neonatal erythropoietin and melatonin combinatorial treatment provides sustained repair of functional deficits in a rat model of cerebral palsy. *Front Neurol*. (2018) 9:233. doi: 10.3389/fneur.2018.00233
39. Marquardt K, Josey M, Kenton JA, Cavanagh JF, Holmes A, Brigman JL. Impaired cognitive flexibility following NMDAR-GluN2B deletion is associated with altered orbitofrontal-striatal function. *Neuroscience*. (2019) 404:338–52. doi: 10.1016/j.neuroscience.2019.01.066
40. Marquardt K, Sigdel R, Brigman JL. Touch-screen visual reversal learning is mediated by value encoding and signal propagation in the orbitofrontal cortex. *Neurobiol Learn Mem*. (2017) 139:179–88. doi: 10.1016/j.nlm.2017.01.006
41. Robinson S, Winer JL, Chan LAS, Oppong AY, Yellowhair TR, Maxwell JR, et al. Extended erythropoietin treatment prevents chronic executive functional and microstructural deficits following early severe traumatic brain injury in rats. *Front Neurol*. (2018) 9:451. doi: 10.3389/fneur.2018.00451
42. Turner KM, Simpson CG, Burne TH. BALB/c mice can learn touchscreen visual discrimination and reversal tasks faster than C57BL/6 mice. *Front Behav Neurosci*. (2017) 11:16. doi: 10.3389/fnbeh.2017.00016
43. Brigman JL, Mathur P, Harvey-White J, Izquierdo A, Saksida LM, Bussey TJ, et al. Pharmacological or genetic inactivation of the serotonin transporter improves reversal learning in mice. *Cereb Cortex*. (2010) 20:1955–63. doi: 10.1093/cercor/bhp266
44. Pappas A, Shankaran S, McDonald SA, Vohr BR, Hintz SR, Ehrenkranz RA, et al. Cognitive outcomes after neonatal encephalopathy. *Pediatrics*. (2015) 135:e624–34. doi: 10.1542/peds.2014-1566
45. Ten VS, Bradley-Moore M, Gingrich JA, Stark RI, Pinsky DJ. Brain injury and neurofunctional deficit in neonatal mice with hypoxic-ischemic encephalopathy. *Behav Brain Res*. (2003) 145:209–19. doi: 10.1016/S0166-4328(03)00146-3
46. Bussey TJ, Holmes A, Lyon L, Mar AC, McAllister KA, Nithianantharajah J, et al. New translational assays for preclinical modelling of cognition in schizophrenia: the touchscreen testing method for mice and rats. *Neuropharmacology*. (2012) 62:1191–203. doi: 10.1016/j.neuropharm.2011.04.011
47. Bussey TJ, Padain TL, Skillings EA, Winters BD, Morton AJ, Saksida LM. The touchscreen cognitive testing method for rodents: how to get the best out of your rat. *Learn Mem*. (2008) 15:516–23. doi: 10.1101/lm.987808
48. Cotter J, Vithanage N, Colville S, Lyle D, Cranley D, Cormack F, et al. Investigating domain-specific cognitive impairment among patients with multiple sclerosis using touchscreen cognitive testing in routine clinical care. *Front Neurol*. (2018) 9:331. doi: 10.3389/fneur.2018.00331
49. Hamilton DA, Brigman JL. Behavioral flexibility in rats and mice: contributions of distinct frontocortical regions. *Genes Brain Behav*. (2015) 14:4–21. doi: 10.1111/gbb.12191
50. Kennerley SW, Behrens TE, Wallis JD. Double dissociation of value computations in orbitofrontal and anterior cingulate neurons. *Nat Neurosci*. (2011) 14:1581–9. doi: 10.1038/nn.2961
51. Rudebeck PH, Saunders RC, Prescott AT, Chau LS, Murray EA. Prefrontal mechanisms of behavioral flexibility, emotion regulation and value updating. *Nat Neurosci*. (2013) 16:1140–5. doi: 10.1038/nn.3440
52. Stalnaker TA, Cooch NK, Schoenbaum G. What the orbitofrontal cortex does not do. *Nat Neurosci*. (2015) 18:620–7. doi: 10.1038/nn.3982
53. Brigman JL, Feyder M, Saksida LM, Bussey TJ, Mishina M, Holmes A. Impaired discrimination learning in mice lacking the NMDA receptor NR2A subunit. *Learn Mem*. (2008) 15:50–4. doi: 10.1101/lm.777308
54. Middleton FA, Strick PL. Basal-ganglia 'projections' to the prefrontal cortex of the primate. *Cereb Cortex*. (2002) 12:926–35. doi: 10.1093/cercor/12.9.926
55. Bergstrom HC, Lipkin AM, Lieberman AG, Pinard CR, Gunduz-Cinar O, Brockway ET, et al. Dorsolateral striatum engagement interferes with early discrimination learning. *Cell Rep*. (2018) 23:2264–72. doi: 10.1016/j.celrep.2018.04.081
56. Yin HH, Mulcare SP, Hilario MR, Clouse E, Holloway T, Davis MI, et al. Dynamic reorganization of striatal circuits during the acquisition and consolidation of a skill. *Nat Neurosci*. (2009) 12:333–41. doi: 10.1038/nn.2261
57. Jantzie LL, Maxwell JR, Newville JC, Yellowhair TR, Kitase Y, Madurai N, et al. Prenatal opioid exposure: the next neonatal neuroinflammatory disease. *Brain Behav Immun*. (2020) 84:45–58. doi: 10.1016/j.bbi.2019.11.007
58. Marquardt K, Cavanagh JF, Brigman JL. Alcohol exposure in utero disrupts cortico-striatal coordination required for behavioral flexibility. *Neuropharmacology*. (2020) 162:107832. doi: 10.1016/j.neuropharm.2019.107832
59. Lee-Kelland R, Jary S, Tonks J, Cowan FM, Thoresen M, Chakkarapani E. School-age outcomes of children without cerebral palsy cooled for neonatal hypoxic-ischaemic encephalopathy in 2008-2010. *Arch Dis Child Fetal Neonatal Ed*. (2019) 105:8–13. doi: 10.1136/archdischild-2018-316509
60. Edwards AB, Feindel KW, Cross JL, Anderton RS, Clark VW, Knuckey NW, et al. Modification to the rice-vannucci perinatal hypoxic-ischaemic encephalopathy model in the P7 rat improves the reliability of cerebral infarct development after 48 hours. *J Neurosci Methods*. (2017) 288:62–71. doi: 10.1016/j.jneumeth.2017.06.016
61. Bailoo JD, Murphy E, Boada-Sana M, Varholick JA, Hintze S, Baussiere C, et al. Effects of cage enrichment on behavior, welfare and outcome variability in female mice. *Front Behav Neurosci*. (2018) 12:232. doi: 10.3389/fnbeh.2018.00232
62. Ball NJ, Mercado E III, Orduna I. Enriched environments as a potential treatment for developmental disorders: a critical assessment. *Front. Psychol*. (2019) 10:466. doi: 10.3389/fpsyg.2019.00466

Conflict of Interest: The authors declare that the research was conducted in the absence of any commercial or financial relationships that could be construed as a potential conflict of interest.

frontiers in Neurology

REVIEW
published: 09 June 2020
doi: 10.3389/fneur.2020.00483

Clinical Implications of Epigenetic Dysregulation in Perinatal Hypoxic-Ischemic Brain Damage

Martín Bustelo[1,2,3,4†], *Melinda Barkhuizen*[1†], *Daniel L. A. van den Hove*[2,5], *Harry Wilhelm. M. Steinbusch*[2], *Martín A. Bruno*[3], *C. Fabián Loidl*[3,4] *and Antonio W. Danilo Gavilanes*[1,6*]

[1] Department of Pediatrics, Maastricht University Medical Center (MUMC), Maastricht, Netherlands, [2] Department of Psychiatry and Neuropsychology, School for Mental Health and Neuroscience (MHeNs), Maastricht University, Maastricht, Netherlands, [3] Instituto de Ciencias Biomédicas, Facultad de Ciencias Médicas, Universidad Católica de Cuyo, San Juan, Argentina, [4] Laboratorio de Neuropatología Experimental, Facultad de Medicina, Instituto de Biología Celular y Neurociencias "Prof. E. De Robertis" (IBCN), Universidad de Buenos Aires, CONICET, Buenos Aires, Argentina, [5] Department of Psychiatry, Psychosomatics and Psychotherapy, University of Würzburg, Würzburg, Germany, [6] Facultad de Ciencias Médicas, Instituto de Investigación e Innovación de Salud Integral, Universidad Católica de Santiago de Guayaquil, Guayaquil, Ecuador

OPEN ACCESS

Edited by:
Claire Thornton,
Royal Veterinary College (RVC),
United Kingdom

Reviewed by:
Wang-Tso Lee,
National Taiwan University Hospital, Taiwan
Ernest Marshall Graham,
Johns Hopkins University,
United States

***Correspondence:**
Antonio W. D. Gavilanes
danilo.gavilanes@mumc.nl

[†]These authors have contributed equally to this work

Specialty section:
This article was submitted to Pediatric Neurology, a section of the journal Frontiers in Neurology

Received: 22 November 2019
Accepted: 04 May 2020
Published: 09 June 2020

Citation:
Bustelo M, Barkhuizen M, van den Hove DLA, Steinbusch HWM, Bruno MA, Loidl CF and Gavilanes AWD (2020) Clinical Implications of Epigenetic Dysregulation in Perinatal Hypoxic-Ischemic Brain Damage. Front. Neurol. 11:483. doi: 10.3389/fneur.2020.00483

Placental and fetal hypoxia caused by perinatal hypoxic-ischemic events are major causes of stillbirth, neonatal morbidity, and long-term neurological sequelae among surviving neonates. Brain hypoxia and associated pathological processes such as excitotoxicity, apoptosis, necrosis, and inflammation, are associated with lasting disruptions in epigenetic control of gene expression contributing to neurological dysfunction. Recent studies have pointed to DNA (de)methylation, histone modifications, and non-coding RNAs as crucial components of hypoxic-ischemic encephalopathy (HIE). The understanding of epigenetic dysregulation in HIE is essential in the development of new clinical interventions for perinatal HIE. Here, we summarize our current understanding of epigenetic mechanisms underlying the molecular pathology of HI brain damage and its clinical implications in terms of new diagnostic, prognostic, and therapeutic tools.

Keywords: hypoxic-ischemic encephalopathy, biomarker, hypoxia, ischemia, microRNAs, histone modifications, DNA methylation

INTRODUCTION

Epigenetics is defined as heritable changes in gene expression that do not result from a change in the DNA sequence (1). Epigenetic regulation plays an essential role during development, and any insult that disrupts physiological developmental epigenetic programming is likely to have long-term consequences. An increasing number of studies link exposure to different adverse factors during early life, including both the gestational and the postnatal period to changes in the epigenome and one's individual suceptibility (2). In this regard, the brain is particularly vulnerable to alterations in the early-life microenvironment, damage induced at this stage may not be evident until the exposure to a new insult triggers it (3).

Perinatal hypoxia represents one of the most common early life insults that ultimately leads to disability or even early death (4, 5). Hypoxia can occur progressively during pregnancy in cases of fetal growth restriction due to placental abnormalities, or can occur acutely during labor and birth, causing peripartum hypoxic-ischemic encephalopathy (HIE). Fetal growth restriction is associated

with stillbirths and permanent neurological disability in survivors (6). Management of fetal growth restriction depends on early detection, and timely delivery before stillbirth occurs (7). Advances in this area have focused on detecting the presence of fetal growth restriction, and the degree of hypoxia present *in utero*.

HIE has a large impact on global child health, with morbidity in 2.5/1,000 live births (4–9 million newborns affected per year worldwide) (8–10). At present, therapeutic hypothermia is the only approved therapy for newborns ≥36 weeks gestational age with moderate-to-severe HIE. Therapeutic hypothermia is thought to work by generally slowing down metabolism and thus counteracting a variety of pathological mechanisms of HIE (11). Several trials have demonstrated that hypothermia is effective in decreasing mortality and decreasing neurocognitive impairments (12, 13), still, this therapy is only partially protective, half of treated newborns still die or develop a lifelong disability, demonstrating the need for the development of other neuroprotective treatment strategies (14).

The features of acute intrapartum hypoxic-ischemia (HI) involve fetal hypoxemia, hypercapnia, and ischemia. In the brain, this leads to metabolic acidosis, cellular necrosis, and activation of apoptotic pathways. After reperfusion/reoxygenation, oxidative metabolism recovers in surviving cells, and most of the neurotoxic cascade is seemingly terminated. This first period immediately following the HI event (0–6 h) is also referred to as the "therapeutic window," where intervention may prevent secondary damage.

Secondary energy failure (6–48 h following HI) involves potent inflammation as well as oxidative stress induced by reactive oxygen species and free radicals, and failure of mitochondrial oxidative phosphorylation due to permeabilization of the mitochondrial membranes. Ultimately, these processes lead to delayed cell death via necrotic and apoptotic pathways (15). Brain injury continues to evolve even months and years after the initial insult, in the tertiary phase, involving neural scarring and persistent inflammation (16). Traditionally epigenetic changes have been attributed to the tertiary phase, its role in the initial phases of HI induced injury is less well-characterized.

Different *in vivo* and *in vitro* models have been used to study the pathological features of HIE. Rodents are the most commonly used animals to model perinatal HI (17), with three major approaches being used. The first model makes use of submersion of the uterine horns containing the term fetal rats in saline. This model mimics a global insult to the fetus at a very low gestational age (18, 19). Considering the fact that brain development in rodents is delayed when compared to that in humans (17), other models use neonatal pups at Postnatal day (P) 3–10 (20) to model insults in the late preterm to term brain. Amongst others, neonatal pups can be subjected to a global hypoxic insult by placing them in a hypoxic chamber, an approach, however, that lacks the ischemic nature of the insult seen in the clinic (20). The most commonly used model, developed by Levine in adult rodents, and adapted by Rice and Vannucci for neonatal rodents (21, 22), induces ischemia by carotid artery occlusion (CAO) followed by exposure to systemic hypoxia (23) inducing an HI insult, here referred as the "HI" model. *In vitro* models exposing neuronal cultures to oxygen-glucose deprivation (OGD)/reoxygenation have also been used as models of HI induced injury (24).

Abbreviations: BBB, blood-brain barrier; DNMTs, DNA methyltransferases; E, embryonic day; HDACs, histone deacetylases; HI, hypoxia-ischemia; HIE, hypoxic-ischemic encephalopathy; HIF, hypoxia inducible factor; HIF-1α, Hypoxia-inducible factor 1α; HRE, hypoxia response element; JmjC, Jumonji-C histone demethylase; KDMs, histone lysine demethylases; P, postnatal day; REST, repressor element-1 (RE1) silencing transcription factor; TETs, ten-eleven translocation enzymes; 5-aza-dC, 5-aza-2′-deoxycytidine.

EPIGENETIC DYSREGULATION IN HYPOXIA-ISCHEMIA

Epigenetic processes regulate both the transcription of the DNA into mRNA and the translation of the mRNA into proteins, acting at multiple levels of control, involving e.g., DNA methylation and hydroxymethylation, chromatin remodeling, and non-coding RNA (ncRNA) regulation (25, 26). As such, DNA is wrapped around histone proteins forming chromatin, where the configuration of chromatin is controlled by post-translational modifications of the associated histone proteins as well as by direct modifications to nucleotides, which collectively form the epigenetic code that controls the transcription of DNA into mRNA (25). This epigenetic code can be modified by "writers," i.e., enzymes which introduce post-translational modifications on the DNA and histones, "erasers," which remove the modifications, and "readers," i.e., specialized proteins which identify and interpret the modifications. The translation of mRNA into proteins is regulated by ncRNAs. HI-induced epigenetic alterations are preserved even in the absence of hypoxia-inducible factors (HIFs) (27, 28) suggesting they may continue to impact upon behavioral phenotypes later in life (**Figure 1**).

Hypoxia-Inducible Factor-1

Hypoxia-inducible factor-1 (HIF-1) is the main effector of cellular hypoxia, being an oxygen-sensitive transcription factor. HIF-1 comprises two subunits, i.e., HIF-1α and HIF-1β (29). The stability and activity of the oxygen-regulated subunit HIF-1α are regulated by post-translational modifications that control its proteasomal degradation. In hypoxia, activation of HIFs is mediated via the inhibition of dioxygenases, such as the Jumonji-C (JmjC) domain-containing histone demethylases. As a result, HIF-1α accumulates, binds to a hypoxic response element (HRE), and leads to the transcriptional induction of several genes involved in adaptation to hypoxia, including genes involved in angiogenesis, iron metabolism, and glucose metabolism.

HIF-1 expression levels, protein stabilization, and its association with HRE are under tight epigenetic regulation, including promoter methylation and microRNA (miRNAs) control (30–32). Conversely, HIF-1 controls the expression of several epigenetic regulators. Studies have shown that DNA methylation regulates HIF-1α transcription regulating the promoter activity at HRE-152 (33) and SP1.

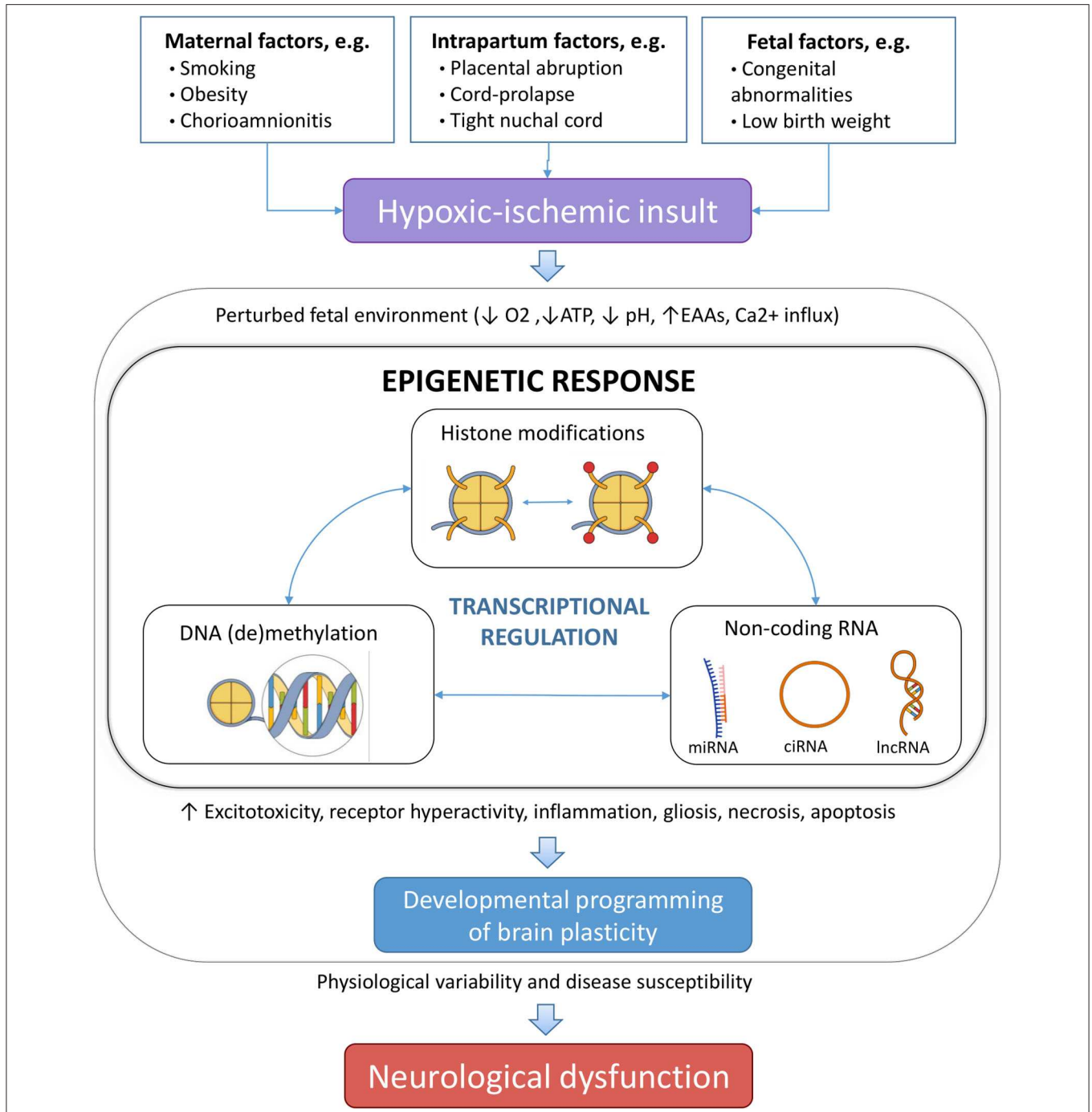

FIGURE 1 | Different risk factors, which can be ante-, peri-, or postnatal can lead to perinatal hypoxia. If prolonged hypoxia results in a perturbed brain environment, leading to modulated epigenetic changes that alter the gene expression profile as an adaption of the fetus to the adverse environment. Different epigenetic mechanisms cooperatively orchestrate this process. As a result, changes in physiology of the neonatal brain can permanently affect the structure and/or functionality, and result in increased disease susceptibility in the offspring. EAAs, excitatory amino acids; miRNA, microRNA; ciRNA, circular RNA; lncRNA, long non-coding RNA.

DNA Methylation

DNA methylation comprises the addition of a methyl group at the carbon 5 position on the pyrimidine ring of cytosines, creating 5-methylcytosine (5-mC) (34). Cytosine methylation provides a stable epigenetic mark with long-term transcriptional effects. DNA methylation is catalyzed by DNA methyltransferases (DNMTs). These enzymes can work in different ways depending on the local chromatin microenvironment, acting as DNA methyltransferase or DNA dehydroxymethylase (35). The methylation status of the DNA is "read" by methyl CpG

binding proteins (MBPs), like the methyl-CpG-binding protein 2 (MECP2) which recruits HDACs to repress transcription (36). Recent evidence indicates that during early postnatal development neuronal genomes accumulate uniquely high levels of two alternative forms of methylation, i.e., non-CpG methylation and DNA hydroxymethylation (37). DNA methylation marks can be "erased" either passively through inhibition of the DNMTs or actively by Ten-eleven translocation (TET) enzymes. TETs are 2-oxoglutarate-dependent dioxygenases that mediate DNA hydroxymethylation and their activity is oxygen-dependent (38).

Non-coding RNAs

In humans, only 1–2% of the genome encodes proteins, while non-coding RNAs (ncRNAs) that do not produce proteins are the great majority of human transcripts (39). As such, ncRNAs, including microRNAs (miRNAs), long non-coding RNAs (lncRNAs), small nucleolar RNAs, and circular RNAs (circRNAs), have important roles in regulating gene expression playing diverse regulatory roles (40). The limited availability of human fetal and neonatal tissue has resulted in studies using animal models and *in vitro* studies as a major alternative for studying the role of ncRNAs in newborns under physiological and pathophysiological conditions.

miRNAs

MiRNAs are a large class of short regulatory RNAs, about 19–22 nucleotides in length, which silence gene expression by binding to the 3′-untranslated region of target genes. The majority of miRNAs are enriched in the developing brain, which signifies their role in neural development (41). Consequently, disruption of miRNAs in the perinatal period is likely to have long-term consequences (42, 43). Several miRNAs termed hypoxamirs have been shown to be induced by hypoxia, and control the cellular response to hypoxia via HIFs. These include miRNAs that regulate HIF1-α signaling (31, 44–50) and miRNAs that contain hypoxia-responsive elements that are transcribed in response to HIF1-α activation and act downstream of the HIFs (31, 47, 49, 51–53). miRNA expression is highly tissue- and disease-specific, which, together with their remarkable stability in circulation, makes them potential diagnostic biomarker candidates, still none has made it to a clinical setting (**Table 1**).

LncRNAs

Long-non coding RNAs (LncRNAs) are ncRNAs larger than 200 nucleotides that act as a competing endogenous RNAs controlling gene expression by sponging miRNAs, and binding and inactivating chromosomes (78). LncRNAs fold into complex secondary and tertiary structures defining their interactions and function, providing a scaffold for proteins to form regulatory complexes (79, 80). Studies have demonstrated that LncRNAs play an important role in the regulation of gene expression, particularly during CNS development (81), with nearly 40% of LncRNAs reported to be specifically expressed in the CNS and involved in brain development and related disorders (82, 83).

Histone Modifications

DNA is wrapped around octamers of histone (H) proteins containing two copies of H2A, H2B, H3, and H4 proteins forming nucleosomes that are bounded by H1 linker histones. H3 and H4 have N-terminal tails that extend beyond the nucleosome and are permissive to modifications, such as acetylation, methylation, glycosylation, ubiquitination, farnesylation, citrullination, and ADP-ribosylation. These modifications alter the charge of the amino acid residues of histones, resulting in relaxed DNA (euchromatin), accessible for the transcriptional machinery, or condensed DNA (heterochromatin) where the transcriptional machinery cannot access (84).

Altogether, these modifications encode the histone code, that, depending on the type and locus of the modifications, the relative location of histones within or toward a gene, and the combination of histone modifications, can lead to enormously diverse readouts (85). Histone modifications can act in different ways depending on the context, increasing the complexity of the histone code. The best-described histone marks in HI brain damage are histone acetylation and methylation.

Histone Methylation

Many enzymes participate in the control of histone methylation, including histone methyltransferases (writers), histone demethylases (erasers), and proteins that recognize the methylated state (readers) (86).

Histone demethylation is carried out by histone lysine demethylases (KDM2–7), which can remove both activating and repressing methyl groups from the chromatin (87, 88). Studies exposing cell lines to hypoxia have shown increased expression of the KDM3 gene, which removes methyl groups from repressive H3K9 sites and activates gene expression (89, 90). Methyl modifications take place mostly on lysine (K) residues of H3 and H4, being the main histone methylation site subject to epigenetic variation H4K20 (91). Interestingly, *in vitro* experiments suggest that JmjC enzymes can act as molecular oxygen sensors in the cell (92).

Histone Acetylation

Histone acetylation by histone acetyltransferases (HATs) relaxes chromatin formation, promoting transcription, whilst the deacetylation of histone tails by histone deacetylases (HDACs) causes the chromatin to condense, thereby inhibiting transcription (93). HATs exert their effects in collaboration with proteins like p300/CBP, PCAF, SRC that can associate and regulate the transcription of HIF-1α (94). HDACs are divided into 4 classes based on their domain organization. Class I, II, and IV HDACs depend on zinc as a co-factor, whilst class III HDACs known as sirtuins (SIRTs), depending on the co-factor NAD+ (95). Class I and class IIa HDACs enhances HIF-1α stability by directly binding to the oxygen-dependent degradation domain of HIF-1α and class IIb HDACs promote HIF-1α transcriptional activity (96, 97).

TABLE 1 | Clinical implications of non-coding RNAs in perinatal hypoxia ischemia studies: SYMBOLS: ↑, Upregulation; ↓, Downregulation; –, Not specified.

	Observed in	Observed effect in HI	Clinical implications	References
Human	Blood plasma	↑miR-210	Therapeutic target	(54)
	Placenta			(55)
			Biomarker	(56)
				(57)
				(58)
	Umbilical cord blood	↓miR-210		(54)
		↓miR-374a		(59)
		↓miR-181b-5p ↓miR-374a-5p ↓miR-376c-3p		(60, 61)
		↓miR-181b ↑miR-210		(60, 61)
	Maternal whole blood			(55)
Pig	Blood plasma			(58)
Rat	Cerebral cortex		Inhibition of miR-210 as therapy	(62)
				(63)
				(64)
		↓miR-139-5p	miR-139-5p agomir as therapy	(65)
		↓miR-129-5p	miR-129-5p mimic as therapy	(66)
		↓miR-23a/b ↑lncRNA-GAS5	↑miR-23a by ↓GAS5 as therapy	(67)
		↓miR-17	IRE1α RNase inhibitor and miR-17-5p mimic as therapy	(68)
		↓miR-17-5p	PPAR-β/δ agonist GW0742 as therapy	(69)
		↑chr6:48820833|48857932	circRNAs as diagnostic tools and therapeutic targets	(70)
	Hippocampus and cortex	↑lncRNAs BC088414	Inhibition of BC088414 as therapy	(71)
	Hippocampus	↓miR124 ↓miR132 ↓miR134	Maternal tRESV supplementation diet as neuroprotective strategy	(72)
	Pineal gland	↑miR-325-3p	Inhibition of miR-325-3p as therapy	(73)
Mice	Cerebral cortex	↓miR-23a/b ↓miR-27a/b	Therapeutic targets	(74)
		↓miR-592-5p	miR-592-5p upregulation as neuroprotective strategy	(75)
	Hippocampus	↑Meg3	↑miR-129-5p silencing of Meg3 as therapy	(76)
In vitro	OGD-induced activated microglial cells	↓miR-21	Ectopic miR-21 as therapy	(77)

HI, hypoxia-ischemia; miR(NA), micro RNA; PPAR-β/δ, Peroxisome proliferator-activated receptor beta or delta; Procr, endothelial protein C receptor; tRESV, trans resveratrol.

POTENTIAL BIOMARKERS

miRNAs

MIR210 is the master hypoxamir and its expression is induced under hypoxia in many cell types. MIR210 acts downstream of HIF-1α, repressing several key processes to lower cellular energy requirements during hypoxia (31, 47, 98, 99). Human studies have consistently shown MIR210 upregulation in placenta (57, 100–103) and plasma (104) from preeclampsia pregnancies, and also in intrauterine growth restriction (56) (**Table 1**). Studies using maternal miRNAs derived from the placenta circulate in the maternal blood during pregnancy and may serve as non-invasive biomarkers. Studies using maternal plasma (57), and blood (55) have shown an elevation in MIR210 in both chronic and acute fetal hypoxia. miRNAs produced in the placenta circulate in the maternal blood during pregnancy and can be used as non-invasive biomarkers for hypoxia *in-utero* and HIE, allowing early interventions.

When perinatal HIE is diagnosed, it is critical to grade the injury to decide whether or not to subject the patient to hypothermic treatment. The ideal biomarker for HIE will quickly define the grade of HIE, and it should discriminate newborns with mild HIE, for whom hypothermia therapy is not indicated, from newborns with moderate HIE, who are eligible for this treatment. Levels of MIR210 in neonatal patient blood in combination with MIR374a, S100B protein, and Neuron-specific enolase (NSE) have shown high accuracy in distinguishing HIE patients from healthy newborns, but also between mild, moderate, and severe HIE (54). These biomarkers also showed prognostic value as their levels correlated with

neonatal behavioral neurological assessment scores. Increased levels of MiR210 were corroborated in plasma using piglet newborn model of HI (58).

Notably, MIR374a is downregulated in the umbilical cord blood after global HIE in humans (59). The extent of down-regulation of MIR374a corresponded to the severity of the insult and, as such, combining the levels of MIR374a with MIR210 may have prognostic value. Other studies in human neonates have shown a correlation between the downregulation of MIR181b, MIR199a, and MIR376c in the umbilical cord blood after HI, and the severity of the hypoxic insult (60, 61). Combining the levels of MIR181b and its target ubiquitin C-terminal hydrolase-L1 (*UCH-L1*) has diagnostic value, possibly enabling discrimination between moderate and severe HIE.

A principal component of HI brain damage is the inflammatory response and associated excitotoxicity (105). HI activates astrocytes and microglia that participate in the inflammatory response leading to increased levels of pro-inflammatory cytokines (106, 107). In this context, a second key hypoxamir is MIR21, a miRNA that could modulate inflammation. MIR-21 also controls several other key processes after HI, including cellular proliferation and migration, mitochondrial function, apoptosis, and HIF-1α stabilization and signaling (47, 49). MIR21 has been shown to be increased in cases of severe preterm fetal growth restriction compared to controls, and combined expression profiles of MIR21 and MIR20b in maternal blood were shown to be associated with the grade of fetal hypoxia at birth (55).

For the use of miRNAs as biomarkers, optimization of protocols for extraction and analysis of circulating miRNAs still needs further improvement toward selectivity and specificity (108). Remarkably, a study in human neonates demonstrated that it is feasible to extract sufficient miRNA from a single dried peripheral blood spot (109), with expression patterns that correlate well with those from EDTA-blood. This method eliminates potential sources of error, associated with blood collection and centrifugation. It is relatively cheap, technically easier to obtain, and easier for transportation and storing. Optimization and standardization of protocols for miRNA analysis will help the implementation into a clinical setting.

One consideration when examining miRNAs profiles after HI is that people of discrepant ethnicities might respond to the injury in different ways, therefore study results obtained in one ethnic group might not be appropriate for another cohort (54). Large-scale studies covering diverse ethnicities should be conducted to address this question.

LncRNAs

In addition to ncRNAs, elevated levels of circulating cell-free fetal DNA (cffDNA) and cell-free fetal RNA (cffRNA) have been proposed as an early indicator of damages caused by perinatal hypoxia, that could be used as early biomarkers for preeclampsia or HIE. A study using newborn piglets exposed to hypoxia-reoxygenation revealed tendencies to higher concentrations of cffDNA in the cerebrospinal fluid in comparison to controls (110). This indicates that CffDNA and cffRNA levels in maternal blood, and also cell-free RNA of placental origin, could have potential applications as biomarkers for the screening and diagnosis of preeclampsia (111).

POTENTIAL TREATMENTS

HIF-1α

In the brains of both fetuses and posnatal (P) 12 rat pups, fetal hypoxia resulted in global DNA hypomethylation and a continuous increase in HIF-1α mRNA and protein, and increased brain injury in response to hypoxia and ischemia (112). In the early stages of neonatal cerebral ischemia, inhibition of HIF-1α has been shown to be neuroprotective. In P7 HI rats inhibition of HIF-1α by 2-methoxyestradiol (2ME2) immediately after HI protected neuronal cells, attenuated blood-brain-barrier (BBB) disruption, and reduced brain edema (113). In contrast, the stabilization of HIF-1α with dimethyloxalylglycine (DMOG), increased BBB permeability and brain edema.

The c-glycosylated flavonoid, vitexin (5, 7, 4-trihydroxyflavone-8-glucoside) is a natural compound found in many medicinal plants, that has HIF-1α inhibitor activity (114). Intraperitoneal administration of vitexin immediately (5 min) after the HI insult in perinatal rats attenuated the increase in HIF-1α and vascular endothelial growth factor (VEGF), reduced infarct size, improved brain edema, BBB disruption, and neuronal cell death, and improved the neurobehavioral outcomes (115). Pretreatment with vitexin before HI showed the same results (116), diminishing the pro-apoptotic signaling pathway by inhibiting the phosphorylation of Ca^{2+}/Calmodulin-dependent protein kinase II, and increasing the BCL-2/BAX protein ratio 24 h after injury. Animals pretreated with vitexin showed reduced brain infarct volume, brain atrophy, and improved neurobehavioral outcomes. Vitexin has also been proposed as a treatment for HI induced epilepsy (117). Treatment with vitexin suppress brain HI induced electrical activity in neonatal rats, by inhibiting the Na-K-Cl cotransporter (NKCC1), and preventing HI induced BBB leakage, and inflammatory cytokine and neutrophil infiltration. These results support further scientific exploration of vitexin as therapy for perinatal for HIE.

DNA (de)Methylation

Defining the direct vs. indirect effects of hypoxia on DNA methylation in HIE populations is challenging. DNA methylation is time, tissue, and cell-type-specific, which poses a challenge in human studies that usually analyze peripheral blood (118). Studies in animal models have shown a causal effect of gestational and perinatal acute hypoxia on the regulation of gene-specific DNA methylation in mediating the neonatal programming of hypoxic sensitivity and the resulting consequences on the developing fetus and offspring. The first report associating DNA methylation to HI brain damage came from a model of ischemia/reperfusion using adult rats, showing that HI generated a 3- to 4-fold increase in methyl group incorporation in the brain (119). Transgenic animals expressing reduced DNA methyltransferase levels did not show this increase in DNA methylation and were resistant to HI brain injury.

In addition, evidence from studies following stroke indicated that the generation of reactive oxygen species (ROS) and

reactive nitrogen species (RNS) directly modify cytosine residues chemically, by promoting DNA hydroxymethylation (120, 121). Moreover, peroxides involved in stroke have been shown to induce nucleobase modifications like 5-chlorocytosine, which mimics 5-mC and induces improper *Dnmt1* methylation within CpG sequences, resulting in gene silencing (122). These findings associated oxidative stress and epigenetic changes via chemical DNA modifications and altering DNA-protein interactions.

In the perinatal period, the majority of studies involving DNA methylation in HI have investigated the effect of a preconditioning stimulus on methylation and subsequent vulnerability to the HI insults. In ischemic tolerance, exposure to a sublethal ischemic (preconditioning) event protects the brain against a subsequent severe ischemic challenge, producing tolerance.

In rat studies, mild fetal asphyxia during the last week of gestation caused global changes in gene transcription at birth, with down-regulation of most mRNA transcripts in the brain, and upregulation of DNMT1 and DMT3L, various HDACs, the Polycomb group ring finger 2 (PCGF2) and the methyl-CpG-binding protein-2 (MeCP2) (123). Fetal asphyxia preconditioning protected against subsequent severe perinatal global HI, reducing postnatal mortality and behavioral deficits after perinatal HI. Concomitantly, fetal asphyctic preconditioning lowered acute cytokine infiltration and modulated the transcriptional response to perinatal asphyxia. This effect was mediated by epigenetic changes, particularly involving histone deacetylation (124–126).

Other evidence suggest that prenatal insults generally tend to increase vulnerability to neonatal HI. In studies using rat models, HI induced gene-specific DNA hypermethylation. In the developing rat fetus, fetal hypoxia (GD 15 to 21) increased methylation of the glucocorticoid receptor (GR) gene (*Nr3c1*) promoter and repression of the GR in the brain, leading to an increased brain vulnerability to hypoxic-ischemic injury (127). In this way, methylation controls the expression patterns of GR, being key in the stress-mediated programming of GR expression (127, 128).

As mentioned, HIF-1α and DNA hypomethylation participate in fetal stress-mediated programming of HI sensitive phenotypes (112). Maternal hypoxia in rats, during the last week of gestation, reduced global methylation levels in the fetal brain and affected methylation of the HIF-1α gene. More specifically, hypomethylation induced by either maternal hypoxia, or pharmacological treatment with the DNMT inhibitor 5-aza-dC increased the vulnerability of the fetus to subsequent neonatal HI and worsened neurobehavioral outcomes in the rat pups. Interestingly, inhibiting HIF-1α with 2ME could counteract some of the damaging effects of hypomethylation.

Prenatal nicotine exposure has shown to increase brain infarct size after subsequent neonatal HI in male rats (129, 130). This increased susceptibility was linked to a down-regulation of angiotensin II receptor expression in the brain and hypermethylation of the angiotensin II type 2-receptor (*At2r*) promoter.

miRNAs

miRNAs and its regulated genes have also been proposed as therapeutic targets. Induction of miRNAs inhibiting pro-apoptotic pathways and inhibition of miRNAs implicated in HI-induced inflammation and apoptosis has shown therapeutic potential in animal models. Further characterization of these findings will help them advance into clinical trials.

MiR139-5p is down-regulated in P10 rat brains after HI treatment, and in cultured neurons exposed to OGD (65). The expression of MiR139-5p correlates inversely with the expression of one of its targets, the pro-apoptotic protein human growth transformation dependent protein (HGTD-P) (131). Interestingly, administration of MiR139-5p agomir attenuates HI brain damage, which is concurrent with the downregulation of HGTD-P expression. This effect was shown even at 12 h after the insult, indicating that targeting epigenetic pathways could extend the therapeutic window in HI brain damage.

The selective α2-adrenoreceptor agonist dexmedetomidine has been shown to provide neuroprotection in HI by inhibiting apoptosis, oxidative activity, Notch/NF-κB activation (132), and inflammation (133). MiR129-5p targets the type III procollagen gene (*COL3A1*) and has shown therapeutic potential in P7 HI rats mimicking and enhancing the neuroprotective effect of dexmedetomidine (66).

Hypoxia-induced brain injury appears to downregulate the expression of the MiR23-27 cluster leading to increased apoptosis. Overexpression of MiR23a/b and MiR27a/b was shown to exert neuroprotective effects in the late stage of mouse gestation (GD20) after global maternal hypoxia, by reducing apoptotic pathways including the expression of Apoptotic protease factor-1 (Apaf-1) (74). Indirectly increasing MiR23a expression by reducing the expression of the lncRNA Growth arrest-specific 5 (GAS5), that binds to MiR23a, reduced infarct size after HI in P10 rats (67).

One pathological mechanism of HI damage is the induction of endoplasmic reticulum stress, which activates the unfolded protein response (UPR). The UPR induces activation of stress sensor signaling pathways, like the RNase inositol requiring enzyme-1 alpha (IRE1α) pathway, leading to inflammation and neuronal cell death. In this context, MiR17-5p, a substrate of IRE1α, is a target that has shown therapeutic potential (68). Animal studies have shown that MiR17-5p mimic before HI, prevented inflammasome activation reducing brain infarct volume. Moreover, intranasal administration of the IRE1α inhibitor STF-083010 1h post-HI attenuated MiR17-5p downregulation and brain injury, and improved neurological behavior outcomes. It has also been reported that activation of the nuclear receptor peroxisome proliferator-activated receptor beta/delta (PPAR-β/δ) in P10 HI rat, by intranasal delivery of the agonist GW0742, could induce MiR17-5p levels (69), diminishing apoptosis, brain infarct area, brain atrophy, and improving neurological function post HI.

In vitro findings showed that primary neonatal rat microglial cells exposed to hypoxia experience downregulation of MiR21 expression and upregulation of one of its targets, the apoptosis-inducing factor Fas ligand (*FasL*) (77). Overexpression of FasL post hypoxic microglial activation increased neuronal apoptosis,

which can be partially reversed by ectopic expression of MiR21. MiR592-5p targets inflammation by targeting the prostaglandin D2 receptor. HI in P7 rats reduces the expression of MiR592-5p and increases prostaglandin D2 expression in the hippocampus, which is detrimental (75), induction of this miRNA could also be beneficial in HI.

MiR124 is the most abundant brain-specific miRNA and plays key roles in neuronal development. Multiple studies have shown a neuroprotective effect of MiR124 in adult HI models (134–137), which has not been validated for the perinatal period. Animal studies showed that MiR124 was down-regulated in the hippocampus after global neonatal hypoxia in rats (72). MiR124 warrants further investigation in neonatal HI models as it may have therapeutic value.

A potential strategy to use miRNAs as therapeutic targets is comprised of inhibiting miRNAs by using antagomirs, or naturally occurring compounds with similar effects such as curcumin or resveratrol. MiR210 expression steadily increases over the first 24 h after HI in P10 rats, disrupting glucocorticoid receptor-mediated neuroprotection and increasing leakiness of the BBB (62–64). Inhibition of MiR210 using an intracerebroventricular injection of complementary locked nucleic acid oligonucleotides increased BDNF signaling, reduced neuronal death and infarct size, and improved functional recovery of the animals. *In vitro* studies also support these findings (138). Although this suggests that MiR210 inhibitors could be used as a potential therapy in HI brain injury, further characterization of its spatiotemporal expression, regulation, targets, and physiological and pathogenic effects in HIE is still required.

NF-κB triggers MiR155, inducing pro-inflammatory effects compromising the BBB integrity. Inhibition of MiR155 is neuroprotective in adult HI models by reducing brain cytokines (139), but its role in neonatal models is underexplored to date. The neuroprotective actions of resveratrol and curcumin in neonatal HI (140–142) may in part be due to the downregulation of MiR155 and MiR21 by resveratrol, and the downregulation of MiR21 by curcumin, combined with epigenetic and anti-oxidant mechanisms (143, 144). MiR153 is reported to be a neuron-related miRNA (50). Inhibition of MiR153 protects neurons against OGD/R-induced injury by increasing the expression of Nuclear factor erythroid 2-related factor 2 (*Nrf2*) and heme oxygenase-1 (*HO-1*) signaling.

Sleep problems associated with circadian rhythm disruptions are common in children after mild-moderate HIE (145), and disruptions in miRNAs likely contribute to these abnormalities. HI in P7 rats leads to an increased expression of MiR325-3p in the pineal gland (73). This disrupts melatonin signaling by targeting Aralkylamine N-acetyltransferase (AANAT), a key protein that controls melatonin synthesis, and this leads to circadian rhythm disturbances. Reducing MiR325-3p has been shown to prevent this impairment after OGD *in vitro*.

Long-Non Coding and Circular RNAs

Studies in human neonates diagnosed with HIE and animal models have shown that lncRNAs are aberrantly expressed under hypoxic conditions and might be implicated in regulating the expression of protein-coding genes involved in pathological processes associated to HI brain damage. A microarray study in human neonates showed that neonatal HI dramatically changed the expression patterns of numerous ncRNAs in peripheral whole blood (146), including 376 lncRNAs and 126 mRNAs involved in the immune system and nervous system. A study on the P7 HI rat cortex identified 7,157 differentially expressed mRNA transcripts, and 328 differentially expressed lncRNAs targeting mRNAs involved in inflammatory and immune responses, wounding, and neurological system processes (147). Specifically, JAK-STAT, NF-κB, and TLR signaling pathways were altered. Targeting genes in these pathways is proposed as a therapeutic strategy.

LncRNAs have shown potential therapeutic applications in animal models. Various studies have pointed to the inhibition of HI-induced lncRNAs as a therapeutic approach to induce neuroprotection. A second microarray profiling study in P10 rats exposed to HI pointed in the same direction, finding expression differences in 322 lncRNAs and 375 coding genes in hippocampal and cortex tissue 24 h after the insult (71). Upregulated protein-coding genes were also involved in inflammation and wounding, while repair and neurogenesis pathways were downregulated. BC088414, which plays a role in apoptosis by regulating caspase 6 (*Casp6*) and in adrenergic signaling by regulating the beta-2 adrenergic receptor (*Adrb2*), was the most significantly upregulated lncRNA. Inhibition of BC088414 with a siRNA in PC12 cells exposed to OGD resulted in the downregulation of *Adrb2* and *Casp6*, increased cell proliferation, and decreased apoptosis.

The lncRNA maternally expressed gene 3 (Meg3) induces cell death in ischemia by binding to the p53 DNA binding domain (148). A study in P7 HI mice hippocampus showed that the Meg3 sponges MiR129-5p, a miRNA with neuroprotective activity, and abolishes the effect of dexmedetomidine therapy (76). The silencing of Meg3 and upregulation of MiR129-5p enhanced the therapeutic effect of dexmedetomidine. Finally, the lncRNA Growth arrest-specific 5 (Gas5) was also shown upregulated in HI models (67). Gas5 sponges MiR23a thereby preventing its neuroprotective action. Inhibition of Gas5 by intracerebroventricular delivery of Gas5 small hairpin RNA has been shown to reduce brain infarct size and diminish functional sequelae in rats, suggesting its use as therapy for the treatment of HI brain injury.

CircRNAs are a subtype of lncRNAs that form a closed loop. CircRNAs play crucial roles as miRNA sponges, and recent studies highlighted the role of these molecules in hypoxic regulation. An exploratory study in P3 HI rats found 98 dysregulated circRNAs in the brain (70). One of the top hits, termed chr6:48820833|48857932, targets HIF-1α signaling by sponging the HIF-1α-targeting-miRNAs MiR433-3p and MiR206-3p. Another study in P10 HI rats discovered a total of 66 circRNAs differentially expressed in HI brain damage rats compared to controls (149). Numerous mRNAs transcribed from the host genes of altered circRNAs were associated with brain damage and neural regeneration processes. These results indicate a novel focus for future studies investigating the molecular mechanism underlying HIE and potentials new biomarkers and treatments through modulating circRNAs.

TABLE 2 | Clinical implications of histone modifications in perinatal hypoxia ischemia studies.

Observed effect in HI	Observed in	Other findings	Clinical implications	References
↓EZH2 ↑H3K27 3me	Rat hippocampus	↑ Pten/Akt/mTOR pathway ↑ Autophagy	Sevofluorane neuroprotection via ↑ EZH2	(152–154)
↓SIRT1	Rat hippocampus and cerebral cortex	↑ Unfolded protein response (UPR)	Melatonin neuroprotection via ↑ SIRT1	(155)
↑ SIRT1	Mice oligodendrocyte progenitor cells	↑ Cdk2/Rb/E2F1 pathway ↑ Oligodendrocyte progenitor cell proliferation	↑ Sirt1 activity for oligodendrocyte recovery	
↑Acetyl-Histone H3 (Ac-H3) ↑Acetyl-Histone H4 (Ac-H4)	Rat	↑Caspase-3 ↑Apopstosis	HDAC activity as target of uridine neuroprotection	(156)
↑Histone 3 deimination (citH3)	Mice hippocampus, cortex, striatum and piriform cortex	↑ TNFα	PAD inhibition as therapeutic target	(157, 158)
↑REST	Hippocampal CA1	↓GluR2 ↓AMPA and NMDA receptors ↑Excitotoxicity	REST inhibition as therapeutic target	(159, 160)

SYMBOLS: ↑, Upregulation; ↓, Downregulation; EZH2, Enhancer of zeste homolog 2; HI, hypoxia-ischemia; HDAC, Histone deacetylase; PAD, protein arginine deiminases; REST, RE1-Silencing Transcription factor; SIRT1, Sirtuin 1; TNFa, Tumor necrosis factor alpha.

Histone Methylation

Enhancer of zeste homolog 2 (EZH2), a catalytic subunit of Polycomb repressive complex 2 (PRC2), plays an important role in mammalian CNS development (150). EZH2 participates in hippocampal learning, memory, and neurogenesis through trimethylation at H3K27 (H3K27me3), which silences downstream genes, including, among others, BDNF and PTEN (151). In HIE, autophagy is increased in the hippocampus, and inhibition of autophagy provides neuroprotection. In this regard, volatile anesthetics, i.e., sevoflurane and isoflurane, have shown to be neuroprotective against HI brain damage in neonatal rats (152, 153) (**Table 2**). Diverse studies have shown sevoflurane inhibits excessive hippocampal autophagy increasing the expression of EZH2, H3K27me3, and decreased expression of PTEN induced by HI, improving the behavioral outcome (154).

Histone Acetylation

Many studies have shown the implications of HATs in perinatal HI damage. Fetal asphyxia in E17 rats leads to an upregulation of class I HDACs HDAC1, HDAC2, HDAC3, and the HAT MYST3 (123). The same stimulus upregulated HDAC1 and class IIb HDAC10 and HDAC11, after severe perinatal asphyxia (126). The HDAC SIRT1 plays an important role in the regulation of oligodendrocyte progenitor cell proliferation and oligodendrocyte regeneration after neonatal brain injury. Neonatal hypoxia in P3 mice has been shown to enhance SIRT1 and SIRT1/Cdk2 complex formation through HIF1α activation, leading to an enhanced oligodendrocyte progenitor cell proliferation (161). Enhancing SIRT1 activity may promote oligodendrocyte recovery after diffuse white matter injury. SIRT1 expression was significantly reduced after neonatal HI in P7 rat pups (155) in cells that activate the unfolded protein response (UPR). In that same study, melatonin neuroprotection involved the prevention of SIRT1 downregulation and UPR activation.

From a therapeutic perspective, HDAC inhibitors (HDACi's) represent the most widely studied epigenetic drugs as several existing marketed drugs and natural dietary metabolites inhibit HDACs. Regarding HI, HDAC inhibition reduces HIF-1α signaling, which is generally protective against HI (96, 112). Numerous HDAC inhibitors have shown beneficial effects in either focal or global neonatal HI. For example, the marketed anticonvulsant sodium valproate inhibits class I HDAC activity and has shown potential in treating neonatal HI in rats (162). Several naturally occurring bioactive molecules, such as trichostatin A (163), sodium butyrate (164), curcumin (142), quercetin (165), resveratrol (72, 140, 141), and uridine (156) have also proven protective effects in focal neonatal HI, the effects of which were shown to be at least partially dependent on HDAC inhibition. The mechanism(s) by which HDACi's provide neuroprotection include prevention of oxidation, suppression of inflammation, and reduction of apoptosis. Importantly, histone acetylation/methylation precedes DNMT or TET methylcytosine dioxygenase binding and promoter methylation/demethylation, and these mechanisms function cooperatively (166). Still, many potential problems remain to be addressed before clinical use of selective HDACi's for the treatment of HIE.

Other Histone Modifications and Epigenetic Complexes

Protein deimination (citrullination) is a post-translational modification that converts the amino acid arginine into citrulline, is caused by Ca^{+2}-regulated peptidylarginine deiminases (PADs), and can act on histone tails.

H3 citrullination (citH3) by PAD4 is associated with gene regulation and the formation of neutrophil extracellular traps in response to infection. PAD activity is induced under HI with or without lipopolysaccharide stimulation. Selective and targeted pharmacological PAD inhibition following HI can be a therapeutic target to enhance neuroprotection (157). Hypothermia following the insult inhibits this pathway and affect the Ca^{2+}-regulated PAD activation (158).

A large degree of epigenetic variation is controlled by epigenetic regulatory complexes. Several epigenetic regulatory complexes may play a role in neonatal HI injuries. The repressor

element-1 (RE1) silencing transcription factor (REST) is the main regulator of neurogenesis and neuronal fate. Neuronal genes controlled by REST contain an RE1 motif. As such, REST assembles to this site with its co-repressor CoREST and recruits a number of epigenetic regulators including HDACs and histone methyltransferases to the promoters of target genes to achieve epigenetic changes (167, 168). It has been demonstrated that REST is a HI-responsive gene, regulating around 20% of the hypoxia-repressed genes. As an example, HI has been shown to upregulate REST expression in the hippocampal CA1, suppressing GluR2 gene expression (159). Interestingly, the downregulation of REST expression with antisense oligodeoxynucleotides has been demonstrated to be neuroprotective 72 h post OGD. REST was also shown to orchestrate epigenetic changes and silencing of miR-132 in insulted CA1 neurons (169) and has been shown to bind directly to the HIF-1α promoter in order to repress HIF-1α transcription after prolonged hypoxia (159, 170, 171). Moreover, REST has been demonstrated to repress the transcription of AMPA and NMDA glutamate receptor subunits (168), which are involved in mediating excitotoxicity after HIE (18). Recently, it has been shown that adult rats overexpress REST after CAO (160), and knocking down REST with an intracerebral siRNA injection increased the expression of its target genes, attenuated apoptosis, and infarct volume, and improved post-ischemic functional recovery. Altogether, although the actual therapeutic potential of REST in the perinatal period has not yet been explored, these data suggest REST reflects a promising new therapeutic target to treat acute hypoxic brain damage.

DISCUSSION

There is an urgent need for new therapies for neonatal HI, as currently, therapeutic hypothermia for term infants is not fully protective against HIE, and the disability burden after neonatal HI remains high. Evidently, epigenetic mechanisms play a key role in the pathological cascade after neonatal HI. The cellular hypoxia response, mediated by HIF-1α and other hypoxia-inducible factors, is controlled by an intricate multi-leveled epigenetic network centered on HIF-1a. A better understanding of this intricate regulatory circuit will provide us with new diagnostic tools and therapeutic approaches for HIE. As an example, HIF-1α signaling controls the expression of various miRNAs, whileHIF-1α by itself is intricately controlled by different miRNAs. Apart from HIF-1α signaling, numerous miRNAs regulate a myriad of other processes relevant for HI, ranging from well-studied processes like inflammation and apoptosis to circadian rhythm disturbances after HIE. Some hypoxia-regulated miRNAs in the maternal blood are promising in terms of identifying pregnancies at risk of fetal hypoxia, permitting early intervention, whereas preclinical interventions using miRNAs are promising in combination with therapeutic hypothermia. Together with miRNAs, HDACs hold promise as biomarkers and therapeutic targets. HDAC inhibitors represent the most advanced agents in this respect as several existing marketed drugs and natural dietary metabolites have been shown to directly inhibit HDACs.

Still, no single epigenetic mark has demonstrated enough reliability and reproducibility to be used as a biomarker or as a therapeutic target in a clinical setting. For this purpose, replication and/or validation studies in larger cohorts are needed. In conclusion, even though numerous advancements have been made in understanding the pathophysiology of perinatal HI brain damage, still our knowledge on the role of epigenetics in HI is very limited. As such, new discoveries on epigenetics may mark the beginning of an etiopathogenic research revolution in neurodevelopmental disorders, and continued exploration of this area is of great promise.

AUTHOR CONTRIBUTIONS

MBu, MBa, MAB, AG, CL, and DH conceived the presented idea. MBu and MBa wrote the first draft. DH and HS edited the draft. AG, MAB, and CL provided funding for the manuscript. All authors read the final version of the manuscript.

FUNDING

This research was partially supported by the Sistema de Investigación y Desarrollo (SINDE) and the Vicerrectorado de Investigación y Posgrado of the Universidad Católica de Santiago de Guayaquil, Guayaquil, Ecuador. MBu was funded by Consejo Nacional de Investigaciones Científicas y Técnicas (CONICET) of Argentina and the Foundation of Pediatrics, Maastricht University Medical Center+ (MUMC+). CL was supported by Universidad de Buenos Aires (UBACyT - 20020160100150BA). All views expressed in this article are those of the authors and do not represent the views of the funding agencies.

REFERENCES

1. Choudhuri S. From Waddington's epigenetic landscape to small noncoding RNA: some important milestones in the history of epigenetics research. *Toxicol Mech Methods*. (2011) 21:252–74. doi: 10.3109/15376516.2011.559695
2. Bolton JL, Molet J, Ivy A, Baram TZ. New insights into early-life stress and behavioral outcomes. *Curr Opin Behav Sci*. (2017) 14:133–9. doi: 10.1016/j.cobeha.2016.12.012
3. Lahiri DK, Maloney B, Zawia NH. The LEARn model: an epigenetic explanation for idiopathic neurobiological diseases. *Mol Psychiatry*. (2009) 14:992. doi: 10.1038/mp.2009.82
4. Nelson KB, Leviton A. How much of neonatal encephalopathy is due to birth asphyxia? *Am J Dis Child*. (1991) 145:1325–31. doi: 10.1001/archpedi.1991.02160110117034
5. Kurinczuk JJ, White-Koning M, Badawi N. Epidemiology of neonatal encephalopathy and hypoxic-ischaemic encephalopathy. *Early Hum Dev*. (2010) 86:329–38. doi: 10.1016/j.earlhumdev.2010.05.010

6. Frøen JF, Gardosi JO, Thurmann A, Francis A, Stray-Pedersen B. Restricted fetal growth in sudden intrauterine unexplained death. *Acta Obstet Gynecol Scand.* (2004) 83:801–7. doi: 10.1111/j.0001-6349.2004.00602.x
7. Maršál K. Obstetric management of intrauterine growth restriction. *Best Pract Res Clin Obstetr Gynaecol*. (2009) 23:857–70. doi: 10.1016/j.bpobgyn.2009.08.011
8. Graham EM, Ruis KA, Hartman AL, Northington FJ, Fox HE. A systematic review of the role of intrapartum hypoxia-ischemia in the causation of neonatal encephalopathy. *Am J Obstet Gynecol.* (2008) 199:587–95. doi: 10.1016/j.ajog.2008.06.094
9. Black RE, Cousens S, Johnson HL, Lawn JE, Rudan I, Bassani DG, et al. Global, regional, and national causes of child mortality in 2008: a systematic analysis. *Lancet*. (2010) 375:1969–87. doi: 10.1016/S0140-6736(10)60549-1
10. Wachtel EV, Hendricks-Muñoz KD. Current management of the infant who presents with neonatal encephalopathy. *Curr Probl Pediatr Adolesc Health Care*. (2011) 41:132–53. doi: 10.1016/j.cppeds.2010.12.002
11. Lemyre B, Chau V. Hypothermia for newborns with hypoxic-ischemic encephalopathy. *Paediatr Child Health*. (2018) 23:285–91. doi: 10.1093/pch/pxy028
12. Natarajan G, Pappas A, Shankaran S. Outcomes in childhood following therapeutic hypothermia for neonatal hypoxic-ischemic encephalopathy (HIE). *Semin Perinatol*. (2016) 40:549–55. doi: 10.1053/j.semperi.2016.09.007
13. Rivero-Arias O, Eddama O, Azzopardi D, Edwards AD, Strohm B, Campbell H. Hypothermia for perinatal asphyxia: trial-based resource use and costs at 6–7 years. *Arch Dis Childh Fetal Neonatal Ed*. (2019) 104:F285–92. doi: 10.1136/archdischild-2017-314685
14. Sarkar S, Barks JD. Systemic complications and hypothermia. *Semin Fetal Neonatal Med*. (2010) 15:270–5. doi: 10.1016/j.siny.2010.02.001
15. Northington FJ, Chavez-Valdez R, Martin LJ. Neuronal cell death in neonatal hypoxia-ischemia. *Ann Neurol.* (2011) 69:743–58. doi: 10.1002/ana.22419
16. Robertson NJ, Cowan FM, Cox IJ, Edwards AD. Brain alkaline intracellular pH after neonatal encephalopathy. *Ann Neurol.* (2002) 52:732–42. doi: 10.1002/ana.10365
17. Semple BD, Blomgren K, Gimlin K, Ferriero DM, Noble-Haeusslein LJ. Brain development in rodents and humans: identifying benchmarks of maturation and vulnerability to injury across species. *Prog Neurobiol.* (2013) 106:1–16. doi: 10.1016/j.pneurobio.2013.04.001
18. Barkhuizen M, Van den Hove D, Vles J, Steinbusch H, Kramer B, Gavilanes A. 25 years of research on global asphyxia in the immature rat brain. *Neurosci Biobehav Rev.* (2017) 75:166–82. doi: 10.1016/j.neubiorev.2017.01.042
19. Vazquez-Borsetti P, Pena E, Rojo Y, Acuna A, Loidl FC. Deep hypothermia reverses behavioral and histological alterations in a rat model of perinatal asphyxia. *J Comp Neurol.* (2019) 527:362–71. doi: 10.1002/cne.24539
20. Takada S, Sampaio C, Allemandi W, Ito P, Takase L, Nogueira M. A modified rat model of neonatal anoxia: development and evaluation by pulseoximetry, arterial gasometry and Fos immunoreactivity. *J Neurosci Methods*. (2011) 198:62–9. doi: 10.1016/j.jneumeth.2011.03.009
21. Rice JE, Vannucci RC, Brierley JB. The influence of immaturity on hypoxic-ischemic brain damage in the rat. *Ann Neurol*. (1981) 9:131–41. doi: 10.1002/ana.410090206
22. Vannucci RC, Vannucci SJ. A model of perinatal hypoxic-ischemic brain damage A. *Ann N Y Acad Sci.* (1997) 835:234–49. doi: 10.1111/j.1749-6632.1997.tb48634.x
23. Edwards AB, Feindel KW, Cross JL, Anderton RS, Clark VW, Knuckey NW, et al. Modification to the Rice-Vannucci perinatal hypoxic-ischaemic encephalopathy model in the P7 rat improves the reliability of cerebral infarct development after 48 hours. *J Neurosci Methods*. (2017) 288:62–71. doi: 10.1016/j.jneumeth.2017.06.016
24. Loetscher PD, Rossaint J, Rossaint R, Weis J, Fries M, Fahlenkamp A, et al. Argon: neuroprotection in *in vitro* models of cerebral ischemia and traumatic brain injury. *Crit Care*. (2009) 13:R206. doi: 10.1186/cc8214
25. Kelly TK, De Carvalho DD, Jones PA. Epigenetic modifications as therapeutic targets. *Nat Biotechnol*. (2010) 28:1069–78. doi: 10.1038/nbt.1678
26. Biswas S, Rao CM. Epigenetic tools (The Writers, The Readers and The Erasers) and their implications in cancer therapy. *Eur J Pharmacol.* (2018) 837:8–24. doi: 10.1016/j.ejphar.2018.08.021
27. Watson JA, Watson CJ, McCann A, Baugh J. Epigenetics: the epicenter of the hypoxic response. *Epigenetics*. (2010) 5:293–6. doi: 10.4161/epi.5.4.11684
28. Tsai YP, Wu KJ. Epigenetic regulation of hypoxia-responsive gene expression: focusing on chromatin and DNA modifications. *Int J Cancer*. (2014) 134:249–56. doi: 10.1002/ijc.28190
29. Ke Q, Costa M. Hypoxia-inducible factor-1. (HIF-1). *Mol Pharmacol.* (2006) 70:1469–80. doi: 10.1124/mol.106.027029
30. Nguyen MP, Lee S, Lee YM. Epigenetic regulation of hypoxia inducible factor in diseases and therapeutics. *Arch Pharm Res*. (2013) 36:252–63. doi: 10.1007/s12272-013-0058-x
31. Ma Q, Xiong F, Zhang L. Gestational hypoxia and epigenetic programming of brain development disorders. *Drug Discov Today*. (2014) 19:1883–96. doi: 10.1016/j.drudis.2014.09.010
32. Hancock RL, Dunne K, Walport LJ, Flashman E, Kawamura AJE. Epigenetic regulation by histone demethylases in hypoxia. *Epigenomics.* (2015) 7:791–811. doi: 10.2217/epi.15.24
33. Koslowski M, Luxemburger U, Türeci Ö, Sahin U. Tumor-associated CpG demethylation augments hypoxia-induced effects by positive autoregulation of HIF-1α. *Oncogene*. (2011) 30:876. doi: 10.1038/onc.2010.481
34. Razin A, Riggs AD. DNA methylation and gene function. *Science*. (1980) 210:604–10. doi: 10.1126/science.6254144
35. van der Wijst MG, Venkiteswaran M, Chen H, Xu G-L, Plösch T, Rots MG. Local chromatin microenvironment determines DNMT activity: from DNA methyltransferase to DNA demethylase or DNA dehydroxymethylase. *Epigenetics*. (2015) 10:671–6. doi: 10.1080/15592294.2015.1062204
36. Monteggia LM, Kavalali ET. Rett syndrome and the impact of MeCP2 associated transcriptional mechanisms on neurotransmission. *Biol Psychiatry.* (2009) 65:204–10. doi: 10.1016/j.biopsych.2008.10.036
37. Kinde B, Gabel HW, Gilbert CS, Griffith EC, Greenberg ME. Reading the unique DNA methylation landscape of the brain: non-CpG methylation, hydroxymethylation, and MeCP2. *Proc Natl Acad Sci USA*. (2015) 112:6800–6. doi: 10.1073/pnas.1411269112
38. Ye D, Xiong Y. Cancer: suffocation of gene expression. *Nature*. (2016) 537:42. doi: 10.1038/nature19426
39. Fu X-D. Non-coding RNA: a new frontier in regulatory biology. *Nat Sci Rev*. (2014) 1:190–204. doi: 10.1093/nsr/nwu008
40. Qu Z, Adelson DL. Evolutionary conservation and functional roles of ncRNA. *Front Genet.* (2012) 3:205–205. doi: 10.3389/fgene.2012.00205
41. Coolen M, Bally-Cuif L. Chapter 18 - MicroRNAs in brain development. In: Sen CK, editor. *MicroRNA in Regenerative Medicine.* Oxford: Academic Press. (2015). p. 447–88.
42. Cui H, Yang L. Analysis of microRNA expression detected by microarray of the cerebral cortex after hypoxic-ischemic brain injury. *J Craniofac Surg.* (2013) 24:2147–52. doi: 10.1097/SCS.0b013e3182a243f3
43. Ponnusamy V, Yip PK. The role of microRNAs in newborn brain development and hypoxic ischaemic encephalopathy. *Neuropharmacology*. (2019) 148:55–65. doi: 10.1016/j.neuropharm.2018.11.041
44. Taguchi A, Yanagisawa K, Tanaka M, Cao K, Matsuyama Y, Goto H, et al. Identification of hypoxia-inducible factor-1α as a novel target for miR-17-92 microRNA cluster. *Cancer Res.* (2008) 68:5540–5. doi: 10.1158/0008-5472.CAN-07-6460
45. Rane S, He M, Sayed D, Vashistha H, Malhotra A, Sadoshima J, et al. Downregulation of miR-199a derepresses hypoxia-inducible factor-1α and Sirtuin 1 and recapitulates hypoxia preconditioning in cardiac myocytes. *Cicul Res*. (2009) 104:879–86. doi: 10.1161/CIRCRESAHA.108.193102
46. Ghosh G, Subramanian IV, Adhikari N, Zhang X, Joshi HP, Basi D, et al. Hypoxia-induced microRNA-424 expression in human endothelial cells regulates HIF-α isoforms and promotes angiogenesis. *J Clin Invest*. (2010) 120:4141–54. doi: 10.1172/JCI42980
47. Nallamshetty S, Chan SY, Loscalzo J. Hypoxia: a master regulator of microRNA biogenesis and activity. *Free Radic Biol Med.* (2013) 64:20–30. doi: 10.1016/j.freeradbiomed.2013.05.022
48. Bartoszewska S, Kochan K, Piotrowski A, Kamysz W, Ochocka RJ, Collawn JF, et al. The hypoxia-inducible miR-429 regulates hypoxia-inducible factor-1 α expression in human endothelial cells through a negative feedback loop. *FASEB J.* (2014) 29:1467–79. doi: 10.1096/fj.14-267054

49. Xu X, Kriegel AJ, Jiao X, Liu H, Bai X, Olson J, et al. miR-21 in ischemia/reperfusion injury: a double-edged sword? *Physiol Genomics*. (2014) 46:789–97. doi: 10.1152/physiolgenomics.00020.2014
50. Ji Q, Gao J, Zheng Y, Liu X, Zhou Q, Shi C, et al. Inhibition of microRNA-153 protects neurons against ischemia/reperfusion injury in an oxygen–glucose deprivation and reoxygenation cellular model by regulating Nrf2/HO-1 signaling. *J Biochem Mol Toxicol*. (2017) 31:e21905. doi: 10.1002/jbt.21905
51. Crosby ME, Kulshreshtha R, Ivan M, Glazer PM. MicroRNA regulation of DNA repair gene expression in hypoxic stress. *Cancer Res*. (2009) 69:1221–9. doi: 10.1158/0008-5472.CAN-08-2516
52. Huang X, Ding L, Bennewith KL, Tong RT, Welford SM, Ang KK, et al. Hypoxia-inducible mir-210 regulates normoxic gene expression involved in tumor initiation. *Mol Cell*. (2009) 35:856–67. doi: 10.1016/j.molcel.2009.09.006
53. Agrawal R, Pandey P, Jha P, Dwivedi V, Sarkar C, Kulshreshtha R. Hypoxic signature of microRNAs in glioblastoma: insights from small RNA deep sequencing. *BMC Genomics*. (2014) 15:686. doi: 10.1186/1471-2164-15-686
54. Wang Z, Liu Y, Shao M, Wang D, Zhang YJB. Combined prediction of miR-210 and miR-374a for severity and prognosis of hypoxic–ischemic encephalopathy. *Brain Behav*. (2018) 8:e00835. doi: 10.1002/brb3.835
55. Whitehead CL, Teh WT, Walker SP, Leung C, Larmour L, Tong SJ. Circulating microRNAs in maternal blood as potential biomarkers for fetal hypoxia *in-utero*. *PLoS ONE*. (2013) 8:e78487. doi: 10.1371/journal.pone.0078487
56. Awamleh Z, Gloor GB, Han VKM. Placental microRNAs in pregnancies with early onset intrauterine growth restriction and preeclampsia: potential impact on gene expression and pathophysiology. *BMC Med Genomics*. (2019) 12:91. doi: 10.1186/s12920-019-0548-x
57. Ishibashi O, Ohkuchi A, Ali MM, Kurashina R, Luo S-S, Ishikawa T, et al. Hydroxysteroid. (17-β) dehydrogenase 1 is dysregulated by miR-210 and miR-518c that are aberrantly expressed in preeclamptic placentas: a novel marker for predicting preeclampsia. *Hypertension*. (2012) 59:265–73. doi: 10.1161/HYPERTENSIONAHA.111.180232
58. Garberg HT, Huun MU, Baumbusch LO, Åsegg-Atneosen M, Solberg R, Saugstad OD. Temporal profile of circulating microRNAs after global hypoxia-ischemia in newborn piglets. *Neonatology*. (2017) 111:133–9. doi: 10.1159/000449032
59. Looney AM, Walsh BH, Moloney G, Grenham S, Fagan A, O'Keeffe GW, et al. Downregulation of umbilical cord blood levels of miR-374a in neonatal hypoxic ischemic encephalopathy. *J Pediatr*. (2015) 167:269–73.e262. doi: 10.1016/j.jpeds.2015.04.060
60. Looney A, O'Sullivan M, Ahearne C, Finder M, Felderhoff-Mueser U, Boylan G, et al. Altered expression of umbilical cord blood levels of miR-181b and its downstream target mUCH-L1 in infants with moderate and severe neonatal hypoxic-ischaemic encephalopathy. *Mol Neurobiol*. 56:3657–63. doi: 10.1007/s12035-018-1321-4
61. O'Sullivan MP, Looney AM, Moloney GM, Finder M, Hallberg B, Clarke G, et al. Validation of altered umbilical cord blood microRNA expression in neonatal hypoxic-ischemic encephalopathy. *JAMA Neurol*. (2018) 76:333–41. doi: 10.1001/jamaneurol.2018.4182
62. Ma Q, Dasgupta C, Li Y, Bajwa NM, Xiong F, Harding B, et al. Inhibition of microRNA-210 provides neuroprotection in hypoxic–ischemic brain injury in neonatal rats. *Neurobiol Dis*. (2016) 89:202–12. doi: 10.1016/j.nbd.2016.02.011
63. Ma Q, Dasgupta C, Li Y, Huang L, Zhang L. MicroRNA-210 suppresses junction proteins and disrupts blood-brain barrier integrity in neonatal rat hypoxic-ischemic brain injury. *Int J Mol Sci*. (2017) 18:1356. doi: 10.3390/ijms18071356
64. Wang L, Ke J, Li Y, Ma Q, Dasgupta C, Huang X, et al. Inhibition of miRNA-210 reverses nicotine-induced brain hypoxic-ischemic injury in neonatal rats. *Int J Biol Sci*. (2017) 13:76. doi: 10.7150/ijbs.17278
65. Qu Y, Wu J, Chen D, Zhao F, Liu J, Yang C, et al. MiR-139-5p inhibits HGTD-P and regulates neuronal apoptosis induced by hypoxia–ischemia in neonatal rats. *Neurobiol Dis*. (2014) 63:184–93. doi: 10.1016/j.nbd.2013.11.023
66. Zhou XM, Liu J, Wang Y, Zhang SL, Zhao X, Zhang MH. microRNA-129-5p involved in the neuroprotective effect of dexmedetomidine on hypoxic-ischemic brain injury by targeting COL3A1 through the Wnt/β-catenin signaling pathway in neonatal rats. *J Cell Biochem*. (2018) 120:6908–19. doi: 10.1002/jcb.26704
67. Zhao R-B, Zhu L-H, Shu J-P, Qiao L-X, Xia Z-K. GAS5 silencing protects against hypoxia/ischemia-induced neonatal brain injury. *Biochem Biophys Res Commun*. (2018) 497:285–91. doi: 10.1016/j.bbrc.2018.02.070
68. Chen D, Dixon BJ, Doycheva DM, Li B, Zhang Y, Hu Q, et al. IRE1alpha inhibition decreased TXNIP/NLRP3 inflammasome activation through miR-17-5p after neonatal hypoxic-ischemic brain injury in rats. *J Neuroinflamm*. (2018) 15:32. doi: 10.1186/s12974-018-1077-9
69. Gamdzyk M, Doycheva DM, Malaguit J, Enkhjargal B, Tang J, Zhang JH. Role of PPAR-beta/delta/miR-17/TXNIP pathway in neuronal apoptosis after neonatal hypoxic-ischemic injury in rats. *Neuropharmacology*. (2018) 140:150–61. doi: 10.1016/j.neuropharm.2018.08.003
70. Zhu L, Zhao R, Huang L, Mo S, Yu Z, Jiang L, et al. Circular RNA expression in the brain of a neonatal rat model of periventricular white matter damage. *J Cell Biochem*. (2018) 49:2264–76. doi: 10.1159/000493829
71. Zhao F, Qu Y, Liu J, Liu H, Zhang L, Feng Y, et al. Microarray profiling and co-expression network analysis of LncRNAs and mRNAs in neonatal rats following hypoxic-ischemic brain damage. *Sci Rep*. (2015) 5:13850. doi: 10.1038/srep13850
72. Isac S, Panaitescu AM, Spataru A, Iesanu M, Totan A, Udriste A, et al. Trans-resveratrol enriched maternal diet protects the immature hippocampus from perinatal asphyxia in rats. *Neurosci Lett*. (2017) 653:308–13. doi: 10.1016/j.neulet.2017.06.003
73. Yang Y, Sun B, Huang J, Xu L, Pan J, Fang C, et al. Up-regulation of miR-325-3p suppresses pineal aralkylamine N-acetyltransferase. (Aanat) after neonatal hypoxia–ischemia brain injury in rats. *Brain Res*. (2017) 1668:28–35. doi: 10.1016/j.brainres.2017.05.001
74. Chen Q, Xu J, Li L, Li H, Mao S, Zhang F, et al. MicroRNA-23a/b and microRNA-27a/b suppress Apaf-1 protein and alleviate hypoxia-induced neuronal apoptosis. *Cell Death Dis*. (2014) 5:e1132. doi: 10.1038/cddis.2014.92
75. Sun L-Q, Guo G-L, Zhang S, Yang L-L. Effects of microRNA-592-5p on hippocampal neuron injury following hypoxic-ischemic brain damage in neonatal mice-involvement of PGD2/DP and PTGDR. *Cell Physiol Biochem*. (2018) 45:458–73. doi: 10.1159/000486923
76. Zhou XM, Liu J, Wang Y, Zhang MH. Silencing of long noncoding RNA MEG3 enhances cerebral protection of dexmedetomidine against hypoxic-ischemic brain damage in neonatal mice by binding to miR-129-5p. *J Cell Biochem*. (2018) 120:7978–88. doi: 10.1002/jcb.28075
77. Zhang L, Dong LY, Li YJ, Hong Z, Wei WS. miR-21 represses FasL in microglia and protects against microglia-mediated neuronal cell death following hypoxia/ischemia. *Glia*. (2012) 60:1888–95. doi: 10.1002/glia.22404
78. Bao M-H, Szeto V, Yang BB, Zhu S-Z, Sun H-S, Feng Z-P. Long non-coding RNAs in ischemic stroke. *Cell Death Dis*. (2018) 9:281. doi: 10.1038/s41419-018-0282-x
79. Schmitz SU, Grote P, Herrmann BG. Mechanisms of long noncoding RNA function in development and disease. *Cell Mol Life Sci*. (2016) 73:2491–509. doi: 10.1007/s00018-016-2174-5
80. Cuevas-Diaz Duran R, Wei H, Kim DH, Wu JQ. Long non-coding RNA s: important regulators in the development, function and disorders of the central nervous system. *Neuropathol Appl Neurobiol*. (2019) 45:538–56. doi: 10.1111/nan.12541
81. An S, Song J-J. The coded functions of noncoding RNAs for gene regulation. *Mol Cells*. (2011) 31:491–6. doi: 10.1007/s10059-011-1004-8
82. Bond AM, VanGompel MJ, Sametsky EA, Clark MF, Savage JC, Disterhoft JF, et al. Balanced gene regulation by an embryonic brain ncRNA is critical for adult hippocampal GABA circuitry. *Nat Neurosci*. (2009) 12:1020. doi: 10.1038/nn.2371
83. Briggs JA, Wolvetang EJ, Mattick JS, Rinn JL, Barry G. Mechanisms of long non-coding RNAs in mammalian nervous system development, plasticity, disease, and evolution. *Neuron*. (2015) 88:861–77. doi: 10.1016/j.neuron.2015.09.045
84. Lawrence M, Daujat S, Schneider R. Lateral thinking: how histone modifications regulate gene expression. *Trends Genet*. (2016) 32:42–56. doi: 10.1016/j.tig.2015.10.007

85. Jenuwein T, Allis CD. Translating the histone code. *Science*. (2001) 293:1074–80. doi: 10.1126/science.1063127
86. Hyun K, Jeon J, Park K, Kim J. Writing, erasing and reading histone lysine methylations. *Exp Mol Med.* (2017) 49:e324. doi: 10.1038/emm.2017.11
87. Johansson C, Tumber A, Che K, Cain P, Nowak R, Gileadi C, et al. The roles of Jumonji-type oxygenases in human disease. *Epigenomics*. (2014) 6:89–120. doi: 10.2217/epi.13.79
88. Salminen A, Kaarniranta K, Hiltunen M, Kauppinen A. Krebs cycle dysfunction shapes epigenetic landscape of chromatin: novel insights into mitochondrial regulation of aging process. *Cell Signal.* (2014) 26:1598–603. doi: 10.1016/j.cellsig.2014.03.030
89. Pollard PJ, Loenarz C, Mole DR, McDonough MA, Gleadle JM, Schofield CJ, et al. Regulation of Jumonji-domain-containing histone demethylases by hypoxia-inducible factor. (HIF)-1α. *Biochem J*. (2008) 416:387–94. doi: 10.1042/BJ20081238
90. Sar A, Ponjevic D, Nguyen M, Box AH, Demetrick DJ. Identification and characterization of demethylase JMJD1A as a gene upregulated in the human cellular response to hypoxia. *Cell Tissue Res.* (2009) 337:223–34. doi: 10.1007/s00441-009-0805-y
91. Balakrishnan L, Milavetz B. Decoding the histone H4 lysine 20 methylation mark. *Crit Rev Biochem Mol Biol.* (2010) 45:440–52. doi: 10.3109/10409238.2010.504700
92. Batie M, Rocha S. JmjC histone demethylases act as chromatin oxygen sensors. *Mol Cell Oncol*. (2019) 6:1608501. doi: 10.1080/23723556.2019.1608501
93. Brandl A, Heinzel T, Krämer, OH. Histone deacetylases: salesmen and customers in the post-translational modification market. *Biol Cell*. (2009) 101:193–205. doi: 10.1042/BC20080158
94. Arany Z, Huang LE, Eckner R, Bhattacharya S, Jiang C, Goldberg MA, et al. An essential role for p300/CBP in the cellular response to hypoxia. *Proc Natl Acad Sci USA*. (1996) 93:12969–73. doi: 10.1073/pnas.93.23.12969
95. Cho Y, Cavalli V. HDAC signaling in neuronal development and axon regeneration. *Curr Opin Neurobiol*. (2014) 27:118–26. doi: 10.1016/j.conb.2014.03.008
96. Kim S-H, Jeong J-W, Park J, Lee J-W, Seo JH, Jung B-K, et al. Regulation of the HIF-1α stability by histone deacetylases. *Oncol Rep*. (2007) 17:647–51. doi: 10.3892/or.17.3.647
97. Schoepflin ZR, Shapiro IM, Risbud MV. Class I and IIa HDACs mediate HIF-1α stability through PHD2-dependent mechanism, while HDAC6, a class IIb member, promotes HIF-1α transcriptional activity in nucleus pulposus cells of the intervertebral disc. *J Bone Miner Res.* (2016) 31:1287–99. doi: 10.1002/jbmr.2787
98. Chan YC, Banerjee J, Choi SY, Sen CK. miR-210: The master hypoxamir. *Microcirculation*. (2012) 19:215–23. doi: 10.1111/j.1549-8719.2011.00154.x
99. Li JY, Yong TY, Michael MZ, Gleadle JM. MicroRNAs: are they the missing link between hypoxia and pre-eclampsia? *Hypertens Pregn*. (2014) 33:102–14. doi: 10.3109/10641955.2013.832772
100. Pineles BL, Romero R, Montenegro D, Tarca AL, Han YM, Kim YM, et al. Distinct subsets of microRNAs are expressed differentially in the human placentas of patients with preeclampsia. *Am J Obstet Gynecol. (*2007) 196:261.e26-6. doi: 10.1016/j.ajog.2007.01.008
101. Zhu X-M, Han T, Sargent IL, Yin G-W, Yao Y-Q. Differential expression profile of microRNAs in human placentas from preeclamptic pregnancies vs normal pregnancies. *Am J Obstetr Gynecol. (*2009) 200:661–7. doi: 10.1016/j.ajog.2008.12.045
102. Mayor-Lynn K, Toloubeydokhti T, Cruz AC, Chegini N. Expression profile of microRNAs and mRNAs in human placentas from pregnancies complicated by preeclampsia and preterm labor. *Reprod Sci*. (2011) 18:46–56. doi: 10.1177/1933719110374115
103. Fu G, Brkic J, Hayder H, Peng C. MicroRNAs in human placental development and pregnancy complications. *Int J Mol Sci.* (2013) 14:5519–44. doi: 10.3390/ijms14035519
104. Zhang Y, Fei M, Xue G, Zhou Q, Jia Y, Li L, et al. Elevated levels of hypoxia-inducible microRNA-210 in pre-eclampsia: new insights into molecular mechanisms for the disease. *J Cell Mol Med.* (2012) 16:249–59. doi: 10.1111/j.1582-4934.2011.01291.x
105. Fernández-López D, Natarajan N, Ashwal S, Vexler ZS. Mechanisms of perinatal arterial ischemic stroke. *J Cerebral Blood Flow Metab*. (2014) 34:921–32. doi: 10.1038/jcbfm.2014.41
106. Badiola N, Malagelada C, Llecha N, Hidalgo J, Comella JX, Sabriá J, et al. Activation of caspase-8 by tumour necrosis factor receptor 1 is necessary for caspase-3 activation and apoptosis in oxygen–glucose deprived cultured cortical cells. *Neurobiol Dis.* (2009) 35:438–47. doi: 10.1016/j.nbd.2009.06.005
107. Algra SO, Groeneveld KM, Schadenberg AW, Haas F, Evens FC, Meerding J, et al. Cerebral ischemia initiates an immediate innate immune response in neonates during cardiac surgery. *J Neuroinflamm*. (2013) 10:796. doi: 10.1186/1742-2094-10-24
108. Keller A, Meese E. Can circulating miRNAs live up to the promise of being minimal invasive biomarkers in clinical settings? *Wiley Interdisc Rev*. (2016) 7:148–56. doi: 10.1002/wrna.1320
109. Ponnusamy V, Kapellou O, Yip E, Evanson J, Wong LF, Michael-Titus A, et al. A study of microRNAs from dried blood spots in newborns after perinatal asphyxia: a simple and feasible biosampling method. *Pediatr Res.* (2015) 79:799–805. doi: 10.1038/pr.2015.276
110. Manueldas S, Benterud T, Rueegg CS, Garberg HT, Huun MU, Pankratov L, et al. Temporal patterns of circulating cell-free DNA (cfDNA) in a newborn piglet model of perinatal asphyxia. *PLoS ONE*. (2018) 13:e0206601. doi: 10.1371/journal.pone.0206601
111. McCarthy FP, Ryan RM, Chappell LC. Prospective biomarkers in preterm preeclampsia: a review. *Pregn Hypertens.* (2018) 14:72–8. doi: 10.1016/j.preghy.2018.03.010
112. Li Y, Ma Q, Halavi S, Concepcion K, Hartman RE, Obenaus A, et al. Fetal stress-mediated hypomethylation increases the brain susceptibility to hypoxic–ischemic injury in neonatal rats. *Exp Neurol.* (2016) 275:1–10. doi: 10.1016/j.expneurol.2015.10.007
113. Chen W, Jadhav V, Tang J, Zhang JH. HIF-1 alpha inhibition ameliorates neonatal brain damage after hypoxic-ischemic injury. *Acta Neurochir Suppl.* (2008) 102:395–9. doi: 10.1007/978-3-211-85578-2_77
114. Choi HJ, Eun JS, Kim BG, Kim SY, Jeon H, Soh Y. Vitexin, an HIF-1α inhibitor, has anti-metastatic potential in PC12 cells. *Mol Cells.* (2006) 22:291–9.
115. Min JW, Hu JJ, He M, Sanchez RM, Huang WX, Liu YQ, et al. Vitexin reduces hypoxia-ischemia neonatal brain injury by the inhibition of HIF-1alpha in a rat pup model. *Neuropharmacology*. (2015) 99:38–50. doi: 10.1016/j.neuropharm.2015.07.007
116. Min JW, Kong WL, Han S, Bsoul N, Liu WH, He XH, et al. Vitexin protects against hypoxic-ischemic injury via inhibiting Ca2+/Calmodulin-dependent protein kinase II and apoptosis signaling in the neonatal mouse brain. *Oncotarget*. (2017) 8:25513–24. doi: 10.18632/oncotarget.16065
117. Luo WD, Min JW, Huang WX, Wang X, Peng YY, Han S, et al. Vitexin reduces epilepsy after hypoxic ischemia in the neonatal brain via inhibition of NKCC1. *J Neuroinflamm*. (2018) 15:186. doi: 10.1186/s12974-018-1221-6
118. Nanduri J, Semenza GL, Prabhakar NR. Epigenetic changes by DNA methylation in chronic and intermittent hypoxia. *Am J Physiol Lung Cell Mol Physiol*. (2017) 313:L1096–100. doi: 10.1152/ajplung.00325.2017
119. Endres M, Meisel A, Biniszkiewicz D, Namura S, Prass K, Ruscher K, et al. DNA methyltransferase contributes to delayed ischemic brain injury. *J Neurosci.* (2000) 20:3175–81. doi: 10.1523/JNEUROSCI.20-09-03175.2000
120. Valinluck V, Tsai H-H, Rogstad DK, Burdzy A, Bird A, Sowers LC. Oxidative damage to methyl-CpG sequences inhibits the binding of the methyl-CpG binding domain. (MBD) of methyl-CpG binding protein 2. (MeCP2). *Nucleic Acids Res.* (2004) 32:4100–8. doi: 10.1093/nar/gkh739
121. Zhao H, Han Z, Ji X, Luo Y. Epigenetic regulation of oxidative stress in ischemic stroke. *Aging Dis.* (2016) 7:295. doi: 10.14336/AD.2015.1009
122. Lao VV, Herring JL, Kim CH, Darwanto A, Soto U, Sowers LC. Incorporation of 5-chlorocytosine into mammalian DNA results in heritable gene silencing and altered cytosine methylation patterns. *Carcinogenesis*. (2009) 30:886–93. doi: 10.1093/carcin/bgp060
123. Cox-Limpens KE, Vles JS, Schlechter J, Zimmermann LJ, Strackx E, Gavilanes AW. Fetal brain genomic reprogramming following asphyctic preconditioning. *BMC Neurosci.* (2013) 14:61. doi: 10.1186/1471-2202-14-61
124. Strackx E, Van den Hove DL, Prickaerts J, Zimmermann L, Steinbusch HW, Blanco CE, et al. Fetal asphyctic preconditioning protects against perinatal

asphyxia-induced behavioral consequences in adulthood. *Behav Brain Res.* (2010) 208:343–51. doi: 10.1016/j.bbr.2009.11.040
125. Vlassaks E, Strackx E, Vles J, Nikiforou M, Martinez-Martinez P, Kramer BW, et al. Fetal asphyctic preconditioning modulates the acute cytokine response thereby protecting against perinatal asphyxia in neonatal rats. *J Neuroinflamm*. (2013) 10:14. doi: 10.1186/1742-2094-10-14
126. Cox-Limpens KE, Vles JS, van den Hove DL, Zimmermann LJ, Gavilanes AW. Fetal asphyctic preconditioning alters the transcriptional response to perinatal asphyxia. *BMC Neurosci.* (2014) 15:67. doi: 10.1186/1471-2202-15-67
127. Gonzalez-Rodriguez PJ, Xiong F, Li Y, Zhou J, Zhang L. Fetal hypoxia increases vulnerability of hypoxic–ischemic brain injury in neonatal rats: role of glucocorticoid receptors. *Neurobiol Dis.* (2014) 65:172–9. doi: 10.1016/j.nbd.2014.01.020
128. McGowan PO, Sasaki A, D'alessio AC, Dymov S, Labonté B, Szyf M, et al. Epigenetic regulation of the glucocorticoid receptor in human brain associates with childhood abuse. *Nat Neurosci.* (2009) 12:342. doi: 10.1038/nn.2270
129. Li Y, Xiao D, Dasgupta C, Xiong F, Tong W, Yang S, et al. Perinatal nicotine exposure increases vulnerability of hypoxic–ischemic brain injury in neonatal rats: role of angiotensin II receptors. *Stroke.* (2012) 43:2483–90. doi: 10.1161/STROKEAHA.112.664698
130. Li Y, Xiao D, Yang S, Zhang L. Promoter methylation represses AT2R gene and increases brain hypoxic–ischemic injury in neonatal rats. *Neurobiol Dis.* (2013) 60:32–8. doi: 10.1016/j.nbd.2013.08.011
131. Qu Y, Mao M, Zhao F, Zhang L, Mu D. Proapoptotic role of human growth and transformation-dependent protein in the developing rat brain after hypoxia-ischemia. *Stroke*. (2009) 40:2843–8. doi: 10.1161/STROKEAHA.109.553644
132. Ren X, Ma H, Zuo Z. Dexmedetomidine postconditioning reduces brain injury after brain hypoxia-ischemia in neonatal rats. *J Neuroimmune Pharmacol.* (2016) 11:238–47. doi: 10.1007/s11481-016-9658-9
133. Liu YJ, Wang DY, Yang YJ, Lei WF. Effects and mechanism of dexmedetomidine on neuronal cell injury induced by hypoxia-ischemia. *BMC Anesthesiol.* (2017) 17:117. doi: 10.1186/s12871-017-0413-4
134. Doeppner TR, Doehring M, Bretschneider E, Zechariah A, Kaltwasser B, Müller B, et al. MicroRNA-124 protects against focal cerebral ischemia via mechanisms involving Usp14-dependent REST degradation. *Acta Neuropathol.* (2013) 126:251–65. doi: 10.1007/s00401-013-1142-5
135. Sun Y, Luo, ZM, Guo XM, Su DF, Liu X. An updated role of microRNA-124 in central nervous system disorders: a review.*Front Cell Neurosci.* (2015) 9:193. doi: 10.3389/fncel.2015.00193
136. Taj SH, Kho W, Riou A, Wiedermann D, Hoehn MJB. MiRNA-124 induces neuroprotection and functional improvement after focal cerebral ischemia. *Biomaterials.* (2016) 91:151–65. doi: 10.1016/j.biomaterials.2016.03.025
137. Doeppner TR, Kaltwasser B, Sanchez-Mendoza EH, Caglayan AB, Bähr M, Hermann DM, et al. Lithium-induced neuroprotection in stroke involves increased miR-124 expression, reduced RE1-silencing transcription factor abundance and decreased protein deubiquitination by GSK3β inhibition-independent pathways. *J Cereb Blood Flow Metab.* (2017) 37:914–26. doi: 10.1177/0271678X16647738
138. Voloboueva LA, Sun X, Xu L, Ouyang Y-B, Giffard RG. Distinct effects of miR-210 reduction on neurogenesis: increased neuronal survival of inflammation but reduced proliferation associated with mitochondrial enhancement. *J Neurosci.* (2017) 37:3072–84. doi: 10.1523/JNEUROSCI.1777-16.2017
139. Pena-Philippides JC, Caballero-Garrido E, Lordkipanidze T, Roitbak T. *In vivo* inhibition of miR-155 significantly alters post-stroke inflammatory response. *J Neuroinflammation.* (2016) 13:287. doi: 10.1186/s12974-016-0753-x
140. West T, Atzeva M, Holtzman DM. Pomegranate polyphenols and resveratrol protect the neonatal brain against hypoxic-ischemic injury. *Dev Neurosci.* (2007) 29:363–72. doi: 10.1159/000105477
141. Karalis F, Soubasi V, Georgiou T, Nakas CT, Simeonidou C, Guiba-Tziampiri O, et al. Resveratrol ameliorates hypoxia/ischemia-induced behavioral deficits and brain injury in the neonatal rat brain. *Brain Res.* (2011) 1425:98–110. doi: 10.1016/j.brainres.2011.09.044
142. Cui X, Song H, Su J. Curcumin attenuates hypoxic-ischemic brain injury in neonatal rats through induction of nuclear factor erythroid-2-related factor 2 and heme oxygenase-1. *Exp Ther Med.* (2017) 14:1512–8. doi: 10.3892/etm.2017.4683
143. Reuter S, Gupta SC, Park B, Goel A, Aggarwal BB. Epigenetic changes induced by curcumin and other natural compounds. *Genes Nutr.* (2011) 6:93. doi: 10.1007/s12263-011-0222-1
144. Vahid F, Zand H, Nosrat–Mirshekarlou E, Najafi R, Hekmatdoost AJG. The role dietary of bioactive compounds on the regulation of histone acetylases and deacetylases: a review. *Gene.* (2015) 562:8–15. doi: 10.1016/j.gene.2015.02.045
145. Ding X, Cheng Z, Sun B, Huang J, Wang L, Han X, et al. Distinctive sleep problems in children with perinatal moderate or mild hypoxic-ischemia. *Neurosci Lett*. (2016) 614:60–4. doi: 10.1016/j.neulet.2015.12.061
146. Dong X, Zhao Y, Huang Y, Yu L, Yang X, Gao FJJ, et al. Analysis of long noncoding RNA expression profiles in the whole blood of neonates with hypoxic-ischemic encephalopathy. *J Cell Biochem*. (2018) 120:8499–509. doi: 10.1002/jcb.28138
147. Zhou H, Wang X, Cheng R, Hou X, Chen Y, Feng Y, et al. Analysis of long non-coding RNA expression profiles in neonatal rats with hypoxic-ischemic brain damage. *J Neurochem*. (2019) 149–346–61. doi: 10.1111/jnc.14689
148. Yan H, Yuan J, Gao L, Rao J, Hu J. Long noncoding RNA MEG3 activation of p53 mediates ischemic neuronal death in stroke. *Neuroscience.* (2016) 337:191–9. doi: 10.1016/j.neuroscience.2016.09.017
149. Jiang L, Li H, Fan Z, Zhao R, Xia Z. Circular RNA expression profiles in neonatal rats following hypoxic-ischemic brain damage. *Int J Mol Med.* (2019) 43:1699–708. doi: 10.3892/ijmm.2019.4111
150. Henriquez B, Bustos FJ, Aguilar R, Becerra A, Simon F, Montecino M, et al. Ezh1 and Ezh2 differentially regulate PSD-95 gene transcription in developing hippocampal neurons. *Mol Cell Neurosci*. (2013) 57:130–43. doi: 10.1016/j.mcn.2013.07.012
151. Zhang J, Ji F, Liu Y, Lei X, Li H, Ji G, et al. Ezh2 regulates adult hippocampal neurogenesis and memory. *J Neurosci.* (2014) 34:5184–99. doi: 10.1523/JNEUROSCI.4129-13.2014
152. Ren X, Wang Z, Ma H, Zuo Z. Sevoflurane postconditioning provides neuroprotection against brain hypoxia–ischemia in neonatal rats. *Neurol Sci*. (2014) 35:1401–4. doi: 10.1007/s10072-014-1726-4
153. Xu Y, Xue H, Zhao P, Yang Y, Ji G, Yu W, et al. Isoflurane postconditioning induces concentration-and timing-dependent neuroprotection partly mediated by the GluR2 AMPA receptor in neonatal rats after brain hypoxia–ischemia. *J Anesth*. (2016) 30:427–36. doi: 10.1007/s00540-015-2132-7
154. Xue H, Xu Y, Wang S, Wu Z-Y, Li X-Y, Zhang Y-H, et al. Sevoflurane post-conditioning alleviates neonatal rat hypoxic-ischemic cerebral injury via Ezh2-regulated autophagy. *Drug Des DevTher.* (2019) 13:1691–706. doi: 10.2147/DDDT.S197325
155. Carloni S, Albertini MC, Galluzzi L, Buonocore G, Proietti F, Balduini W. Melatonin reduces endoplasmic reticulum stress and preserves sirtuin 1 expression in neuronal cells of newborn rats after hypoxia–ischemia. *J Pineal Res.* (2014) 57:192–9. doi: 10.1111/jpi.12156
156. Koyuncuoglu T, Turkyilmaz M, Goren B, Cetinkaya M, Cansev M, Alkan T. Uridine protects against hypoxic-ischemic brain injury by reducing histone deacetylase activity in neonatal rats. *Restor Neurol Neurosci.* (2015) 33:777–84. doi: 10.3233/RNN-150549
157. Lange S, Rocha-Ferreira E, Thei L, Mawjee P, Bennett K, Thompson PR, et al. Peptidylarginine deiminases: novel drug targets for prevention of neuronal damage following hypoxic ischemic insult. (HI) in neonates. *J Neurochem.* (2014) 130:555–62. doi: 10.1111/jnc.12744
158. Lange S. Peptidylarginine deiminases as drug targets in neonatal hypoxic-ischemic encephalopathy. *Front Neurol.* (2016) 7:22. doi: 10.3389/fneur.2016.00022
159. Calderone A, Jover T, Noh KM, Tanaka H, Yokota H, Lin Y, et al. Ischemic insults derepress the gene silencer REST in neurons destined to die. *J Neurosci.* (2003) 23:2112–21. doi: 10.1523/JNEUROSCI.23-06-02112.2003
160. Morris-Blanco KC, Kim T, Bertogliat MJ, Mehta SL, Chokkalla AK, Vemuganti R. Inhibition of the epigenetic regulator REST ameliorates ischemic brain injury. *Mol Neurobiol.* (2019) 56:2542–50. doi: 10.1007/s12035-018-1254-y

161. Jablonska B, Gierdalski M, Chew L-J, Hawley T, Catron M, Lichauco A, et al. Sirt1 regulates glial progenitor proliferation and regeneration in white matter after neonatal brain injury. *Nat Commun.* (2016) 7:13866. doi: 10.1038/ncomms13866
162. Kabakus N, Ay I, Aysun S, Söylemezoglu F, Özcan A, Celasun B. Protective effects of valproic acid against hypoxic-ischemic brain injury in neonatal rats. *J Child Neurol.* (2005) 20:582–7. doi: 10.1177/08830738050200070801
163. Fleiss B, Nilsson MKL, Blomgren K, Mallard C. Neuroprotection by the histone deacetylase inhibitor trichostatin A in a model of lipopolysaccharide-sensitised neonatal hypoxic-ischaemic brain injury. *J Neuroinflamm.* (2012) 9:70. doi: 10.1186/1742-2094-9-70
164. Jaworska J, Zalewska T, Sypecka J, Ziemka-Nalecz M. Effect of the HDAC inhibitor, sodium butyrate, on neurogenesis in a rat model of neonatal hypoxia–ischemia: potential mechanism of action. *Mol Neurobiol.* (2019) 56:6341–70. doi: 10.1007/s12035-019-1518-1
165. Qu X, Qi D, Dong F, Wang B, Guo R, Luo M, et al. Quercetin improves hypoxia-ischemia induced cognitive deficits via promoting remyelination in neonatal rat. *Brain Res.* (2014) 1553:31–40. doi: 10.1016/j.brainres.2014.01.035
166. Zhang Y, Reinberg D. Transcription regulation by histone methylation: interplay between different covalent modifications of the core histone tails. *Genes Dev*. (2001) 15:2343–60. doi: 10.1101/gad.927301
167. Qureshi IA, Gokhan S, Mehler MF. REST and CoREST are transcriptional and epigenetic regulators of seminal neural fate decisions. *Cell Cycle*. (2010) 9:4477–86. doi: 10.4161/cc.9.22.13973
168. Noh KM, Hwang JY, Follenzi A, Athanasiadou R, Miyawaki T, Greally JM, et al. Repressor element-1 silencing transcription factor. (REST)-dependent epigenetic remodeling is critical to ischemia-induced neuronal death. *Proc Natl Acad Sci USA*. (2012) 109:E962–71. doi: 10.1073/pnas.1121568109
169. Hwang J-Y, Kaneko N, Noh K-M, Pontarelli F, Zukin RS. The gene silencing transcription factor REST represses miR-132 expression in hippocampal neurons destined to die. *J Mol Biol.* (2014) 426:3454–66. doi: 10.1016/j.jmb.2014.07.032
170. Cavadas MA, Mesnieres M, Crifo B, Manresa MC, Selfridge AC, Scholz CC, et al. REST mediates resolution of HIF-dependent gene expression in prolonged hypoxia. *Sci Rep*. (2015) 5:17851. doi: 10.1038/srep17851
171. Cavadas MA, Mesnieres M, Crifo B, Manresa MC, Selfridge AC, Keogh CE, et al. REST is a hypoxia-responsive transcriptional repressor. *Sci Rep.* (2016) 6:31355. doi: 10.1038/srep31355

Conflict of Interest: The authors declare that the research was conducted in the absence of any commercial or financial relationships that could be construed as a potential conflict of interest.

frontiers in Pediatrics

ORIGINAL RESEARCH
published: 23 June 2020
doi: 10.3389/fped.2020.00238

Treatment for Post-hemorrhagic Ventricular Dilatation: A Multiple-Treatment Meta-Analysis

Liam Mahoney[1,2], *Karen Luyt*[3], *David Harding*[3] and *David Odd*[4*†]

[1] Neonatal Unit, North Bristol NHS Trust, Bristol, United Kingdom, [2] Academic Department of Paediatrics, Brighton and Sussex Medical School, Brighton, United Kingdom, [3] Bristol Medical School, University of Bristol, Bristol, United Kingdom, [4] School of Medicine, University of Cardiff, Cardiff, United Kingdom

Objective: To perform a systematic review and multiple-treatment meta-analysis for the treatment of premature infants with post-hemorrhagic ventricular dilatation (PHVD), to prevent death or long-term neuro-disability.

Design/Method: A systematic review was performed using PubMed, EMBASE, and the Cochrane Library. A free-word search was performed to identify likely relevant literature intervention trials of PHVD in preterm infants. Initially, network mapping was performed followed by performing a Bayesian random-effects model using the Markov chain Monte Carlo method. Areas under the cumulative ranking curve (SUCRA) were calculated as a measure of the probability that each intervention was likely to be the 1st, 2nd, 3rd, etc. best therapy. Primary outcome measure was death or moderate or severe neurodevelopmental outcome at or beyond 12 months of corrected age.

Results: Ten different trials were identified, enrolling 700 individuals (449 for the primary outcome). Seven intervention categories were identified, and of the 15 possible pair comparisons, 6 have been studied directly. In the multiple-treatment meta-analysis, no comparison reached conventional levels of statistical significance. Drainage Irrigation and Fibrinolytic Therapy (DRIFT) had the highest probability of being the best treatment for the primary outcome (82.1%), followed by CSF removal (10.8%), conservative management (6.7%), and then diuretic therapy (0.4%).

Conclusions: PHVD is a significant cause of death and disability in developed countries, yet few therapeutic options have so far been trialed. While new therapies are urgently needed for these infants, at present, NMA shows that DRIFT appears to be the most likely candidate to improve outcomes after sIVH.

Keywords: premature birth, brain injury, preterm, intraventricular hemorrhage, post-hemorrhagic ventricular dilatation

OPEN ACCESS

Edited by:
Changlian Zhu,
Third Affiliated Hospital of Zhengzhou University, China

Reviewed by:
Betty Vohr,
Ministry of Health, Turkey
Fuat Emre Canpolat,
Ministry of Health, Turkey

***Correspondence:**
David Odd
oddd@cardiff.ac.uk

†Present address:
David Odd,
Division of Population Medicine, School of Medicine, Cardiff University, Cardiff, United Kingdom

Specialty section:
This article was submitted to Neonatology, a section of the journal Frontiers in Pediatrics

Received: *19 December 2019*
Accepted: *20 April 2020*
Published: *23 June 2020*

Citation:
Mahoney L, Luyt K, Harding D and Odd D (2020) Treatment for Post-hemorrhagic Ventricular Dilatation: A Multiple-Treatment Meta-Analysis. Front. Pediatr. 8:238. doi: 10.3389/fped.2020.00238

INTRODUCTION

Around 1 in 10 infants is born preterm, and survival of these infants has increased significantly over the last two decades (1, 2). However, brain injury, associated with two different patterns of damage, periventricular leukomalacia (PVL) and intraventricular hemorrhage (IVH), is common in infants born preterm, with potentially devastating personal impacts and significant

population effects. While the risk of PVL in infants below 32 weeks has halved over the last two decades, the risk of IVH has stayed similar despite improvements in antenatal and neonatal care and while new interventions, such as delayed cord clamping, antenatal steroids, and intrapartum care, appear to reduce the risk of IVH, the overall risk of IVH remains high (3–6).

Consequently, it now represents the most common cause of neurological disability in the survivors (7). Those infants who develop severe intraventricular hemorrhage (sIVH) are at high risk of developing post-hemorrhagic ventricular dilatation (PHVD), a condition with high rates of long-term disability with conditions such as cerebral palsy (CP), sensory problems, and cognitive deficits (8, 9). In addition to the personal impact, the care of these premature infants who grow up with potentially disabling brain injury is expensive, with economic impacts to health care, the families involved, educational systems, and society at large (10, 11).

However, while reducing neonatal brain injury remains a research priority, no standardized treatment for these vulnerable infants appears to exist, although a number of treatments designed to prevent ongoing brain injury after sIVH and subsequent PHVD have been studied (12–26). This work aims to use Network Meta-analysis (NMA) methodology to allow the comparison of different treatment modalities for PHVD, combining the direct evidence of comparisons trailed, and deriving indirect assessments to help identify the most efficacious treatment. To our knowledge, NMA has not been applied to interventions targeted at preventing the complications and the neurodevelopmental sequelae after development of PHVD.

METHODS AND MATERIALS

Study Selection and Data Collection

Criteria for inclusion were based on previous meta-analyses in this area and methodology was based on the Preferred Reporting Items for Systematic Reviews and Meta-Analyses guidelines (27–30). Systematic review was performed by all three authors using PubMed (1966–2018), EMBASE (1974–2018), and the Cochrane Library. A free-word search was performed (**Appendix 1**) to identify likely relevant literature. The search strategy was piloted to ensure that it identified studies already known by the authors to be relevant. Searches were limited to those with English language abstracts and for research in human subjects.

Three quantitative analyses were of interest: (i) death, (ii) neurodevelopmental disability, and (iii) ventriculo-peritoneal shunt surgery. The titles obtained from database searching were sifted to exclude duplicates and those clearly not relevant to the review. Abstracts of those remaining were examined and tested against the inclusion criteria.

- Randomized or quasi-randomized controlled trials for the treatment of PHVD
- At least one measure out of
    - Neurodevelopmental outcomes at or beyond 12 months of age
    - Mortality
    - Ventriculo-peritoneal shunt surgery
- Randomized or quasi-randomized intervention trials

Full texts were obtained for those articles likely to be eligible and reviewed once more. The process was performed independently by all three authors. References in the papers were checked to identify any other possible relevant studies. Data were extracted on the characteristics of the individual studies. All three authors independently reviewed the papers identified and confirmed eligibility and the quality rating. Studies were assessed on a quality rating of adequate, unclear, or inadequate on the categories of random allocation, concealment, and blinding. Primary outcome measure was death or moderate or severe neurodevelopmental outcome at or beyond 12 months of corrected age (using any standardized measure). Where developmental outcomes were reported in a number of papers, the reported primary outcome of the study was used. An arbitrary control group was defined as treatment for PHVD only being instigated once head growth was excessive or there were clinical signs or raised intracranial pressure mandating treatment. Other interventions were grouped by consensus by two of the authors prior to analyses being performed (DO and DH). Intention-to-treat analysis was used where available. All three authors assessed the risk of bias in trials using the Cochrane risk of bias tool, with discrepancies resolved by consensus (31). Where composite outcomes of death and/or VP shunt or disability were not provided, they were calculated if possible from the presented data. Where data were unavailable, we assumed that infants who died before discharge from the neonatal unit did not receive VP shunts. Authors of included papers were not approached for missing data or where queries about a studies' methodology due to the length of time since the publications of many of the manuscripts included.

Statistical Analysis

Network mapping was performed with the size of the nodes proportional to the sample size and the thickness of the connecting lines proportional to the number of trials. We then performed a Bayesian random-effects model using the Markov chain Monte Carlo method. The results were reported as OR with 95% confidence intervals. We used $p < 0.05$ as a conventional level of significance. The areas under the cumulative ranking curve (SUCRA) were calculated as a measure of the probability that each intervention was the best for each of the outcome measures, and for the primary outcome, we also derived the probabilities that each therapy is likely to be the 1st, 2nd, 3rd, etc. best therapy (32).

Analyses were repeated for the following outcomes:

1. Death or moderate or severe neurodevelopmental impairment at or beyond 12 months of age
2. Moderate or severe neurodevelopmental impairment at or beyond 12 months of age
3. Death in the neonatal period, or before 1 year of age
4. Requiring ventriculo-peritoneal shunt surgery in the neonatal period, or before 1 year of age
5. Requiring ventriculo-peritoneal shunt surgery or death in the neonatal period, or before 1 year of age

An assumption behind multiple-treatment meta-analysis is that direct and indirect evidence on comparisons do not disagree (coherence). To estimate this, we planned to calculate the direct and indirect OR where possible; however, due to the limited amount of studies reporting the primary outcome, we were unable to test if the direct and indirect assessments were coherent.

Finally, an *a priori* sensitivity analysis was planned excluding those studies that were considered "inadequate" on any quality measures. All analyses were performed using Stata 14. Results are presented as OR (95% confidence interval).

Public and Patient Involvement

Patients or members of the public were not involved in the design, or conduct, reporting, or dissemination plan of this research.

RESULTS

Literature Search

Databases were searched on 10/09/2018 and, after removal of duplicates, produced a list of 3445 publications. Of these, 36 abstracts were screened, and of these, a total of 11 full-text papers were reviewed, all of which fulfilled the inclusion criteria (13, 14, 16–22, 24, 25). Four systematic reviews were identified (27, 29, 33, 34) and a further three likely papers were identified from the references of the full-text papers and the existing reviews. These three additional papers were reviewed and all were included in the analysis, leaving a total of 14 papers [**Appendix 2**; (13–26)] from 10 different trials. The earliest publication dates were from 1980 (15), and the most recent dates were from 2019 (20). Overall, 700 individuals were randomly assigned and were included in at least one multiple-treatment meta-analysis, although only 449 infants have been enrolled in trials that have reported the primary outcome. All studies were two-armed trials. Further details are shown in **Appendix 3**.

Six categories of intervention were identified by the authors:

1) Control (defined as above) (13–17, 19–21, 23–26)
2) Tapping of CSF prior to symptoms or excessive head growth (16, 17)
3) Diuretic therapy (23–25)
4) Drainage Irrigation and Fibrinolytic Therapy (DRIFT) (13, 18, 19)
5) Fibrinolytic therapy (21, 22)

After discussion between authors regarding one paper randomizing infants between CSF tapping at conventional levels (2 above) and early tapping, and an additional category was added (6) (Early CSF tapping) to accommodate this intervention (20).

A total of four studies reported an eligible neurodevelopmental measure (13, 19, 24–26), while all reported mortality or shunt usage during the neonatal period or during the first year of life. Five studies were European (13, 17, 20, 22, 24), four were based in the USA (14, 15, 23, 26), and 1 was based in Turkey (21). All studies use some form of imaging to diagnose IVH. All studies but two had a control group compatible with our pre-defined criteria; Luciano, in contrast, randomized between diuretic treatment in one arm and streptokinase in the other (22) and De Vries used two different thresholds of CSF tapping (discussed above) (20). One study (15) used an alternative number to allocate treatment arms, while a further three did not specify the randomization methods (21, 23, 35). VP shunt criteria were defined in all studies except two (15, 21). Of the four trials that reported neurodevelopmental data, three were considered adequate (13, 16, 17, 19, 24, 25) and one was unclear (26). No trial was able to blind clinicians to the intervention. A summary of quality assessments is shown in **Figure 1**.

Individual Study Findings

Two studies investigated the use of furosemide and acetazolamide vs. standard treatment/LPs. Libenson (23) included a total of 16 infants who received either acetazolamide and frusemide, or daily LPs. They reported a reduction in VP shunts (10 vs. 50%) although there was crossover between treatment arms. Kennedy et al. (24, 25) also compared acetazolamide and frusemide to a control group and reported a higher rate of death and/or ventricular shunt placement in the intervention arm [RR 1.42 (1.06–1.90); $p = 0.026$] and worse developmental outcomes [e.g., RR 1.67 (1.23–2.28) for motor impairment]. Mantovani et al. (15), Dykes et al. (26), Anwar et al. (14), and the Ventriculomegaly Trial Group (16) compared frequent LP to conservative treatment, but none reported a difference in VP shunts or death between these treatment arms. De Vries et al. (20) randomized 126 infants with PHVD to intervention of repeat CSF tapping to two different thresholds with no difference in the primary outcome of VP shunt or death ($p = 0.45$). Two small studies have investigated the use of intraventricular streptokinase; Luciano et al. (22) found no difference in the rate of VP shunt between the two groups while Yapicioglu et al. (21) reported an increased need for VP shunt in the streptokinase group (83 vs. 50%). Finally, the DRIFT study included a total of 70 infants who were randomized to either intraventricular drainage, irrigation, and fibrinolytic therapy with tissue plasminogen activator (DRIFT) or to standard treatment (13). This study was closed early due a minimum chance that the short-term primary outcome would identify a difference between groups (VP shunt or death). There was no difference in the primary outcome of reducing the rates of VP shunt surgery or death but an analysis of developmental outcomes in infants at 2 years corrected age found evidence of improved neurodevelopment [adjusted OR of 0.17 (0.05–0.57)].

Quantitative Synthesis

Figure 2 shows the resultant network of eligible comparisons from the multiple-treatment meta-analysis.

Of the 15 possible pair comparisons, 6 have been studied directly. **Table 1** summarizes the results of the multiple-treatment meta-analysis for the pre-specified outcomes [e.g., compared to control diuretics, which appeared to have a higher OR of the primary outcome (OR 1.17 (0.99–1.39)], while compared to diuretics, DRIFT had a lower OR [OR 0.69 (0.44–1.07)]. Repeating the analysis for the other outcomes showed similar results. No comparison reached conventional levels of statistical significance.

	Random Sequence Generation (selection bias)	Allocation Concealment (selection bias)	Blinding of participants and personnel (performance bias)	Blinding of outcome assessment (detection bias)	Incomplete data (attrition bias)	Selective reporting (reporting bias)
Mantovani 1980	-	-	-	N/A	N/A	N/A
Anwar 1985	+	?	-	N/A	N/A	N/A
Dykes 1989	+	?	-	?	?	?
Whitelaw 1990 and 1993	+	+	-	+	+	+
Luciano 1997	?	?	-	N/A	N/A	N/A
Kennedy 1998 and 2001	+	+	-	+	+	+
Libenson 1999	?	?	-	N/A	N/A	N/A
Yapicioglu 2003	?	?	-	N/A	N/A	N/A
Whitelaw 2007 and 2010	+	+	-	+	+	+
deVries 2018	+	+	-	N/A	N/A	N/A

Key: + = Adequate, ? = Unclear, - = Inadequate

FIGURE 1 | Quality measures.

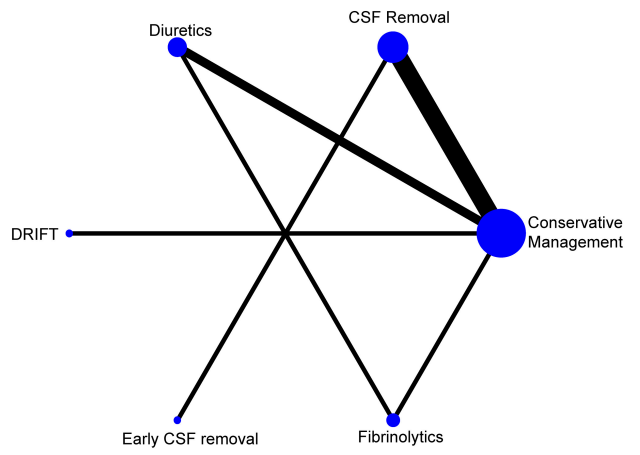

FIGURE 2 | Network eligible comparisons for the multiple-treatment meta-analysis.

Table 2 and **Figure 3** shows the SURCRA for each treatment and outcomes measured. DRIFT had the highest probability of being the best treatment for the primary outcome (82.1%), followed by CSF removal (10.8%), conservative management (6.7%), and then diuretic therapy (0.4%). No study was able to blind clinicians delivering the treatment, and so no additional analysis was performed.

DISCUSSION

We have found in this work that little evidence exists to directly differentiate any proposed or trialed therapy for PHVD. Diuretic therapy appeared to be detrimental, and ranking of therapies appeared to show that DRIFT may by the most efficacious. However, despite the significant impact of this disease, only 700 infants have ever been enrolled in an intervention trial, and further studies are desperately needed.

Limitations of this work include the heterogeneity of the infants enrolled, in part due to the wide time frame recruitment across the studies (1980–2019). Neonatal care has changed significantly during this time, with new therapies such as antenatal steroids and surfactant, and the reduction in other treatments such as postnatal steroids. Despite this, the control arm of these trials appears remarkably similar over the 40 years investigated, with VP shunt insertion after development of PHVD still the standard treatment of choice. The biggest and perhaps most influential trials have all been performed in the last 20 years and had infants of similar gestation, with similar control group interventions. We have used a random effects model to allow for increased uncertainty in this work, but the lack of precision is likely due to the small numbers included (around 700 infants involved in these randomized controlled trials) rather than heterogeneity.

The timing of intervention in each study makes the comparison of treatments in this using this methodology difficult. For example, in some of the trials, lumbar punctures were used to

TABLE 1 | Comparisons between different treatment groups for direct and indirect outcome measures.

Treatment comparison	Moderate or severe neuro-disability, or death		Moderate or severe neuro-disability		VP shunt or death		VP shunt		Death	
	OR (95% CI)	*p*	OR (95% CI)	*p*	OR (95% CI)	*p*	OR (95% CI)	*p*	OR (95% CI)	*p*
Compared to Control										
CSF removal	1.01 (0.86–1.19)	0.921	0.87 (0.45–1.70)	0.689	0.96 (0.8–1.15)	0.652	0.97 (0.75–1.24)	0.791	0.91 (0.53–1.57)	0.739
Diuretics	1.17 (0.99–1.39)	0.062	1.05 (0.47–2.34)	0.905	1.20 (0.93–1.54)	0.165	1.07 (0.79–1.44)	0.676	1.58 (0.81–3.08)	0.179
DRIFT	0.80 (0.53–1.22)	0.302	0.87 (0.35–2.17)	0.759	0.97 (0.62–1.53)	0.91	1.04 (0.6–1.79)	0.89	0.58 (0.15–2.28)	0.439
Early CSF removal					0.80 (0.47–1.37)	0.421	0.80 (0.39–1.67)	0.556	0.77 (0.26–2.32)	0.645
Fibrinolytics					1.20 (0.52–2.77)	0.675	1.41 (0.70–2.84)	0.342	1.26 (0.20–7.76)	0.806
Compared to CSF Removal										
Diuretics	1.16 (0.92–1.47)	0.20	1.20 (0.42–3.42)	0.73	1.25 (0.91–1.70)	0.16	1.1 (0.75–1.63)	0.62	1.73 (0.73–4.10)	0.21
DRIFT	0.80 (0.51–1.24)	0.32	0.99 (0.32–3.09)	0.99	1.02 (0.62–1.65)	0.95	1.07 (0.59–1.96)	0.81	0.64 (0.15–2.78)	0.55
Early CSF removal					0.84 (0.51–1.39)	0.49	0.83 (0.42–1.65)	0.60	0.85 (0.33–2.20)	0.73
Fibrinolytics					1.25 (0.53–2.94)	0.61	1.45 (0.69–3.07)	0.33	1.38 (0.21–9.22)	0.74
Compared to Diuretic										
DRIFT	0.69 (0.44–1.07)	0.10	0.82 (0.24–2.79)	0.76	0.81 (0.48–1.37)	0.44	0.97 (0.52–1.82)	0.94	0.37 (0.08–1.68)	0.20
Early CSF removal					1.49 (0.37–1.21)	0.19	0.75 (0.34–1.66)	0.48	0.49 (0.14–1.77)	0.28
Fibrinolytics					1.00 (0.45–2.23)	1.00	1.32 (0.64–2.71)	0.45	0.80 (0.13–4.91)	0.81
Compared to DRIFT										
Early CSF removal					0.82 (0.41–1.66)	0.59	0.77 (0.31–1.92)	0.58	1.32 (0.23–7.59)	0.76
Fibrinolytics					1.23 (0.47–3.19)	0.67	1.35 (0.56–3.29)	0.51	2.15 (0.22–20.84)	0.51
Compared to Early CSF Removal										
Fibrinolytics					1.49 (0.55–4.04)	0.43	1.75 (0.63–4.83)	0.28	1.63 (0.19–13.62)	0.65

TABLE 2 | SUCRA for probability of most efficacious treatment for different outcomes.

Treatment	Outcome				
	Moderate/severe neuro-disability or death	Moderate/severe neuro-disability	Death	VP shunt	VP shunt or death
Control	0.6	0.4	0.5	0.5	0.5
CSF removal	0.5	0.6	0.6	0.6	0.6
Diuretic treatment	0.1	0.4	0.2	0.4	0.2
DRIFT	0.9	0.6	0.8	0.5	0.6
Early CSF removal	–	–	0.6	0.7	0.8
Fibrinolytics	–	–	0.4	0.2	0.3

reduce the size of already distended ventricles compared (13) to preventing further enlargement through early intervention (23). The differences in the randomization thresholds may contribute to some of the variation seen in the outcome measured (e.g., the percentage of VP shunts required).

PHVD remains a significant problem in the developed world. There are around 8,000 preterm infants born 32 weeks gestation in England alone each year, and around 483 (6%) of these develop a sIVH (7). Overall, around 700 infants a year develop sIVH after birth, and most of these will develop some degree of motor or cognitive disability (13). In all the work reviewed here, mortality was high, and many infants who survive have complex developmental needs, a population impact likely higher than neonatal hypoxic–ischemic encephalopathy (36) or Trisomy 21 (37), with a corresponding burden to the NHS (in future healthcare needs) and society. With this in mind, we find the lack of recent trials disappointing, and this appears to be a vital area for new biomedical research.

In this work, DRIFT is likely to be the most efficacious treatment. Recent presentation of a secondary analysis of school age neurodevelopmental outcomes from this trial appears to show similar results to those used in this work on a subset of the initial trial group (38). While this recent work was a secondary analysis, the results are in parallel with those at 2 years, with children assessed at 10 years, after adjusting for gender, birthweight, and grade of IVH, with cognitive quotient being, on average, 23.47 points higher than those who received standard treatment ($p = 0.009$).

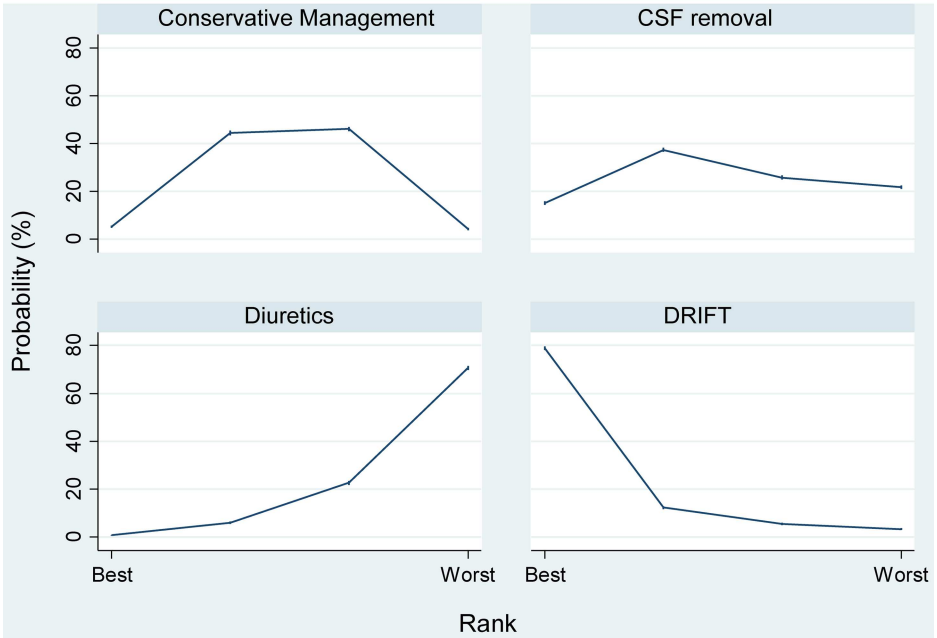

FIGURE 3 | Probabilities of each therapy being the 1st, 2nd, 3rd, or 4th best treatment for the prevention of moderate/severe neuro-disability or death.

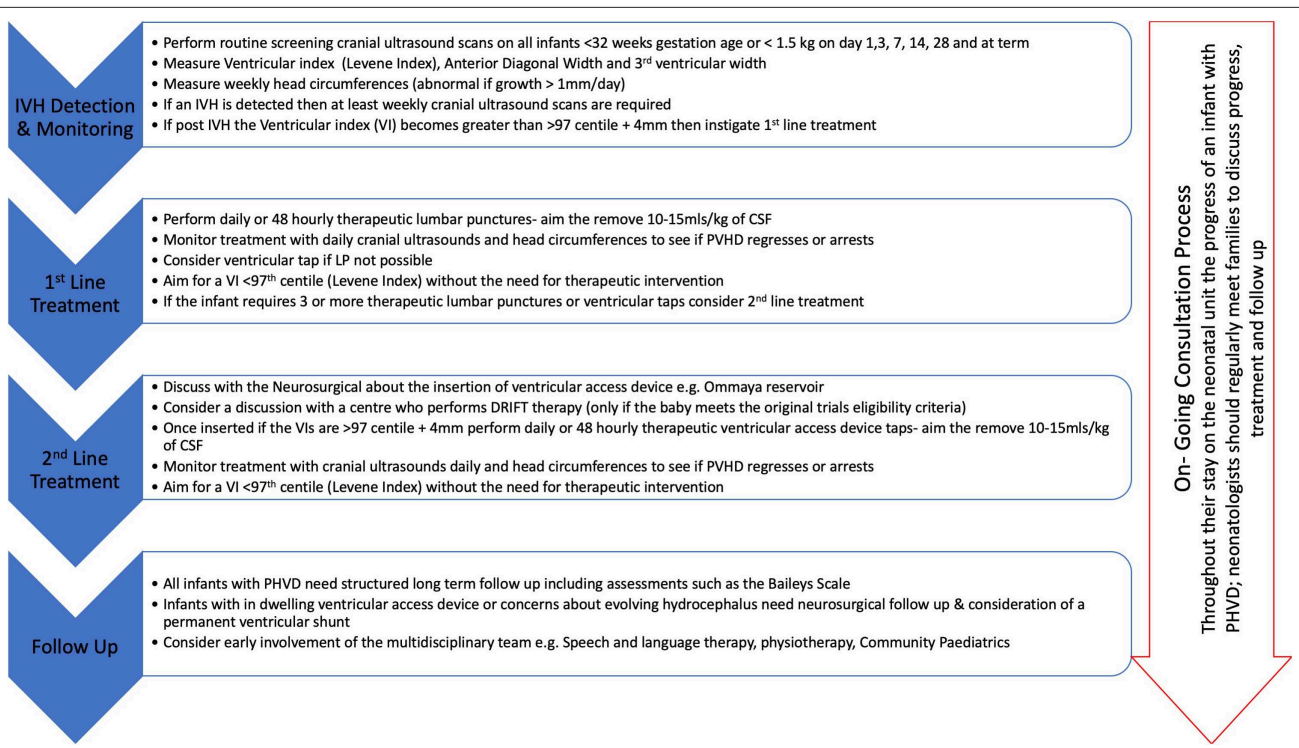

FIGURE 4 | Proposed strategy for the management of PHVD.

DRIFT is however a complex intervention and involves 72 h of intensive nursing and medical care. The process of DRIFT was modified during the trial due to concerns over secondary bleeds, and the trial was stopped early due to likely futility in reaching a difference in the short-term primary outcome of shunt or death. As an alternative approach, some units have

reported success with more rapid clot removal (e.g., through endoscopes) or percutaneous methods of treating intra- and extra-axial intracranial hemorrhage, although no RCT has yet been published with these novel treatments (39, 40). Equally, the ELVIS trial (20) has completed its recruitment and later neurodevelopmental outcomes are expected to be published soon. These results are eagerly awaited as a sub-study of the ELVIS trial has reported that, in the high-threshold group (LPs when the VI > p97 + 4 mm and anterior horn width >10 mm), there was more brain injury and higher ventricular volumes compared to the low-threshold groups (VI > p97 and anterior horn width >6 mm) (41). There is also interest surrounding stem cell treatment after sIVH; however, this has only been reported in phase 1 trial (42). In lieu of the results of this research, **Figure 4** shows a proposed strategy for PHVD.

PHVD is a significant cause of death and disability in developed countries, yet few therapeutic options have so far been trialed. Only 700 infants have been enrolled in intervention trials, while <500 have had longer-term developmental measures reported. While new therapies are urgently needed for these infants, at present, NMA shows that DRIFT appears to be the most likely candidate to improve outcomes after sIVH, but further work is needed to implement this in routine healthcare and promising newer therapies remain untrialed.

DATA AVAILABILITY STATEMENT

The raw data supporting the conclusions of this article will be made available by the authors, without undue reservation, to any qualified researcher.

AUTHOR CONTRIBUTIONS

DO, DH, and LM: conception, design, collection, and assembly of data. DO, DH, LM, and KL: analysis and interpretation of the data, drafting of the article, critical revision of the article for important intellectual content and final approval.

SUPPLEMENTARY MATERIAL

The Supplementary Material for this article can be found online at: https://www.frontiersin.org/articles/10.3389/fped.2020.00238/full#supplementary-material

REFERENCES

1. Santhakumaran S, Statnikov Y, Gray D, Battersby C, Ashby D, Modi N. Survival of very preterm infants admitted to neonatal care in England 2008-2014: time trends and regional variation. *Arch Dis Child Fetal Neonatal Ed*. (2018) 103:F208–15. doi: 10.1136/archdischild-2017-312748
2. Younge N, Goldstein RF, Bann CM, Hintz SR, Patel RM, Smith PB, et al. Survival and neurodevelopmental outcomes among periviable infants. *N Engl J Med*. (2017) 376:617–28. doi: 10.1056/NEJMoa1605566
3. Stoll BJ, Hansen NI, Bell EF, Walsh MC, Carlo WA, Shankaran S, et al. Trends in care practices, morbidity, and mortality of extremely preterm Neonates, 1993-2012. *JAMA*. (2015) 314:1039–51. doi: 10.1001/jama.2015.10244
4. Nagano N, Saito M, Sugiura T, Miyahara F, Namba F, Ota E. Benefits of umbilical cord milking versus delayed cord clamping on neonatal outcomes in preterm infants: a systematic review and meta-analysis. *PLoS ONE*. (2018) 13:e0201528. doi: 10.1371/journal.pone.0201528
5. Shepherd E, Salam RA, Middleton P, Makrides M, Mcintyre S, Badawi N, et al. Antenatal and intrapartum interventions for preventing cerebral palsy: an overview of cochrane systematic reviews. *Cochrane Database Syst Rev*. (2017) 8:CD012077. doi: 10.1002/14651858.CD012077.pub2
6. Gamaleldin I, Harding D, Siassakos D, Draycott T, Odd D. Significant intraventricular hemorrhage is more likely in very preterm infants born by vaginal delivery: a multi-centre retrospective cohort study. *J Matern Neonatal Med*. (2019) 32:477–82. doi: 10.1080/14767058.2017.1383980
7. Gale C, Statnikov Y, Jawad S, Uthaya SN, Modi N, Modi N, et al. Neonatal brain injuries in England: population-based incidence derived from routinely recorded clinical data held in the national neonatal research database. *Arch Dis Child Fetal Neonatal Ed*. (2018) 103:F301–6. doi: 10.1136/archdischild-2017-313707
8. Radic JAE, Vincer M, McNeely PD. Outcomes of intraventricular hemorrhage and posthemorrhagic hydrocephalus in a population-based cohort of very preterm infants born to residents of Nova Scotia from 1993 to 2010. *J Neurosurg Pediatr*. (2015) 15:580–8. doi: 10.3171/2014.11.PEDS14364
9. Srinivasakumar P, Limbrick D, Munro R, Mercer D, Rao R, Inder T, et al. Posthemorrhagic ventricular dilatation-impact on early neurodevelopmental outcome. *Am J Perinatol*. (2013) 30:207–14. doi: 10.1055/s-0032-1323581
10. Christian EA, Jin DL, Attenello F, Wen T, Cen S, Mack WJ, et al. Trends in hospitalization of preterm infants with intraventricular hemorrhage and hydrocephalus in the United States, 2000-2010. *J Neurosurg Pediatr*. (2016) 17:260–9. doi: 10.3171/2015.7.PEDS15140
11. Kruse M, Michelsen SI, Flachs EM, Brønnum-Hansen H, Madsen M, Uldall P. Lifetime costs of cerebral palsy. *Dev Med Child Neurol*. (2009) 51:622–8. doi: 10.1111/j.1469-8749.2008.03190.x
12. Department of Health and Social Care and The Rt Hon Jeremy Hunt MP. *New Ambition to Halve Rate of Stillbirths and Infant Deaths*. London.
13. Whitelaw A, Jary S, Kmita G, Wroblewska J, Musialik-Swietlinska E, Mandera M, et al. Randomized trial of drainage, irrigation and fibrinolytic therapy for premature infants with posthemorrhagic ventricular dilatation: developmental outcome at 2 years. *Pediatrics*. (2010) 125:e852–8. doi: 10.1542/peds.2009-1960
14. Anwar M, Kadam S, Hiatt IM, Hegyi T. Serial lumbar punctures in prevention of post-hemorrhagic hydrocephalus in preterm infants. *J Pediatr*. (1985) 107:446–50. doi: 10.1016/S0022-3476(85)80532-1
15. Mantovani JF, Pasternak JF, Mathew OP, Allan WC, Mills MT, Casper J, et al. Failure of daily lumbar punctures to prevent the development of hydrocephalus following intraventricular hemorrhage. *J Pediatr*. (1980) 97:278–81. doi: 10.1016/S0022-3476(80)80495-1
16. Randomised trial of early tapping in neonatal posthaemorrhagic ventricular dilatation. Ventriculomegaly trial group. *Arch Dis Child*. (1990) 65:3–10. doi: 10.1136/adc.65.1_spec_no.3
17. Whitelaw A. Randomised trial of early tapping in neonatal posthaemorrhagic ventricular dilatation: results at 30 months. *Arch Dis Child*. (1994) 70:F129–36. doi: 10.1136/fn.72.3.f211
18. Whitelaw A, Pople I, Cherian S, Evans D, Thoresen M. Phase 1 trial of prevention of hydrocephalus after intraventricular hemorrhage in newborn infants by drainage, irrigation, and fibrinolytic therapy. *Pediatrics*. (2003) 111(4 Pt 1):759–65. doi: 10.1542/peds.111.4.759
19. Whitelaw A, Evans D, Carter M, Thoresen M, Wroblewska J, Mandera M, et al. Randomized clinical trial of prevention of hydrocephalus after intraventricular hemorrhage in preterm infants: brain-washing versus tapping fluid. *Pediatrics*. (2007) 119:e1071–8. doi: 10.1542/peds.2006-2841
20. De Vries LS, Groenendaal F, Liem KD, Heep A, Brouwer AJ, Van 'T Verlaat E, et al. Treatment thresholds for intervention in posthaemorrhagic ventricular dilation: a randomised controlled trial. *Arch Dis Child Fetal Neonatal Ed*. (2019) 104:F70–5. doi: 10.1136/archdischild-2017-314206
21. Yapicioglu H, Narli N, Satar M, Soyupak S, Altunbasak S. Intraventricular streptokinase for the treatment of posthaemorrhagic

hydrocephalus of preterm. *J Clin Neurosci*. (2003) 10:297–9. doi: 10.1016/S0967-5868(03)00028-6
22. Luciano R, Velardi F, Romagnoli C, Papacci P, De Stefano V, Tortorolo G. Failure of fibrinolytic endoventricular treatment to prevent neonatal post haemorrhagic hydrocephalus. *A case control trial. Child's Nerv Syst*. (1997) 6:1. doi: 10.1007/s003810050045
23. Libenson MH, Kaye EM, Rosman NP, Gilmore HE. Acetazolamide and furosemide for posthemorrhagic hydrocephalus of the newborn. *Pediatr Neurol*. (1999) 20:185–91. doi: 10.1016/S0887-8994(98)00127-1
24. Kennedy CR, Ayers S, Campbell MJ, Elbourne D, Hope P, Johnson A. Randomized, controlled trial of acetazolamide and furosemide in posthemorrhagic ventricular dilation in infancy: follow-up at 1 year. *Pediatrics*. (2001) 108:597–607. doi: 10.1542/peds.108.3.597
25. Kennedy CR, Campbell M, Elbourne D, Hope P, Johnson A. International randomised controlled trial of acetazolamide and furosemide in posthaemorrhagic ventricular dilatation in infancy. *Lancet*. (1998) 352:433–40. doi: 10.1016/S0140-6736(97)12390-X
26. Dykes FD, Dunbar B, Lazarra A, Ahmann PA. Posthemorrhagic hydrocephalus in high-risk preterm infants: natural history, management, and long-term outcome. *J Pediatr*. (1989) 114(4 Pt 1):611–8. doi: 10.1016/S0022-3476(89)80707-3
27. Whitelaw A, Odd DE. Intraventricular streptokinase after intraventricular hemorrhage in newborn infants. *Cochrane Database Syst Rev*. (2007) 17:CD000498. doi: 10.1002/14651858.CD000498.pub2
28. Whitelaw A. Repeated lumbar or ventricular punctures in newborns with intraventricular hemorrhage. *Cochrane Database Syst Rev*. (2017) 4:CD000216. doi: 10.1002/14651858.cd000216
29. Whitelaw A, Brion LP, Kennedy CR, Odd D. Diuretic therapy for newborn infants with posthemorrhagic ventricular dilatation. *Cochrane Database Syst Rev*. (2001) CD002270. doi: 10.1002/14651858.cd002270
30. Moher D, Liberati A, Tetzlaff J, Altman DG, Altman D, Antes G, et al. Preferred reporting items for systematic reviews and meta-analyses: the PRISMA statement. *PLoS Med*. (2009) 6:e1000097. doi: 10.1371/journal.pmed.1000097
31. Higgins JPT, Green S, editors. *Cochrane Handbook for Systematic Reviews of Interventions Version 5.1.0*. Cochrane Collaboration (2011).
32. Salanti G, Ades AE, Ioannidis JPA. Graphical methods and numerical summaries for presenting results from multiple-treatment meta-analysis: an overview and tutorial. *J Clin Epidemiol*. (2011) 64:163–71. doi: 10.1016/j.jclinepi.2010.03.016
33. Whitelaw A, Lee-Kelland R. Repeated lumbar or ventricular punctures in newborns with intraventricular haemorrhage. *Cochrane Database Syst Rev*. (2017) 4:CD000216. doi: 10.1002/14651858.CD000216.pub2
34. Haines SJ, Lapointe M. Fibrinolytic agents in the management of posthemorrhagic hydrocephalus in preterm infants: the evidence. *Child's Nerv Syst*. (1999) 15:226–34. doi: 10.1007/s003810050378
35. Latini G, Dipaola L, De Felice C. First day of life reference values for pleth variability index in spontaneously breathing term newborns. *Neonatology*. (2012) 101:179–82. doi: 10.1159/000331774
36. Azzopardi D, Strohm B, Marlow N, Brocklehurst P, Deierl A, Eddama O, et al. Effects of hypothermia for perinatal asphyxia on childhood outcomes. *N Engl J Med*. (2014) 371:140–9. doi: 10.1056/NEJMoa1315788
37. Wu J, Morris JK. The population prevalence of down's syndrome in England and wales in 2011. *Eur J Hum Genet*. (2013) 21:1016–9. doi: 10.1038/ejhg.2012.294
38. Luyt K, Jary S, Lea C, Young GJ, Odd D, Miller H, et al. Ten-year follow-up of a randomised trial of drainage, irrigation and fibrinolytic therapy (DRIFT) in infants with post-haemorrhagic ventricular dilatation. *Health Technol Assess*. (2019) 23:1–116. doi: 10.3310/hta23040
39. Etus V, Kahilogullari G, Karabagli H, Unlu A. Early endoscopic ventricular irrigation for the treatment of neonatal posthemorrhagic hydrocephalus: a feasible treatment option or not? A multicenter study. *Turk Neurosurg*. (2018) 28:137–41. doi: 10.5137/1019-5149.JTN.18677-16.0
40. Cizmeci MN, Thewissen L, Zecic A, Woerdeman PA, Boer B, Baert E, et al. Bedside ultrasound-guided percutaneous needle aspiration of intra- and extra-axial intracranial hemorrhage in neonates. *Neuropediatrics*. (2018) 49:238–45. doi: 10.1055/s-0038-1641568
41. Cizmeci MN, Khalili N, Claessens NHP, Groenendaal F, Liem KD, Heep A, et al. Assessment of brain injury and brain volumes after posthemorrhagic ventricular dilatation: a nested substudy of the randomized controlled ELVIS trial. *J Pediatr*. (2019) 208:191–7.e2. doi: 10.1016/j.jpeds.2018.12.062
42. Ahn SY, Chang YS, Sung SI, Park WS. Mesenchymal stem cells for severe intraventricular hemorrhage in preterm infants: phase i dose-escalation clinical trial. *Stem Cells Transl Med*. (2018) 7:847–56. doi: 10.1002/sctm.17-0219

Conflict of Interest: The authors declare that the research was conducted in the absence of any commercial or financial relationships that could be construed as a potential conflict of interest.

frontiers in Pediatrics

ORIGINAL RESEARCH
published: 26 June 2020
doi: 10.3389/fped.2020.00272

Perinatal Opioid Exposure Primes the Peripheral Immune System Toward Hyperreactivity

Jessie Newville[1], *Jessie R. Maxwell*[1,2], *Yuma Kitase*[3], *Shenandoah Robinson*[4,5] *and Lauren L. Jantzie*[3,4,5,6]*

[1] Department of Neurosciences, University of New Mexico School of Medicine, Albuquerque, NM, United States, [2] Departments of Pediatrics, University of New Mexico School of Medicine, Albuquerque, NM, United States, [3] Division of Neonatal-Perinatal Medicine, Department of Pediatrics, Johns Hopkins University School of Medicine, Baltimore, MD, United States, [4] Division of Pediatric Neurosurgery, Department of Neurosurgery, Johns Hopkins University School of Medicine, Baltimore, MD, United States, [5] Department of Neurology, Johns Hopkins University School of Medicine, Baltimore, MD, United States, [6] Department of Neurology, Kennedy Krieger Institute, Baltimore, MD, United States

The increased incidence of opioid use during pregnancy warrants investigation to reveal the impact of opioid exposure on the developing fetus. Exposure during critical periods of development could have enduring consequences for affected individuals. Particularly, evidence is mounting that developmental injury can result in immune priming, whereby subsequent immune activation elicits an exaggerated immune response. This maladaptive hypersensitivity to immune challenge perpetuates dysregulated inflammatory signaling and poor health outcomes. Utilizing an established preclinical rat model of perinatal methadone exposure, we sought to investigate the consequences of developmental opioid exposure on *in vitro* activation of peripheral blood mononuclear cells (PBMCs). We hypothesize that PBMCs from methadone-exposed rats would exhibit abnormal chemokine and cytokine expression at baseline, with exaggerated chemokine and cytokine production following immune stimulation compared to saline-exposed controls. On postnatal day (P) 7, pup PMBCs were isolated and cultured, pooling three pups per *n*. Following 3 and 24 h, the supernatant from cultured PMBCs was collected and assessed for inflammatory cytokine and chemokine expression at baseline or lipopolysaccharide (LPS) stimulation using multiplex electrochemiluminescence. Following 3 and 24 h, baseline production of proinflammatory chemokine and cytokine levels were significantly increased in methadone PBMCs ($p < 0.0001$). Stimulation with LPS for 3 h resulted in increased tumor necrosis factor (TNF-α) and C-X-C motif chemokine ligand 1 (CXCL1) expression by 3.5-fold in PBMCs from methadone-exposed PBMCs compared to PBMCs from saline-exposed controls ($p < 0.0001$). Peripheral blood mononuclear cell hyperreactivity was still apparent at 24 h of LPS stimulation, evidenced by significantly increased TNF-α, CXCL1, interleukin 6 (IL-6), and IL-10 production by methadone PMBCs compared to saline control PBMCs ($p < 0.0001$). Together, we provide evidence of increased production of proinflammatory molecules from methadone PBMCs at baseline, in addition to sustained hyperreactivity relative to saline-exposed controls. Exaggerated peripheral immune responses exacerbate inflammatory signaling, with subsequent consequences on many organ systems throughout the body, such as the developing nervous system. Enhanced

OPEN ACCESS

Edited by:
Lewis Phillip Rubin, MedStar Georgetown University Hospital, United States

Reviewed by:
Robert Galinsky, Hudson Institute of Medical Research, Australia
Sinno Simons, Erasmus Medical Center, Netherlands

***Correspondence:**
Lauren L. Jantzie
ljantzie@jhmi.edu

Specialty section:
This article was submitted to Neonatology, a section of the journal Frontiers in Pediatrics

Received: *07 January 2020*
Accepted: *29 April 2020*
Published: *26 June 2020*

Citation:
Newville J, Maxwell JR, Kitase Y, Robinson S and Jantzie LL (2020) Perinatal Opioid Exposure Primes the Peripheral Immune System Toward Hyperreactivity. Front. Pediatr. 8:272. doi: 10.3389/fped.2020.00272

understanding of these inflammatory mechanisms will allow for appropriate therapeutic development for infants who were exposed to opioids during development. Furthermore, these data highlight the utility of this *in vitro* PBMC assay technique for future biomarker development to guide specific treatment for patients exposed to opioids during gestation.

Keywords: methadone, lymphocyte, PBMC, SPIHR, blood mononuclear cell, neuroinflammation, neonatal abstinence syndrome, prenatal

INTRODUCTION

The incidence of opioid abuse in the United States has steadily increased since 2000, today reaching epidemic proportions (1, 2). The crisis is illustrated by data demonstrating that the number of opioid-related hospitalizations increased by 64%, and the number of deaths due to opioid overdose increased by 27% between the years of 2005 and 2014 (3, 4). Mirroring the national trend, opioid use by pregnant women has escalated to alarming rates (5). Opioid use in this population increased 5-fold from 2000 to 2009 (6), and the prevalence of women with opioid use disorders at delivery hospitalizations quadrupled between 1999 and 2014 (7).

Prenatal opioid exposure results from maternal use or abuse of illicit opioids, such as heroin, and prescription opioids including oxycodone, hydrocodone, morphine, codeine, and fentanyl (8). In addition, the maternal use of buprenorphine or methadone, two synthetic opioids commonly used in opioid maintenance therapy for individuals suffering from opioid use disorder (9, 10), also contribute to prenatal opioid exposure. The growing rate of women using opioids during pregnancy has led to an increase in adverse neonatal outcomes (11, 12). Recent studies showing an association between opioid use during pregnancy and poor health outcomes for both pregnant women and infants highlight prenatal opioid exposure as a serious public health concern (13, 14). Opioid-exposed infants represent an extremely vulnerable patient population (15), with 50–80% experiencing neonatal abstinence syndrome (16). Indeed, prenatal opioid exposure is associated with increased risk of fetal growth restriction, preterm birth, and lifelong motor and cognitive deficits (17–25). The devastating consequences of opioid exposure on the physical health and developmental outcomes of exposed children strengthen the need to advance scientific understanding of the underpinnings of opioid-induced neural injury and to advance biomarker development in this patient population.

Insult during the prenatal period affects ongoing developmental processes in the fetus, leading to lifelong consequences and health challenges. Both the central nervous system (CNS) and the immune system undergo complex and incremental steps toward maturation during gestation (26–28). New advances in molecular neuroscience have begun to elucidate the importance of the multifaceted interplay of central and peripheral immune system in regulating and supporting ongoing brain development. Moreover, these advances highlight the neurodevelopmental consequences of perinatal immune activation following perinatal insult (29–33). The findings from both clinical and preclinical studies implicate perinatal immune activation in the pathophysiology of numerous neurodevelopmental disorders, such as cerebral palsy, autism spectrum disorders, Down syndrome, and fetal alcohol spectrum disorders (33–41).

Previously, we reported evidence of neural injury and reduced cognitive functioning in a model of prenatal opioid exposure, with multiple assays reflecting significant neuroinflammation (42). In the aforementioned study, analysis of serum inflammatory cytokine expression of opioid-exposed animals compared to saline-exposed controls demonstrated elevated levels of interleukin 1β (IL-1β), tumor necrosis factor α (TNF-α), IL-6, and C-X-C motif chemokine ligand 1 (CXCL1), indicating systemic inflammatory response syndrome induced by opioid exposure. Additionally, initial *in vitro* assessment of isolated PBMC from opioid-exposed animals challenged with lipopolysaccharide (LPS) suggested heightened immune reactivity and immune priming toward exaggerated responses to stimuli (42).

Here, we extend our investigation of opioid-induced inflammation by thoroughly defining the peripheral immune signaling and reactivity of opioid-exposed PBMCs using an established *in vitro* assay and biomarker platform (35, 37, 43–50). These data enhance the understanding of important inflammatory mechanisms, an essential step to inform future development of appropriate therapeutic interventions for infants who are exposed to opioids during gestation.

MATERIALS AND METHODS

Animals

Sprague–Dawley rat dams and litters were maintained in a 12-h dark–light cycle (lights on at 0800 h), temperature, and humidity-controlled facility with food and water available *ad libitum*. All experiments were performed in strict accordance with protocols approved by the Institutional Animal Care and Use Committee at the University of New Mexico Health Sciences Center. Protocols were developed and performed consistent with National Research Council and ARRIVE guidelines (51).

Opioid Administration

Methadone is a full μ-, δ-, and κ-opioid receptor agonist, similar to heroin, morphine, and fentanyl, whereas buprenorphine is a partial μ-opioid receptor agonist and κ-opioid receptor antagonist (52). The use of methadone in our experiments allows us avoid differential pharmacology related to partial antagonism and study the effects from of full agonism at the predominant opioid receptor subtypes. As previously published (42), osmotic

minipumps (model 2004; Alzet, Cupertino, CA, USA) primed with 12 mg/kg of methadone or normal saline were implanted in embryonic day (E) 16 timed-pregnant rat dams (Charles River Laboratories, Wilmington, MA, USA) (**Figure 1**). Implantation on E16 allows *in utero* opioid exposure from E16 to birth and postnatal opioid exposure via milk from birth to postnatal day (P) 7 (blood collection). These minipumps allow for continual infusion of methadone or saline at a rate of 0.25 μL per hour for a maximum of 28 days. Under isoflurane-induced anesthesia, dams underwent a minipump placement procedure. Subcutaneous minipump placement was achieved by transverse 1.5-cm incision. The subcutaneous area was opened by careful blunt dissection, and the prefilled, primed osmotic minipump was placed in the opened space. Following closure of the incision with sutures, dams were then returned to their respective home cages, where their recovery was closely monitored. When pups were born on E22, they then received methadone through milk ingestion. Postnatal methadone exposure was confirmed by measuring the concentration of methadone in dam and offspring urine (42). As previously reported, this paradigm of opioid exposure results in significant pup weight loss at the neonatal and perinatal period. Opioid exposure via 12 mg/kg minipump results in a significant 10% reduction in offspring weight at P1 and 23% reduction in weight by P21 compared to saline exposed controls (42). These preclinical data reflect data from clinical studies showing that infants of mothers who exclusively used opioids suffered from a 2 to 10% decrease in birth weight compared to healthy controls (53, 54). Further, another study found that infants of mothers on methadone replacement therapy suffered a 19% reduction in birth weight compared to age-matched controls (55). Thus, this model replicates the systemic consequences of extended prenatal opioid exposure observed in human infants.

Peripheral Blood Mononuclear Cell Isolation

At P7, rats are developmentally equivalent to human infants between approximately 32 and 38 weeks' gestation (56–62). From P7 to P10 in rats and 36–40 weeks' gestation in humans (term infant), overall brain growth peaks while important neural developmental processes, such as gliogenesis and expansion of axonal and dendritic density, occur (60, 63–65, 65–69). During this same developmental period, consolidation of the immune system in humans and rats occurs, whereby the functional capacity of immune cells evolves, and the number of circulating leukocytes, neutrophils, and monocytes increases (26–28, 60, 70–72). At P7, PBMC isolation was performed as previously published (41). Venous blood was collected from the right atrium of deeply anesthetized P7 pups and pooled across three animals in pyrogen-free K2 EDTA Vacutainer tubes (366643; Becton Dickson, Franklin Lakes, NJ, USA). Each n represents PBMCs isolated from blood pooled across three separate animals. In this study, equal numbers of male and female pups were used throughout. Peripheral blood mononuclear cells were isolated by Ficoll gradient separation (37), whereby equal volumes of peripheral blood and RPMI 1640 media (Gibco, Waltham, MA, USA) were combined and layered atop 3 mL of Ficoll-Plaque Plus (17144002; GE Healthcare, Chicago, IL, USA) within sterile 15-mL conical tubes. Following centrifugation at 400 *g* for 30 min at room temperature, the PBMC cell layer was transferred to a new centrifuge tube and resuspended in three volumes of RPMI media. Two wash cycles were performed, consisting of centrifugation at 400 *g* for 10 min at room temperature, disposal of the supernatant, and resuspension of the pellet in three volumes of RPMI media. Isolated PBMCs resuspended in media were plated in triplicates at a density of 1×10^6 cells/mL on 3.5-cm Petri dishes.

Peripheral Blood Mononuclear Cell Treatment With LPS

Plated PBMCs from saline and methadone groups were stimulated with 10, 50, or 100 ng/mL of LPS to generate a dose response curve. Based on TNF-α secretion levels at 3 h, we determined that stimulation with 100 ng of LPS was ideal to produce a robust PBMC secretory response in both treatment groups. Therefore, consistent with previous studies, 100 ng of LPS was used for LPS challenge experiments (41, 45, 73). Supernatant samples were collected at 3 and 24 h in sterile 2-mL Eppendorf tubes, snap frozen on dry ice, and stored at −80°C until biochemical analysis.

Multiplex Electrochemiluminescent Immunoassay

To capture the secretory activity of PBMCs prior to protein synthesis, and then after protein synthesis, the supernatants from plated PBMCs were assayed at 3 and 24 h, respectively. Subsequently, secreted cytokine and chemokine expression was quantified using a V-PLEX Proinflammatory Panel 2 Rat Kit (K15059D; Meso Scale Diagnostics, Rockville, MD, USA) created to detect levels of interferon γ, IL-1β, IL-4, IL-5, IL-10, IL-13, IL-6, CXCL1, and TNF-α. The V-PLEX multielectrochemiluminescent immunoassay (MECI) was performed according to manufacturer instructions with <5% interassay variation. Specifically, supernatants from cultured PBMCs were diluted 1:4 and, together with prepared standards, were loaded in duplicate onto the manufacturer-provided blocked and washed 96-well plates. Then, following a series of washes and incubation with the antibody detection solution, plates were washed and loaded with the manufacturer-provided Read Buffer and read on a Quickplex SQ 120 Imager. Here, we report data on the levels of TNF-α and CXCL1 production at 3 h and TNF-α, CXCL1, IL-6, and IL-10 at 24 h. Of note, levels of IL-6 and IL-10 at 3 h were below the detectable limit in baseline conditions, as were other cytokine levels in the panel.

Statistical Analyses

To determine appropriate sample size, statistical power was calculated using G*Power 3.1.9.7 (Institut für Psychologie, Kiel, Germany) (74), using estimated means from previous studies (33, 42). Here, we prepared an n of three per treatment group, whereby each n represents isolated PBMCs from three animals pooled into one sample. Comparisons to determine statistical significance, defined as $p < 0.05$, were performed within Prism 7.05 (GraphPad software, San Diego, CA, USA). For comparisons

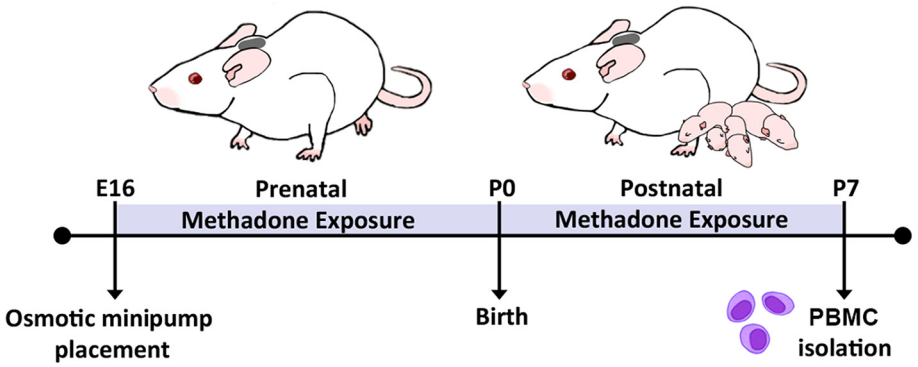

FIGURE 1 | Experimental timeline. Perinatal methadone exposure was accomplished by minipump implantation on E16, permitting pup exposure to methadone during critical stages of immune and neurological maturation. On P7, PBMCs from methadone- or saline-exposed pups were isolated for culture and biochemical analysis.

between saline and methadone PMBC secretion, a Student *t*-test was used to determine significance. For statistical analysis of the dose response to LPS, a one-way analysis of variance (ANOVA) with Bonferroni multiple comparisons was performed. To make comparisons between treatments (baseline secretion vs. LPS-stimulated secretion) and to make comparisons between time points (3- vs. 24-h secretion), two-way ANOVA was performed with Bonferroni *post-hoc* analyses.

RESULTS

Methadone Alters Baseline Peripheral Immune System Signaling

At 3 h, unstimulated PBMCs from methadone-exposed pups produced significantly augmented levels of the inflammatory cytokine TNF-α (methadone: 3.589 pg/mL, saline: 0.8142 pg/mL, *t*-test, $p < 0.0001$), as well as CXCL1 (methadone: 1.280 pg/mL, saline: 0.0, *t*-test, $p = 0.0004$) (**Figure 2A**).

After 24 h, the level of TNF-α secreted by saline PBMCs was 41% increased from levels measured at 3 h, whereas methadone PBMCs demonstrated a 152% increase from levels measured at 3 h (two-way ANOVA, $p < 0.0001$). Increased production of TNF-α by methadone PBMCs at 24 h (methadone: 9.047 pg/mL, saline: 1.148 pg/mL, *t*-test, $p < 0.0001$) was accompanied by increased secretion of CXCL1 by methadone PBMCs relative to saline PBMCs (methadone: 2.950 pg/mL, saline: 0.0 pg/mL, *t*-test, $p = 0.0004$) (**Figure 2B**). By 24 h, CXCL1 secretion by methadone PBMCs was 130% increased from measurement at 3 h (*t*-test, $p < 0.0002$), whereas levels of CXCL1 production by saline PBMCs remained below detectable levels at both the 3- and 24-h time points. Moreover, after 24 h in culture, methadone PBMCs demonstrated additional evidence of dysregulated immune signaling, evident by increased IL-6 (methadone: 39.82 pg/mL, saline: 0.0 pg/mL, *t*-test, $p < 0.0001$) and decreased IL-10 expression (methadone: 0.0 pg/mL, saline: 1.712 pg/mL, *t*-test, $p = 0.0001$) (**Figure 2C**). Together, these data show significantly altered baseline production of inflammatory signaling molecules by methadone-derived PBMCs at 3 and 24 h compared to controls.

Methadone Primes the Peripheral Immune System Toward Hyperreactivity

To illuminate potential discrepancies in reactivity to immune stimulus between treatment groups, PBMCs from methadone and saline exposed pups were challenged with LPS *in vitro*. By increasing the dose of LPS from 10, to 50, to 100 ng/mL, we observed a dose-dependent increase in TNF-α secretion from both saline and methadone PBMCs, compared to PMBCs in media alone (one-way ANOVA, $p < 0.0001$) (**Figure 3**). In this assay, addition of media alone resulted in levels of TNF-α production that were not statistically different from baseline levels of TNF-α measured at 3 h, as reported earlier in this study (one-way ANOVA, $p > 0.05$). With each dose of LPS, PBMCs derived from methadone-exposed animals produced greater levels of TNF-α compared to saline PBMCs (one-way ANOVA, $p < 0.001$). As 100 ng/mL LPS elicited a significant response in PBMCs from both methadone- and saline-exposed pups, we stimulated a separate cohort of PBMCs with this dose and measured cytokine and chemokine levels at 3 and 24 h.

At 3 h following stimulation with 100 ng/mL LPS, TNF-α (methadone: 215.8 pg/mL, saline: 59.08 pg/mL, *t*-test, $p < 0.0001$) and CXCL1 (methadone: 53.29 pg/mL, saline: 14.33 pg/mL, *t*-test, $p < 0.0001$) production by PBMCs from P7 methadone-exposed pups was increased compared to PBMCs from saline-exposed controls, representing a 265 and 272% increase, respectively (**Figure 4A**). Compared to baseline levels of unstimulated PBMCS, LPS-stimulated PBMCs derived from both saline and methadone animals produced significantly increased levels of TNF-α and CXCL1 3 h (two-way ANOVA, $p < 0.0001$).

Following 24 h of LPS stimulation, levels of TNF-α (methadone: 412.6 pg/mL, saline: 102.8 pg/mL, *t*-test, $p < 0.0001$) and CXCL1 (methadone: 231.6 pg/mL, saline: 38.34 pg/mL, *t*-test, $p < 0.0001$) produced by methadone PBMCs were increased by 301 and 504%, respectively, compared to levels from saline PBMCs (**Figure 4B**). Compared to measurements taken at 3 h following LPS stimulation, TNF-α secretion at 24 h increased by 74% in saline PBMCs, whereas methadone PBMCs demonstrated a 91% increase (two-way ANOVA, $p < 0.0001$). A similar pattern arose with CXCL1 production.

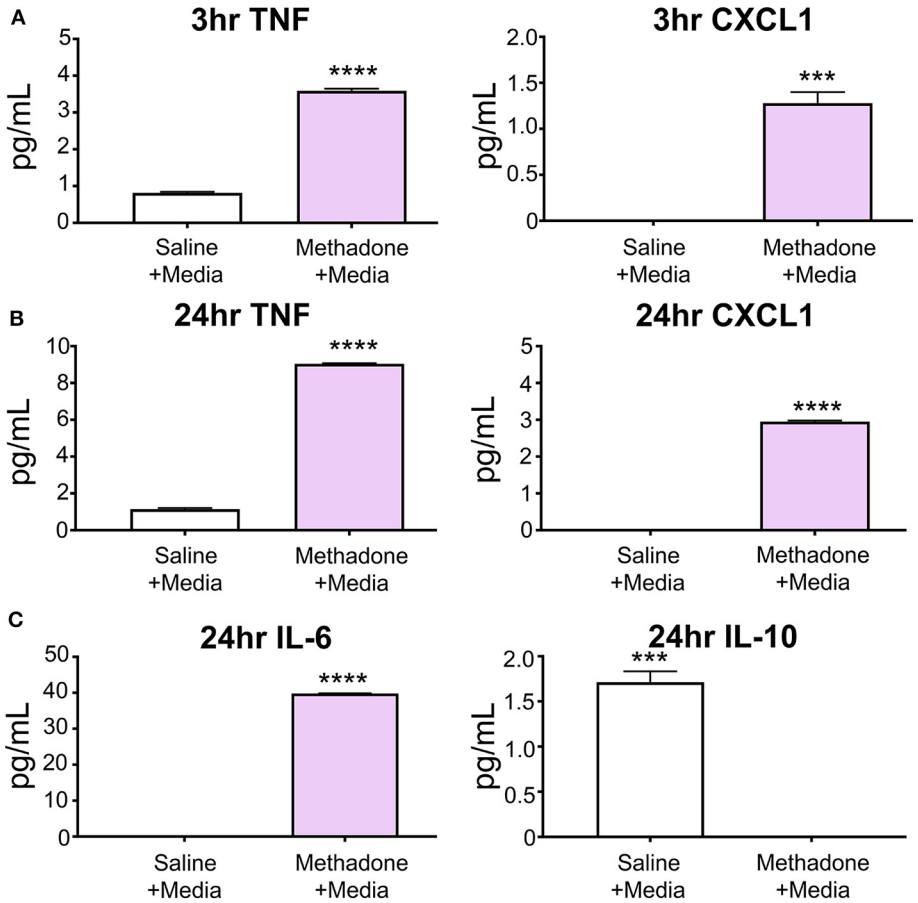

FIGURE 2 | At baseline, PBMCs from methadone-exposed pups demonstrated dysregulated production of inflammatory signaling molecules. **(A)** At 3 h following isolation from P7 pups and plating in media alone, PBMCs from methadone-exposed pups produced significantly increased levels of TNF-α and CXCL1, compared to PBMCs from saline-exposed control PBMCs. **(B)** After 24 h, TNF-α and CXCL1 levels from methadone PBMCs compared to saline were further augmented. **(C)** Additionally, methadone PBMCs produced significantly higher levels of IL-6 and significantly lower levels of IL-10, compared to saline controls ($n = 3$ per treatment group, ***$p < 0.001$, ****$p < 0.0001$).

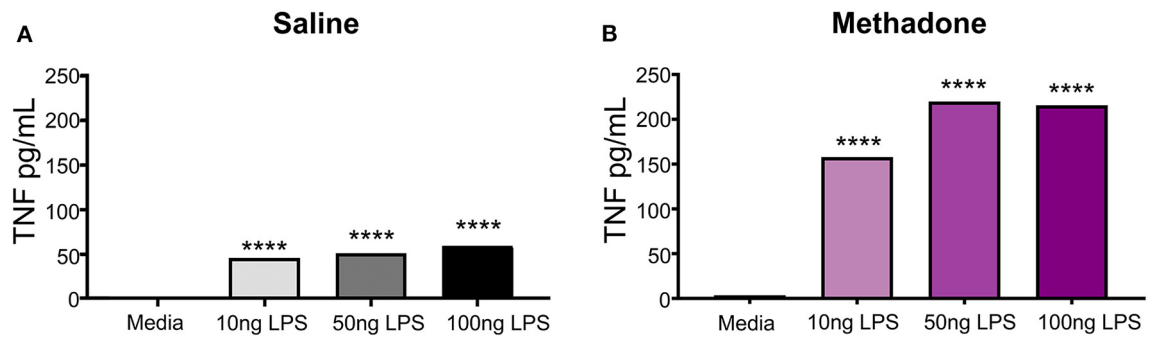

FIGURE 3 | Peripheral blood mononuclear cells isolated from P7 pups exhibit LPS induced dose-responsive increases in TNF-α production. **(A)** Increasing doses of LPS (10, 50, or 100 ng/mL) elicited significantly augmented secretion of TNF-α from saline and **(B)** methadone PBMCs, compared to PMBCs in media alone ($n = 3$ per treatment group, 1 way ANOVA, ****$p < 0.0001$).

By 24 h, CXCL1 production by saline PBMCs increased 164% from levels measured at 3 h, whereas CXCL1 produced by LPS-challenged methadone PBMCs rose 334% (two-way ANOVA, $p < 0.0001$). At 24 h, we also found significantly increased levels of IL-6 (methadone: 409.4 pg/mL, saline: 111.7 pg/mL, t-test, $p < 0.0001$) and IL-10 (methadone: 20.35 pg/mL, saline: 1.442

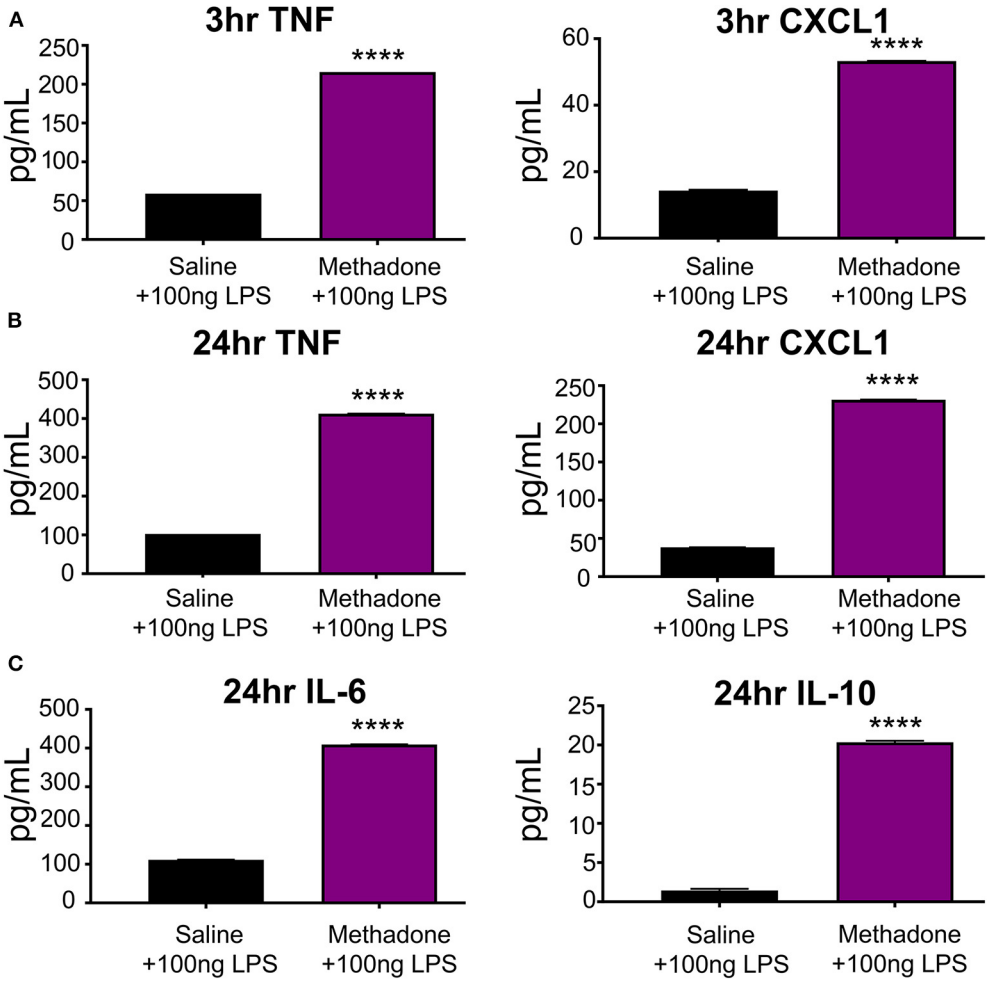

FIGURE 4 | Stimulation with LPS revealed hyperreactivity of PBMCs from methadone-exposed pups. **(A)** At 3 h, TNF-α and CXCL1 production by PBMCs from P7 methadone-exposed pups was significantly increased compared to PBMCs from saline exposed controls. **(B)** After 24 h, TNF-α and CXCL1 levels from methadone PBMCs were significantly increased compared to saline levels. **(C)** Additionally, production of IL-6 and IL-10 by methadone PBMCs was significantly augmented, compared to saline controls ($n = 3$ per treatment group, unpaired t-test, $^{****}p < 0.0001$).

pg/mL, t-test, $p < 0.0001$) from methadone PBMCs, compared to saline controls (**Figure 4C**).

DISCUSSION

As the opioid crisis continues to grow, increasing numbers of pregnant women and infants are affected. While mounting evidence indicates that prenatal opioid exposure is associated with significant and long-lasting neurological injury (17–19, 25), information on the pathophysiology of opioid exposure during the perinatal period is limited. Increasing our understanding of the cellular and molecular mechanisms that are impacted in circumstances of *in utero* opioid exposure is important for the development and implementation of informed clinical practices, in addition to the improvement of therapeutic options to support opioid-exposed infants.

Using the same model of perinatal opioid exposure employed in the current study, we previously provided evidence of neuroinflammation, microstructural brain injury, persistent cognitive deficits, and peripheral immune activation following perinatal opioid exposure (42). Here, we expand our understanding of the systemic immune dysfunction through an in-depth characterization of peripheral immune cell activity and reactivity following perinatal methadone exposure. Utilizing a clinically applicable *in vitro* cell culture protocol and translational multiplex immunoassay inflammatory biomarker panel (36, 37, 75–80), we found that at baseline PBMCs derived from methadone-exposed P7 pups hypersecreted proinflammatory molecules. Consistent with our previous findings that PBMCs derived from methadone-exposed rats secreted increased levels of TNF-α at 3 and 24 h after collection (42), here, we demonstrate that methadone PBMCs also secrete

elevated levels of CXCL1 at 3 h. Increased expression of TNF-α and CXCL1 relative to PBMCs derived from saline-exposed controls was still evident at 24 h, demonstrating sustained peripheral immune activation of methadone-derived PBMCs at P7. Interestingly, after 24 h in culture, we observe additional evidence of dysregulated immune signaling with elevated IL-6 and diminished IL-10 in methadone-exposed animals relative to saline controls, in addition to the increased TNF-α and CXCL1 levels from methadone PBMCs. Despite probing for the presence of IL-6 and IL-10 at 3 h, the levels from both saline- and methadone-derived PBMCs remained below the detectable limits of the MECI. In summary, this evidence of elevated PBMC baseline production of known proinflammatory molecules TNF-α, CXCL1, and IL-6, with decreased levels of anti-inflammatory IL-10 from methadone-exposed animals, likely contributes to a proinflammatory environment within the systemic circulation (81).

To further characterize altered immune function, we stimulated cultured PBMCs with 100 ng/mL of LPS to represent an immune challenge and then quantified the chemokine and cytokine profile signature. While the addition of 100 ng/mL of LPS is a supraphysiological dose, it was formulated in consideration of our previous work (41, 42) and based on the dose response measured in TNF-α secretion to 10, 50, and 100 ng/mL of LPS that we performed in this study. We demonstrate that 100 ng/mL produces a robust PBMC response in the *in vitro* PBMC culture assay we performed, allowing us to examine chemokine and cytokine production by PBMCs from both saline and methadone treatment groups. Following 3 h of LPS stimulation, we detected levels of TNF-α and CXCL1 that were elevated from baseline in both methadone- and saline-exposed groups. Lipopolysaccharide-stimulated methadone PBMCs produced significantly more TNF-α and CXCL1 compared to PBMCs from stimulated saline control PBMCs. At 24 h, hyperreactivity of methadone PBMCs was evident from significantly elevated levels of TNF-α, CXCL1, IL-6, and IL-10 compared to saline controls. Taken together, these data provide evidence of increased sensitivity and a priming effect to subsequent inflammatory challenge in PBMCs from methadone-exposed pups. This suggests a mechanism of deleterious feed-forward inflammatory pathophysiology and fetal programming of immune system activation induced by methadone. Indeed, immune plasticity altered by methadone exposure may have long-lasting effects on the inflammatory responses of circulating leukocytes later in life. Future studies that assess the secretome and reactivity of PBMCs derived from opioid-exposed subjects at later developmental time points beyond P7 would be important to answer these questions.

Importantly, our *in vitro* approach allowed us to study PBMC responsiveness and sensitivity in isolation of potential confounders such as Toll-like receptor–stimulating agents in the peripheral circulation (82). Our *in vitro* data showing increased proinflammatory signaling at baseline from methadone-exposed PBMCs, without any immune stimulation, are distinct to this paradigm of perinatal injury and highlight this *in vitro* assay for use as a potential biomarker. The *in vitro* LPS challenge we perform here is a method that has been used clinically in children with developmental disorders and brain injury (35, 37). For instance, in a clinical study of children born preterm with cerebral palsy (37) and preclinical model reminiscent of preterm CNS injury (41), PBMCs were assayed consistent with the *in vitro* approach employed in the current study. Interestingly, in these studies, baseline secretion of PBMCs did not differ between treatment groups (37, 41). Only after stimulation with LPS did appreciable differences in PBMC chemokine and cytokine production appear in subjects with cerebral palsy (37), similar to preclinical studies (41, 45, 73). Perinatal insult–specific PBMC properties, revealed using this *in vitro* approach, support the potential use of secreted protein profiles from isolated PBMCs as a biomarker to discern distinct pathologies and potentially guide clinical treatment. Indeed, elucidating these profiles of immune signaling molecules holds potential for use as a biomarker to determine vulnerability to sustained peripheral immune hyperreactivity. Specifically, biomarkers in neonates could provide estimation of extent of immune system abnormalities and CNS injury and provide pharmacodynamic support to guide duration or degree of treatment for neonatal opioid withdrawal syndrome or supportive care in neonatal intensive care units. In this context, durable changes in PBMC reactivity may be an effective biomarker, and clinical utility may prove high given the ease of access to these cells and well-defined clinical stimulation protocols (37, 43). However, while these *in vitro* PBMC assays are clinically relevant, they are distinctly different than studying the complex, multidimensional *in vivo* response to inflammation, sepsis, and systemic sensitization catalyzed by an LPS challenge. Unquestionably, further study is required to validate how circulating leukocytes respond to LPS immune challenges *in vivo* and in the context of complex inflammatory networks, systemic circulating factors, and all cells that express TLR4.

Peripheral blood mononuclear cell hypersecretion of proinflammatory molecules and PBMC hyperreactivity resultant of gestational opioid exposure have important implications for the developing CNS. Our previous preclinical report strongly implicates brain injury secondary to opioid-induced systemic and neuroinflammation (42). In alignment with the aforementioned study, we now provide evidence of PBMC hypersection and hyperreactivity, which could contribute to increased systemic inflammation during the term equivalent developmental time point, coinciding with the brain growth spurt, peak myelination and gliogenesis, and astrocyte production (60, 63, 65–69, 83). Increased chemokine and cytokine production by PBMCs during the perinatal period jeopardizes proper neural cell development and circuitry maturation. Indeed, inflammation during perinatal development results in lasting neurological impairment (77, 80, 84, 85). While future studies are needed to clarify if methadone elicits PBMC systemic inflammation via PBMC activation throughout the methadone exposure, it is well-established that elevated levels of circulating inflammatory proteins during later stages in brain development (late third trimester, term equivalent) are associated with brain injury,

characterized by increased structural and functional neurological deficits (80, 84, 86–89). Specifically, in a recent study of systemic TNF-α inhibition in preterm fetal sheep exposed to LPS-induced inflammation, researchers identified circulating TNF-α as a critical contributor to neuroinflammation and pathogenesis of impaired neurodevelopment (90). Cytokine and chemokines produced by circulating leukocytes are able to cross the blood–brain barrier via selective transporters (91). Furthermore, as in the specific case of TNF-α, increased levels can contribute to impairment of the blood–brain barrier function (92–94), allowing for increased proinflammatory molecule access to the developing CNS. Opioids are able to cross from maternal circulation through the placenta to fetal circulation owing to their low molecular weight, moderate lipid solubility, and low protein binding (95). Once in fetal circulation, opioids are able to cross the fetal blood-brain barrier by means of numerous transporters (96, 97). Thus, not only are developing neural cells and circuitry exposed to elevated levels of proinflammatory molecules in the context of opioid exposure, but they are directly exposed to opioids as well. In the developing CNS, neurons in addition to oligodendrocytes, astrocytes, and microglia express opioid receptors (98). Intriguingly, oligodendrocytes express opioid receptors in a maturation-dependent manner, in which immature stages of oligodendrocytes have increased opioid receptor expression (98), rendering this population more vulnerable to opioid exposure. Ultimately, exposure to opioids in conjunction with the proinflammatory profile produced by opioid exposure characterized in the current investigation could contribute to observed brain injury in preclinical studies (42), as well as clinical studies indicating particular vulnerability to major white matter tracts in infants exposed to opioids during brain development (20, 22, 24, 25).

Similar to the CNS, the immune system develops and matures over the course of gestation and the perinatal period. Dysregulated chemokines and cytokine production, and changes in immune cells themselves, culminate in impaired immune function that can last decades (35, 37). Similar to neural cells, leukocytes are uniquely responsive to their environment. Indeed, immune plasticity altered by prenatal insults may have long-term effects on the inflammatory responses of circulating leukocytes, which may serve as a biomarker of persistent or prior neuroinflammation and brain injury (99, 100). Infants exposed to intrauterine inflammation are at an increased risk of neurodevelopmental disorders (101). Notably, newborns that have elevated levels of biomarkers of systemic inflammation on two occasions 1 week apart are at a higher risk of brain injury and impaired neurodevelopment (77, 80, 84) Thus, understanding the homeostatic regulation of central and peripheral inflammatory cells in infants following opioid exposure, and the long-term consequences of their dysregulation, is essential (102). Significantly, an increase in chemokines/cytokines can contribute to perinatal brain injury by multiple overlapping mechanisms, including direct initiation of programed cell death pathways, microglial activation, immune cell recruitment, mitochondrial damage, and endoplasmic reticulum stress (85, 103, 104).

There are important limitations to this present study. For instance, here PBMCs were isolated from pooled peripheral blood from term equivalent male and female rats, limiting the ability to elucidate differences between individual animals and between male and female rat pups. Evidence from studies examining PBMCs isolated from adult humans suggests that sex differences in stimulated PBMC properties and secretion exist (105–107). While sex differences in secretion of PBMCs isolated at neonatal time points are not well-defined (35, 37), evidence exists demonstrating sex-specific differences in brain inflammation following circulating myeloid cells depletion in neonatal mice (108) and that inflammatory responses following immune cell activation in the immature brain differ between males and females, as reviewed by Mallard et al. (109). Thus, separate pooling of males and female peripheral blood from P7 pups for sex-specific analysis represents an important future direction. Additionally, although pooling of blood from multiple P7 rat pups was necessary in these experiments to collect an adequate PBMC fraction following differential centrifugation, analysis at later time points with larger animals would not require pooling, allowing for analysis of individual animal PBMC secretion and reactivity. Peripheral blood mononuclear cells represent a heterogeneous population of mononuclear cells in the peripheral circulation composed of T cells, T regulatory cells, T helper cells, B cells, and natural killer/dendritic cells/monocytes (110). Undoubtedly, flow cytometric studies beyond the scope of the present investigation are needed to define the precise immune cell population composition of PBMCs isolated from animals exposed to opioids during development.

In the current study, pregnant ram dams were implanted with methadone administering osmotic minipumps on E16 prior to complete oligodendrocyte, microglial, and astrocyte maturation (60), limiting rat pup opioid exposure to E16 through P7 when PBMCs were collected. This prenatal and postnatal opioid exposure paradigm accomplishes opioid exposure up until the equivalent end of the human third trimester. Future studies should now aim to commence opioid exposure from the onset of pregnancy (E0), thereby encompassing the entirety of brain and immune development.

In conclusion, we provide evidence in support of a systemic inflammatory response to perinatal opioid exposure, characterized by immune cell reprogramming and priming. This evidence may in part contribute to the neurological injury following developmental opioid exposure characterized in our previous preclinical study (42). The current study with the study by Jantzie et al. (42) joins a host of new and intriguing investigations that link developmental neurological injuries including cerebral palsy (37) and Down syndrome (35) with underlying systemic inflammation resultant of abnormal PBMC activity. Treatments that reduce inflammation or support developing neural cells in the context of inflammation could rescue the poor neural outcomes observed in preclinical and clinical investigations of perinatal opioid exposure. Our future studies will aim to identify appropriate therapies that target these proinflammatory mechanisms

underlying brain injury associated with *in utero* opioid exposure (33, 111–114).

DATA AVAILABILITY STATEMENT

The datasets generated for this study are available on request to the corresponding author.

ETHICS STATEMENT

The animal study was reviewed and approved by the Institutional Animal Care and Use Committee (IACUC) at the University of New Mexico Health Sciences Center.

AUTHOR CONTRIBUTIONS

LJ conceptualized the hypothesis and supervised the experiments. JN, JM, YK, SR, and LJ designed and performed the experiments. SR and LJ interpreted the data. JN, LJ, and SR wrote the manuscript. All authors contributed to manuscript revision and approved the final version.

FUNDING

This study was supported by generous funding from the National Institutes of Health 1R01HL139492 to LJ, Dedicated Health Research Funds from the University of New Mexico, and the Department of Pediatrics at the University of New Mexico Health Sciences Center. The authors are grateful for support from Departments of Pediatrics and Neurosciences at the University of New Mexico, and from the Departments of Neurosurgery, Neurology and Pediatrics at Johns Hopkins University and the Kennedy Krieger Institute.

ACKNOWLEDGMENTS

We are grateful for the technical expertise of Tracylyn Yellowhair and Dr.Ksenia Matlowska.

REFERENCES

1. Lyden J, Binswanger IA. The United States opioid epidemic. *Semin Perinatol.* (2019) 43:123–31. doi: 10.1053/j.semperi.2019.01.001
2. US Department of Health and Human Services. *HHS Acting Secretary Declares Public Health Emergency to Address National Opioid Crisis*. (2017). Available online at: https://www.hhs.gov/about/news/2017/10/26/hhs-acting-secretary-declares-public-health-emergency-address-national-opioid-crisis.html (accessed February 22, 2019).
3. Seth P, Rudd RA, Noonan RK, Haegerich TM. Quantifying the epidemic of prescription opioid overdose deaths. *Am J Public Health*. (2018) 108:500–2. doi: 10.2105/AJPH.2017.304265
4. Weiss AJ, Bailey MK, O'Malley LO, Barrett ML, Elixhauser A, Steiner CA. *Patient Characteristics of Opioid-Related Inpatient Stays and Emergency Department Visits Nationally and by State, 2014*. (2017). Available online at: https://www.hcup-usahrqgov/faststats/landingjsp (accessed April 22, 2019).
5. Krans EE, Patrick SW. Opioid use disorder in pregnancy: health policy and practice in the midst of an epidemic. *Obstet Gynecol*. (2016) 128:4–10. doi: 10.1097/AOG.0000000000001446
6. Patrick SW, Schumacher RE, Benneyworth BD, Krans EE, McAllister JM, Davis MM. Neonatal abstinence syndrome and associated health care expenditures: United States, 2000-2009. *JAMA*. (2012) 307:1934–40. doi: 10.1001/jama.2012.3951
7. Haight SC, Ko JY, Tong VT, Bohm MK, Callaghan WM. Opioid use disorder documented at delivery hospitalization — United States, 1999–2014. *MMWR Morb Mortal Wkly Rep*. (2018) 67:845–9. doi: 10.15585/mmwr.mm6731a1
8. Reddy UM, Davis JM, Ren Z, Greene MF. Opioid use in pregnancy, neonatal abstinence syndrome, and childhood outcomes: executive summary of a joint workshop by the eunice kennedy shriver national institute of child health and human development, american congress of obstetricians and gynecologists, american academy of pediatrics, society for maternal-fetal medicine, centers for disease control and prevention, and the march of dimes foundation. *Obstet Gynecol*. (2017) 130:10–28. doi: 10.1097/AOG.0000000000002054
9. Mattick RP, Breen C, Kimber J, Davoli M. Methadone maintenance therapy versus no opioid replacement therapy for opioid dependence. *Cochrane Database Syst Rev*. (2009) 2009:CD002209. doi: 10.1002/14651858.CD002209.pub2
10. Zedler BK, Man AL, Kim MM, Amick HR, Joyce AR, Murrelle EL, et al. Buprenorphine compared with methadone to treat pregnant women with opioid use disorder: a systematic review and meta-analysis of safety in the mother, fetus and child. *Addiction*. (2016) 111:2115–28. doi: 10.1111/add.13462
11. Monnelly VJ, Hamilton R, Chappell FM, Mactier H, Boardman JP. Childhood neurodevelopment after prescription of maintenance methadone for opioid dependency in pregnancy: a systematic review and meta-analysis. *Dev Med Child Neurol*. (2019) 61:750–60. doi: 10.1111/dmcn.14117
12. Patrick SW, Davis MM, Lehmann CU, Cooper WO. Increasing incidence and geographic distribution of neonatal abstinence syndrome: United States 2009 to 2012. *J Perinatol*. (2015) 35:650–5. doi: 10.1038/jp.2015.36
13. Maeda A, Bateman BT, Clancy CR, Creanga AA, Leffert LR. Opioid abuse and dependence during pregnancy: temporal trends and obstetrical outcomes. *Anesthesiology*. (2014) 121:1158–65. doi: 10.1097/ALN.0000000000000472
14. Ross EJ, Graham DL, Money KM, Stanwood GD. Developmental consequences of fetal exposure to drugs: what we know and what we still must learn. *Neuropsychopharmacology*. (2015) 40:61–87. doi: 10.1038/npp.2014.147
15. Osborn DA, Jeffery HE, Cole MJ. Opiate treatment for opiate withdrawal in newborn infants. *Cochrane Database Syst Rev*. (2010) 10:CD002059. doi: 10.1002/14651858.CD002059.pub3
16. Ko JY, Patrick SW, Tong VT. Incidence of neonatal abstinence syndrome - 28 states, 1999-2013. *MMWR Morb Mortal Wkly Rep*. (2016) 65:799–802. doi: 10.15585/mmwr.mm6531a2
17. Azuine RE, Ji Y, Chang H, Kim Y, Ji H, DiBari J, et al. Prenatal risk, factors, and perinatal and postnatal outcomes associated with maternal opioid exposure in an urban, low-income, multiethnic, U. S population. *JAMA Netw Open*. (2019) 2:e196405. doi: 10.1001/jamanetworkopen.2019.6405
18. Feder KA, Letourneau EJ, Brook J. Children in the opioid epidemic: addressing the next generation's public health crisis. *Pediatrics*. (2019) 144:e20181656. doi: 10.1542/peds.2018-1656
19. Hudak ML, Tan RC, The Committee on Drugs and the Committee on Fetus and Newborn. Neonatal drug withdrawal. *Pediatrics*. (2012) 129:e540–60. doi: 10.1542/peds.2011-3212
20. Monnelly VJ, Anblagan D, Quigley A, Cabez MB, Cooper ES, Mactier H, et al. Prenatal methadone exposure is associated with altered neonatal brain development. *NeuroImage Clin*. (2018) 18:9–14. doi: 10.1016/j.nicl.2017.12.033
21. Salzwedel AP, Grewen KM, Vachet C, Gerig G, Lin W, Gao W. Prenatal drug exposure affects neonatal brain functional connectivity. *J Neurosci*. (2015) 35:5860–9. doi: 10.1523/JNEUROSCI.4333-14.2015
22. Sirnes E, Oltedal L, Bartsch H, Eide GE, Elgen IB, Aukland SM. Brain morphology in school-aged children with prenatal opioid

exposure: a structural MRI study. *Early Hum Dev*. (2017) 106–7:33–9. doi: 10.1016/j.earlhumdev.2017.01.009
23. Sirnes E, Griffiths ST, Aukland SM, Eide GE, Elgen IB, Gundersen H. Functional MRI in prenatally opioid-exposed children during a working memory-selective attention task. *Neurotoxicol Teratol*. (2018) 66:46–54. doi: 10.1016/j.ntt.2018.01.010
24. Walhovd KB, Westlye LT, Moe V, Slinning K, Due-Tonnessen P, Bjornerud A, et al. White matter characteristics and cognition in prenatally opiate- and polysubstance- exposed children: a diffusion tensor imaging study. *Am J Neuroradiol*. (2010) 31:894–900. doi: 10.3174/ajnr.A1957
25. Yeoh SL, Eastwood J, Wright IM, Morton R, Melhuish E, Ward M, et al. Cognitive and motor outcomes of children with prenatal opioid exposure: a systematic review and meta-analysis. *JAMA Netw Open*. (2019) 2:e197025. doi: 10.1001/jamanetworkopen.2019.7025
26. Davies NP, Buggins AG, Snijders RJ, Jenkins E, Layton DM, Nicolaides KH. Blood leucocyte count in the human fetus. *Arch Dis Child*. (1992) 67:399–403. doi: 10.1136/adc.67.4_Spec_No.399
27. Madse-Bouterse SA, Romero R, Tarca AL, Kusanovic JP, Espinoza J, Kim CJ, et al. The transcriptome of the fetal inflammatory response syndrome. *Am J Reprod Immunol*. (2009) 63:73–92. doi: 10.1111/j.1600-0897.2009.00791.x
28. Zakharova LA, Malyukova IV, Proshlyakova EV, Potapova AA, Sapronova AY, Ershov PV, et al. Hypothalamo-pituitary control of the cell-mediated immunity in rat embryos: role of LHRH in regulation of lymphocyte proliferation. *J Reprod Immunol*. (2000) 47:17–32. doi: 10.1016/S0165-0378(00)00057-7
29. Hasegawa K, Ichiyama T, Isumi H, Nakata M, Sase M, Furukawa S. NF-κB activation in peripheral blood mononuclear cells in neonatal asphyxia. *Clin Exp Immunol*. (2003) 132:261–4. doi: 10.1046/j.1365-2249.2003.02127.x
30. Knuesel I, Chicha L, Britschgi M, Schobel SA, Bodmer M, Hellings JA, et al. Maternal immune activation and abnormal brain development across CNS disorders. *Nat Rev Neurol*. (2014) 10:643–60. doi: 10.1038/nrneurol.2014.187
31. Marc T. Brain development and the immune system: an introduction to inflammatory and infectious diseases of the child's brain. *Handb Clin Neurol*. (2013) 112:1087–9. doi: 10.1016/B978-0-444-52910-7.00026-X
32. Tanabe S, Yamashita T. The role of immune cells in brain development and neurodevelopmental diseases. *Int Immunol*. (2018) 30:437–44. doi: 10.1093/intimm/dxy041
33. Yellowhair TR, Noor S, Maxwell JR, Anstine CV, Oppong AY, Robinson S, et al. Preclinical chorioamnionitis dysregulates CXCL1/CXCR2 signaling throughout the placental-fetal-brain axis. *Exp Neurol*. (2019) 301:110–9. doi: 10.1016/j.expneurol.2017.11.002
34. Eliwan HO, Watson WRG, Regan I, Philbin B, O'Hare FM, Strickland T, et al. Pediatric intensive care: immunomodulation with activated protein c *ex vivo*. *Front Pediatr*. (2019) 7:386. doi: 10.3389/fped.2019.00386
35. Huggard D, McGrane F, Lagan N, Roche E, Balfe J, Leahy TR, et al. Altered endotoxin responsiveness in healthy children with down syndrome. *BMC Immunol*. (2018) 19:31. doi: 10.1186/s12865-018-0270-z
36. Kuban KC, Joseph RM, O'Shea TM, Heeren T, Fichorova RN, Douglass L, et al. Circulating inflammatory-associated proteins in the first month of life and cognitive impairment at age 10 years in children born extremely preterm. *J Pediatr*. (2017) 180:116–23.e1. doi: 10.1016/j.jpeds.2016.09.054
37. Lin CY, Chang YC, Wang ST, Lee TY, Lin CF, Huang C-C. Altered inflammatory responses in preterm children with cerebral palsy. *Ann Neurol*. (2010) 68:204–12. doi: 10.1002/ana.22049
38. Noor S, Milligan E. Lifelong impacts of moderate prenatal alcohol exposure on neuroimmune function. *Front Immunol*. (2018) 9:1107. doi: 10.3389/fimmu.2018.01107
39. Parker-Athill EC, Tan J. Maternal immune activation and autism spectrum disorder: interleukin-6 signaling as a key mechanistic pathway. *Neurosignals*. (2010) 18:113–28. doi: 10.1159/000319828
40. Rossignol DA. A review of research trends in physiological abnormalities in autism spectrum disorders: immune dysregulation, inflammation, oxidative stress, mitochondrial dysfunction and environmental toxicant exposures. *Mol Psychiatry*. (2012) 17:389–401. doi: 10.1038/mp.2011.165
41. Yellowhair TR, Noor S, Mares B, Jose C, Newville JC, Maxwell JR, et al. Chorioamnionitis in rats precipitates extended postnatal inflammatory lymphocyte hyperreactivity. *Dev Neurosci*. (2019) 40:523–33. doi: 10.1159/000497273
42. Jantzie LL, Maxwell JR, Newville JC, Yellowhair TR, Kitase Y, Madurai N, et al. Prenatal opioid exposure: the next neonatal neuroinflammatory disease. *Brain Behav Immun*. (2020)84:45–58. doi: 10.1016/j.bbi.2019.11.007
43. Huggard D, Koay WJ, Kelly L, McGrane F, Ryan E, Lagan N, et al. Altered toll-like receptor signalling in children with down syndrome. *Mediators Inflamm*. (2019) 2019:4068734. doi: 10.1155/2019/4068734
44. Jyonouchi H, Sun S, Le H. Proinflammatory and regulatory cytokine production associated with innate and adaptive immune responses in children with autism spectrum disorders and developmental regression. *J Neuroimmunol*. (2001) 120:170–9. doi: 10.1016/S0165-5728(01)00421-0
45. Kowalski ML, Wolska A, Grzegorczyk J, Hilt J, Jarzebska M, Drobniewski M, et al. Increased responsiveness to toll-like receptor 4 stimulation in peripheral blood mononuclear cells from patients with recent onset rheumatoid arthritis. *Mediators Inflamm*. (2008) 2008:132732. doi: 10.1155/2008/132732
46. Maes OC, Chertkow HM, Wang E, Schipper HM. Stress gene deregulation in alzheimer peripheral blood mononuclear cells. In: Basu S, Wiklund L, editors. *Studies on Experimental Models. Oxidative Stress in Applied Basic Research and Clinical Practice*. Totowa, NJ: Humana Press (2011). p. 251–63.
47. Moore DF, Li H, Jefferies N, Wright V, Cooper RA, Elkahloun A, et al. Using peripheral blood mononuclear cells to determine a gene expression profile of acute ischemic stroke: a pilot investigation. *Circulation*. (2005) 111:212–21. doi: 10.1161/01.CIR.0000152105.79665.C6
48. Nagabhushan M, Mathews HL, Witek-Janusek L. Aberrant nuclear expression of ap-1 and nfkb in lymphocytes of women stressed by the experience of breast biopsy. *Brain Behav Immun*. (2001) 15:78–84. doi: 10.1006/brbi.2000.0589
49. Segman RH, Shefi N, Goltser-Dubner T, Friedman N, Kaminski N, Shalev AY. Peripheral blood mononuclear cell gene expression profiles identify emergent post-traumatic stress disorder among trauma survivors. *Mol Psychiatry*. (2005) 10:500–13. doi: 10.1038/sj.mp.4001636
50. Witek-Janusek L, Gabram S, Mathews HL. Psychologic stress, reduced NK cell activity, and cytokine dysregulation in women experiencing diagnostic breast biopsy. *Psychoneuroendocrinology*. (2007) 32:22–35. doi: 10.1016/j.psyneuen.2006.09.011
51. Kilkenny C, Browne WJ, Cuthill IC, Emerson M, Altman DG. Improving bioscience research reporting: the ARRIVE guidelines for reporting animal research. *PLoS Biol*. (2010) 8:e1000412. doi: 10.1371/journal.pbio.1000412
52. Nelson LS, Olsen D. Opioids. In: Hoffman RS, Howland M, Lewin NA, Nelson LS, Goldfrank LR, editors. *Goldfrank's Toxicologic Emergencies*. 10th ed. New York, NY: McGraw-Hill (2015). p. 559–78.
53. Garrison L, Leeman L, Savich RD, Gutierrez H, Rayburn WF, Bakhireva LN. Fetal growth outcomes in a cohort of polydrug- and opioid-dependent patients. *J Reprod Med*. (2016) 16:311–9.
54. Jansson LM, Pietro JA, Elko A, Williams EL, Milio L, Velez M. Pregnancies exposed to methadone, methadone and other illicit substances, and poly-drugs without methadone: a comparison of fetal neurobehaviors and infant outcomes. *Drug Alcohol Depend*. (2012) 122:213–9. doi: 10.1016/j.drugalcdep.2011.10.003
55. Greig E, Ash A, Douiri A. Maternal and neonatal outcomes following methadone substitution during pregnancy. *Arch Gynecol Obstet*. (2012) 286:843–51. doi: 10.1007/s00404-012-2372-9
56. Clancy B, Darlington RB, Finlay BL. Translating developmental time across mammalian species. *Neuroscience*. (2001) 105:7–17. doi: 10.1016/S0306-4522(01)00171-3
57. Mallard C, Vexler Z. Modeling ischemia in the immature brain: how translational are animal models? *Stroke*. (2015) 46:3006–11. doi: 10.1161/STROKEAHA.115.007776
58. Patel SD, Pierce L, Ciardiello AJ, Vannucci SJ. Neonatal encephalopathy: pre-clinical studies in neuroprotection. *Biochem Soc Trans*. (2014) 42:564–8. doi: 10.1042/BST20130247
59. Salmaso N, Jablonska B, Scafidi J, Vaccarino FM, Gallo V. Neurobiology of premature brain injury. *Nat Neurosci*. (2014) 17:341–6. doi: 10.1038/nn.3604
60. Semple BD, Blomgren K, Gimlin K, Ferriero DM, Noble-Haeusslein LJ. Brain development in rodents and humans: identifying benchmarks of maturation and vulnerability to injury across species. *Prog Neurobiol*. (2013) 106–7:1–16. doi: 10.1016/j.pneurobio.2013.04.001

61. Tucker AM, Aquilina K, Chakkarapani E, Hobbs CE, Thoresen M. Development of amplitude-integrated electroencephalography and interburst interval in the rat. *Pediatr Res*. (2009) 65:62–6. doi: 10.1203/PDR.0b013e3181891316
62. Vannucci RC, Connor JR, Mauger DT, Palmer C, Smith MB, Towfighi J, et al. Rat model of perinatal hypoxic-ischemic brain damage. *J Neurosci Res*. (1999) 55:158–63. doi: 10.1002/(SICI)1097-4547(19990115)55:2<158::AID-JNR3>3.0.CO;2-1
63. Dobbing J, Sands J. Comparative aspects of brain growth spurt. *Early Hum Dev*. (1979) 311:79–83. doi: 10.1016/0378-3782(79)90022-7
64. Downes N, Mullins P. The development of myelin in the brain of the juvenile rat. *Toxicol Pathol*. (2013) 42:913–22. doi: 10.1177/0192623313503518
65. Bockhorst KH, Narayana PA, Liu R, Ahobila-Vijjula P, Ramu J, Kamel M, et al. Early postnatal development of rat brain: *in vivo* diffusion tensor imaging. *J Neurosci Res*. (2008) 86:1520–8. doi: 10.1002/jnr.21607
66. Catalani A, Sabbatini M, Consoli C, Cinque C, Tomassoni D, Azmitia E, et al. Glial fibrillary acidic protein immunoreactive astrocytes in developing rat hippocampus. *Development*. (2002) 123:481–90. doi: 10.1016/S0047-6374(01)00356-6
67. Cowan WM. The development of the brain. *Sci Am*. (1979) 241:113–33. doi: 10.1038/scientificamerican0979-112
68. Dean JM, Moravec MD, Grafe M, Abend N, Ren J, Gong X, et al. Strain-specific differences in perinatal rodent oligodendrocyte lineage progression and its correlation with human. *Dev Neurosci*. (2011) 33:251–60. doi: 10.1159/000327242
69. Kriegstein A, Alvarez-Buylla A. The glial nature of embryonic and adult neural stem cells. *Annu Rev Neurosci*. (2009) 32:149–84. doi: 10.1146/annurev.neuro.051508.135600
70. Hagberg H, Mallard C, Ferriero DM, Vannucci SJ, Levison SW, Vexler ZS, et al. The role of inflammation in perinatal brain injury. *Nat Rev Neurol*. (2015) 11:192–208. doi: 10.1038/nrneurol.2015.13
71. Holsapple MP, West LJ, Landreth KS. Species comparison of anatomical and functional immune system development. *Birth Defects Res B Dev Reprod Toxicol*. (2003) 68:321–34. doi: 10.1002/bdrb.10035
72. Lai JCY, Rocha-Ferreira E, Ek CJ, Wang X, Hagberg H, Mallard C. Immune responses in perinatal brain injury. *Brain Behav Immun*. (2017) 63:210–23. doi: 10.1016/j.bbi.2016.10.022
73. Ayer JG, Song C, Steinbeck K, Celermajer DS, Ben Freedman S. Increased tissue factor activity in monocytes from obese young adults. *Clin Exp Pharmacol Physiol*. (2010) 37:1049–54. doi: 10.1111/j.1440-1681.2010.05430.x
74. Faul F, Erdfelder E, Lang AG, Buchner A. G*Power 3: a flexible statistical power analysis program for the social, behavioral, and biomedical sciences. *Behav Res Methods*. (2007) 39:175–91. doi: 10.3758/bf03193146
75. Dammann O, Phillips TM, Allred EN, O'Shea TM, Paneth N, Van Marter LJ, et al. Mediators of fetal inflammation in extremely low gestational age newborns. *Cytokine*. (2001) 13:234–9. doi: 10.1006/cyto.2000.0820
76. Kuban KC, Jara H, O'Shea TM, Heeren T, Joseph RM, Fichorova RN, et al. Association of circulating proinflammatory and anti-inflammatory protein biomarkers in extremely preterm born children with subsequent brain magnetic resonance imaging volumes and cognitive function at age 10 years. *J Pediatr*. (2019) 210:81–90.e3. doi: 10.1016/j.jpeds.2019.03.018
77. Leviton A, Kuban KC, Allred EN, Fichorova RN, O'Shea TM, Paneth N, et al. Early postnatal blood concentrations of inflammation-related proteins and microcephaly two years later in infants born before the 28th post-menstrual week. *Early Hum Dev*. (2011) 87:325–30. doi: 10.1016/j.earlhumdev.2011.01.043
78. Leviton A, Allred EN, Fichorova RN, VanderVeen DK, O'Shea TM, Kuban K, et al. Early postnatal IGF-1 and IGFBP-1 blood levels in extremely preterm infants: relationships with indicators of placental insufficiency and with systemic inflammation. *Am J Perinatol*. (2019) 36:1442–52. doi: 10.1055/s-0038-1677472
79. O'Shea TM, Joseph RM, Kuban KC, Allred EN, Ware J, Coster T, et al. Elevated blood levels of inflammation-related proteins are associated with an attention problem at age 24 mo in extremely preterm infants. *Pediatr Res*. (2014) 75:781–7. doi: 10.1038/pr.2014.41
80. Leviton A, Kuban K, O'Shea TM, Paneth N, Fichorova R, Allred EN, et al. The relationship between early concentrations of 25 blood proteins and cerebral white matter injury in preterm newborns: the ELGAN study. *J Pediatr*. (2011) 158:897–903 e1–5. doi: 10.1016/j.jpeds.2010.11.059
81. Turner MD, Nedjai B, Hurst T, Pennington DJ. Cytokines and chemokines: at the crossroads of cell signalling and inflammatory disease. *Biochem Biophys Acta*. (2014) 1843:2563–82. doi: 10.1016/j.bbamcr.2014.05.014
82. O'Neill LAJ, Bowie AG. The family of five: TIR-domain-containing adaptors in Toll-like receptor signalling. *Nat Rev Immunol*. (2007) 7:353–64. doi: 10.1038/nri2079
83. Baloch S, Verma R, Huang H, Khurd P, Clark S, Yarowsky P, et al. Quantification of brain maturation and growth patterns in C57Bl/6 mice via computational neuroanatomy of diffusion tensor images. *Cerebral Cortex*. (2009) 19:675–87. doi: 10.1093/cercor/bhn112
84. O'Shea TM, Allred EN, Kuban KC, Dammann O, Paneth N, Fichorova R, et al. Elevated concentrations of inflammation-related proteins in postnatal blood predict severe developmental delay at 2 years of age in extremely preterm infants. *J Pediatr*. (2012) 160:395–401 e4. doi: 10.1016/j.jpeds.2011.08.069
85. McAdams RM, Juul SE. The role of cytokines and inflammatory cells in perinatal brain injury. *Neurol Res Int*. (2015) 2012:561494. doi: 10.1155/2012/561494
86. Leviton A, Fichorova R, Yamamoto Y, Allred EN, Dammann O, Hecht J, et al. Inflammation-related proteins in the blood of extremely low gestational age newborns. The contribution of inflammation to the appearance of developmental regulation. *Cytokine*. (2011) 53:66–73. doi: 10.1016/j.cyto.2010.09.003
87. Kuban KC, O'Shea TM, Allred EN, Fichorova RN, Heeren T, Paneth N, et al. The breadth and type of systemic inflammation and the risk of adverse neurological outcomes in extremely low gestation newborns. *Pediatr Neurol*. (2015) 52:42–8. doi: 10.1016/j.pediatrneurol.2014.10.005
88. Leviton A, Allred EN, Fichorova RN, Kuban KC, Michael O'Shea T, Dammann O, et al. Systemic inflammation on postnatal days 21 and 28 and indicators of brain dysfunction 2years later among children born before the 28th week of gestation. *Early Hum Dev*. (2016) 93:25–32. doi: 10.1016/j.earlhumdev.2015.11.004
89. Dammann O, Allred EN, Fichorova RN, Kuban K, O'Shea TM, Leviton A, et al. Duration of systemic inflammation in the first postnatal month among infants born before the 28th week of gestation. *Inflammation*. (2016) 39:672–7. doi: 10.1007/s10753-015-0293-z
90. Galinsky R, Dhillon SK, Dean JM, Davidson JO, Lear CA, Wassink G, et al. Tumor necrosis factor inhibition attenuates white matter gliosis after systemic inflammation in preterm fetal sheep. *J Neuroinflamm*. (2020) 17:1–16. doi: 10.1186/s12974-020-01769-6
91. Pan W, Stone KP, Hsuchou H, Manda VK, Kastin AJ. Cytokine signaling modulates blood-brain barrier function. *Curr Pharm Des*. (2011) 17:3729–40. doi: 10.2174/138161211798220918
92. Rosenberg GA, Estrada EY, Dencoff JE, Stetler-Stevenson WG. Tumor necrosis factor-alpha-induced gelatinase B causes delayed opening of the blood-brain barrier: an expanded therapeutic window. *Brain Res*. (1995) 703:151–5. doi: 10.1016/0006-8993(95)01089-0
93. Tsao N, Hsu HP, Wu CM, Liu CC, Lei HY. Tumour necrosis factor-alpha causes an increase in blood-brain barrier permeability during sepsis. *J Med Microbiol*. (2001) 50:812–21. doi: 10.1099/0022-1317-50-9-812
94. Zhao C, Ling Z, Newman MB, Bhatia A, Carvey PM. TNF-alpha knockout and minocycline treatment attenuates blood-brain barrier leakage in MPTP-treated mice. *Neurobiol Dis*. (2007) 26:36–46. doi: 10.1016/j.nbd.2006.11.012
95. Griffiths SK, Campbell JP. Placental structure, function and drug transfer. *BJA Educ*. (2014) 15:84–9. doi: 10.1093/bjaceaccp/mku013
96. Chaves C, Remiao F, Cisternino S, Decleves X. Opioids and the blood-brain barrier: a dynamic interaction with consequences on drug disposition in brain. *Curr Neuropharmacol*. (2017) 15:1156–73. doi: 10.2174/1570159X15666170504095823
97. Gharavi R, Hedrich W, Wang H, Hassan HE. Transporter-mediated disposition of opioids: implications for clinical drug interactions. *Pharm Res*. (2015) 32:2477–502. doi: 10.1007/s11095-015-1711-5
98. Hutchinson MR, Shavit Y, Grace PM, Rice KC, Maier SF, Watkins LR. Exploring the neuroimmunopharmacology of opioids: an integrative review of mechanisms of central immune signaling and their implications for

opioid analgesia. *Pharmacol Rev*. (2011) 63:772–810. doi: 10.1124/pr.110.004135
99. Bilbo SD, Biedenkapp JC, Der-Avakian A, Watkins LR, Rudy JW, Maier SF. Neonatal infection-induced memory impairment after lipopolysaccharide in adulthood is prevented via caspase-1 inhibition. *J Neurosci*. (2005) 25:8000–9. doi: 10.1523/JNEUROSCI.1748-05.2005
100. Bilbo SD, Levkoff LH, Mahoney JH, Watkins LR, Rudy JW, Maier SF. Neonatal infection induces memory impairments following an immune challenge in adulthood. *Behav Neurosci*. (2005) 119:293–301. doi: 10.1037/0735-7044.119.1.293
101. Yanni D, Korzeniewski SJ, Allred EN, Fichorova RN, O'Shea TM, Kuban K, et al. Both antenatal and postnatal inflammation contribute information about the risk of brain damage in extremely preterm newborns. *Pediatr Res*. (2017) 82:691–6. doi: 10.1038/pr.2017.128
102. Claus CP, Tsuru-Aoyagi K, Adwanikar H, Walker B, Whetstone W, Noble-Haeusslein LJ. Age is a determinant of the inflammatory response and loss of cortical volume after traumatic brain injury. *Dev Neurosci*. (2010) 32:454–65. doi: 10.1016/j.nbd.2014.12.003
103. Fleiss B, Gressens P. Tertiary mechanisms of brain damage: a new hope for treatment of cerebral palsy? *Lancet Neurol*. (2012) 11:556–66. doi: 10.1016/S1474-4422(12)70058-3
104. Thornton C, Rousset CI, Kichev A, Miyakuni Y, Vontell R, Baburamani AA, et al. Molecular mechanisms of neonatal brain injury. *Neurol Res Int*. (2012) 2012:506320. doi: 10.1155/2012/506320
105. Asai K, Hiki N, Mimura Y, Ogawa T, Unou K, Kaminishi M. Gender differences in cytokine secretion by human peripheral blood mononuclear cells: role of estrogen in modulating LPS-induced cytokine secretion in an *ex vivo* septic model. *Shock*. (2001) 16:340–3. doi: 10.1097/00024382-200116050-00003
106. Da Pozzo E, Giacomelli C, Cavallini C, Martini C. Cytokine secretion responsiveness of lymphomonocytes following cortisol cell exposure: sex differences. *PLoS ONE*. (2018) 13:e0200924. doi: 10.1371/journal.pone.0200924
107. Silaidos C, Pilatus U, Grewal R, Matura S, Lienerth B, Pantel J, et al. Sex-associated differences in mitochondrial function in human peripheral blood mononuclear cells (PBMCs) and brain. *Biol Sex Dif*. (2018) 9:34. doi: 10.1186/s13293-018-0193-7
108. Smith PLP, Mottahedin A, Svedin P, Mohn CJ, Hagberg H, Ek J, et al. Peripheral myeloid cells contribute to brain injury in male neonatal mice. *J Neuroinflammation*. (2018) 15:301. doi: 10.1186/s12974-018-1344-9
109. Mallard C, Tremblay ME, Vexler ZS. Microglia and neonatal brain injury. *Neuroscience*. (2019) 405:68–76. doi: 10.1016/j.neuroscience.2018.01.023
110. Finak G, Langweiler M, Jaimes M, Malek M, Taghiyar J, Korin Y, et al. Standardizing flow cytometry immunophenotyping analysis from the human immunophenotyping consortium. *Sci Rep*. (2016) 6:20686. doi: 10.1038/srep20686
111. Carloni S, Proietti F, Longini M, Marseglia L, D'Angelo G, Balduini W, et al. Melatonin pharmacokinetics following oral administration in preterm neonates. *Molecules*. (2017) 22:2115. doi: 10.3390/molecules22122115
112. Jantzie LL, Oppong AY, Conteh FS, Yellowhair TR, Kim J, Fink G, et al. Repetitive neonatal erythropoietin and melatonin combinatorial treatment provides sustained repair of functional deficits in a rat model of cerebral palsy. *Front Neurol*. (2018) 9:233. doi: 10.3389/fneur.2018.00233
113. Juul SE, Comstock BA, Heagerty PJ, Mayock DE, Goodman AM, Hauge S, et al. High-dose erythropoietin for asphyxia and encephalopathy (HEAL): a randomized controlled trial - background, aims, and study protocol. *Neonatology*. (2018) 133:331–8. doi: 10.1159/000486820
114. Robinson S, Conteh FS, Oppong AY, Yellowhair TR, Newville JC, El Demerdash N, et al. Extended combined neonatal treatment with erythropoietin plus melatonin prevents posthemorrhagic hydrocephalus of prematurity in rats. *Front Cell Neurosci*. (2019) 12:322. doi: 10.3389/fncel.2018.00322

Conflict of Interest: The authors declare that the research was conducted in the absence of any commercial or financial relationships that could be construed as a potential conflict of interest.

frontiers in Pediatrics

REVIEW
published: 15 July 2020
doi: 10.3389/fped.2020.00359

Murine Models for the Study of Fetal Alcohol Spectrum Disorders: An Overview

Laura Almeida[1,2,3†], *Vicente Andreu-Fernández*[1,4,5*†], *Elisabet Navarro-Tapia*[1,3,5], *Rosa Aras-López*[1,6], *Mariona Serra-Delgado*[3], *Leopoldo Martínez*[1,6,7], *Oscar García-Algar*[1,5,8‡] *and María Dolores Gómez-Roig*[1,2,3*‡]

[1] Maternal and Child Health and Development Network II (SAMID II), Instituto de Salud Carlos III (ISCIII), Barcelona, Spain, [2] Fundació Sant Joan de Déu, Barcelona, Spain, [3] BCNatal Barcelona Center for Maternal Fetal and Neonatal Medicine, Hospital Sant Joan de Déu and Hospital Clínic, Barcelona, Spain, [4] Nutrition and Health Deparment, Valencian International University (VIU), Valencia, Spain, [5] Grup de Recerca Infancia i Entorn (GRIE), Institut D'investigacions Biomèdiques August Pi i Sunyer (IDIBAPS), Barcelona, Spain, [6] Congenital Malformations Lab, Institute of Medicine and Molecular Genetic (INGEMM), Institute for Health Research of La Paz Universitary Hospital (IdiPAZ), Madrid, Spain, [7] Department of Pediatric Surgery, Hospital Universitario La Paz, Madrid, Spain, [8] Department of Neonatology, Hospital Clínic-Maternitat, ICGON, IDIBAPS, BCNatal, Barcelona, Spain

OPEN ACCESS

Edited by:
Changlian Zhu,
Third Affiliated Hospital of Zhengzhou University, China

Reviewed by:
Maurizio Elia,
Oasi Research Institute (IRCCS), Italy
Joana Gil-Mohapel,
University of Victoria, Canada

***Correspondence:**
Vicente Andreu-Fernández
viandreu@clinic.cat
María Dolores Gómez-Roig
lgomezroig@sjdhospitalbarcelona.org

[†] These authors have contributed equally to this work

[‡] These authors share last authorship

Specialty section:
This article was submitted to Pediatric Neurology, a section of the journal Frontiers in Pediatrics

Received: 09 December 2019
Accepted: 29 May 2020
Published: 15 July 2020

Citation:
Almeida L, Andreu-Fernández V, Navarro-Tapia E, Aras-López R, Serra-Delgado M, Martínez L, García-Algar O and Gómez-Roig MD (2020) Murine Models for the Study of Fetal Alcohol Spectrum Disorders: An Overview. Front. Pediatr. 8:359. doi: 10.3389/fped.2020.00359

Prenatal alcohol exposure is associated to different physical, behavioral, cognitive, and neurological impairments collectively known as fetal alcohol spectrum disorder. The underlying mechanisms of ethanol toxicity are not completely understood. Experimental studies during human pregnancy to identify new diagnostic biomarkers are difficult to carry out beyond genetic or epigenetic analyses in biological matrices. Therefore, animal models are a useful tool to study the teratogenic effects of alcohol on the central nervous system and analyze the benefits of promising therapies. Animal models of alcohol spectrum disorder allow the analysis of key variables such as amount, timing and frequency of ethanol consumption to describe the harmful effects of prenatal alcohol exposure. In this review, we aim to synthetize neurodevelopmental disabilities in rodent fetal alcohol spectrum disorder phenotypes, considering facial dysmorphology and fetal growth restriction. We examine the different neurodevelopmental stages based on the most consistently implicated epigenetic mechanisms, cell types and molecular pathways, and assess the advantages and disadvantages of murine models in the study of fetal alcohol spectrum disorder, the different routes of alcohol administration, and alcohol consumption patterns applied to rodents. Finally, we analyze a wide range of phenotypic features to identify fetal alcohol spectrum disorder phenotypes in murine models, exploring facial dysmorphology, neurodevelopmental deficits, and growth restriction, as well as the methodologies used to evaluate behavioral and anatomical alterations produced by prenatal alcohol exposure in rodents.

Keywords: prenatal alcohol exposure, fetal alcohol spectrum disorders, fetal alcohol syndrome, alcohol consumption patterns, facial dysmorphology, neurodevelopmental disorders, fetal growth restriction, models of fetal alcohol spectrum disorders

INTRODUCTION

Alcohol is a known teratogen. Its frequent use during pregnancy impacts the normal development of human fetuses promoting severe developmental alterations and generating a wide range of physical, behavioral, cognitive, and neurological impairments. In 1968, Lemoine et al. established an association between prenatal alcohol exposure (PAE) with certain neurodevelopmental disabilities (1). However, it was not until 1973 when Jones and Smith provided the initial characterization of fetal alcohol syndrome (FAS) (2), defined as growth restriction, facial dysmorphologies (wide-spaced eyes, mid-facial hypoplasia, and a smooth philtrum), and central nervous system (CNS) disorders, resulting in motor, cognitive and behavioral disorders (3). Subsequent observational studies identified and characterized the umbrella term fetal alcohol spectrum disorder (FASD) (4) that includes: FAS (the most deleterious manifestation of FASD), partial FAS (pFAS) (an intermediate phenotype defined by the absence of some FAS characteristics), alcohol-related birth defects (ARBD) (certain physical impairments are exhibited), and alcohol-related neurological disorders (ARND) (behavioral and learning neuropsychological alterations, usually without facial dysmorphology) (5).

Thus, behavioral deficits in FASD subjects associate with structural changes in brain organogenesis: the *Corpus callosum* may lose its structure (agenesis) and generate cognitive deficits linked to attention, executive and psychosocial functions, language, and reading comprehension (6); cerebellum and anterior part of the vermis may suffer hypoplasia and affect motor skills and learning capacity (7). Moreover, proven asymmetry of the hippocampus in FAS children may also affect their memory (8). The degree of structural abnormalities in the brain correlates with the severity of FAS-like facial features, and this in turn, with more serious behavioral problems (9).

According to the World Health Organization, PAE is the main preventable cause of intellectual disability in the western world (10–12). A recent meta-analysis estimated global prevalence of alcohol use during pregnancy to be 9.8% (13). Therefore, PAE-related disorders may lead to major problems for the social environment as well as economic setbacks for the public health system.

Animal models play a key role in the study of FASD by allowing the development of novel diagnostic and therapeutic tools. Researchers have used a great variety of organisms to mimic the physical and behavioral characteristics found in PAE and FASD phenotypes. Inbred strains of rodents are genetically homogenous populations that facilitate result reproducibility and interpretation in studies designed to evaluate the impact of environmental insults such as ethanol. Moreover, the alcohol intake pattern can be more precisely defined (timing and dose), allowing the identification of time-sensitive windows and thresholds of harmful doses during pregnancy. Rodents have been widely used in FASD research to assess the way PAE-related impairments affect metabolic pathways, molecular biology, cell signaling, synaptic plasticity, and cognition during fetal development, promoting the study of variables affected by alcohol exposure at neuroanatomical, neurochemical and behavioral levels (14).

In this review, we focus on rodent FAS-like phenotype neurodevelopmental disabilities, taking into account facial dysmorphology and fetal growth restriction. We examine every stage of brain development, considering changes caused by PAE in different neural cell lineages, molecular pathways and oxidative stress epigenetic variations. We also review the experimental methodologies used to generate rodent FASD-like phenotypes, including advantages and disadvantages of the different routes by which alcohol has been administered. Finally, we revise anatomical and behavioral alterations, as well as the methodologies used to assess these features in murine models.

FASD-LIKE ANIMAL MODELS

FASD studies in humans have common limitations due to the complexity in correctly measuring certain variables such as maternal diet or health, or the volume and timing of ethanol exposure during pregnancy. These difficulties may be resolved by using animal models, simple, effective, and reliable tools for alcohol research. These models are useful for understanding the molecular mechanisms underlying alcohol teratogenicity and for monitoring cognitive and behavioral changes. Animal models also allow assessing different therapeutic approaches in preclinical studies, for initial screening of the compounds and strategies for future human clinical studies.

The invertebrate *Caenorhabditis elegans* is a simple model for development and is commonly chosen to study the effects of ethanol on molecular pathways. However, the embryos develop outside the body, exact ethanol concentrations administered cannot be finely controlled (15), and the way alcohol is metabolized differs substantially from that in humans (15). The zebrafish (*Danio rerio*) has several physiological and genetic similarities with humans (16), which makes it a suitable alternative as model of vertebrate. Regarding the effects of ethanol, there are further advantages: substantial knowledge of all stages of development, short developmental period, and produce large amounts of offspring (17). Zebrafish eggs and embryos are transparent (just like in nematodes) making embryonic development easy to follow, facilitating exposure to alcohol of the embryos during different and precise developmental periods, and easy determination of physical malformations and simple behaviors (16, 18). By contrast, the chorion of the egg acts as a barrier and large volumes of ethanol are necessary to ensure its penetration (17).

Mammals offer significant advantages in the study of brain structures or complex behaviors (19). Although primates could be the gold standard, there are some disadvantages, mainly the long duration of the studies and ethical limitations (19). Rodents are the most employed mammals for FASD research because they are easy to handle, have a short gestational period, and produce large numbers of offspring. Rats offer the advantages of being larger and with a more sophisticated behavior in comparison to mice. Regardless, mice (particularly the C57BL/6 strain) are the most commonly used mammal

due to their ease of care, availability of transgenic and disease models, short lifespan, and basic physiology and genetics similar to that of humans. Teratogenic effects of alcohol exposure in mice have been reported, including craniofacial malformations, altered neurogenesis processes, and soft-tissue and skeletal abnormalities (20, 21). The main disadvantage in using rodents for FASD research is that the third trimester equivalent to human development in rodents occurs after birth. Thus, there are differences in the processes of absorption, distribution, metabolism and elimination in rodents in comparison to the human utero, with no influence of the placental barrier. Interestingly, C57BL/6J is the strain with the highest preference for alcohol (22).

In following sections, we discuss details that need to be considered when a murine model is chosen for a FASD study.

Alcohol Exposure Patterns

Drinking patterns are characterized by the amount and frequency of ethanol taken. This is measured by blood alcohol concentration (BAC) and expressed as weight of alcohol per unit of volume of blood.

Kelly et al. showed that binge-like alcohol exposure is more harmful than non-binge exposure in rat brain development after exposure to the same dose of ethanol. The authors administered doses of 6.6 g/kg/day of ethanol to neonatal rats using artificial rearing, following one of two possible patterns. A continuous pattern (24 h per day) for several days, which resulted in an average BAC peak of 79–97 mg/dL or an acute exposure pattern (8 h per day) for the same period of time, resulting in an average BAC peak of 56–415 mg/dL. Lower brain growth was observed in the acute exposure group in comparison to the continuous pattern (23). Other findings support the hypothesis that lower daily doses of ethanol following a binge-like pattern leads to lower brain weight and cell loss in different brain areas than higher non-binge doses. Three groups of ethanol-exposed rat pups were compared. One group was exposed to 4.5 g/kg/day in a condensed pattern (4 h per day), the second group was exposed to the same dose although administered in a less condensed pattern (8 h per day), and the third group was exposed to a higher dose of alcohol (i.e., 6.6 g/kg/day) administered in a continuous pattern (24 h per day). The resulting average BACs peaks were 361, 190, and 39 mg/dL, respectively. The authors found that pups exposed to 4.5 g/kg/day over 4 h had the lowest brain weight, followed by the second group. The animals that ingested highest doses of ethanol throughout the 24 h had the highest brain weights (24). These results demonstrate that ethanol intake under a binge-like pattern is more harmful than higher doses taken for longer periods of time due to higher BAC peaks in shorter periods of time.

Control Group

Several studies have assessed the influence of nutritional intake on the teratogenic effects of alcohol (25, 26). Alcohol can replace other nutrients because of its caloric content and may interfere with the absorption of other nutrients due to its inflammatory effects on the stomach (27).

Pair-fed control has been used in some FASD-like animal model experiments since it acts as a calorie-matched control group. A carbohydrate substance (e.g., maltose dextrin or sucrose) is usually employed to replace ethanol-derived calories in the diet (28). A pair-fed group may also allow monitoring a stress condition. On the other hand, the pair-fed group is considered as an imperfect control group, since the pattern of food consumption in this group is different from a physiological intake. Individuals in pair-fed controls consume the assigned food as soon as it is available, creating additional stress associated to food restriction. In addition, in the pair-fed group it is not possible to match the effect of alcohol on the absorption of other nutrients because of its inflammatory effects. Thus, some researchers have suggested the use of a basal control group known as non-handle, *ad libitum*, or *sham*, in which the intake of nutrients resembles the physiological one. This is useful to avoid biases caused by ethanol interference in nutrient absorption (29). Consequently, the use of a pair-fed group and an *ad libitum* control group should be considered as an alternative when designing a FASD murine model study.

Route of Administration and Dosage Forms

Several modes of ethanol administration methods have been described, particularly in rodent gestation. Ethanol delivery methods directly affect variables such as the alcohol exposure pattern, exact amount of alcohol taken, and generated stress. All these variables must be taken into account during experimental design. Voluntary ethanol feeding and intragastric gavage are the most physiological administration methods. Voluntary ethanol feeding (30, 31) is a safe technique when low stable BAC levels want to be reached. Conversely, intragastric gavage (29) offers a more accurate control of doses and timing, and reaches higher BACs. Inhalation (32) or injection (33) offer some advantages compared to voluntary ethanol drinking and intragastric gavage due to their time efficiency. Artificial rearing is a useful method when the aim of the study is alcohol administration in a third trimester equivalent model (29, 34, 35). Briefly, the choice of method must consider the purpose of the experiment and the researcher's experience. **Table 1** [based on a previous review (45)] summarizes the characteristics of the main routes of alcohol administration in rodents and dosage forms, focusing mainly on mice.

Blood Alcohol Concentration

BAC depends on several factors such as dosage, pattern of exposure, metabolic rate, food consumption, tolerance and genetics (46, 47). As mentioned above, BAC peaks are higher when ethanol is administered in a binge-like pattern, even with low doses of alcohol (24). There are several types of methods for measuring BAC: headspace gas chromatography (HS-GC), headspace solid-phase microextraction (HS-SPME), capillary gas chromatography, or enzymatic ADH immunoassays (48). Immunoassays are not as accurate as mass spectrometry and are susceptible to bias by overestimating alcohol concentration due to non-specific interferences. On the other hand, immunoassays are sufficiently accurate, easy to use in any laboratory, and require a small amount of sample ($\sim$100 μL). Immunoassays

TABLE 1 | Characteristics of the different routes of ethanol administration in mice.

Administration route	Characteristics	Reached BAC	Advantages	Disadvantages
Voluntary ethanol feeding	Oral, self-administration. Pre-gestational alcohol consumption is usually introduced (36). Sometimes, ethanol is added to flavored liquid nutritional formulas (Liquid-diet or Sustacal) to allow easy self-administration (37, 38). 10–20% (vol/vol) ethanol solution (36). Possibility of isovolumic and isocaloric pair-fed diet (e.g., maltose-dextrin) in controls (28). Drinking in the dark (DID) procedure mimics binge-like pattern (39).	50–100 mg/dL when ethanol intake is 1–2 g/Kg [10% (vol/vol) ethanol solution]	Prevent the stress caused by other invasive methods. Safe technique. Easy to carry out. Gradual BAC increase. Low, stable BAC levels. Used prenatally.	Lower ethanol BAC achieved compared to other administration routes. Not useful for binge drinking pattern. Difficult control of dose and timing. No proper control of dose in breastfeeding pups. Not recommended postnatally. Lower BAC achieved if saccharin or a sucrose-sweetened solution is added to the alcohol.
Intragastric gavage	Administration of ethanol into the stomach using a gavage needle. Administered volumes <2 mL/100 Kg body weight (40). Allowed alcohol concentration <31.5% (vol/vol) (40). Ethanol dose 2–6 g/Kg/day (28). Ethanol vehicle (water, saline solution, or nutritional formula) (28).	250–300 mg/dL (60 min) for administration doses of 3.8 g/Kg [21% (wt./vol) ethanol solution]	Useful for binge drinking pattern. Accurate control of dose and timing. Reliable high BAC. Useful for pre- and postnatal administration.	Inhibition of suckling behavior in neonates. Stressful procedure for animals. Invasive procedure.
Inhalation	Inhalation chamber filled with ethanol vapor (41). Sometimes, administration of pyrazole to obtain stable BACs (32, 42).	150–250 mg/dl when volatized ethanol (ethanol 95%) is delivered to the chamber at a rate of 10 l/min	Reliable high BAC. Not a stressful technique for animals. Time and labor efficient. Useful for pre- and postnatal administration. Higher BACs in neonates compared to mothers.	Does not mimic the routes of intake in humans. Special equipment required. Interindividual variations.
Intraperitoneal injection	Ethanol solution injection in intraperitoneal space (43). Single or multiple doses for several days during pregnancy.	350–400 mg/dL (60 min) for administration doses of 3.8 g/Kg [21% (wt./vol) ethanol solution]	Rapid increase in BAC. Time efficient. Useful for pre- and postnatal administration. Useful for binge drinking pattern.	Handling-induced stress. Different intake routes in humans. This administration route produces higher BAC in fetuses than other routes using the same PAE. Higher incidence of malformations when used during first trimester equivalent.
Artificial rearing	Intragastric gavage ethanol discharge in pups while being kept in a special setting to mimic maternal environment (29, 34, 44). Placement of gastrostomy catheters.	150 mg/Kg when ethanol solution of 2,5 g/Kg is administered or 420 mg/Kg when ethanol solution of 7,5 g/Kg is administered*	Accurate control of dose and timing. Useful for postnatal administration. Mimics human third trimester.	Invasive and expensive technique. Social factors removed due to isolation of pups.

**Data obtained from experiments with rats (no available data for mice). BAC, blood alcohol concentration; Vol, volume; Wt, weight.*

are currently the most commonly used method for determining BACs in peripheral blood.

In animal models, BAC is defined as the amount of ethanol per unit of blood (usually mg/dL), measured when ethanol concentration reaches the highest level in peripheral circulation (49). In rodents, peak concentration is detected between 30 and 150 min (50–100 min in mice and 50–150 min in rats) following administration. The timeline of BAC depends on the administration route, the dosage and the species (rate of ethanol metabolism is 550 and 300 mg/Kg/h in mice and rats, respectively) (50). Severe neurotoxicity is typically linked to binge-like episodes causing higher BACs (i.e., BAC over 300 mg/dl in rats). However, continuous alcohol exposure, reaching lower BAC levels (i.e., BAC below 40 mg/dl in rats) despite higher doses, induces more subtle brain injuries (23, 24).

DEVELOPMENTAL STAGES OF THE FETAL BRAIN

During the development of the CNS throughout pregnancy, there are vulnerable periods sensitive to environmental insults. PAE affects brain organogenesis differently depending on the dosage, timing, developmental stage (moment), and location of the cell

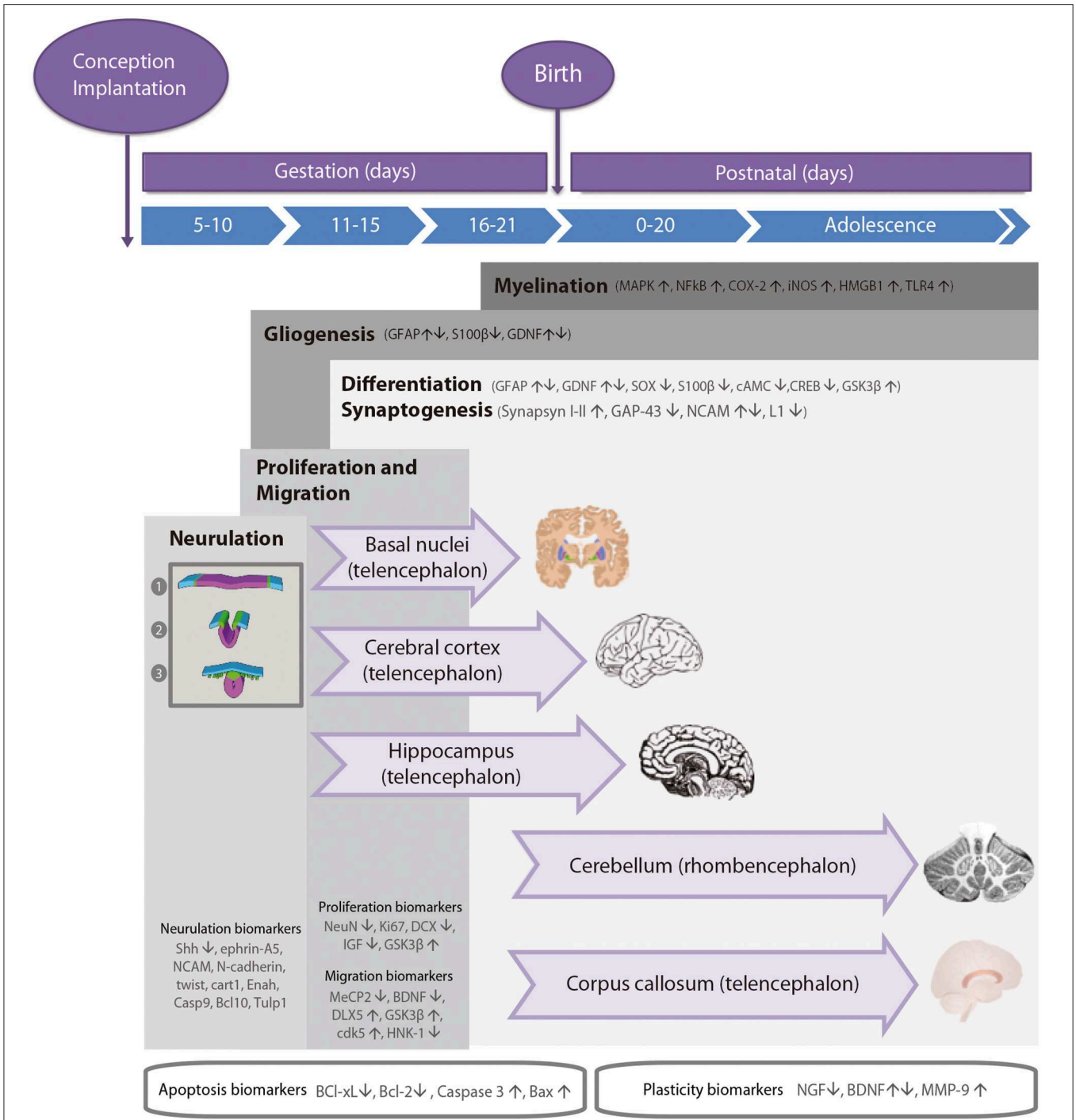

FIGURE 1 | Timeline of neurodevelopmental processes and brain neurogenesis in fetal rodents by areas sensitive to alcohol injury. Proteins in neurulation, proliferation, migration, differentiation, synaptogenesis, gliogenesis, and myelination neurodevelopmental processes. Changes in the levels of these biomarkers (up- or down-regulation) caused by prenatal alcohol exposure are represented by arrows. Stages of neurulation: (1) Neuroectodermal tissues differentiate from the ectoderm and thicken into the neural plate. The neural plate border separates the ectoderm from the neural plate. (2) The neural plate bends dorsally, with the two ends eventually joining at the neural plate borders, forming the neural crest. (3) The closure of the neural tube disconnects the neural crest from the epidermis. Neural crest cells differentiate to form the peripheral nervous system.

types involved in the biological stages (**Figure 1**). Key processes such as proliferation (51), migration (52), differentiation (53), synaptogenesis (54, 55), gliogenesis, myelination (56), and apoptosis (57, 58) are altered by PAE leading to congenital abnormalities and functional deficits in the CNS during fetal development (**Figure 2**) (74, 75).

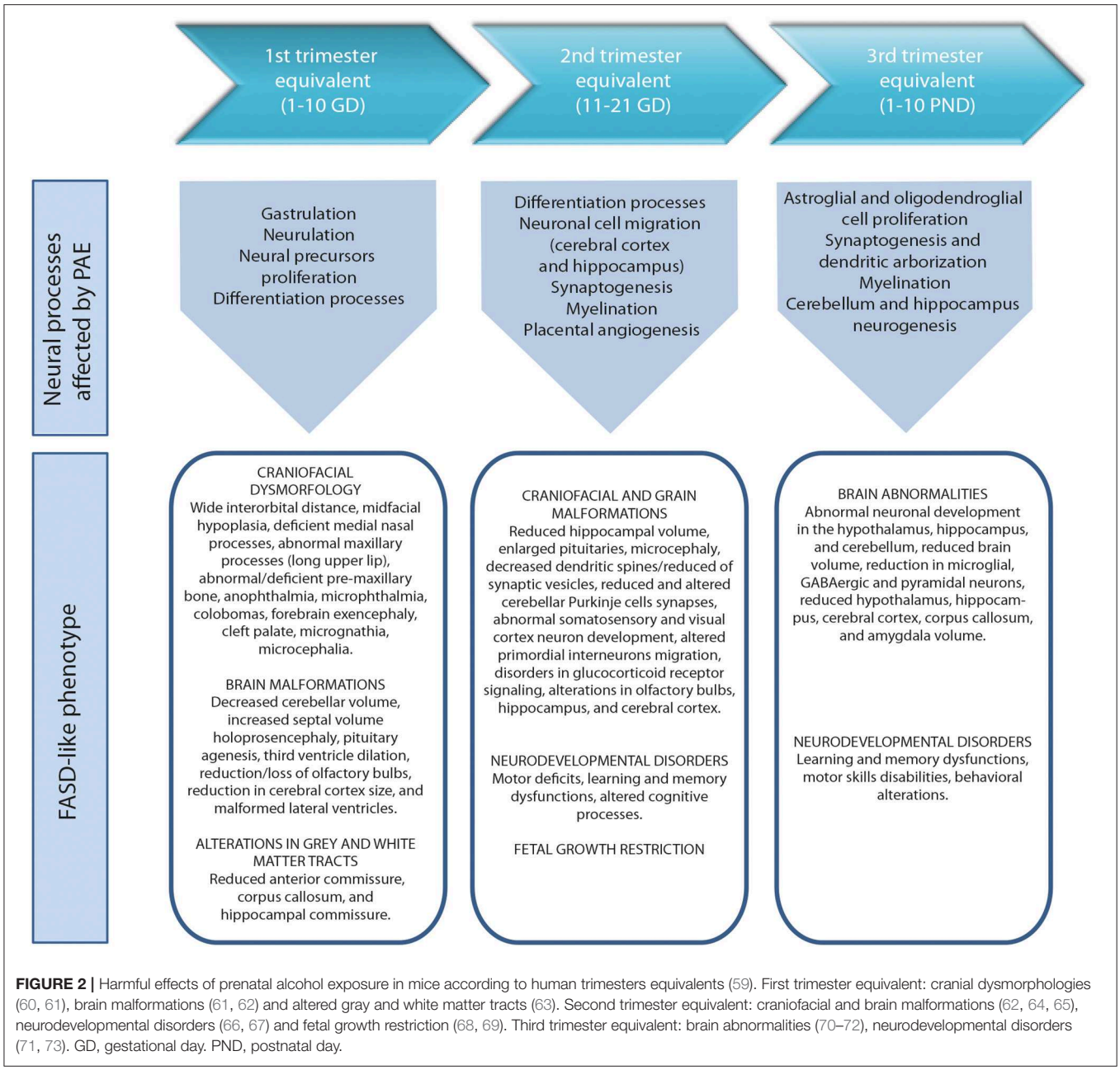

FIGURE 2 | Harmful effects of prenatal alcohol exposure in mice according to human trimesters equivalents (59). First trimester equivalent: cranial dysmorphologies (60, 61), brain malformations (61, 62) and altered gray and white matter tracts (63). Second trimester equivalent: craniofacial and brain malformations (62, 64, 65), neurodevelopmental disorders (66, 67) and fetal growth restriction (68, 69). Third trimester equivalent: brain abnormalities (70–72), neurodevelopmental disorders (71, 73). GD, gestational day. PND, postnatal day.

The anatomies of human and rodent brains show analogous structures and similar stages of development. However, they also exhibit some anatomical and functional differences. Human pregnancy consists of three pre-natal trimesters in which the brain rapidly grows between week 25 and 38. Several differentiation and proliferations processes occur in the third trimester of gestation, with maximum brain growth rate at birth and gradual decrease in early life (59, 76). Rat and mouse pregnancies are shorter than human pregnancies (rats: 21–23 days; mice: 20–22 days) and newborns undergo substantial brain development following birth (56, 57). The first trimester (59) in human pregnancy corresponds to gestational days (GDs) 1–10/11 in rat and mouse. The second trimester equivalent corresponds to GDs 11–21/22 (mice usually give birth on GD 21 and rats on GD 22), and the third trimester equivalent correlates to postnatal days (PNDs) 1–10. The ontogeny of specific behaviors can be used to draw inferences regarding the maturation of specific brain structures or neural circuits in rodents and humans. Despite the similarities between human and rodent brain development it is important to consider that rodents do not exactly mimic the developmental phases of human gestation (**Figure 1**).

Cellular precursors of the brain and the spinal cord develop through neurulation in early embryogenesis (**Figure 1**). The cellular fate of neurulation is the formation of the notochord,

which defines the primitive axis of the embryo and determines the vertebral system. The neural tube closure starts in the hindbrain area above the origin of the notochord, and continues anteriorly and posteriorly, making a caudal-to-rostral gradient in the developing brain. Neural tube formation finishes at gestational day (GD) 10–11 in rodents (77). Early in the second week of pregnancy (GD 7 in mouse, GD 9.5 in rats), neurogenesis and subsequent cell migration shape specific areas of the CNS in the forebrain, midbrain, and hindbrain, promoting distinct series of developmental processes (77). Therefore, the second critical developmental stage for PAE occurs between GD 5 and 11, implying alterations in organogenesis, neural tube formation and proliferation of neuronal precursors in areas adjacent to the neural tube. High levels of alcohol exposure during this stage not only cause major neural tube defects, but also lead to facial dysmorphologies similar to those observed in children affected with FAS.

The second critical developmental stage occurs between GD 11 and 21. During this period, most CNS areas are involved in distinct differentiation processes and several neuronal cell types emerge and migrate to specific areas of the brain (including the cerebral cortex and the hippocampus; **Figure 1**). The developmental phase of the different cell lineages varies according to its spatial location in separate brain areas. PAE particularly affects the neurulation, proliferation, and migration processes of the neocortex, cerebellum, hippocampus, and the basal ganglia. The last decisive developmental period occurs from GD 18 to postnatal day (PND) 9 and is characterized by the proliferation of astroglial and oligodendroglial cells, synaptogenesis, and dendritic arborization, which produce an increase in brain weight. At the same time, neurogenesis continues in the cerebellum and the dentate gyrus (DG) of the hippocampus. Alcohol exposure during third trimester induces severe neuronal loss, reactive gliosis, impaired myelination, as well as damage to the prefrontal cortex, hippocampal and cerebellar regions (64, 78, 79).

Proliferation

Neurogenesis is a highly regulated process whose timing and phases depend on the anterior-posterior gradient in the neuronal axis and the regions of the brain formed during organogenesis. Most cell proliferation processes take place throughout all the stages of neurodevelopment (80), although the most expansive phase occurs in the second half of pregnancy (mice: GD 10–21, rats: GD 11–22). This is a key developmental period due to ethanol toxicity vulnerability of neuronal precursors and brain structures (51), which may cause permanent alterations and profound behavioral deficits. For that reason, the consequences of PAE on proliferation and differentiation processes are assessed not only during fetal development but also later in life. As shown in **Figure 1**, several biomarkers help identify and evaluate neurogenesis and proliferation processes during neurodevelopment.

NeuN is expressed in nearly all post-mitotic neurons representing a reliable marker of mature neurons (81). This protein may also act as a biomarker of neuronal integrity, as it decreases in brain regions such as the hippocampus following ethanol exposure in rats (81–83). Ki67 has been thoroughly analyzed as a proliferation biomarker during neurogenesis in PAE studies.

Several authors have studied the effect of PAE on different regions of the hippocampus with different results. Some have found a reduced number of granular cells in the DG and pyramidal cells in specific regions of the rat hippocampus after GD 1–GD 20 plus PND 4–10 of ethanol exposure (24, 84), and during the third trimester equivalent (24, 83, 84), with no changes in the number of hippocampal neurons after GD 1–20 ethanol exposure (84, 85). Komada et al. showed a reduced proliferation rate (measured by Ki67) in mouse telencephalon after PAE on GD 6–18 (86). Conversely, West et al. showed an increase in the number of granular cells of the DG in rat hippocampus after ethanol exposure during the third trimester equivalent (87). Thus, early disturbances in proliferation after PAE may differ depending on the developmental period in which exposure to ethanol occurs.

Some of the effects of PAE on the hippocampus can be identified from birth, but others are more subtle and difficult to detect in the early stages. The consequences of PAE on hippocampal cell proliferation and survival in young adult animals are not always persistent (29, 35, 88). Interestingly, no changes in hippocampal cell proliferation (assessed by Ki67 and BrdU), but an increase in immature neurons of adult hippocampus in rats prenatally exposed to alcohol, have been described, probably due to a compensatory mechanism against PAE effects (29). Other authors have shown alterations in cell proliferation [measured by Ki67 (35) and BrdU (35, 88)] and increased neuronal maturation in the DG of the hippocampus in young adult rats prenatally exposed to ethanol. More recently, Gil-Mohapel et al. described significant decreases in adult hippocampal neurogenesis in aged rats after PAE (during first and second trimester equivalent), not previously seen in younger animals. These findings suggest a more conserved neurogenesis capacity in the early stages of life (89). Moreover, Delatour et al. analyzed Ki67 levels in pyramidal cells in adolescent mice exposed to ethanol at GD 13.5–16.5 and showed there were no changes when compared to controls (90). Once again, it seems that alterations in hippocampal neurogenesis vary according to the timing of ethanol exposure.

Coleman et al. examined the long-term effects on adult hippocampal neurogenesis after ethanol exposure in PND 7 in male and female mice. Increased Ki67 levels were found in the DG in males but not in females (70). This reveals gender differences regarding susceptibility to PAE.

PAE also affects the activity of enzymes involved in neurogenesis and proliferation, promoting hippocampal function behavioral disorders. Glycogen synthase kinase-3β (GSK3β) is highly expressed during brain development [from GD18 to PND10 in rats (91) and GD16 to PD18 in mice (92)] modulating different developmental processes such as neurogenesis, differentiation and neuronal survival. GSK3β activation sensitizes neurons to ethanol-induced injury, deregulating cell proliferation mechanisms (93). Increased levels of GSK3β post-PAE activates apoptosis in neural progenitor cells, decreasing neurogenesis and differentiation in immature

brains. Additionally, ethanol decreases the insulin-like growth factor (IGF) receptor signaling, affecting neural proliferation and decreasing the transcription of c-myc, c-fos, and c-jun51 in cell cultures (94).

Current evidence indicates that prenatal and neonatal alcohol exposure reduces the number of mature and immature neurons. Interestingly, this reduction is subtle when ethanol exposure is not continuous. Nonetheless, the brain region, developmental stage, and cell type are key factors when analyzing results of the biomarkers in proliferation processes.

Migration

Migration from the ventricular and germinal layers occurs radially in the medial/dorsal neocortex and tangentially in other regions of the forebrain (95). On GD 5, superficial layers are still not clearly defined (96). On GD 14.5 (mice) or GD17 (rats), the first cell lineages reach the area that will form the laminae of the cortical plate. Throughout the rest of the gestation period until adulthood, the cortical plate gets thicker and more cells migrate from the ventricular zone (97). When proliferation is disrupted, migration is also affected (**Figure 1**). PAE alters proliferation and migration processes (52), affecting neural crest migration and causing cytoskeletal rearrangements. These phenomena destabilize the formation of focal adhesions in cell lineages, reducing their capacity for directional migration. Moreover, the activity of glycogen synthase kinase 3 (GSK3) and cyclin-dependent kinase 5 (cdk5) modulate microtubule-associated protein 1B (MAP1B) phosphorylation, involved in the regulation of microtubules and actin filaments in neurons, needed in migration processes (98). *In vitro*, ethanol inhibits neurite outgrowth by activating GSK3β (99). Conversely, PAE promotes GABAergic interneuron migration by inducing epigenetic alterations in the methylation pattern of the MeCP2-BDNF/DLX5 pathway. MeCP2 regulates the expression of the brain-derived neurotrophic factor (BDNF), a marker of neuronal plasticity and cellular survival known to influence GABAergic interneuron migration (100). MeCP2 has been shown to regulate DLX5 transcription, a transcription factor involved in the migration and maturation of GABAergic interneurons in mouse models (101). The human natural killer-1 (HNK-1) carbohydrate is also used as a biomarker in migration processes studies involving cranial neural crest cells (102). Results indicate reduced levels of HNK-1 in a model of chick embryos exposed to 2% ethanol, which suggests that PAE may disrupt cranial neural crest cell migration.

Long-term effects of PAE on migration have also been evaluated. Miller et al. describe the harmful effects of alcohol on proliferation and migration in rats prenatally exposed to alcohol. The authors found a delay in migration of early and late-generated neurons in rats following PAE between GD 6 and GD 21. Ethanol blocks neuronal migration, probably by leading to a desynchronization of cortical development that interferes with the establishment of a normal neural network (52). Skorput et al. studied the effects of PAE on GABAergic interneurons in mice. They found an increase in BrdU labeling in the medial ganglionic eminence showing an increase in neurogenesis, as well as an increase in parvalbumin-expressing GABAergic interneurons in the medial pre-frontal cortex in adults. These results support the contribution of GABAergic interneuron migration disorders to persistent alterations in cortical development in adulthood (103).

In summary, migration is a set of complex processes regulated by different molecular pathways that are disrupted in several checkpoints when ethanol exposure occurs.

Differentiation

Processes of neuroblast differentiation initiate after neuronal precursors have completed their last division and are ready to migrate to a specific area (104–106). Depending on the fate (brain area) of migration, neuronal precursors may differentiate into neurons, astrocytes, or oligodendrocytes (107). The differentiation of the cerebral cortex implies the formation of laminae in the radial domain from the ventricular zone to the pial surface and the subdivision of functional areas in the tangential domain, in rostrocaudal and mediolateral axes. In this process, the laminar fate is determined by cell-to-cell interactions and cell autonomous restriction on their development (104).

Several proteins, used as biomarkers, are involved in the differentiation processes. Doublecortin (DCX) has been studied in depth as an endogenous marker of immature neurons. The effects of pre-natal chronic ethanol consumption on adult neurogenesis (PND 56) has been assessed in C57BL/6J mice, revealing a decrease of DCX in the hippocampus after PAE (82). Quantification of immature neurons labeled with DCX in mouse was lower in the group of individuals exposed to alcohol in the prenatal period compared to controls. Moreover, DCX levels were lower in males than in females (108). Broadwater et al. obtained similar results after PAE by oral gavage on PND28–48, with decreased DCX levels in the DG of adolescent mice. Furthermore, after interrupting ethanol exposure, reduced levels of differentiated neurons in adulthood were found in rats (109). Elibol-Can et al. observed slight changes in the number of granular cells labeled with DCX in hippocampal DG on PND 30. The authors reported a decrease in the volume of the hippocampus in rats after a daily dose of 6 g/Kg ethanol during second trimester equivalent (110). Likewise, Hamilton et al. studied the long term-effects of single or continuous exposure to alcohol during the third trimester equivalent in mice and the effect of voluntary exercise as a therapy. Mice were exposed to ethanol on PND 7 or PND 5, 7, and 9 and DCX measured in adulthood. No differences in DCX levels were found in ethanol exposed groups. Nevertheless, the group exposed to ethanol during PND 5, 7, and 9 showed alterations in the results obtained in Rotarod and passive avoidance behavioral tests, which measure motor coordination and memory, respectively (111). Conversely, Coleman et al. observed increased levels of DCX after ethanol exposure in the DG in adult PND 7 male mice, but not in females (70).

Long-term effects of PAE have also been studied using other biomarkers. Choi et al. assessed the effects of PAE on BrdU levels in adult mice exposed to ethanol during the two trimester equivalents. No differences in neuronal proliferation nor differentiation were found after evaluating BrdU levels (31). Boehme et al. studied BDNF levels of rats exposed to ethanol during the three trimester equivalents. They found no changes

in BDNF levels of animals exposed to ethanol in the prenatal period. However, increased BDNF levels were observed in groups assigned to voluntary exercise (35). Gil-Mohapel et al. reported increases in NeuroD levels in adult rats exposed to ethanol during the three trimester equivalents. The increase in differentiation processes are probably due to the increase in immature neurons showed in prenatally exposed groups (29). The changes observed in the differentiation processes in adult rodents exposed to ethanol during the prenatal period vary according to the used biomarker. The increase in neuronal differentiation may occur as a compensation of the cellular loss in fetal life.

Responsive element binding protein (CREB) and cAMP signaling is directly correlated to neurogenesis, differentiation, neuronal connectivity, and plasticity (112). Ethanol exposure disrupts the activity of adenylyl cyclase (AC) reducing cAMP/CREB signaling and therefore altering the differentiation processes during neurodevelopment (112). *In vivo* and *in vitro* studies have shown that acute alcohol exposure enhances agonist-stimulated AC catalytic activity, while chronic alcohol exposure produces adaptive changes in AC (113–115). Additionally, GSK3β over-expression in neural cells disrupts CNS maturation and differentiation processes in mouse at PND 60–120 (116).

The glial cell-derived neurotrophic factor (GDNF) is a growth factor necessary for the development, differentiation, proliferation, and function of midbrain dopaminergic neurons. The GDNF signaling pathway is initiated by the binding of GDNF to its co-receptor, GDNF family receptor-α 1 (GFRα1), which leads to the recruitment of the RET receptor tyrosine kinase. The activation of RET promotes the up-regulation of downstream signaling pathways such as ERK1/2 (117) and P13K (118), firing the activity of dopaminergic neurons. Moderate administration of alcohol increases GDNF expression, exerting a protective function against PAE. However, after acute (binge) ethanol exposure in rats, GDNF expression decreases and its protective function diminished (119). A recent study performed in adult rats exposed to alcohol showed a decrease in DNA methylation as the leading cause of GDNF epigenetic changes following alcohol exposure (120).

Alcohol has deleterious effects on astrocytes despite them being less susceptible than neurons to moderate alcohol consumption (121). Glial cell alterations due to PAE lead to changes in neuron-glia interactions, which causes developmental defects of the brain (122). Glial fibrillary acidic protein (GFAP) is a biomarker of mature astrocytes commonly evaluated in differentiation processes during development. *In vitro* studies using primary cultures of astrocytes from 21-day old fetuses show initial increased values of GFAP levels post-ethanol exposure (123), although these GFAP values decrease after 3 weeks (123). GFAP levels in rat neonates have been shown to increase following ethanol exposure in different brain areas, e.g., the hippocampus, cerebellum, and cortex as per different administration routes (124–126). The results in *in vitro* models suggest different effects of ethanol on astrocytes depending on the neurodevelopmental stage. Moreover, some researchers have found increased GFAP expression associated to gliosis after chronic (moderate) and acute low ethanol exposures, in mice (127, 128). These results indicate a high risk of neurodevelopmental disease in acute PAE or heavy drinkers. Conversely, no changes were observed in GFAP expression after low chronic ethanol exposure (127). S100β is a classical biomarker astrocytes, as the expression levels of S100β in these glial cells is very high. During neurite outgrowth, S100β is also secreted by proliferating astrocytes from cortical neurons. The accumulation of this protein in mature glial cells is associated with microtubule network and neurotrophic activity (129). Reduced levels of S100β were reported in mice after ethanol exposure (130), indicating a depletion in the number of proliferating astrocytes and an impairment in the differentiation processes. Otherwise, Sox2 and Oct4 transcription factors regulate the embryonic stem cell pluripotency and the fate of cell lineages by a narrow range of dose-effect (131). Excess of Oct4 compared to Sox2 leads cells to mesoendoderm differentiation, while the other way round, i.e., higher levels of Sox2, promotes neuroectoderm formation. Ethanol exposure of embryonic stem cells in early differentiation generates imbalances between Oct4 and Sox2, which modifies the cellular fate from neuroectoderm to mesoendoderm, altering the formation of the ectoderm lineage and its derived progenitors. The Oct4/Sox2 imbalance is considered one of the leading causes of developmental delay and anatomical disabilities of the CNS observed in FAS phenotypes (131).

Synaptogenesis

The developmental process of synaptogenesis involves biochemical and morphological changes in pre- and post-synaptic components. In rodents, maturation of synaptic connections occurs during the postnatal period (**Figure 1**) (132) and depends on the physicochemical compatibility of pre- and post-synaptic components and the exclusion of inadequate connections. Less harmful effects of alcohol exposure on synaptogenesis have been observed when administered after birth (54, 55), although during neuronal development ethanol seriously alters some mechanisms related to synaptogenesis (54, 55). In a study using a rat model in which individuals were exposed to ethanol 4 weeks before and during pregnancy, the ultrastructural analysis of the cerebellum at PND 7 showed a delayed synaptogenesis and immature appearance of the presynaptic grid (55). PAE affects the expression levels of synaptic proteins such as synapsin 1 and of other proteins of the pre-synaptic (GAP-43, synaptophysin, synaptotagmin) or post-synaptic machinery (MAP 2 and neurogranin). Moreover, ethanol interferes with the function of adhesion molecules such as NCAM (in chick embryo model) (133) and L1 (in mouse model) (134) involved in cell-cell interactions. During the neural processes of migration and morphogenesis, both proteins are involved in the organization and function of synaptic networks, which determine neuronal plasticity. Several studies in animal models (zebrafish) and cell cultures show decreased levels of NCAM after ethanol exposure (135, 136). In other studies, different patterns of NCAM expression were detected according to the developmental stage on which PAE occurs (133) or the NCAM isoform analyzed. For example, the highly sialylated form of NCAM is overexpressed after ethanol exposure but the NCAM 180 and NCAM 140 isoforms appear down-regulated in

a rat model (137). Other studies in animal models (mice and rats) have shown down-regulation of L1 following ethanol exposure (134, 138).

Gliogenesis and Myelination

Glial cells provide nutrients and physical support to neurons and regulate the presence of different proteins and components in the extracellular fluid surrounding neurons and synapses in the brain. They are essential for a normal development and function of the central nervous system (139). Neuroblast migration occurs through a scaffold provided by radial glia (140). Microglia have macrophage functions and astrocytes preserve the ionic and trophic balance of the extracellular medium (141). Oligodendrocytes synthesize myelin, therefore, this cell lineage preserves the myelin sheath and provides trophic support (142). Schwann cells and oligodendrocytes are in charge of the isolation and myelination of neuronal axons (143). Oligodendrocyte progenitor cells proliferate and differentiate into mature oligodendrocytes capable of myelinogenesis (144). Thus, myelination begins later in neurodevelopment than other processes such as proliferation and migration and progresses throughout adolescence in rodents (145, 146). The development of these cell lineages occurs at the same time as neurogenesis in several areas of the central nervous system (141). These lineages are characterized by distinct developmental stages and sequential expression of different developmental biomarkers such as the nerve growth factor (NGF), neurotrophins (NT-3 and NT-4), the brain derived neurotrophic factor (BDNF), and the IGF-1 and IGF-2 factors. The BDNF is one of the most studied neurotrophins. Alcohol alters the levels of BDNF and its receptor tyrosine kinase B (TrkB). PAE induces decreased levels of BDNF in the cortex and in the hippocampus in rats at PND 7–8 (147). Some studies in rats show that TrkB levels decrease in specific brain regions, e.g., in the hippocampus (147, 148) and increase in the cortex (148). The BDNF and its receptor are targets for ethanol damage. Consequently, imbalances between them may contribute to the development of FASD-like phenotypes, even in cases in which the levels of one of them remain unaltered. In general, the up-regulation of these neurotrophic factors show protective effects during development, promoting myelination, cell survival, and neural regeneration in pathological conditions (149).

Lancaster et al. showed that PAE reduces myelinogenesis and its persistence after birth in a rat model (56). Severe impairments in gliosis and a reduction of proteins related to myelin integrity (myelin-associated glycoprotein, myelin basic protein, myelin proteolipid protein, and myelin regulatory factor) was observed in male adult mice exposed to a binge (acute) pattern of PAE during gestation and lactation. This damage was followed by behavioral alterations in executive function and motor coordination (79). These changes could be associated to the behavioral disabilities observed in FASD individuals. It has also been shown that exposure to alcohol activates toll-like receptor 4 signaling pathways (MAPK, NFκB) in a mouse model, leading to an increased expression of pro-inflammatory mediators (COX-2, iNOS, HMGB1) and cytokines. Inflammation processes cause myelinogenesis imbalances, impairments in synaptic links, and activation of the cell death mechanism (150).

Trophic Support

CNS remodeling is a continuous process that not only takes place during development, but also throughout adulthood in response to environmental influences or genetically programmed events. Alcohol alters synaptic plasticity and neural function (151). Several proteins used as biomarkers participate in neural plasticity processes. Histone deacetylase 2 alters the GluN2A/GluN2B balance [the major subunits of functional N-methyl-D-aspartate (NMDA) receptors] through changes in GluN2B expression, which leads to memory-impairing effects (152). The neurotrophin family of proteins includes NGF, BDNF, NT-3, NT-4/5, and NT-6. It is well-known that NGF and BDNF play important roles in PAE and FASD pathogenesis. Various studies have shown that PAE disrupts neurotrophin pathways, thus affecting the organogenesis and development of brain structures in rodents (153, 154). NGF and BDNF exert their biological effects by activating some members of the tropomyosin-related kinase (Trk) family. NGF activates TrkA and BDNF binds to TrkB (155). Stressful events, neurological injuries, or neuroendocrine alterations in rats increase blood levels of NGF (156). Thus, NGF expression and the functional activity of NGF-target cells in the CNS are seriously affected by alcohol consumption. BDNF regulates neural cell survival and differentiation as well as several functions related to neural plasticity such as learning and memory (157). A recent study found that BDNF levels in the pre-frontal cortex were significantly lower in the group of mice treated with ethanol in comparison to the control group (158). The study concluded that the impairment in learning and memory observed in mice exposed to ethanol was associated to changes in BDNF levels. Stragier et al. showed that chronic and moderate alcohol consumption in C57BL/6J mice promotes a chromatin-remodeling process, leading to up-regulation of BDNF signaling. The authors suggest that this epigenetic regulation is an adaptive process to balance cognitive disorders induced by alcohol (159). Another study in mouse observed a reduction in ethanol dependence after BDNF infusion in the pre-frontal cortex (160), evidencing that BDNF levels in specific brain areas play a role in alcohol dependence. Boehme et al. studied the changes produced by voluntary exercise in hippocampal BDNF levels. Ethanol was delivered by intragastric gavage during the three trimester equivalents and individuals had free access to voluntary exercise on a running wheel during adulthood. Results showed increased BDNF levels in young adult females after voluntary exercise (35). Recent studies suggest that matrix metalloproteinase-9 (MMP-9), a Zn $(2)^{+}$ dependent extracellular endopeptidase, participates in neuronal plasticity, specifically in memory and learning (161, 162). Acute and chronic ethanol exposure up-regulates the MMP-9 levels in the brain, particularly in the medial pre-frontal cortex and hippocampus, in rats (163). The vascular endothelial growth factor (VEGF) is involved in the activity, plasticity and survival of microvessels. Mice prenatally exposed to alcohol have reduced cortical vascular density, affected microvascular structure, and altered expression of VEGF and its receptor.

VEGF may prevent microvessel plasticity disorders and death. As a mouse model shows, PAE exerts its deleterious effects on the microvascular network, which suggests that vascular defects contribute to alcohol-induced brain injury (164). *In vitro* studies show that ethanol also alters the expression and function of IGF-I and IGF-II, leading to birth defects such as low head circumference at birth and microcephaly. These insulin-like growth factors are used by the organism as a general signal of cell survival, so that reduced IGF-I or IGF-II signaling by PAE in neurons activates cell death mechanisms by apoptosis or necrosis (165). Other biomarkers such as DYRK1A act as general inhibitors of neural plasticity. Its over-expression in different brain areas due to environmental insults or stress conditions reduces neural plasticity in neurons promoting cognitive problems and intellectual disability (166–168). Recent studies have demonstrated that some DYRK1A inhibitors such as the antioxidant Epigallocatechin gallate (EGCG) improve long-term outcomes related with memory and executive function in individuals with Down syndrome (166–168). Although it is currently under study, the inhibition of DYRK1A could improve the cognitive performance in pathologies associated to the loss of neuronal functions and plasticity, e.g., FASD, Autism, or Down Syndrome (169). Furthermore, EGCG increases NGF expression by downregulation MMP-9. These proteins have been associated with FASD alterations during neurodevelopment (170).

Synaptic Plasticity

Synaptic plasticity is the process through which long-term changes in synaptic communication occur (171).

Fontaine et al. studied the effect of prenatal exposure to ethanol in a rat model during the two trimester equivalent and PND 21–28 on long-term potentiation, long-term depression, and depotentiation in the medial perforant path input to the DG of the hippocampus. Impairment of long-term potentiation was seen in both males and females, while long-term depression was only observed in males. The results suggest that PAE causes sex specific impairment in synaptic plasticity in long-term depression (172). Wong et al. focused their study in the contribution of microglia in synaptic plasticity. Using a third trimester equivalent mice model, ethanol was injected following a binge-drinking pattern. The authors found a deficit in experience-dependent synaptic plasticity in the visual cortex with no correlation to microglial function (173). Shivakumar et al. administered ethanol to mice at PND 7, and showed that ethanol exposure produces epigenetic changes that inhibit the activation of several synaptic plasticity genes. Coadministration of trichostatin A prevents learning and memory disorders in adult mice (174).

PAE negatively affects synaptic plasticity. Epigenetic changes, as well as damage to the microglia, may partially explain synaptic plasticity disorders in FASD models.

Apoptosis

Apoptosis is a critical pathway in fetal neurodevelopment. Programmed cell death systematically removes a large number of neural precursors in embryonic structures formed during development. PAE activates and deregulates cell death mechanisms leading to the loss of cell lineages in the hippocampus, basal ganglia, or cerebellum and disappearance of critical structures in the brain such as the *corpus callosum* (57, 58). The activation of apoptosis is produced by an increase of reactive oxygen species (ROS) generated in ethanol metabolism (see section Oxidative Stress). ROS activate intrinsic and extrinsic apoptotic pathways, reducing the expression and function of the anti-apoptotic proteins Bcl-xL and Bcl-2 in a rat model (175). A study using a mouse model shows that the function of the pro-apoptotic effectors Bak and Bax is directly influenced by alcohol due to alterations in mitochondrial membrane fluidity and dysfunctions in mitochondrial respiration, which leads to the activation of the caspase cascade and subsequent generation of the active form of the effector caspase 3 (176). Consequently, some researchers have developed mitochondrial protective strategies to prevent alcohol-induced damage. Certain molecules, e.g., nicotinamide (177), can stabilize mitochondrial membranes while others, e.g., antioxidants, prevent mitochondrial dysfunction induced by the production of ROS following ethanol exposure, in mouse. In addition, ethanol activates specific cell death pathways. More specifically, ethanol induces the phosphorylation of c-jun N-terminal-kinase, a mitogen-activated protein kinase associated with apoptosis and GDNF may interfere with the activation of the c-jun N-terminal-kinase molecular pathway to prevent ethanol-induced apoptosis. Unlike other neurotoxic substances, ethanol does not interfere with the phosphorylation of the extracellular signal-regulated kinases involved in the regulation of cell survival (178).

PATHOPHYSIOLOGY

There are multiple pathological effects derived from alcohol exposure during fetal development depending on the studied organ, region and cell type, as well as the stage of pregnancy in which the fetus is exposed to ethanol (179). The following sections provide a detailed description of the teratogenic effects of PAE.

Oxidative Stress

Ethanol is metabolized in the liver of adult individuals via the alcohol dehydrogenase (ADH) and aldehyde dehydrogenase (ALDH) families of enzymes (**Figure 3**), leading to moderate ROS production, e.g., hydrogen peroxide (H_2O_2) and hydroxyl radicals (OH-). ROS are eliminated by endogenous antioxidant mechanisms directed by catalase, superoxide dismutase (SOD) and the antioxidant molecule glutathione (GSH) (180). After a high intake of alcohol, the catalytic activity of ADH and ALDH becomes saturated and an alternative pathway mediated by the cytochrome P450 2E1 enzyme is up-regulated to metabolize ethanol to acetaldehyde, producing high amounts of ROS. ROS-sensing transcription factors, such as the nuclear erythroid 2-related factor 2, activate the oxidative stress response mechanisms when moderate levels of alcohol-derived ROS are present, up-regulating antioxidant enzymes and proteins involved in DNA repair. Imbalances between ROS-producing pathways (following PAE) vs. the endogenous antioxidant and DNA repair mechanisms promotes down-regulation of detoxification pathways (180, 181). The decrease of the

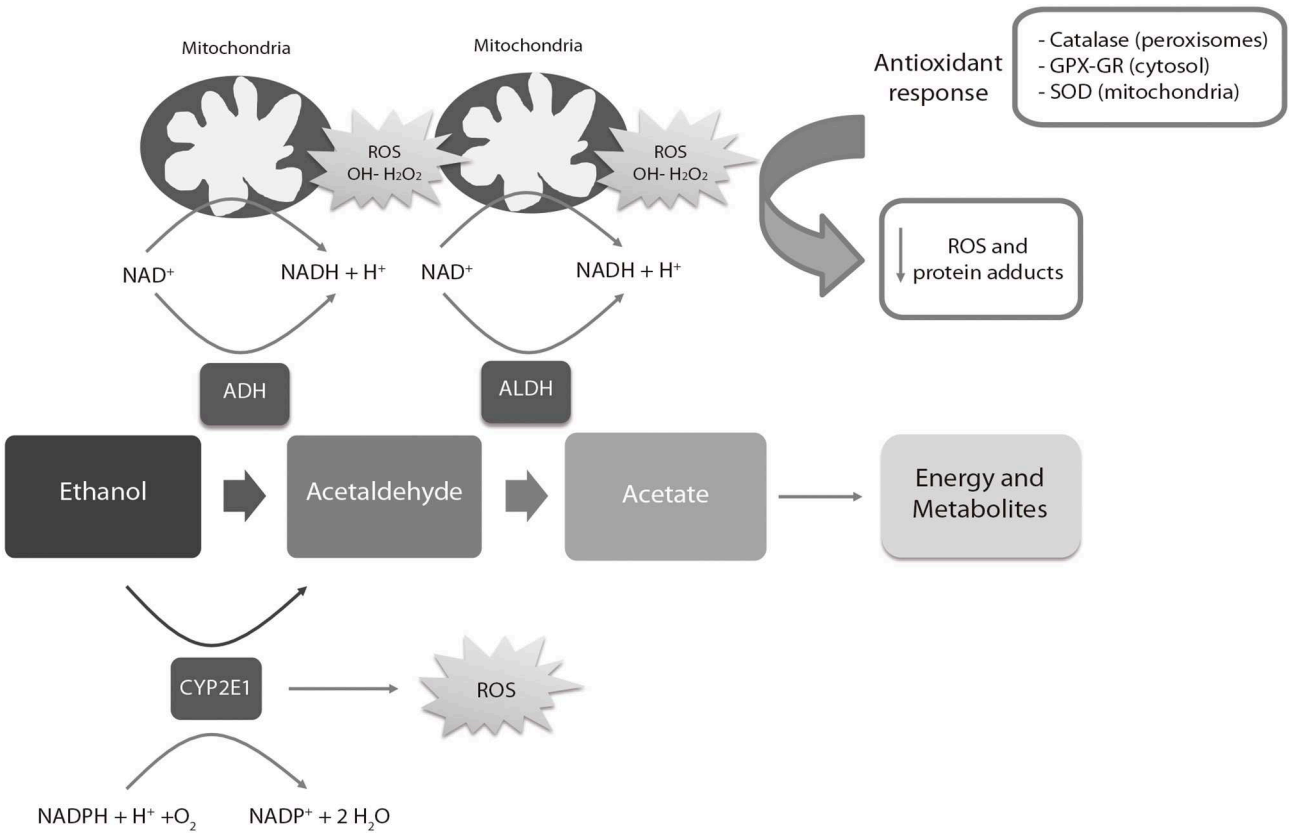

FIGURE 3 | Liver metabolic pathway of alcohol. ADH, alcohol dehydrogenase; ALDH, aldehyde dehydrogenase; ROS, reactive oxygen species; SOD, Superoxide Dismutase; GPX, Glutathione peroxidase; GR, Glutathione reductase. The ADH, ALDH enzymes and the P450 2E1 cytochrome participate in the oxidative metabolism of alcohol. The activity of the P450 2E1 cytochrome in alcohol metabolism and the re-oxidation of NADH via the electron transport chain in the mitochondria results in the formation of ROS. Catalase in peroxisomes, SOD in mitochondria and GPX-GR in cytosol are activated by an increase of oxidative stress to reduce the levels of ROS. High amounts of ROS lead to a down-regulation (negative feedback) of the antioxidant response.

antioxidant system affects specific regions of the CNS such as the cerebellum, hippocampus and cortex, as well as the placenta (182, 183). The fetal brain is particularly sensitive to PAE because the ADH isoform expressed in this tissue during development is a class II isoenzyme ADH4. This isoform is less efficient for alcohol catabolism than other isoforms expressed in adults (184). The mechanisms involved in antioxidant response are physiologically downregulated during development (185–188), contributing to brain vulnerability by ethanol. The excess of ethanol also activates the lactate pathway in the fetal liver, generating a deficit of glucose in the bloodstream that affects especially the nervous tissues (189). Imbalances of ROS activate the mechanisms of inflammation (190) mediated by cytokines such as IL-6 or the NLRP3 inflammasome, a multi-protein intracellular complex responsible for processing and secreting the pro-inflammatory cytokines IL-1β and IL-18 (191).

Tissue homeostasis is also affected by ROS (192), causing changes in critical cell functions as signal transduction related to the metabolism of macromolecules (lipids, proteins, RNA, and DNA) (190). AS an example, ROS promote the modification of 8-oxoguanine in DNA during embryogenesis (193, 194), which is corrected by the enzyme oxoguanine glycosylase 1 (195). Calcium homeostasis and protein folding, modification and secretion in endoplasmic reticulum are also altered by ROS, as well as mitochondrial respiration, affecting its morphology and function. Moreover, activation of autophagy, programmed (apoptosis) and non-programmed (necrosis) cell death are also promoted by oxidative stress (192, 196, 197).

Some studies have assessed the long-term consequences of PAE on oxidative stress and the intracellular redox state. Dembele et al. found an relation between continuous administration of PAE with increased levels of oxidative stress in adult rats (PND 90), characterized by high levels of protein carbonyls, lipid peroxides, high expression of SOD, and low levels of GSH (198). Similar results have been reported by other authors, who showed an association between chronic PAE at different concentrations with increased levels of distinct oxidative stress and lipid peroxidation markers in adolescent and adult rodents (199, 200). Chu et al. found a correlation between PAE and apoptotic (p53) and DNA oxidation markers (8-hydroxydeoxyguanosine) in adult rats (200). Brocardo et al. reported depressive and anxiety-like behaviors and high levels of lipid and protein peroxidation

in adult rats (PND60) who were given ethanol throughout the three-trimester equivalents (201). Their findings also indicate an association between voluntary exercise, which increased the endogenous antioxidant pathways in brain, and the reduction of oxidative stress and depressive/anxiety-like behaviors. Similarly, binge drinking model of PAE (GD 17–18) increased the levels of lipid peroxidation and oxidative stress, apoptotic activation via caspase-3 activity, and DNA fragmentation, decreasing antioxidant molecules as GSH (202, 203).

Dysregulation of the Neuroimmune System

Ethanol exposure activates the innate neuroimmune system, causing brain damage and neurodegeneration (150, 204). Alcohol intake triggers the stimulation of microglia and astrocytes, promoting neuroinflammation with the consequent production of pro-inflammatory cytokines and chemokines (e.g., TNF-α, IL-2, IL-6, IL-8, Il-10, IL-1RA, IFN-γ, or MCP-1) (150, 204).

Toll-like receptor 4 and NOD-like receptors have an important function in glial cell stimulation and alcohol-mediated neuroinflammation. Ethanol activates toll-like receptor 4 signaling pathways mediated by NFκB and MAPK, which leads to the up-regulation of cytokines and pro-inflammatory mediators such as HMGB1, COX-2, and iNOS (150). The activation of these inflammation pathways generate severe impairments on synaptic and myelin proteins as well as neural damage (150). Moreover, the increased caspase-3 activity in the prefrontal cortex indicates apoptotic cell death secondary to PAE-related neuroinflammation (205). Regarding myelination and white matter structure, PAE causes neuroimmune changes such as reductions in myelin-associated glycoprotein levels, myelin basic protein and myelin proteolipid protein. Alterations in oligodendrocytes that interfere in the myelination process affecting neural transmission and cognitive development have also been described (79, 205).

Neurotransmitter Disorders

Neuronal cells and neuroanatomical structures are particularly susceptible to toxic compounds during embryonic development, explained by the high sensitivity of the processes during brain formation. Neuronal damage triggers tissue degeneration by inflammation and massive cell death (apoptosis and necrosis) (182, 206). The loss of some progenitor cell lines seriously affects proliferation, migration, and differentiation of mature neuronal cells, essential to configure the distinct regions of the brain and make them functional (207). The high sensitivity to increases in oxidative stress is the main cause of cell death in these parental lineages. This occurs because they lack the molecules and enzymes required for an antioxidant response, i.e., catalase and superoxide dismutase (181). High levels of ROS affect the mitochondrial function in neurons and leads to the activation of apoptosis (208).

In a prenatal ethanol-exposed brain, differentiation from multipotent glial cells to astrocytes occurs prematurely, preventing the correct completion of migration processes (209). These astrocytes are therefore incorrectly located in the brain, causing motor, and cognitive disorders, promoting cell death of these neuronal groups and triggering harmful effects such as the agenesis of the *corpus callosum* (209). Moreover, primary cultures of hippocampal neurons exposed to ethanol show reduced levels of the glucose transporter GLU1 necessary for the correct growth and development of most cell types present in the brain whose main carbon source is glucose (210). Alcohol also alters the levels of neurotransmitters, namely serotonin, dopamine, and glutamate (211). Exposure to alcohol delays serotonin synthesis, blocking the stimulation of astrocytes and the release of the growth factors needed for proper neurodevelopment (212). Ethanol reduces the number of glutamate receptors (NMDA), which in turn affects other neurotransmitter routes generating important alterations in the transmission of nerve signals (213). The acetaldehyde produced by the metabolism of local ethanol in fetal hippocampus inhibits neurosteroid synthesis and blocks NMDA receptors in pyramidal neurons, contributing to synaptic dysfunction associated with severe alcohol intoxication (214). Furthermore, a recent *in vitro* study with rat brain slices exposed to 70 mM ethanol indicates that the combined overexpression of GABA receptors and inhibition of NMDA receptors results in alcohol-induced neurodegeneration during synaptogenesis (215). Consequently, the administration of single doses of an NMDA antagonist in Sprague Dawley rats causes apoptotic neurodegeneration in young animals, although no impairments were identified in adult individuals. Therefore, the NMDA antagonist acts on the CNS in a similar way ethanol does (216).

PAE has neuroapoptotic effects on the up-regulation of GABAergic transmission and deficit of NMDA receptors. The impairment produced by ethanol on developing neurons depends on the specific neural lineage and is age-dependent. A study performed in mice exposed to moderate amounts of alcohol showed that the subunits of NMDA receptors GluN1 and GluN3A are up-regulated after PAE in the DG. The study also found a decrease of GluN2B levels in the synaptic membrane (217).

Epigenetic Modifications

During fetal development, epigenetic mechanisms establish the whole pattern of gene expression for the tissues, organs and cell types that constitute the complete organism. These mechanisms involve the methylation of DNA, modifications of N-terminal tails in histones, and the regulation of micro and non-coding RNA.

In DNA methylation, methyl groups (CH_3), a product of folate metabolism, are added to the cytosines (C) present in the regions known as CpG islands of the DNA helix. This phenomenon is mediated by methyl-transferases (DNMT) and demethylases such as TET2 (218). DNMT3a and 3b set the complete genome expression patterns during fetal development and DNMT1 maintains this pattern in postnatal stages (219). Usually, the clusters of CpG islands match with promoter regions to regulate the expression of the genes involved in a specific pathway or signaling (220). In general, methylation is associated with gene silencing and demethylation with active transcription. Histones regulate the dynamics of chromatin in remodeling processes between heterochromatin, inaccessible to DNA polymerases, and the expanded chromatin (euchromatin) that allows gene expression. Histone structure and function is regulated through

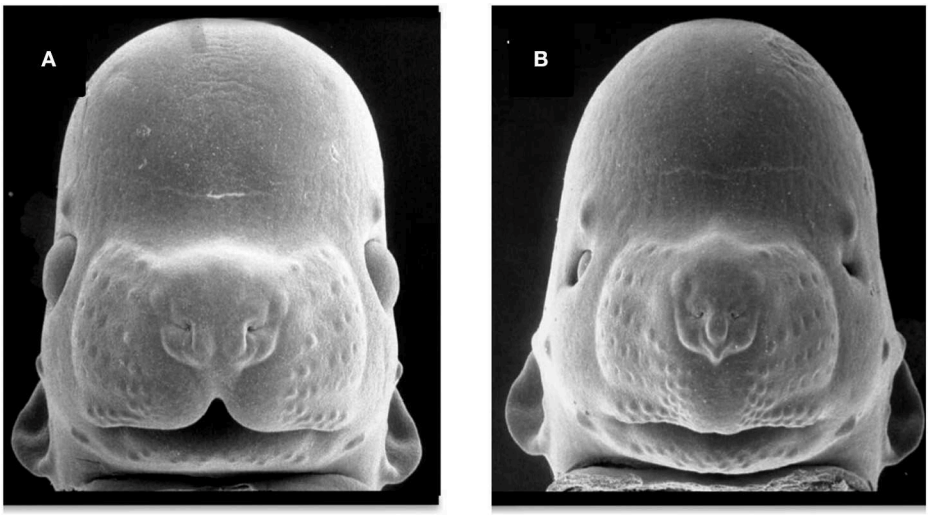

FIGURE 4 | Facial dysmorphology induced by prenatal ethanol exposure. Representative examples of a control animal **(A)** and a fetus severely affected by ethanol exposure **(B)**. FAS-like phenotype **(B)** is defined by microcephaly, short palpebral fissures, thin upper vermillion, and smooth philtrum. FAS-like facial features are induced in the mouse by maternal alcohol exposure on gestational day 7 and 8.5 (equivalent to the third gestational week in humans). Courtesy of Prof. Kathie Sulik, University of North Carolina-Chapel Hill (271) (https://www.teratology.org/primer/fas.asp).

different post-translational modifications in their N-terminal tail such as methylation, acetylation, and phosphorylation, mainly in the amino acids lysine, arginine, and serine. All these reversible modifications are carried out by different enzymes such as kinases, acetyl-transferases or methyl-transferases depending on the requirements of the cell (221). Otherwise, non-coding and microRNAs regulate protein translation and mRNA stability, acting post-transcriptionally as inhibitors of mRNA by direct interaction (222).

Ethanol and ROS can modify the activity of methyltransferases and demethylases, directly affecting the global DNA methylation pattern during development. A recent study performed in mice after PAE found 118 differentially methylated regions (DMRs) related to transcription factor binding sites (223). The pathways affected by these DMRs were epigenetic remodeling, hormonal signaling, metabolism, and immune response, revealing persistent occurrence of these alterations in all developmental stages (223). Demethylation following ethanol exposure causes a decrease in IGF-2 levels *in utero*, generating an important delay in growth and leading to skeletal malformations (224).

PAE influences the activity of enzymes such as histone acetyltransferase and histone deacetylase, which modify the composition of the amino-terminal tails in histones (225). Moreover, the acetylation of histones H3 and H4 has been directly related to alterations in the development of the cerebellum, cardiac defects, and hepatic damage (226, 227). Cantacorps et al. (228) showed that a binge PAE pattern in mice alters histone acetylation (lysine 5 and 12 in histone H4) in the pre-frontal cortex and the hippocampus. These long-term epigenetic modifications are associated with cognitive and behavioral impairments in offspring. Ethanol exposure alters the expression pattern during development, affecting non-coding and microRNAs expression (229). PAE generates a decrease in the expression of miR135, miR9, miR21, and miR355. The absence and deregulation of these microRNAs generate early maturation of the progenitor stem cells and an increase in cell apoptosis, producing severe impairments in fetal brain development (230). The high variability of the described epigenetic changes is associated to the dose of ethanol received, the time of exposure and the gestational stage in which alcohol intake occurs.

DIAGNOSIS OF FASD

PAE results in a wide range of phenotypic manifestations and behavioral deficits in the offspring we describe below.

Craniofacial Anomalies

The key facial features used for a clinical diagnosis of FAS in humans include short palpebral fissures, a thin upper vermilion, and a smooth philtrum (231). Considering previous studies in humans (232, 233), Fang et al. described, for first time in 2009, a validated facial image analysis method based on a multi-angle image classification using micro-video images of mouse embryos. This method, validated later by other researchers, allows discerning between embryos that have been exposed or not to ethanol (232, 233). Rodents provide not only a validated model to study how PAE alters morphogenetic processes, but it also allows making an association between a facial feature alteration and the structure/function in the CNS.

Alcohol exposure during essential periods of embryonic development results in craniofacial dysmorphology (**Figure 4**). Several studies have used chick and murine PAE models to demonstrate the correlation between craniofacial anomalies,

apoptosis induction, and altered migration of neural crest cells (234–236). A series of facial anomalies may present in FASD associated to PAE during the premigratory period of neural crest cells (**Figure 2**). At this stage, ethanol induces calcium transients that activate CaMKII that mediates the loss of transcriptionally active β-catenin, which produces the apoptosis of populations of neural crest cells. Genetic factors play an important role in the vulnerability to alcohol-induced craniofacial dysmorphology. Sonic Hedgehog signaling, platelet-derived growth factor subunit A, Vang-like protein 2, or ribosomal biogenesis genes are of special importance in neural crest development (237). Studies using FASD-like phenotype rodent models, in which dose and timing of ethanol exposure is controlled, show structural alterations in head and face (238, 239) similar to anomalies observed in humans (240).

Several studies have examined the craniofacial anomalies in FASD-like rodent models. According to Godin et al., intraperitoneal administration of two injections of ethanol at 2.9 g/Kg in mice on GD 7 (equivalent to post-fertilization week 3 in humans), generates a series of facial dysmorphologies similar to those seen in FAS children. These defects include median facial cleft, cleft palate, micrognathia, pituitary agenesis, and third ventricular dilatation and heterotopias (33). However, intraperitoneal alcohol exposure of two 25% dosages of ethanol at 2.9 g/Kg delayed to GD 8.5 in mice produces a different pattern of dysmorphologies such as shortening of the palpebral fissures, mild hypoplasia and shortened upper lip, but a preserved philtrum (60). Variations in FAS-like facial phenotypes depend on exposure timing, implying different facial features when considering this variable (**Figure 2**). New techniques for FASD diagnosis include methods to identify potentially at-risk individuals based on the identification of subtle and subclinical facial characteristics (241). Scientists have developed a computerized system for detecting facial characteristics using three-dimensional facial imaging and computer-based dense-surface modeling (241, 242). This approach has been compared against standard dysmorphology physical examination for FAS diagnosis revealing high similarities (243). More recently, new techniques based on MicroCT 3D scan performed on pups prenatally exposed to alcohol have been developed (244). This method showed that craniofacial bones might be a reliable and sensitive indicator of PAE in mouse pups exposed to 4.2% alcohol v/v for 2 weeks before the pregnancy and GD 7–16. The same study also confirmed that the neurocranium (cranial skeleton) is more sensitive to alcohol than the viscerocranium (facial skeleton). Other researchers characterized concurrent face-brain phenotypes in mouse fetuses exposed to two 25% intraperitoneal dosages of ethanol at 2.9 g/Kg on GD 7 or GD 8.5 and using MRI imaging and dense surface modeling-based shape analysis (60). Differences in facial phenotype linked to GD of ethanol exposure were found, being more subtle when the exposure was on GD 8.5. Both phenotypes were associated with unique volumetric and shape abnormalities of the septal region, pituitary, and olfactory bulbs. These findings illustrate the need of increasing the current diagnostic criteria to better capture the full range of facial and brain dysmorphology in FASD.

Brain and Neurobehavioral Deficits

Brain organogenesis is the most severely affected process by alcohol exposure (245) and there is a general consensus in relation to the effects of PAE on the hippocampus, cerebellum, and the *corpus callosum* (246, 247). Important asymmetry of the hippocampus is observed in FAS children, with the left lobe being smaller than the right lobe (8). The cerebellum, associated with balance, coordination and learning capacity, and the anterior part of the vermis develop hypoplasia when exposed to ethanol (7).

The *corpus callosum* is particularly vulnerable to ethanol exposure and, in some cases, may lead to total (agenesis) or partial (hypoplasia) loss of structure (248). The most affected areas of the *corpus callosum* areas are the front (genu) and back (splenium and isthmus), appearing smaller and displaced from the usual spatial location in the brain (6). Basal ganglia is responsible for motor and cognitive abilities, presenting a smaller size in patients with FAS, particularly the area of the caudal nucleus associated to cognitive abilities such as spatial capacity (249). A recent study using three-dimensional surface MRI techniques showed abnormalities in the cortical folding (gyrification) of FASD children. These findings are directly correlated with IQ (250). Future research with MRI techniques to evaluate rodent gyrification may prove to be useful to increase the knowledge on the relationship between cortical development involvement and cognitive disorders in humans.

Broadly, the timing of the ethanol exposure (251) has a clear impact on the CNS and elicits specific brain and behavioral deficits and disorders in motor and cognitive functions (14) (**Figure 2**).

Different standardized tests in rodents have been used to assess FASD-related abnormalities. As the hippocampus is one of the most damages structures when exposed to ethanol, most studies assessed hippocampal function. Spatial learning is commonly evaluated to demonstrate hippocampal disorders (45, 79, 252). Different authors describe long-term motor coordination impairments, learning and memory deficiencies in adult male mice prenatally exposed to alcohol (79), behavioral effects in rats following short-term PAE (253), or depressive-like behaviors in adult rats exposed to ethanol across the three-trimester equivalents (201). To identify the outcomes of gestational alcohol exposure, a summary of behavioral characteristics after alcohol exposure is needed. **Table 2** summarizes the standardized behavioral tests used in rodents to analyze the harmful effects of PAE.

Fetal Growth Restriction

Ethanol interference with maternal nutrition may differ. As a source of energy, alcohol blocks the absorption of other nutrients, including proteins, and hinders intestinal transport of essential nutrients. Due to its effects on liver, alcohol causes metabolic and nutrient utilization alterations. PAE causes maternal nutritional deficiencies that result in fetal growth deficiencies (26).

PAE also impairs placental angiogenesis (269) and consequently fetal growth restriction (FGR) (270). The growth curves defined by Dilworth et al. are a useful tool to define the frequency distribution of mouse weight. Any fetus with a weight below the fifth centile was considered growth restricted (68).

TABLE 2 | Standardized experimental methodologies for assessing behavioral effects of prenatal alcohol exposure in murine models.

Skills affected by PAE	Disorders	Behavioral test	Description
Motor skills Cerebellum (Purkinje cells) (254)	Motor hyperactivity, poor motor coordination, altered accuracy of saccadic eye movements, and deficits in postural balance are impaired motor skills observed in individuals exposed to ethanol during early life. PAE-related motor deficits are more apparent in early life than in adulthood.	The rotarod (79)	For this test, a bar that can rotate at an accelerated or a fixed speed is used. The latency of the fall of the rodent placed in the bar is measured. Measurements provide an idea of motor coordination.
		Swimming test (255)	It consists of a Perspex tank where rodents are placed and must swim to an escape platform. The sequence is recorded and later analyzed to assess the latency to reach the platform and the number of fore and hind limb strokes.
		Raised beam test	Rodents are placed on the bar and their ability to cross it is measured along with paw slips and traverse time. It provides an indication of their balance.
		Footprint analysis	After their paws are painted or dipped in ink, rodents leave a trail of footprints when they walk or run along a corridor to a goal box. Measurements of stride length, base width, and fore and hind paws overlap give an indication of gait. Automated versions of the task use video processing of footage taken from below the rodents.
Learning and memory Hippocampus (dentate gyrus) (256, 257)	Hippocampal cell loss, altered neuronal morphology, decreased synaptic density, and reduced trophic support.	Simple maze task (258, 259)	A T-maze (or the variant Y-maze) is a simple maze used in animal cognition experiments. It is shaped like the letter T (or Y), providing the subject, typically a rodent, with a straightforward choice. T-mazes are used to study how rodents function with memory and spatial learning by applying different stimuli. The different tasks, such as left-right discrimination and forced alternation, are mainly used with rodents to test reference and working memory.
		Morris water maze (71, 252)	MWM is a test of spatial learning for rodents that relies on distal cues to navigate from a start point around the perimeter of an open swimming box to locate a submerged escape platform. The test allows measuring spatial learning and reference memory.
		Fear conditioning (260)	This test is a form of Pavlovian learning based on the conditioning of an innate response to fear consisting in a complete lack of movements. During an initial phase, the animal is exposed to a conditioned stimulus paired with an aversive experience (unconditioned stimulus). The test measures the fear response in mice replaced in the same location with and without the previous stimulus.
		Object recognition (79, 261)	In an initial session, the rodent is presented with two similar objects. One of the objects is replaced by a new object in the second session. The test measures the amount of time taken to explore the new object.

(Continued)

TABLE 1 | Continued

Skills affected by PAE	Disorders	Behavioral test	Description
Executive function frontal cortex and extra-frontal cortex (262)	Disorders in cognitive control of behavior, including basic cognitive processes such as attentional control, cognitive inhibition, inhibitory control, working memory, and cognitive flexibility.	Passive avoidance (263)	Mice learn to inhibit the natural tendency to explore new environments where a negative stimulus was previously obtained. The test consists of a chamber divided in two compartments separated by a gate. Animals are allowed to explore both compartments in the initial phase. In the following phase, they obtain a negative stimulus in one of the compartments. Animals will learn to associate certain properties of the chamber with the negative stimulus. The test measures the latency to cross the gate between the two compartments when the animal is placed in the compartment where no aversive stimulus were obtained.
		Simple maze task (258, 259)	See description in learning and memory.
		Morris water maze (71, 252, 264)	See description in learning and memory.
		Prepulse inhibition (265)	PPI is a neurological phenomenon in which a soft pre-stimulus (pre-pulse) inhibits the reaction of the animal to a subsequent strong stimulus (pulse) often using the startle reflex. Stimuli may be acoustic, tactile, or luminous.
Social behavior (251)	Poor social skills and inappropriate social interactions.	Observation (251)	Feeding difficulties in neonates and lack of parental care. Aggressive behaviors in adults and reversed behaviors between males and females.
Affective behavior (201)	Anxiety- and depressive-like behaviors (201)	Elevated-plus maze (266)	The device is made up of open arms and closed arms, crossed in the middle perpendicularly to each other. Mice have access to all of the arms. The number of entries into the open arms and the time spent in each arm are used as a measure of anxiety-like behavior.
		Forced-swim test (267)	The test is based on the assumption that an animal placed in a container filled with water will try to escape. However, it will eventually exhibit immobility that may be considered a measure of depressive-like behavior.
Olfaction (253)	Injury of the olfactory circuits.	Classical conditioning tasks (268)	An odor is paired with a tempting or aversive stimulus and the response of the animal to the odor is followed by the tester.

PAE, prenatal alcohol exposure.

Middaugh et al. characterized the impaired growth of C57BL/6 mice prenatally exposed to alcohol (271) showing the influence of alcohol on fetal growth when administered in the second and third trimester equivalents (271, 272).

Other authors have described the effects of ethanol on trophoblasts and placental permeability. Gundogan showed an altered branching morphogenesis in the labyrinthine zone and the suppression of invasive trophoblastic precursors. This altered process compromised fetal growth and placentation in a dose-response manner (69). The permeability inducer VEGF was up-regulated in mouse placenta after acute alcohol exposure. Permeability was also affected by altered structures in the barriers that separate feto-maternal blood circulation (273). Therefore, altered growth factors in conjunction with malformations of the placental barrier may contribute to placental malfunction and permeability alterations in the feto-maternal barrier.

Biomarkers for PAE

A biomarker is objectively measured and assessed as an indicator of a normal biological or pathogenic process, or a pharmacologic response to a therapeutic intervention (274). Here we will use the term biomarker as the molecular or genetic indicator that

identifies prenatal exposure to ethanol. In murine models, the researcher controls the dose and timing of alcohol exposure and eliminates other variables (e.g., other drugs) that may skew the results. This, and the possibility of getting multiple matrices from the rodents, will allow to obtain appropriate biomarkers for PAE detection.

Some authors have demonstrated a significant decrease of alpha-fetoprotein, a perinatal stress biomarker, in the amniotic fluid of B6J litters exposed to alcohol on Day 8 of gestation, although no differences were found in the B6N substrain (275). Other biomarkers, such as fatty acid ethyl esters (FAEEs), a product of non-oxidative ethanol metabolism and a validated biomarker for PAE, have been detected in mouse heart, liver, placenta, and fetal tissues, 1 h after maternal ethanol exposure. FAEEs were shown to persist for at least seven days in the placenta of the mice and at least 14 days in fetal rat organs (276). Unfortunately, FAEEs cannot be measured in neonatal rodents due to the lack of neonatal hair. By contrast, guinea pigs allow a good approximation since they are born with hair (277). Some authors have shown that FAEE concentrations in exposed offspring samples taken at PND 1 were more than 15-fold higher than their control counterparts (278).

On the other hand, changes in selective neurotransmitters from fetal brains of prenatal alcohol-treated C57BL/6 mice were also observed. Authors showed significant reductions in dopamine, norepinephrine, epinephrine, serotonin, and GABA levels in E13 fetal brains. These results would explain the main causes of abnormalities in brain function and behavior found in fetal alcohol spectrum disorders (279).

In recent years, epigenetic studies in rodents highlight the potential of DNA methylation, histone modification, or non-coding RNA species as biomarkers of PAE. Most of these studies have evaluated general changes for each epigenetic modification. DNA methylation has been the most analyzed marker for PAE-induced epigenetic dysregulation, showing that PAE promotes a global pattern of hypomethylation on fetal DNA during pregnancy affecting critical genes such as *bdnf* (280). Haycock et al. demonstrated that genomic imprinting was also deregulated by PAE, in mouse embryos (281). Low levels of *igf2* expression correlates with PAE due to a specific CpG hypomethylation found in its promoter region (224). *Pomc* expression in neurons, related to stress response, is also reduced by CpG hypermethylation in its promoter (282). The authors suggest that this alteration can be transmitted to offspring, raising the hypothesis that the effect of PAE not only occurs when the fetus is exposed to alcohol but also throughout its whole life and future progeny. Hence, the use of these epigenetic changes using CpG methylations as biomarkers of PAE may be a challenge to consider.

Regarding histone modifications, several studies have found PAE-specific alterations on PAE on H3K9ac, H3K4me2, H3K27me3, and H3K9me2, particularly in the brain. These changes are related to alcohol response mechanisms, e.g., H3K9ac, which has been shown to increase after PAE down-regulates genes related to alcohol response (283, 284). Moreover, the increase of H3K4me2 promotes the up-regulation of genes related to alcohol response (284). A general increase of H3K27me2 was observed in the brain in response to PAE (285), more specifically in the hippocampus and neocortex. H3K9me2 also increased after alcohol exposure suggesting persistent alterations in the expression pattern for a long period, and as such has it being considered as a potential biomarker of PAE (286).

Alterations in non-coding RNA expression following PAE have been assessed in rodents. Results show that PAE causes the suppression of several miRNA such as miR-21 and miR335 in fetal neuronal and progenitor stem cells (230, 287). PAE also suppresses the expression of miR-9 and miR-153 and increases the levels of miR-10a during pregnancy (287, 288). Similar results have been reported in zebrafish after PAE (289) and in a rodent model of alcohol use disorder (290). However, due to the heterogeneity, the low reproducibility and the lack of correlations in the results from the different studies, no consensus has been reached for non-coding RNA, showing the complexity of epigenetic interactions when they are altered by PAE.

Animal models play an important role in the identification and validation of new candidate biomarkers, e.g., selective neurotrasmitters, igf1, igf2, and miRNA. In humans, only the direct biomarkers fatty acid FAEEs, ethyl glucuronide, ethyl sulfate, and phosphatidylethanol in biological matrices are validated to detect PAE (291). The low levels of *igf2* expression after PAE (224) in mouse are in line with the results of a recent publication that compared the levels of IGF I and IGF II in the FASD pediatric population with children objectively non-exposed to ethanol (292). These results highlight the potential use of IGF-I and IGF-II as surrogate biomarkers of the damage induced by PAE. Furthermore, BDNF levels in rodent models are known to be disrupted during acute/chronic and prenatal alcohol consumption (293). Thus, changes of BDNF levels in the meconium, cord blood, or in the mother's/infant's serum are used as potential biomarkers of PAE in humans based on rodents results (293, 294). Moreover, magnetic resonance spectroscopy studies in rodents have shown that neurotransmitter biomarkers of FAS including choline, acetyl choline, N-acetyl aspartate, and glutamate, a precursor for the synthesis of GABA, are significantly reduced in FAS (295). Reduced levels of glutamate, taurine, and N-methyl D-aspartic acid receptor have also been observed in FAS children (296, 297). PAE alters the methionine-homocysteine pathway in rodents and humans. Thus, s-adenosylmethionine, which acts as donor of methyl groups to DNA methylases, may be a promising clinical biomarker of FASD (298).

DISCUSSION

FASD is a growing problem in our society. Diagnostic difficulties, limited knowledge on the underlying mechanisms of ethanol toxicity, and absence of effective strategies to treat this pathology is a serious medical matter. There is a wide range of FASD-like animal models, and researchers must be very precise and choose the one that suits best the objective of the study. Invertebrates and simple vertebrates allow alcohol exposure and the assessment of physical malformations and simple behaviors at different developmental periods (299). However,

when studying brain structures or complex behaviors, mammals offer significant advantages compared to the above mentioned models (19). Further insights on FASD is possible with murine models as they allow evaluating the specificity of dose-dependent alcohol teratogenic effects, the timing and developmental stage of fetuses, brain structures, and complex behaviors. Rodents are useful for exploring promising treatments that may help minimize the effects of PAE. C57BL/6 mice are one of the most commonly used mammals in FASD research because they are easy to handle when searching for malformations or complex behaviors after alcohol exposure. A wide range of precise methodologies and experimental protocols have been performed using these animal models. In this review, we have described and compared these protocols to provide a framework that allows researchers to make the correct choice of animal model in their research project.

Rodents and humans have similar stages of brain development, differing in birth timing. The third trimester equivalent in rodents is postnatal. It seems clear that facial dysmorphology appears when ethanol exposure occurs during first trimester equivalent (33, 60, 236, 300). However, it is difficult to establish the optimal period for ethanol exposure when brain and behavioral alterations are explored, because brain developmental processes occur continuously throughout the second and third trimester equivalent. The criteria to choose an appropriate FAS-like model will depend on the experimental design and research questions, for which different patterns of alcohol exposure, tissue analysis, molecular mechanisms, or cell types assessment will be needed.

The pattern of ethanol exposure and dosages are important parameters. Some studies support the hypothesis that a lower daily dose of alcohol administered in a binge-like pattern results in lower brain weight and greater cell loss than a higher daily dose administered in a non-binge-like pattern, as binge-like patterns lead to higher BAC peaks (24, 301).

It is essential to identify FASD manifestations in the experimental models to reach the objectives of the research. Different biomarkers are involved in the distinct stages of brain development (summarized in **Figure 1**), which can be of help when studying the effects of ethanol intake during pregnancy. FAS biomarkers are useful to evaluate the effects of experimental therapies. There is a wide spectrum of techniques to assess facial dysmorphology, e.g., the validated facial image analysis method based on a multi-angle image classification using micro-video images of mouse embryos (233), and other experimental novel techniques based on MicroCT 3D (244). To assess neurodevelopment and behavior of FASD-like rodent models, several standardized behavioral measurements have been described (302, 303) (summarized in **Table 2**), which allow evaluating the different spheres affected by PAE. When choosing the most appropriate test, the skills the researcher wants to analyze must be taken into consideration. The Morris water maze allows an accurate evaluation of a set of cognitive and motor behaviors affected by PAE. It is necessary to underline the existence of other useful alternatives to evaluate these behaviors.

Fetal growth is impaired by the harmful effects alcohol exerts on angiogenesis. Fetal growth restriction may be evaluated through standardized fetal measurements in defined frequency distribution curves (68), or by assessing the placenta using biomarkers and histopathological analysis.

The use of animal models results essential in pre-clinical studies to evaluate the toxicity of potential pharmacological tools. Animal models also provide an insight into the molecular mechanisms altered by alcohol as per the developmental timing of exposure, pattern of exposure, and dosage. Thus, any experimental breakthrough may be directly applied in clinical care to improve the diagnosis and treatment of FASD patients.

This review contains updated information on FAS-like model in rodents, aiming to be a useful reference for researchers working with FASD-like murine models. This is not a systematic review, although we have performed an in-depth narrative review on the topic. We have reviewed methodologies and protocols as per the objectives of the study in order to obtain robust conclusions for future studies. This work will facilitate decision-making when designing a FASD experiment in rodents by exploring and summarizing the currently available information on prenatal alcohol effects in each pregnancy equivalent trimester.

Additional knowledge on cellular, biochemical, genetic and molecular mechanisms, and pathways altered by PAE is necessary. This will allow further experimental research with murine models aiming to improve diagnostic strategies, prevention and treatment for alcohol-related problems.

AUTHOR CONTRIBUTIONS

LA and VA-F drafted the initial manuscript and conceptualized the topics, tables, and figures. MG-R, OG-A, VA-F, and LM conceptualized, designed, and coordinated the review. EN-T, LA, RA-L, and MS-D revised the different versions of the manuscript and prepared the figures and tables. All authors critically reviewed the manuscript and approved the final version for publication.

FUNDING

This work was supported by Red de Salud Materno-Infantil y del Desarrollo (SAMID) (RD12/0026/0003 and RD16/0022/0002) from Instituto de Salud Carlos III and the PI15/01179 grant from Instituto de Salud Carlos III.

ACKNOWLEDGMENTS

English language review/editing supplied by Dainora Jaloveckas (Ciencia Traducida—https://cienciatrad.wordpress.com/). We also want to thank Mrs. Luisa Martínez Colom for her support.

REFERENCES

1. Lemoine P, Harousseau H, Borteyru JP, Menuet JC. Les enfants des parents alcoholiques : anomolies observees à propos de 127 cas (The children of alcoholic parents: anomalies observed in 127 cases). *Quest Med.* (1968) 25:476–82. doi: 10.1097/00007691-200304000-00002
2. Jones K, Smith D. Recognition of the fetal alcohol syndrome in early infancy. *Lancet.* (1973) 302:999–1001. doi: 10.1016/S0140-6736(73)91092-1
3. Sokol RJ, Delaney-Black V, Nordstrom B. Fetal alcohol spectrum disorder. *JAMA.* (2003) 290:2996–9. doi: 10.1001/jama.290.22.2996
4. Sampson PD, Streissguth AP, Bookstein FL, Little RE, Clarren SK, Dehaene P, et al. Incidence of fetal alcohol syndrome and prevalence of alcohol-related neurodevelopmental disorder. *Teratology.* (1997) 56:317–26. doi: 10.1002/(SICI)1096-9926(199711)56:5<317::AID-TERA5>3.0.CO;2-U
5. Hoyme HE, Kalberg WO, Elliott AJ, Blankenship J, Buckley D, Marais A-S, et al. Updated clinical guidelines for diagnosing fetal alcohol spectrum disorders. *Pediatrics.* (2016) 138:e20154256. doi: 10.1542/peds.2015-4256
6. Sowell ER, Mattson SN, Thompson PM, Jernigan TL, Riley EP, Toga AW. Mapping callosal morphology and cognitive correlates: effects of heavy prenatal alcohol exposure. *Neurology.* (2001) 57:235–44. doi: 10.1212/WNL.57.2.235
7. Sowell ER, Jernigan TL, Mattson SN, Riley EP, Sobel DF, Jones KL. Abnormal development of the cerebellar vermis in children prenatally exposed to alcohol: size reduction in lobules I-V. *Alcohol Clin Exp Res.* (1996) 20:31–4. doi: 10.1111/j.1530-0277.1996.tb01039.x
8. Riikonen R, Salonen I, Partanen K, Verho S. Brain perfusion SPECT and MRI in foetal alcohol syndrome. *Dev Med Child Neurol.* (1999) 41:652–9. doi: 10.1017/S0012162299001358
9. Riley EP, Court A, Diego S, Warren KR. Fetal alcohol spectrum disorders: an overview. *Neuropsychol Rev.* (2011) 21:73–80. doi: 10.1007/s11065-011-9166-x
10. May PA, Gossage JP. Estimating the prevalence of fetal alcohol syndrome - a summary. *Alcohol Res Heal.* (2001) 25:159–67.
11. Lange S, Probst C, Gmel G, Rehm J, Burd L, Popova S. Global prevalence of fetal alcohol spectrum disorder among children and youth: a systematic review and meta-analysis. *JAMA Pediatr.* (2017) 171:948–56. doi: 10.1001/jamapediatrics.2017.1919
12. Cowan AE. Syndromes of intellectual disability. In: Gentile JP, Cowan AED, Editors. *Guide to Intellectual Disabilities.* Springer International Publishing. (2019). p. 203–13. doi: 10.1007/978-3-030-04456-5_15
13. Popova S, Lange S, Probst C, Gmel G, Rehm J. Estimation of national, regional, and global prevalence of alcohol use during pregnancy and fetal alcohol syndrome: a systematic review and meta-analysis. *Lancet Glob Heal.* (2017) 5:e290–9. doi: 10.1016/S2214-109X(17)30021-9
14. Marquardt K, Brigman JL. The impact of prenatal alcohol exposure on social, cognitive and affective behavioral domains: insights from rodent models. *Alcohol.* (2016) 51:1–15. doi: 10.1016/j.alcohol.2015.12.002
15. Davis JR, Li Y, Rankin CH. Effects of developmental exposure to ethanol on caenorhabditis elegans. *Alcohol Clin Exp Res.* (2008) 32:853–67. doi: 10.1111/j.1530-0277.2008.00639.x
16. Meyers JR. Zebrafish: development of a vertebrate model organism. *Curr Protoc Essent Lab Tech.* (2018) 16:e19. doi: 10.1002/cpet.19
17. Ali S, Champagne DL, Spaink HP, Richardson MK. Zebrafish embryos and larvae: a new generation of disease models and drug screens. *Birth Defects Res C Embryo Today Rev.* (2011) 93:115–33. doi: 10.1002/bdrc.20206
18. Loucks E, Ahlgren S. Assessing teratogenic changes in a zebrafish model of fetal alcohol exposure. *J Vis Exp.* (2012) 61:3704. doi: 10.3791/3704
19. Schneider ML, Moore CF, Adkins MM. The effects of prenatal alcohol exposure on behavior: rodent and primate studies. *Neuropsychol Rev.* (2011) 21:186–203. doi: 10.1007/s11065-011-9168-8
20. Boehm SL, Lundahl KR, Caldwell J, Gilliam DM. Ethanol teratogenesis in the C57BL/6J, DBA/2J, and A/J inbred mouse strains. *Alcohol.* (1997) 14:389–95. doi: 10.1016/S0741-8329(97)87950-5
21. Sulik K, Johnston M, Webb M. Fetal alcohol syndrome: embryogenesis in a mouse model. *Science.* (1981) 214:936–8. doi: 10.1126/science.6795717
22. Yoneyama N, Crabbe JC, Ford MM, Murillo A, Finn DA. Voluntary ethanol consumption in 22 inbred mouse strains. *Alcohol.* (2008) 42:149–60. doi: 10.1016/j.alcohol.2007.12.006
23. Kelly SJ, Pierce DR, West JR. Microencephaly and hyperactivity in adult rats can be induced by neonatal exposure to high blood alcohol concentrations. *Exp Neurol.* (1987) 96:580–93. doi: 10.1016/0014-4886(87)90220-2
24. Bonthius DJ, West JR. Alcohol-induced neuronal loss in developing rats: increased brain damage with binge exposure. *Alcohol Clin Exp Res.* (1990) 14:107–18. doi: 10.1111/j.1530-0277.1990.tb00455.x
25. Dreosti IE. Nutritional factors underlying the expression of the fetal alcohol syndrome. *Ann N Y Acad Sci.* (1993) 678:193–204. doi: 10.1111/j.1749-6632.1993.tb26122.x
26. Fisher SE. Selective fetal malnutrition: the fetal alcohol syndrome. *J Am Coll Nutr.* (1988) 7:101–6. doi: 10.1080/07315724.1988.10720225
27. Sebastiani G, Borrás-Novell C, Casanova MA, Tutusaus MP, Martínez SF, Roig MDG, et al. The effects of alcohol and drugs of abuse on maternal nutritional profile during pregnancy. *Nutrients.* (2018) 10:1008. doi: 10.3390/nu10081008
28. Berman RF, Hannigan JH. Effects of prenatal alcohol exposure on the hippocampus: Spatial behavior, electrophysiology, and neuroanatomy. *Hippocampus.* (2000) 10:94–110. doi: 10.1002/(SICI)1098-1063(2000)10:1<94::AID-HIPO11>3.0.CO;2-T
29. Gil-Mohapel J, Boehme F, Patten A, Cox A, Kainer L, Giles E, et al. Altered adult hippocampal neuronal maturation in a rat model of fetal alcohol syndrome. *Brain Res.* (2011) 1384:29–41. doi: 10.1016/j.brainres.2011.01.116
30. Kleiber ML, Wright E, Singh SM. Maternal voluntary drinking in C57BL/6J mice: advancing a model for fetal alcohol spectrum disorders. *Behav Brain Res.* (2011) 223:376–87. doi: 10.1016/j.bbr.2011.05.005
31. Choi IY, Allan AM, Cunningham LA. Moderate fetal alcohol exposure impairs the neurogenic response to an enriched environment in adult mice. *Alcohol Clin Exp Res.* (2005) 29:2053–62. doi: 10.1097/01.alc.0000187037.02670.59
32. Pal N, Alkana RL. Use of inhalation to study the effect of ethanol and ethanol dependence on neonatal mouse development without maternal separation: a preliminary study. *Life Sci.* (1997) 61:1269–81. doi: 10.1016/S0024-3205(97)00672-3
33. Godin EA, O'Leary-Moore SK, Khan AA, Parnell SE, Ament JJ, Dehart DB, et al. Magnetic resonance microscopy defines ethanol-induced brain abnormalities in prenatal mice: effects of acute insult on gestational day 7. *Alcohol Clin Exp Res.* (2010) 34:98–111. doi: 10.1111/j.1530-0277.2009.01071.x
34. Beierle EA, Chen MK, Hartwich JE, Iyengar M, Dai W, Li N, et al. Artificial rearing of mouse pups: development of a mouse pup in a cup model. *Pediatr Res.* (2004) 56:250–5. doi: 10.1203/01.PDR.0000132753.81333.39
35. Boehme F, Gil-Mohapel J, Cox A, Patten A, Giles E, Brocardo PS, et al. Voluntary exercise induces adult hippocampal neurogenesis and BDNF expression in a rodent model of fetal alcohol spectrum disorders. *Eur J Neurosci.* (2011) 33:1799–811. doi: 10.1111/j.1460-9568.2011.07676.x
36. Allan AM, Chynoweth J, Tyler LA, Caldwell KK. A mouse model of prenatal ethanol exposure using a voluntary drinking paradigm. *Alcohol Clin Exp Res.* (2003) 27:2009–16. doi: 10.1097/01.ALC.0000100940.95053.72
37. Lieber CS, DeCarli LM. The feeding of alcohol in liquid diets: two decades of applications and 1982 update. *Alcohol Clin Exp Res.* (1982) 6:523–31. doi: 10.1111/j.1530-0277.1982.tb05017.x
38. Cassells B, Wainwright P, Blom K. Heredity and alcohol-induced brain anomalies: effects of alcohol on anomalous prenatal development of the corpus callosum and anterior commissure in BALB c and C57BL 6 mice. *Exp Neurol.* (1987) 95:587–604. doi: 10.1016/0014-4886(87)90301-3
39. Thiele TE, Crabbe JC, Boehm SL. Drinking in the dark (DID): a simple mouse model of binge-like alcohol intake. *Curr Protoc Neurosci.* (2014) 68:9491. doi: 10.1002/0471142301.ns0949s68
40. Bertola A, Mathews S, Ki SH, Wang H, Gao B. Mouse model of chronic and binge ethanol feeding (the NIAAA model). *Nat Protoc.* (2013) 8:627–37. doi: 10.1038/nprot.2013.032
41. Sidhu H, Kreifeldt M, Contet C. Affective disturbances during withdrawal from chronic intermittent ethanol inhalation in C57BL/6J and DBA/2J male mice. *Alcohol Clin Exp Res.* (2018) 42:1281–90. doi: 10.1111/acer.13760
42. Maldonado-Devincci AM, Kampov-Polevoi A, McKinley RE, Morrow DH, O'Buckley TK, Morrow AL. Chronic intermittent ethanol exposure alters stress effects on (3α,5α)-3-hydroxy-pregnan-20-one (3α,5α-THP) immunolabeling of amygdala neurons in C57BL/6J

Mice. *Front Cell Neurosci.* (2016) 10:40. doi: 10.3389/fncel.2016.00040
43. Webster WS, Walsh DA, McEwen SE, Lipson AH. Some teratogenic properties of ethanol and acetaldehyde in C57BL/6J mice: implications for the study of the fetal alcohol syndrome. *Teratology.* (1983) 27:231–43. doi: 10.1002/tera.1420270211
44. Bonthius DJ, West JR. Blood alcohol concentration and microencephaly: a dose-response study in the neonatal rat. *Teratology.* (1988) 37:223–31. doi: 10.1002/tera.1420370307
45. Gil-Mohapel J, Boehme F, Kainer L, Christie BR. Hippocampal cell loss and neurogenesis after fetal alcohol exposure: Insights from different rodent models. *Brain Res Rev.* (2010) 64:283–303. doi: 10.1016/j.brainresrev.2010.04.011
46. Abel EL. Alcohol-induced changes in blood gases, glucose, and lactate in pregnant and nonpregnant rats. *Alcohol.* (1996) 13:281–5. doi: 10.1016/0741-8329(95)02056-X
47. Hannigan JH. What research with animals is telling us about alcohol-related neurodevelopmental disorder. *Pharmacol Biochem Behav.* (1996) 55:489–99. doi: 10.1016/S0091-3057(96)00251-1
48. Zailer E, Diehl BWK. Alternative determination of blood alcohol concentration by 1H NMR spectroscopy. *J Pharm Biomed Anal.* (2016) 119:59–64. doi: 10.1016/j.jpba.2015.11.030
49. Serbus DC, Young MW, Light KE. Blood ethanol concentrations following intragastric intubation of neonatal rat pups. *Neurobehav Toxicol Teratol.* (1986) 8:403–6.
50. Livy DJ, Parnell SE, West JR. Blood ethanol concentration profiles: a comparison between rats and mice. *Alcohol.* (2003) 29:165–71. doi: 10.1016/S0741-8329(03)00025-9
51. Miller MW. Limited ethanol exposure selectively alters the proliferation of precursor cells in the cerebral cortex. *Alcohol Clin Exp Res.* (1996) 20:139–43. doi: 10.1111/j.1530-0277.1996.tb01056.x
52. Miller MW. Migration of cortical neurons is altered by gestational exposure to ethanol. *Alcohol Clin Exp Res.* (1993) 17:304–14. doi: 10.1111/j.1530-0277.1993.tb00768.x
53. Vallés S, Sancho-Tello M, Miñana R, Climent E, Renau-Piqueras J, Guerri C. Glial fibrillary acidic protein expression in rat brain and in radial glia culture is delayed by prenatal ethanol exposure. *J Neurochem.* (1996) 67:2425–33. doi: 10.1046/j.1471-4159.1996.67062425.x
54. Lancaster F, Delaney C, Samorajski T. Synaptic density of caudate-putamen and visual cortex following exposure to ethanol in utero. *Int J Dev Neurosci.* (1989) 7:581–9. doi: 10.1016/0736-5748(89)90017-8
55. Volk B. Cerebellar histogenesis and synaptic maturation following pre- and postnatal alcohol administration. An electron-microscopic investigation of the rat cerebellar cortex. *Acta Neuropathol.* (1984) 63:57–65. doi: 10.1007/BF00688471
56. Lancaster FE, Mayur BK, Patsalos PN, Samorajski T, Wiggins RC. The synthesis of myelin and brain subcellular membrane proteins in the offspring of rats fed ethanol during pregnancy. *Brain Res.* (1982) 235:105–13. doi: 10.1016/0006-8993(82)90199-8
57. Hoffman PL, Tabakoff B. To be or not to be: how ethanol can affect neuronal death during development. *Alcohol Clin Exp Res.* (1996) 20:193–5. doi: 10.1111/j.1530-0277.1996.tb01065.x
58. Liesi P. Ethanol-exposed central neurons fail to migrate and undergo apoptosis. *J Neurosci Res.* (1997) 48:439–48. doi: 10.1002/(SICI)1097-4547(19970601)48:5<439::AID-JNR5>3.0.CO;2-F
59. West JR. Fetal alcohol-induced brain damage and the problem of determining temporal vulnerability: a review. *Alcohol Drug Res.* (1987) 7:423–41. doi: 10.1080/09595238880000141
60. Lipinski RJ, Hammond P, O'Leary-Moore SK, Ament JJ, Pecevich SJ, Jiang Y, et al. Ethanol-induced face-brain dysmorphology patterns are correlative and exposure-stage dependent. *PLoS ONE.* (2012) 7:e43067. doi: 10.1371/journal.pone.0043067
61. Sulik KK, Johnston MC. Sequence of developmental alterations following acute ethanol exposure in mice: craniofacial features of the fetal alcohol syndrome. *Am J Anat.* (1983) 166:257–69. doi: 10.1002/aja.1001660303
62. Parnell SE, Holloway HE, Baker LK, Styner MA, Sulik KK. Dysmorphogenic effects of first trimester-equivalent ethanol exposure in mice: a magnetic resonance microscopy-based study. *Alcohol Clin Exp Res.* (2014) 38:2008–14. doi: 10.1111/acer.12464
63. Cao W, Li W, Han H, O'Leary-Moore SK, Sulik KK, Allan Johnson G, et al. Prenatal alcohol exposure reduces magnetic susceptibility contrast and anisotropy in the white matter of mouse brains. *Neuroimage.* (2014) 102:748–55. doi: 10.1016/j.neuroimage.2014.08.035
64. Nirgudkar P, Taylor DH, Yanagawa Y, Valenzuela CF. Ethanol exposure during development reduces GABAergic/glycinergic neuron numbers and lobule volumes in the mouse cerebellar vermis. *Neurosci Lett.* (2016) 632:86–91. doi: 10.1016/j.neulet.2016.08.039
65. El Shawa H, Abbott CW, Huffman KJ. Prenatal ethanol exposure disrupts intraneocortical circuitry, cortical gene expression, and behavior in a mouse model of FASD. *J Neurosci.* (2013) 33:18893–905. doi: 10.1523/JNEUROSCI.3721-13.2013
66. Kajimoto K, Allan A, Cunningham LA. Fate analysis of adult hippocampal progenitors in a murine model of fetal alcohol spectrum disorder (FASD). *PLoS ONE.* (2013) 8:e73788. doi: 10.1371/journal.pone.0073788
67. Morton RA, Diaz MR, Topper LA, Valenzuela CF. Construction of vapor chambers used to expose mice to alcohol during the equivalent of all three trimesters of human development. *J Vis Exp.* (2014) 89:51839. doi: 10.3791/51839
68. Dilworth MR, Kusinski LC, Baker BC, Renshall LJ, Greenwood SL, Sibley CP, et al. Defining fetal growth restriction in mice: a standardized and clinically relevant approach. *Placenta.* (2011) 32:914–6. doi: 10.1016/j.placenta.2011.08.007
69. Gundogan F, Gilligan J, Qi W, Chen E, Naram R, De La Monte SM. Dose effect of gestational ethanol exposure on placentation and fetal growth. *Placenta.* (2015) 36:523–30. doi: 10.1016/j.placenta.2015.02.010
70. Coleman LG, Oguz I, Lee J, Styner M, Crews FT. Postnatal day 7 ethanol treatment causes persistent reductions in adult mouse brain volume and cortical neurons with sex specific effects on neurogenesis. *Alcohol.* (2012) 46:603–12. doi: 10.1016/j.alcohol.2012.01.003
71. Karacay B, Mahoney J, Plume J, Bonthius DJ. Genetic absence of nNOS worsens fetal alcohol effects in mice. II: microencephaly and neuronal losses. *Alcohol Clin Exp Res.* (2015) 39:221–31. doi: 10.1111/acer.12615
72. Smiley JF, Saito M, Bleiwas C, Masiello K, Ardekani B, Guilfoyle DN, et al. Selective reduction of cerebral cortex GABA neurons in a late gestation model of fetal alcohol spectrum disorder. *Alcohol.* (2015) 49:571–80. doi: 10.1016/j.alcohol.2015.04.008
73. Wilson DA, Masiello K, Lewin MP, Hui M, Smiley JF, Saito M. Developmental ethanol exposure-induced sleep fragmentation predicts adult cognitive impairment. *Neuroscience.* (2016) 322:18–27. doi: 10.1016/j.neuroscience.2016.02.020
74. Brocardo PS, Gil-Mohapel J, Wortman R, Noonan A, McGinnis E, Patten AR, et al. The effects of ethanol exposure during distinct periods of brain development on oxidative stress in the adult rat brain. *Alcohol Clin Exp Res.* (2017) 41:26–37. doi: 10.1111/acer.13266
75. May PA, Blankenship J, Marais AS, Gossage JP, Kalberg WO, Joubert B, et al. Maternal alcohol consumption producing fetal alcohol spectrum disorders (FASD): quantity, frequency, and timing of drinking. *Drug Alcohol Depend.* (2013) 133:502–12. doi: 10.1016/j.drugalcdep.2013.07.013
76. Dobbing J, Sands J. Comparative aspects of the brain growth spurt. *Early Hum Dev.* (1979) 3:79–83. doi: 10.1016/0378-3782(79)90022-7
77. Zohn IE, Sarkar AA. Modeling neural tube defects in the mouse. *Curr Top Dev Biol.* (2008) 84:1–35. doi: 10.1016/S0070-2153(08)00601-7
78. Goodlett CR, Leo JT, O'Callaghan JP, Mahoney JC, West JR. Transient cortical astrogliosis induced by alcohol exposure during the neonatal brain growth spurt in rats. *Dev Brain Res.* (1993) 72:85–97. doi: 10.1016/0165-3806(93)90162-4
79. Cantacorps L, Alfonso-Loeches S, Moscoso-Castro M, Cuitavi J, Gracia-Rubio I, López-Arnau R, et al. Maternal alcohol binge drinking induces persistent neuroinflammation associated with myelin damage and behavioural dysfunctions in offspring mice. *Neuropharmacology.* (2017) 123:368–84. doi: 10.1016/j.neuropharm.2017.05.034
80. Angevine JB, Bodian D, Coulombre AJ, Edds MV, Hamburger V, Jacobson M, et al. Embryonic vertebrate central nervous system: revised terminology. *Anat Rec.* (1970) 166:257–61. doi: 10.1002/ar.1091660214

81. Reynolds AR, Saunders MA, Berry JN, Sharrett-Field LJ, Winchester S, Prendergast MA. Broad-spectrum protein kinase inhibition by the staurosporine analog KT-5720 reverses ethanol withdrawal-associated loss of NeuN/Fox-3. *Alcohol.* (2017) 64:37–43. doi: 10.1016/j.alcohol.2017.05.006
82. Ji Z, Yuan L, Lu X, Ding H, Luo J, Ke ZJ. Binge alcohol exposure causes neurobehavioral deficits and GSK3β activation in the hippocampus of adolescent rats. *Sci Rep.* (2018) 8:3088. doi: 10.1038/s41598-018-21341-w
83. Klintsova AY, Helfer JL, Calizo LH, Dong WK, Goodlett CR, Greenough WT. Persistent impairment of hippocampal neurogenesis in young adult rats following early postnatal alcohol exposure. *Alcohol Clin Exp Res.* (2007) 31:2073–82. doi: 10.1111/j.1530-0277.2007.00528.x
84. Livy DJ, Miller EK, Maier SE, West JR. Fetal alcohol exposure and temporal vulnerability: effects of binge-like alcohol exposure on the developing rat hippocampus. *Neurotoxicol Teratol.* (2003) 25:447–58. doi: 10.1016/S0892-0362(03)00030-8
85. Maier SE, West JR. Regional differences in cell loss associated with binge-like alcohol exposure during the first two trimesters equivalent in the rat. *Alcohol.* (2001) 23:49–57. doi: 10.1016/S0741-8329(00)00133-6
86. Komada M, Hara N, Kawachi S, Kawachi K, Kagawa N, Nagao T, et al. Mechanisms underlying neuro-inflammation and neurodevelopmental toxicity in the mouse neocortex following prenatal exposure to ethanol. *Sci Rep.* (2017) 7:4934. doi: 10.1038/s41598-017-04289-1
87. West JR, Hamre KM, Cassell MD. Effects of ethanol exposure during the third trimester equivalent on neuron number in rat hippocampus and dentate gyrus. *Alcohol Clin Exp Res.* (1986) 10:190–7. doi: 10.1111/j.1530-0277.1986.tb05070.x
88. Redila VA, Olson AK, Swann SE, Mohades G, Webber AJ, Weinberg J, et al. Hippocampal cell proliferation is reduced following prenatal ethanol exposure but can be rescued with voluntary exercise. *Hippocampus.* (2006) 16:305–11. doi: 10.1002/hipo.20164
89. Gil-Mohapel J, Titterness AK, Patten AR, Taylor S, Ratzlaff A, Ratzlaff T, et al. Prenatal ethanol exposure differentially affects hippocampal neurogenesis in the adolescent and aged brain. *Neuroscience.* (2014) 273:174–88. doi: 10.1016/j.neuroscience.2014.05.012
90. Delatour LC, Yeh PW, Yeh HH. Ethanol exposure in utero disrupts radial migration and pyramidal cell development in the somatosensory cortex. *Cereb Cortex.* (2019) 29:2125–39. doi: 10.1093/cercor/bhy094
91. Leroy K, Brion JP. Developmental expression and localization of glycogen synthase kinase-3β in rat brain. *J Chem Neuroanat.* (1999) 16:279–93. doi: 10.1016/S0891-0618(99)00012-5
92. Coyle-Rink J, Del Valle L, Sweet T, Khalili K, Amini S. Developmental expression of Wnt signaling factors in mouse brain. *Cancer Biol Ther.* (2002) 1:640–5. doi: 10.4161/cbt.313
93. Luo J. GSK3β in ethanol neurotoxicity. *Mol Neurobiol.* (2009) 40:108–21. doi: 10.1007/s12035-009-8075-y
94. Resnicoff M, Sell C, Ambrose D, Baserga R, Rubin R. Ethanol inhibits the autophosphorylation of the insulin-like growth factor 1 (IGF-1) receptor and IGF-1-mediated proliferation of 3T3 cells. *J Biol Chem.* (1993) 268:21777–82.
95. O'Rourke NA, Dailey ME, Smith SJ, McConnell SK. Diverse migratory pathways in the developing cerebral cortex. *Science.* (1992) 258:299–302. doi: 10.1126/science.1411527
96. Vorhees C V. Principles of behavioral teratology. In: Riley EP, Vorhees CV Editors. *Handbook of Behavioral Teratology*. Boston, MA: Springer US. (1986). p. 23–48. doi: 10.1007/978-1-4613-2189-7_2
97. Stagni F, Giacomini A, Guidi S, Ciani E, Bartesaghi R. Timing of therapies for down syndrome: the sooner, the better. *Front Behav Neurosci.* (2015) 9:265. doi: 10.3389/fnbeh.2015.00265
98. González-Billault C, Del Río JA, Ureña JM, Jiménez-Mateos EM, Barallobre MJ, Pascual M, et al. A role of MAP1B in reelin-dependent neuronal migration. *Cereb Cortex.* (2005) 15:1134–45. doi: 10.1093/cercor/bhh213
99. Chen G, Bower KA, Xu M, Ding M, Shi X, Ke ZJ, et al. Cyanidin-3-glucoside reverses ethanol-induced inhibition of neurite outgrowth: role of glycogen synthase kinase 3 beta. *Neurotox Res.* (2009) 15:321–31. doi: 10.1007/s12640-009-9036-y
100. Martinowich K, Hattori D, Wu H, Fouse S, He F, Hu Y, et al. DNA methylation-related chromatin remodeling in activity-dependent BDNF gene regulation. *Science.* (2003) 302:890–3. doi: 10.1126/science.1090842
101. Horike SI, Cai S, Miyano M, Cheng JF, Kohwi-Shigematsu T. Loss of silent-chromatin looping and impaired imprinting of DLX5 in Rett syndrome. *Nat Genet.* (2005) 37:31–40. doi: 10.1038/ng1491
102. Zhang P, Wang G, Lin Z, Wu Y, Zhang J, Liu M, et al. Alcohol exposure induces chick craniofacial bone defects by negatively affecting cranial neural crest development. *Toxicol Lett.* (2017) 281:53–64. doi: 10.1016/j.toxlet.2017.09.010
103. Skorput AGJ, Yeh HH. Chronic gestational exposure to ethanol leads to enduring aberrances in cortical form and function in the medial prefrontal cortex. *Alcohol Clin Exp Res.* (2016) 40:1479–88. doi: 10.1111/acer.13107
104. Eagleson KL, Lillien L, Chan A V, Levitt P. Mechanisms specifying area fate in cortex include cell-cycle-dependent decisions and the capacity of progenitors to express phenotype memory. *Development.* (1997) 124:1623–30.
105. McConnell SK. The specification of neuronal identity in the mammalian cerebral cortex. *Experientia.* (1990) 46:922–9. doi: 10.1007/BF01939385
106. Martín-Ibáñez R, Guardia I, Pardo M, Herranz C, Zietlow R, Vinh N-N, et al. Insights in spatio-temporal characterization of human fetal neural stem cells. *Exp Neurol.* (2017) 291:20–35. doi: 10.1016/j.expneurol.2017.01.011
107. Gage FH. Mammalian neural stem cells. *Science.* (2000) 287:1433–8. doi: 10.1126/science.287.5457.1433
108. Olateju OI, Spocter MA, Patzke N, Ihunwo AO, Manger PR. Hippocampal neurogenesis in the C57BL/6J mice at early adulthood following prenatal alcohol exposure. *Metab Brain Dis.* (2018) 33:397–410. doi: 10.1007/s11011-017-0156-4
109. Broadwater MA, Liu W, Crews FT, Spear LP. Persistent loss of hippocampal neurogenesis and increased cell death following adolescent, but not adult, chronic ethanol exposure. *Dev Neurosci.* (2014) 36:297–305. doi: 10.1159/000362874
110. Elibol-Can B, Dursun I, Telkes I, Kilic E, Canan S, Jakubowska-Dogru E. Examination of age-dependent effects of fetal ethanol exposure on behavior, hippocampal cell counts, and doublecortin immunoreactivity in rats. *Dev Neurobiol.* (2014) 74:498–513. doi: 10.1002/dneu.22143
111. Hamilton GF, Bucko PJ, Miller DS, DeAngelis RS, Krebs CP, Rhodes JS. Behavioral deficits induced by third-trimester equivalent alcohol exposure in male C57BL/6J mice are not associated with reduced adult hippocampal neurogenesis but are still rescued with voluntary exercise. *Behav Brain Res.* (2016) 314:96–105. doi: 10.1016/j.bbr.2016.07.052
112. Rashid MA, Kim H-Y. N-Docosahexaenoylethanolamine ameliorates ethanol-induced impairment of neural stem cell neurogenic differentiation. *Neuropharmacology.* (2016) 102:174–85. doi: 10.1016/j.neuropharm.2015.11.011
113. Gobejishvili L, Barve S, Joshi-Barve S, Uriarte S, Song Z, McClain C. Chronic ethanol-mediated decrease in cAMP primes macrophages to enhanced LPS-inducible NF-κB activity and TNF expression: relevance to alcoholic liver disease. *Am J Physiol Liver Physiol.* (2006) 291:G681–8. doi: 10.1152/ajpgi.00098.2006
114. Hoffman PL, Tabakoff B. Ethanol and guanine nucleotide binding proteins: a selective interaction. *FASEB J.* (1990) 4:2612–22. doi: 10.1096/fasebj.4.9.2161371
115. Rabin RA. Chronic ethanol exposure of PC 12 cells alters adenylate cyclase activity and intracellular cyclic AMP content. *J Pharmacol Exp Ther.* (1990) 252:1021–7.
116. Spittaels K, Van den Haute C, Van Dorpe J, Geerts H, Mercken M, Bruynseels K, et al. Glycogen synthase kinase-3β phosphorylates protein tau and rescues the axonopathy in the central nervous system of human four-repeat tau transgenic mice. *J Biol Chem.* (2000) 275:41340–9. doi: 10.1074/jbc.M006219200
117. Faccidomo S, Besheer J, Stanford PC, Hodge CW. Increased operant responding for ethanol in male C57BL/6J mice: specific regulation by the ERK1/2, but not JNK, MAP kinase pathway. *Psychopharmacology.* (2009) 204:135–47. doi: 10.1007/s00213-008-1444-9
118. Villegas SN, Njaine B, Linden R, Carri NG. Glial-derived neurotrophic factor (GDNF) prevents ethanol (EtOH) induced B92 glial cell death by both PI3K/AKT and MEK/ERK signaling pathways. *Brain Res Bull.* (2006) 71:116–26. doi: 10.1016/j.brainresbull.2006.08.014

119. Ahmadiantehrani S, Barak S, Ron D. GDNF is a novel ethanol-responsive gene in the VTA: implications for the development and persistence of excessive drinking. *Addict Biol.* (2014) 19:623–33. doi: 10.1111/adb.12028
120. Maier HB, Neyazi M, Neyazi A, Hillemacher T, Pathak H, Rhein M, et al. Alcohol consumption alters Gdnf promoter methylation and expression in rats. *J Psychiatr Res.* (2020) 121:1–9. doi: 10.1016/j.jpsychires.2019.10.020
121. Guerri C, Pascual M, Renau-Piqueras J. Glia and fetal alcohol syndrome. *Neurotoxicology.* (2001) 22:593–9. doi: 10.1016/S0161-813X(01)00037-7
122. González A, Pariente JA, Salido GM. Ethanol stimulates ROS generation by mitochondria through Ca2+ mobilization and increases GFAP content in rat hippocampal astrocytes. *Brain Res.* (2007) 1178:28–37. doi: 10.1016/j.brainres.2007.08.040
123. Sáez R, Burgal M, Renau-Piqueras J, Marqués A, Guerri C. Evolution of several cytoskeletal proteins of astrocytes in primary culture: effect of prenatal alcohol exposure. *Neurochem Res.* (1991) 16:737–47. doi: 10.1007/BF00965682
124. Fletcher TL, Shain W. Ethanol-induced changes in astrocyte gene expression during rat central nervous system development. *Alcohol Clin Exp Res.* (1993) 17:993–1001. doi: 10.1111/j.1530-0277.1993.tb05654.x
125. Goodlett CR, Peterson SD, Lundahl KR, Pearlman AD. Binge-like alcohol exposure of neonatal rats via intragastric intubation induces both Purkinje cell loss and cortical astrogliosis. *Alcohol Clin Exp Res.* (1997) 21:1010–7. doi: 10.1111/j.1530-0277.1997.tb04246.x
126. Topper LA, Baculis BC, Valenzuela CF. Exposure of neonatal rats to alcohol has differential effects on neuroinflammation and neuronal survival in the cerebellum and hippocampus. *J Neuroinflammation.* (2015) 12:160. doi: 10.1186/s12974-015-0382-9
127. Lundgaard I, Wang W, Eberhardt A, Vinitsky HS, Reeves BC, Peng S, et al. Beneficial effects of low alcohol exposure, but adverse effects of high alcohol intake on glymphatic function. *Sci Rep.* (2018) 8:2246. doi: 10.1038/s41598-018-20424-y
128. Alfonso-Loeches S, Ureña-Peralta JR, Morillo-Bargues MJ, La Cruz JO De, Guerri C. Role of mitochondria ROS generation in ethanol-induced NLRP3 inflammasome activation and cell death in astroglial cells. *Front Cell Neurosci.* (2014) 8:216. doi: 10.3389/fncel.2014.00216
129. Marshak DR. S100 beta as a neurotrophic factor. *Prog Brain Res.* (1990) 86:169–81. doi: 10.1016/S0079-6123(08)63175-1
130. Wilhelm CJ, Hashimoto JG, Roberts ML, Bloom SH, Andrew MR, Wiren KM. Astrocyte dysfunction induced by alcohol in females but not males. *Brain Pathol.* (2016) 26:433–51. doi: 10.1111/bpa.12276
131. Ogony JW, Malahias E, Vadigepalli R, Anni H. Ethanol alters the balance of Sox2, Oct4, and nanog expression in distinct subpopulations during differentiation of embryonic stem cells. *Stem Cells Dev.* (2013) 22:2196–210. doi: 10.1089/scd.2012.0513
132. Jacobson M. Formation of dendrites and development of synaptic connections. In: Rao MS, Jacobson M, Editors. *Developmental Neurobiology*. Boston, MA: Springer US. (1991). p. 223–83. doi: 10.1007/978-1-4757-4954-0_6
133. Kentroti S, Rahman H, Grove J, Vernadakis A. Ethanol neuronotoxicity in the embryonic chick brain in ovo and in culture: interaction of the neural cell adhesion molecule (NCAM). *Int J Dev Neurosci.* (1995) 13:859–70. doi: 10.1016/0736-5748(95)00065-8
134. Dou X, Menkari C, Mitsuyama R, Foroud T, Wetherill L, Hammond P, et al. L1 coupling to ankyrin and the spectrin-actin cytoskeleton modulates ethanol inhibition of L1 adhesion and ethanol teratogenesis. *FASEB J.* (2018) 32:1364–74. doi: 10.1096/fj.201700970
135. Miller MW, Luo J. Effects of ethanol and transforming growth factor beta (TGF beta) on neuronal proliferation and nCAM expression. *Alcohol Clin Exp Res.* (2002) 26:1281–125. doi: 10.1111/j.1530-0277.2002.tb02668.x
136. Mahabir S, Chatterjee D, Misquitta K, Chatterjee D, Gerlai R. Lasting changes induced by mild alcohol exposure during embryonic development in BDNF, NCAM and synaptophysin-positive neurons quantified in adult zebrafish. *Eur J Neurosci.* (2018) 47:1457–73. doi: 10.1111/ejn.13975
137. Miñana R, Climent E, Barettino D, Segui JM, Renau-Piqueras J, Guerri C. Alcohol exposure alters the expression pattern of neural cell adhesion molecules during brain development. *J Neurochem.* (2000) 75:954–64. doi: 10.1046/j.1471-4159.2000.0750954.x
138. Littner Y, Tang N, He M, Bearer CF. L1 cell adhesion molecule signaling is inhibited by ethanol *in vivo*. *Alcohol Clin Exp Res.* (2013) 37:383–9. doi: 10.1111/j.1530-0277.2012.01944.x
139. Watson WE. Physiology of neuroglia. *Physiol Rev.* (1974) 54:245–71. doi: 10.1152/physrev.1974.54.2.245
140. Soriano E, Alvarado-Mallart RM, Dumesnil N, Del Río JA, Sotelo C. Cajal-retzius cells regulate the radial glia phenotype in the adult and developing cerebellum and alter granule cell migration. *Neuron.* (1997) 18:563–77. doi: 10.1016/S0896-6273(00)80298-6
141. Cuadros MA, Navascués J. The origin and differentiation of microglial cells during development. *Prog Neurobiol.* (1998) 56:173–89. doi: 10.1016/S0301-0082(98)00035-5
142. Oluich LJ, Stratton JAS, Xing YL, Ng SW, Cate HS, Sah P, et al. Targeted ablation of oligodendrocytes induces axonal pathology independent of overt demyelination. *J Neurosci.* (2012) 32:8317–30. doi: 10.1523/JNEUROSCI.1053-12.2012
143. Salzer JL. Schwann cell myelination. *Cold Spring Harb Perspect Biol.* (2015) 7:a020529. doi: 10.1101/cshperspect.a020529
144. From R, Eilam R, Bar-Lev DD, Levin-Zaidman S, Tsoory M, Lopresti P, et al. Oligodendrogenesis and myelinogenesis during postnatal development effect of glatiramer acetate. *Glia.* (2014) 62:649–65. doi: 10.1002/glia.22632
145. Miller RH, Ono K. Morphological analysis of the early stages of oligodendrocyte development in the vertebrate central nervous system. *Microsc Res Tech.* (1998) 41:441–53. doi: 10.1002/(SICI)1097-0029(19980601)41:5<441::AID-JEMT10>3.0.CO;2-N
146. Wiggins RC. Myelin development and nutritional insufficiency. *Brain Res.* (1982) 257:151–75. doi: 10.1016/0165-0173(82)90016-9
147. Feng MJ, Yan SE, Yan QS. Effects of prenatal alcohol exposure on brain-derived neurotrophic factor and its receptor tyrosine kinase B in offspring. *Brain Res.* (2005) 1042:125–32. doi: 10.1016/j.brainres.2005.02.017
148. Moore DB, Madorsky I, Paiva M, Heaton MB. Ethanol exposure alters neurotrophin receptor expression in the rat central nervous system: effects of neonatal exposure. *J Neurobiol.* (2004) 60:114–26. doi: 10.1002/neu.20010
149. Lessmann V, Gottmann K, Malcangio M. Neurotrophin secretion: current facts and future prospects. *Progr Neurobiol.* (2003) 69:341–74. doi: 10.1016/S0301-0082(03)00019-4
150. Montesinos J, Pascual M, Pla A, Maldonado C, Rodríguez-Arias M, Miñarro J, et al. TLR4 elimination prevents synaptic and myelin alterations and long-term cognitive dysfunctions in adolescent mice with intermittent ethanol treatment. *Brain Behav Immun.* (2015) 45:233–44. doi: 10.1016/j.bbi.2014.11.015
151. Koob GF. Alcoholism: allostasis and Beyond. *Alcohol Clin Exp Res.* (2003) 27:232–43. doi: 10.1097/01.ALC.0000057122.36127.C2
152. Drissi I, Deschamps C, Fouquet G, Alary R, Peineau S, Gosset P, et al. Memory and plasticity impairment after binge drinking in adolescent rat hippocampus: GluN2A/GluN2B NMDA receptor subunits imbalance through HDAC2. *Addict Biol.* (2019) 25:e12760. doi: 10.1111/adb.12760
153. Fiore M, Laviola G, Aloe L, di Fausto V, Mancinelli R, Ceccanti M. Early exposure to ethanol but not red wine at the same alcohol concentration induces behavioral and brain neurotrophin alterations in young and adult mice. *Neurotoxicology.* (2009) 30:59–71. doi: 10.1016/j.neuro.2008.11.009
154. Aloe L. Alcohol intake during prenatal life affects neuroimmune mediators and brain neurogenesis. *Ann Ist Super Sanita.* (2006) 42:17–21.
155. Freund-Michel V, Frossard N. The nerve growth factor and its receptors in airway inflammatory diseases. *Pharmacol Ther.* (2008) 117:52–76. doi: 10.1016/j.pharmthera.2007.07.003
156. Aloe L. Alcohol intake during prenatal life affects neuroimmune mediators and brain neurogenesis. *Ann Ist Super Sanita.* (2006) 42:17–21.
157. Kojima M, Mizui T. BDNF propeptide. In: Litwack G, Editor. *Vitamins and Hormones.* Academic Press. (2017). p. 19–28. doi: 10.1016/bs.vh.2016.11.006
158. Pautassi RM, Suárez AB, Hoffmann LB, Rueda AV, Rae M, Marianno P, et al. Effects of environmental enrichment upon ethanol-induced conditioned place preference and pre-frontal BDNF levels in adolescent and adult mice. *Sci Rep.* (2017) 7:8574. doi: 10.1038/s41598-017-08795-0
159. Stragier E, Martin V, Davenas E, Poilbout C, Mongeau R, Corradetti R, et al. Brain plasticity and cognitive functions after ethanol consumption in C57BL/6J mice. *Transl Psychiatry.* (2015) 5:e696. doi: 10.1038/tp.2015.183

160. Haun HL, Griffin WC, Lopez MF, Solomon MG, Mulholland PJ, Woodward JJ, et al. Increasing brain-derived neurotrophic factor (BDNF) in medial prefrontal cortex selectively reduces excessive drinking in ethanol dependent mice. *Neuropharmacology.* (2018) 140:35–42. doi: 10.1016/j.neuropharm.2018.07.031
161. Rivera S, Khrestchatisky M, Kaczmarek L, Rosenberg GA, Jaworski DM. Metzincin proteases and their inhibitors: foes or friends in nervous system physiology? *J Neurosci.* (2010) 30:15337–57. doi: 10.1523/JNEUROSCI.3467-10.2010
162. Liu W-T, Han Y, Liu Y-P, Song AA, Barnes B, Song X-J. Spinal matrix metalloproteinase-9 contributes to physical dependence on morphine in mice. *J Neurosci.* (2010) 30:7613–23. doi: 10.1523/JNEUROSCI.1358-10.2010
163. Yin L, Li F, Li J, Yang X, Xie X, Xue L, et al. Chronic intermittent ethanol exposure induces upregulation of matrix metalloproteinase-9 in the rat medial prefrontal cortex and hippocampus. *Neurochem Res.* (2019) 44:1593–601. doi: 10.1007/s11064-019-02783-8
164. Jégou S, El Ghazi F, De Lendeu PK, Marret S, Laudenbach V, Uguen A, et al. Prenatal alcohol exposure affects vasculature development in the neonatal brain. *Ann Neurol.* (2012) 72:952–60. doi: 10.1002/ana.23699
165. Cui SJ, Tewari M, Schneider T, Rubin R. Ethanol promotes cell death by inhibition of the insulin-like growth factor I receptor. *Alcohol Clin Exp Res.* (1997) 21:1121–7. doi: 10.1111/j.1530-0277.1997.tb04262.x
166. de la Torre R, de Sola S, Hernandez G, Farré M, Pujol J, Rodriguez J, et al. Safety and efficacy of cognitive training plus epigallocatechin-3-gallate in young adults with down's syndrome (TESDAD): a double-blind, randomised, placebo-controlled, phase 2 trial. *Lancet Neurol.* (2016) 15:801–10. doi: 10.1016/S1474-4422(16)30034-5
167. De Toma I, Ortega M, Aloy P, Sabidó E, Dierssen M. DYRK1A overexpression alters cognition and neural-related proteomic pathways in the hippocampus that are rescued by green tea extract and/or environmental enrichment. *Front Mol Neurosci.* (2019) 12:272. doi: 10.3389/fnmol.2019.00272
168. Souchet B, Duchon A, Gu Y, Dairou J, Chevalier C, Daubigney F, et al. Prenatal treatment with EGCG enriched green tea extract rescues GAD67 related developmental and cognitive defects in Down syndrome mouse models. *Sci Rep.* (2019) 9:3914. doi: 10.1038/s41598-019-40328-9
169. Solzak JP, Liang Y, Zhou FC, Roper RJ. Commonality in down and fetal alcohol syndromes. *Birth Defects Res A Clin Mol Teratol.* (2013) 97:187–97. doi: 10.1002/bdra.23129
170. Wyganowska-Swiatkowska M, Matthews-Kozanecka M, Matthews-Brzozowska T, Skrzypczak-Jankun E, Jankun J. Can EGCG alleviate symptoms of down syndrome by altering proteolytic activity? *Int J Mol Sci.* (2018) 19:248. doi: 10.3390/ijms19010248
171. Bettio L, Thacker JS, Hutton C, Christie BR. Modulation of synaptic plasticity by exercise. *Int Rev Neurobiol.* (2019) 147:295–322. doi: 10.1016/bs.irn.2019.07.002
172. Fontaine CJ, Pinar C, Yang W, Pang AF, Suesser KE, Choi JSJ, et al. Impaired bidirectional synaptic plasticity in juvenile offspring following prenatal ethanol exposure. *Alcohol Clin Exp Res.* (2019) 43:2153–66. doi: 10.1111/acer.14170
173. Wong EL, Lutz NM, Hogan VA, Lamantia CE, McMurray HR, Myers JR, et al. Developmental alcohol exposure impairs synaptic plasticity without overtly altering microglial function in mouse visual cortex. *Brain Behav Immun.* (2018) 67:257–78. doi: 10.1016/j.bbi.2017.09.003
174. Shivakumar M, Subbanna S, Joshi VBB. Postnatal ethanol exposure activates HDAC-mediated histone deacetylation, impairs synaptic plasticity gene expression and behavior in mice. *Int J Neuropsychopharmacol.* (2020) 23:324–38. doi: 10.1093/ijnp/pyaa017
175. Lee HY, Naha N, Kim JH, Jo MJ, Min KS, Seong HH, et al. Age- and area-dependent distinct effects of ethanol on Bax and Bcl-2 expression in prenatal rat brain. *J Microbiol Biotechnol.* (2008) 18:1590–8.
176. Britton SM, Miller MW. Neuronal loss in the developing cerebral cortex of normal and bax-deficient mice: effects of ethanol exposure. *Neuroscience.* (2018) 369:278–91. doi: 10.1016/j.neuroscience.2017.11.013
177. Ieraci A, Herrera DG. Nicotinamide protects against ethanol-induced apoptotic neurodegeneration in the developing mouse brain. *PLoS Med.* (2006) 3:547–57. doi: 10.1371/journal.pmed.0030101
178. McAlhany RE, West JR, Miranda RC. Glial-derived neurotrophic factor (GDNF) prevents ethanol-induced apoptosis and JUN kinase phosphorylation. *Dev Brain Res.* (2000) 119:209–16. doi: 10.1016/S0165-3806(99)00171-6
179. Ornoy A, Ergaz Z. Alcohol abuse in pregnant women: effects on the fetus and newborn, mode of action and maternal treatment. *Int J Environ Res Public Health.* (2010) 7:364–79. doi: 10.3390/ijerph7020364
180. Zakhari S. Overview: how is alcohol metabolized by the body? *Alcohol Res Health.* (2006) 29:245–54. doi: 10.1159/000095013
181. Wu D, Cederbaum AI. Alcohol, oxidative stress, and free radical damage. *Alcohol Res Health.* (2003) 27:277–84.
182. Heaton M, Paiva M, Mayer J, Miller R. Ethanol-mediated generation of reactive oxygen species in developing rat cerebellum. *Neurosci Lett.* (2002) 334:83–6. doi: 10.1016/S0304-3940(02)01123-0
183. Kay HH, Tsoi S, Grindle K, Magness RR. Markers of oxidative stress in placental villi exposed to ethanol. *J Soc Gynecol Investig.* (2006) 13:118–21. doi: 10.1016/j.jsgi.2005.11.007
184. Haselbeck RJ, Duester G. ADH4-lacZ transgenic mouse reveals alcohol dehydrogenase localization in embryonic midbrain/hindbrain, otic vesicles, and mesencephalic, trigeminal, facial, and olfactory neural crest. *Alcohol Clin Exp Res.* (1998) 22:1607–13. doi: 10.1111/j.1530-0277.1998.tb03955.x
185. Gupta KK, Gupta VK, Shirasaka T. An update on fetal alcohol syndrome-pathogenesis, risks, and treatment. *Alcohol Clin Exp Res.* (2016) 40:1594–602. doi: 10.1111/acer.13135
186. Myllynen P, Pasanen M, Pelkonen O. Human placenta: a human organ for developmental toxicology research and biomonitoring. *Placenta.* (2005) 26:361–71. doi: 10.1016/j.placenta.2004.09.006
187. Guerri C, Bazinet A, Riley EP. Foetal alcohol spectrum disorders and alterations in brain and behaviour. *Alcohol Alcohol.* (2009) 44:108–14. doi: 10.1093/alcalc/agn105
188. Heller M, Burd L. Review of ethanol dispersion, distribution, and elimination from the fetal compartment. *Birth Defects Res A Clin Mol Teratol.* (2014) 100:277–83. doi: 10.1002/bdra.23232
189. Streissguth AP, Landesman-Dwyer S, Martin JC, Smith DW. Teratogenic effects of alcohol in humans and laboratory animals. *Science.* (1980) 209:353–61. doi: 10.1126/science.6992275
190. Wells PG, Bhatia S, Drake DM, Miller-Pinsler L. Fetal oxidative stress mechanisms of neurodevelopmental deficits and exacerbation by ethanol and methamphetamine. *Birth Defects Res C Embryo Today Rev.* (2016) 108:108–30. doi: 10.1002/bdrc.21134
191. Hoyt LR, Randall MJ, Ather JL, Depuccio DP, Landry CC, Qian X, et al. Mitochondrial ROS induced by chronic ethanol exposure promote hyper-activation of the NLRP3 inflammasome. *Redox Biol.* (2017) 12:883–96. doi: 10.1016/j.redox.2017.04.020
192. Yang F, Luo J. Endoplasmic reticulum stress and ethanol neurotoxicity. *Biomolecules.* (2015) 5:2538–53. doi: 10.3390/biom5042538
193. Miller-Pinsler L, Wells PG. Deficient DNA repair exacerbates ethanol-initiated DNA oxidation and embryopathies in ogg1 knockout mice: gender risk and protection by a free radical spin trapping agent. *Arch Toxicol.* (2016) 90:415–25. doi: 10.1007/s00204-014-1397-1
194. Wong AW, McCallum GP, Jeng W, Wells PG. Oxoguanine glycosylase 1 protects against methamphetamine-enhanced fetal brain oxidative DNA damage and neurodevelopmental deficits. *J Neurosci.* (2008) 28:9047–54. doi: 10.1523/JNEUROSCI.2557-08.2008
195. Wells PG, McCallum GP, Chen CS, Henderson JT, Lee CJJ, Perstin J, et al. Oxidative stress in developmental origins of disease: teratogenesis, neurodevelopmental deficits, and cancer. *Toxicol Sci.* (2009) 108:4–18. doi: 10.1093/toxsci/kfn263
196. Chen G, Ke Z, Xu M, Liao M, Wang X, Qi Y, et al. Autophagy is a protective response to ethanol neurotoxicity. *Autophagy.* (2012) 8:1577–89. doi: 10.4161/auto.21376
197. Luo J. Autophagy and ethanol neurotoxicity. *Autophagy.* (2014) 10:2099–108. doi: 10.4161/15548627.2014.981916
198. Dembele K, Yao XH, Chen L, Nyomba BLG. Intrauterine ethanol exposure results in hypothalamic oxidative stress and neuroendocrine alterations

in adult rat offspring. *Am J Physiol - Regul Integr Comp Physiol.* (2006) 291:R796–802. doi: 10.1152/ajpregu.00633.2005
199. Petkow VV, Stoianovski D, Petkov VD VI. Lipid peroxidation changes in the brain in fetal alcohol syndrome. *Biull Eksp Biol Med.* (1992) 113:500–2.
200. Chu J, Tong M, Monte SM. Chronic ethanol exposure causes mitochondrial dysfunction and oxidative stress in immature central nervous system neurons. *Acta Neuropathol.* (2007) 113:659–73. doi: 10.1007/s00401-007-0199-4
201. Brocardo PS, Boehme F, Patten A, Cox A, Gil-Mohapel J, Christie BR. Anxiety- and depression-like behaviors are accompanied by an increase in oxidative stress in a rat model of fetal alcohol spectrum disorders: protective effects of voluntary physical exercise. *Neuropharmacology.* (2012) 62:1607–18. doi: 10.1016/j.neuropharm.2011.10.006
202. Ramachandran V, Perez A, Chen J, Senthil D, Schenker S. *In utero* ethanol exposure causes mitochondrial dysfunction, which can result in apoptotic cell death in fetal brain: a potential role for 4-hydroxynonenal. *Alcohol Clin Exp Res.* (2001) 25:862–71. doi: 10.1111/j.1530-0277.2001.tb02292.x
203. Dong J, Sulik KK, Chen S. The role of NOX enzymes in ethanol-induced oxidative stress and apoptosis in mouse embryos. *Toxicol Lett.* (2010) 193:94–100. doi: 10.1016/j.toxlet.2009.12.012
204. Bjørkhaug ST, Neupane SP, Bramness JG, Aanes H, Skar V, Medhus AW, et al. Plasma cytokine levels in patients with chronic alcohol overconsumption: relations to gut microbiota markers and clinical correlates. *Alcohol.* (2019) 85:35–40. doi: 10.1016/j.alcohol.2019.10.002
205. Alfonso-Loeches S, Pascual M, Gómez-Pinedo U, Pascual-Lucas M, Renau-Piqueras J, Guerri C. Toll-like receptor 4 participates in the myelin disruptions associated with chronic alcohol abuse. *Glia.* (2012) 60:948–64. doi: 10.1002/glia.22327
206. Cartwright MM, Smith SM. Increased cell death and reduced neural crest cell numbers in ethanol-exposed embryos: partial basis for the fetal alcohol syndrome phenotype. *Alcohol Clin Exp Res.* (1995) 19:378–86. doi: 10.1111/j.1530-0277.1995.tb01519.x
207. Dunty WC, Chen SY, Zucker RM, Dehart DB, Sulik KK. Selective vulnerability of embryonic cell populations to ethanol-induced apoptosis: implications for alcohol-related birth defects and neurodevelopmental disorder. *Alcohol Clin Exp Res.* (2001) 25:1523–35. doi: 10.1111/j.1530-0277.2001.tb02156.x
208. Marin-Garcia J, Ananthakrishnan R, Goldenthal MJ. Mitochondrial dysfunction after fetal alcohol exposure. *Alcohol Clin Exp Res.* (1996) 20:1029–32. doi: 10.1111/j.1530-0277.1996.tb01942.x
209. Miller MW, Robertson S. Prenatal exposure to ethanol alters the postnatal development and transformation of radial glia to astrocytes in the cortex. *J Comp Neurol.* (1993) 337:253–66. doi: 10.1002/cne.903370206
210. Hu IC, Singh SP, Snyder AK. Effects of ethanol on glucose transporter expression in cultured hippocampal neurons. *Alcohol Clin Exp Res.* (1995) 19:1398–402. doi: 10.1111/j.1530-0277.1995.tb00998.x
211. Maier SE, Chen WJA, West JR. Prenatal binge-like alcohol exposure alters neurochemical profiles in fetal rat brain. *Pharmacol Biochem Behav.* (1996) 55:521–9. doi: 10.1016/S0091-3057(96)00282-1
212. Zhou FC, Sari Y, Powrozek TA. Fetal alcohol exposure reduces serotonin innervation and compromises development of the forebrain along the serotonergic pathway. *Alcohol Clin Exp Res.* (2005) 29:141–9. doi: 10.1097/01.ALC.0000150636.19677.6F
213. Ikonomidou C, Bittigau P, Ishimaru MJ, Wozniak DF, Koch C, Genz K, et al. Ethanol-induced apoptotic neurodegeneration and fetal alcohol syndrome. *Science.* (2000) 287:1056–60. doi: 10.1126/science.287.5455.1056
214. Tokuda K, Izumi Y, Zorumski CF. Locally-generated acetaldehyde contributes to the effects of ethanol on neurosteroids and long-term potentiation in the hippocampus. *Neurol Clin Neurosci.* (2013) 1:138–47. doi: 10.1111/ncn3.39
215. Sanderson JL, Donald Partridge L, Fernando Valenzuela C. Modulation of GABAergic and glutamatergic transmission by ethanol in the developing neocortex: an in vitro test of the excessive inhibition hypothesis of fetal alcohol spectrum disorder. *Neuropharmacology.* (2009) 56:541–55. doi: 10.1016/j.neuropharm.2008.10.012
216. Farber NB, Heinkel C, Dribben WH, Nemmers B, Jiang X. In the adult CNS, ethanol prevents rather than produces NMDA antagonist-induced neurotoxicity. *Brain Res.* (2004) 1028:66–74. doi: 10.1016/j.brainres.2004.08.065
217. Brady ML, Diaz MR, Iuso A, Everett JC, Valenzuela CF, Caldwell KK. Moderate prenatal alcohol exposure reduces plasticity and alters NMDA receptor subunit composition in the dentate gyrus. *J Neurosci.* (2013) 33:1062–7. doi: 10.1523/JNEUROSCI.1217-12.2013
218. Li E, Bestor TH, Jaenisch R. Targeted mutation of the DNA methyltransferase gene results in embryonic lethality. *Cell.* (1992) 69:915–26. doi: 10.1016/0092-8674(92)90611-F
219. Watanabe D, Suetake I, Tada T, Tajima S. Stage- and cell-specific expression of Dnmt3a and Dnmt3b during embryogenesis. *Mech Dev.* (2002) 118:187–90. doi: 10.1016/S0925-4773(02)00242-3
220. Rodenhiser D, Mann M. Epigenetics and human disease: translating basic biology into clinical applications. *CMAJ.* (2006) 174:341–8. doi: 10.1503/cmaj.050774
221. Kouzarides T. Chromatin modifications and their function. *Cell.* (2007) 128:693–705. doi: 10.1016/j.cell.2007.02.005
222. Resendiz M, Mason S, Lo C-L, Zhou FC. Epigenetic regulation of the neural transcriptome and alcohol interference during development. *Front Genet.* (2014) 5:285. doi: 10.3389/fgene.2014.00285
223. Lussier AA, Bodnar TS, Mingay M, Morin AM, Hirst M, Kobor MS, et al. Prenatal alcohol exposure: profiling developmental dna methylation patterns in central and peripheral tissues. *Front Genet.* (2018) 9:610. doi: 10.3389/fgene.2018.00610
224. Downing C, Johnson TE, Larson C, Leakey TI, Siegfried RN, Rafferty TM, et al. Subtle decreases in DNA methylation and gene expression at the mouse Igf2 locus following prenatal alcohol exposure: effects of a methyl-supplemented diet. *Alcohol.* (2011) 45:65–71. doi: 10.1016/j.alcohol.2010.07.006
225. Mandal C, Halder D, Jung KH, Chai YG. *In utero* alcohol exposure and the alteration of histone marks in the developing fetus: an epigenetic phenomenon of maternal drinking. *Int J Biol Sci.* (2017) 13:1100–8. doi: 10.7150/ijbs.21047
226. Zhong L, Zhu J, Lv T, Chen G, Sun H, Yang X, et al. Ethanol and its metabolites induce histone lysine 9 acetylation and an alteration of the expression of heart development-related genes in cardiac progenitor cells. *Cardiovasc Toxicol.* (2010) 10:268–74. doi: 10.1007/s12012-010-9081-z
227. Guo W, Crossey EL, Zhang L, Zucca S, George OL, Valenzuela CF, et al. Alcohol exposure decreases CREB binding protein expression and histone acetylation in the developing cerebellum. Cai H, editor. *PLoS ONE.* (2011) 6:e19351. doi: 10.1371/journal.pone.0019351
228. Cantacorps L, Alfonso-Loeches S, Guerri C, Valverde O. Long-term epigenetic changes in offspring mice exposed to alcohol during gestation and lactation. *J Psychopharmacol.* (2019) 33:1562–72. doi: 10.1177/0269881119856001
229. Laufer BI, Mantha K, Kleiber ML, Diehl EJ, Addison SMF, Singh SM. Long-lasting alterations to DNA methylation and ncRNAs could underlie the effects of fetal alcohol exposure in mice. *DMM Dis Model Mech.* (2013) 6:977–92. doi: 10.1242/dmm.010975
230. Sathyan P, Golden HB, Miranda RC. Competing interactions between micro-RNAs determine neural progenitor survival and proliferation after ethanol exposure: evidence from an *ex vivo* model of the fetal cerebral cortical neuroepithelium. *J Neurosci.* (2007) 27:8546–57. doi: 10.1523/JNEUROSCI.1269-07.2007
231. Astley SJ, Clarren SK. Measuring the facial phenotype of individuals with prenatal alcohol exposure: correlations with brain dysfunction. *Alcohol Alcohol.* (2001) 36:147–59. doi: 10.1093/alcalc/36.2.147
232. Anthony B, Vinci-Booher S, Wetherill L, Ward R, Goodlett C, Zhou FC. Alcohol-induced facial dysmorphology in C57BL/6 mouse models of fetal alcohol spectrum disorder. *Alcohol.* (2010) 44:659–71. doi: 10.1016/j.alcohol.2010.04.002
233. Fang S, Liu Y, Huang J, Vinci-Booher S, Anthony B ZF. Facial image classification of mouse embryos for the animal model study of fetal alcohol syndrome. *Proc Symp Appl Comput.* (2009) 2009:852–6. doi: 10.1145/1529282.1529463
234. Cartwright MM, Smith SM. Stage-dependent effects of ethanol on cranial neural crest cell development: partial basis for the phenotypic variations

observed in fetal alcohol syndrome. *Alcohol Clin Exp Res.* (1995) 19:1454–62. doi: 10.1111/j.1530-0277.1995.tb01007.x
235. Chen SY, Periasamy A, Yang B, Herman B, Jacobson K, Sulik KK. Differential sensitivity of mouse neural crest cells to ethanol-induced toxicity. *Alcohol.* (2000) 20:75–81. doi: 10.1016/S0741-8329(99)00058-0
236. Sulik KK. Genesis of alcohol-induced craniofacial dysmorphism. *Exp Biol Med).* (2005) 230:366–75. doi: 10.1177/15353702-0323006-04
237. Smith SM, Garic A, Flentke GR, Berres ME. Neural crest development in fetal alcohol syndrome. *Birth Defects Res C Embryo Today Rev.* (2014) 102:210–20. doi: 10.1002/bdrc.21078
238. Ogawa T, Kuwagata M, Ruiz J, Zhou FC. Differential teratogenic effect of alcohol on embryonic development between C57BL/6 and DBA/2 mice: a new view. *Alcohol Clin Exp Res.* (2005) 29:855–63. doi: 10.1097/01.ALC.0000163495.71181.10
239. Zhou FC, Sari Y, Powrozek T, Goodlett CR, Li T-K. Moderate alcohol exposure compromises neural tube midline development in prenatal brain. *Brain Res Dev Brain Res.* (2003) 144:43–55. doi: 10.1016/S0165-3806(03)00158-5
240. Sulik KK. Critical periods for alcohol teratogenesis in mice, with special reference to the gastrulation stage of embryogenesis. *Ciba Found Symp.* (1984) 105:124–41. doi: 10.1002/9780470720868.ch8
241. Murawski NJ, Moore EM, Thomas JD, Riley EP. Advances in diagnosis and treatment of fetal alcohol spectrum disorders: from animal models to human studies. *Alcohol Res.* (2015) 37:97–108.
242. Fang S, McLaughlin J, Fang J, Huang J, Autti-Rm I, Fagerlund A, et al. Automated diagnosis of fetal alcohol syndrome using 3D facial image analysis. *Orthod Craniofac Res.* (2008) 11:162–71. doi: 10.1111/j.1601-6343.2008.00425.x
243. Suttie M, Foroud T, Wetherill L, Jacobson JL, Molteno CD, Meintjes EM, et al. Facial dysmorphism across the fetal alcohol spectrum. *Pediatrics.* (2013) 131:e779–88. doi: 10.1542/peds.2012-1371
244. Shen L, Ai H, Liang Y, Ren X, Anthony CB, Goodlett CR, et al. Effect of prenatal alcohol exposure on bony craniofacial development: a mouse MicroCT study. *Alcohol.* (2013) 47:405–15. doi: 10.1016/j.alcohol.2013.04.005
245. Caputo C, Wood E, Jabbour L. Impact of fetal alcohol exposure on body systems: a systematic review. *Birth Defects Res C Embryo Today Rev.* (2016) 108:174–80. doi: 10.1002/bdrc.21129
246. Tran TD, Stanton ME, Goodlett CR. Binge-like ethanol exposure during the early postnatal period impairs eyeblink conditioning at short and long CS–US intervals in rats. *Dev Psychobiol.* (2007) 49:589–605. doi: 10.1002/dev.20226
247. Weinberg J, Sliwowska JH, Lan N, Hellemans KGC. Prenatal alcohol exposure: foetal programming, the hypothalamic-pituitary-adrenal axis and sex differences in outcome. *J Neuroendocrinol.* (2008) 20:470–88. doi: 10.1111/j.1365-2826.2008.01669.x
248. Roebuck TM, Mattson SN, Riley EP. A review of the neuroanatomical findings in children with fetal alcohol syndrome or prenatal exposure to alcohol. *Alcohol Clin Exp Res.* (1998) 22:339–44. doi: 10.1111/j.1530-0277.1998.tb03658.x
249. Archibald SL, Fennema-Notestine C, Gamst A, Riley EP, Mattson SN, Jernigan TL. Brain dysmorphology in individuals with severe prenatal alcohol exposure. *Dev Med Child Neurol.* (2001) 43:148–54. doi: 10.1111/j.1469-8749.2001.tb00179.x
250. Hendrickson TJ, Mueller BA, Sowell ER, Mattson SN, Coles CD, Kable JA, et al. Cortical gyrification is abnormal in children with prenatal alcohol exposure. *NeuroImage Clin.* (2017) 15:391–400. doi: 10.1016/j.nicl.2017.05.015
251. Kelly SJ, Goodlett CR, Hannigan JH. Animal models of fetal alcohol spectrum disorders: impact of the social environment. *Dev Disabil Res Rev.* (2009) 15:200–8. doi: 10.1002/ddrr.69
252. Wagner JL, Zhou FC, Goodlett CR. Effects of one- and three-day binge alcohol exposure in neonatal C57BL/6 mice on spatial learning and memory in adolescence and adulthood. *Alcohol.* (2014) 48:99–111. doi: 10.1016/j.alcohol.2013.12.001
253. Vorhees CV FK. Effects of short-term prenatal alcohol exposure on maze, activity, and olfactory orientation performance in rats. *Neurobehav Toxicol Teratol.* (1986) 8:23–8.
254. Maier SE, Miller JA, Blackwell JM, West JR. Fetal alcohol exposure and temporal vulnerability: regional differences in cell loss as a function of the timing of binge-like alcohol exposure during brain development. *Alcohol Clin Exp Res.* (1999) 23:726–34. doi: 10.1111/j.1530-0277.1999.tb04176.x
255. Caldwell KK, Sheema S, Paz RD, Samudio-Ruiz SL, Laughlin MH, et al. Fetal alcohol spectrum disorder-associated depression: evidence for reductions in the levels of brain-derived neurotrophic factor in a mouse model. *Pharmacol Biochem Behav.* (2008) 90:614–24. doi: 10.1016/j.pbb.2008.05.004
256. Lv K, Yang C, Xiao R, Yang L, Liu T, Zhang R, et al. Dexmedetomidine attenuates ethanol-induced inhibition of hippocampal neurogenesis in neonatal mice. *Toxicol Appl Pharmacol.* (2020) 390:114881. doi: 10.1016/j.taap.2020.114881
257. Hiller-Sturmhöfel S, Spear LP. Binge drinking's effects on the developing brain-animal models. *Alcohol Res.* (2018) 39:77–86.
258. Waddell J, Mooney SM. Choline and working memory training improve cognitive deficits caused by prenatal exposure to ethanol. *Nutrients.* (2017) 9:1080. doi: 10.3390/nu9101080
259. Shoji H, Hagihara H, Takao K, Hattori S, Miyakawa T. T-maze forced alternation and left-right discrimination tasks for assessing working and reference memory in mice. *J Vis Exp.* (2012) 2012:e3300. doi: 10.3791/3300
260. Hunt PS, Jacobson SE, Torok EJ. Deficits in trace fear conditioning in a rat model of fetal alcohol exposure: dose-response and timing effects. *Alcohol.* (2009) 43:465–74. doi: 10.1016/j.alcohol.2009.08.004
261. Leger M, Quiedeville A, Bouet V, Haelewyn B, Boulouard M, Schumann-Bard P, et al. Object recognition test in mice. *Nat Protoc.* (2013) 8:2531–7. doi: 10.1038/nprot.2013.155
262. Patten AR, Fontaine CJ, Christie BR. A comparison of the different animal models of fetal alcohol spectrum disorders and their use in studying complex behaviors. *Front Pediatr.* (2014) 2:93. doi: 10.3389/fped.2014.00093
263. Hamilton GF, Hernandez IJ, Krebs CP, Bucko PJ, Rhodes JS. Neonatal alcohol exposure reduces number of parvalbumin-positive interneurons in the medial prefrontal cortex and impairs passive avoidance acquisition in mice deficits not rescued from exercise. *Neuroscience.* (2017) 352:52–63. doi: 10.1016/j.neuroscience.2017.03.058
264. Vorhees C V, Williams MT. Morris water maze: procedures for assessing spatial and related forms of learning and memory. *Nat Protoc.* (2006) 1:848–58. doi: 10.1038/nprot.2006.116
265. Woolfrey KM, Musisca NJ, Hunt PS, Burk JA. Early postnatal ethanol administration does not affect prepulse inhibition in rats. *Physiol Behav.* (2005) 84:747–52. doi: 10.1016/j.physbeh.2005.03.003
266. Komada M, Takao K, Miyakawa T. Elevated plus maze for mice. *J Vis Exp.* (2008) 2008:1088. doi: 10.3791/1088
267. Yankelevitch-Yahav R, Franko M, Huly A, Doron R. The forced swim test as a model of depressive-like behavior. *J Vis Exp.* (2015) 2015:52587. doi: 10.3791/52587
268. Akers KG, Kushner SA, Leslie AT, Clarke L, van der Kooy D, Lerch JP, et al. Fetal alcohol exposure leads to abnormal olfactory bulb development and impaired odor discrimination in adult mice. *Mol Brain.* (2011) 4:29. doi: 10.1186/1756-6606-4-29
269. Lecuyer M, Laquerrière A, Bekri S, Lesueur C, Ramdani Y, Jégou S, et al. PLGF, a placental marker of fetal brain defects after in utero alcohol exposure. *Acta Neuropathol Commun.* (2017) 5:44. doi: 10.1186/s40478-017-0444-6
270. Gomez-Roig MD, Marchei E, Sabra S, Busardò FP, Mastrobattista L, Pichini S, et al. Maternal hair testing to disclose self-misreporting in drinking and smoking behavior during pregnancy. *Alcohol.* (2018) 67:1–6. doi: 10.1016/j.alcohol.2017.08.010
271. Middaugh LD, Boggan WO. Postnatal growth deficits in prenatal ethanol-exposed mice: characteristics and critical periods. *Alcohol Clin Exp Res.* (1991) 15:919–26. doi: 10.1111/j.1530-0277.1991.tb05189.x
272. Tran TD, Cronise K, Marino MD, Jenkins WJ, Kelly SJ. Critical periods for the effects of alcohol exposure on brain weight, body weight, activity and investigation. *Behav Brain Res.* (2000) 116:99–110. doi: 10.1016/S0166-4328(00)00263-1
273. Haghighi Poodeh S, Salonurmi T, Nagy I, Koivunen P, Vuoristo J, Räsänen J, et al. Alcohol-induced premature permeability

in mouse placenta-yolk sac barriers *in vivo*. *Placenta.* (2012) 33:866–73. doi: 10.1016/j.placenta.2012.07.008
274. Atkinson AJ, Colburn WA, DeGruttola VG, DeMets DL, Downing GJ, Hoth DF, et al. Biomarkers and surrogate endpoints: preferred definitions and conceptual framework. *Clin Pharmacol Ther.* (2001) 69:89–95. doi: 10.1067/mcp.2001.113989
275. Datta S, Turner D, Singh R, Ruest LB, Pierce WM, Knudsen TB. Fetal alcohol syndrome (FAS) in C57BL/6 mice detected through proteomics screening of the amniotic fluid. *Birth Defects Res A Clin Mol Teratol.* (2008) 82:177–86. doi: 10.1002/bdra.20440
276. Bearer CF, Gould S, Emerson R, Kinnunen P, Cook CS. Fetal alcohol syndrome and fatty acid ethyl esters. *Pediatr Res.* (1992) 31:492–5. doi: 10.1203/00006450-199205000-00017
277. Kulaga V, Caprara D, Iqbal U, Kapur B, Klein J, Reynolds J, et al. Fatty acid ethyl esters (FAEE); comparative accumulation in human and guinea pig hair as a biomarker for prenatal alcohol exposure. *Alcohol Alcohol.* (2006) 41:534–9. doi: 10.1093/alcalc/agl048
278. Caprara DL, Brien JF, Iqbal U, Reynolds JN, Klein J, Koren G. A guinea pig model for the identification of in utero alcohol exposure using fatty acid ethyl esters in neonatal hair. *Pediatr Res.* (2005) 58:1158–63. doi: 10.1203/01.pdr.0000185201.83801.ed
279. Sari Y, Hammad LA, Saleh MM, Rebec G V., Mechref Y. Alteration of selective neurotransmitters in fetal brains of prenatally alcohol-treated C57BL/6 mice: quantitative analysis using liquid chromatography/tandem mass spectrometry. *Int J Dev Neurosci.* (2010) 28:263–9. doi: 10.1016/j.ijdevneu.2010.01.004
280. Maire SE, Cramer JA, West JR, Sohrabji F. Alcohol exposure during the first two trimesters equivalent alters granule cell number and neurotrophin expression in the developing rat olfactory bulb. *J Neurobiol.* (1999). 41:414–23. doi: 10.1002/(SICI)1097-4695(19991115)41:3<414::AID-NEU9>3.0.CO;2-F
281. Haycock PC, Ramsay M. Exposure of mouse embryos to ethanol during preimplantation development: effect on DNA methylation in the H19 imprinting control region 1. *Biol Reprod.* (2009) 81:618–27. doi: 10.1095/biolreprod.108.074682
282. Govorko D, Bekdash RA, Zhang C, Sarkar DK. Male germline transmits fetal alcohol adverse effect on hypothalamic proopiomelanocortin gene across generations. *Biol Psychiatry.* (2012) 72:378–88. doi: 10.1016/j.biopsych.2012.04.006
283. Kim J-S, Shukla SD. Histone H3 modifications in rat hepatic stellate cells by ethanol. *Alcohol.* (2005) 40:367–72. doi: 10.1093/alcalc/agh170
284. Pal-Bhadra M, Bhadra U, Jackson DE, Mamatha L, Park PH, Shukla SD. Distinct methylation patterns in histone H3 at Lys-4 and Lys-9 correlate with up- & down-regulation of genes by ethanol in hepatocytes. *Life Sci.* (2007) 81:979–87. doi: 10.1016/j.lfs.2007.07.030
285. Subbanna S, Nagre NN, Shivakumar M, Umapathy NS, Psychoyos D, Basavarajappa BS. Ethanol induced acetylation of histone at G9a exon1 and G9a-mediated histone H3 dimethylation leads to neurodegeneration in neonatal mice. *Neuroscience.* (2014) 258:422–32. doi: 10.1016/j.neuroscience.2013.11.043
286. Veazey KJ, Parnell SE, Miranda RC, Golding MC. Dose-dependent alcohol-induced alterations in chromatin structure persist beyond the window of exposure and correlate with fetal alcohol syndrome birth defects. *Epigenetics Chromatin.* (2015) 8:39. doi: 10.1186/s13072-015-0031-7
287. Balaraman S, Winzer-Serhan UH, Miranda RC. Opposing actions of ethanol and nicotine on microRNAs are mediated by nicotinic acetylcholine receptors in fetal cerebral cortical-derived neural progenitor cells. *Alcohol Clin Exp Res.* (2012) 36:1669–77. doi: 10.1111/j.1530-0277.2012.01793.x
288. Wang L-L, Zhang Z, Li Q, Yang R, Pei X, Xu Y, et al. Ethanol exposure induces differential microRNA and target gene expression and teratogenic effects which can be suppressed by folic acid supplementation. *Hum Reprod.* (2009) 24:562–79. doi: 10.1093/humrep/den439
289. Tal TL, Franzosa JA, Tilton SC, Philbrick KA, Iwaniec UT, Turner RT, et al. MicroRNAs control neurobehavioral development and function in zebrafish. *FASEB J.* (2012) 26:1452–61. doi: 10.1096/fj.11-194464
290. Nunez YO, Truitt JM, Gorini G, Ponomareva ON, Blednov YA, Harris RA, et al. Positively correlated miRNA-mRNA regulatory networks in mouse frontal cortex during early stages of alcohol dependence. *BMC Genomics.* (2013) 14:725. doi: 10.1186/1471-2164-14-725
291. Bager H, Christensen LP, Husby S, Bjerregaard L. Biomarkers for the detection of prenatal alcohol exposure: a review. *Alcohol Clin Exp Res.* (2017) 41:251–61. doi: 10.1111/acer.13309
292. Andreu-Fernández V, Bastons-Compta A, Navarro-Tapia E, Sailer S, Garcia-Algar O. Serum concentrations of IGF-I/IGF-II as biomarkers of alcohol damage during foetal development and diagnostic markers of foetal alcohol syndrome. *Sci Rep.* (2019) 9:1562. doi: 10.1038/s41598-018-38041-0
293. Silva-Peña D, García-Marchena N, Alén F, Araos P, Rivera P, Vargas A, et al. Alcohol-induced cognitive deficits are associated with decreased circulating levels of the neurotrophin BDNF in humans and rats. *Addict Biol.* (2019) 24:1019–33. doi: 10.1111/adb.12668
294. Carito V, Ceccanti M, Ferraguti G, Coccurello R, Ciafrè S, Tirassa P, et al. NGF and BDNF alterations by prenatal alcohol exposure. *Curr Neuropharmacol.* (2019) 17:308–17. doi: 10.2174/1570159X15666170825101308
295. O'Leary-Moore SK, McMechan AP, Galloway MP, Hannigan JH. Neonatal alcohol-induced region-dependent changes in rat brain neurochemistry measured by high-resolution magnetic resonance spectroscopy. *Alcohol Clin Exp Res.* (2008) 32:1697–707. doi: 10.1111/j.1530-0277.2008.00747.x
296. Olney JW, Wozniak DF, Jevtovic-Todorovic V, Farber NB, Bittigau P, Ikonomidou C. Glutamate and GABA receptor dysfunction in the fetal alcohol syndrome. *Neurotox Res.* (2002) 4:315–25. doi: 10.1080/1029842021000010875
297. Chandrasekar R. Alcohol and NMDA receptor: current research and future direction. *Front Mol Neurosci.* (2013) 6:14. doi: 10.3389/fnmol.2013.00014
298. Chater-Diehl EJ, Laufer BI, Singh SM. Changes to histone modifications following prenatal alcohol exposure: an emerging picture. *Alcohol.* (2017) 60:41–52. doi: 10.1016/j.alcohol.2017.01.005
299. Bilotta J, Saszik S, Givin CM, Hardesty HR, Sutherland SE. Effects of embryonic exposure to ethanol on zebrafish visual function. *Neurotoxicol Teratol.* (2002) 24:759–66. doi: 10.1016/S0892-0362(02)00319-7
300. Parnell SE, O'Leary-Moore SK, Godin EA, Dehart DB, Johnson BW, Allan Johnson G, et al. Magnetic resonance microscopy defines ethanol-induced brain abnormalities in prenatal mice: effects of acute insult on gestational day 8. *Alcohol Clin Exp Res.* (2009) 33:1001–11. doi: 10.1111/j.1530-0277.2009.00921.x
301. Pierce DR, West JR. Differential deficits in regional brain growth induced by postnatal alcohol. *Neurotoxicol Teratol.* (1987) 9:129–41. doi: 10.1016/0892-0362(87)90089-4
302. Carter RJ, Morton J, Dunnett SB. Motor coordination and balance in rodents. In: Wiley A, Editor. *Current Protocols in Neuroscience*. Hoboken, NJ: John Wiley and Sons, Inc. (2001). p. 8.12. doi: 10.1002/0471142301.ns0812s15
303. Brooks SP, Dunnett SB. Tests to assess motor phenotype in mice: a user's guide. *Nat Rev Neurosci.* (2009) 10:519–29. doi: 10.1038/nrn2652

Conflict of Interest: The authors declare that the research was conducted in the absence of any commercial or financial relationships that could be construed as a potential conflict of interest.

frontiers in Neurology

ORIGINAL RESEARCH
published: 15 July 2020
doi: 10.3389/fneur.2020.00590

Preeclampsia Drives Molecular Networks to Shift Toward Greater Vulnerability to the Development of Autism Spectrum Disorder

Qinglian Xie[1], *Zhe Li*[2], *Yan Wang*[1], *Shan Zaidi*[3], *Ancha Baranova*[3,4], *Fuquan Zhang*[5]* and *Hongbao Cao*[3,6]*

[1] Department of Outpatient, West China Hospital of Sichuan University, Chengdu, China, [2] Mental Health Center and National Clinical Research Center for Geriatrics, West China Hospital of Sichuan University, Chengdu, China, [3] School of Systems Biology, George Mason University, Fairfax, VA, United States, [4] Research Centre for Medical Genetics, Moscow, Russia, [5] Department of Psychiatry, The Affiliated Brain Hospital of Nanjing Medical University, Nanjing, China, [6] Department of Psychiatry, First Hospital/First Clinical Medical College of Shanxi Medical University, Taiyuan, China

Preeclampsia (PE) confers a significant risk for subsequent diagnosis with autism spectrum disorder (ASD), with the mechanisms underlying this observation being largely unknown. To identify molecular networks affected by both PE and ASD, we conducted a large-scale literature data mining and a gene set enrichment analysis (GSEA), followed by an expression mega-analysis in 13 independently profiled ASD datasets. Sets of genes implicated in ASD and in PE significantly overlap (156 common genes; $p = 3.14E^{-67}$), with many biological pathways shared (94 pathways; $p < 1.00E^{-21}$). A set of PE-driven molecular triggers possibly contributing to worsening the risk of subsequent ASD was identified, possibly representing a regulatory shift toward greater vulnerability to the development of ASD. Mega-analysis of expression highlighted RPS4Y1, an inhibitor of STAT3 that is expressed in a sexually dimorphic manner, as a contributor to both PE and ASD, which should be evaluated as a possible contributor to male predominance in ASD. A set of PE-driven molecular triggers may shift the developing brain toward a greater risk of ASD. One of these triggers, chromosome Y encoded gene RPS4Y1, an inhibitor of STAT3 signaling, warrants evaluation as a possible contributor to male predominance in ASD.

Keywords: autism, autism spectrum disorder, preeclampsia, GSEA, extreme male brain theory

OPEN ACCESS

Edited by:
Changlian Zhu,
Third Affiliated Hospital of Zhengzhou University, China

Reviewed by:
Rosa Marotta,
University of Magna Graecia, Italy
Jakub Mieczkowski,
Medical University of Gdansk, Poland

***Correspondence:**
Fuquan Zhang
zhangfq@njmu.edu.cn
Hongbao Cao
caohon2010@gmail.com

Specialty section:
This article was submitted to Pediatric Neurology, a section of the journal Frontiers in Neurology

Received: *09 January 2020*
Accepted: *22 May 2020*
Published: *15 July 2020*

Citation:
Xie Q, Li Z, Wang Y, Zaidi S, Baranova A, Zhang F and Cao H (2020) Preeclampsia Drives Molecular Networks to Shift Toward Greater Vulnerability to the Development of Autism Spectrum Disorder. Front. Neurol. 11:590. doi: 10.3389/fneur.2020.00590

INTRODUCTION

Autism spectrum disorders (ASD) are a range of neurodevelopmental mental disorders affecting nearly 1% of the global population (62.2 million globally) (1) and more than 2% of children (about 1.5 million) in the United States of America (www.hrsa.gov). Studies in recent years revealed hundreds of genes linked to ASD, paving the way for understanding the pathological mechanisms of the disease (2–4).

Preeclampsia (PE) is a disorder of pregnancy that increases the risk of poor outcomes for both the newborn and the mother. In PE, patients commonly present with high blood pressure, then their condition aggravates with the reduction *in utero* placental blood flow (1). Recent studies indicate that PE is one of the important risk factors for ASD (5, 6). However, the underlying mechanisms are largely unknown.

ASD and PE do share at least some pathophysiological pathways. For example, one of the core clinical features of PE is a systemic inflammation in a mother (Shennan et al., 2015). In turn, prenatal exposure to inflammation leads to exaggerated stress response and cytokine expression in a newborn (7). As these changes persist long-term, they may undermine normal postnatal development of the brain (8), increasing the chances for subsequent ASD diagnosis. It is likely, however, that the molecular networks connecting PE and ASD are not limited to relatively non-specific inflammatory signaling. Identification of the shared pathways may aid in understanding the mechanisms of PE-dependent delay in brain development or its contribution to ASD-specific defects while providing possible therapeutic targets involved in the pathogenesis of both diseases.

To dissect the association between PE and ASD at the genetic level, we employed the Pathway Studio (www.pathwaystudio.com) knowledge database to undertake large-scale literature mining effort and integrated its results with an analysis of multiple PE and ASD expression datasets. We identified a set of PE-driven molecular triggers, possibly contributing to worsening the risk of subsequent ASD through a regulatory shift toward greater vulnerability to the development of ASD. Chromosome Y-encoded gene RPS4Y1, an inhibitor of STAT3 signaling, was highlighted as a PE-driven contributor to ASD phenotypes. RPS4Y1 warrants evaluation as a possible contributor to male predominance in ASD.

MATERIALS AND METHODS

This study utilized the following workflow. First, the molecules involved in either PE or ASD were extracted in the Pathway Studio environment; common molecules and pathways connecting with both diseases were identified. All data and analysis results were organized in a database ASD_PE. The downloadable form of these two databases is available at gousinfo.com/database/Data_Genetic/ASD_PE.xlsx. Then, each PE-specific gene was tested in expression mega-analysis performed across 13 independently obtained, publicly available ASD datasets retrieved from Gene Expression Omnibus (GEO) (https://www.ncbi.nlm.nih.gov/geo/). Thereafter, functional network analysis was performed to study the pathogenic significance of identified genes for ASD-related processes.

Disease-Gene Relation Data

Disease-gene relation data for both ASD and PE were acquired through large-scale literature data analysis assisted by the Pathway Studio environment (www.pathwaystudio.com) commonly utilized for modeling the relationships between proteins, genes, complexes, cells, tissues, and diseases (9). Extracted relation data were uploaded in ASD_PE. For each of the genes linked to any of these two diseases, supporting references were examined and collated (ASD_PE: Ref4PE; Ref4ASD), including titles of the references and the related sentences describing the disease-gene relationship. Fisher's exact test was employed to compare the significance of the overlap between ASD genes and PE genes (https://david.ncifcrf.gov/content.jsp?file=functional_annotation.html).

TABLE 1 | A summary of the datasets utilized in expression mega-analysis.

Study Name	Dataset GEOID	#Control	#Case	Country
Nishimura et al. (2007)	GSE7329	15	15	USA
Hu et al. (2009)	GSE15402	29	26	USA
Hu et al. (2009)	GSE15402	29	30	USA
Hu et al. (2009)	GSE15451	17	21	USA
Alter et al. (2011)	GSE25507	64	82	USA
Kuwano et al. (2011)	GSE26415	42	21	Japan
Voineagu et al. (2011)	GSE28521	40	39	USA
Colak and Kaya, (2014)	GSE29691	13	2	Saudi Arabia
Luo et al. (2012)	GSE37772	206	233	USA
Ginsberg et al. (2012)	GSE38322	18	18	USA
Pramparo et al. (2015)	GSE42133	56	91	USA
Griesi-Oliveira et al. (2014)	GSE62632	12	6	USA
François et al. (2014)	GSE63524	5	6	France
Liu et al. (2017)	GSE65106	38	21	USA

Mega-Analysis of Expression Datasets

To compile the list of gene expression datasets, a publicly available GEO database was searched using keywords "autism spectrum disorder" and "ASD," which has returned 321 entries. This search covered the entire content of GEO and had no selection bias. Further filtering was performed according to the following criteria: (1) The data type is RNA expression; (2) the study design is case vs. control; (3) the original datasets and format files are available; and (4) the sample organism is Homo sapiens. A total of 14 datasets satisfied all the criteria listed and were pipelined into the mega-analysis of expression patterns as raw data files (**Table 1**).

For across-dataset mega-analysis, the expression data were normalized and log2-transformed. The mega-analysis workflow pools individual gene expression measurements while correcting for between-study variation (10). For each expression dataset, the log-fold change (LFC) in ASD samples was calculated and used as the index of effect size. Both the fixed-effect model and random-effects model (11) were tested to study the effect size of PE-related genes on ASD, and their outputs compared. For each model, the heterogeneity of study inputs was calculated. Analyses were conducted using MATLAB (R2017a) mega-analysis package. To note, we used the term "mega-analysis" instead of "meta-analysis" to address the fact that the LFC of expression for each gene was calculated from the original datasets rather than using the values extracted from existing publications, which is the major difference between the two terms.

In mega-analysis, each gene was evaluated according to the following criteria: (1) The results were calculated from at least half of the studies; (2) $p < 0.05$; and (3) effect size (LFC) > 0.59 or < -1.00. When a gene has an effect size LFC > 0.59 or < -1.00, it means that the change in the expression level of the gene had increased by more than 50% or decreased by more than 50%. While ASD_PE→Mega-analysis presents mega-analysis outputs for the entire set of the analyzed genes, here we will discuss only the genes that satisfy the significance criteria outlined above.

TABLE 2 | Genetic pathways enriched with 156 genes contributing to both preeclampsia and ASD.

Name	GO ID	# of Entities	Overlap	*p*-value
GO: response to toxic substance	0009636	634	52	4.86E–38
GO: response to extracellular stimulus	0009991	761	53	1.61E–35
GO: response to nutrient levels	0031667	730	52	2.16E–35
GO: positive regulation of locomotion	0040017	666	49	8.86E–34
GO: positive regulation of cell motility	2000147	630	48	8.87E–34
GO: aging	0016280	493	44	1.43E–33
GO: positive regulation of cell migration	0030335	603	47	1.47E–33
GO: positive regulation of cellular component movement	0051272	650	48	2.4E–33
GO: regulation of response to external stimulus	0032101	977	55	6.88E–33
GO: regulation of secretion	0051046	985	54	1.25E–31

For each pathway/GO term, the p-value was calculated using the Fisher exact test against the hypothesis that a randomly selected gene group of the same size (N = 156) can generate a similar or higher overlap with the corresponding pathway/GO term. All these pathways/GO terms passed the FDR correction (q = 0.05).

Gene Set Enrichment Analysis (GSEA) and Shortest Path Analysis

To gain functional insights into genes implicated both in ASD and in PE, we conducted a gene set enrichment analysis (GSEA) in the Pathway Studio environment, with enrichment *p*-values being corrected according to the Benjamini–Hochberg procedure (12). In addition to GSEA, for a gene showing significance in the mega-analysis, which was not yet described as an ASD contributor, a literature-based functional pathway analysis was conducted using the "Shortest Path" module of Pathway Studio (www.pathwaystudio.com).

Multiple Linear Regression Analysis

A multiple linear regression analysis was employed to study the possible influence of the following three factors on the gene expression change: sample size, population region, and study date. *P*-values and 95% confidence interval (CI) were reported for each of these factors. The analysis was performed in Matlab (R 2017a) with the "regress" statistical analysis package.

RESULTS

Common Genes for PE and ASD

As could be seen in the ASD_PE database, a total of 1,188 genes were associated with PE (see ASD_PE: PE_Genes and Ref4PE), and a total of 624 genes were associated with ASD (ASD_PE: ASD_Genes and Ref4ASD), with a significant overlap ($N = 156$, Fisher's exact test $p = 3.14E{-}67$; ASD_PE: common genes). To investigate the pathways shared by PE and ASD, a set of 156 common genes associated with both ASD and PE was submitted to a Gene Set Enrichment Analysis (GSEA) executed by using Pathway Studio. A total of 116 out of these 156 genes were shared among the top 10 most significantly enriched pathways ($p < 1.20E{-}31$, $q = 0.05$ for FDR), which are presented in **Table 2**. The full 94 pathways/gene sets enriched with $p < 1.00e{-}20$, which encompassed 144 out of 156 genes, were presented in ASD_PE→Common Pathways. Notably, a majority of the shared pathways highlighted by the GSEA approach were related to responses to some kind of external stimuli, including toxic ones, and to various aspects of the migration of cells. For detailed information regarding these significantly enriched pathways, please refer to ASD_PE→Common Pathways.

We also identified six positive regulators for ASD that have been stimulated by PE condition and one inhibitor (IGF1) that has been deactivated during PE (**Figure 1**). The detailed information of the pathway presented in **Figure 1** can be found in ASD_PE→Prognostic pathway, including the type of the relationship, supporting references, and related sentences from the references where the relationship has been identified.

Co-directionality of the PE and ASD Phenotype Interaction

Pathway analysis has also identified multiple molecules influenced by both PE and ASD (**Figure 2**). Notably, these interactions were predominantly co-directional. A total of 25 molecules upregulated in ASD were stimulated in PE, and a total of 13 molecules suppressed in ASD were negatively affected by PE. The detailed information regarding the network presented in **Figure 2** can be found in ASD_PE→Diagnostic pathway, with each network-related entry including the type of the relationship, supporting references, and related sentences from the references where the relationship has been identified.

Mega-Analysis of Gene Expression Pattern Identified *RPS4Y1* as a Novel Contributor to ASD

Only one gene, RPS4Y1, has satisfied the significance criteria outlined in the Methods section as it was significantly overexpressed in ASD samples assessed in 8 out of 14 studies. To note, the other six studies have not included RPS4Y1 in the respective lists of assessed signals. Analysis of study heterogeneity showed a significant between-datasets variance of expression levels for this gene (ISq = 89.46, p Q > 7.74E−12), and therefore, a random-effects model was selected. Multiple linear regression analysis indicated that the expression levels of RPS4Y1 were significantly influenced by the sample size and population region (country) ($p = 9.76E{-}3$ and 6.19E−6, respectively), but not by the year when the study was performed ($p = 0.94$). Dataset-specific effect sizes, 95% confidence intervals, and weights of the gene are shown in **Figure 3A**.

DISCUSSION

Previous studies showed that postnatal exposure to PE is a significant risk factor for ASD with mechanistic connections being not yet described (5, 6, 13). In an attempt to identify novel, not-yet-described molecular pathways that link preeclampsia to subsequently diagnosed ASD phenotypes, we employed natural

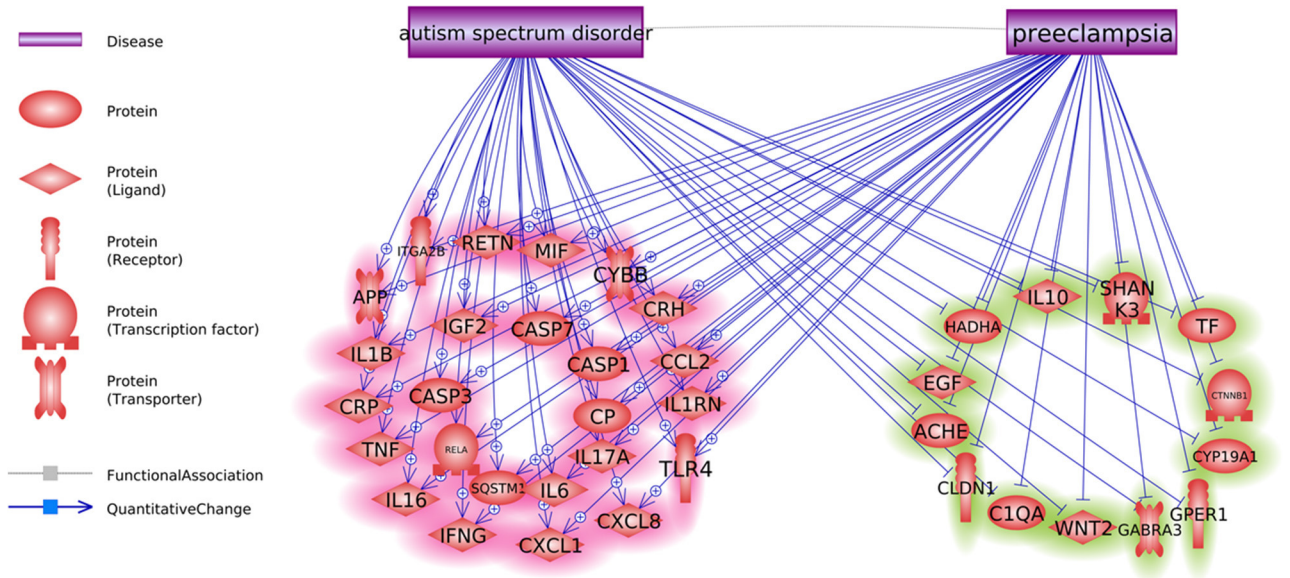

FIGURE 1 | Co-directional regulatory influences exerted by PE and ASD.

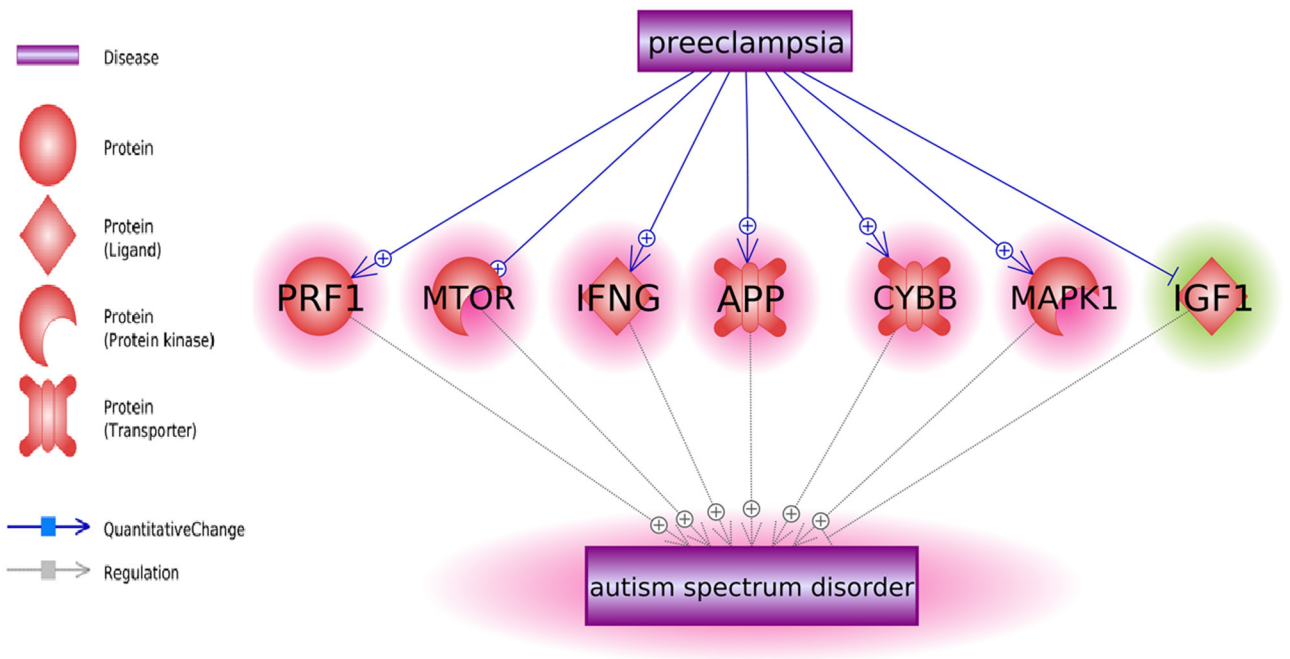

FIGURE 2 | The set of molecular triggers contributing to PE-driven regulatory shift contributing to increased risk of subsequent ASD diagnosis.

language programming environment Pathway Studio to perform large-scale exploration of previous knowledge concerning both of these conditions.

Notably, sets of genes linked to PE and to ASD demonstrated significant overlaps (see **Figure 1**, $p = 3.14E{-}67$; shared genes: $N = 156$). This set of shared genes was significantly enriched in the pathways previously implicated with both PE and ASD, such as response to nutrient levels [(14); Sharp et al., 2018], positive regulation of locomotion (15, 16), and aging [(17); Ruggieri et al., 2019]. Overall, the results of GSEA suggest that pathophysiological mechanisms of PE and ASD are partially shared.

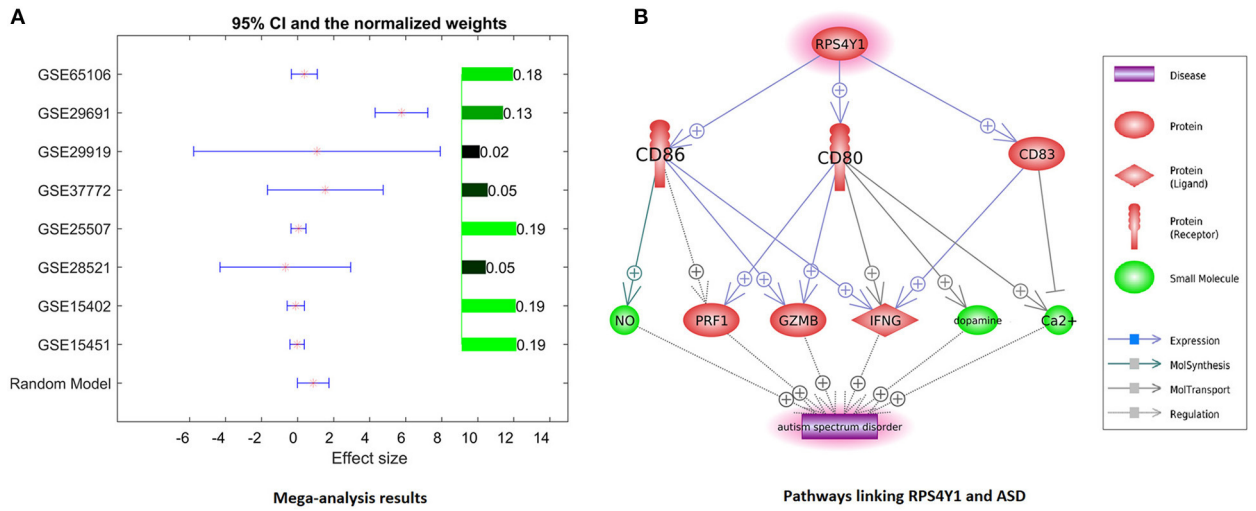

FIGURE 3 | Evidence of preeclampsia-related gene *RPS4Y1* involvement in ASD phenotypes. **(A)** Dataset-specific effect sizes, 95% confidence intervals, and weights of RPS4Y1. **(B)** Molecular network connecting *RPS4Y1* and ASD.

Some molecules contributing to both PE and ASD were highlighted as molecular triggers set by PE and possibly contributing to a worsening risk of subsequent ASD (**Figure 1**). This set includes six ASD-positive regulators that have been stimulated by PE condition and one inhibitor (IGF1) that has been deactivated during PE. Moreover, a bulk of regulatory interactions exerted by PE condition was co-directional with that observed in ASD phenotypes. For example, in PE patients, serum levels of transferrin do decrease (18), a phenomenon suggested as a negative contributor to intrauterine growth (19). At the same time, lower than normal levels of transferrin (Chauhan et al., 2004) or the defects in its saturation (20) are commonly seen in children with ASD diagnosis (21). Similarly, levels of IL6, TNF-alpha, and IL17 are repeatedly reported as elevated in both PE and ASD [Kara et al., 2019; (22–27)].

As PE etiologically precedes the diagnosis of ASD, this finding may be interpreted as a PE-driven regulatory shift toward greater vulnerability to the development of ASD, which may occur even by quantifiable at the time of the late pregnancy or delivery (**Figures 1**, **2**).

For further analysis, genes shared between curated PE- and ASD-specific gene sets were removed from consideration in order to ensure that uncovered PE-related contributors to ASD had not been already described as such. A total of 1,032 genes involved in preeclampsia but not in ASD were highlighted by Pathway Studio data mining. In subsequent mega-analysis of expression, each of these genes was investigated for consistent evidence of the changes in their expression in ASD phenotypes across 14 mRNA expression datasets acquired from GEO (**Table 1**). This analysis highlighted only one novel gene, *RPS4Y1*, which passed the preselected criterion of the significance of the association. *RPS4Y1* is a member of the S4E family of ribosomal proteins, which promotes PE by impairing STAT3 (Signal Transducer and Activator of Transcription 3) signaling and suppressing migration and invasion of trophoblast cells (28). **Figure 3B** shows that the product of *RPS4Y1* may also promote the development of ASD through the activation of multiple membrane proteins, including CD86, CD80, and CD83. In turn, these membrane molecules activate other molecular players previously implicated in ASD, such as ion transport pumps (29), and affect the release of nitric oxide (30). Importantly, all three of these membrane proteins promote the activity of interferon-gamma, which has been suggested to associate with increased oxidative stress in ASD (31), and also being produced at substantially elevated steady-state levels by natural killer (NK) cells of high-functioning adult individuals with ASD (32). Additional information regarding the activation of the IFNG pathway is provided in ASD_PE→RPS4Y1_Pathway.

Given the 4:1 male predominance for ASD (33), the involvement of sex-linked genes in these phenotypes is very likely. The *RPS4Y* gene is located on chromosome Y and encodes the ubiquitously expressed ribosomal protein gene. Interestingly, the expression of this gene in the process of neural differentiation increases even more (34). XY males express two RPS4-encoding genes (*RPS4Y* and *RPS4X*), whereas XX females express only one copy of *RPS4X* due to X-inactivation; thus, indicating that the levels of RPS4 protein in males vs. females are greater to begin with (35). In XYY individuals, known to score significantly higher on various autism-related scales, *RPS4Y* is expressed at the levels approximately 2-fold of that in age-matched, typically developing male controls (36). Exposure to PE may be viewed as yet another way to increase the expression of RPS4Y in affected fetuses systemically. Interestingly, Y-chromosome harbors another autism-related gene, *NLGN4Y*, which encodes a trans-synaptic cell adhesion molecule that stabilizes excitatory and inhibitory synaptic activity. Gene dosage of *NLGN4Y* is defined in a manner similar to that of *RPS4Y*. The involvement of *NLGN4Y* in autistic phenotypes is widely discussed, as it has been found mutated in some rare family clusters of autism (37). It is likely that the genetic contribution to the predominance of

autistic males depends on more than one gene, thus justifying the addition of *RPS4Y*, which is normally expressed at the very high levels throughout human tissues, including the brain, to the list of the candidates in need of further exploration.

There were several limitations of this study that need to be addressed in future work. First, the expression datasets employed in the analysis were lack of age and sex information. The influence of age and sex on the identified ASD potential genes should be explored with relevant data. Second, the pathways connecting RPS4 and ASD were built based on literature data. Experiment data were needed to confirm these relations in the case of ASD (e.g., using co-expression analysis to confirm the gene–gene relations within the pathway).

CONCLUSION

In conclusion, a large-scale literature mining effort and analysis of expression data allowed us to identify a set of PE-driven molecular triggers, shifting the developing brain toward a risk of ASD. In particular, chromosome Y-encoded gene RPS4Y1, an inhibitor of STAT3 signaling, was highlighted as PE-driven contributor to ASD phenotypes. RPS4Y1 warrants evaluation as a possible contributor to male predominance in ASD.

DATA AVAILABILITY STATEMENT

Publicly available datasets were analyzed in this study. This data can be found here: gousinfo.com/database/Data_Genetic/ASD_PE.xlsx; www.ncbi.nlm.nih.gov/geo/.

AUTHOR CONTRIBUTIONS

QX, HC, and FZ designed the study and collected the data. AB, SZ, QX, ZL, HC, and FZ performed the data analysis and contributed to the writing of the manuscript. AB and SZ provided functional analysis of RPS4Y1 and edited the manuscript into its final shape. QX and FZ contributed to the acquisition of funding that supported this study. All authors read and approved the final manuscript.

FUNDING

AB was partially supported by an Egg Nutrition Center (ENCs) grant to study the influence of the choline on ASD-related sensory phenotypes; FZ was partially supported by the National Natural Science Foundation of China (No. 81471364).

REFERENCES

1. Eiland E, Nzerue C, Faulkner M. Preeclampsia 2012. *J Pregnan*. (2012) 2012:586578. doi: 10.1155/2012/586578
2. Nisar S, Hashem S, Bhat A, Syed N, Yadav S, Azeem M, et al. Association of genes with phenotype in autism spectrum disorder. *Aging*. (2019) 11:10742–70. doi: 10.18632/aging.102473
3. Rylaarsdam L, Guemez-Gamboa A. Genetic causes and modifiers of autism spectrum disorder. *Front Cell Neurosci*. (2019) 13:385. doi: 10.3389/fncel.2019.00385
4. Lovato D, Herai R, Pignatari G, Beltrão-Braga P. The relevance of variants with unknown significance for autism spectrum disorder considering the genotype–phenotype interrelationship. *Front Psychiatr*. (2019) 10:409. doi: 10.3389/fpsyt.2019.00409
5. Dachew B, Mamun A, Maravilla J, Alati R. Pre-eclampsia and the risk of autism-spectrum disorder in offspring: meta-analysis. *Br J Psychiatr*. (2018) 212:142–7. doi: 10.1192/bjp.2017.27
6. Getahun D, Fassett M, Peltier M, Wing D, Xiang A, Chiu V, et al. Association of perinatal risk factors with autism spectrum disorder. *Am J Perinatol*. (2017) 34:295–304. doi: 10.1055/s-0036-1597624
7. Driscoll D, Felice V, Kenny L, Boylan G, O'Keeffe G. Mild prenatal hypoxia-ischemia leads to social deficits and central and peripheral inflammation in exposed offspring. *Brain Behav Immun*. (2018) 69:418–27. doi: 10.1016/j.bbi.2018.01.001
8. Gustafsson H, Sullivan E, Nousen E, Sullivan C, Huang E, Rincon M, et al. Maternal prenatal depression predicts infant negative affect via maternal inflammatory cytokine levels. *Brain Behav Immun*. (2018) 73:470–81. doi: 10.1016/j.bbi.2018.06.011
9. Nikitin A, Egorov S, Daraselia N, Mazo I. Pathway studio–the analysis and navigation of molecular networks. *Bioinformatics*. (2003) 19:2155–7. doi: 10.1093/bioinformatics/btg290
10. Seifuddin F, Pirooznia M, Judy J, Goes F, Potash J, Zandi P. Systematic review of genome-wide gene expression studies of bipolar disorder. *BMC Psychiatr*. (2013) 13:213. doi: 10.1186/1471-244X-13-213
11. Borenstein M, Hedges L, Higgins J, Rothstein H. A basic introduction to fixed-effect and random-effects models for meta-analysis. *Res Synthes Methods*. (2010) 1:97–111. doi: 10.1002/jrsm.12
12. Reiner A, Yekutieli D, Benjamini Y. Identifying differentially expressed genes using false discovery rate controlling procedures. *Bioinformatics*. (2003) 19:368–75. doi: 10.1093/bioinformatics/btf877
13. Kim J, Son M, Son C, Radua J, Eisenhut M, Gressier F, et al. Environmental risk factors and biomarkers for autism spectrum disorder: an umbrella review of the evidence. *Lancet Psychiatr*. (2019) 6:590–600. doi: 10.1016/S2215-0366(19)30181-6
14. Kim J, Kim Y, Lee R, Moon J, Jo I. Serum levels of zinc, calcium, and iron are associated with the risk of preeclampsia in pregnant women. *Nutr Res*. (2012) 32:764–9. doi: 10.1016/j.nutres.2012.09.007
15. Connolly C, Conger S, Montoye A, Marshall M, Schlaff R, Badon S, et al. Walking for health during pregnancy: a literature review and considerations for future research. *J Sport Health Sci*. (2019) 8:401–11. doi: 10.1016/j.jshs.2018.11.004
16. Urdaneta K, Castillo M, Montiel N, Semprún-Hernández N, Antonucci N, Siniscalco D. Autism spectrum disorders: potential neuro-psychopharmacotherapeutic plant-based drugs. *ASSAY Drug Deve Technol*. (2018) 16:433–44. doi: 10.1089/adt.2018.848
17. Nakashima A, Tsuda S, Kusabiraki T, Aoki A, Ushijima A, Shima T, et al. Current understanding of autophagy in pregnancy. *Int J Mol Sci*. (2019) 20:2342. doi: 10.3390/ijms20092342
18. Aksoy H, Taysi S, Altinkaynak K, Bakan E, Bakan N, Kumtepe Y. Antioxidant potential and transferrin, ceruloplasmin, and lipid peroxidation levels in women with preeclampsia. *J Investig Med*. (2003) 51:284–7. doi: 10.1136/jim-51-05-15
19. Wu Y, Sakamoto H, Kanenishi K, Li J, Khatun R, Hata T. Transferrin microheterogeneity in pregnancies with preeclampsia. *Clin Chim Acta*. (2003) 332:103–10. doi: 10.1016/s0009-8981(03)00134-7
20. Luck A, Bobst C, Kaltashov I, Mason A. Human serum transferrin: is there a link among autism, high oxalate levels, and iron deficiency anemia? *Biochemistry*. (2013) 52:8333–41. doi: 10.1021/bi401190m
21. Bjørklund G, Meguid N, El-Ansary A, El-Bana M, Dadar M, Aaseth J, et al. Diagnostic and severity-tracking biomarkers for autism spectrum disorder. *J Mol Neurosci*. (2018) 66:492–511. doi: 10.1007/s12031-018-1192-1
22. El Shahaway A, Yahia S, Abdelrhman A, Elhady R. Role of maternal serum interleukin 17 in preeclampsia: diagnosis and prognosis. *J Inflamm Res*. (2019) 12:175–80. doi: 10.2147/JIR.S206800

23. Daneva AM, Hadži-Lega M, Stefanovic M. Correlation of the system of cytokines in moderate and severe preeclampsia. *Clin Exp Obste Gynecol*. (2016) 43:220–224. doi: 10.12891/ceog2077.2016
24. Salazar Garcia M, Mobley Y, Henson J, Davies M, Skariah A, Dambaeva S, et al. Early pregnancy immune biomarkers in peripheral blood may predict preeclampsia. *J Reprod Immunol*. (2018) 125:25–31. doi: 10.1016/j.jri.2017.10.048
25. Black K, Horowitz J. Inflammatory markers and preeclampsia: a systematic review. *Nursing Res*. (2018) 67:242–51. doi: 10.1097/NNR.0000000000000285
26. Wei H, Alberts I, Li X. Brain IL-6 and autism. *Neuroscience*. (2013) 252:320–5. doi: 10.1016/j.neuroscience.2013.08.025
27. Eftekharian M, Ghafouri-Fard S, Noroozi R, Omrani M, Arsang-jang S, Ganji M, et al. Cytokine profile in autistic patients. *Cytokine*. (2018) 108:120–126. doi: 10.1016/j.cyto.2018.03.034
28. Chen X, Tong C, Li H, Peng W, Li R, Luo X, et al. Dysregulated expression of RPS4Y1 (ribosomal protein S4, Y-linked 1) impairs STAT3 (signal transducer and activator of transcription 3) signaling to suppress trophoblast cell migration and invasion in preeclampsia. *Hypertension*. (2018) 71:481–90. doi: 10.1161/HYPERTENSIONAHA.117.10250
29. Ji L, Chauhan A, Brown W, Chauhan V. Increased activities of Na+/K+-ATPase and Ca2+/Mg2+-ATPase in the frontal cortex and cerebellum of autistic individuals. *Life Sci*. (2009) 85:788–93. doi: 10.1016/j.lfs.2009.10.008
30. Yui K, Kawasaki Y, Yamada H, Ogawa S. Oxidative stress and nitric oxide in autism spectrum disorder and other neuropsychiatric disorders. *CNS Neurol Disord Drug Targets*. (2016) 15:587–96. doi: 10.2174/1871527315666160413121751
31. Tostes M, Teixeira H, Gattaz W, Brandão M, Raposo N. Altered neurotrophin, neuropeptide, cytokines and nitric oxide levels in autism. *Pharmacopsychiatry*. (2012) 45:241–3. doi: 10.1055/s-0032-1301914
32. Bennabi M, Tarantino N, Gaman A, Scheid I, Krishnamoorthy R, Debré P, et al. Persistence of dysfunctional natural killer cells in adults with high-functioning autism spectrum disorders: stigma/consequence of unresolved early infectious events? *Mol Autism*. (2019) 10:22. doi: 10.1186/s13229-019-0269-1
33. Newschaffer C, Croen L, Daniels J, Giarelli E, Grether J, Levy S, et al. The epidemiology of autism spectrum disorders. *Ann Rev Pub Health*. (2007) 28:235–58. doi: 10.1146/annurev.publhealth.28.021406.144007
34. Vakilian H, Mirzaei M, Tabar M, Pooyan P, Rezaee L, Parker L, et al. DDX3Y, a male-specific region of Y chromosome gene, may modulate neuronal differentiation. *J Proteome Res*. (2015) 14:3474–83. doi: 10.1021/acs.jproteome.5b00512
35. Staedtler F, Hartmann N, Letzkus M, Bongiovanni S, Scherer A, Marc P, et al. Robust and tissue-independent gender-specific transcript biomarkers. *Biomarkers*. (2013) 18:436–45. doi: 10.3109/1354750X.2013.811538
36. Ross J, Tartaglia N, Merry D, Dalva M, Zinn A. Behavioral phenotypes in males with XYY and possible role of increased NLGN4Y expression in autism features: NLGN4Y overexpression in XYY. *Genes Brain Behav*. (2015) 14:137–44. doi: 10.1111/gbb.12200
37. Yan J, Noltner K, Feng J, Li W, Schroer R, Skinner C, et al. Neurexin 1α structural variants associated with autism. *Neurosci. Lett*. (2008) 438:368–70. doi: 10.1016/j.neulet.2008.04.074

Conflict of Interest: The authors declare that the research was conducted in the absence of any commercial or financial relationships that could be construed as a potential conflict of interest.

frontiers in Cellular Neuroscience

ORIGINAL RESEARCH
published: 28 July 2020
doi: 10.3389/fncel.2020.00212

Establishment of a Novel Fetal Growth Restriction Model and Development of a Stem-Cell Therapy Using Umbilical Cord-Derived Mesenchymal Stromal Cells

Yuma Kitase[1,2], Yoshiaki Sato[1], Sakiko Arai[1,2], Atsuto Onoda[1,3], Kazuto Ueda[1], Shoji Go[1], Haruka Mimatsu[1,2], Mahboba Jabary[1,2], Toshihiko Suzuki[1], Miharu Ito[1], Akiko Saito[1], Akihiro Hirakawa[4], Takeo Mukai[5], Tokiko Nagamura-Inoue[5], Yoshiyuki Takahashi[2], Masahiro Tsuji[6] and Masahiro Hayakawa[1]*

[1]*Division of Neonatology, Center for Maternal-Neonatal Care, Nagoya University Hospital, Nagoya, Japan,* [2]*Department of Pediatrics, Nagoya University Graduate School of Medicine, Nagoya, Japan,* [3]*Faculty of Pharmaceutical Sciences, Sanyo-Onoda City University, Yamaguchi, Japan,* [4]*Clinical Research Center, Division of Biostatistics and Data Science, Medical and Dental University, Tokyo, Japan,* [5]*Department of Cell Processing and Transfusion, Institute of Medical Science, University of Tokyo, Tokyo, Japan,* [6]*Department of Food and Nutrition, Faculty of Home Economics, Kyoto Women's University, Kyoto, Japan*

OPEN ACCESS

Edited by:
Changlian Zhu,
Third Affiliated Hospital of Zhengzhou University, China

Reviewed by:
Emilio A. Herrera,
University of Chile, Chile
Man Xiong,
Fudan University, China

***Correspondence:**
Yoshiaki Sato
yoshiaki@med.nagoya-u.ac.jp

Specialty section:
This article was submitted to Cellular Neuropathology, a section of the journal Frontiers in Cellular Neuroscience

Received: *05 January 2020*
Accepted: *16 June 2020*
Published: *28 July 2020*

Citation:
Kitase Y, Sato Y, Arai S, Onoda A, Ueda K, Go S, Mimatsu H, Jabary M, Suzuki T, Ito M, Saito A, Hirakawa A, Mukai T, Nagamura-Inoue T, Takahashi Y, Tsuji M and Hayakawa M (2020) Establishment of a Novel Fetal Growth Restriction Model and Development of a Stem-Cell Therapy Using Umbilical Cord-Derived Mesenchymal Stromal Cells. Front. Cell. Neurosci. 14:212. doi: 10.3389/fncel.2020.00212

Fetal growth restriction (FGR) is a major complication of prenatal ischemic/hypoxic exposure and affects 5%–10% of pregnancies. It causes various disorders, including neurodevelopmental disabilities due to chronic hypoxia, circulatory failure, and malnutrition *via* the placenta, and there is no established treatment. Therefore, the development of treatments is an urgent task. We aimed to develop a new FGR rat model with a gradual restrictive load of uterus/placental blood flow and to evaluate the treatment effect of the administration of umbilical cord-derived mesenchymal stromal cells (UC-MSCs). To create the FGR rat model, we used ameroid constrictors that had titanium on the outer wall and were composed of C-shaped casein with a notch and center hole inside that gradually narrowed upon absorbing water. The ameroid constrictors were attached to bilateral ovarian/uterine arteries on the 17th day of pregnancy to induce chronic mild ischemia, which led to FGR with over 20% bodyweight reduction. After the intravenous administration of 1×10^5 UC-MSCs, we confirmed a significant improvement in the UC-MSC group in a negative geotaxis test at 1 week after birth and a rotarod treadmill test at 5 months old. In the immunobiological evaluation, the total number of neurons counted *via* the stereological counting method was significantly higher in the UC-MSC group than in the vehicle-treated group. These results indicate that the UC-MSCs exerted a treatment effect for neurological impairment in the FGR rats.

Keywords: umbilical cord-derived mesenchymal stromal cells, fetal growth restriction, mesenchymal stem cell, neurodevelopment, stem cells

INTRODUCTION

Fetal growth restriction (FGR) causes a wide variety of complications due to prenatal hypoxic/ischemic exposure and is defined as a fetal weight lower than the 10th percentile of the population of the gestation period (Jang et al., 2015). It affects about 20 million infants each year in the world (de Onis et al., 1998; Froen et al., 2004). The causes of FGR include chromosomal abnormalities (Lin and Santolaya-Forgas, 1998), genetic syndromes (Abuzzahab et al., 2003), intrauterine infections (Neerhof, 1995), multiple gestation pregnancies (Blickstein, 2004), and inborn errors of metabolism (Abuzzahab et al., 2003) as fetal factors; maternal factors include clinical diseases (Galan et al., 2001; Infante-Rivard et al., 2002; McCowan et al., 2003), nutritional disorders (Schulz, 2010), and drug use (Lieberman et al., 1994). Among these causes, hypertensive disease of pregnancy (HDP), which develops at a higher rate compared with the other causes, is the main cause of maternal, fetal, and neonatal morbidity and mortality; such fetuses are at an increased risk of FGR, prematurity, and intrauterine death (Kintiraki et al., 2015).

HDP induces chronic ischemia/hypoxia in the uterus (Naderi et al., 2017), to which exposure during the fetal period causes various disorders, including hypoglycemia, feeding intolerance, pulmonary hemorrhage (Sharma et al., 2016a,b), and, in particular, neuro-behavioral abnormalities (Padidela and Bhat, 2003). Neurological developmental disorders include poor exercise quality and developmental retardation (Zuk et al., 2004; Bergvall et al., 2006), and impaired intelligence/cognition, academic problems, mental problems, and obstacles to adaptation in society last for a lifetime (Sharma et al., 2016a). In this way, FGR increases neonatal mortality and morbidity as well as the risk of long-lasting problems in life.

The present study focuses on the neurodevelopmental disorders in FGR associated with chronic mild intrauterine hypoperfusion. Some infants with FGR exhibit abnormalities upon neurological examination, including a lower degree of organization and degraded neurobehavioral profiles, particularly in the orientation and motor domains (Feldman and Eidelman, 2006). Moreover, it is well known that children born with FGR exhibit long-term global cognitive impairment and short-term memory difficulties (Geva et al., 2006). Despite such a diverse range of serious diseases that last for a lifetime, there are few established treatments for neonates with FGR. Aggressive postnatal nutrition, constant rehabilitation, and growth hormone administration for physical growth are often conducted for FGR, but these are just supportive rather than fundamental treatments. Therefore, the development of a novel treatment is an urgent task.

Chronic placental dysfunction is a common cause of FGR, and inadequate blood flow to the placenta during pregnancy results in an inadequate supply of nutrients and oxygen to maintain proper fetal growth (Wixey et al., 2017). Several studies have reported on various FGR models, e.g., exposure to low-concentration oxygen (Morton et al., 2010; Dolinsky et al., 2011), ligation of the uterine artery with silk threads (Ruff et al., 2017), and administration of a synthetic thromboxane A_2 analog (STA_2) (Saito et al., 2009). However, considering the blood flow to placentas in FGR, these models do not properly mimic FGR associated with HDP, in which chronic ischemia occurs in the uterus. Therefore, to understand the pathophysiology of FGR more accurately and/or develop a novel therapy for FGR with an animal model, it is necessary to establish a proper model with a chronic decrease of blood flow to the uterus.

In recent years, many reports have demonstrated the effectiveness of stem cell therapy in repairing cells and tissues (Schwarz et al., 1999; Orlic et al., 2001; Wagenaar et al., 2017). Mesenchymal stromal cells (MSCs) have been reported to be a potential source of therapies for various conditions such as stroke, Parkinson's disease, and myocardial infarction (Schwarz et al., 1999; Chen et al., 2001; Orlic et al., 2001) and can differentiate into various mesodermal tissue cells or neuronal cells (Uccelli et al., 2008). Moreover, MSCs secrete various factors that not only suppress inflammation but also enhance neurogenesis and angiogenesis (Cunningham et al., 2018). Also, MSCs have a low risk of rejection and graft-vs.-host disease (Le Blanc and Ringden, 2005; Götherstrom, 2007). Therefore, we have hypothesized that the ability of MSCs to differentiate into various tissues and anti-inflammatory effects is effective against the tissue injury and persistent inflammation associated with chronic ischemia in FGR. Therefore, MSC-based cell therapy has the potential to be a promising treatment for FGR.

Of the various MSCs, we used umbilical cord-derived MSCs (UC-MSCs) in the present study. The advantages of UC-MSCs are as follows: a noninvasive collection procedure for autologous or allogeneic use, multipotency and low immunogenicity with a good immunosuppressive ability (Girdlestone et al., 2009; Nagamura-Inoue and He, 2014) that is greater in Wharton's Jelly-derived MSC than in bone marrow-derived mesenchymal stem cell (BM-MSC; Prasanna et al., 2010), easy storage, and few ethical problems for collection and usage. In addition to those advantages, UC-MSCs have demonstrated the ability to accumulate in damaged tissue and differentiate into three different germ layers that induce tissue repair (Nagamura-Inoue and He, 2014). Moreover, UC-MSCs also have a higher proliferative ability than various other MSCs (Hsieh et al., 2010; Sriramulu et al., 2018).

The purposes of the present study are to create a novel FGR rat model with a gradual restrictive load of the uterus/placental blood flow and to evaluate the treatment effects of UC-MSCs administration for the FGR model rats.

MATERIALS AND METHODS

Animals

The animal experiment protocols adopted in the present study were approved by the Institutional Review Board of Nagoya University (Nagoya, Aichi Prefecture, Japan; permit numbers: 27354-2015, 28001-2016, and 29096-2017). The number of animals was kept to the minimum required to achieve statistical significance. Sprague Dawley dams were obtained from Japan SLC Inc. (Shizuoka, Japan). All the rats were allowed free access to food and water and housed in a temperature-controlled room (23°C) under 12:12 h light/dark conditions (9.00 a.m.–9.00 p.m.).

We used a total of five dams for the sham group and nine dams for the FGR model i.e., vehicle and UC-MSC groups. Also, we used five dams (three for the sham; fetus $n = 12$ and two for the FGR; fetus $n = 7$) for the measurement of the uterus blood flow. We used 37 pups for the shams group, 18 for the vehicle group, and 15 for the UC-MSC group as negative geotaxis. Then, we separated males and females and used seven males for the sham group, nine for the vehicle group, and seven for the UC-MSC group as well as females for the immunohistological evaluations (eight for the sham group, three for the vehicle group and four for the UC-MSC group). We also used all of the females and males to evaluate the survival rate and safety. The minimal sample size of seven in each group was calculated to achieve an 80% power of testing with an α error rate of 5.0%. This was conducted under the assumption (and based on the preliminary experiments) that the effect size was 1.5 in the rotarod treadmill test, which is a primary endpoint.

Ameroid Constrictor *in vitro*

To induce chronic ischemia, we chose a tool known as an ameroid constrictor (AC; **Figure 1A**). The AC contains casein inside and is covered with a wide titanium ring approximately 3.0 mm in diameter and 1.3 mm in width, with a notch and a hole in the center of 0.4 mm in diameter (SW-MICE-0.4-SS, Tokyo Instruments Inc., Japan). This casein protein swells slowly when it absorbs water. AC was put into physiological saline at 37°C and the diameter of the center hole was measured every 24 h.

Surgical Procedure and Implantation of AC

To create an FGR rat model, we induced anesthesia in a rat with 2%–2.5% isoflurane and, then, maintained the anesthesia at around 2% on pregnancy day 17, which is equivalent to 20–25 weeks pregnant in humans (Salmaso et al., 2014), when severe gestation HDP often develops (Li et al., 2020). After confirming that the rat did not respond to painful stimuli, we disinfected its abdomen with alcohol and removed the hair with electric hair clippers, taking care not to damage the teats. Next, we incised the skin and muscular layers about 1.5 cm in the median, somewhat above the second papillary level from the bottom, and confirmed the number of fetuses by pulling out the left and right uteruses. Afterward, we put one uteruses back on one side of the abdominal cavity, while the uteruses on the other side were kept out, covered with gauze, and then humidified and warmed with warm physiological saline and a light bulb. We sequentially peeled the left and right ovarian and uterine arteries from the accompanying veins. Following this, we placed ACs in each of the four arteries (**Figure 1B**). After placing the ACs, we sewed the muscular and skin layers *via* continuous suturing and closed the incision. Regarding the sham group, we took out the uteruses and counted the number of fetuses. Then, we only waited for 15 min, keeping them humidified and warmed without any treatments, before placing the uteruses back into the abdomen and closing the incision. To reduce stress to the rats, we put nest material in the cage on pregnancy day 15 and made maximum efforts to avoid unnecessary stimulation.

Blood Flow Change in Uterus With AC *in vivo*

To confirm the changes in blood flow to the uterus derived from the AC attachment, we measured the flow using a laser blood flowmeter ω zone® (OMEGA WAVE, Inc., Tokyo, Japan), which is used to estimate blood perfusion by the speckle contrast (Fredriksson and Larsson, 2017). We defined a circle region of interest (ROI) on the inside of the uterus to cover the whole fetus. We then measured the blood flow in four fetuses in the top and bottom of the bilateral uteri (**Figure 2A**) in each rat before and after AC attachment on gestational day 17 and on gestational days 18, 19, and 20.

UC-MSCs

The collection of human umbilical cord tissue and MSC culturing for the present study were approved by the Ethics Committee of the Institute of Medical Science, University of Tokyo, Yamaguchi Hospital, NTT Medical Center Hospital, and Nagoya University Hospital, Japan. The frozen UC-MSCs ready to use were provided by IMSUT CORD in IMSUT. Briefly, the human umbilical cord was collected from babies at the cesarean sections after written informed consent from pregnant mothers. After collecting, the umbilical cord tissue was frozen until use (Shimazu et al., 2015). The frozen-thawed UC tissues were cut into 1- to 2-mm^3 fragments, covered by Cellamigo® (Tsubakimoto Co., Osaka, Japan) for improved explant isolation (Mori et al., 2015). Tissue fragments were cultured with RM medium (ROHTO Pharmaceutical Co., Ltd., Japan), which is a serum-free culture medium. The fibroblast-like adherent cells that migrated from the tissue fragments were harvested using TrypLE Select (Life Technologies) and these cells were defined as passage 1 cells. The harvested cells were passaged until passage four when the cells were used as UC-MSCs for the experimental analyses. The UC-MSCs were cryopreserved in cryoprotectant, STEM-CELLBANKER® (ZENOAQ Resource Co., Ltd.) and thawed just before use. The cryoprotectant was used as the vehicle in the control group.

Administration of Treatment and Experimental Design

After AC attachment at pregnancy day 17, we waited for spontaneous delivery. All pups born from rats with ACs were allocated to two equivalent groups at P4 (postnatal day 4), i.e., the UC-MSC group and the vehicle group, based on gender and body weight. Male rats were used for behavioral experiments and females for a histological examination. We administered 1×10^5 UC-MSCs *via* the right jugular vein in the UC-MSC group and only STEM-CELLBANKER® in the vehicle group at P4, which is the same as the preterm of humans and corresponds to the time when the adverse effects on neural development easily develop (Baschat, 2011). The right external jugular vein was exposed under general anesthesia using isoflurane (3.0% for induction and 2.0% for maintenance) on a heating plate set on 37°C and then injection was conducted using a 35-gauge needle. We subsequently performed behavioral experiments at P8–11 and 5 months after birth with the male rats and an

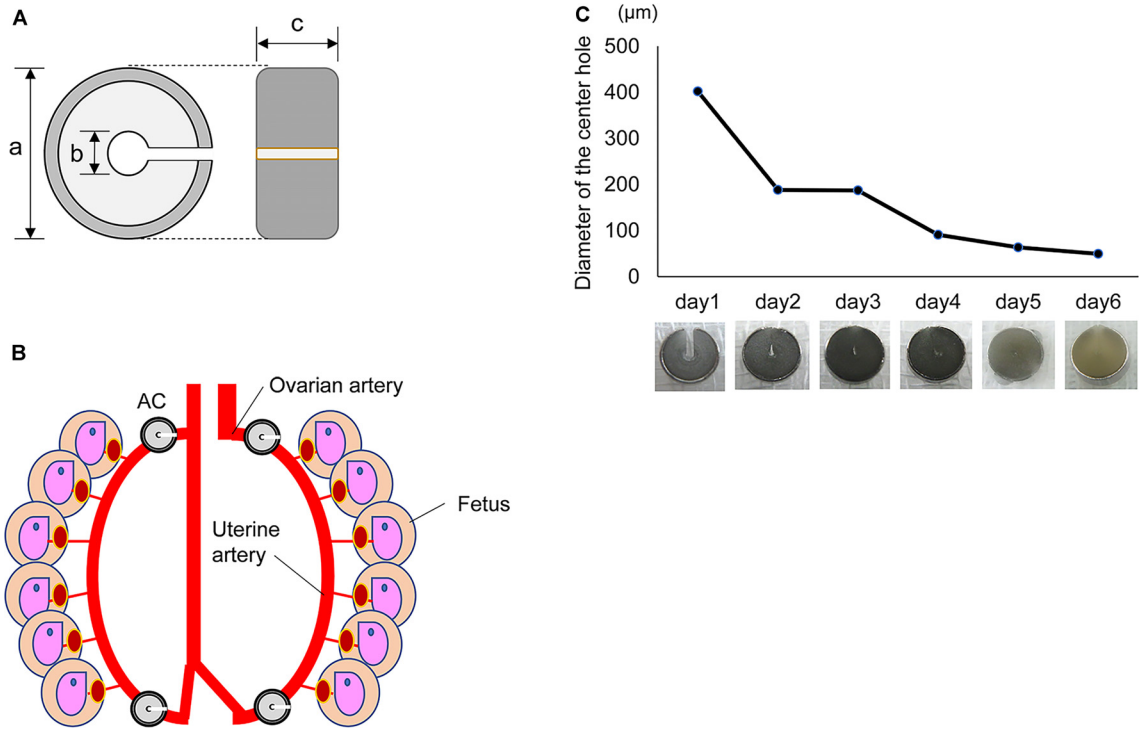

FIGURE 1 | Characters of the Ameroid constrictor. **(A)** Ameroid constrictor. An ameroid constrictor (AC) contains casein inside, has a notch and a hole in the center and is covered with a wide titanium ring. Its size is approximately 3.0 mm in diameter (a); the tool has a center hole of 0.4 mm (b) and a width of about 1.3 mm (c). This casein protein swells slowly when it absorbs water. **(B)** Installation of AC. The figure shows that the left and right ovarian/uterine arteries were sequentially detached from the vein, and an AC was placed in each of the four locations of the artery. **(C)** The change of diameter in AC. The graph shows the diameter of the center hole in an AC in a physiological saline environment of 37°C *in vitro*. The hole shrank to approximately 1/5 its original size in 1 day and to about 1/10 in 3 days. The photograph below shows the change of its shape over time in saline at 37°C.

immunohistological examination 2 months after birth with the female rats.

Tissue Preparation and Immunohistochemistry

For the immunohistological evaluation, we used anti-neuronal nuclei (NeuN) antibody (clone A60, EMD Millipore, Burlington, MA, USA), a marker for neurons. The histological and immunohistochemical procedures were performed as previously described (Osato et al., 2010) with minor modifications. Briefly, 2 months after birth, all the female rats were administered pentobarbital sodium intraperitoneally for anesthetization before being sacrificed; then, it was perfused intracardially, first with normal saline and next with 4% paraformaldehyde in phosphate buffer. The rats' whole brains were collected and immersed overnight in the same paraformaldehyde solution. Subsequently, the brains were transferred to 10% sucrose, stirred gently before sinking, and transferred to 20% sucrose and, finally, to 30%. Next, 40-μm coronal sections were cut throughout the brain every 600 μm.

The sections were blocked with 0.6% H_2O_2 in phosphate-buffered saline (PBS), then blocked using 3% normal donkey serum with 0.1% Triton-X100 in PBS for 30 min. These sections were incubated overnight at 4°C with a primary antibody (1:400; mouse anti-NeuN) in 3% donkey serum and PBS. On the second day, the sections were further incubated with a secondary antibody (1:1,000; biotinylated donkey anti-mouse; Jackson ImmunoResearch Laboratories, West Grove, PA, USA) with 3% donkey serum and 0.1% Triton-X100 in PBS for 60 min. After using Avidin-Biotin-Peroxidase (Vectastain Elite ABC Kit; Vector Laboratories, Burlingame, CA, USA) for 60 min, peroxidase detection was performed for 15 min (0.25 mg/ml DAB, 0.01% H_2O_2, 0.04% $NiCl_2$).

Furthermore, we evaluated the volumes of the cortex, hippocampus, and corpus callosum as well as the number of S100-positive, Iba-1-positive, and double-positive cells for ED-1+/Iba-1+ and CD206+/Iba-1+ using three sections per rat, 20 sections (600 μm) apart, at the hippocampal and basal ganglia level. We applied the same staining protocol to anti-S100 as that applied to anti-NeuN using a primary antibody (rabbit anti-S100; 1:1,000; Dako Cytomation, Glostrup, Denmark) and secondary antibody (1:1,000; biotinylated donkey anti-rabbit; Jackson ImmunoResearch Laboratories, West Grove, PA, USA). We performed triple staining using anti-Iba-1 (1:1,000 Abcam ab5076, Cambridge, UK), anti-ED-1 (1:300; EMD Millipore, Burlington, MA, USA), and anti-CD206 (1:100; Abcam, Cambridge, UK) with overnight incubation at 4°C, followed by incubation with Alexa Fluor goat 546, Alexa

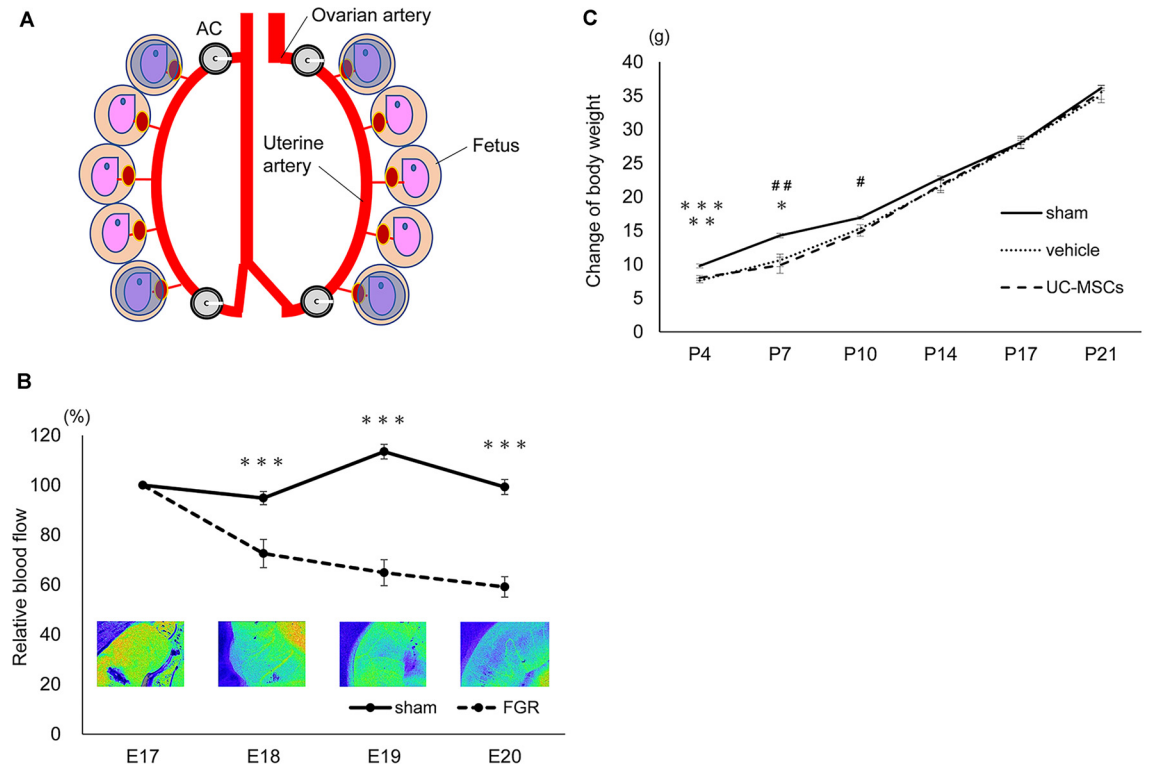

FIGURE 2 | Characters of the fetal growth restriction (FGR) model using the Ameroid constrictor. **(A)** The measurement area. We applied circle ROIs (blue circles) on the inside of the whole uteri and measured the four fetuses: top and bottom of the bilateral uteri before and after AC attachment on embryonic day 17 (E17) as well as E18, 19, and 20. **(B)** The changes in blood flow over time. The measurement of the blood flow every 24 h after the attachment of the AC in the sham group (n = 12) and the FGR group (n = 7). In the FGR group, the blood flow gradually decreased over time, and on the 20th day of pregnancy, just before birth, the blood flow had decreased to about 60% (sham, n = 12; FGR, n = 7). ***sham vs. FGR, $p < 0.001$. **(C)** The body weight change of each group. At P4 and P7 days of age, the mean body weight of the sham group was significantly higher than that of the vehicle and the umbilical cord-derived mesenchymal stromal cell (UCMSC) groups. Both the vehicle group and the UC-MSC group subsequently caught up with the sham group, and the significant difference disappeared (sham, n = 21; vehicle, n = 26; UC-MSCs, n = 23). *sham vs. vehicle, $p < 0.05$; #sham vs. UC-MSCs, $p < 0.05$; **sham vs. UC-MSCs, $p < 0.01$; ##sham vs. UC-MSCs, $p < 0.01$; ***sham vs. vehicle, $p < 0.001$.

Fluor mice 488, and Alexa Fluor rabbit 647 (1:500) antibodies, respectively, for 1 h at room temperature. The sections were then mounted using ProLong Gold Antifade reagent containing DAPI (Thermo Fisher Scientific Inc., Waltham, MA).

Cell Counting and Volume Measurement

We counted the NeuN-positive cells throughout the hippocampus and cortex *via* unbiased stereological counting techniques as discussed below (Stereo Investigator version 10 stereology software, Micro Bright Field Europe EK, Magdeburg, Germany). After outlining the borders of the hippocampus and the cortex, the computer program overlaid the outlined area with a grid system of counting frames. Cells within these frames as well as those touching two out of four predetermined sides of the frames were counted. The total number of NeuN-positive cells was calculated according to Cavalieri's principle using the following formula: $tN = \Sigma n \times P$, wherein tN = the total number, Σn = the sum of the number of positive cells in each section, and P = the inverse of the sampling fraction (Osato et al., 2010).

We placed squares (600 × 600 μm) in the bilateral cortex (**Supplementary Figure S1**) and counted all S100- and Iba-1-positive cells inside each square. The cell counts were expressed as densities. To calculate the Iba-1+/ED-1+ and Iba-1+/CD206+ cells, at least 50 Iba-1-positive cells per animal were analyzed. The ratios of Iba-1+/ED-1+ cells to Iba-1+ cells and Iba-1+/CD206+ cells to Iba-1+ cells were assessed using a fluorescence microscope (IX83, Olympus Co, Tokyo, Japan) and multiplied by the number of Iba-1-positive cells.

The areas of the cortex and corpus callosum were measured using a Stereo Investigator and the volume of each region was then determined according to the Cavalieri principle: $V = \Sigma A \times P$, where V = total volume, ΣA = sum of the area measurements, and P = inverse of the sampling fraction.

Behavioral Tests

Negative Geotaxis

For all rats, we performed a negative geotaxis test for four consecutive days, from P8 to P11 (Saito et al., 2009). We placed an anti-slip mat on a 30° slope, facing each rat's head downward.

We measured the time it took each rat to rotate 180° and face their head upward. We scored using zero to five points based on the rotation time: five points for 0–15 s, four points for 15–30 s, three points for 30–45 s, two points for 45–60 s, one point for over 60 s, and zero points for no reaction or falling.

Rotarod Treadmill Test

A rotarod treadmill was used to measure the duration of time that each rat could stay on an automatic rotating rod to check their balance, coordination, and stamina. The rats were placed on rotating rods that accelerated from 4 to 40 rpm for 5 min. On the first day, only training (at 4 rpm) was performed to help the animals get used to the environment and rods; the examination was carried out over the following 2 days. We measured twice a day, with a break time of 4 h per day, totaling four observations over 2 days. The amount of time each animal remained on the rod was measured.

Statistical Analysis

All data were expressed as mean ± standard error. One-way analysis of variance was performed when comparing three groups. *Post hoc* comparisons were made using Tukey's test. A significant difference was observed at $p < 0.05$. All statistical analyses were performed using JMP 13 (SAS Institute Inc., Cary, NC, USA).

RESULTS

Changes in the Inner Hole of an AC *in vitro*

First, we examined how an AC (**Figure 1A**) changes *in vitro*. We placed an AC into physiological saline at 37°C and measured the diameter of the center hole every 24 h. The hole narrowed to approximately 1/5 of its original size after 24 h and to 1/10 after 3 days. The hole of the AC closed completely within 1 week (**Figure 1C**).

Uterine Blood Flow Changes Due to AC Attachment

The blood flow was measured using a laser blood flowmeter after attaching the ACs to the rats on pregnancy day 17 (**Figure 1B**). The sham group showed almost no change in blood flow. Although no change in blood flow was observed immediately after AC attachment, the flow decreased to 72.5 ± 5.7% after 24 h (sham 94.8 ± 2.7 $p < 0.001$), to 64.8 ± 5.2% after 48 h (sham 113.5 ± 2.9 $p < 0.001$), and to 59.1 ± 4.1% after 72 h (sham 99.3 ± 3.9 $p < 0.001$) compared with the initial blood flow before the attachment of ACs (**Figure 2B**).

Survival Rate and Body Weight

The survival rate and weight of the sham group ($n = 21$), vehicle group ($n = 23$) and UC-MSC group ($n = 26$) were compared. To create FGR rats, we performed a surgical operation on 2 rats (dams) for the sham and 6 rats (dams) for the AC attachment. All dams delivered on pregnancy day 21 in both groups.

Regarding the sham group, 21 fetuses in total were confirmed, and all pups were born. No deaths were observed during the observation period thereafter.

In the AC-mounted group, 50 rats (63.3%) of 79 fetuses confirmed upon the operation for AC attachment were born. According to the protocol of the present study, all FGR rats were mixed at P4 and divided into two equivalent groups based on their body weights. Overall, 5 of 24 animals (20.8%) in the vehicle group and 4 out of 26 (15.4%) in the UC-MSC group died by P21. Afterward, all animals in both groups survived to the end of the observation period, i.e., to 310 days of age.

At P4, the mean bodyweight of the sham group was higher (9.8 ± 0.3 g) than that of the vehicle group (7.6 ± 0.3 g; $p < 0.001$) and the UC-MSC group (8.0 ± 0.4 g; $p < 0.01$). The body weight at P7 in the sham group was 14.3 ± 0.3 g vs. 10.6 ± 0.9 g in the vehicle group ($p < 0.05$) and 9.9 ± 1.2 g in the UC-MSC group ($p < 0.01$). Moreover, at P10, the body weight was 16.9 ± 0.2 g in the sham group vs. 15.3 ± 0.6 g in the vehicle group (n.s.) and 14.8 ± 0.6 g in the UC-MSC group ($p < 0.05$). The body weight in both the vehicle and UC-MSC groups subsequently caught up to that of the sham group, and the significant difference among the groups disappeared (**Figure 2C**).

Behavioral Tests

Negative Geotaxis

To evaluate both the effect of FGR and the treatment effect of UC-MSCs on the maturity of vestibular receptors, central sensory function, and motor function, a negative geotaxis test was performed at P8–11. The time it took the rats to rotate 180°, with the head facing downward on a 30° slope, was measured.

No significant difference was observed among the sham group ($n = 37$), vehicle group ($n = 18$), and UC-MSC group ($n = 15$) at P8. The scores in the vehicle group were significantly lower than those in the sham group at P9, P10 and P11 (2.3 ± 0.3 vs. 3.7 ± 0.2 at P9, $p < 0.001$; 2.6 ± 0.3 vs. 3.6 ± 0.2 at P10, $p < 0.05$; 2.9 ± 0.2 vs. 4.2 ± 0.2 at P11, $p < 0.001$, respectively). However, the UC-MSC group's scores were significantly higher compared with those of the vehicle group at P11 (4.1 ± 0.3 vs. 2.9 ± 0.2, $p < 0.01$, respectively; **Figure 3A**).

Rotarod Treadmill Test

To evaluate balance, exercise coordination, durability, and learning, a rotarod treadmill test were performed at P154–155. The time it took the rats to fall from a forcibly rotating rod was evaluated. The test was conducted twice a day, with a break time of 4 h a day, for a total of four times in total over two consecutive days at 5 months after birth. Compared with the average duration of the sham group, that of the vehicle group ($n = 9$) was shorter (sham vs. vehicle, 110.8 ± 9.6 vs. 86.9 ± 8.5 s, respectively), while that of UC-MSC group ($n = 7$) was significantly longer (UC-MSC vs. vehicle 124.9 ± 9.6 vs. 86.9 ± 8.5 s, $p < 0.05$, respectively; **Figure 3B**).

Immunohistological Evaluation

An immunohistological evaluation using an anti-NeuN antibody, which recognizes neuron-specific nuclear proteins, was performed to histologically evaluate the impact of FGR and the UC-MSC treatment on the brain. Representative photomicrographs of NeuN-positive cells in the hippocampus (**Figure 4A**), and cortex (**Figure 4B**) are shown. The total

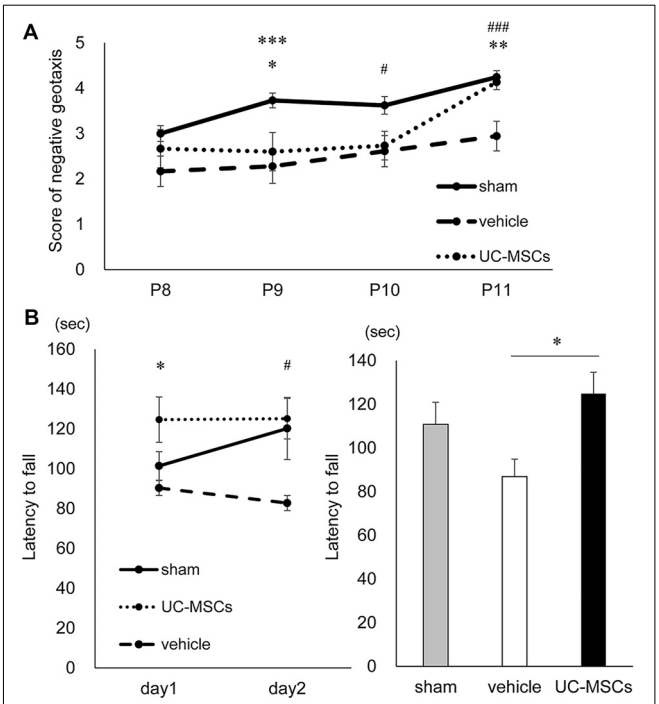

FIGURE 3 | Behavioral tests. **(A)** Negative geotaxis. At postnatal day 9, both the vehicle group and the UC-MSC group were significantly lower scores than the sham group. At postnatal day 10, the vehicle group was significantly lower than the sham group. At postnatal day 11, the vehicle group was significantly lower than the sham group, and the UC-MSC group significantly improved over the vehicle group. Sham group is represented by a solid line, vehicle group by a dashed line and UC-MSC group by a dotted line (sham, $n = 37$; vehicle, $n = 18$; UC-MSCs, $n = 15$). *sham vs. UC-MSCs, $p < 0.05$; #sham vs. vehicle, $p < 0.05$; **UC-MSCs vs. vehicle, $p < 0.01$; ***sham vs. vehicle, $p < 0.001$; ###sham vs. vehicle, $p < 0.001$. **(B)** Rotarod treadmill test. The average daily values were calculated. The left bar graph shows a daily average, and the right bar graph does an average of total observations. The duration was shortened in the vehicle group and prolonged in the UC-MSC group at P154-155. Sham group is represented by a solid line, vehicle group by a dashed line and UC-MSC group by a dotted line (sham, $n = 7$; vehicle, $n = 9$; UC-MSCs $n = 7$). *UC-MSCs vs. vehicle, $p < 0.05$; #UC-MSCs vs. vehicle, $p < 0.05$.

number of neurons was counted *via* the stereology method. To start, the total number of neurons in the hippocampus was evaluated. The number of positive cells for NeuN in the hippocampus was significantly lower in the vehicle group than in the sham group (141,960 ± 7,626 cells vs. 226,988 ± 16,751 cells, $p < 0.05$), whereas there was no significant difference between the UC-MSC group and the sham group (177,720 ± 8,631 cells vs. 226,988 ± 16,751 cells, n.s.; **Figure 4C**). Next, the number of positive cells for NeuN in the cerebral cortex was evaluated. As in the hippocampus, the total was significantly smaller in the vehicle group than in the sham group (3,670,185 ± 195,271 cells vs. 7,698,468 ± 221,946 cells, $p < 0.001$), and a significant improvement was observed in the UC-MSC group (3,670,185 ± 195,271 cells vs. 5,408,288 ± 252,595 cells, respectively, $p < 0.01$; **Figure 4D**).

We also evaluated the number of cells that were positive for S100, which is a marker for astroglia that is used to determine the effect on astrogliosis, and Iba-1, which is a marker for pan-microglia to determine the effect on microglia, in the cortex. The numbers of S100 positive cells was not significantly different among the three groups (**Figure 5A**). However, the number of Iba-1+ cells in the UC-MSC group was significantly higher than that of the sham group (7,511.3 ± 632.1 cells/mm^3 vs. 4,003.1 ± 678.8 cells/mm^3, $p < 0.05$; **Figure 5B**). Therefore, we also evaluated microglia M1 and M2 polarization by counting the number of cells that were double-positive for ED-1+/Ib-1+ and CD206+/Ib-1+, which are markers M1 microglia and M2 microglia, respectively. The numbers of ED-1+/Iba-1+ cells in both the vehicle group and the UC-MSC group were significantly higher compared with the sham group (**Figure 5C**, vehicle vs. sham, 3.70 ± 0.93 cells/mm^3 vs. 0.81 ± 0.44 cells/mm^3 $p < 0.05$; UC-MSC vs. sham, 3.47 ± 0.69 cells/mm^3 vs. 0.81 ± 0.44 cells/mm^3, $p < 0.05$), but there was no significant difference between the vehicle group and the UC-MSC group. The number of CD206+/Iba-1+ cells was significantly higher in the UC-MSC group than in the sham group, but there was no significant difference between the vehicle and sham groups (**Figure 5D**, 14.58 ± 2.37 cells/mm^3 vs. 4.39 ± 1.11 cells/mm^3, $p < 0.05$). The volumes of the cortex, hippocampus, and corpus callosum were calculated. We found no significant difference among the sham, vehicle, and UC-MSC groups in either the hippocampus, cortex, or corpus callosum (**Supplementary Figure S2**).

DISCUSSION

In the present study, we aimed to create and establish a novel FGR rat model in which the uterine blood flow decreased gradually to investigate the neurological effects of the administration of UC-MSCs for the established FGR model as well as to verify the therapeutic effect of the UC-MSC treatment. To create an appropriate FGR model, we applied a slowly progressive ischemic burden to rats using ACs whose inner central hole gradually narrowed. The rats born with this treatment showed a significant reduction in body weight compared with the sham group, and we confirmed that those who received the ischemic burden in the uterus showed significant abnormalities upon behavioral and immunohistochemical evaluations. Moreover, we confirmed the therapeutic effects of UC-MSCs on the FGR model.

Thus far, a model in which pregnant rats were exposed to hypoxia (Jang et al., 2015), a model in which either a uterine artery was occluded by an atraumatic clamp for 60 min (Kazemi-Darabadi and Akbari, 2020) or a uterine artery and vein were ligated with a thread (Tashima et al., 2001), a model in which STA_2 was used (Saito et al., 2009), and a model in which microcoils were attached to a uterine and ovarian arteries (Ohshima et al., 2016) have been reported. Herrera et al. (2016) studied a guinea pig model with ACs attaching only to the uterine artery during the second trimester and reported that during pregnancy, the umbilical doppler blood flow decreased, and immediately before birth, the fetuses showed weight loss of approximately 30% and the heart, lungs, liver, and kidneys were significantly reduced in weight, which is similar to that

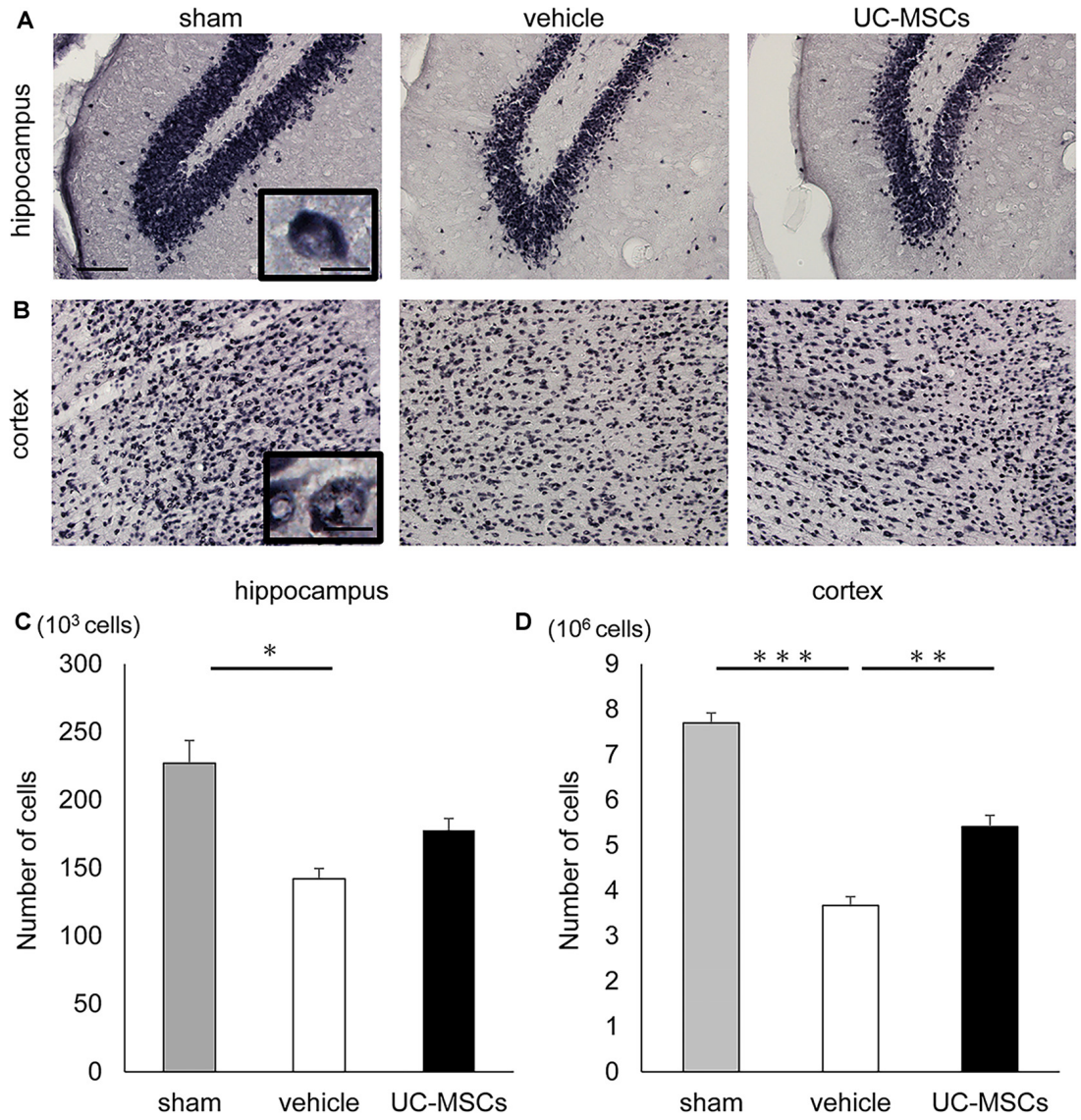

FIGURE 4 | Effects of UC-MSC treatment on neurons in FGR. Representative photomicrographs of the hippocampus **(A)** and part of the cortex **(B)** 2 months after birth. Scale bar = 100 μm. The inset shows a higher magnification view. Scale bar = 10 μm. **(C)** The number of positive cells for NeuN in the hippocampus was significantly lower in the vehicle group than in the sham group, although there was no significant difference between the UC-MSC group and the sham group (sham, $n = 8$; vehicle, $n = 3$; UC-MSCs $n = 4$). $^{*}p < 0.05$. **(D)** The number of positive cells for NeuN in the cortex was significantly lower in the vehicle group than that in the sham group, and a significant amelioration was observed in the UC-MSC group (sham, $n = 8$; vehicle, $n = 3$; UC-MSCs $n = 4$). $^{**}p < 0.01$, $^{***}p < 0.001$.

observed in our study; however, they reported no findings regarding neuromotor development. The attaching of ACs to the uterine artery affected the blood flow of each organ and reduced their weight (Herrera et al., 2016). On the contrary, in our FGR model, we attached ACs to not only the uterine but also the ovarian arteries during the third trimester, and the blood flow to the rats' uteruses was decreased to about 60% before birth *via* ACs whose center hole gradually narrowed. Furthermore, similar to other models (Tashima et al., 2001; Saito et al., 2009; Ohshima et al., 2016), we were able to reproduce a weight loss of over 20%. Although the degree of weight loss was different among litters, the functional impairment induced by chronic intrauterine hypoperfusion was observed in each litter (**Supplementary Figure S3**). The primary characteristic of the FGR model in the present study was the gradual reduction of blood flow in the uterine and ovarian arteries to the rats' uteruses.

In the management of HDP, blood flow to the fetus is one of the most important factors determining whether pregnancy can continue (Schwarze et al., 2005). Usually, the blood flow is gradually decreased, and blood flow interruption and sudden blood flow reduction are rare. As such, compared with FGR models using permanent ligations or temporary clamping of uterine arteries, our FGR model more precisely mimicked pathological conditions, as the blood flow to the animals' uteruses

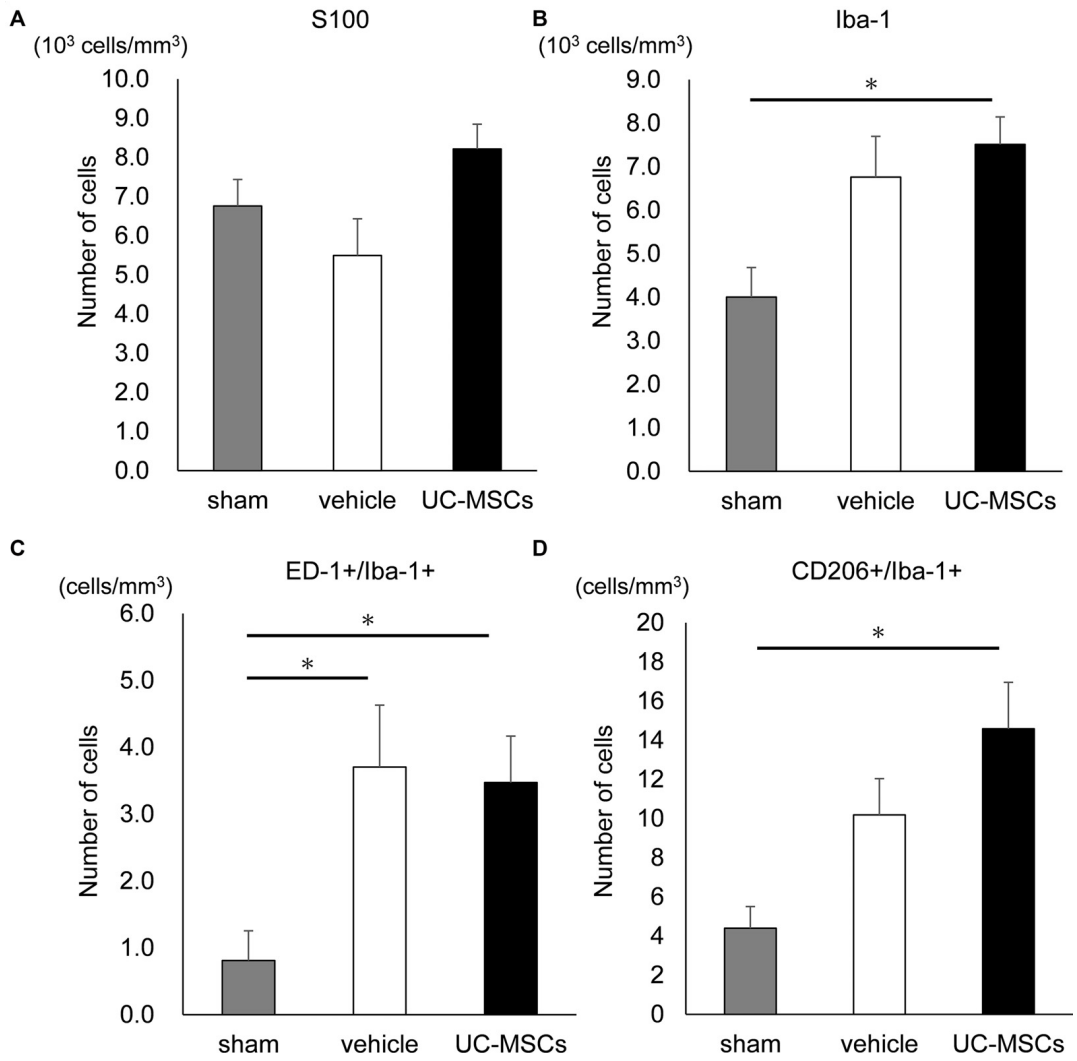

FIGURE 5 | Effects of UC-MSC treatment on astroglia and microglia in FGR. **(A)** There was no significant difference among the three groups in the number of S100 positive cells in the cortex. **(B)** The number of Iba-1 positive cells in the cortex was significantly higher in the UC-MSC group compared to the sham group (sham, $n = 8$; vehicle, $n = 3$; UC-MSCs, $n = 4$). $^*p < 0.05$. The number of ED-1 and Iba-1 double-positive cells **(C)** and CD206 and Iba-1 double-positive cells **(D)** in the cortex with fluorescent immunostaining. The number of ED-1+/Iba-1+ in both the UC-MSCs and the vehicle were significantly higher than that in the sham (sham, $n = 8$; vehicle, $n = 3$; UC-MSCs, $n = 4$). $^*p < 0.05$, whereas that of CD206+/Iba-1+ in the UC-MSCs was significantly higher than that in the sham (sham, $n = 8$; vehicle, $n = 3$; UC-MSCs, $n = 4$). $^*p < 0.05$.

was gradually reduced. The hypoperfused placenta releases inflammatory and anti-angiogenic factors that cause systemic inflammation, vascular dysfunction, high blood pressure, and maternal organ damage (LaMarca et al., 2016). In dogs, bilateral ligation of the uterine ovarian artery and obstruction of the abdominal aorta below the renal artery induced hypertension, proteinuria, and glomerular endotheliosis (Abitbol, 1981). Ligation of the unilateral uterine artery of a baboon also reproduced preeclampsia-like symptoms (Makris et al., 2007). Moreover, the development of FGR in an HDP mother was previously found to be associated with reduced uteroplacental blood flow and placental insufficiency and characterized by decreased oxygen and nutrient delivery to the fetus (Herrera et al., 2014). Although our model was not exactly an HDP model as we did not measure blood pressure and proteinuria in rats with AC in the present study, our model might represent the pathogenesis of HDP.

It is well known that children born with FGR display difficulties in coordination, lateralization, and abundance of associated movements (Leitner et al., 2000). Our model confirmed a significant delay in negative geotaxis as a primitive reflex as in the other model (Saito et al., 2009). Moreover, we revealed impairments of balance, coordination, durability, and learning memory with a rotarod treadmill test in the chronic phase, 5 months after birth. Our FGR rat model displayed similar symptoms as those in children with FGR. However, more experiments are needed to confirm whether our FGR model can display other such symptoms, including cognitive function and

behavioral problems, which are partially shown in other FGR models (Tashima et al., 2001; Saito et al., 2009; Pham et al., 2015; Ohshima et al., 2016). In a study that compared the total brain volume in humans using MRI, including a reduction in cortical gray and white matter volume, the small for gestational age (SGA) group showed a total brain volume reduction of almost 6% compared with the non-SGA control group. Thus, it has been reported that cerebral cortex volume is significantly affected by FGR (Østgård et al., 2014). Other studies have reported that SGA causes a decreased white matter volume in the cerebrum and cerebellum, a decreased basal ganglia volume, and a decreased overall cortical surface area (De Bie et al., 2011). In the present study, since both the numbers of neurons in the hippocampus and cortex were significantly reduced, the FGR model has a gray matter injury. To evaluate a white matter injury, we measured the volume of the corpus callosum but we did not find a significant difference among the three groups. Although our FGR model may be unlikely to have a white matter injury, a more detailed evaluation regarding white matter injury is required. Clinical studies have shown that FGR is also associated with diffuse white matter lesions, microglial activation, astrogliosis, and loss of pre-oligodendrocytes followed by a delay in myelination (Olivier et al., 2007), and decreased hippocampal volume (Lodygensky et al., 2008). Other FGR models display white matter (Ohshima et al., 2016) and hippocampal (Ruff et al., 2017) injuries and glial activation (Pham et al., 2015). Further detailed evaluations should be performed to demonstrate how our FGR model histologically mimics FGR in clinical settings.

In the present study, we also observed the therapeutic effects of UC-MSCs on primitive reflexes and motor function. In particular, the FGR model in which UC-MSCs were administered had a significantly large number of neurons. The FGR model delayed neurological maturation and impaired the behavioral deficit, and that administration of UC-MSCs ameliorated the neurological development delay and exerted a significant treatment effect on the deficit, even in the long term, i.e., 5 months after birth. The major mechanisms that may cause FGR brain cell death and injury are presumed to be excitotoxicity, oxidative stress, necrotic and apoptotic degeneration, and neuroinflammation (Rees et al., 2011; Miller et al., 2016). Chronic blood flow disturbances result in decreased oxygen delivery to the brain and decreased glucose and amino acid delivery, potentially affecting immature neurons and glial cells (Rees et al., 2011).

A previous study on the neurological effects of prenatal hypoxia on guinea pig brains showed that brain-derived neurotrophic factor (Bdnf) was significantly lower in the FGR group, and it was also reported that the Bdnf and Tropomyosin receptor kinase B protein levels were reduced in FGR fetuses (Dieni and Rees, 2005; Ke et al., 2011). The UC-MSCs express neurotrophic factors, and it has been reported that the UC-MSC-conditioned medium promotes Schwann cell viability and proliferation through increased levels of nerve growth factor and Bdnf expression due to the paracrine effect of UC-MSC on nerve regeneration (Guo et al., 2015). Our previous study also found that Bdnf and hepatocyte growth factor increased significantly in the serum, cerebrospinal fluid, and brain tissue of mice after intravenous administration of UC-MSCs in a neonatal intraventricular hemorrhage model and that periventricular reactive gliosis, hypomyelination, and periventricular cell death observed after IVH were significantly attenuated (Mukai et al., 2017). Generally, Bdnf is associated with neuronal cell proliferation, survival, and differentiation and is expressed in developing and adult brains (Lee et al., 2002; Pollock et al., 2016). As such, it also relieved hippocampal neuronal loss and promoted neurogenesis in the IVH model (Ko et al., 2018), enhanced proliferation in neuronal populations in the cerebellum and hippocampus (Nonomura et al., 1996; Labelle and Leclerc, 2000; Ko et al., 2018), and ameliorated hypomyelination (Xiao et al., 2010; Peckham et al., 2016). Also, the hepatocyte growth factor is known as a neurotrophic factor of motor, sensory, and parasympathetic neurons (Liu et al., 2010) and affects the development and growth of oligodendrocytes and the proliferation of myelin-forming Schwann cells (Yan and Rivkees, 2002). In a previous study with traumatic brain injury model rats, UC-MSC administration up-regulated neurotrophic factors, such as Bdnf and hepatocyte growth factor, and improved the neurological severity (Qi et al., 2018). In the present study, neurotrophic factors secreted by the UC-MSCs likely suppressed the neuroinflammation induced by chronic ischemia. The results of perinatal brain injury heavily involve microglia; proinflammatory M1 microglia first respond to stimuli such as hypoxic ischemia and infection and then involve the production of inflammatory cytokines that ultimately exacerbate brain injury. After the pro-inflammatory phase, the anti-inflammatory M2 microglia initiates the production of anti-inflammatory molecules that promote tissue repair and nerve regeneration (Hagberg et al., 2015). Exosomes derived from Human Wharton's jelly mesenchymal stem cells reduce microglia-mediated neuroinflammation with perinatal brain injury (Thomi et al., 2019). In the present study, there was no significant effect of UC-MSCs on M1 microglia. However, the number of M2 microglia was significantly higher in the administration of UC-MSCs than the sham. One possible mechanism for the improvement of the behaviors in the present study might be *via* M2 microglia activated by UC-MSCs. The inflammation and apoptosis in the acute and subacute phases could not be evaluated directly in the present study, but the decrease in the number of neurons was improved, and the number of M2 microglia, which result in an anti-inflammatory effect, was increased by UC-MSC administration. We speculated that UC-MSC treatment resulted in a reduction in cell death and/or an ameliorated suppressed neurogenesis *via* suppression of inflammation, which led to behavioral improvement. In the subsequent studies, we will evaluate the effect on inflammation and apoptosis in detail.

There are several limitations. The present study demonstrated the efficacy of xenograft administration of human UC-MSCs to rats. Before pursuing clinical application, it will be necessary to confirm the safety and efficacy of the human cells used in the clinical trial in a non-clinical study with an animal model. On the other hand, when we administer human cells to rats, we must consider the effects of xenografting. Although the effect of xenograft administration may be small as UC-MSCs

have immunomodulatory properties (Nagamura-Inoue and He, 2014), subsequent studies should evaluate the treatment effect using rat derived UC-MSCs.

Regarding the change of the inner diameter of ACs, we only used *in vitro* and not *in vivo* confirmation and this was another drawback of the study. A mouse model of subcortical infarcts using AC (inner diameter: 0.5 mm) reported that the center hole was not completely occluded a week after implantation *in vivo* (Hattori et al., 2015). Although we used a different AC size (inner diameter: 0.4 mm), the AC *in vivo* could be occluded slower than *in vitro*. However, the actual blood flow is more important than the change of AC, and we think the change of AC *in vitro* in the present study may be a reference value.

We administered UC-MSCs on day 4 but were not able to evaluate other treatment times. The third trimester is critical timing for glial cell proliferation and dendritic branching of synapse formation (de Graaf-Peters and Hadders-Algra, 2006). Since FGR injury developed in utero, it may be presumed that earlier timing after birth could be better, but one of the reasons that we selected P4 for the administration of the cells in the present study was due to technical limitations as the size of the pups was too small for us to intravenously administer. We need to further examine the optical number of cells, number of administrations, and timing for UC-MSC treatment.

Also, concerning the immunohistological evaluation, although there were statistically significant differences in some analyses with a limited number of samples, a confirmatory evaluation with a larger number of samples should be performed in the subsequent study.

In conclusion, we established a novel FGR rat model that mimics FGR associated with chronic mild intrauterine hypoperfusion. Also, the intravenous administration of UC-MSCs led to a significant amelioration of the reduced number of neurons and impaired behaviors induced by FGR.

DATA AVAILABILITY STATEMENT

The datasets generated for this study are available on request to the corresponding author.

ETHICS STATEMENT

The animal study was reviewed and approved by the Institutional Review Board of Nagoya University.

AUTHOR CONTRIBUTIONS

YK, YS, MT, MI, AS, YT, and MH designed the study. YK, AO, and MJ made FGR model rats. YK, SA, SG, HM, and TS conducted the experiments with immunohistochemistry, behavioral tests. KU, TM, and TN-I conducted UC-MSCs cell culture. YK and YS analyzed the data. YK, HM, and AH performed statistical analyses. YK and YS wrote the manuscript draft. MI, AS, YT, and HM critically revised the manuscript. All authors contributed to manuscript revision, read and approved the submitted version.

ACKNOWLEDGMENTS

We are grateful to Ms. Azusa Okamoto and Ms. Tomoko Yamaguchi for their skillful technical assistance.

SUPPLEMENTARY MATERIAL

The Supplementary Material for this article can be found online at: https://www.frontiersin.org/articles/10.3389/fncel.2020.00212/full#supplementary-material.

REFERENCES

Abitbol, M. M. (1981). A simplified technique to produce toxemia in the pregnant dog. *Am. J. Obstet. Gynecol.* 139, 526–534. doi: 10.1016/0002-9378(81)90512-3

Abuzzahab, M. J., Schneider, A., Goddard, A., Grigorescu, F., Lautier, C., Keller, E., et al. (2003). IGF-I receptor mutations resulting in intrauterine and postnatal growth retardation. *N. Engl. J. Med.* 349, 2211–2222. doi: 10.1056/NEJMoa010107

Baschat, A. A. (2011). Neurodevelopment following fetal growth restriction and its relationship with antepartum parameters of placental dysfunction. *Ultrasound Obstet. Gynecol.* 37, 501–514. doi: 10.1002/uog.9008

Bergvall, N., Iliadou, A., Johansson, S., Tuvemo, T., and Cnattingius, S. (2006). Risks for low intellectual performance related to being born small for gestational age are modified by gestational age. *Pediatrics* 117, e460–e467. doi: 10.1542/peds.2005-0737

Blickstein, I. (2004). Is it normal for multiples to be smaller than singletons? *Best. Pract. Res. Clin. Obstet. Gynaecol.* 18, 613–623. doi: 10.1016/j.bpobgyn.2004.04.008

Chen, J., Li, Y., Wang, L., Zhang, Z., Lu, D., Lu, M., et al. (2001). Therapeutic benefit of intravenous administration of bone marrow stromal cells after cerebral ischemia in rats. *Stroke* 32, 1005–1011. doi: 10.1161/01.str.32.4.1005

Cunningham, C. J., Redondo-Castro, E., and Allan, S. M. (2018). The therapeutic potential of the mesenchymal stem cell secretome in ischaemic stroke. *J. Cereb. Blood Flow Metab.* 38, 1276–1292. doi: 10.1177/0271678x18776802

De Bie, H. M., Oostrom, K. J., Boersma, M., Veltman, D. J., Barkhof, F., Delemarre-Van De Waal, H. A., et al. (2011). Global and regional differences in brain anatomy of young children born small for gestational age. *PLoS One* 6:e24116. doi: 10.1371/journal.pone.0024116

de Graaf-Peters, V. B., and Hadders-Algra, M. (2006). Ontogeny of the human central nervous system: what is happening when? *Early Hum. Dev.* 82, 257–266. doi: 10.1016/j.earlhumdev.2005.10.013

de Onis, M., Blossner, M., and Villar, J. (1998). Levels and patterns of intrauterine growth retardation in developing countries. *Eur. J. Clin. Nutr.* 52, S5–S15.

Dieni, S., and Rees, S. (2005). BDNF and TrkB protein expression is altered in the fetal hippocampus but not cerebellum after chronic prenatal compromise. *Exp. Neurol.* 192, 265–273. doi: 10.1016/j.expneurol.2004.06.003

Dolinsky, V. W., Rueda-Clausen, C. F., Morton, J. S., Davidge, S. T., and Dyck, J. R. (2011). Continued postnatal administration of resveratrol prevents diet-induced metabolic syndrome in rat offspring born growth restricted. *Diabetes* 60, 2274–2284. doi: 10.2337/db11-0374

Feldman, R., and Eidelman, A. I. (2006). Neonatal state organization, neuromaturation, mother-infant interaction, and cognitive development in small-for-gestational-age premature infants. *Pediatrics* 118, e869–e878. doi: 10.1542/peds.2005-2040

Fredriksson, I., and Larsson, M. (2017). Vessel packaging effect in laser speckle contrast imaging and laser Doppler imaging. *J. Biomed. Opt.* 22, 1–7. doi: 10.1117/1.jbo.22.10.106005

Froen, J. F., Gardosi, J. O., Thurmann, A., Francis, A., and Stray-Pedersen, B. (2004). Restricted fetal growth in sudden intrauterine unexplained death. *Acta Obstet. Gynecol. Scand.* 83, 801–807. doi: 10.1111/j.0001-6349.2004.00602.x

Galan, H. L., Rigano, S., Radaelli, T., Cetin, I., Bozzo, M., Chyu, J., et al. (2001). Reduction of subcutaneous mass, but not lean mass, in normal fetuses in Denver, Colorado. *Am. J. Obstet. Gynecol.* 185, 839–844. doi: 10.1067/mob.2001.117350

Geva, R., Eshel, R., Leitner, Y., Fattal-Valevski, A., and Harel, S. (2006). Memory functions of children born with asymmetric intrauterine growth restriction. *Brain Res.* 1117, 186–194. doi: 10.1016/j.brainres.2006.08.004

Girdlestone, J., Limbani, V. A., Cutler, A. J., and Navarrete, C. V. (2009). Efficient expansion of mesenchymal stromal cells from umbilical cord under low serum conditions. *Cytotherapy* 11, 738–748. doi: 10.3109/14653240903079401

Götherstrom, C. (2007). Immunomodulation by multipotent mesenchymal stromal cells. *Transplantation* 84, S35–S37. doi: 10.1097/01.tp.0000269200.67707.c8

Guo, Z. Y., Sun, X., Xu, X. L., Zhao, Q., Peng, J., and Wang, Y. (2015). Human umbilical cord mesenchymal stem cells promote peripheral nerve repair *via* paracrine mechanisms. *Neural Regen Res.* 10, 651–658. doi: 10.4103/1673-5374.155442

Hagberg, H., Mallard, C., Ferriero, D. M., Vannucci, S. J., Levison, S. W., Vexler, Z. S., et al. (2015). The role of inflammation in perinatal brain injury. *Nat. Rev. Neurol.* 11, 192–208. doi: 10.1038/nrneurol.2015.13

Hattori, Y., Enmi, J., Kitamura, A., Yamamoto, Y., Saito, S., Takahashi, Y., et al. (2015). A novel mouse model of subcortical infarcts with dementia. *J. Neurosci.* 35, 3915–3928. doi: 10.1523/JNEUROSCI.3970-14.2015

Herrera, E. A., Alegria, R., Farias, M., Diaz-Lopez, F., Hernandez, C., Uauy, R., et al. (2016). Assessment of *in vivo* fetal growth and placental vascular function in a novel intrauterine growth restriction model of progressive uterine artery occlusion in guinea pigs. *J. Physiol.* 594, 1553–1561. doi: 10.1113/jp271467

Herrera, E. A., Krause, B., Ebensperger, G., Reyes, R. V., Casanello, P., Parra-Cordero, M., et al. (2014). The placental pursuit for an adequate oxidant balance between the mother and the fetus. *Front. Pharmacol.* 5:149. doi: 10.3389/fphar.2014.00149

Hsieh, J. Y., Fu, Y. S., Chang, S. J., Tsuang, Y. H., and Wang, H. W. (2010). Functional module analysis reveals differential osteogenic and stemness potentials in human mesenchymal stem cells from bone marrow and Wharton's jelly of umbilical cord. *Stem Cells Dev.* 19, 1895–1910. doi: 10.1089/scd.2009.0485

Infante-Rivard, C., Rivard, G. E., Yotov, W. V., Genin, E., Guiguet, M., Weinberg, C., et al. (2002). Absence of association of thrombophilia polymorphisms with intrauterine growth restriction. *N. Engl. J. Med.* 347, 19–25. doi: 10.1056/NEJM200207043470105

Jang, E. A., Longo, L. D., and Goyal, R. (2015). Antenatal maternal hypoxia: criterion for fetal growth restriction in rodents. *Front. Physiol.* 6:176. doi: 10.3389/fphys.2015.00176

Kazemi-Darabadi, S., and Akbari, G. (2020). Evaluation of magnesium sulfate effects on fetus development in experimentally induced surgical fetal growth restriction in rat. *J. Matern. Fetal Neonatal. Med.* 33, 2459–2465. doi: 10.1080/14767058.2018.1554048

Ke, X., McKnight, R. A., Caprau, D., O'Grady, S., Fu, Q., Yu, X., et al. (2011). Intrauterine growth restriction affects hippocampal dual specificity phosphatase 5 gene expression and epigenetic characteristics. *Physiol. Genomics* 43, 1160–1169. doi: 10.1152/physiolgenomics.00242.2010

Kintiraki, E., Papakatsika, S., Kotronis, G., Goulis, D. G., and Kotsis, V. (2015). Pregnancy-induced hypertension. *Hormones* 14, 211–223. doi: 10.14310/horm.2002.1582

Ko, H. R., Ahn, S. Y., Chang, Y. S., Hwang, I., Yun, T., Sung, D. K., et al. (2018). Human UCB-MSCs treatment upon intraventricular hemorrhage contributes to attenuate hippocampal neuron loss and circuit damage through BDNF-CREB signaling. *Stem Cell Res. Ther.* 9:326. doi: 10.1186/s13287-018-1052-5

Labelle, C., and Leclerc, N. (2000). Exogenous BDNF, NT-3 and NT-4 differentially regulate neurite outgrowth in cultured hippocampal neurons. *Brain Res. Dev. Brain Res.* 123, 1–11. doi: 10.1016/s0165-3806(00)00069-9

LaMarca, B., Amaral, L. M., Harmon, A. C., Cornelius, D. C., Faulkner, J. L., and Cunningham, M. W. Jr., et al. (2016). Placental ischemia and resultant phenotype in animal models of preeclampsia. *Curr. Hypertens Rep.* 18:38. doi: 10.1007/s11906-016-0633-x

Le Blanc, K., and Ringden, O. (2005). Immunobiology of human mesenchymal stem cells and future use in hematopoietic stem cell transplantation. *Biol. Blood Marrow. Transplant.* 11, 321–334. doi: 10.1016/j.bbmt.2005.01.005

Lee, J., Duan, W., and Mattson, M. P. (2002). Evidence that brain-derived neurotrophic factor is required for basal neurogenesis and mediates, in part, the enhancement of neurogenesis by dietary restriction in the hippocampus of adult mice. *J. Neurochem.* 82, 1367–1375. doi: 10.1046/j.1471-4159.2002.01085.x

Leitner, Y., Fattal-Valevski, A., Geva, R., Bassan, H., Posner, E., Kutai, M., et al. (2000). Six-year follow-up of children with intrauterine growth retardation: long-term, prospective study. *J. Child Neurol.* 15, 781–786. doi: 10.1177/088307380001501202

Li, X., Zhang, W., Lin, J., Liu, H., Yang, Z., Teng, Y., et al. (2020). Hypertensive disorders of pregnancy and risks of adverse pregnancy outcomes: a retrospective cohort study of 2368 patients. *J. Hum. Hypertens.* doi: 10.1038/s41371-020-0312-x [Epub ahead of print].

Lieberman, E., Gremy, I., Lang, J. M., and Cohen, A. P. (1994). Low birthweight at term and the timing of fetal exposure to maternal smoking. *Am. J. Public Health* 84, 1127–1131. doi: 10.2105/ajph.84.7.1127

Lin, C. C., and Santolaya-Forgas, J. (1998). Current concepts of fetal growth restriction: part I. Causes, classification, and pathophysiology. *Obstet. Gynecol.* 92, 1044–1055. doi: 10.1016/s0029-7844(98)00328-7

Liu, A. M., Lu, G., Tsang, K. S., Li, G., Wu, Y., Huang, Z. S., et al. (2010). Umbilical cord-derived mesenchymal stem cells with forced expression of hepatocyte growth factor enhance remyelination and functional recovery in a rat intracerebral hemorrhage model. *Neurosurgery* 67, 357–365; discussion 365–356. doi: 10.1227/01.neu.0000371983.06278.b3

Lodygensky, G. A., Seghier, M. L., Warfield, S. K., Tolsa, C. B., Sizonenko, S., Lazeyras, F., et al. (2008). Intrauterine growth restriction affects the preterm infant's hippocampus. *Pediatr. Res.* 63, 438–443. doi: 10.1203/PDR.0b013e318165c005

Makris, A., Thornton, C., Thompson, J., Thomson, S., Martin, R., Ogle, R., et al. (2007). Uteroplacental ischemia results in proteinuric hypertension and elevated sFLT-1. *Kidney Int.* 71, 977–984. doi: 10.1038/sj.ki.5002175

McCowan, L. M., Craigie, S., Taylor, R. S., Ward, C., Mclintock, C., and North, R. A. (2003). Inherited thrombophilias are not increased in "idiopathic" small-for-gestational-age pregnancies. *Am. J. Obstet. Gynecol.* 188, 981–985. doi: 10.1067/mob.2003.218

Miller, S. L., Huppi, P. S., and Mallard, C. (2016). The consequences of fetal growth restriction on brain structure and neurodevelopmental outcome. *J. Physiol.* 594, 807–823. doi: 10.1113/jp271402

Mori, Y., Ohshimo, J., Shimazu, T., He, H., Takahashi, A., Yamamoto, Y., et al. (2015). Improved explant method to isolate umbilical cord-derived mesenchymal stem cells and their immunosuppressive properties. *Tissue Eng. Part C Methods* 21, 367–372. doi: 10.1089/ten.tec.2014.0385

Morton, J. S., Rueda-Clausen, C. F., and Davidge, S. T. (2010). Mechanisms of endothelium-dependent vasodilation in male and female, young and aged offspring born growth restricted. *Am. J. Physiol. Regul. Integr. Comp. Physiol.* 298, R930–R938. doi: 10.1152/ajpregu.00641.2009

Mukai, T., Mori, Y., Shimazu, T., Takahashi, A., Tsunoda, H., Yamaguchi, S., et al. (2017). Intravenous injection of umbilical cord-derived mesenchymal stromal cells attenuates reactive gliosis and hypomyelination in a neonatal intraventricular hemorrhage model. *Neuroscience* 355, 175–187. doi: 10.1016/j.neuroscience.2017.05.006

Naderi, S., Tsai, S. A., and Khandelwal, A. (2017). Hypertensive disorders of pregnancy. *Curr. Atheroscler. Rep.* 19, 15–15. doi: 10.1007/s11883-017-0648-z

Nagamura-Inoue, T., and He, H. (2014). Umbilical cord-derived mesenchymal stem cells: their advantages and potential clinical utility. *World J. Stem Cells* 6, 195–202. doi: 10.4252/wjsc.v6.i2.195

Neerhof, M. G. (1995). Causes of intrauterine growth restriction. *Clin. Perinatol.* 22, 375–385. doi: 10.1016/s0095-5108(18)30289-6

Nonomura, T., Kubo, T., Oka, T., Shimoke, K., Yamada, M., Enokido, Y., et al. (1996). Signaling pathways and survival effects of BDNF and NT-3 on cultured cerebellar granule cells. *Brain Res. Dev. Brain Res.* 97, 42–50. doi: 10.1016/s0165-3806(96)00130-7

Ohshima, M., Coq, J. O., Otani, K., Hattori, Y., Ogawa, Y., Sato, Y., et al. (2016). Mild intrauterine hypoperfusion reproduces neurodevelopmental disorders observed in prematurity. *Sci. Rep.* 6:39377. doi: 10.1038/srep39377

Olivier, P., Baud, O., Bouslama, M., Evrard, P., Gressens, P., and Verney, C. (2007). Moderate growth restriction: deleterious and protective effects on white matter damage. *Neurobiol. Dis.* 26, 253–263. doi: 10.1016/j.nbd.2007.01.001

Orlic, D., Kajstura, J., Chimenti, S., Jakoniuk, I., Anderson, S. M., Li, B., et al. (2001). Bone marrow cells regenerate infarcted myocardium. *Nature* 410, 701–705. doi: 10.1038/35070587

Osato, K., Sato, Y., Ochiishi, T., Osato, A., Zhu, C., Sato, M., et al. (2010). Apoptosis-inducing factor deficiency decreases the proliferation rate and protects the subventricular zone against ionizing radiation. *Cell Death Dis.* 1:e84. doi: 10.1038/cddis.2010.63

Østgård, H. F., Løhaugen, G. C., Bjuland, K. J., Rimol, L. M., Brubakk, A. M., Martinussen, M., et al. (2014). Brain morphometry and cognition in young adults born small for gestational age at term. *J. Pediatr.* 165, 921.e1–927.e1. doi: 10.1016/j.jpeds.2014.07.045

Padidela, R. N., and Bhat, V. (2003). Neurobehavioral assessment of appropriate for gestational and small for gestational age babies. *Indian Pediatr.* 40, 1063–1068.

Peckham, H., Giuffrida, L., Wood, R., Gonsalvez, D., Ferner, A., Kilpatrick, T. J., et al. (2016). Fyn is an intermediate kinase that BDNF utilizes to promote oligodendrocyte myelination. *Glia* 64, 255–269. doi: 10.1002/glia.22927

Pham, H., Duy, A. P., Pansiot, J., Bollen, B., Gallego, J., Charriaut-Marlangue, C., et al. (2015). Impact of inhaled nitric oxide on white matter damage in growth-restricted neonatal rats. *Pediatr. Res.* 77, 563–569. doi: 10.1038/pr.2015.4

Pollock, K., Dahlenburg, H., Nelson, H., Fink, K. D., Cary, W., Hendrix, K., et al. (2016). Human mesenchymal stem cells genetically engineered to overexpress brain-derived neurotrophic factor improve outcomes in Huntington's disease mouse models. *Mol. Ther.* 24, 965–977. doi: 10.1038/mt.2016.12

Prasanna, S. J., Gopalakrishnan, D., Shankar, S. R., and Vasandan, A. B. (2010). Pro-inflammatory cytokines, IFNγ and TNFα, influence immune properties of human bone marrow and Wharton jelly mesenchymal stem cells differentially. *PLoS One* 5:e9016. doi: 10.1371/journal.pone.0009016

Qi, L., Xue, X., Sun, J., Wu, Q., Wang, H., Guo, Y., et al. (2018). The promising effects of transplanted umbilical cord mesenchymal stem cells on the treatment in traumatic brain injury. *J. Craniofac. Surg.* 29, 1689–1692. doi: 10.1097/scs.0000000000005042

Rees, S., Harding, R., and Walker, D. (2011). The biological basis of injury and neuroprotection in the fetal and neonatal brain. *Int. J. Dev. Neurosci.* 29, 551–563. doi: 10.1016/j.ijdevneu.2011.04.004

Ruff, C. A., Faulkner, S. D., Rumajogee, P., Beldick, S., Foltz, W., Corrigan, J., et al. (2017). The extent of intrauterine growth restriction determines the severity of cerebral injury and neurobehavioural deficits in rodents. *PLoS One* 12:e0184653. doi: 10.1371/journal.pone.0184653

Saito, A., Matsui, F., Hayashi, K., Watanabe, K., Ichinohashi, Y., Sato, Y., et al. (2009). Behavioral abnormalities of fetal growth retardation model rats with reduced amounts of brain proteoglycans. *Exp. Neurol.* 219, 81–92. doi: 10.1016/j.expneurol.2009.04.012

Salmaso, N., Jablonska, B., Scafidi, J., Vaccarino, F. M., and Gallo, V. (2014). Neurobiology of premature brain injury. *Nat. Neurosci.* 17, 341–346. doi: 10.1038/nn.3604

Schulz, L. C. (2010). The Dutch Hunger Winter and the developmental origins of health and disease. *Proc. Natl. Acad. Sci. U S A* 107, 16757–16758. doi: 10.1073/pnas.1012911107

Schwarz, E. J., Alexander, G. M., Prockop, D. J., and Azizi, S. A. (1999). Multipotential marrow stromal cells transduced to produce L-DOPA: engraftment in a rat model of Parkinson disease. *Hum. Gene Ther.* 10, 2539–2549. doi: 10.1089/10430349950016870

Schwarze, A., Gembruch, U., Krapp, M., Katalinic, A., Germer, U., and Axt-Fliedner, R. (2005). Qualitative venous Doppler flow waveform analysis in preterm intrauterine growth-restricted fetuses with ARED flow in the umbilical artery—correlation with short-term outcome. *Ultrasound Obstet. Gynecol.* 25, 573–579. doi: 10.1002/uog.1914

Sharma, D., Farahbakhsh, N., Shastri, S., and Sharma, P. (2016a). Intrauterine growth restriction—part 2. *J. Matern. Fetal Neonatal. Med.* 29, 4037–4048. doi: 10.3109/14767058.2016.1154525

Sharma, D., Shastri, S., and Sharma, P. (2016b). Intrauterine growth restriction: antenatal and postnatal aspects. *Clin. Med. Insights Pediatr.* 10, 67–83. doi: 10.4137/cmped.s40070

Shimazu, T., Mori, Y., Takahashi, A., Tsunoda, H., Tojo, A., and Nagamura-Inoue, T. (2015). Serum- and xeno-free cryopreservation of human umbilical cord tissue as mesenchymal stromal cell source. *Cytotherapy* 17, 593–600. doi: 10.1016/j.jcyt.2015.03.604

Sriramulu, S., Banerjee, A., Di Liddo, R., Jothimani, G., Gopinath, M., Murugesan, R., et al. (2018). Concise review on clinical applications of conditioned medium derived from human umbilical cord-mesenchymal stem cells (UC-MSCs). *Int. J. Hematol. Oncol. Stem Cell Res.* 12, 230–234.

Tashima, L., Nakata, M., Anno, K., Sugino, N., and Kato, H. (2001). Prenatal influence of ischemia-hypoxia-induced intrauterine growth retardation on brain development and behavioral activity in rats. *Biol. Neonate* 80, 81–87. doi: 10.1159/000047125

Thomi, G., Surbek, D., Haesler, V., Joérger-Messerli, M., and Schoeberlein, A. (2019). Exosomes derived from umbilical cord mesenchymal stem cells reduce microglia-mediated neuroinflammation in perinatal brain injury. *Stem Cell Res. Ther.* 10:105. doi: 10.1186/s13287-019-1207-z

Uccelli, A., Moretta, L., and Pistoia, V. (2008). Mesenchymal stem cells in health and disease. *Nat. Rev. Immunol.* 8, 726–736. doi: 10.1038/nri2395

Wagenaar, N., Nijboer, C. H., and van Bel, F. (2017). Repair of neonatal brain injury: bringing stem cell-based therapy into clinical practice. *Dev. Med. Child Neurol.* 59, 997–1003. doi: 10.1111/dmcn.13528

Wixey, J. A., Chand, K. K., Colditz, P. B., and Bjorkman, S. T. (2017). Review: neuroinflammation in intrauterine growth restriction. *Placenta* 54, 117–124. doi: 10.1016/j.placenta.2016.11.012

Xiao, J., Wong, A. W., Willingham, M. M., Van Den Buuse, M., Kilpatrick, T. J., and Murray, S. S. (2010). Brain-derived neurotrophic factor promotes central nervous system myelination *via* a direct effect upon oligodendrocytes. *Neurosignals* 18, 186–202. doi: 10.1159/000323170

Yan, H., and Rivkees, S. A. (2002). Hepatocyte growth factor stimulates the proliferation and migration of oligodendrocyte precursor cells. *J. Neurosci. Res.* 69, 597–606. doi: 10.1002/jnr.10323

Zuk, L., Harel, S., Leitner, Y., and Fattal-Valevski, A. (2004). Neonatal general movements: an early predictor for neurodevelopmental outcome in infants with intrauterine growth retardation. *J. Child Neurol.* 19, 14–18. doi: 10.1177/088307380401900103011

Conflict of Interest: The authors declare that the research was conducted in the absence of any commercial or financial relationships that could be construed as a potential conflict of interest.

The handling Editor declared a past collaboration with one of the authors YS.

frontiers in Cellular Neuroscience

ORIGINAL RESEARCH
published: 07 August 2020
doi: 10.3389/fncel.2020.00249

Type 2 Innate Lymphoid Cells Accumulate in the Brain After Hypoxia-Ischemia but Do Not Contribute to the Development of Preterm Brain Injury

*Aura Zelco[1], Eridan Rocha-Ferreira[2], Arshed Nazmi[1], Maryam Ardalan[1], Tetyana Chumak[1], Gisela Nilsson[1], Henrik Hagberg[2], Carina Mallard[1] and Xiaoyang Wang[1,3]**

[1] Department of Physiology, Institute of Neuroscience and Physiology, Sahlgrenska Academy, University of Gothenburg, Gothenburg, Sweden, [2] Centre of Perinatal Medicine & Health, Institute of Clinical Sciences, Sahlgrenska Academy, University of Gothenburg, Gothenburg, Sweden, [3] Henan Key Laboratory of Child Brain Injury, Institute of Neuroscience and Third Affiliated Hospital of Zhengzhou University, Zhengzhou, China

OPEN ACCESS

Edited by:
Chao Chen,
Children's Hospital of Fudan University, China

Reviewed by:
Hector Rosas-Hernandez,
National Center for Toxicological Research (FDA), United States
Josephine Herz,
Essen University Hospital, Germany

***Correspondence:**
Xiaoyang Wang
xiaoyang.wang@fysiologi.gu.se

Specialty section:
This article was submitted to Cellular Neuropathology, a section of the journal Frontiers in Cellular Neuroscience

Received: 19 February 2020
Accepted: 17 July 2020
Published: 07 August 2020

Citation:
Zelco A, Rocha-Ferreira E, Nazmi A, Ardalan M, Chumak T, Nilsson G, Hagberg H, Mallard C and Wang X (2020) Type 2 Innate Lymphoid Cells Accumulate in the Brain After Hypoxia-Ischemia but Do Not Contribute to the Development of Preterm Brain Injury. Front. Cell. Neurosci. 14:249. doi: 10.3389/fncel.2020.00249

Background: The immune system of human and mouse neonates is relatively immature. However, innate lymphoid cells (ILCs), commonly divided into the subsets ILC1, ILC2, and ILC3, are already present in the placenta and other fetal compartments and exhibit higher activity than what is seen in adulthood. Recent reports have suggested the potential role of ILCs, especially ILC2s, in spontaneous preterm labor, which is associated with brain damage and subsequent long-term neurodevelopmental deficits. Therefore, we hypothesized that ILCs, and especially ILC2s, play a role in preterm brain injury.

Methods: C57Bl/6J mice at postnatal day 6 were subjected to hypoxia-ischemia (HI) insult induced by left carotid artery ligation and subsequent exposure to 10% oxygen in nitrogen. The presence of ILCs and ILC2s in the brain was examined at different time points after HI. The contribution of ILC2s to HI-induced preterm brain damage was explored using a conditionally targeted ILC2-deficient mouse strain ($Ror\alpha^{fl/fl}IL7r^{Cre}$), and gray and white-matter injury were evaluated at 7 days post-HI. The inflammatory response in the injured brain was assessed using immunoassays and immunochemistry staining.

Results: Significant increases in ILCs and ILC2s were observed at 24 h, 3 days, and 7 days post-HI in the injured brain hemisphere compared with the uninjured hemisphere in wild-type mice. ILC2s in the brain were predominantly located in the meninges of the injured ipsilateral hemispheres after HI but not in the brain parenchyma. Overall, we did not observe changes in cytokine/chemokine levels in the brains of $Ror\alpha^{fl/fl}IL7r^{Cre}$ mice compared with wild type animals apart from IL-13. Gray and white-matter tissue loss in the brain was not affected after HI in $Ror\alpha^{fl/fl}IL7r^{Cre}$ mice. Correspondingly, we

did not find any differences in reactive microglia and astrocyte numbers in the brain in *Rorα*$^{fl/fl}$*IL7r*^{Cre} mice compared with wild-type mice following HI insult.

Conclusion: After HI, ILCs and ILC2s accumulate in the injured brain hemisphere. However, ILC2s do not contribute to the development of brain damage in this mouse model of preterm brain injury.

Keywords: preterm brain injury, innate lymphoid cells, hypoxia-ischemia, innate immunity, newborns

INTRODUCTION

Preterm infants are highly susceptible to brain damage, which may lead to long-term neurodevelopmental deficits such as cerebral palsy and cognitive impairments. Therapeutic hypothermia is used for term newborns, and other strategies such as erythropoietin are being tested; however, there are still no effective treatments for brain damage in preterm newborns (Shankaran et al., 2005; Zhu et al., 2009; Shankaran, 2015; Natalucci et al., 2016; Song et al., 2016; Juul et al., 2020). The mechanisms underlying perinatal brain damage are not fully understood, but hypoxia-ischemia (HI) and maternal/neonatal inflammation have been suggested as major etiological factors. Apoptosis, mitochondrial dysfunction, excitotoxicity, and impaired oligodendrocyte maturation are also implicated in the injury process, as is the involvement of immune cells (Yang et al., 2014; Hagberg et al., 2015; Zhang et al., 2017; Albertsson et al., 2018; Herz et al., 2018; Nazmi et al., 2018).

Since their discovery about a decade ago, innate lymphoid cells (ILCs), which are part of the innate immune system, have been studied intensively. ILCs lack antigen recognition and therefore can respond quickly to a variety of stimuli in their immediate surroundings (Spits et al., 2013; Vivier et al., 2018). ILCs are usually divided into subtypes based on the expression of the transcription factors that regulate their development, cytokine production, and function. These cells mirror the T-helper (Th) cells of the adaptive immune system in terms of their cytokine production and functions (Almeida and Belz, 2016). Type 1 ILCs (ILC1s), including natural killer cells, respond similarly to Th1 cells. ILC2s mirror Th2 cells with the production of cytokines such as interleukin (IL)-4, IL-5, and IL-13, which are involved in allergic inflammation. ILC3s are similar to Th17 cells and secrete IL-17 and IL-22 upon activation (Spits et al., 2013; Vivier et al., 2018). The immune response in neonates is biased toward the Th2 type (Adkins et al., 2004; Debock and Flamand, 2014), but after HI insult there is a Th1/Th17-type immune response in the neonatal mouse brain (Albertsson et al., 2014; Yang et al., 2014) and blockage of lymphocyte trafficking to the brain is neuroprotective (Yang et al., 2014). Further, the Th2 cytokines IL-4 and IL-13 have been found to protect the mouse brain from injury (Walsh et al., 2015; Kolosowska et al., 2019).

ILCs have been shown to play an important role in the immune response against viruses, allergens, and lung and intestinal inflammation (Nussbaum et al., 2013; Bernink et al., 2014; Oliphant et al., 2014; Besnard et al., 2015). Furthermore, ILCs develop early in ontogeny and are present already in the placenta and in other fetal compartments like the thymus, the liver, cord blood, and bone marrow (Forsberg et al., 2014; Jones et al., 2018; Miller et al., 2018; Xu et al., 2018) and therefore might be especially important for immune responses in early life. Recent studies have shown that ILC2s are involved in asthma-like responses after neonatal hyperoxia (Cheon et al., 2018) and that together with ILC3s they are increased when spontaneous preterm birth occurs (Xu et al., 2018), suggesting the possible involvement of these cells in injurious events around birth. Additionally, ILCs, in particular ILC2s, have been found in the murine central nervous system (Mair and Becher, 2014; Besnard et al., 2015; Russi et al., 2015; Fung et al., 2020), especially in the meninges (Gadani et al., 2017; Russi et al., 2018), and they are involved in the neuroinflammatory response associated with experimental autoimmune encephalomyelitis (Mair and Becher, 2014), aging (Fung et al., 2020), and cerebral malaria (Besnard et al., 2015). In a mouse model of spinal cord injury, meningeal ILC2s are functionally activated, enter the injury site, and produce type 2 cytokines that up-regulate inflammatory genes and improve recovery, thus suggesting that these cells can also play a beneficial role in preventing CNS injury (Gadani et al., 2017).

Given the early development and functional maturity of ILCs in ontogeny, the rapid response of ILCs to insults in various tissues, and their potential role in cerebral pathologies, we hypothesize that ILCs accumulate in the brain after HI insult and are involved in the injury process in the mouse model of preterm brain injury.

MATERIALS AND METHODS

Experimental Animals

Mice were bred at our animal facility (Experimental Biomedicine, University of Gothenburg), and pups of both sexes were used. C57Bl/6J mice (Charles River, Germany) were used for flow cytometry experiments and meningeal immunofluorescence staining. The transgenic mouse strain *Rorα*$^{fl/fl}$*IL7r*^{Cre}, that were generated by crossing *Rorα*$^{fl/fl}$ mice and *IL7-Cre* mice, was a kind gift from Professor Andrew McKenzie (Cambridge University, United Kingdom). The floxed gene was retinoid-related orphan receptor alpha (RORα), a transcription factor that is critical for ILC2 development. The Cre-recombinase enzyme was linked to interleukin-7 receptor (IL7R), a transmembrane receptor restricted to the lymphoid lineage. This combination leads to impairment of ILC2s, as described previously (Oliphant et al., 2014). *Rorα*$^{fl/fl}$*IL7r*$^{+/Cre}$ (ILC2-impaired) and *Rorα*$^{fl/fl}$*IL7r*$^{+/+}$

(wild-type controls) mouse littermates were used in the experiments. These mice were phenotypically indistinguishable from commercially available C57Bl/6J mice. Genotyping of *Rorα*$^{fl/fl}$ mice was undertaken using PCR primers (5′ TGA GTG GTA ACA CCA CGG CAC GC 3′ and 5′ TGG AGC AGA ATC ATC CAG GAG GCC 3′), giving a wild-type product of 573 bp and a targeted product of ∼650 bp. For genotyping of *IL7-Cre* mice, the PCR primers were 5′ CCT GAA AAC TTT GCC CCC TCC ATA 3′, 5′ CCA TAG AAT AGT GCA GCC TTG CCT C 3′, and 5′ AGC GAA AGC TCT ACC CAG AGC 3′, and these generated a wild-type product of 584 bp and a targeted product of 680 bp.

The animal facility had a 12-h light-dark cycle, and the mice had free access to standard chow (B&K, Solna, Sweden) and water. All experiments were performed with the approval of the Regional Animal Ethical Committee of Gothenburg (ethical permit numbers 58/2016 and 2042/18). The experimental design and the number of animals used for each experiment are shown in **Figure 1**.

Hypoxic-Ischemic Model

The day of birth was defined as postnatal day (PND)0. At PND6, HI surgery was performed as described previously (Albertsson et al., 2014). The pups were anesthetized with isoflurane (5% for induction and 3% for maintenance) and underwent unilateral left carotid artery ligation followed by xylocaine as the local anesthetic. After recovering with their dam for 1 h, the pups were transferred to a humidified chamber for exposure to 70 min of hypoxia (10% O_2 in N_2, 36.0 ± 0.5°C) (Rice et al., 1981). Before and after the hypoxia, the pups rested for 10 min at 36.0 ± 0.5°C in the chamber. The pups were then returned to the dam's cage until being sacrificed.

IL-33 Stimulation of ILC2 Expansion

To test the Cre efficiency in neonatal ILC2-impaired mice, we challenged wild type and ILC2-impaired pups with IL-33, which promotes ILC2 expansion (Oliphant et al., 2014). Briefly, the pups received intraperitoneal (i.p.) injections of either mouse recombinant IL-33 (0.04 μg/μl/g body weight in PBS, BioLegend) or PBS alone (n = 6–9/group) every 24 h from PND3 to PND6 for a total of four injections. The pups were sacrificed 24 h after the last injection (PND7), and their lungs were collected for flow cytometry analysis to determine the number of IL-33–induced ILC2s.

Flow Cytometry Experiments

Flow cytometry was used to investigate the presence of all ILCs in the brains of C57Bl/6J mice at 6 h, 24 h, 3 days, and 7 days after HI with naïve littermates as controls (n = 6–8/group). Transcardial saline perfusion was performed after i.p. injection of pentobarbital (50 mg/ml, Abcur AB, Helsingborg, Sweden). The brains were dissected out, the cerebellum was removed, and the ipsilateral and contralateral hemispheres, including the meninges, were processed separately to obtain single-cell suspensions as described previously (Zhang et al., 2017; Nazmi et al., 2018). In brief, brain homogenate samples were incubated with an enzymatic solution composed of 0.01% papain, 0.01% DNase I (Worthington, NJ, United States), 0.1% Dispase II (Roche, Sweden), and 12.4 mM $MgSO_4$ in Ca^{2+}/Mg^{2+}-free HBSS (Thermo Fisher Scientific, Sweden) at 37°C for 20 min. The monocyte population was then separated on a Percoll gradient (30/70%). After blocking non-specific binding with Fc block (C16/32; clone 2.4G2; cat. 553142, BD Pharmingen), the following primary antibodies were used: anti-lineage cocktail (FITC; CD3, CD5, B220, CD11b, CD11c, Gr-1, TCRgd, and Ter-119; cat. 22-7770-72, eBioscience), anti-CD45 (APCcy7; clone 30-F77; cat. 103115, BioLegend) and anti-CD90 (Thy1.2, PEcy7; cat. ABIN477038, eBioscience). ILC2s were identified by the addition of anti-SCA-1 (PE; clone D7; cat. 108107, BioLegend), anti-NKp46 (BV510; clone 29A1.4; cat. 563455; BD Biosciences), anti-KLRG1 (APC; clone 2F1; cat. 561620, BD Biosciences), and anti-GATA3 PE (Catalog # 12-9966-42, eBiosciences) antibodies. For intracellular staining, the permeabilization and fixation procedure was performed according to manufacturer's protocol. Briefly, after incubation with 250 μl of BD Cytofix/Cytoperm solution, the cells were washed in 1 × BD Perm/Wash buffer (BD Biosciences, CA, United States) and resuspended in 100 μl of 1 × BD Perm/Wash buffer before the GATA3 intracellular staining. The samples were run on a BD FACSCanto II^{TM} flow cytometer. Fluorescence-minus-one controls for each antibody were run together with each experiment. Lung tissues in which ILC2s were enriched were included as positive controls for all brain tissue flow cytometry experiments, and the data were analyzed with the FlowJo v10 software (Tree Star, Ashland, OR, United States).

The lung single-cell suspensions were prepared following a previously described method (Moro et al., 2015) with minor modifications. Briefly, after perfusion the lungs were extracted, minced into small pieces, and then digested for 45 min at 37°C with the same enzyme mix used for the brain dissociation. The supernatant was incubated with Red Blood Cell Lysing Buffer (R7757, Sigma-Aldrich, Sweden) at room temperature. Samples were then stained and analyzed as above.

Immunoassay for Cytokines and Chemokines

Samples were collected at 6 h, 48 h, and 7 days after HI from wild type and ILC2-impaired mice (n = 7/group) for immunoassays of cytokine and chemokine protein expression. In summary, after pentobarbital i.p. injection the animals underwent transcardial saline perfusion. The ipsilateral and contralateral hemispheres, including the meninges, were collected separately and stored at -80°C until processing. The Bio-Plex Pro^{TM} Mouse Cytokine 23-plex Assay (#m60009rdpd, Bio-Rad, **Table 1**) was used according to the manufacturer's instructions.

Immunohistochemistry and Immunofluorescence Staining

At PND13 (7 days after HI), wild type and ILC2-impaired mice were deeply anesthetized by i.p. injection with pentobarbital and then perfused-fixed with 5% buffered formaldehyde (Histofix,

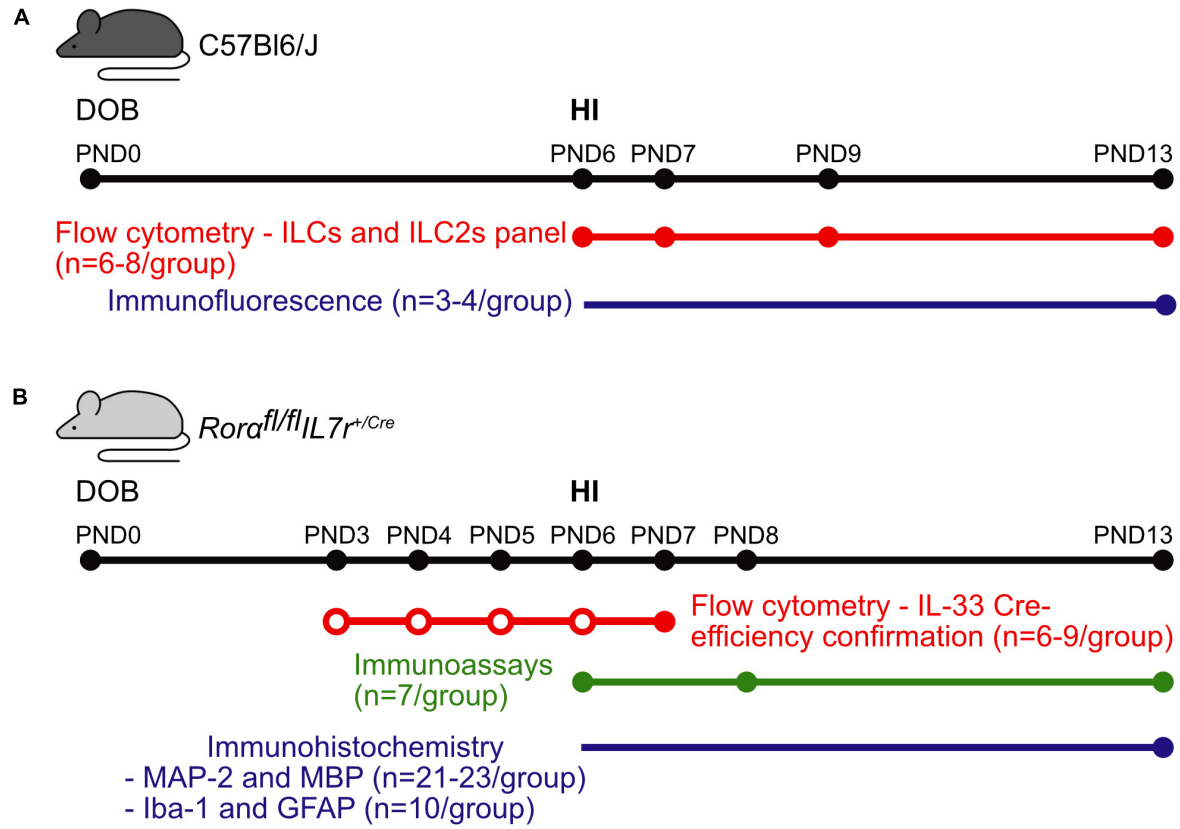

FIGURE 1 | Graphical abstract of the experiments. Representative scheme of the methods, numbers of animals, and time points used for experiments in **(A)** the C57Bl6/J mouse strain and **(B)** the *Rorα*$^{fl/fl}$*IL7r*^{Cre} mouse strain. Colored dots correspond the data collection time points for the respective methods, while the empty dots correspond to the IL-33 injections. Abbreviations: DOB: date of birth, PND: postnatal day, IL-33: interleukin-33, HI: hypoxia-ischemia.

TABLE 1 | Cytokines and chemokines analyzed with the Bio-Plex Pro^{TM} Mouse Cytokine 23-plex Immunoassay.

Abbreviation	Cytokine/Chemokine	Abbreviation	Cytokine/Chemokine
IL-1α	Interleukin 1α	IL-17	Interleukin 17
IL-1β	Interleukin 1β	Eotaxin	Eotaxin
IL-2	Interleukin 2	G-CSF	Granulocyte-colony stimulating factor
IL-3	Interleukin 3	GM-CSF	Granulocyte-macrophage colony-stimulating factor
IL-4	Interleukin 4	IFN-γ	Interferon γ
IL-5	Interleukin 5	KC	Chemokine (C-X-C motif) ligand 1
IL-6	Interleukin 6	MCP-1	Monocyte chemoattractant protein 1
IL-9	Interleukin 9	MIP-1α	Macrophage inflammatory protein 1α
IL-10	Interleukin 10	MIP-1β	Macrophage inflammatory protein 1β
IL-12(p40)	Interleukin 12 p40	RANTES	Regulated on activation, normal T cell expressed and secreted
IL-12(p70)	Interleukin 12 p70	TNF-α	Tumor necrosis factor α
IL-13	Interleukin 13		

Histolab, Sweden). For Immunohistochemistry staining, the brains with meninges were collected and stored at 4°C in Histofix before paraffin-embedding and sectioning. Coronal sections of the forebrain were cut with a thickness of 7 μm. To obtain a representation of the areas of interest, the staining was performed for evaluating gray matter on every 50th section (6 sections/animal). For white-matter assessment, and microglial and astrocyte assessments, every 100th section was used (3 sections/animal). Briefly, the sections were de-paraffinized followed by antigen retrieval and 3% H_2O_2 in phosphate buffer. After blocking, sections were incubated with mouse anti-microtubule-associated protein 2 (MAP-2, 1:1,000 dilution; M4403, Sigma-Aldrich, United States), mouse anti-myelin basic protein (MBP, 1:1,000 dilution;

SMI-94 Covance, United States), rabbit anti-ionized calcium binding adaptor molecule 1 (Iba-1, 1:2000 dilution, 019-19741, FUJIFILM *Wako* Chemicals, United States), and rabbit anti-Glial fibrillary acidic protein (GFAP, 1:500, Z0334, Dako, Denmark) primary antibodies overnight at 4°C. The following day, the sections were incubated with the corresponding secondary antibodies for 1 h at room temperature. The sections were then incubated for 1 h in ABC Elite, and the immunoreactivity was visualized with 0.5 mg/ml 3.3-diaminobenzidine in a buffer consisting of $NiSO_4$, β-D-glucose, NH_4Cl, and β-D-glucose oxidase (all from Sigma-Aldrich, Sweden).

Immunofluorescence was performed to identify ILC2s at 7 days after HI ($n = 3$/group). After saline perfusion, the meninges from each hemisphere were peeled off from the parenchyma and placed separately on a glass slide. Brains and lungs were collected as well and stored in Histofix followed by sucrose 30%. Both tissues were then frozen in isopentane and cut at 30 μm of thickness. After fixation and blocking with 5% donkey serum at room temperature for 1 h, the tissues were incubated with rat anti-mouse CD3 (1:500 dilution, cat. 100202, BioLegend) and rabbit anti-mouse ST2 (1:250 dilution, PA5-20077, Invitrogen) primary antibodies overnight at 4°C. The tissues were then incubated for 1 h at room temperature with donkey anti-rat Alexa Fluor 488® (1:1,500 dilution, A21208, Invitrogen) and donkey anti-rabbit Alexa Fluor 594® (1:1,500 dilution, A21207, Invitrogen) secondary antibodies. Lung tissue was used as the positive control, and omitting the primary antibodies was used as the negative control (**Supplementary Figure 1**). The slides were then stained with DAPI and afterward mounted with coverslips and ProLong™ gold antifade reagent (P36930, Invitrogen).

Quantification of Gray and White-Matter Tissue Loss

Gray-matter tissue loss was assessed by measuring MAP-2^+ areas, either as a percentage of volume (mm^3) or area (mm^2) for each stained section at different levels as described previously (Zhang et al., 2017; Albertsson et al., 2018). Images of the stained sections were acquired with an Olympus Optical microscope using a 1.25 × objective lens. MAP-2^+ areas were delineated using ImageJ software (Rasband, W.S., US National Institutes of Health, United States[1]).

To assess white-matter injury, a newly established automated segmentation method, MyelinQ, was used to measure the size of the MBP$^+$ areas (Mottahedin et al., 2018). Briefly, we captured images of each section using a 5 × objective lens with the newCAST software (Visiopharm, Denmark) on a modified Leica microscope (Leica DM6000 B, Germany) equipped with a motorized stage (Ludl MAC 5000, United States) and a digital camera (Leica DFC 295, Germany). MyelinQ was used for automatic detection of MBP$^+$ areas in the whole brain hemisphere.

For the quantification of gray and white-matter loss, the sizes of the MAP-2^+ and MBP$^+$ areas in the contralateral and ipsilateral hemispheres were measured separately in order to calculate the tissue damage in the ipsilateral hemisphere against the internal control (the contralateral hemisphere). The total tissue loss was calculated with the following formula (Albertsson et al., 2014):

$$(\text{contralateral area} - \text{ipsilateral area})/\text{contralateral area} \times 100\%$$

The total tissue loss volume was calculated as:

$$\text{Volume} = \text{sum of section area} \times \text{section thickness} \times (1/\text{sampling fraction})$$

Quantification of Iba-1 Positive Brain Region and GFAP-Positive Astrocytes

The border zone between the injured and non-injured brain areas in the ipsilateral hemispheres, as well as the corresponding brain regions in the contralateral brain hemispheres were selected for analysis. Using ImageJ software (v1.52a, NIH, United States), GFAP-positive astrocytes were counted on captured images with an Olympus Optical microscope using a 40× objective lens from selected areas in two regions of interest per section (in total 6 regions of interest per brain), and expressed as cell density (cells/mm^2). The Iba-1–positive stained brain regions were measured on the images which were captured by a 20× objective lens from eight regions of interest per brain. Analysis was performed on the images with final resolution of 1360 × 1024 pixel after adjusting threshold of positive stained areas on ImageJ. Data were expressed as the ratio between Iba-1 stained area and total regions of interest.

Meningeal ILC2 Cell Counting

A systematic set of Z-stacks of three regions of interest per hemisphere were acquired with a 20× objective lens on LSM 800 confocal microscope (Carl Zeiss, Germany). ILC2s (defined as CD3$^-$ST2$^+$) were blindly counted in the height of the Z (z step = 1 μm), and volumes of each regions of interest were calculated. Estimation of number density was performed by applying the following formula (McNaught and Wilkinson, 1997) of paired regions of interests from contralateral and ipsilateral meninges:

$$N = \Sigma Q^- / V$$

N is the total number of cells per volume of brain region; ΣQ^- is the number of counted cells; V is the volume of regions of interest per sampling frame.

Statistical Analysis

All statistical analyses were performed with IBM SPSS Statistics 25 (IBM Corp, Armonk, NY, United States). Data were tested for normal distribution through the generation of QQ plots, and equality of variance was assessed by Leven's test. If normally distributed, the data were analyzed with the corresponding parametric test, while in the case when the data were non-normally distributed, appropriate non-parametric tests were applied. All data are presented as boxplots (5th –

[1]https://imagej.nih.gov/ij/, 1997–2016

95th percentiles). Statistical significance was considered as p-values < 0.05.

RESULTS

The Frequencies of ILCs and ILC2s Increased in the Neonatal Mouse Brain After HI Injury

ILC2s are the subtype that are most frequently observed in the adult mouse brain compared to ILC1s and ILC3s (Russi et al., 2015; Gadani et al., 2017). To determine if ILCs were present in the neonatal mouse brain, we performed flow cytometry analysis on single-cell suspensions isolated from brain homogenate (**Figures 2A–C**, **Supplementary Figure 2**), and measured the frequencies of both ILCs and ILC2s in naïve mice (n = 6/time point) and in mice at 6 h (n = 8), 24 h (n = 7), 3 days (n = 8), and 7 days (n = 7) after HI. Because of the lack of single specific markers, we selected a panel of surface markers in the FACS analysis for their identification, and ILCs were defined as $CD45^+Lin^-Thy1.2^+$ (Pelly et al., 2016) and ILC2s were defined as $CD45^+Lin^-Thy1.2^+SCA\text{-}1^+NKp46^-KLRG1^+$ (Cardoso et al., 2017).

For both ILCs and ILC2s, we did not detect any differences between naive and contralateral brain hemispheres at any time points after HI; therefore, data from naïve mice are not shown. The frequencies of ILCs were significantly increased in the brain hemisphere ipsilateral to the injury compared to the uninjured contralateral hemisphere at 24 h ($p < 0.001$), 3 days ($p = 0.010$), and 7 days ($p < 0.001$) after HI, but not at 6 h after HI (**Figure 2B**). Quantification of ILC2s showed a significant increase in the ipsilateral hemisphere compared with the uninjured contralateral hemisphere at 6 h ($p = 0.011$), 3 days ($p = 0.020$), and 7 days ($p < 0.001$) after HI (**Figure 2C**).

Furthermore, the frequencies of both ILCs (**Figure 2B**) and ILC2s (**Figure 2C**) in the ipsilateral hemisphere of HI mice showed an increasing trend over time, with the highest at 7 days after HI for both populations. We observed a first small peak for ILCs at 24 h, which was higher than 6 h ($p < 0.001$) and the subsequent 3 days ($p = 0.031$) time points. The ILCs showed a second peak and were significantly greater at 7 days compared with 6 h ($p < 0.001$), 24 h ($p = 0.009$), and 3 days ($p = 0.002$) after HI (**Figure 2B**). ILC2s instead increased drastically only at 7 days compared with 6 h ($p <$ 0,001), 24 h ($p = 0.002$), and 3 days ($p = 0.002$) after HI (**Figure 2C**). The increased ILC2s at 7 days after HI in the ipsilateral hemisphere were further confirmed using intracellular staining for GATA3, the key transcription factor and master regulator that is critical for the development and maintenance of ILC2s (Yagi et al., 2014) (**Supplementary Figure 3**).

ILC2s are known to be enriched in the meninges compared with the brain parenchyma (Gadani et al., 2017; Russi et al., 2018). We examined the presence of ILC2s at 7 days after HI, when ILC2 accumulation in the brain peaked, using immunofluorescent staining of the meninges compared to naïve mice (**Figures 3A–E**). ILC2s were found mostly in the meninges of the ipsilateral hemisphere after HI (**Figures 3C–E**) and only few cells in the meninges contralaterally (**Figures 3B,E**, $p = 0.013$), or in naïve mice (**Figure 3A**). In addition, we did not observe ILC2s in the brain parenchyma in either the naïve mice or after HI (data not shown). Because we observed this increase of ILC2s in the injured brain, their role in brain injury after HI was further investigated.

ILC2-Impaired Neonatal Mice Did Not Respond to IL-33 Stimulation

To explore the role of ILC2s in neonatal brain injury, we used the ILC2-deficient mouse strain $Ror\alpha^{fl/fl}IL7r^{Cre}$ (Oliphant et al., 2014). To confirm the ILC2 deficiency in the newborn mice, which has not been investigated previously, we used IL-33, which is known to efficiently induce the expansion and activation of ILC2s (Oliphant et al., 2014; Van Dyken et al., 2014; Besnard et al., 2015; Bartemes et al., 2017), including ILC2s in the CNS (Gadani et al., 2017). We performed IL-33 stimulation experiments to compare the ILC2 response in wild type mice and $Ror\alpha^{fl/fl}IL7r^{Cre}$ mice (**Figures 4A,B**, **Supplementary Figure 4**). Naïve mouse pups without any injection showed similar amount of ILC2s between genotypes, and PBS injections did not evoke ILC2s expansion, as shown by similar amount of ILC2s as in naïve mice (**Figure 4B**). In contrast, IL-33 triggered massive ILC2 expansion in wild type animals (n = 7), but failed to do so in $Ror\alpha^{fl/fl}IL7r^{Cre}$ mouse pups (n = 9, $p = 0.006$) (**Figure 4B**), thus confirming that the ILC2 expansion in response to IL-33 stimulation in $Ror\alpha^{fl/fl}IL7r^{Cre}$ mouse pups was significantly impaired.

ILC2 Impairment Attenuated the IL-13 Increase After HI

To illustrate the inflammatory response in the brain after HI, we performed a Bio-Plex Pro™ Mouse Cytokine 23-plex Assay using brain homogenate from wild type and $Ror\alpha^{fl/fl}IL7r^{Cre}$ mice. This method allowed the study of 23 different cytokine/chemokines at the same time (**Table 1**) at 6 h, 48 h, and 7 days after HI (n = 7/group) (**Figures 4C–F**). IL-13 protein levels in the brain were significantly lower at 6 h after HI in $Ror\alpha^{fl/fl}IL7r^{Cre}$ mice compared with wild-type mice ($p = 0.046$) (**Figures 4C,F**), while no significant differences were observed for any other cytokine/chemokine between wild type and $Ror\alpha^{fl/fl}IL7r^{Cre}$ mice (**Figures 4C–E**) in the ipsilateral hemispheres at any of the time points analyzed.

ILC2 Impairment Did Not Affect Tissue Loss or the Neuroinflammatory Response in the Neonatal Mouse Brain After HI

Next, we investigated the involvement of ILC2s in HI-induced preterm brain injury using the $Ror\alpha^{fl/fl}IL7r^{Cre}$ mouse strain. Brain injury was evaluated at 7 days after HI for both the gray and white matter. ILC2 impairment did not impact the severity of gray-matter injury either in terms of total tissue loss (**Figure 5B**) or at different brain levels (**Figure 5C**) as evaluated by immunohistochemical staining of the neuronal marker MAP-2 (**Figures 5A–C**). To evaluate white-matter

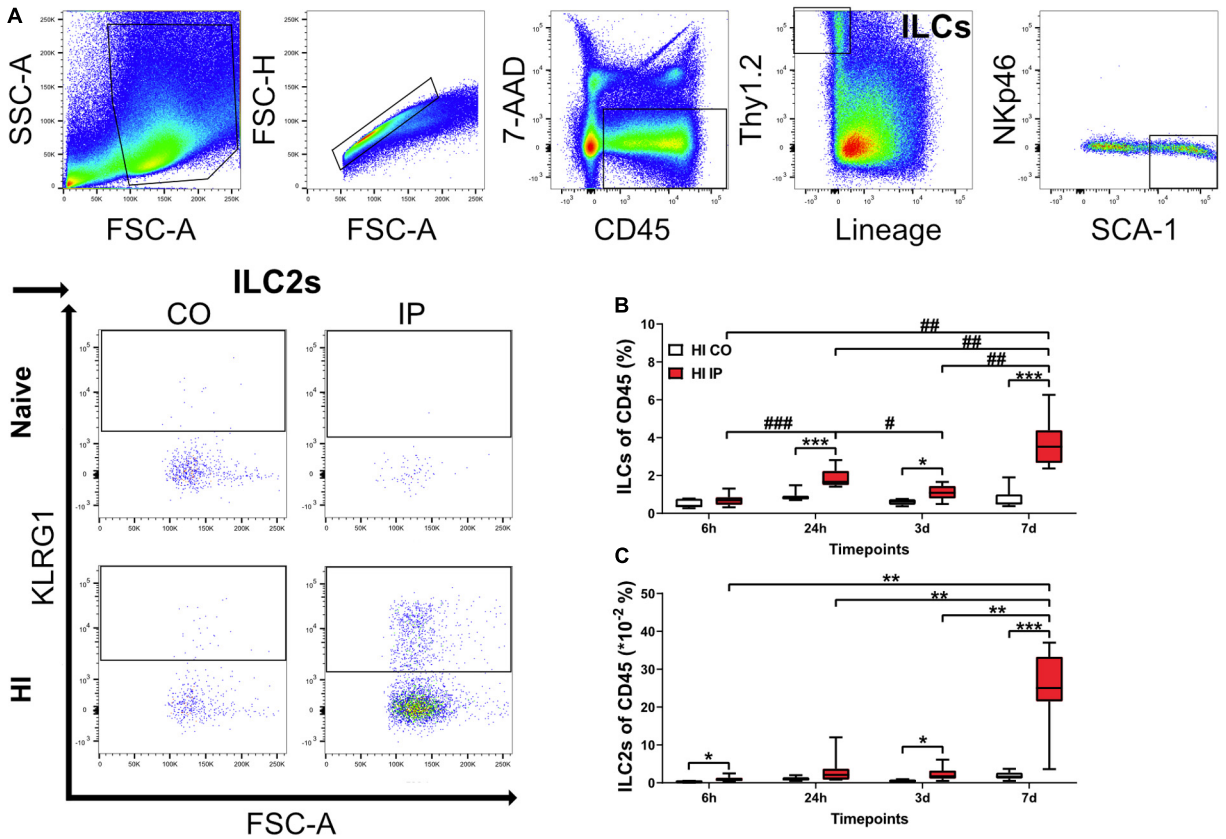

FIGURE 2 | ILCs and ILC2s increased in the ipsilateral hemispheres in the neonatal mouse brain in a time-dependent fashion after HI injury. Single-cell suspensions generated from brain homogenates were analyzed using flow cytometry in mouse pups at different time points after HI, with naïve C57Bl6/J mouse littermates as controls (n = 6–8/group). **(A)** Representative flow cytometry plots showing the gating strategy for ILCs and ILC2s. Both are represented as percentages of the CD45$^+$ population. ILCs **(B)** and ILC2s **(C)** in the ipsilateral and contralateral hemisphere at 24 h, 3 days, and 7 days after HI. A mixed model ANOVA with Games-Howell post-hoc were used. *#: $p < 0.05$, **##: $p < 0.01$, ***###: $p < 0.001$. in panels (**B,C**). Abbreviations: N: naïve, HI: hypoxia-ischemia, IP: ipsilateral hemisphere, CO: contralateral hemisphere.

injury, we performed MBP immunohistochemical staining (**Figure 5D**), and the MBP$^+$ white-matter volumes in the whole brain hemisphere (**Figure 5E**) and areas at different levels (**Figure 5F**) were measured. Similarly, ILC2 impairment did not affect the tissue loss in white matter in the whole brain hemisphere (**Figures 5E,F**) or in the subcortical white-matter area (data not shown). Further, no sex difference was noted regarding either the gray or white-matter injury after HI (data not shown).

To explore the neuroinflammatory response in *Rorα*$^{fl/fl}$*IL7r*^{Cre} after HI insult, we examined the microglia and astrocyte reactivity using immunochemistry staining for the microglia marker Iba-1 and the astrocyte marker GFAP. At 7 days after HI, there were significantly increased staining for microglia (**Figures 5G–K**) and number of astrocytes (**Figures 5L–P**) in the ipsilateral hemispheres in both the wild type (microglia: p = 0.001, astrocytes: p = 0.015) and *Rorα*$^{fl/fl}$*IL7r*^{Cre} mice (microglia: p = 0.003, astrocytes: $p < 0.001$); however, no differences were observed for microglia or astrocytes after HI between the wild type and *Rorα*$^{fl/fl}$*IL7r*^{Cre} mice in either of the two brain hemispheres.

DISCUSSION

ILCs and ILC2s have previously been found in the mouse brain and have recently been studied in adult murine models of various brain pathologies (Mair and Becher, 2014; Besnard et al., 2015; Hatfield and Brown, 2015; Russi et al., 2015; Gadani et al., 2017; Russi et al., 2018; Romero-Suarez et al., 2019; Fung et al., 2020). Here we found accumulation of these cells in the meninges after HI injury in neonatal mice, and to our knowledge this is the first study to investigate their presence and function in a neonatal mouse model of brain injury.

Among ILCs, ILC2 is the most abundant subtype in the healthy adult mouse brain (Gadani et al., 2017; Russi et al., 2018). ILC2s have been shown to be increased in tissues in different disease models such as spinal cord injury (Gadani et al., 2017), experimental autoimmune encephalomyelitis (Russi et al., 2015; Russi et al., 2018), experimental cerebral malaria (Besnard et al., 2015), and aging (Fung et al., 2020). In our study, ILCs and ILC2s were present in the normal neonatal mouse brain, and after HI insult ILCs and particularly ILC2s accumulated in the injured brain, which agrees with previous studies

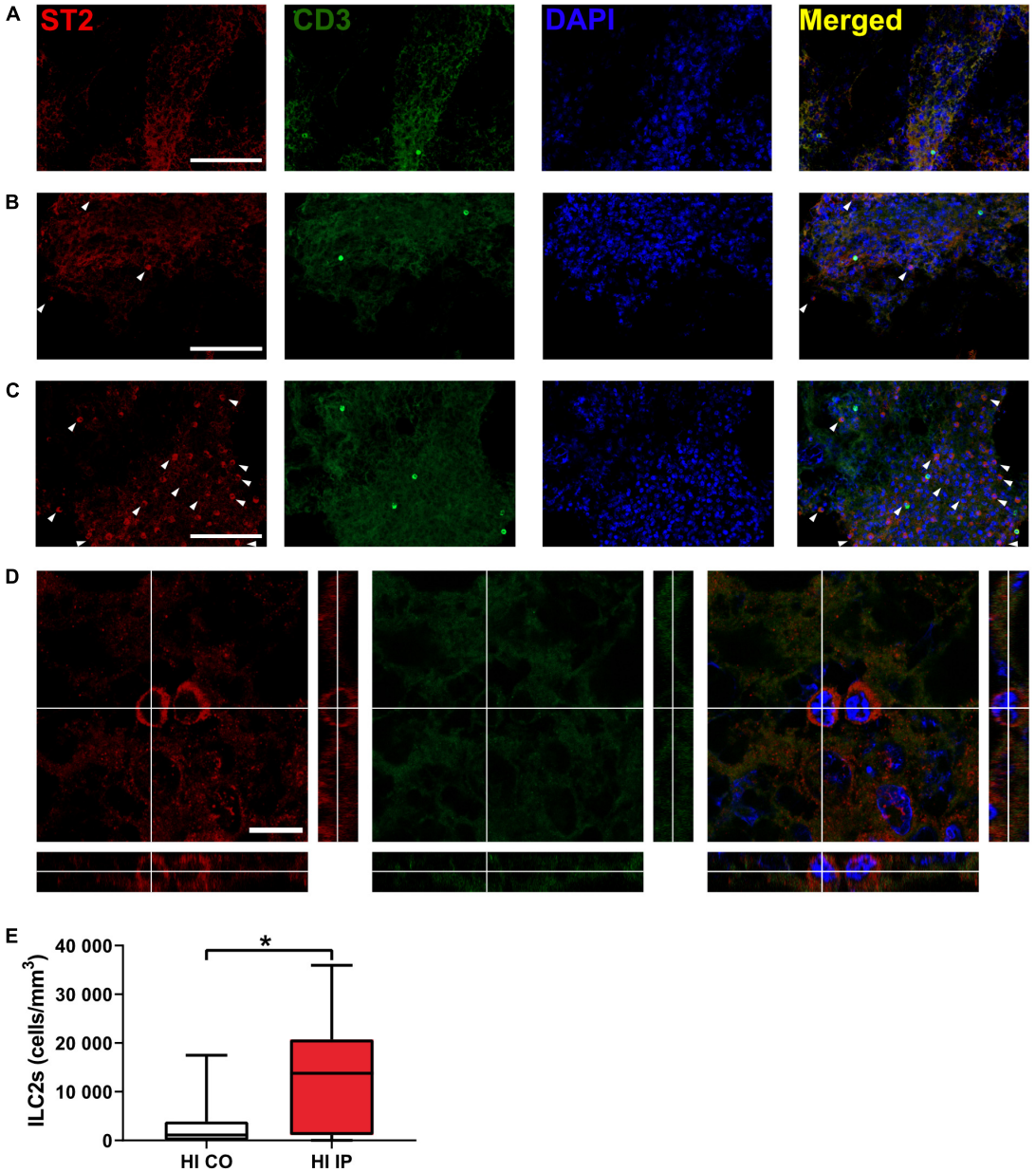

FIGURE 3 | The presence of ILC2s in the meninges in neonatal mice after HI. Representative confocal images of immunofluorescent staining showing the presence of ILC2s ($CD3^-ST2^+$, arrowheads) in the meninges taken from brain hemispheres in a naïve mouse **(A)** and from the contralateral hemisphere **(B)** and ipsilateral hemisphere **(C)** in a mouse at 7 days after HI. **(D)** High magnification orthogonal views of cells stained with ST2. The merged picture shows cytoplasm localization of ST2 surrounding $DAPI^+$ nuclei. Scale bars: **(A–C)** 100 μm; **(D)** 10 μm. **(E)** The number density of ILC2-positive cells in the meninges in the ipsilateral hemisphere and contralateral hemispheres after HI. Paired *t*-test was used. $^*p < 0.05$. Abbreviations: HI: hypoxia-ischemia, IP: ipsilateral hemisphere, CO: contralateral hemisphere.

(Mair and Becher, 2014; Hatfield and Brown, 2015; Romero-Suarez et al., 2019). This accumulation occurred in a time-dependent manner, and reached the highest level at 7 days after HI. This indicated that ILCs, and especially ILC2s, are stimulated and expanded by HI-induced tissue injury. ILC2s are recognized as tissue-resident cells (Moro et al., 2010; Neill et al., 2010; Price et al., 2010; Molofsky et al., 2013) and are expanded upon IL-33 stimulation in both the peripheral tissue (Oliphant et al., 2014; Van Dyken et al., 2014; Besnard et al., 2015; Bartemes et al., 2017) and the CNS (Gadani et al., 2017). In the current study, we found that neonatal ILC2s in the lung tissue in the wild type mice were also expanded by IL-33 stimulation, which did not occur in the ILC2-deficient mice. Together, this supports the hypothesis that ILC2s in both the peripheral nervous system and CNS are able to respond and expand to either a stimulator like IL-33 and/or

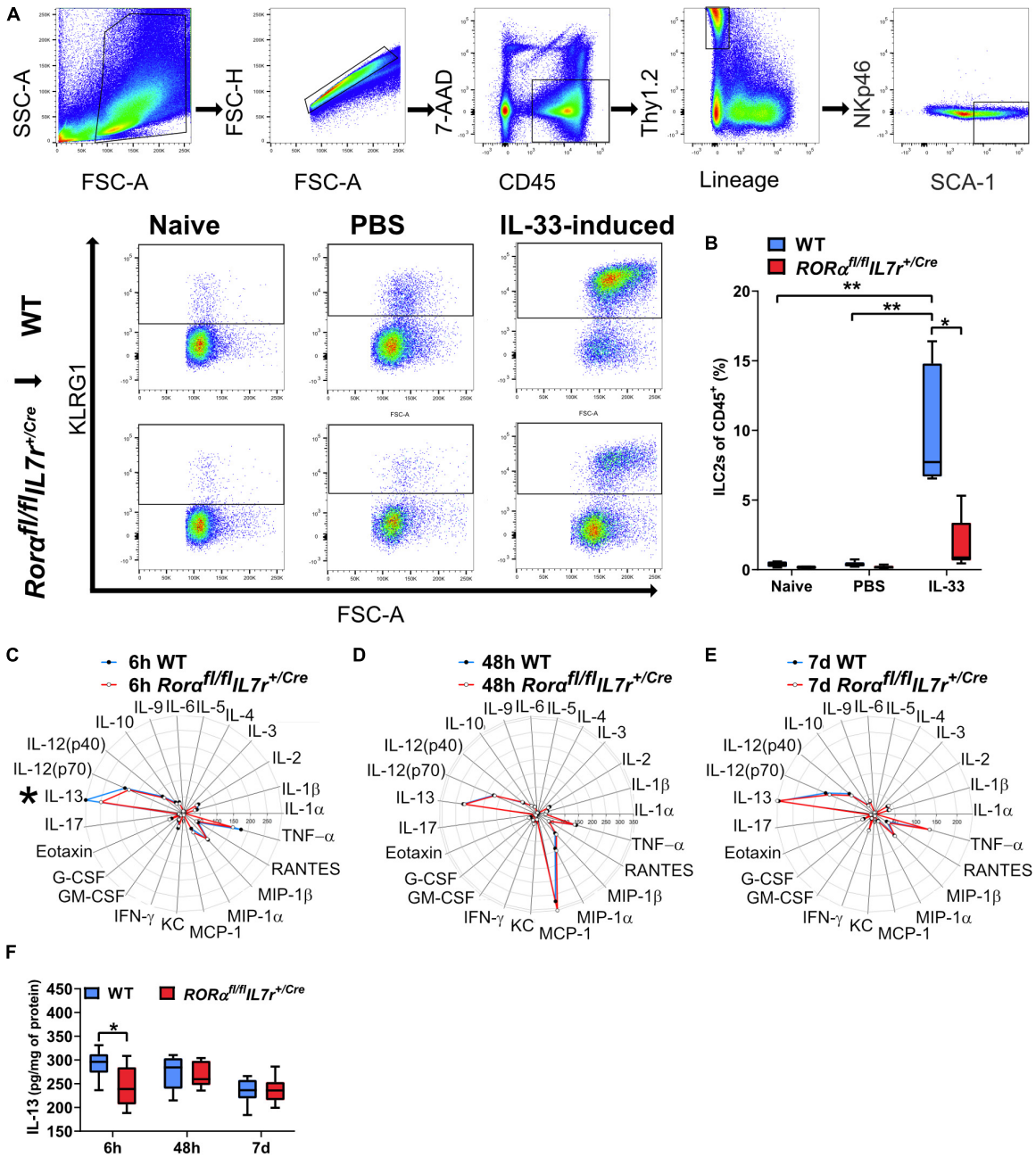

FIGURE 4 | ILC2s in *Rorα*$^{fl/fl}$*IL7r*^{Cre} mice did not expand after IL-33 stimulation, but their cytokine/chemokine profile in the brain after HI was similar to wild-type mice. **(A)** Representative flow cytometry plots show the gating strategy for IL-33–stimulated ILC2 expansion in the lungs (n = 7–9/group). **(B)** IL-33–stimulated ILC2 expansion in wild-type and *Rorα*$^{fl/fl}$*IL7r*^{Cre} mouse pups. **(C–E)** Radar plots from immunoassays show the cytokine/chemokine changes in the ipsilateral hemisphere from the wild type and *Rorα*$^{fl/fl}$*IL7r*^{Cre} mouse pups at 6 h **(C)**, 48 h **(D)**, and 7 days **(E)** after HI. **(F)** IL-13 in the ipsilateral hemispheres in the wild type and *Rorα*$^{fl/fl}$*IL7r*^{Cre} mice at different time points after HI. *$p < 0.05$, **$p < 0.01$. Mann–Whitney U-tests were used in **(B)**, and 2-Way ANOVA with Games-Howell post-hoc were used in **(F)**. Abbreviations: HI: hypoxia-ischemia, IP: ipsilateral hemisphere, WT: wild type.

stress induced by tissue injury and that they are functional already in early life.

To identify the localization of ILC2 in the neonatal mouse brain, we performed immunofluorescence staining and found that – similar to previous findings (Gadani et al., 2017) – ILC2s in the neonatal mouse brain were resident in the meninges and were seldom found in the brain parenchyma under either normal conditions or after HI-induced brain injury, thus suggesting a role for meningeal immune cells as sentinels for brain-derived alarmins as part of the immune response after brain injury in neonates.

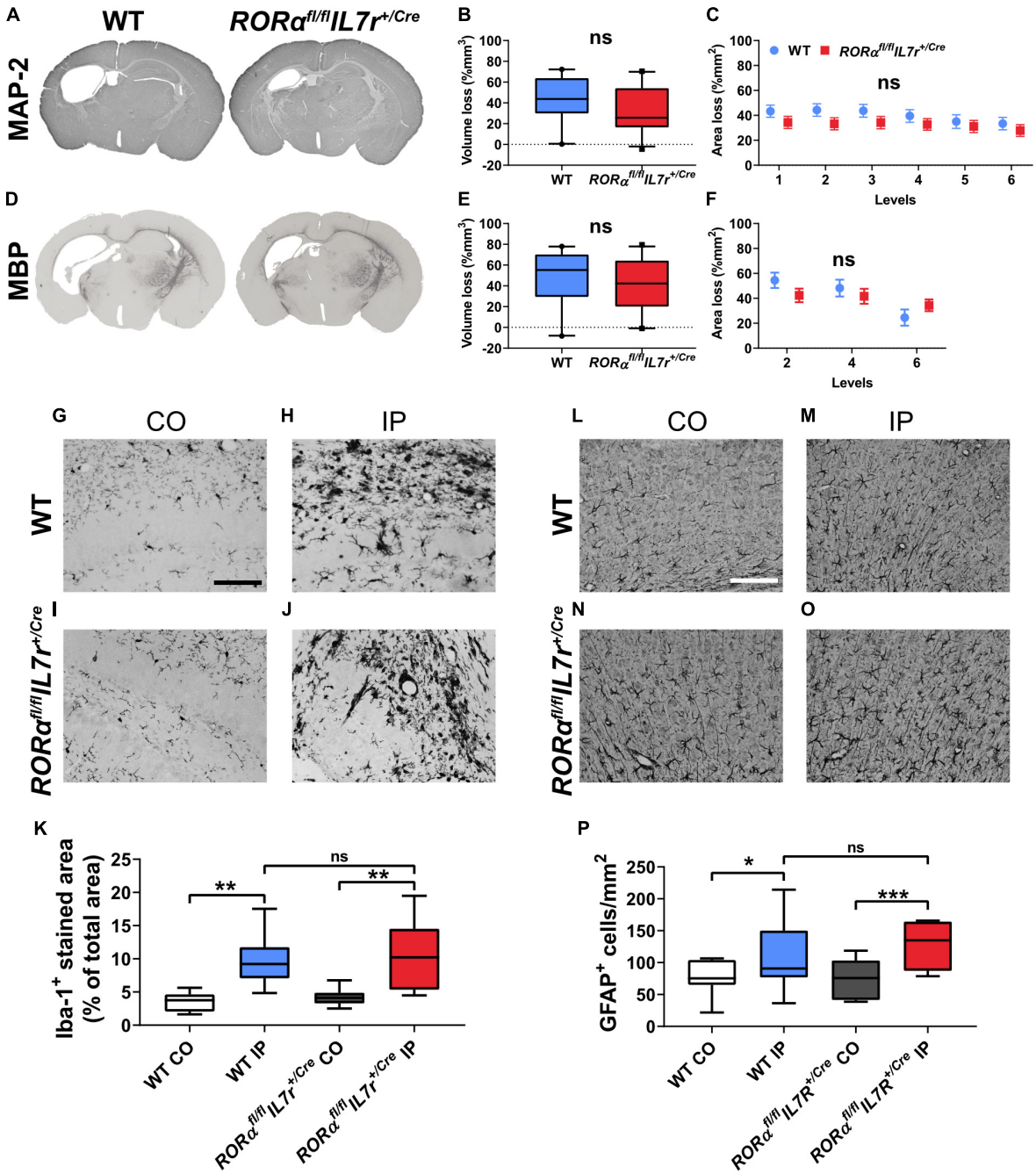

FIGURE 5 | ILC2 impairment did not affect brain tissue loss 7 days after HI. **(A,D)** Representative pictures show immunochemistry staining for MAP-2 **(A)** and MBP **(D)**. Gray matter **(A–C)** in *Rorα*$^{fl/fl}$*IL7r*^{Cre} mice (n = 23) after HI compared to WT littermates (n = 21) in terms of brain tissue volume loss **(B)** or area loss per level **(C)**. White matter **(D–F)** tissue loss in the whole hemisphere in terms of tissue volume loss **(E)** or area loss at each level **(F)** in the wild type and *Rorα*$^{fl/fl}$*IL7r*^{Cre} mice. Representative images **(G–J,L–O)** and quantification **(K,P)** of Iba-1^{+} cells **(G–K)** and GFAP^{+} astrocytes **(L–P)** in the wild type and *Rorα*$^{fl/fl}$*IL7r*^{Cre} mouse pups at 7 days after HI. Paired t-test was used for comparisons between brain hemispheres, and independent t-test was used for comparisons between genotypes. Scale bars: 100 μm. Abbreviations: MAP-2: microtubule-associated protein-2, MBP: myelin basic protein; WT: wild type, IP: ipsilateral hemisphere. CO: contralateral hemisphere. *$p < 0.05$, **$p < 0.01$, ***$p < 0.001$.

In the current study, among all the cytokine/chemokines examined, we found a small yet significant decrease in expression of IL-13 in the ILC2-deficient mice compared with the wild type mice. IL-13 is considered an anti-inflammatory cytokine and an important modulator of peripheral allergic reactions. In the brain, IL-13 contributes to the death of activated microglia (Yang et al., 2002; Yang et al., 2006) and potentiates the effects of oxidative stress on neurons during neuroinflammation

(Park et al., 2009), and both neuroprotective and neurotoxic effects of IL-13 have been proposed. IL-13 has been previously found to be increased both in the serum of term newborns (Orrock et al., 2016; Al-Shargabi et al., 2017; Massaro et al., 2018) and in brain mRNA levels in mice (Albertsson et al., 2014) early after HI injury. In newborns, increased serum IL-13 levels are associated with worse brain injury (Massaro et al., 2018), reduced heart rate variability metrics (Al-Shargabi et al., 2017), and adverse outcome after 24 h of therapeutic hypothermia (Orrock et al., 2016). ILC2s are one of the major producers of IL-13 in response to insults in different tissues (Fallon et al., 2006; Price et al., 2010; Klein Wolterink et al., 2012; Kabata et al., 2018), including in a model of spinal cord injury, where IL-13^{+} cells were found to make up the majority ILC2s (Gadani et al., 2017). The reduction in IL-13 protein levels that we observed here might suggest that ILC2s have a detrimental role. However, in spite of the observed significant increase in ILC2s in the brain after the HI insult, ILC2 impairment did not affect the HI-induced inflammatory responses in the brain or the extent of brain injury after HI in neonatal mice. Similarly, a previous study showed that ILCs infiltrated the brain in an experimental autoimmune encephalomyelitis model but did not affect the severity of injury (Mair and Becher, 2014). Further, we did not observe any sex differences regarding to the degree of injury in the brain of ILC2-deficient mice compared with wild-type mice, although it has been reported previously that the role of ILC2 is sex-dependent under certain circumstances (Bartemes et al., 2017; Russi et al., 2018). Even though ILCs were increased in the CNS after insult, it is possible that there are still not enough ILCs to affect the brain damage development in a substantial manner. Indeed, ILC2s reside mainly in the meninges and choroid plexus, and not in the parenchyma, and their frequencies are generally low in relation to the whole leukocyte population (Hatfield and Brown, 2015; Gadani et al., 2017; Russi et al., 2018; Fung et al., 2020).

ILC2s were the main cell type shown to be responsible for allergic response in a mouse model of lung inflammation (Van Dyken et al., 2014). However, genetic ablation of ILC2s triggered an increase in gamma delta T-cells, thus revealing compensatory mechanisms among innate immune cells (Van Dyken et al., 2014). Another example of cross talk between ILC2s and other innate immune cells was found in a murine model of experimental autoimmune encephalomyelitis where both mast cells and ILC2s were coordinated in the development of brain damage (Russi et al., 2018). We speculate that such cross talk and compensatory mechanisms between ILC2s and other innate immune cells might be among the reasons why ILC2 impairment did not impact HI-induced brain injury in neonatal mice.

In addition, the role of other ILCs such as ILC1 and ILC3 remains an important topic for future study. The lymphoid tissue inducer cells comprise the ILC3 population. They present as early as the embryonic stage and play an important role in intestinal homeostasis after birth (Eberl, 2012), this might indicate the importance of ILC3s in the immune response in the perinatal period during development. In the current study, we did not observe any obvious increase of ILC1 and ILC3 in the brain after HI (data not shown), which might be due to the time points at which ILC1 and ILC3 levels were assessed. Furthermore, whether or not there are compensatory changes in ILC1 and ILC3 that contribute to the lack of an effect from ILC2 deficiency also needs to be explored in the future.

Exploration of the neuroinflammatory response after HI by immunohistochemistry revealed increased numbers of astrocytes and staining for microglia in the ipsilateral hemisphere at 7 days after HI in both ILC2-deficient and wild-type mice, and this agreed with previous findings (Doverhag et al., 2010; Bonestroo et al., 2013). However, there was no significant difference in astrocytes and microglia in either of the brain hemispheres between wild type and ILC2-deficient mice, and these results are thus in line with our findings that no significant differences were observed for cytokines/chemokines between wild type and ILC2-deficient mice apart from IL-13 and that there were no differences in the severity of brain injury between the two mouse genotypes.

We found increased accumulation of ILC2s in the injured brain after HI, but ILC2 deficiency did not affect the severity of the injury. We found no differences in the neuroinflammatory response after HI between ILC2-deficient and wild-type mice that might partly explain the lack of effect of ILC2 deficiency on brain injury. However, the in-depth molecular mechanisms behind these findings are not known. A limitation of the study is that we only assessed effect of ILC2 deficiency on brain injury at 7 days after HI. We cannot exclude the possibility that ILC2 deficiency might have an effect at a later time point after HI.

In conclusion, ILCs and ILC2s accumulate in the injured brain after HI insult in the neonatal mouse brain. However, ILC2s did not affect the major inflammatory response in the brain and did not contribute to the development of brain damage in this mouse model of preterm brain injury.

DATA AVAILABILITY STATEMENT

All datasets generated for this study are included in the article/**Supplementary Material**.

ETHICS STATEMENT

The animal study was reviewed and approved by the Regional Animal Ethical Committee of Gothenburg (ethical permit numbers: 58/2016 and 2042/18).

AUTHOR CONTRIBUTIONS

XW conceptualized the study. AZ, ER-F, and AN designed the experiments and performed the flow cytometry experiments. AZ and ER-F performed the HI model. AZ performed the protein assays, immunohistochemistry, and immunofluorescence staining. AZ and TC performed fluorescent imaging and analyzed the immunofluorescence data. AZ and MA performed the statistical analysis. AZ and XW drafted the manuscript. All authors contributed to data interpretation and critical revision of the manuscript and approved the submitted version.

FUNDING

This work was supported by the Swedish Research Council (2018-02682 to XW), the Brain Foundation (FO2017-0102 to XW), grants from the Swedish state under the agreement between the Swedish Government and the county councils, the ALF-agreement (ALFGBG-813291 to XW), the National Natural of Science Foundation of China (81771418 to XW), H&K Jacobssons stiftelse (to AZ, 7/h18), Wilhelm & Martina Lundgren's Foundation (to AZ, 2017-1972), and the Frimurare Barnhus Foundation (150511 to AN).

ACKNOWLEDGMENTS

We thank Anna-Lena Leverin (Department of Physiology, Sahlgrenska Academy, University of Gothenburg) for help with the protein assays and Kajsa Groustra (Experimental Biomedicine, Sahlgrenska Academy, University of Gothenburg) for assistance with animal maintenance and breeding. The *Rorα*$^{fl/fl}$*IL7r*^{Cre} mouse strain was a kind gift from Dr. Andrew McKenzie (Cambridge University, United Kingdom) with the kind permission from Hans-Reimer Rodewald (Deutsches Krebsforschungszentrum, Heidelberg, Germany) for the use of *IL7rCre* mice in the ILC2-impaired mouse strain. We also thank Anna Rehammar from Mathematical Sciences, Chalmers University of Technology and University of Gothenburg, and Thomas Karlsson from Biostatistics, School of Public Health and Community Medicine, Institute of Medicine, University of Gothenburg for the statistic consultations.

SUPPLEMENTARY MATERIAL

The Supplementary Material for this article can be found online at: https://www.frontiersin.org/articles/10.3389/fncel.2020.00249/full#supplementary-material

FIGURE S1 | Representative images show the positive controls (lung tissue, **A**), and negative controls omitting the primary antibodies for the immunofluorescent staining of ST2 and CD3 for lung tissue **(B)** and meninges **(C)**. Arrow head: ST2+ ILC2s, star: CD3+ cells. Scale bars: 50 μm.

FIGURE S2 | Representative flow cytometry plots for fluorescence-minus-one controls (FMO) used in flow cytometry experiments.

FIGURE S3 | (A) Representative flow cytometry plots for intracellular staining of GAGA-3. **(B)** The frequency of Lin$^-$CD45$^+$GATA3$^+$ ILC2s at 7 days post HI in the neonatal wild-type mice. Paired *t*-test was used in B for comparison between hemispheres. $^*p < 0.05$.

FIGURE S4 | Representative flow cytometry plots for fluorescence-minus-one controls (FMO) used in flow cytometry experiments for the lung tissue IL-33 experiments.

REFERENCES

Adkins, B., Leclerc, C., and Marshall-Clarke, S. (2004). Neonatal adaptive immunity comes of age. *Nat. Rev. Immunol.* 4, 553–564. doi: 10.1038/nri1394

Albertsson, A., Bi, D., Duan, L., Zhang, X., Leavenworth, J. W., Qiao, L., et al. (2014). The immune response after hypoxia-ischemia in a mouse model of preterm brain injury. *J. Neuroinflamm.* 11:153.

Albertsson, A., Zhang, X., Vontell, R., Bi, D., Bronson, R. T., Supramaniam, V., et al. (2018). Gammadelta T cells contribute to injury in the developing brain. *Am. J. Pathol.* 188, 757–767.

Almeida, F. F., and Belz, G. T. (2016). Innate lymphoid cells: models of plasticity for immune homeostasis and rapid responsiveness in protection. *Mucosal Immunol.* 9, 1103–1112. doi: 10.1038/mi.2016.64

Al-Shargabi, T., Govindan, R. B., Dave, R., Metzler, M., Wang, Y., Du Plessis, A., et al. (2017). Inflammatory cytokine response and reduced heart rate variability in newborns with hypoxic-ischemic encephalopathy. *J. Perinatol.* 37, 668–672. doi: 10.1038/jp.2017.15

Bartemes, K., Chen, C. C., Iijima, K., Drake, L., and Kita, H. (2017). IL-33-responsive group 2 innate lymphoid cells are regulated by female sex hormones in the uterus. *J. Immunol.* 200, 229–236. doi: 10.4049/jimmunol.1602085

Bernink, J. H., Germar, K., and Spits, H. (2014). The role of ILC2 in pathology of type 2 inflammatory diseases. *Curr. Opin. Immunol.* 31, 115–120. doi: 10.1016/j.coi.2014.10.007

Besnard, A. G., Guabiraba, R., Niedbala, W., Palomo, J., Reverchon, F., Shaw, T. N., et al. (2015). IL-33-mediated protection against experimental cerebral malaria is linked to induction of type 2 innate lymphoid cells, M2 macrophages and regulatory T cells. *PLoS Pathog.* 11:e1004607. doi: 10.1371/journal.ppat.1004607

Bonestroo, H. J., Nijboer, C. H., Van Velthoven, C. T., Kavelaars, A., Hack, C. E., Van Bel, F., et al. (2013). Cerebral and hepatic inflammatory response after neonatal hypoxia-ischemia in newborn rats. *Dev. Neurosci.* 35, 197–211. doi: 10.1159/000346685

Cardoso, V., Chesne, J., Ribeiro, H., Garcia-Cassani, B., Carvalho, T., Bouchery, T., et al. (2017). Neuronal regulation of type 2 innate lymphoid cells via neuromedin U. *Nature* 549, 277–281. doi: 10.1038/nature23469

Cheon, I. S., Son, Y. M., Jiang, L., Goplen, N. P., Kaplan, M. H., Limper, A. H., et al. (2018). Neonatal hyperoxia promotes asthma-like features through IL-33-dependent ILC2 responses. *J. Allergy Clin. Immunol.* 142, 1100–1112. doi: 10.1016/j.jaci.2017.11.025

Debock, I., and Flamand, V. (2014). Unbalanced neonatal CD4(+) T-cell immunity. *Front. Immunol.* 5:393. doi: 10.3389/fimmu.2014.00393

Doverhag, C., Hedtjarn, M., Poirier, F., Mallard, C., Hagberg, H., Karlsson, A., et al. (2010). Galectin-3 contributes to neonatal hypoxic-ischemic brain injury. *Neurobiol. Dis.* 38, 36–46. doi: 10.1016/j.nbd.2009.12.024

Eberl, G. (2012). Development and evolution of RORgammat+ cells in a microbe's world. *Immunol. Rev.* 245, 177–188. doi: 10.1111/j.1600-065x.2011.01071.x

Fallon, P. G., Ballantyne, S. J., Mangan, N. E., Barlow, J. L., Dasvarma, A., Hewett, D. R., et al. (2006). Identification of an interleukin (IL)-25-dependent cell population that provides IL-4, IL-5, and IL-13 at the onset of helminth expulsion. *J. Exp. Med.* 203, 1105–1116.

Forsberg, A., Bengtsson, M., Eringfalt, A., Ernerudh, J., Mjosberg, J., and Jenmalm, M. C. (2014). GATA binding protein 3(+) group 2 innate lymphoid cells are present in cord blood and in higher proportions in male than in female neonates. *J. Allergy Clin. Immunol.* 134, 228–230.

Fung, I. T. H., Sankar, P., Zhang, Y., Robison, L. S., Zhao, X., D'souza, S. S., et al. (2020). Activation of group 2 innate lymphoid cells alleviates aging-associated cognitive decline. *J. Exp. Med.* 217:e20190915.

Gadani, S. P., Smirnov, I., Smith, A. T., Overall, C. C., and Kipnis, J. (2017). Characterization of meningeal type 2 innate lymphocytes and their response to CNS injury. *J. Exp. Med.* 214, 285–296. doi: 10.1084/jem.20161982

Hagberg, H., Mallard, C., Ferriero, D. M., Vannucci, S. J., Levison, S. W., Vexler, Z. S., et al. (2015). The role of inflammation in perinatal brain injury. *Nat. Rev. Neurol.* 11, 192–208.

Hatfield, J. K., and Brown, M. A. (2015). Group 3 innate lymphoid cells accumulate and exhibit disease-induced activation in the meninges in EAE. *Cell Immunol.* 297, 69–79. doi: 10.1016/j.cellimm.2015.06.006

Herz, J., Koster, C., Crasmoller, M., Abberger, H., Hansen, W., Felderhoff-Muser, U., et al. (2018). Peripheral T cell depletion by FTY720 exacerbates

hypoxic-ischemic brain injury in neonatal mice. *Front. Immunol.* 9:1696. doi: 10.3389/fimmu.2018.01696

Jones, R., Cosway, E. J., Willis, C., White, A. J., Jenkinson, W. E., Fehling, H. J., et al. (2018). Dynamic changes in intrathymic ILC populations during murine neonatal development. *Eur. J. Immunol.* 48, 1481–1491. doi: 10.1002/eji.201847511

Juul, S. E., Comstock, B. A., Wadhawan, R., Mayock, D. E., Courtney, S. E., Robinson, T., et al. (2020). A randomized trial of erythropoietin for neuroprotection in preterm infants. *N. Engl. J. Med.* 382, 233–243.

Kabata, H., Moro, K., and Koyasu, S. (2018). The group 2 innate lymphoid cell (ILC2) regulatory network and its underlying mechanisms. *Immunol. Rev.* 286, 37–52. doi: 10.1111/imr.12706

Klein Wolterink, R. G., Kleinjan, A., Van Nimwegen, M., Bergen, I., De Bruijn, M., Levani, Y., et al. (2012). Pulmonary innate lymphoid cells are major producers of IL-5 and IL-13 in murine models of allergic asthma. *Eur. J. Immunol.* 42, 1106–1116. doi: 10.1002/eji.201142018

Kolosowska, N., Keuters, M. H., Wojciechowski, S., Keksa-Goldsteine, V., Laine, M., Malm, T., et al. (2019). Peripheral administration of IL-13 induces anti-inflammatory microglial/macrophage responses and provides neuroprotection in ischemic stroke. *Neurotherapeutics* 16, 1304–1319. doi: 10.1007/s13311-019-00761-0

Mair, F., and Becher, B. (2014). Thy1+ Sca1+ innate lymphoid cells infiltrate the CNS during autoimmune inflammation, but do not contribute to disease development. *Eur. J. Immunol.* 44, 37–45. doi: 10.1002/eji.201343653

Massaro, A. N., Wu, Y. W., Bammler, T. K., Comstock, B., Mathur, A., Mckinstry, R. C., et al. (2018). Plasma biomarkers of brain injury in neonatal hypoxic-ischemic encephalopathy. *J Pediatr* 194, 67.e1–75.e1.

McNaught, A. D., and Wilkinson, A. (1997). *Compendium of Chemical Terminology*. Oxford: Blackwell Science Oxford.

Miller, D., Motomura, K., Garcia-Flores, V., Romero, R., and Gomez-Lopez, N. (2018). Innate lymphoid cells in the maternal and fetal compartments. *Front. Immunol.* 9:2396. doi: 10.3389/fimmu.2018.02396

Molofsky, A. B., Nussbaum, J. C., Liang, H. E., Van Dyken, S. J., Cheng, L. E., Mohapatra, A., et al. (2013). Innate lymphoid type 2 cells sustain visceral adipose tissue eosinophils and alternatively activated macrophages. *J. Exp. Med.* 210, 535–549. doi: 10.1084/jem.20121964

Moro, K., Ealey, K. N., Kabata, H., and Koyasu, S. (2015). Isolation and analysis of group 2 innate lymphoid cells in mice. *Nat. Protoc.* 10, 792–806. doi: 10.1038/nprot.2015.047

Moro, K., Yamada, T., Tanabe, M., Takeuchi, T., Ikawa, T., Kawamoto, H., et al. (2010). Innate production of T(H)2 cytokines by adipose tissue-associated c-Kit(+)Sca-1(+) lymphoid cells. *Nature* 463, 540–544. doi: 10.1038/nature08636

Mottahedin, A., Zhang, X., Zelco, A., Ardalan, M., Lai, J. C. Y., Mallard, C., et al. (2018). A novel image segmentation method for the evaluation of inflammation-induced cortical and hippocampal white matter injury in neonatal mice. *J. Chem. Neuroanat.* 96, 79–85. doi: 10.1016/j.jchemneu.2018.12.009

Natalucci, G., Latal, B., Koller, B., Ruegger, C., Sick, B., Held, L., et al. (2016). Effect of early prophylactic high-dose recombinant human erythropoietin in very preterm infants on neurodevelopmental outcome at 2 years: a randomized clinical trial. *Jama* 315, 2079–2085.

Nazmi, A., Albertsson, A., Rocha-Ferreira, E., Zhang, X., Vontell, R., Zelco, A., et al. (2018). Lymphocytes contribute to the pathophysiology of neonatal brain injury. *Front. Neurol.* 9:159. doi: 10.3389/fneur.2018.00159

Neill, D. R., Wong, S. H., Bellosi, A., Flynn, R. J., Daly, M., Langford, T. K., et al. (2010). Nuocytes represent a new innate effector leukocyte that mediates type-2 immunity. *Nature* 464, 1367–1370. doi: 10.1038/nature08900

Nussbaum, J. C., Van Dyken, S. J., Von Moltke, J., Cheng, L. E., Mohapatra, A., Molofsky, A. B., et al. (2013). Type 2 innate lymphoid cells control eosinophil homeostasis. *Nature* 502, 245–248. doi: 10.1038/nature12526

Oliphant, C. J., Hwang, Y. Y., Walker, J. A., Salimi, M., Wong, S. H., Brewer, J. M., et al. (2014). MHCII-mediated dialog between group 2 innate lymphoid cells and CD4(+) T cells potentiates type 2 immunity and promotes parasitic helminth expulsion. *Immunity* 41, 283–295. doi: 10.1016/j.immuni.2014.06.016

Orrock, J. E., Panchapakesan, K., Vezina, G., Chang, T., Harris, K., Wang, Y., et al. (2016). Association of brain injury and neonatal cytokine response during therapeutic hypothermia in newborns with hypoxic-ischemic encephalopathy. *Pediatr. Res.* 79, 742–747. doi: 10.1038/pr.2015.280

Park, K. W., Baik, H. H., and Jin, B. K. (2009). IL-13-induced oxidative stress via microglial NADPH oxidase contributes to death of hippocampal neurons in vivo. *J. Immunol.* 183, 4666–4674. doi: 10.4049/jimmunol.0803392

Pelly, V. S., Kannan, Y., Coomes, S. M., Entwistle, L. J., Ruckerl, D., Seddon, B., et al. (2016). IL-4-producing ILC2s are required for the differentiation of TH2 cells following *Heligmosomoides polygyrus* infection. *Mucosal Immunol.* 9, 1407–1417. doi: 10.1038/mi.2016.4

Price, A. E., Liang, H. E., Sullivan, B. M., Reinhardt, R. L., Eisley, C. J., Erle, D. J., et al. (2010). Systemically dispersed innate IL-13-expressing cells in type 2 immunity. *Proc. Natl. Acad. Sci. U.S.A.* 107, 11489–11494. doi: 10.1073/pnas.1003988107

Rice, J. E., Vannucci, R. C., and Brierley, J. B. (1981). The influence of immaturity on hypoxic-ischemic brain damage in the rat. *Annal. Neurol.* 9, 131–141. doi: 10.1002/ana.410090206

Romero-Suarez, S., Del Rio Serrato, A., Bueno, R. J., Brunotte-Strecker, D., Stehle, C., Figueiredo, C. A., et al. (2019). The central nervous system contains ILC1s that differ from NK cells in the response to inflammation. *Front. Immunol.* 10:2337. doi: 10.3389/fimmu.2019.02337

Russi, A. E., Ebel, M. E., Yang, Y., and Brown, M. A. (2018). Male-specific IL-33 expression regulates sex-dimorphic EAE susceptibility. *Proc. Natl. Acad. Sci. U.S.A.* 115, E1520–E1529.

Russi, A. E., Walker-Caulfield, M. E., Ebel, M. E., and Brown, M. A. (2015). Cutting edge: c-Kit signaling differentially regulates type 2 innate lymphoid cell accumulation and susceptibility to central nervous system demyelination in male and female SJL mice. *J. Immunol.* 194, 5609–5613. doi: 10.4049/jimmunol.1500068

Shankaran, S. (2015). Therapeutic hypothermia for neonatal encephalopathy. *Curr. Opin. Pediatr.* 27, 152–157. doi: 10.1097/mop.0000000000000199

Shankaran, S., Laptook, A., Ehrenkran, Z. R., Tyson, J., Mcdonald, S., Donovan, E., et al. (2005). Whole-Body hypothermia for neonates with hypoxic–ischemic encephalopathy. *N. Engl. J. Med.* 353, 1574–1584.

Song, J., Sun, H., Xu, F., Kang, W., Gao, L., Guo, J., et al. (2016). Recombinant human erythropoietin improves neurological outcomes in very preterm infants. *Ann. Neurol.* 80, 24–34. doi: 10.1002/ana.24677

Spits, H., Artis, D., Colonna, M., Diefenbach, A., Di Santo, J. P., Eberl, G., et al. (2013). Innate lymphoid cells–a proposal for uniform nomenclature. *Nat. Rev. Immunol.* 13, 145–149. doi: 10.1038/nri3365

Van Dyken, S. J., Mohapatra, A., Nussbaum, J. C., Molofsky, A. B., Thornton, E. E., Ziegler, S. F., et al. (2014). Chitin activates parallel immune modules that direct distinct inflammatory responses via innate lymphoid type 2 and gammadelta T cells. *Immunity* 40, 414–424. doi: 10.1016/j.immuni.2014.02.003

Vivier, E., Artis, D., Colonna, M., Diefenbach, A., Di Santo, J. P., Eberl, G., et al. (2018). Innate lymphoid cells: 10 years on. *Cell* 174, 1054–1066.

Walsh, J. T., Hendrix, S., Boato, F., Smirnov, I., Zheng, J., Lukens, J. R., et al. (2015). MHCII-independent CD4+ T cells protect injured CNS neurons via IL-4. *J. Clin. Invest.* 125:2547. doi: 10.1172/jci82458

Xu, Y., Romero, R., Miller, D., Silva, P., Panaitescu, B., Theis, K. R., et al. (2018). Innate lymphoid cells at the human maternal-fetal interface in spontaneous preterm labor. *Am. J. Reprod. Immunol.* 79:e12820. doi: 10.1111/aji.12820

Yagi, R., Zhong, C., Northrup, D. L., Yu, F., Bouladoux, N., Spencer, S., et al. (2014). The transcription factor GATA3 is critical for the development of all IL-7Ralpha-expressing innate lymphoid cells. *Immunity* 40, 378–388. doi: 10.1016/j.immuni.2014.01.012

Yang, D., Sun, Y. Y., Bhaumik, S. K., Li, Y., Baumann, J. M., Lin, X., et al. (2014). Blocking lymphocyte trafficking with FTY720 prevents inflammation-sensitized hypoxic-ischemic brain injury in newborns. *J. Neurosci.* 34, 16467–16481. doi: 10.1523/jneurosci.2582-14.2014

Yang, M. S., Ji, K. A., Jeon, S. B., Jin, B. K., Kim, S. U., Jou, I., et al. (2006). Interleukin-13 enhances cyclooxygenase-2 expression in activated rat brain microglia: implications for death of activated microglia. *J. Immunol.* 177, 1323–1329. doi: 10.4049/jimmunol.177.2.1323

Yang, M. S., Park, E. J., Sohn, S., Kwon, H. J., Shin, W. H., Pyo, H. K., et al. (2002). Interleukin-13 and -4 induce death of activated microglia. *Glia* 38, 273–280. doi: 10.1002/glia.10057

Zhang, X., Rocha-Ferreira, E., Li, T., Vontell, R., Jabin, D., Hua, S., et al. (2017). gammadeltaT cells but not alphabetaT cells contribute to sepsis-induced white matter injury and motor abnormalities in mice. *J. Neuroinflamm.* 14:255.

Zhu, C., Kang, W., Xu, F., Cheng, X., Zhang, Z., Jia, L., et al. (2009). Erythropoietin improved neurologic outcomes in newborns with hypoxic-ischemic encephalopathy. *Pediatrics* 124, e218–e226. doi: 10.1542/peds.2008-3553

Conflict of Interest: The authors declare that the research was conducted in the absence of any commercial or financial relationships that could be construed as a potential conflict of interest.

frontiers in Pediatrics

ORIGINAL RESEARCH
published: 21 August 2020
doi: 10.3389/fped.2020.00485

Prediction of Delayed Neurodevelopment in Infants Using Brainstem Auditory Evoked Potentials and the Bayley II Scales

Xiaoyan Wang[1], *Xianming Carroll*[2]*, *Hong Wang*[1], *Ping Zhang*[1], *Jonathan Nimal Selvaraj*[3] *and Sandra Leeper-Woodford*[4]

[1] Department of Child Health, Hubei Maternal and Child Health Hospital, Wuhan, China, [2] Department of Public Health, Mercer University College of Health Professions, Atlanta, GA, United States, [3] College of Life Science, Hubei University, Wuhan, China, [4] Department of Biomedical Sciences, Mercer University School of Medicine, Macon, GA, United States

Background: Brainstem auditory evoked potentials (BAEP) provide an objective analysis of central nervous system function and development in infants. This study proposed to examine the relationship between infant BAEP values at age 6 months, and their neurodevelopment at age 2 years assessed by the mental development indices (MDI), a form of Bayley Scales of Infant Development. We hypothesized that in infants with BAEP values outside normal range, there may be neurodevelopmental delays, as shown by their MDI scores.

Methods: An exploratory investigation was conducted using preterm (28–36 weeks gestation; 95 cases) and term infants (≥37 weeks gestation; 100 cases) who were born with specific perinatal conditions. BAEP values were recorded in these infants from 1 to 8 months of age, and compared with MDI scores in these infants at age 2 years. A multivariate linear regressions model was performed to test the associations between all variables and MDI scores. Stratified linear regression was used to test the interactions between gestational age and BAEP values with MDI scores. Significance was determined at a $p < 0.05$.

Results: We found that BAEP values were inversely associated with MDI scores in premature infants ($\beta = -1.89$; 95% confidence interval $= -3.42$ to -0.36), and that the effect of gestational age and BAEP values on the MDI scores is decreased by 1.89 points due to the interaction between these two variables. In premature babies, the lower the BAEP value below the mean, the greater the decrease in MDI score at age 2 years. Asphyxia and lower socioeconomic status in the family were also covariates associated with lower MDI scores at age 2 years.

Conclusion: The data provided evidence that BAEP values outside the normal range in premature infants at age 6 months may predict developmental delays in cognitive and motor skills, as shown by MDI scores. We propose that BAEP assessment may be utilized as a potential indicator for neurodevelopment, and suggest that early intellectual

OPEN ACCESS

Edited by:
Changlian Zhu,
Third Affiliated Hospital of Zhengzhou University, China

Reviewed by:
Maria Lorella Gianni,
University of Milan, Italy
Jean-Baptist Du Prel,
University of Wuppertal, Germany

***Correspondence:**
Xianming Carroll
carroll_x@mercer.edu

Specialty section:
This article was submitted to Pediatric Neurology, a section of the journal Frontiers in Pediatrics

Received: *20 December 2019*
Accepted: *10 July 2020*
Published: *21 August 2020*

Citation:
Wang X, Carroll X, Wang H, Zhang P, Selvaraj JN and Leeper-Woodford S (2020) Prediction of Delayed Neurodevelopment in Infants Using Brainstem Auditory Evoked Potentials and the Bayley II Scales. Front. Pediatr. 8:485. doi: 10.3389/fped.2020.00485

and public health interventions should be encouraged to enrich neurodevelopment in premature babies with BAEP values outside the normal range.

Keywords: pediatric neurodevelopment, brainstem auditory evoked potentials (BAEP), Bayley Scales of Infant Development, premature birth, perinatal conditions

INTRODUCTION

There has been a rapid increase in survival rates of premature infants in recent decades because of the advancement in neonatal intensive care. Certain unexpected medical issues occur in newborn infants which affect the long-term learning ability in children (1–4). If not addressed properly in the early stages of infant development, these medical issues in early infancy can have long-term effects on neurodevelopment (1–6).

Abnormality in the brainstem auditory evoked potentials (BAEP) is considered to be an early indicator for cognitive related brain issues in premature infants and those with perinatal issues (7). BAEP may be used to assess auditory function in infants and children, and is considered as a clinically useful method for evaluation of cognitive development (8). In a number of studies, BAEP values have been found to be outside the normal range in individuals with autism, intellectual and language retardation, and attention deficit/hyperactivity disorder (9, 10). Because of the widespread acceptance of BAEP as a clinical tool assessing early cognitive brain issues, we proposed to utilize BAEP in our investigation of neurodevelopment in infants with perinatal issues.

The Bayley Scales of Infant Development (BSID) is considered a clinically valid measurement for assessing infant developmental progress (11–15). In our study, we used the modified Bayley II scale which is used in Chinese hospitals to assess the neurodevelopment of premature infants between 1 and 42 months of age (11–15). The BSID-II includes the mental developmental index (MDI), which indicates adaptive behavior, language, and exploration activities, and the psychomotor developmental index (PDI) to assess gross and fine movements (11–16).

Because perinatal issues in newborns may lead to higher risks for negative neurological effects in these infants (1), we propose that assessments of infant BAEP values, in combination with gestational age and certain perinatal conditions, may provide potential predictors for later neurodevelopmental delays. Beyond prematurity and perinatal conditions at birth, there are multiple individual factors that likely influence early cognitive development, including socioeconomic conditions (17, 18) and parental education (19–23). Because of this, our current analyses will also include certain socioeconomic conditions as factors in the prediction of early childhood cognitive development.

Monitoring these predictors could possibly guide us on how to improve the neurological development of those children at high risk for delayed development. Our study investigates the predictive value of comparing BAEP indices at age 6 months to the MDI and PDI scores at age 2 years, in term and preterm infants born with certain perinatal conditions. We hypothesized that in infants with BAEP values outside the normal range, there may be developmental delays in cognitive and motor skills, as shown by the MDI and PDI scores in these babies. We propose that by using these assessments, we may be able to predict alterations in the neurodevelopment of infants exposed to compromising medical conditions at birth.

MATERIALS AND METHODS

Study Design and Sample Enrollment

This study was designed as an explorative investigation. We conducted this retrospective study at Hubei Maternal and Child Health Hospital, Wuhan, Hubei Province, China. The study samples included preterm infants (95 cases; 28–36 weeks gestational age), and term infants (100 cases; $\geq$37 weeks gestational age) who were born between June 1st, 2014 to October 31st, 2015.

Our hospital has 30,000 births per year, and accounts for half of all newborns in Wuhan. The incidence of premature infants born in the Obstetrics Department of our hospital is 3.0–8.0%. Our Child Health Department works together with the Neonatal Department to plan long-term follow-up programs for all infants with high-risk factors. The Neonatal Department of our hospital also accepts premature babies transferred from the other hospitals in Hubei province, and these infants are transferred to our Child Health Department for follow-up after age 1-month. The infants randomly selected for this study were among our long-term follow-up infant population. A total of 230 infants selected for this study were to be followed up to at least 2 years of age, with the repeated BAEP examinations done regularly. However, due to various reasons, including parents relocating to other provinces, or not wanting to continue the repeated BAEP tests, 35 infants were lost to follow-up. As a result, only 195 infants remained to complete our study. The consent rate for participation was 85.7%.

Because there is information sharing between the Neonatal Department and our Child Health Department, we were able to access the essential medical, socioeconomic, and demographic information on file for the newborns selected for our study. All parents of newborns with perinatal conditions had filled out questionnaires prior to the infant follow-up programs, and we did not see these until after our random selection of infants for the current study. The questionnaires included socioeconomic and demographic information. Gender was the only demographic variable in our study, and maternal education, paternal education, maternal occupation, paternal occupation, and household income were considered as SES variables in this study. Parental education was assigned as

being either compulsory education (<9 years, low level), high school education (9–12 years, middle level), or some college or advanced training (>12 years, high level) (24). Parental occupation was assigned as three levels: unemployment, manual labor, and professional. Household income was defined as <3,000 Yuan/month, 3,000–5,999 Yuan/month, and ≥6,000 Yuan/month; three levels, in which 1.00 USD was equal to 6.23 RMB (Yuan) in 2015. Higher levels of parental education, professional jobs, and income ≥6,000 Yuan/month were indicative of higher SES as the reference category.

The assessment forms also included whether the mothers had issues of hypertension, diabetes, or history of miscarriage, threatened abortion, intrauterine distress, or jaundice. These maternal conditions were found in the mothers of both preterm and term infants, and future studies may provide further information on the effects of these maternal issues on neurodevelopment in preterm and term infants. The infants included in this current study experienced perinatal issues such as infection, jaundice, asphyxia, respiratory failure, or intracranial hemorrhage around the time of delivery, and they were followed in our clinic up to the age of 2 years. For these perinatal conditions, the disease classification method currently used in our hospital is The International Classification of Diseases, an internationally unified disease classification method developed by the World Health Organization (WHO). The 10th revision of the "International Statistical Classification of Diseases and Related Health Problems" (25) is common worldwide, and is collectively referred to as ICD-10. Our hospital used the ICD-10 to classify disease conditions according to the etiology, pathology, clinical manifestations, and anatomical location of the disease, making this an organized method for disease coding in our health systems. In both the preterm and term groups in our study, all infants had been given the appropriate interventions for their medical conditions at birth. For infants with staged developmental delay, our doctors and nurses provide special training programs such as help for 3-month-old infants who are unable to raise their head, and, for 6-month-old infants who cannot sit without being supported, we offer training sessions to help these infants sit alone.

For this study, the selected infants had recovered from their neonatal treatment, were discharged from the hospital, and their vital signs were stable. Because these infants had been at high risk during the perinatal period, follow-up of these infants continued at our hospital until they were 2 years old. The criteria for exclusion from our study were babies born in our hospital with hearing impairments, cerebral palsy, severe cardiopulmonary disease, severe malformation or genetic metabolic diseases. Our study included regular follow-up examinations, monitoring infant growth and development level, feeding and exercise guidance, health education guidance for parents, and early rehabilitation training for infants with poor development level. Our main task was to promote normal growth and development in all infants. Because all families of infants in this study were given the same intervention guidance, including nutrition advice, infant muscle movement training, and early parent-child education information, the intervention measures were not taken into account for our study analyses.

This investigation was approved by the Ethics Committee of Hubei Maternal and Child Health Hospital. Informed consent of parents was obtained for all infants. We only tested infants with perinatal issues, and followed the "Ethical Review Measures for Biomedical Research Involving Human Beings." The principle of this ethical review is to respect the voluntary will of the subjects and abide by the principles of benefit, non-harm and justice. For this reason, our study had no control group of healthy infants because this would not be beneficial for normal infants to undergo the numerous tests and assessments.

Because of these required constraints on testing healthy infants, the controls used for this study were those normal scale ranges built into each of the assessment tests utilized for this study. For BAEP assessment of hearing loss in infants, it is clinically acceptable to check the latencies of waves I, III, and V, interpeak latencies of I–III, III–V, and I–V for abnormalities of BAEPs (7, 8, 26–28). For this assessment, wave latencies of III and V, and interpeak latencies of more than two standard deviations between waves I–III, and I–V, or III–V are considered as abnormal (7, 8, 26–28). The BSID II used for neurodevelopment assessment includes the mental development index (MDI) indicating the scale of adaptive behaviors, language, and exploration activities, and the psychomotor development index (PDI) for assessment of gross and fine movements (11–16). The MDI and PDI scores assigned to each infant ranged from 120 (excellent development) to ≤69 (developmental delay) (11–16). All procedures and methods were performed in accordance with the approved guidelines.

BAEP Assessment

The auditory function of all infants in this study was assessed by using BAEP assessments at 1–8 months after birth. The BAEP assessment is considered an effective tool in screening for possible hearing loss in children with conditions such as meningitis, where it has been found that the frequency of BAEP impairment or hearing loss was 34.6 and 30.8%, respectively (29). The BAEP has been used to assess the hearing abilities in infants 6 months old, and in those older who have motor or intellectual problems (30). While BAEP assessments at 1, 3, 6, and 8 months are used to determine auditory function, age 6 months is the critical period for infant physical exams, and a number of deficits at birth are resolved by age 6 months. For these reasons, we focused our BAEP analyses in **Tables 5–7** and **Figures 1–4** on the infants tested at age 6 months.

In our study, BAEP was recorded using the Navigator PRO brainstem auditory evoked potential system (Bio-logic Inc., USA). The recording electrode was placed in the midline of the forehead, and the reference electrode was placed at the bilateral mastoid. Electrode impedance was reduced to <5 kΩ, which was maintained during the whole session of the BAEP recording. The acoustic stimuli were given through TIP-50 earphones using a click sound stimulus. Band pass filter was 0.1–3 kHz, superimposition was 1,024–2,048 times, and stimulation rate was 30.1 times/s, and the sweep duration was 10 ms.

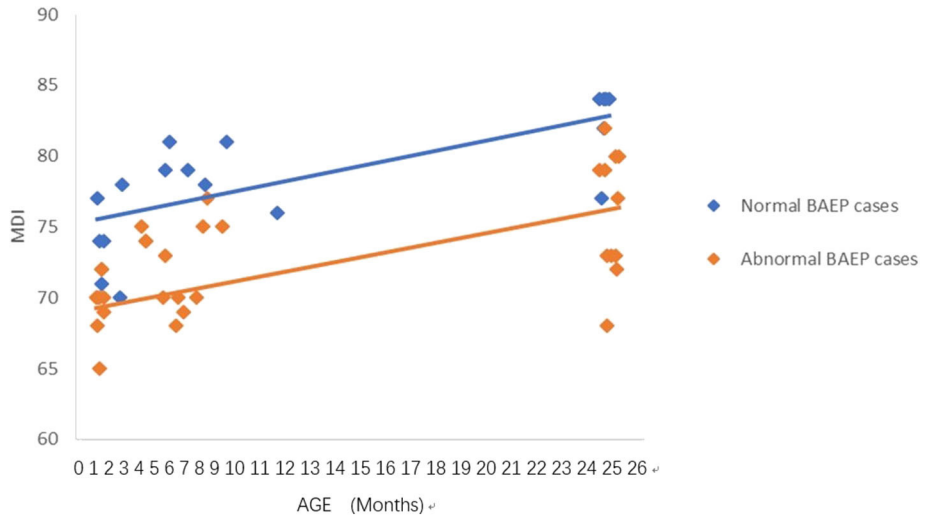

FIGURE 1 | Mental Development Index (MDI) in preterm infants with perinatal asphyxia; comparisons of infants with Brainstem Auditory Evoked Potential (BAEP) within (normal), or outside (abnormal) normal range values. Each data point represents an individual infant case prior to 11 months of age and at 24 months. There is a trend of increased MDI in infants with perinatal asphyxia from below 1 year of age to age 2. From age one to two, there is a trend of higher MDI in infants with perinatal asphyxia and normal BAEP values compared with those infants with abnormal BAEP values.

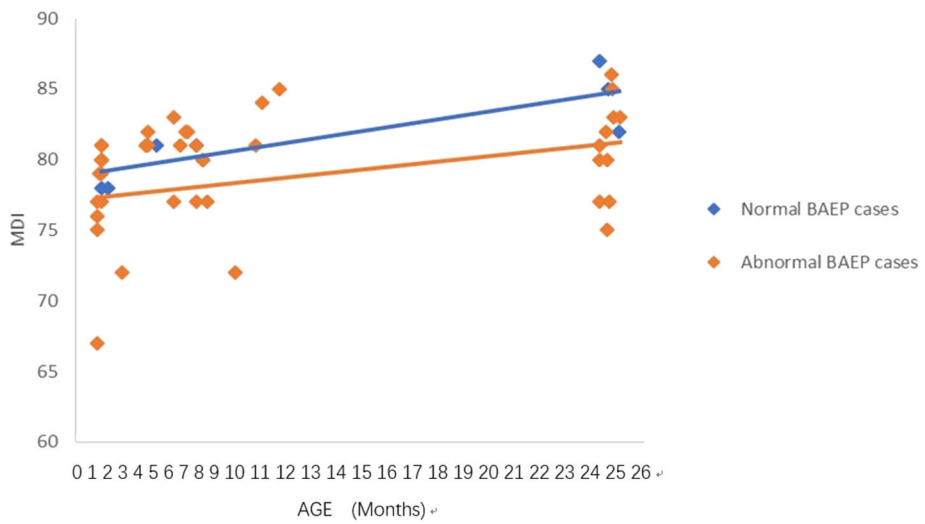

FIGURE 2 | Mental Development Index (MDI) in preterm infants with perinatal respiratory failure; comparisons of infants with Brainstem Auditory Evoked Potential (BAEP) within (normal), or outside (abnormal) normal range values. Each data point represents an individual infant case prior to 11 months of age and at 24 months. There is a trend of increased MDI in infants with perinatal respiratory failure from below 1 year of age to age 2. From age one to two, there is a trend of higher MDI in infants with perinatal respiratory failure and normal BAEP values compared with those infants with abnormal BAEP values.

The BAEP assessments were performed in a sound-insulated room with a noise level below 30 dBA. The I, III, V wave latency and I–III, III–V, I–V wave interval were recorded under 80 dBnHL short-sound stimulation. The waves (I–V) are usually recorded in the first 10 ms following broad-band and high-intensity clicks. The latencies of waves I, III, and V, interpeak latencies of I-III, III–V, and I–V, and the amplitude ratio of wave V to wave I are assessed for abnormalities of BAEPs (7, 8, 26–28). Recordings are obtained and compared with respect to midline forehead and mastoids. Evaluating different components of the latencies and amplitudes of the waves allows for evidence of impaired neural function in the auditory brainstem as evidenced by delayed latencies and reduced amplitudes of the component waves (7, 8, 26–28).

BAEP impairment is determined by latencies of waves I, III, and V that are increased beyond 2 S.D. of age-matched normal infant values, with normal interpeak latencies of I–III, III–V, and I–V, and hearing thresholds elevated to above 40 dB. Wave

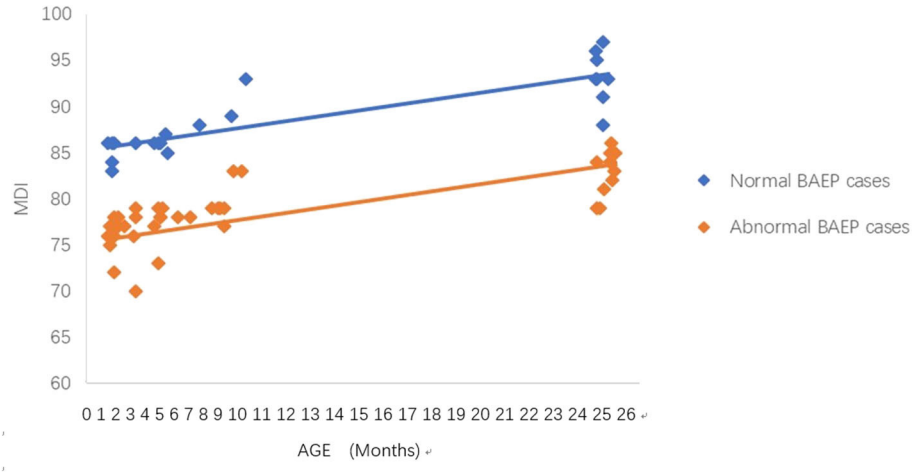

FIGURE 3 | Mental Development Index (MDI) in term infants with perinatal asphyxia; comparisons of infants with Brainstem Auditory Evoked Potential (BAEP) within (normal), or outside (abnormal) normal range values. Each data point represents an individual infant case prior to 11 months of age and at 24 months. There is a trend of increased MDI in infants with perinatal asphyxia from below 1 year of age to age 2. From age one to two, there is a trend of higher MDI in infants with perinatal asphyxia and normal BAEP values compared with those infants with abnormal BAEP values.

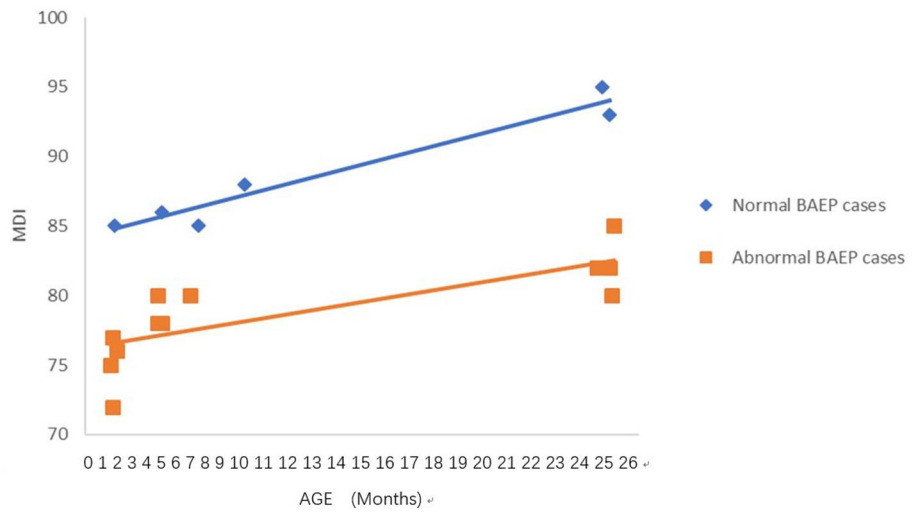

FIGURE 4 | Mental Development Index (MDI) in term infants with perinatal respiratory failure; comparisons of infants with Brainstem Auditory Evoked Potential (BAEP) within (normal), or outside (abnormal) normal range values. Each data point represents an individual infant case prior to 11 months of age and at 24 months. There is a trend of increased MDI in infants with perinatal respiratory failure from below 1 year of age to age 2. From age one to two, there is a trend of higher MDI in infants with perinatal respiratory failure and normal BAEP values compared with those infants with abnormal BAEP values.

latencies of III and V, and interpeak latencies of more than two standard deviations between waves I–III, and I–V, or III–V were considered as abnormal in our BAEP assessments (7, 8, 26–28). Abnormal BAEP is also noted by hearing thresholds increased to >40 dB, with normal latencies and interpeak latencies; or increased latencies of wave V or III (or both) and increased interpeak latencies of waves I-V and III-V, with elevated or normal hearing thresholds (7, 8). Duplicate recordings were made in response to each stimulus condition to recheck the reproducibility. BAEP was monitored in infants at 1, 3, 6, and 8 months of age.

BSID II Neurodevelopmental Assessment

The Bayley Scales of Infant Development (BSID II) is used for neurodevelopment assessment, and is the most widely used measure to assess neurodevelopment of infants before the age of three (11–16). As noted in these previous studies, the BSID-I can be used for assessing infants between 2 and 30 months of age, while the BSID-II and Bayley-III can assess infants ranging between 1 and 42 months of age. In this study, we used BSID II for assessment of the infants, and analyzed the results with respect to different medical conditions of the infants during the time of delivery. The BSID-II is primarily used in China, and we

used the revised edition prepared by Hunan Medical University (11–13). Our trained medical professionals are qualified to do the BSID-II assessment for neurodevelopment assessment in infants. The BSID II included the MDI, to evaluate and score adaptive behaviors, language and exploration activities, and the PDI to determine gross and fine movements (11–13). The MDI and PDI scores assigned are: ≥120 is excellent development, 119–90 is moderate development, 80–89 is between moderate and critical, 70–79 is critical, and ≤69 is developmental delay (11–14, 16).

Data Analysis

The age of premature infants was calculated after correcting for gestational age. The BAEP assessments were presented from infants at 1–8 months of age, and the BSID II scores were from infants at ages 1 month, 3 months, 6 months, and 2 years. The relationship between the normal and abnormal BAEP assessment at the 6th month of age, and the MDI/PDI scores for neurodevelopment at age 2 years were also monitored with respect to the different conditions at birth. Because a recent meta-analysis study which reviewed BSID-II results indicated that MDI scores correlated strongly with later cognitive functions, explaining 37% of variance, while PDI scores only correlated later motor outcomes with 12% of the variance (16), we compared only the MDI scores with the BAEP assessments in **Table 5** and **Figures 1**–**4**. We did, however, analyze both MDI and PDI scores with the BAEP assessments in **Tables 6**, **7**. To eliminate evaluator bias in our study, only the researchers who designed the study and collected data knew the birth status of the infants, and the clinic doctors and nurses who were unaware of the perinatal status of the infants conducted the tests, or evaluated and recorded the assessment scores.

Statistical Analysis

All statistical analyses were performed using SPSS version 19.0 (IBM SPSS Statistics, IBM Corporation, Armonk, NY). Chi-square tests and Cochrane's *Q*-tests were used for the comparisons of the same gestational groups over time. Using repeated measure ANOVA to analyze differences in the same groups over time, we examined MDI and PDI between term and preterm infants of different gestational ages (1 month, 3 months, 6 months, 8 months, and 2 years). Student *t*-tests were then used to examine the significance of the MDI at age 2 years, in the preterm and term infants exposed at birth to infection, jaundice, asphyxia, respiratory failure, or intracranial hemorrhage, with respect to whether each of the infants had normal or abnormal BAEP assessments at age 6 months. We constructed scatter plots to focus on the analyses of the MDI and BAEP assessments on preterm and term infants with asphyxia or respiratory failure because more infants with these conditions showed BAEP values outside of the normal range (see **Table 5**). We analyzed the trends in MDI scores at different ages in infants with perinatal asphyxia or respiratory failure, by comparing those with BAEP values outside the normal range (abnormal BAEP cases), vs. those with normal BAEP values (normal BAEP cases) (**Figures 1**–**4**).

Two steps of linear regression models were applied for further analyses of our data. In the first step, the association of all variables related to MDI and PDI was calculated in the multivariate linear regression model (31), including BAEP values at age 6 months and the other potential confounding factors, gestational age, SES (maternal education, paternal education, maternal occupation, paternal occupation, household income), and perinatal conditions (infection, jaundice, asphyxia, respiratory failure, intracranial hemorrhage). In the next step, we conducted the stratified linear regression model (32) to test our hypothesis that an interaction exists between gestational age and BAEP value at age 6 months on the MDI and PDI outcomes. We created the interaction term gestational age*BAEP for these two variables as the predictor, and MDI or PDI as the outcome in the stratified linear regression. Regression coefficients (β), 95% confidence intervals (CIs), and *p*-values were reported. All statistical tests were considered to be significant when less than an alpha level of 0.05 on a two-tailed test.

RESULTS

Descriptive Statistics

Characteristics of Study Sample

Demographic information and SES variables of 95 preterm infants (28–36 weeks gestational age) and 100 term infants (≥37 weeks gestational age) are shown in **Table 1**. The percent within the different gestational groups was used for each demographic and SES variable to compare the gestational groups with respect to their socio-demographic conditions. There is a higher percent of less educated mothers (36.0%) and fathers (28.0%) in the very premature gestational group compared with the less educated mothers (5.0%) and fathers (8.0%) in the later stage gestational groups (**Table 1**). There is also a higher percent of low income families (40.0%) in the very premature gestational group compared with the low income families (10.0%) in the later stage gestational group (**Table 1**).

The clinical characteristics of 95 preterm infants and 100 term infants are shown in **Table 2**. Among the 95 preterm infants, the mean gestational age was 34.8 ± 3.82 weeks, the mean birth weight was 2.65 ± 0.41 kg, and the mean hospitalization time was 7.57 ± 2.35 days. The term and preterm infants had neonatal conditions including infection, jaundice, asphyxia, respiratory failure, and intracranial hemorrhage around the time of delivery. We calculated the percent within each gestational group instead of the total percent to make it easier to compare the frequency of the different perinatal conditions between the different gestational groups. When compared with the term newborns, the preterm infants in the study had more issues of jaundice (88.0%), followed by asphyxia (68.0 %), infection (60.0%), respiratory failure (52.0%), and intracranial hemorrhage (32.0%), as shown in **Table 2**.

BAEP Assessment

BAEP assessments were recorded in all term and preterm infants included in this study. Some infants in our study had to be excluded from the data analysis because they were unavailable for one or more of their BAEP assessment appointments. For this reason, 5% of these data were missing. We conducted Cochrane's *Q*-test for comparisons of the same gestational groups over time by analyzing the BAEP values outside the normal

TABLE 1 | Demographic information and socioeconomic status of 95 preterm infants and 100 term infants.

Gestational age (*n*)	Gender		Socioeconomic status									
	Male *n* (%)	Female *n* (%)	Maternal education *n* (%)		Paternal education *n* (%)		Maternal occupation *n* (%)		Paternal occupation *n* (%)		Household income (Yuan/month) *n* (%)	
28–32 weeks (25)	14 (56.0)	11 (44.0)	Low	9 (36.0)	Low	7 (28.0)	Unemployed	10 (40.0)	Unemployed	7 (28.0)	<3,000	10 (40.0)
			Middle	12 (48.0)	Middle	12 (48.0)	Manual labor	10 (40.0)	Manual labor	8 (32.0)	3,000–5,999	10 (40.0)
			High	4 (16.0)	High	6 (24.0)	Professional	5 (20.0)	Professional	10 (40.0)	≥6,000	5 (20.0)
33–34 weeks (28)	16 (57.1)	12 (42.9)	Low	0 (0)	Low	2 (7.1)	Unemployed	3 (10.7)	Unemployed	1 (3.6)	<3,000	1 (3.6)
			Middle	12 (42.9)	Middle	9 (32.1)	Manual labor	10 (35.7)	Manual labor	12 (42.8)	3,000–5,999	15 (53.6)
			High	16 (57.1)	High	17 (60.8)	Professional	15 (53.6)	Professional	15 (53.6)	≥6,000	12 (42.8)
35–36 weeks (42)	22 (52.4)	20 (47.6)	Low	2 (4.8)	Low	2 (4.8)	Unemployed	8 (19.0)	Unemployed	10 (23.8)	<3,000	2 (4.8)
			Middle	16 (38.1)	Middle	13 (31.0)	Manual labor	9 (21.4)	Manual labor	15 (35.7)	3,000–5,999	25 (59.5)
			High	24 (57.1)	High	27 (64.2)	Professional	25 (59.6)	Professional	17 (40.5)	≥6,000	15 (35.7)
≥37 weeks (100)	55 (55.0)	45 (45.0)	Low	5 (5.0)	Low	8 (8.0)	Unemployed	19 (19.0)	Unemployed	14 (14.0)	<3,000	10 (10.0)
			Middle	10 (10.0)	Middle	16 (16.0)	Manual labor	15 (15.0)	Manual labor	14 (14.0)	3,000–5,999	76 (76.0)
			High	85 (85.0)	High	76 (76.0)	Professional	66 (66.0)	Professional	72 (72.0)	≥6,000	14 (14.0)

Term infants, ≥37 weeks gestational age; preterm infants, 28–36 weeks gestational age (number of weeks mother is pregnant). Maternal/Paternal education (number of years spent in school): Low ≤9 years; Middle 10–12 years; High >12 years. 1.00 USD equal to 6.23 RMB (Yuan) in 2015. n, number of infants in each category. %, percent within the different gestational groups for each socio-demographic characteristic.

TABLE 2 | Clinical characteristics of 95 preterm infants and 100 term infants.

Gestational age (*n*)	Delivery mode *n* (%)		Birth weight (kg)	Days of hospitalization	Infection	Jaundice	Asphyxia	Respiratory failure	Intracranial hemorrhage
	Vaginal delivery	Cesarean birth			*n* (%)	*n* (%)	*n* (%)	*n* (%)	*n* (%)
28–32 weeks (25)	8 (32.0)	17 (68.0)	1.97–2.42	7–22	15 (60.0)	22 (88.0)	17 (68.0)	13 (52.0)	8 (32.0)
33–34 weeks (28)	9 (32.1)	19 (67.9)	1.85–2.56	5–15	12 (42.9)	15 (53.6)	13 (46.4)	15 (53.6)	7 (25.0)
35–36 weeks (42)	13(31.0)	29 (69.0)	2.49–3.10	3–7	3 (7.1)	5 (11.9)	12 (28.6)	7 (16.7)	3 (7.1)
≥37 weeks (100)	18 (18.0)	82 (82.0)	2.90–4.10	1–7	3 (3.0)	10 (10.0)	26 (26.0)	7 (7.0)	2 (2.0)

Term infants, ≥37 weeks gestational age; preterm infants, 28–36 weeks gestational age. n, number of infants in each category. %, percent within each gestational group to compare the frequency of the different perinatal conditions between the different gestational groups.

range across each of the infant age groups. We also conducted chi-square tests for comparisons of the BAEP values outside the normal range across the gestational age groups. When comparing these BAEP values in the different gestational age groups, significant results were observed at ages 3 months $p = 0.001$, 6 months $p = 0.005$, and 8 months $p < 0.0001$ (**Table 3**). Our results indicate that BAEP values outside the normal range tends to be higher and remains increased during the early growth period in preterm infants compared to term infants (**Table 3**).

Neurodevelopment Assessment Based on BSID-II

The BSID-II neurodevelopment assessment of the infants varied according to gestational age (**Table 4**). The MDI/PDI scores in the infants born at 28–32 weeks gestation showed an increased trend from the 1st month of age (78.36 ± 8.51/77.08 ± 8.89) to the 6th month (85.95 ± 5.73/85.33 ± 7.11), and this was increased further at age 2 years (90.66 ± 4.10/91.10 ± 3.26) (**Table 4**). In the infants born at 35–36 weeks, there were also trends for higher MDI/PDI scores during the growth period, at 1 month (81.80 ± 2.67/80.42 ± 2.64), 6 months (87.21 ± 1.11/86.24 ±1.15), and at age 2 years (94.13 ± 4.80/94.53 ± 4.72). In the term infants, MDI/PDI scores were higher than in preterm infants at age 1 month, and were increased to a greater extent at age 2 years (98.55 ± 4.64/99.81 ± 3.92). Overall, these data show that the neurodevelopment of premature infants of different gestational ages gradually increases with age, and that their developmental level gradually approaches that of the term infants (**Table 4**). However, when compared to the neurodevelopment of term infants at each of the respective age groups, these data also reveal that there are trends for differences in the neurodevelopmental levels of premature infants at 1-month, 3-months, 6-months, and 2 years of age (**Table 4**).

TABLE 3 | Brainstem Auditory Evoked Potential (BAEP) assessment for 95 preterm infants and 100 term infants.

Gestational age (*n*)	BAEP value outside normal range at age 1 month *n* (%)	BAEP value outside normal range at age 3 months *n* (%)	BAEP value outside normal range at age 6 months *n* (%)	BAEP value outside normal range at age 8 months *n* (%)	Cochrane's *Q*	**p*-value
28–32 weeks (25)	22 (85.7)	21 (82.7)	20 (80.0)	19 (75.0)	40.33	<0.001
33–34 weeks (28)	28 (100)	17 (61.8)	16 (57.0)	13 (45.0)	34.70	<0.001
35–36 weeks (42)	35 (82.6)	20 (47.4)	17 (42.0)	13 (32.0)	40.52	<0.001
≥37 weeks (100)	81 (80.7)	61 (60.5)	54 (54.1)	25 (24.5)	107.21	<0.001
χ^2	2.16	7.62	6.55	8.79		
***p*-value	0.080	0.001	0.005	<0.0001		

*Comparisons of BAEP value outside normal range across the infant age groups are presented horizontally (Cochrane's Q-test, Cochrane's Q-value; *p-value). Comparisons of BAEP value outside normal range across the gestational age groups are presented vertically (chi-square-test, χ^2-value; **p-value). Term infants, ≥37 weeks gestational age; preterm infants, 28–36 weeks gestational age. n, number of infants in each category. %, percent within each gestational group. *p-value was obtained from Cochrane's Q-test; **p-value was obtained from chi-square test for categorical variables. Significant level $p < 0.05$.*

TABLE 4 | Neurodevelopment assessment using Mental Development Index (MDI) and Psychomotor Development Index (PDI) for 95 preterm infants and 100 term infants.

Gestational age (*n*)	MDI/PDI at age 1 month (mean ± *SD*)	MDI/PDI at age 3 months (mean ± *SD*)	MDI/PDI at age 6 months (mean ± SD)	MDI/PDI at age 2 years (mean ± *SD*)	**F*-value	**p*-value
28–32 weeks (25)	78.36 ± 8.51/77.08 ± 8.89	82.60 ± 4.65/80.05 ± 5.31	85.95 ± 5.73/85.33 ± 7.11	90.76 ± 4.10/91.10 ± 3.26	29.02/21.86	<0.001/<0.001
33–34 weeks (28)	80.98 ± 6.00/79.70 ± 5.58	85.76 ± 4.91/85.10 ± 4.10	86.57 ± 2.35/85.26 ± 2.60	90.93 ± 5.57/94.36 ± 6.67	38.12/49.29	<0.001/<0.001
35–36 weeks (42)	81.80 ± 2.67/80.42 ± 2.64	84.96 ± 2.20/84.38 ± 2.44	87.21 ± 1.11/86.24 ± 1.15	94.13 ± 4.80/94.53 ± 4.72	51.53/90.42	<0.001/<0.001
≥37 weeks (100)	90.22 ± 2.18/90.61 ± 3.26	91.11 ± 3.35/90.87 ± 2.59	90.35 ± 4.87/91.17 ± 3.37	98.55 ± 4.64/99.81 ± 3.92	27.70/99.65	<0.001/<0.001
***F*-value	73.19/93.97	101.96/47.57	47.96/101.47	18.10/27.87		
***p*-value	<0.0001/<0.0001	<0.0001/<0.0001	<0.0001/<0.0001	<0.0001/<0.0001		

*Comparisons of MDI/PDI across the infant age groups are presented horizontally (*F-value; *p-value). Comparisons of MDI/PDI across the gestational age groups are presented vertically (**F-value; **p-value). Term infants, ≥37 weeks gestational age; preterm infants, 28–36 weeks gestational age. MDI or PDI Index: ≥120 is excellent, 119–90 is moderate development, 80–89 is between moderate and critical, 70–79 is critical, and ≤69 is developmental delay. n, number of infants in each category. p-value was obtained from ANOVA. Significant level $p < 0.05$.*

Neurodevelopment MDI Scores With BAEP, and Prematurity, Asphyxia, and Respiratory Failure at Birth

In these comparisons, we used only the MDI scores because a recent study indicated that MDI scores correlated strongly with later cognitive functions, while PDI scores were less correlated with later motor functions (16). For this reason, we compared only the MDI scores with the BAEP assessment data in **Table 5**. As shown in this table, in the asphyxia and respiratory failure categories there were significant decreases in the MDI scores of both preterm and term infants with these perinatal conditions. We found that these conditions at birth may also impact the BAEP scores in both preterm and term infants (**Table 5**). In preterm infants who experienced asphyxia, the number of BAEP values outside the normal range at age 6 months (32 infants) was higher, and the MDI scores were significantly lower in this group at age 2 years (76.36 ± 3.66), when compared to those preterm infants with asphyxia at birth who were assessed with normal range BAEP values (10 infants; MDI scores, 82.30 ± 5.67) (**Table 5**). Similarly, in term infants with asphyxia at birth and BAEP values outside the normal range at age 6 months (13 infants), lower MDI scores were observed at age 2 years (83.12 ± 5.66), but significantly higher MDI scores were observed in the 13 infants with asphyxia at birth and BAEP in the normal range (93.42 ± 5.45) (**Table 5**). In the preterm infants who experienced respiratory failure at birth, the MDI score at age 2 years was 80.36 ± 7.66 in those with BAEP values outside the normal range at age 6 months (25 infants), but the MDI showed higher scores in those 10 preterm infants with respiratory failure at birth and normal range BAEP values (84.44 ± 5.55) (**Table 5**).

To analyze the trends in MDI scores at different ages, we constructed scatter plots to present data from the same infants

TABLE 5 | Brainstem Auditory Evoked Potential (BAEP) value at age 6 months vs. Mental Development Index (MDI) at age 2 years in preterm infants and term infants with respect to perinatal condition.

Gestational age (weeks)	Perinatal condition	BAEP value outside normal range at age 6 months *n* (%)	MDI at age 2 years (mean ± SD)	BAEP value normal range at age 6 months *n* (%)	MDI at age 2 years (mean ± SD)
28–36	Infection	2 (1.0)	80.63 ± 5.21	28 (14.4)	89.75 ± 5.25
	Jaundice	3 (1.5)	83.43 ± 3.56	39 (20.0)	94.30 ± 7.74
	Asphyxia	32 (16.4)	76.36 ± 3.66*	10 (5.1)	82.30 ± 5.67*
	Respiratory failure	25 (12.8)	80.36 ± 7.66*	10 (5.1)	84.44 ± 5.55*
	Intracranial hemorrhage	2 (1.0)	90.35 ± 7.57	16 (8.2)	92.28 ± 4.52
≥37	Infection	1 (0.5)	90	2 (1.0)	93.89 ± 9.75
	Jaundice	1 (0.5)	92	9 (4.6)	93.62 ± 5.66
	Asphyxia	13 (6.7)	83.12 ± 5.66*	13 (6.7)	93.42 ± 5.45*
	Respiratory failure	5 (2.6)	81.15 ± 5.64*	2 (1.0)	95.78 ± 4.52*
	Intracranial hemorrhage	1 (0.5)	90	1 (0.5)	93

*Comparisons of MDI scores of infants with BAEP value outside normal range vs. infants with normal range BAEP (*significant p-value). Term infants, ≥37 weeks gestational age; preterm infants, 28–36 weeks gestational age. MDI Index: ≥120 is excellent, 119–90 is moderate development, 80–89 is between moderate and critical, 70–79 is critical, and ≤69 is developmental delay. n, number of infants in each category. %, percent within each category. *p-value was obtained from student t-test. Significant level *$p < 0.05$.*

prior to 11 months of age and at age 24 months (**Figures 1**–**4**). In these figures, with age as the horizontal axis and MDI as the vertical axis, the trend of MDI scores in specific infants as they increased in age was investigated in the different groups (term/preterm, respiratory failure/asphyxia, BAEP within normal range, or outside normal range). **Figures 1**–**4** show that the MDI scores of infants with BAEP outside the normal range were lower than in infants with normal range BAEP in all four subgroups. Whether they are full-term or premature infants, and regardless of whether there is a history of asphyxia or respiratory failure, the MDI scores of infants with BAEP outside the normal range did not reach the developmental level of infants with normal range BAEP values (**Figures 1**–**4**).

Multiple Linear Regression Analysis

Multivariate Linear Regression Model

Table 6 shows the results of two multivariate linear regression models in the overall sample of infants in our study, with all factors as the independent variables, and MDI and PDI as the outcome variables. The independent variables entered into the model included gestational age, SES (maternal education, paternal education, maternal occupation, paternal occupation, household income), perinatal conditions (infection, jaundice, asphyxia, respiratory failure, intracranial hemorrhage), and BAEP values at 6 months of age. Model 1 entered the main effects of all factors related to MDI scores. Model 2 entered the main effects of all factors related to PDI scores.

In **Table 6**, we found that gestational age was very strongly associated with MDI scores (β = 0.36; 95% CI = 0.13–0.50) and PDI scores (β = 0.29; 95% CI = 0.07–0.41). We also found that SES indicators (maternal education and household income) are associated with MDI scores but not PDI scores, with respect to maternal education (β = 1.50; 95% CI = 0.59–3.91) and household income (β = 1.42; 95% CI = 0.19–2.60), respectively. In addition, our data showed that asphyxia was inversely associated with MDI scores (β = −1.27; 95% CI = −2.45 to −0.27), which means that infants born with asphyxia are predicted to have low MDI scores an average of 1.27 times more than the infants without asphyxia (**Table 6**). In the multivariate linear regression model, we did not find that the BAEP value at age 6 months was significantly related to MDI scores, but the $p = 0.084$ may possibly be due to the interactive correlations of two independent variables such as gestational age and BAEP value. In this case, we will continue to conduct further analyses to reveal the interactions between gestational age and BAEP values on MDI and PDI scores.

Stratified Linear Regression Model

Table 7 shows a summary of the results for the stratified linear regression models. In Model 3 and Model 4, gestational age*BAEP value at age 6 months was the predictive variable, and MDI and PDI were the outcome variables. The interactions of BAEP values and gestational age were estimated in MDI scores and PDI scores, respectively.

We found that in the preterm infant group, the BAEP value at age 6 months was an independent factor and inversely associated with MDI scores at age 2 (β = −1.89; 95% CI = −3.42 to −0.36, $p = 0.015$; **Table 7**). In the term infant group, there was no statistical significance (β = 0.28; 95% CI = −1.52 to 2.08, $p = 0.725$) between BAEP value and MDI scores as shown in **Table 7**. These findings suggest that in premature infants there is a significant difference in the magnitude of the association between BAEP values at age 6 months and MDI scores in gestational age, and that a BAEP value outside the normal range at age 6 months may possibly be a predictor of lower MDI scores at age 2 years in these babies. As noted in **Table 7**, the effect of gestational age and BAEP on the MDI score is decreased by 1.89 points due to the interaction between these two variables, in that, the decrease in MDI score in infants with a lower BAEP value is dependent on gestational age, and vice versa. Also, the lower the BAEP value was below the mean, correlated with a greater decrease in MDI score with gestational age. There was no significant difference in the relationship between BAEP at age 6 months and PDI score in either preterm or term infants (**Table 7**).

TABLE 6 | Multivariate linear regression model.

Factors	MDI (n =195) Model 1					PDI (n = 195) Model 2				
	Unstandardized coefficients		95% CI	t	p	Unstandardized coefficients		95% CI	t	p
	β	SE (b)				β	SE (b)			
Gestational age	0.36***	0.09	0.13 to 0.50	4.21	**0.000**	0.29***	0.08	0.07 to 0.41	3.70	**0.000**
Maternal education	1.50*	0.74	0.59 to 3.91	2.02	**0.045**	0.57	0.68	−0.91 to 2.14	0.84	0.403
Paternal education	−0.81	0.98	−2.45 to 1.54	−0.82	0.411	−0.40	0.90	−2.10 to 1.56	−0.44	0.660
Maternal occupation	−0.03	0.80	−2.57 to 0.94	−0.04	0.968	0.94	0.73	−0.76 to 2.47	1.29	0.199
Paternal occupation	1.76	1.05	−0.88 to 3.42	1.67	0.096	0.76	0.96	−1.29 to 2.65	0.79	0.430
Household income	1.42*	0.63	0.19 to 2.60	2.26	**0.025**	0.75	0.58	−0.63 to 1.94	1.30	0.195
Infection	1.42	1.04	−0.61 to 3.59	1.36	0.175	1.75	0.96	−0.16 to 3.69	1.84	0.068
Jaundice	0.41	0.78	−1.31 to 2.18	0.52	0.601	0.39	0.71	−2.05 to 1.16	0.55	0.586
Asphyxia	−1.27*	0.64	−2.45 to −0.27	−1.99	**0.048**	−0.77	0.58	−2.31 to 0.18	−1.32	0.189
Respiratory failure	−1.41	0.91	−3.24 to 0.43	−1.55	0.123	−0.56	0.83	−2.24 to 1.14	−0.67	0.501
Intracranial hemorrhage	−3.80	2.47	−8.99 to 0.95	−1.54	0.126	−1.56	2.26	−6.06 to 3.07	−0.69	0.492
BAEP (6 months)	−1.00	0.58	−1.96 to 0.36	−1.74	0.084	−0.86	0.53	−1.81 to 0.32	−1.63	0.106

*All factors associated with Mental Development Index (MDI) and Psychomotor Development Index (PDI) at age 2 years. Gestational age—number of weeks mother is pregnant. BAEP (6 months)—Brainstem Auditory Evoked Potential at age 6 months. Model 1: Outcome—MDI; Model 2: Outcome—PDI. β–Unstandardized regression coefficient. SE(b)—Standard Error of value of b. Significant level *$p < 0.05$; ***$p < 0.001$ (bolded figures when $p < 0.05$).*

TABLE 7 | Stratified linear regression model.

Gestational age (n)	MDI Model 3					PDI Model 4				
	β	*SE*	95% CI	t	p	β	*SE*	95% CI	t	p
28–36 weeks (95)	−1.89*	0.76	−3.42 to −0.36	−2.50	**0.015**	−0.74	0.68	−2.11 to 0.63	−1.13	0.263
≥37 weeks (100)	0.28	0.91	−1.52 to 2.08	−0.35	0.725	−0.77	0.85	−2.52 to 0.98	−1.23	0.223

*Brainstem Auditory Evoked Potential (BAEP) at age 6 months in Preterm and Term Infants Associated with Mental Development Index (MDI) and Psychomotor Development Index (PDI) at age 2 years. Model 3: Outcome—MDI; Model 4: Outcome—PDI. Predictor variable—Brainstem Auditory Evoked Potential (BAEP) at age 6 months. Covariates entered into the model—SES (maternal education, paternal education, maternal occupation, paternal occupation, household income) and perinatal conditions (infection, jaundice, asphyxia, respiratory failure, intracranial hemorrhage). Term infants, ≥37 weeks gestational age; preterm infants, 28–36 weeks gestational age. n, number of infants in each category. β–Regression coefficient. SE—Standard Error. Significant level *$p < 0.05$ (bolded figures when $p < 0.05$).*

DISCUSSION

In this study, we found that BAEP values at age 6 months in premature infants is inversely associated with MDI scores at age 2 years. The effect of gestational age and BAEP value on the MDI score is decreased by 1.89 points due to the interaction between these two variables (**Table 7**). In premature babies, the lower their BAEP values were below the mean, the more the decrease was in their MDI scores at age 2 years. These results support our hypothesis that BAEP values outside the normal range at age 6 months have a predictive effect on neurodevelopmental delay, as shown by MDI scores, especially in premature newborns. In this study, we found that prematurity in newborns was strongly associated with low MDI and PDI scores in these infants at age 2 years. We also found that infants who experienced asphyxia at birth were more likely to have low MDI scores at age 2 years. In addition, our data revealed that infants born in families from lower SES, as indicated by maternal education and household income, were more likely to have low MDI scores at age 2 years (**Table 6**).

BAEP Value Predicts MDI Score in Premature Infants

There is increasing evidence that the issues related to cognitive and motor function performance in early childhood are related to clinical conditions during preterm or term birth (1, 33). Gestational age was found to have an effect on BAEP assessments in infants, and was also strongly associated with MDI and PDI scores as shown in our data ($p = 0.000$; **Table 6**). In our stratified multiple linear regression model, our data revealed that BAEP values outside the normal range in infants at age 6 months were more likely associated with developmental delays in cognitive skills, as shown by MDI scores in these infants (**Table 7**). In these analyses, we found that the BAEP values were inversely associated with MDI scores in preterm infants, but no significant differences were observed between BAEP and MDI scores in term infants. These data suggest that BAEP values at 6 months of age may be used as predictors for neurodevelopmental delay at age 2 years, especially for premature infants. We will expand the sample size in future studies to investigate whether this same significance is also present in term infants.

The younger the fetus, the more chances of brain cell damage caused by various conditions due to immature development (7, 34). Infants in these previous studies exhibited lower auditory function scores in the first year of infancy, and this was correlated with their lower MDI/PDI indicators of cognitive and motor development. Our current investigation provides evidence that infants may have issues of cognitive and motor function performance if they experience prematurity. A significant number of preterm infants in our study exhibited BAEP values outside the normal range in the first year of infancy, and this was correlated with their lower MDI/PDI scores in the BSID assessments of cognitive and motor development. We also observed that the majority of preterm infants who experienced asphyxia at birth and had BAEP values outside the normal range at age 6 months exhibited lower MDI/PDI scores, suggesting that there may be altered cognitive and motor functions, especially in language development in these infants at age 2. Our results indicate that BAEP values outside the normal range could be a potential indicator for altered cognitive and motor function in these infants at later ages.

In our study, we used the modified Bayley II scale which is used in Chinese hospitals to assess the neurodevelopment in premature infants. With our results utilizing the Bayley-II scale, we provided evidence that this assessment may be used to predict abnormalities in infant neurodevelopment, yet further studies are needed to compare with assessments reported using the Bayley III scale. Previous studies have shown that the Bayley-III scale could be effective in measuring developmental functions with respect to examiner observations, and parent-reported behaviors (12, 35). But, while this scale may be used to collectively assess language development, many larger studies are needed to prove its effectiveness (12, 35). Previous publications have indicated that the BSID-II has higher predictive abilities for future functioning, while others favor BSID-III (12, 13, 36, 37). There are indications that BSID-II might underestimate development and BSID-III might overestimate development (12, 13, 38). In previous studies, the Bayley III scale identified significantly fewer children with disabilities with respect to low birth weight preterm infants, and the authors proposed that intervention may be essential for these infants at the time of discharge from the neonatal intensive care unit (39, 40). The Bayley-II and brain magnetic resonance imaging to assess the neurodevelopmental outcomes have mostly been applied to infants exposed to asphyxia (41, 42). In our study using the Bayley-II assessment, we identified a number of cases with neurodevelopmental issues especially in the infants exposed to asphyxia.

The MDI/PDI scores of cognitive and motor function vary during the stages of early infant development (43, 44). A previous study indicated that variation in the PDI score for psychomotor function is less significant compared to the MDI score for mental/cognitive function in low birth weight infants (44). In this study, we found similar results consistent with this previous study that PDI score for psychomotor function is less significant compared to the MDI score (**Table 7**). In our current study, we found that preterm infants with BAEP values outside the normal range had significantly lower MDI scores, compared to those of term infants.

Studies using the Bayley II scale consistently identified high rates of cognitive impairments among preterm or low birth rate infants (45). In our study, the cognitive impairments tend be higher in preterm infants subjected to asphyxia or respiratory failure, based on the Bayley II assessment. Other studies have shown that there is a reduction in cognitive impairment level from 39% at 20 months to 16% at 8 years, based on the Bayley II assessment in extremely low birth weight infants (46). In our study, the MDI/PDI values for cognitive and motor scores that were observed at age 2 years might have shown increases at the later stages of development, if these infants had been exposed to early interventions such as cognitive and motor exercises, physical therapy sessions, and learning games with parents to improve their developing cognitive and motor skills.

Asphyxia Associated With MDI Score

Our investigation has shown that perinatal issues such as prematurity and asphyxia may be negatively associated with MDI scores. Infants born with asphyxia had low MDI scores an average of 1.27 times more than the infants without asphyxia (**Table 6**). Previous publications have reported that as a result of perinatal asphyxia in infants, alterations of the putamen and thalamus of the brain, and atrophic areas in the brainstem were observed (47). Studies using magnetic resonance imaging in newborns with perinatal asphyxia showed lesions in basal ganglia, thalamus, brainstem tectum, parasagittal cortex, and the midline cerebrum, but found no lesions in basal ganglia and parasagittal regions (48). According to previous studies, perinatal asphyxia may cause lesions in the central generators of brainstem auditory-evoked response components, such as the cochlear nuclei, superior olive, and inferior colliculus (48). In addition, it was found that auditory-evoked response abnormalities in the brainstem occurred more frequently after severe, prolonged asphyxia (48).

Other studies have also proposed that following perinatal hypoxemia, damage to the neonatal auditory system, including the cochlea, may result in hearing deficits (48). Children who experienced perinatal asphyxia tended to exhibit hearing loss and neurodevelopmental deficits when compared to those not exposed to asphyxia (26, 34). In reported cases of perinatal asphyxia, infants generally recovered without neurological defects, but neurodevelopmental deficits due to brain hypoxia-ischemia were noted in some of these infants (27, 28).

In our current study, the data revealed abnormal brainstem auditory-evoked responses in infants exposed to perinatal conditions such as asphyxia, and we proposed that this auditory assessment may be used to predict delays in their neurodevelopment. Our results support using the early BAEP assessments in infants as indicators of possible delays in neurodevelopment of infants with perinatal conditions such as asphyxia, as well as, prematurity and respiratory failure. To further support this proposal, **Figures 1–4** in our results show that the cognitive development of infants was lower in the infants who had BAEP values outside of the normal range, and that this was observed in all of the perinatal categories, including term, preterm, asphyxia, and respiratory failure.

Further studies using a larger number of infants, including those with perinatal infection, intracranial bleeding, jaundice, and perhaps other conditions at birth will be pursued in future investigations.

SES Related to MDI Scores

We had proposed that SES indicators are related to prematurity in newborns, and our data revealed that a higher percent of less educated mothers and low income families had infants in the very premature gestational group, when compared with less educated mothers and low income families with infants in the later stage gestational group (**Table 1**). After analyzing the data, we also found that SES indicators such as maternal education and household income were associated with infants having lower MDI scores, as shown by the lower MDI scores in infants from families in the lower SES group (**Table 6**).

These results are consistent with previous studies showing that SES variables likely influence early cognitive development, especially when the variables measured are maternal education (49) and household income (43). In our investigation (as shown in **Table 6**), we found that the infants with less educated mothers were 1.5 times more likely to have low MDI scores than the infants with more educated mothers. In addition, the infants in families with low income were 1.42 times more likely to have low MDI scores than the infants in families with higher income.

Maternal education has been shown to be a strong correlate of children's language, cognitive, and academic development. A longitudinal database (19) from the National Institute of Child Health and Human Development Study found that maternal education is associated with concurrent improvements in school readiness, language skills, and the quality of home environments in children at age 3. Other studies where interventions supporting parent-child interactions to enhance motor control and coordination are provided weekly at home from the age of 6–12 months, the overall cognitive level, especially in verbal performance, was higher at age 4 (29, 50–53). Previous investigations on low birth weight infants showed that their behavioral characteristics are also affected by family SES, which may play a role in delayed cognitive developmental at 18–22 months (52, 53). In two studies, high doses of DHA supplementation were given at an early age and found to be beneficial for improving mental development, especially in girls (50, 51). From the results of our current study, we propose that to improve their cognitive level during the stages of infant growth, early interventions are highly essential in infants with abnormal BAEP assessments and low MDI/PDI scores.

Limitations of the Study

One of our limitations is that this is an exploratory investigation and retrospective study, the study findings should be proved in confirmatory studies in the future. In addition to this limitation, while we randomly selected our study sample, we were limited by the selection criteria that only allowed us to choose infants with perinatal issues. For this reason, selection bias may have influenced the representativeness of our study. Also, because we followed the "Ethical Review Measures for Biomedical Research Involving Human Beings" to respect the voluntary will of the subjects and abide by the principles of benefit, non-harm, and justice, we were unable to have a control group of normal infants because our study would not benefit healthy infants by administering numerous tests and assessments. Future case-control studies may also be needed to investigate the odds radios which would be more rigorous than the analyses used in the current study, with respect to the association between independent and dependent variables.

Another limitation is the relatively small number of preterm infants with clinical issues at birth enrolled in our study to examine the BAEP and MDI/PDI scores. Further studies will be needed to include higher numbers of infants with jaundice, infection, and intracranial bleeding. We were not informed of the severity of intracranial hemorrhage of the infants in our study because they had been released from the hospital following normalization of their cranial MRIs. In our next study, we will take multiple factors into consideration, including more detailed information on the severity of intracranial hemorrhage and the other perinatal conditions.

We used the Bayley II scale in the assessments, and, in studies by others using the Bayley III scale, our data may not be comparable because the Bayley III scale might reveal different results with respect to the current data. We have been using the Bayley II scale in assessments at our hospital for many years, and our trained professionals are skilled to conduct the Bayley II assessments. A comparison study between the Bayley II scale and he Bayley III scale assessments might be interesting to conduct in this area of research.

In addition, issues related to environmental factors and parental lifestyle factors such as domestic smoking, alcohol use, and nutritional factors may need to be taken into consideration in future studies of cognitive and motor neurodevelopment in infants and children. Future large scale, long-term studies are needed to provide further information concerning neurodevelopmental outcomes from birth to childhood.

CONCLUSION

Our study found that BAEP values outside the normal range at age 6 months have a predictive effect on developmental delays in cognitive and motor skills, as shown by MDI scores, especially in premature newborns. Preventive prenatal care and early diagnoses and treatments during the perinatal period could possibly help prevent later problems with neurodevelopment in early childhood. For infants who experience prematurity and asphyxia, early interventions to improve cognitive and motor skills development for these infants might help to attenuate the abnormal neurodevelopmental issues that develop at later stages in these premature infants. In addition, for families with lower SES, early public health interventions, such as parental instruction with respect to teaching skills and games to enrich infant learning, may facilitate cognitive and motor development in babies with BAEP values that predict developmental delays and lower MDI scores.

DATA AVAILABILITY STATEMENT

The data analyzed during the current study are not publicly available, because they include personal identifiers and medical information that cannot be released, but are available from the first author on reasonable request.

ETHICS STATEMENT

The studies involving human participants were reviewed and approved by Institutional Ethics Committee of Hubei Maternal and Child Health Hospital. Written informed consent to participate in this study was provided by the participants' legal guardian/next of kin.

AUTHOR CONTRIBUTIONS

XW designed the study, performed the experiments, and helped with manuscript preparation. XC revised the subsequent drafts of the manuscript, helped with statistical analysis, and was responsible for the final submission. HW provided general support for the research project. PZ collected and analyzed the data. JS wrote the first draft of the manuscript. SL-W reviewed and edited the subsequent drafts of the manuscript. All authors read and approved the final version of the manuscript.

FUNDING

This research has been supported by the China Center for Disease Control and Prevention for the technology research projects for early childhood development from 2017 to 2018 (2017FYE004). This funding source had no role in the study design, data collection, statistical analysis, data interpretation, or writing the manuscript.

ACKNOWLEDGMENTS

We appreciate Dr. Xiaoxuan Zheng from Hubei Maternal and Child Health Hospital for help with the statistical analysis for the revised submission. We are particularly grateful to all the pediatricians, nurses who participated in patient recruitment and data collection at Hubei Maternal and Child Health Hospital.

REFERENCES

1. Marlow N, Hennessy EM, Bracewell MA, Wolke D. EPICure Study Group. Motor and executive function at 6 years of age after extremely preterm birth. *Pediatrics*. (2007) 120:793–804. doi: 10.1542/peds.2007-0440
2. Sammallahti S, Pyhälä R, Lahti M, Lahti J, Pesonen AK, Heinonen K, et al. Infant growth after preterm birth and neurocognitive abilities in young adulthood. *J Pediatr*. (2014) 165:1109–15.e3. doi: 10.1016/j.jpeds.2014.08.028
3. Wood N, Costeloe K, Gibson A, Hennessy E, Marlow N, Wilkinson A. The EPICure study: associations and antecedents of neurological and developmental disability at 30 months of age following extremely preterm birth. *Arch Dis Child Fetal Neonatal Ed*. (2005) 90:F134–40. doi: 10.1136/adc.2004.052407
4. Vohr BR, Wright LL, Dusick AM, Mele L, Verter J, Steichen JJ, et al. Neurodevelopmental and functional outcomes of extremely low birth weight infants in the national institute of child health and human development neonatal research network, 1993-1994. *Pediatrics*. (2000) 105:1216–26. doi: 10.1542/peds.105.6.1216
5. Saugstad OD. Hypoxanthine as an indicator of hypoxia: its role in health and disease through free radical production. *Pediatr Res*. (1988) 23:143–50. doi: 10.1203/00006450-198802000-00001
6. Pierrat V, Haouari N, Liska A, Thomas D, Subtil D, Truffert P, et al. Prevalence, causes, and outcome at 2 years of age of newborn encephalopathy: population based study. *Arch Dis Child Fetal Neonatal Ed*. (2005) 90:F257–61. doi: 10.1136/adc.2003.047985
7. Karmel BZ, Gardner JM, Zappulla RA, Magnano CL, Brown EG. Brain-stem auditory evoked responses as indicators of early brain insult. *Electroencephalogr Clin Neurophysiol*. (1988) 71:429–42. doi: 10.1016/0168-5597(88)90047-0
8. Bao X, Wong V. Brainstem auditory-evoked potential evaluation in children with meningitis. *Pediatr Neurol*. (1998) 19:109–12. doi: 10.1016/S0887-8994(98)00032-0
9. Judith MG, Bernard ZK, Robert LF. Neonatal brainstem function and 4-month arousal-modulated. *Attention Are Jointly Associated With Autism Autism Res*. (2013) 6:11–22. doi: 10.1002/aur.1259
10. Miron O, Roth D-A, Gabis LV, Henkin Y, Shefer S, Dinstein I. Prolonged auditory brainstem responses in infants with autism. *Autism Res*. (2016) 9:689–95. doi: 10.1002/aur.1561
11. Bayley N. *Bayley Scales of Infant Development*. 2nd ed. San Antonio, TX: The Psychological Corporation (1993).
12. Yi YG, Sung IY, Yuk JS. Comparison of second and third editions of the Bayley scales in children with suspected developmental delay. *Ann Rehabil Med*. (2018) 42:313–20. doi: 10.5535/arm.2018.42.2.313
13. Lindsey JC, Brouwers P. Intrapolation and extrapolation of age-equivalent scores for the Bayley II: a comparison of two methods of estimation. *Clin Neuropharmacol*. (1999) 22:44–53. doi: 10.1097/00002826-199901000-00009
14. Sattler JM, Dumont R. *Assessment of Children*. San Diego, CA: Jerome M. Sattler (1992).
15. Bayley N. *Bayley Scales of Infant and Toddler Development 3rd Edition (Bayley-III)*. San Antonio, TX: The Psychological Corporation (2006). doi: 10.1037/t14978-000
16. Luttikhuizen dos Santos ES, de Kieviet JF, Konigs M, van Elburg RM, and Oosterlaan J. Predictive value of the Bayley scales of infant development on development of very preterm/very low birth weight children: a meta-analysis. *Early Hum Dev*. (2013) 89:487–96. doi: 10.1016/j.earlhumdev.2013.03.008
17. Kopp CB, Vaughn BE. Sustained attention during exploratory manipulation as a predictor of cognitive competence in preterm infants. *Child Develop*. (1982) 53:174–82. doi: 10.2307/1129650
18. McLoyd V. Socioeconomic disadvantage and child development. *Am Psychol*. (1998) 53:185–204. doi: 10.1037/0003-066X.53.2.185
19. Magnuson KA, Sexton H, Davis-Kean PE, Huston AC. Increases in maternal education and children's language skills at age 3: evidence from the NICHD study. *Merrill Palmer Q*. (2009) 55:319–50. doi: 10.1353/mpq.0.0024
20. Cohen SE, Parmelee AH. Prediction of five-year Stanford-Binet scores in preterm infants. *Child Develop*. (1983) 54:1242–53. doi: 10.2307/1129679
21. Kaufman AS, Wang J. Sex, race, and education differences on the K-BIT at ages 4 to 90 years. *J Psychoeduc Assess*. (1992) 10:219–29. doi: 10.1177/073428299201000302
22. Sellers AH, Burns WJ, Guyrke J. Differences in young children's IQs on the Wechsler Preschool and Primary Scale of Intelligence-Revised as a function of stratification variables. *Appl Neuropsychol*. (2002) 9:65–73. doi: 10.1207/S15324826AN0902_1
23. Roberts E, Bornstein MH, Slater AM, Barrett J. Early cognitive development and parental education. *Infant Child Develop*. (1999) 8:49–62. doi: 10.1002/(SICI)1522-7219(199903)8:1<49::AID-ICD188>3.0.CO;2-1

24. du Prel Carroll X, Yi H, Liang Y, Pang K, Leeper-Woodford S, Riccardi P, et al. Family-environmental factors associated with attention deficit hyperactivity disorder in Chinese children: a case-control study. *PLoS ONE*. (2012) 7:e50543. doi: 10.1371/journal.pone.0050543
25. Brämer GR. International statistical classification of diseases and related health problems. *Tenth Revision World Health Stat Q*. (1988) 41:32–6.
26. Jiang ZD. Long-term effect of perinatal and postnatal asphyxia on developing human auditory brainstem responses: peripheral hearing loss. *Int J Pediatr Otorhinolaryngol*. (1995) 33:225–38. doi: 10.1016/0165-5876(95)01213-3
27. Jiang ZD, Liu XY, Shi BP, Lin L, Bu CF, Wilkinson AR. Brainstem auditory outcomes and correlation with neurodevelopment after perinatal asphyxia. *Pediatr Neurol*. (2008) 39:189–95. doi: 10.1016/j.pediatrneurol.2008.06.013
28. Jiang ZD, Chen C. Short-term outcome of functional integrity of the auditory brainstem in term infants who suffer perinatal asphyxia. *J Neurol Sci*. (2017) 376:219–24. doi: 10.1016/j.jns.2017.03.036
29. Martínez-Cruz CF, Poblano A, Fernández-Carrocera LA. Risk factors associated with sensorineural hearing loss in infants at the neonatal intensive care unit: 15-year experience at the National Institute of Perinatology (Mexico City). *Arch Med Res*. (2008) 39:686–94. doi: 10.1016/j.arcmed.2008.06.004
30. American Academy of Pediatrics, Joint Committee on Infant Hearing. Year 2007 position statement: principles and guidelines for early hearing detection and intervention programs. *Pediatrics*. (2007) 120:898–921. doi: 10.1542/peds.2007-2333
31. Rose O, Blanco E, Martinez SM, Sim EK, Castillo M. Developmental scores at 1 year with increasing gestational age, 37–41 weeks. *Pediatrics*. (2013) 131:e1475. doi: 10.1542/peds.2012-3215
32. Assari S, Caldwell CH. Teacher discrimination reduces school performance of African American youth: role of gender. *Brain Sci.*. (2018) 8:183. doi: 10.3390/brainsci8100183
33. Anderson P, Doyle LW. Victorian infant collaborative study group. Neurobehavioral outcomes of school-age children born extremely low birth weight or very preterm in the 1990s. *JAMA*. (2003) 289:3264–72. doi: 10.1001/jama.289.24.3264
34. Zhang L, Jiang ZD. Development of the brainstem auditory pathway in low birthweight and perinatally asphyxiated children with neurological sequelae. *Early Hum Dev*. (1992) 30:61–73.
35. Messinger D, Lambert B, Bauer CR, Bann CM, Kasey Hamlin-Smith K, Abhik Das A. The relationship between behavior ratings and concurrent and subsequent mental and motor performance in toddlers born at extremely low birth weight. *J Early Interv*. (2010) 32:214–33. doi: 10.1177/1053815110380917
36. Moore T, Johnson S, Haider S, Hennessy E, Marlow N. Relationship between test scores using the second and third editions of the bayley scales in extremely preterm children. *J Pediatr*. (2012) 160:553–8. doi: 10.1016/j.jpeds.2011.09.047
37. Lowe JR, Erickson SJ, Schrader R, Duncan AF. Comparison of the Bayley II mental developmental index and the Bayley III cognitive scale: are we measuring the same thing? *Acta Paediatr*. (2012) 101:e55–8. doi: 10.1111/j.1651-2227.2011.02517.x
38. Bos AF. Bayley-II or Bayley-III: what do the scores tell us? *Dev Med Child Neurol*. (2013) 55:978–9. doi: 10.1111/dmcn.12234
39. Vohr BR, Stephens BE, Higgins RD, Bann CM, Hintz SR, Das A, et al. Are outcomes of extremely preterm infants improving? Impact of bayley assessment on outcomes. *J Pediatr*. (2012) 161:222–8.e3. doi: 10.1016/j.jpeds.2012.01.057
40. Huggard D, Slevin M, Vavasseur C. Neurodevelopmental outcome of preterm babies of 1999-2009. *Ir Med J*. (2014) 107:166–8.
41. Barkovich AJ, Hajnal BL, Vigneron D, Sola A, Partridge JC, Allen F, et al. Prediction of neuromotor outcome in perinatal asphyxia: evaluation of MR scoring systems. *AJNR Am J Neuroradiol*. (1998) 19:143–9.
42. Miller SP, Ramaswamy V, Michelson D, Barkovich AJ, Holshouser B, Wycliffe N, et al. Patterns of brain injury in term neonatal encephalopathy. *J Pediatr*. (2005) 146:453–60. doi: 10.1016/j.jpeds.2004.12.026
43. Lowe J, Woodward B, Papile LA. Emotional regulation and its impact on development in extremely low birth weight infants. *J Dev Behav Pediatr*. (2005) 26:209–13. doi: 10.1097/00004703-200506000-00008
44. Lowe J, Erickson SJ, Maclean P. Cognitive correlates in toddlers born very low birth weight and full-term. *Infant Behav Dev*. (2010) 33:629–34. doi: 10.1016/j.infbeh.2010.07.016
45. Stoll BJ, Hansen NI, Bell EF, Shankaran S, Laptook AR, Walsh MC, et al. Neonatal outcomes of extremely preterm infants from the NICHD Neonatal Research Network. *Pediatrics*. (2010) 126:443–56. doi: 10.1542/peds.2009-2959
46. Galicia-Connolly E, Shamseer L, Vohra S. Complementary, holistic, and integrative medicine: therapies for neurodevelopment in preterm infants. *Pediatr Rev*. (2012) 33:276–8. doi: 10.1542/pir.33-6-276
47. Natsume J, Watanabe K, KuniyoshiKuno K, Hayakawa F, Hashizume Y. Clinical, neurophysiologic, and neuropathological features of an infant with brain damage of total asphyxia type (Myers). *Pediatr Neurol*. (1995) 13:61–4. doi: 10.1016/0887-8994(95)00054-J
48. Pasternak JF, Predey TA, Mikhael MA. Neonatal asphyxia: vulnerability of basal ganglia, thalamus, and brainstem. *Pediatr Neurol*. (1991) 7:147–9. doi: 10.1016/0887-8994(91)90014-C
49. Chatoor I, Surles J, Ganiban J, Beker L, McWade Paez L, Kerzner B. Failure to thrive and cognitive development in toddlers with infantile anorexia. *Pediatrics*. (2004) 113:e440–7. doi: 10.1542/peds.113.5.e440
50. Lauritzen L, Brambilla P, Mazzocchi A, Harsløf LB, Ciappolino V, Agostoni C. DHA effects in brain development and function. *Nutrients*. (2016) 8:6. doi: 10.3390/nu8010006
51. Innis SM. Dietary (n-3) fatty acids and brain development. *J Nutr*. (2007) 137:855–9. doi: 10.1093/jn/137.4.855
52. Ross GS, Foran LM, Barbot B, Sossin KM, Perlman JM. Using cluster analysis to provide new insights into development of very low birthweight (VLBW) premature infants. *Early Hum Dev*. (2016) 92:45–9. doi: 10.1016/j.earlhumdev.2015.11.005
53. Goodwin LK, Iannacchione MA, Hammond WE, Crockett P, Maher S, Schlitz K. Data mining methods find demographic predictors of preterm birth. *Nurs Res*. (2001) 50:340–5. doi: 10.1097/00006199-200111000-00003

Conflict of Interest: The authors declare that the research was conducted in the absence of any commercial or financial relationships that could be construed as a potential conflict of interest.

frontiers in Pediatrics

CLINICAL TRIAL
published: 09 October 2020
doi: 10.3389/fped.2020.517207

Randomized Control Trial of Postnatal rhIGF-1/rhIGFBP-3 Replacement in Preterm Infants: *Post-hoc* Analysis of Its Effect on Brain Injury

Sandra Horsch[1,2], Alessandro Parodi[3], Boubou Hallberg[2], Mariya Malova[3], Isabella M. Björkman-Burtscher[4,5], Ingrid Hansen-Pupp[6], Neil Marlow[7], Kathryn Beardsall[8], David Dunger[8], Mirjam van Weissenbruch[9], Lois E. H. Smith[10], Mohamed Hamdani[11], Alexandra Mangili[12], Norman Barton[11], Luca A. Ramenghi[3,13], Ann Hellström[14], David Ley[6] and the ROPP-2008-01 Study Team*

[1] HELIOS Klinikum Berlin-Buch, Berlin, Germany, [2] Department of Clinical Science, Intervention and Technology (CLINTEC), Karolinska Institutet, Stockholm, Sweden, [3] Neonatal Intensive Care Unit, Department Mother and Child, IRCCS (Istituto di Ricovero e Cura a Carattere Scientifico) Istituto Giannina Gaslini, Genoa, Italy, [4] Department of Clinical Sciences Lund, Radiology, Skåne University Hospital, Lund University, Lund, Sweden, [5] Clinical Sciences, Radiology, Sahlgrenska Academy, Gothenburg University, Gothenburg, Sweden, [6] Department of Clinical Sciences Lund, Pediatrics, Skåne University Hospital, Lund University, Lund, Sweden, [7] Department of Academic Neonatology, UCL Elizabeth Garrett Anderson Institute for Women's Health, University College London, London, United Kingdom, [8] Department of Paediatrics, University of Cambridge, Cambridge, United Kingdom, [9] Department of Pediatrics, Division of Neonatology, Vrije Universiteit University Medical Center, Amsterdam UMC, Amsterdam, Netherlands, [10] Harvard Medical School, Boston Children's Hospital, Boston, MA, United States, [11] Global Clinical Development, Rare Metabolic Diseases, Shire, a Takeda Company, Lexington, MA, United States, [12] Global Clinical Development, Rare Metabolic Diseases, Shire, a Takeda Company, Zurich, Switzerland, [13] Department of Neurosciences, Rehabilitation, Ophthalmology, Genetics, Maternal and Child Health (DINOGMI), University of Genoa, Genoa, Italy, [14] Institute of Neuroscience and Physiology, Sahlgrenska Academy, Gothenburg, Sweden

OPEN ACCESS

Edited by:
Changlian Zhu,
Third Affiliated Hospital of Zhengzhou University, China

Reviewed by:
Sanjeet K. Panda,
Texas Tech University Health Sciences Center El Paso, United States
Ömer Erdeve,
Ankara University, Turkey

***Correspondence:**
Sandra Horsch
s.horsch@gmx.de

Specialty section:
This article was submitted to Neonatology, a section of the journal Frontiers in Pediatrics

Received: *06 December 2019*
Accepted: *01 September 2020*
Published: *09 October 2020*

Citation:
Horsch S, Parodi A, Hallberg B, Malova M, Björkman-Burtscher IM, Hansen-Pupp I, Marlow N, Beardsall K, Dunger D, van Weissenbruch M, Smith LEH, Hamdani M, Mangili A, Barton N, Ramenghi LA, Hellström A, Ley D and the ROPP-2008-01 Study Team (2020) Randomized Control Trial of Postnatal rhIGF-1/rhIGFBP-3 Replacement in Preterm Infants: Post-hoc Analysis of Its Effect on Brain Injury. Front. Pediatr. 8:517207. doi: 10.3389/fped.2020.517207

Background: Postnatal insulin-like growth factor-1 (IGF-1) replacement with recombinant human (rh)IGF-1 and IGF binding protein-3 (rhIGF-1/rhIGFBP-3) is being studied as a potential treatment to reduce comorbidities of prematurity. We have recently reported on a phase II, multicenter, randomized, controlled trial comparing postnatal rhIGF-1/rhIGFBP-3 replacement with standard of care (SOC) in extremely preterm infants (NCT01096784). Maximum severity of retinopathy of prematurity was the primary endpoint of the trial and presence of GMH-IVH/PHI one of the pre-specified secondary endpoints. Infants therefore received serial cranial ultrasound scans (CUS) between birth and term age. In this *post-hoc* analysis we present a detailed analysis of the CUS data of this trial and evaluate the effect of postnatal rhIGF-1/rhIGFBP-3 replacement on the incidence of different kinds of brain injury in extremely preterm infants.

Methods: This report is an exploratory *post-hoc* analysis of a phase II trial in which infants <28 weeks gestational age were randomly allocated to rhIGF-1/rhIGFBP-3 or SOC. Serial cranial ultrasounds were performed between birth and term-equivalent age. Presence of germinal matrix hemorrhage and intraventricular hemorrhage (GMH-IVH), periventricular hemorrhagic infarction (PHI), post-hemorrhagic ventricular dilatation, and white matter injury (WMI) were scored by two independent masked readers.

Results: The analysis included 117 infants; 58 received rhIGF-1/rhIGFBP-3 and 59 received SOC. A trend toward less grade II–III GMH-IVH and PHI was observed in treated

infants vs. SOC. A subanalysis of infants without evidence of GMH-IVH at study entry (n = 104) showed reduced progression to GMH-IVH in treated infants (25.0% [13/52] vs. 40.4% [21/52]; not significant). No effects of rhIGF-1/rhIGFBP-3 on WMI were observed.

Conclusion: The potential protective effect of rhIGF-1/rhIGFBP-3 on the occurrence of GMH-IVH/PHI appeared most pronounced in infants with no evidence of GMH-IVH at treatment start.

Keywords: neonate, brain injury, cerebral hemorrhage, recombinant human IGF-1, extremely preterm

INTRODUCTION

Despite advances in neonatal care and the widespread use of antenatal steroids, prematurity-related brain injuries such as germinal matrix hemorrhage and intraventricular hemorrhage (GMH-IVH), periventricular hemorrhagic infarction (PHI), post-hemorrhagic ventricular dilatation (PHVD), and white matter injury (WMI) remain common in extremely preterm infants (1–3). These events are highly related to short- and long-term adverse neurodevelopmental outcomes (4–6). It is therefore important to evaluate novel strategies to prevent brain injury in these vulnerable infants.

Postnatal levels of insulin-like growth factor-1 (IGF-1) in extremely premature infants are lower than intrauterine levels at a corresponding gestational age (GA) (7). IGF-1 is a major fetal growth factor involved in a number of processes that include metabolism, growth, and differentiation (8). Postnatal IGF-1 replacement with a complex of recombinant human (rh)IGF-1 and IGF binding protein-3 (rhIGF-1/rhIGFBP-3) is being studied as a potential treatment to reduce comorbidities associated with premature birth. A phase II, multicenter, randomized, controlled trial recently compared postnatal rhIGF-1/rhIGFBP-3 replacement with standard of care (SOC) in extremely preterm infants (NCT01096784) (9). The maximum severity of retinopathy of prematurity was the primary endpoint of the trial and presence of GMH-IVH detected by cranial ultrasound scans (CUS) was a pre-specified secondary endpoint. Results of that trial showed a trend toward reduction in IVH favoring active treatment. The study was not powered for a reduction in IVH and some study infants already had evidence of GMH-IVH at study entry, which also may have influenced the results. The reason that some study infants had evidence of GMH-IVH at study entry is because the baseline scan was read locally to allow enrollment decisions within the first 24 h after birth. The effect of postnatal IGF-1 replacement on incidence of PHVD and WMI detected by CUS has not yet been reported.

We conducted *post-hoc* analyses of data from that trial to clarify the findings relative to GMH-IVH, and to further evaluate the effect of postnatal rhIGF-1/rhIGFBP-3 replacement on the incidence of prematurity-related brain injury (GMH-IVH, PHI, PHVD, and WMI), as assessed by CUS.

METHODS

Study Design and Patient Population

The methods, study design, and results from the primary analyses of the phase II study were reported previously (9). In brief, this was a multicenter, randomized, SOC concurrent control, assessor-masked study of rhIGF-1/rhIGFBP-3 (mecasermin rinfabate, 50 μg/ml solution) in extremely preterm infants (ClinicalTrials.gov, NCT01096784). Eligible infants had a GA at birth ranging from 23 weeks + 0 days to 27 weeks + 6 days. Exclusion criteria included detectable gross malformation, known or suspected chromosomal abnormality, clinically significant neurological disease, GMH-IVH grade II or III, or PHI (infants with grade I GMH-IVH were included). Infants in the active treatment group received a standardized dosage of 250 μg/kg per day of rhIGF-1/rhIGFBP-3 via continuous intravenous infusion in addition to SOC from ≤24 h of birth until a post-menstrual age (PMA) of 29 weeks + 6 days. Infants in the control group received SOC based on their individual medical needs and according to local protocols. The primary endpoint of the phase II study was maximum severity of retinopathy of prematurity (ROP). Secondary endpoints included IVH, time to discharge from neonatal care, bronchopulmonary dysplasia, and growth parameters (9). A *post-hoc* analysis was conducted to further explore the phase II study findings relative to IVH.

Written informed consent was provided by all infants' parents/guardians. The study was reviewed/approved by all relevant institutional review boards/independent ethics committees of all participating centers.

Detection and Assessment of Brain Injury on CUS

As part of the phase II trial, CUS examinations were performed to detect and assess cerebral hemorrhage at study entry (day 0); at postnatal days 3, 7, 14, and 21 (±1 day); and at PMA of 40 weeks (± 4 days). As initially reported, a single reader (masked to treatment) evaluated all ultrasound images for the highest grade of GMH-IVH, according to Papile and Bowerman methods (10, 11). No IVH and grade I IVH were grouped together. As a *post-hoc* follow up, CUS was re-examined for GMH-IVH and PHI for each scan by two independent readers, who were masked to treatment allocation. In addition, CUS images were analyzed for the presence of PHVD and WMI. GMH-IVH was graded according to Volpe (12); PHI was graded

TABLE 1 | Cranial ultrasound image grading systems.

GMH-IVH graded according to Volpe method (12)	
Severity	**Description**
Grade I	GMH with no or minimal IVH (<10% of ventricular area on parasagittal view)
Grade II	IVH in 10–50% of ventricular area on parasagittal view
Grade III	IVH in >50% of ventricular area on parasagittal view; usually distends lateral ventricle
Grade IV (IVH and PHI)	IVH compounded by hemorrhagic venous infarction in the periventricular white matter
PHI graded according to Dudink method (13)	
Localization	Caudate vein infarct
	Temporal vein infarct
	Anterior terminal vein infarct
	Complete terminal vein infarct
Severity	**Description**
Limited PHI	Only caudate vein or temporal vein affected; small anterior terminal vein infarction
Extensive PHI	Complete terminal vein infarction or combination of caudate vein, temporal vein, anterior vein infarctions
PHVD graded according to Davies method (14)	
Severity	**Description**
0	Normal, AHW <3 mm
1	Mild, AHW 3 to <5 mm
2	Moderate AHW 5–10 mm
3	Severe AHW >10 mm
White matter injury	
Schematic description	
•	Persistent periventricular hyperechogenicity, no cysts, no obvious white matter loss (white matter loss was identified as ventricular dilatation without hemorrhage)
•	Persistent periventricular hyperechogenicity evolving into diffuse white matter loss, but no cysts
•	Persistent periventricular hyperechogenicity evolving into small localized frontoparietal cystic lesions (limited cystic PVL)
•	Persistent periventricular hyperechogenicity evolving into extensive cystic lesions (extensive cystic PVL)
Scoring[a]	**Description**
0	Persistent periventricular hyperechogenicity or punctate lesions without overt white matter loss, no cysts
1	Persistent periventricular hyperechogenicity or extensive punctate lesions evolving in a white matter loss without cysts
2	Limited cystic PVL
3	Extensive cystic PVL
Brain injury severity score	
0	No brain abnormalities
1	GMH, periventricular hyperechogenicity without white or gray matter loss, and mild-moderate cerebral injury
2	IVH II, mild PHVD, stroke of a perforating artery
3	IVH III, persistent moderate PHVD without shunt or Rickham device, persistent periventricular hyperechogenicities with diffuse white and/or gray matter loss at term cranial ultrasound
4	Limited PHI, limited PVL, PHVD with shunt or Rickham device, anterior cerebral artery stroke, posterior cerebral artery stroke, severe cerebellar injury
5	Unilateral extensive PHI, extensive cystic PVL, mild cerebral artery stroke, severe global brain atrophy[b]
6	Bilateral extensive PHI

AHW, anterior horn width; GMH, germinal matrix hemorrhage; IVH, intraventricular hemorrhage; PHI, periventricular hemorrhagic infarction; PHVD, post-hemorrhagic ventricular dilatation; PVL, periventricular leukomalacia.

*[a]Grade 0 and grade I persistent periventricular hyperechogenicity were combined for presentation in **Figure 1**; grade II and grade III were combined for cystic PVL.*

[b]Severe global brain atrophy defined as a combination of global loss of gray and white matter, delayed cortical folding, and enlarged lateral ventricles and subarachnoid spaces.

by localization and extent of the lesion according to Dudink (13). PHVD was measured by anterior horn width (AHW) according to Davies, and graded as follows: normal, <3 mm; mild, AHW 3 to <5 mm; moderate, AHW 5–10 mm; severe, AHW >10 mm [(14); **Table 1**]. WMI was schematically described according to Govaert and de Vries (15), with presentation as persistent periventricular hyperechogenicity, white matter loss, or cystic periventricular leukomalacia (PVL). White matter loss was identified as ventricular dilatation without hemorrhage on CUS. WMI was scored using a four-grade classification. A seven-grade brain injury severity score was developed by one of the authors (SH) for use in the current study (not previously published). The brain injury severity score utilized a classification system where each grade reflected a greater degree of brain injury (**Table 1**). The brain injury severity score was recorded for each infant at 40 weeks PMA. Information on surgical intervention in infants with PHVD (e.g., shunt, Rickham device) was collected prospectively. Any discrepancy between the two readers was resolved by consensus agreement.

Statistical Analysis

The current study included *post-hoc* analysis of brain injury severity distribution, and a further subanalysis on GMH-IVH progression in those infants without hemorrhage on the baseline CUS. The severity distribution for GMH-IVH analysis included all eligible infants in the phase II study. The distribution of GMH-IVH according to treatment group was determined from the maximum-grade hemorrhage observed for each infant in the study population after randomization. A consensus maximum GMH-IVH grade for each infant was defined based on the highest grade of GMH-IVH observed by joint masked reader review of all scans performed for that infant between day 0 and PMA 40 weeks (even in the event that some scans were missing). In the subanalysis, the preventative effect of treatment with rhIGF-1/rhIGFBP-3 on GMH-IVH was assessed based on the progression of cerebral hemorrhage during the study among

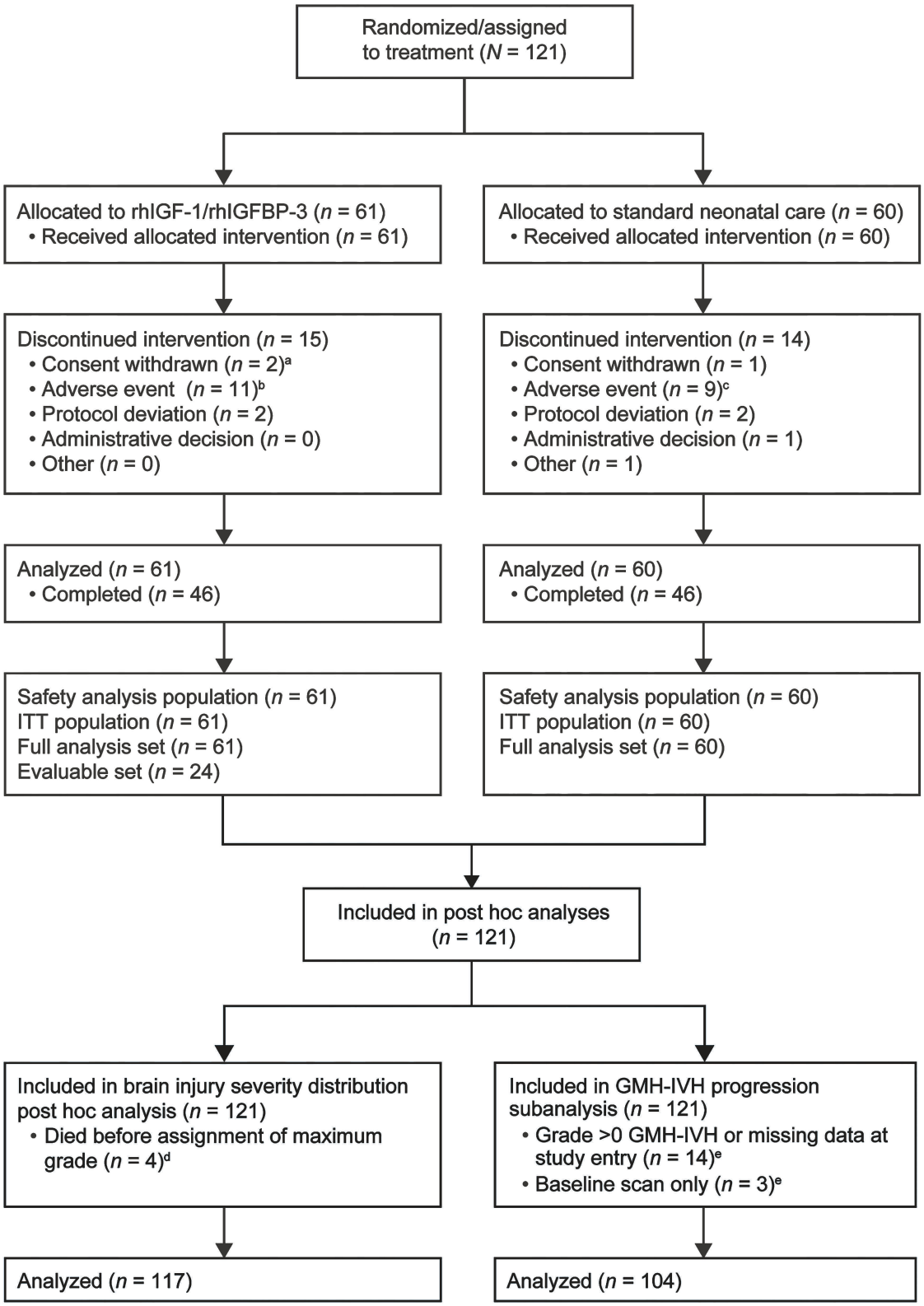

FIGURE 1 | Flowchart of infants included in the phase II study (9), the *post-hoc* analysis, and the subanalysis. GMH-IVH, germinal matrix hemorrhage and intraventricular hemorrhage; rhIGF-1, recombinant human insulin-like growth factor-1; rhIGFBP-3, recombinant human insulin-like growth factor binding protein-3.

(Continued)

FIGURE 1 | [a]One infant had a serious adverse event with fatal outcome, but the primary reason for discontinuation was withdrawal of consent. [b]All infants discontinued due to a serious adverse event with fatal outcome. [c]Seven of nine discontinuations were due to serious adverse events with fatal outcome. [d]For the distribution analysis ($n = 117$), each infant was classified based on the maximum grade of GMH-IVH observed between day 0 and week 40 during a joint masked consensus review of all available scans for that infant; one infant receiving standard of care and three infants receiving rhIGF-1/rhIGFBP-3 died within 72 h of randomization and did not have an assigned maximum grade. [e]The progression analysis ($n = 104$) was based on a comparison of longitudinal scans with the baseline grade 0 scan for each eligible infant; 17 infants were excluded for the progression analysis: grade 0 → missing ($n = 3$); grade I → grade I ($n = 4$); grade I → grade II ($n = 2$); grade II → grade II ($n = 3$); grade II → grade IV ($n = 1$); grade III → grade IV ($n = 1$); grade IV → grade IV ($n = 1$); missing → grade 0 ($n = 1$); missing → grade III ($n = 1$). Reprinted from Ley et al. (9), Copyright 2019, with permission from Elsevier. https://www.sciencedirect.com/science/article/pii/S0022347618315403.

infants with no evidence of GMH-IVH or PHI (classified as grade 0 GMH-IVH) at study entry. Progression to GMH-IVH in infants with no evidence of hemorrhage at baseline was analyzed based on the highest grade identified at any subsequent scan after the baseline scan. The final analysis in the current study included two different subgroups; 117 infants were included in the *post-hoc* analysis for brain injury, and 104 infants were included in the GMH-IVH progression analysis.

The Fisher exact test was performed to test the significance of the difference between the rhIGF-1/rhIGFBP-3 treatment and SOC groups. A $p \leq 0.05$ was regarded as significant. The grade of GMH-IVH (grades I–III) or PHI was summarized descriptively by treatment group and GA strata. Weighted kappa statistics were used to measure interrater agreement between the two readers. No power calculations were performed for comparing GMH-IVH in this *post-hoc* analysis, since it was a secondary endpoint; the trial was only powered for the primary endpoint of maximum severity of retinopathy of prematurity in the primary phase II study.

RESULTS

Brain Injury Severity Distribution Analysis ($n = 117$)

A total of 121 infants were enrolled in the original phase II trial, and details of patient disposition among these infants have been previously reported (9). In the current study, 117 infants were assigned a maximum grade of GMH-IVH and were included in the analysis for presence of brain injury (**Figure 1**). Four infants died within 72 h of randomization and were not assigned a maximum grade. The cause of death was respiratory failure in each circumstance; baseline CUS revealed no evidence of hemorrhage. Fifty-eight of 117 infants received rhIGF-1/rhIGFBP-3 and 59 received SOC. Thirty-two of 58 (55.2%) treated infants and 31 of 59 (52.5%) control infants were born before 26 weeks GA (**Table 2**).

TABLE 2 | Demographic characteristics and maternal/perinatal histories of infants included in the *post-hoc* analysis ($n = 117$).

Characteristic	Standard of care ($n = 59$)	rhIGF-1/rhIGFBP-3 ($n = 58$)
Sex, *n* (%)		
Male	38 (64.4)	38 (65.5)
Female	21 (35.6)	20 (34.5)
GA group, *n* (%)		
<26 weeks	31 (52.5)	32 (55.2)
≥26 weeks	28 (47.5)	26 (44.8)
GA (weeks)		
Mean (SD)	25 (1)	26 (1)
Weight at birth (g)		
Mean (SD)	803 (175)	782 (186)
Race, *n* (%)		
Asian	5 (8.5)	4 (6.9)
Black or African American	9 (15.3)	4 (6.9)
White	41 (69.5)	47 (81.0)
Other	4 (6.8)	3 (5.2)
Mode of delivery, *n* (%)		
Vaginal	27 (45.8)	24 (41.4)
Cesarean section	32 (54.2)	34 (58.6)
Maternal infections, *n* (%)	14 (23.7)	10 (17.2)
Clinical chorioamnionitis, *n* (%)	6 (10.2)	9 (15.5)
Maternal antibiotics, *n* (%)	38 (64.4)	29 (50.0)
Antenatal steroids, *n* (%)	59 (100)	58 (100.0)
Fertility therapy, *n* (%)	8 (13.6)	8 (13.8)
In vitro fertilization	6 (10.2)	8 (13.8)
Ovulation stimulation	2 (3.4)	0
Preterm labor, *n* (%)	52 (88.1)	47 (81.0)
Preterm premature rupture of membranes, *n* (%)	20 (33.9)	16 (27.6)
Preeclampsia, *n* (%)	5 (8.5)	7 (12.1)
Apgar score at 5 min		
Median (range)	7.0 (2.0–10.0)	8.0 (1.0–10.0)

GA, gestational age; rhIGF-1, recombinant human insulin-like growth factor-1; rhIGFBP-3, recombinant human insulin-like growth factor binding protein-3; SD, standard deviation.

GMH-IVH or PHI

A smaller proportion of treated infants had grade II–III GMH-IVH or PHI, compared with control infants; the differences were not statistically significant (**Figure 2**). Across all GAs, a higher frequency of grade II–III GMH-IVH or PHI was observed among infants receiving SOC vs. rhIGF-1/rhIGFBP-3 (**Figure 3**). Among infants <25 weeks GA, a smaller proportion of rhIGF-1/rhIGFBP-3–treated infants had grade II–III GMH-IVH or PHI compared with controls (15.0% [$n = 3/20$] vs. 36.4% [$n = 8/22$], respectively; not statistically significant).

PHVD and WMI

Overall, the proportion of infants with PHVD was lower among treated infants vs. controls (not statistically significant; **Figure 2**). Mild PHVD (AHW 3–5 mm) occurred in 1.7% ($n = 1/58$) of infants in the treated group and 15.3% ($n = 9/59$) in the SOC group. Moderate PHVD (AHW 5–10 mm) occurred in 8.6%

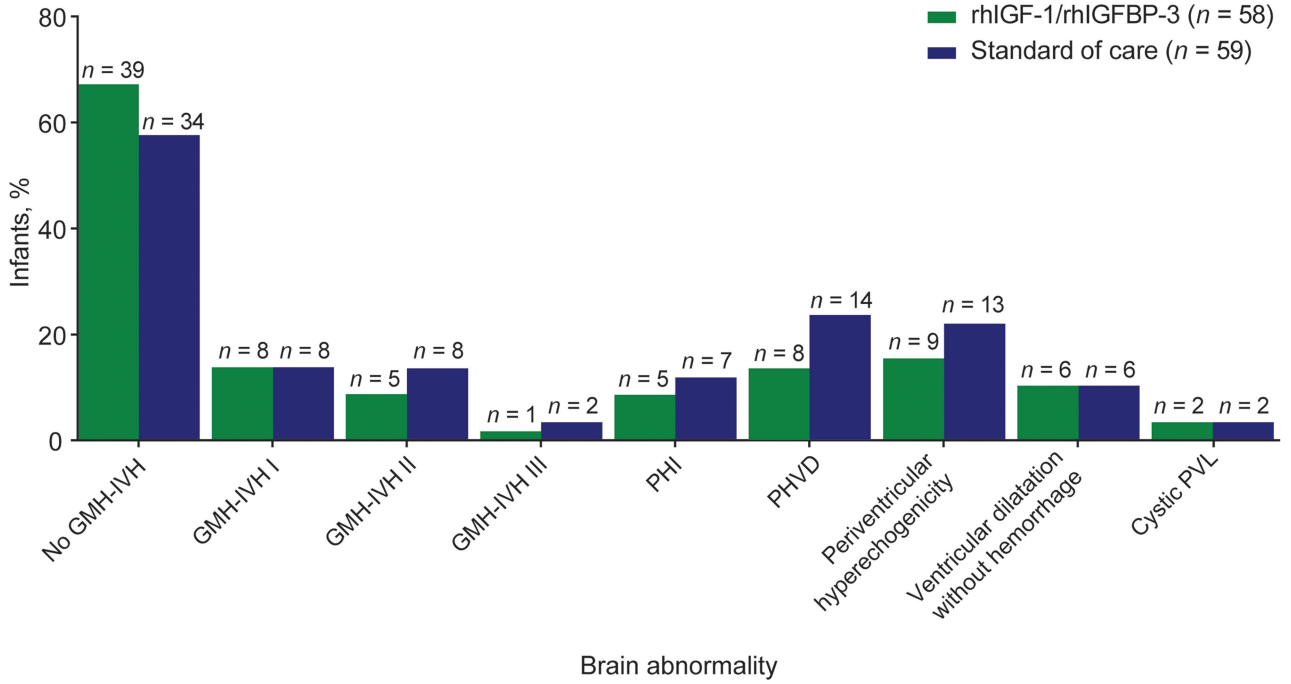

FIGURE 2 | Distribution of brain abnormalities among extremely preterm infants receiving rhIGF-1/rhIGFBP-3 or standard of care.[a] GMH-IVH, germinal matrix hemorrhage and intraventricular hemorrhage; PHI, periventricular hemorrhagic infarction; PHVD, post-hemorrhagic ventricular dilatation; PVL, periventricular leukomalacia; rhIGF-1, recombinant human insulin-like growth factor-1; rhIGFBP-3, recombinant human insulin-like growth factor binding protein-3. [a]Based on the maximum-grade hemorrhage for each infant observed in cranial ultrasound on study days 0, 3, 7, 14, and 21, and at 40 weeks post-menstrual age.

($n = 5/58$) in the treated group and 6.8% ($n = 4/59$) in the SOC group. Severe PHVD (AHW >10 mm) was low in both the treated and SOC groups: 3.4% ($n = 2/58$) vs. 1.7% ($n = 1/59$), respectively (these findings were not statistically significant). A smaller proportion of infants in the rhIGF-1/rhIGFBP-3 group had periventricular hyperechogenicity than among controls: 15.5% ($n = 9/58$) vs. 22% ($n = 13/59$), respectively (not statistically significant; **Figure 2**). The proportion of treated vs. control infants with ventricular dilatation without hemorrhage (mild and moderate) was equal (10.3% [$n = 6/58$] vs. 10.2% [$n = 6/59$], respectively). No infants had severe dilatation without hemorrhage. The proportion of treated vs. control infants with cystic PVL (limited and extensive) was equal (3.4% [$n = 2/58$] vs. 3.4% [$n = 2/59$], respectively).

Brain Injury Score

Compared with control infants, a higher proportion of infants in the rhIGF-1/rhIGFBP-3 group had a brain injury severity score of 0 (53.4 % [$n = 31/58$] vs. 42.4% [$n = 25/59$], respectively; **Figure 4**). The proportion of infants with a severity score ≥3 was slightly higher among treated infants (25.9% [$n = 15/58$]) than control infants (22.0% [$n = 13/59$]). These differences were not statistically significant.

Overall, findings from the brain injury severity distribution analysis among 117 infants showed no significant effect on brain injury among treated infants vs. infants receiving SOC.

Subanalysis on the Preventative Effect of rhIGF-1/rhIGFBP-3 on GMH-IVH ($n = 104$)

Of the total phase II study population ($n = 121$), 107 infants had no evidence of GMH-IVH on CUS at study entry (14 infants had evidence of GMH-IVH grade >0 or missing data at study entry). Three infants had a baseline scan only and were excluded from the subanalysis. One infant, excluded from the distribution analysis due to lack of assignment of maximum grade owing to poor quality of day 3 CUS, was included in the progression analysis. A total of 104 infants were, therefore, included in the subanalysis of GMH-IVH progression (**Figure 1**). Of these infants with no GMH-IVH at study entry, 70 remained hemorrhage free over the course of the study (39 infants in the rhIGF-1/rhIGFBP-3 group; 31 in the SOC group), while 34 developed GMH-IVH (13 in the rhIGF-1/rhIGFBP-3 group; 21 in the SOC group; **Table 3**).

Among infants in the SOC group whose mothers had infections, a significantly higher proportion developed GMH-IVH than remained GMH-IVH free (38.1% [$n = 8/21$] vs. 12.9% [$n = 4/31$], respectively; $p = 0.05$). The difference in the proportion of treated infants with maternal infections who developed hemorrhages or remained hemorrhage free was not statistically significant. A higher frequency of clinical chorioamnionitis and maternal antibiotic use was observed among infants who developed IVH/PHI in both the SOC and rhIGF-1/rhIGFBP-3 treatment groups, compared with infants

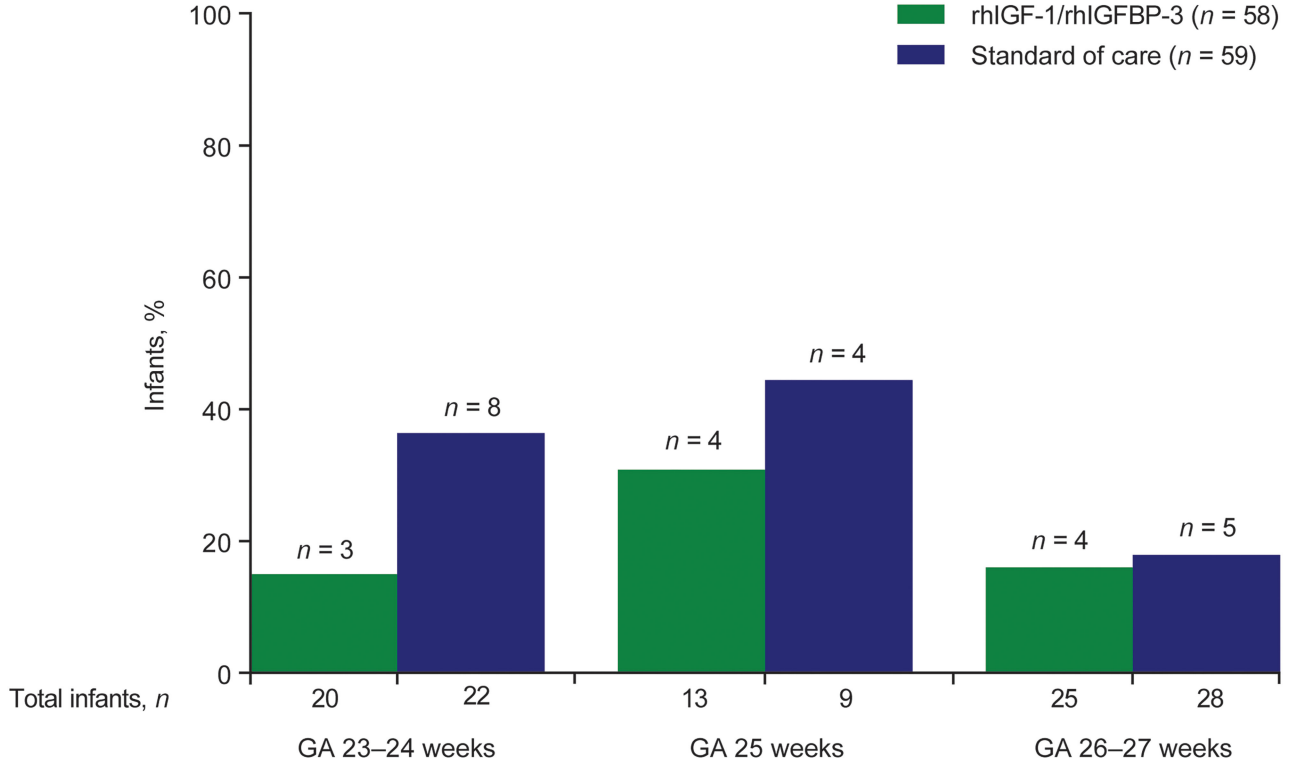

FIGURE 3 | Distribution of GMH-IVH grade II–III or PHI among infants assigned a maximum grade ($n = 117$), by treatment group and gestational age. GA, gestational age; GMH-IVH, germinal matrix hemorrhage and intraventricular hemorrhage; PHI, periventricular hemorrhagic infarction; rhIGF-1, recombinant human insulin-like growth factor-1; rhIGFBP-3, recombinant human insulin-like growth factor binding protein-3.

who remained hemorrhage free (not statistically significant; **Table 3**).

GMH-IVH Progression

Among 104 infants who had no evidence of GMH-IVH on CUS at study entry, there was a trend toward less progression to GMH-IVH grade I–III or PHI among treated infants compared with SOC (25.0% [$n = 13/52$] vs. 40.4% [$n = 21/52$], respectively; $p = 0.14$; percentage risk difference, −15.4%; confidence interval [CI], −34.6 to 4.8%; **Figure 5**).

DISCUSSION

To our knowledge, this is the first multicenter, randomized, controlled trial to evaluate the effect of postnatal rhIGF-1/rhIGFBP-3 replacement on brain injury in extremely preterm infants, as assessed by serial CUS. Among the full population in the current study ($n = 117$), we observed a lower prevalence of grade II–III GMH-IVH and PHI in infants receiving rhIGF-1/rhIGFBP-3 vs. infants receiving SOC. The prevalence of grade I GMH-IVH and WMI (cystic PVL and white matter loss) was broadly comparable between groups.

Post-hoc analysis of the serial CUS imaging data from the phase II trial (9) by two independent central readers revealed that 12 infants (6 in the treatment group, 6 in the control group) had pre-existing GMH-IVH before treatment with rhIGF-1/rhIGFBP-3 commenced, which may have attenuated the observed protective effect of rhIGF-1/rhIGFBP-3 replacement on the occurrence of GMH-IVH. Therefore, we performed a further exploratory *post-hoc* analysis, including a subcohort of infants without pre-existing GMH-IVH ($n = 104$), in order to study the potentially preventive effect of rhIGF-1/rhIGFBP-3 replacement. In this subcohort, 25.0% in the treatment group vs. 40.4% in the SOC group developed GMH-IVH or PHI. Although not statistically significant, we believe that the potentially beneficial effect of rhIGF-1/rhIGFBP-3 replacement in preventing GMH-IVH is more pronounced in the *post-hoc* analysis than we were able to demonstrate in the clinical trial. No power calculations were performed for comparing GMH-IVH (the study was powered for the retinopathy of prematurity endpoint in the primary study only). Dose-response characteristics for this potentially beneficial effect will be further explored in a larger clinical trial that is currently underway (EudraCT number: 2018-001393-16). If the protective effect of rhIGF-1/rhIGFBP-3 can be confirmed in a larger cohort of preterm infants, early administration of the drug may be beneficial to reduce GMH-IVH occurrence.

While severe GMH-IVH (grade III and PHI) is commonly used as an outcome parameter in clinical trials, low-grade GMH-IVH (i.e., grade I and II) is not always considered a

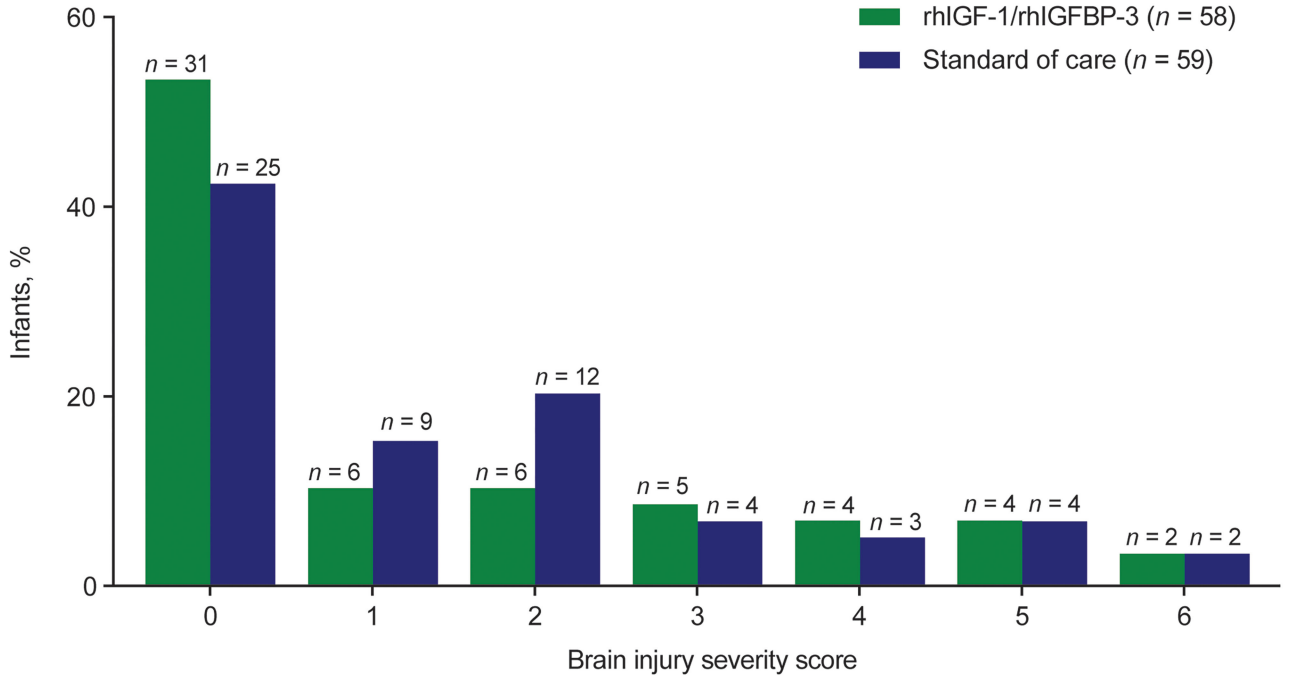

FIGURE 4 | Brain injury severity score among infants assigned a maximum grade ($n = 117$), by treatment group. rhIGF-1 recombinant human insulin-like growth factor-1, rhIGFBP-3 recombinant human insulin-like growth factor binding protein-3.

relevant neonatal morbidity. Indeed, it has become customary to inform parents that an uncomplicated, limited GMH-IVH has no relevance in relation to long-term outcomes. However, recent data have associated low-grade hemorrhage with neurodevelopmental impairment in preterm infants (16). A meta-analysis by Mukerji et al. found an increased risk for moderate to severe neurodevelopmental impairment at 18–24 months (adjusted odds ratio, 1.39; 95% CI, 1.09–1.77) in infants with mild (grade I and/or II) periventricular/intraventricular hemorrhage compared with infants without hemorrhage (17). Even though the meta-analysis was based on a limited amount of data, low-grade GMH-IVH might in the future need to be taken into account when considering clinical outcome.

The exact neurobiological basis of the adverse effect of uncomplicated low-grade GMH-IVH on neurodevelopmental outcome still needs to be elucidated, but it is likely multifactorial, and there are several pathogenetic mechanisms that have been related to the observed brain injury after low-grade GMH-IVH. The destruction of the germinal matrix itself may result in a relevant loss of glial precursor cells, leading to impaired myelination, and cortical development (18, 19). Low-grade GMH-IVH can be followed by abnormal microstructural alterations in periventricular and subcortical white matter (20). Even limited amounts of intraventricular blood can further trigger inflammation in adjacent white matter through activated microglia, passage of red blood cells, and red blood cell degradation; the resulting perilesional tissue injury may be secondary to free radical release and the presence of free iron (21–24). In this context, we believe it is important to include low-grade GMH-IVH as an outcome variable, although careful long-term neurodevelopmental follow up of larger cohorts is needed to prove this assumption.

Infants who experience PHVD after GMH-IVH carry a higher risk of adverse neurodevelopmental outcomes than infants without PHVD (25–27). In our cohort, 13.8% of infants receiving rhIGF-1/rhIGFBP-3 developed some degree of PHVD, compared with 23.7% of infants receiving SOC. However, the difference was mainly due to an increased incidence of mild PHVD in the control group, which is in line with the finding of a higher prevalence of low-grade GMH-IVH in the control group. The incidence of severe PHVD (AHW >10 mm) was low, and comparable in both groups (2 infants in the treatment group vs. 1 infant in the control group). Therefore, the clinical relevance of the observed difference in subtle cases of PHVD between groups remains speculative.

WMI is common in preterm infants (28, 29). The cystic form of WMI, also known as cystic PVL, is highly associated with cerebral palsy (28, 30). It can be reliably detected by serial CUS imaging (31). Today, due to advances in neonatal care, it has become a rare disease (32). The incidence of cystic PVL was 3.4% in each of the study groups (rhIGF-1/rhIGFBP-3 and SOC) in the current study, which is comparable to data from population-based cohorts (1, 3). The non-cystic form of WMI, the more common type of WMI in preterm infants today, can present on CUS as persisting periventricular hyperechogenicity. The incidence of periventricular hyperechogenicity was 15.5% in the treatment group vs. 22.0% in the SOC group in the current study. Non-cystic WMI can lead to impaired brain growth and

TABLE 3 | Demographics, characteristics, and maternal/perinatal histories of infants with no GMH-IVH at study entry who either remained hemorrhage free or developed GMH-IVH after study entry ($n = 104$).

Characteristic	Infants who remained GMH-IVH free ($n = 70$)		Infants who developed GMH-IVH ($n = 34$)	
	Standard of care ($n = 31$)	rhIGF-1/rhIGFBP-3 ($n = 39$)	Standard of care ($n = 21$)	rhIGF-1/rhIGFBP-3 ($n = 13$)
Sex, *n* (%)				
Male	18 (58.1)	26 (66.7)	16 (76.2)	8 (61.5)
Female	13 (41.9)	13 (33.3)	5 (23.8)	5 (38.5)
GA group, *n* (%)				
<26 weeks	11 (35.5)	19 (48.7)	16 (76.2)	9 (69.2)
≥26 weeks	20 (64.5)	20 (51.3)	5 (23.8)	4 (30.8)
GA (weeks)				
Mean (SD)	26 (1)	26 (1)	25 (1)	25 (1)
Weight at birth (g)				
Mean (SD)	836 (182)	779 (173)	747 (145)	816 (221)
Race, *n* (%)				
Asian	2 (6.5)	3 (7.7)	3 (14.3)	1 (7.7)
Black or African American	5 (16.1)	1 (2.6)	4 (19.0)	3 (23.1)
White	22 (71.0)	32 (82.1)	13 (61.9)	9 (69.2)
Other	2 (6.5)	3 (7.7)	1 (4.8)	0
Mode of delivery, *n* (%)				
Vaginal	14 (45.2)	14 (35.9)	8 (38.1)	8 (61.5)
Cesarean section	17 (54.8)	25 (64.1)	13 (61.9)	5 (38.5)
Maternal infections, *n* (%)	4 (12.9)	5 (12.8)	8 (38.1)	4 (30.8)
Clinical chorioamnionitis, *n* (%)	2 (6.5)	3 (7.7)	2 (9.5)	4 (30.8)
Maternal antibiotics, *n* (%)	17 (54.8)	18 (46.2)	17 (81.0)	8 (61.5)
Antenatal steroids, *n* (%)	31 (100)	39 (100)	21 (100)	13 (100)
Fertility therapy, *n* (%)	7 (22.6)	4 (10.3)	1 (4.8)	3 (23.1)
In vitro fertilization	5 (16.1)	4 (10.3)	1 (4.8)	3 (23.1)
Ovulation stimulation	2 (6.5)	0	0	0
Preterm labor, *n* (%)	27 (87.1)	29 (74.4)	19 (90.5)	13 (100)
Premature rupture of membranes, *n* (%)	9 (29.0)	9 (23.1)	8 (38.1)	6 (46.2)
Preeclampsia, *n* (%)	2 (6.5)	6 (15.4)	2 (9.5)	0
Apgar score at 5 min				
Median (range)	7.0 (2.0–10.0)	8.0 (3.0–10.0)	7.0 (4.0–10.0)	6.0 (1.0–9.0)

GA, gestational age; GMH-IVH, germinal matrix hemorrhage and intraventricular hemorrhage; rhIGF-1, recombinant human insulin-like growth factor-1; rhIGFBP-3, recombinant human insulin-like growth factor binding protein-3; SD, standard deviation.

development and brain atrophy. One of the sonographic signs of impaired brain development or loss of gray and white matter volume is ventricular dilatation without hemorrhage on the term-age ultrasound. This finding on term-age CUS has been shown to correlate to long-term outcomes (33, 34). The prevalence of ventricular dilatation without hemorrhage was identical in both groups in the current trial (rhIGF-1/rhIGFBP-3 10.3% vs. SOC 10.2%). Therefore, we could not find evidence of either adverse or beneficial effects of rhIGF-1/rhIGFBP-3 replacement on cystic or non-cystic WMI with serial CUS.

The present data suggest that postnatal replacement therapy with rhIGF-1/rhIGFBP-3 may have a beneficial effect on causal mechanisms involved in the development of preterm GMH-IVH. The rupture of vessels leading to GMH-IVH has been attributed to an increased vulnerability of the germinal matrix vasculature to fluctuations in cerebral blood flow (35). The vasculature of the germinal matrix is in a highly proliferative phase and exhibits a paucity of pericytes and an immature basal lamina low in fibronectin (35). Further, circulating IGF-1 deficiency has been shown to compromise the structural integrity of the cerebral vasculature, resulting in decreased cerebral capillary density and impaired cerebral myogenic autoregulation in preclinical studies (36–38). The relationship between decreased circulating levels of IGF-I and structural or functional aspects of the immature blood-brain barrier remain to be elucidated.

The strength of this study is the multicenter, randomized, controlled study design. Centers in five European countries and the United States participated in the trial, which underlines the generalizability of our findings. Furthermore, CUS was performed serially from birth to term age and analyzed

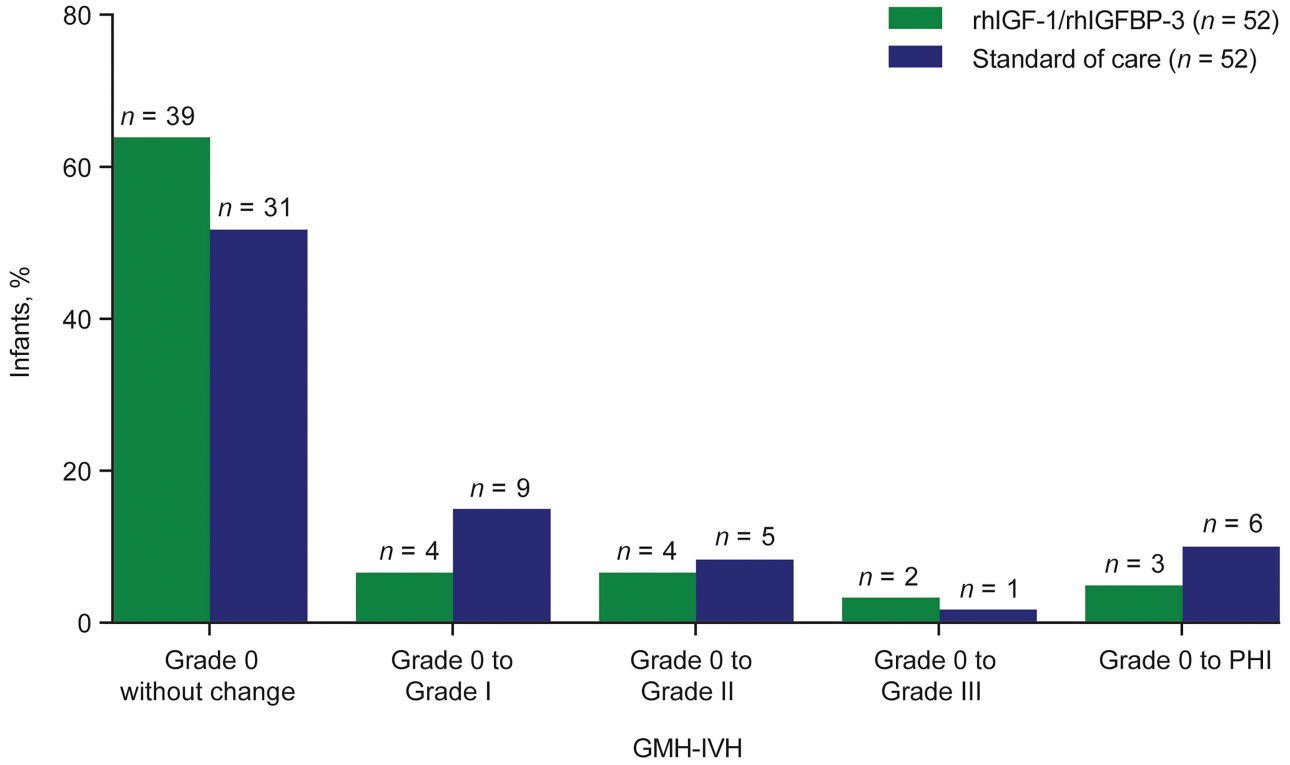

FIGURE 5 | Progression of GMH-IVH among infants with no evidence of GMH-IVH on cranial ultrasound at study entry ($n = 104$).[a] GMH-IVH, germinal matrix hemorrhage and intraventricular hemorrhage; PHI, periventricular hemorrhagic infarction; rhIGF-1, recombinant human insulin-like growth factor-1; rhIGFBP-3, recombinant human insulin-like growth factor binding protein-3. [a]Seventeen infants were excluded for the progression analysis: grade 0 → missing ($n = 3$); grade I → grade I ($n = 4$); grade I → grade II ($n = 2$); grade II → grade II ($n = 3$); grade II → grade IV ($n = 1$); grade III → grade IV ($n = 1$); grade IV → grade IV ($n = 1$); missing → grade 0 ($n = 1$); missing → grade III ($n = 1$).

independently by two masked readers, increasing reliability in detection of not only mild hemorrhage, but also cystic and non-cystic forms of WMI as well as severe brain atrophy.

Limitations include the relatively small sample size in our treated and SOC cohorts, which could be a possible explanation as to why a number of our results did not reach significance. The trial was powered for the primary endpoint: maximum severity of retinopathy of prematurity. Presence of GMH-IVH was one of the pre-specified secondary endpoints, but the study was not powered for IVH reduction, nor for reduction of the other types of prematurity-related brain injury. It is therefore important that a larger clinical trial is underway that is planning to enroll ∼600 infants (EudraCT number: 2018-001393-16; NCT03253263). An additional consideration is that CUS was performed using the anterior fontanel as an acoustic window. Additional visualization of the posterior fossa via mastoid fontanel would have improved detection of cerebellar injury (39, 40) but was not part of the initial study protocol. Another limitation is that brain injury was evaluated by CUS only. Magnetic resonance imaging (MRI) as a complementary imaging modality would have certainly increased the sensitivity and accuracy of the detection of prematurity-related brain injury, and would have allowed detailed segmentation of different brain regions and volumetric studies, as well as quantification of white matter changes. However, acquiring high quality MRI data in a multicenter study setting can be challenging compared to sequential CUS. The advantage of CUS is that it is a bedside tool that is nearly universally available in neonatal intensive care units, and allows frequent serial imaging with minimal disturbance of the infants and thereby gives valuable information on the timing and evolution of brain injury. This can be crucial especially in intervention studies like ours where timing of brain injury in relation to drug application is an important aspect.

CONCLUSIONS

In this first multicenter, randomized, controlled trial comparing rhIGF-1/rhIGFBP-3 replacement therapy with standard treatment in extremely preterm infants, a trend toward less grade II–III GMH-IVH and PHI in the treatment group was observed across GAs. The potential protective effect of rhIGF-1/rhIGFBP-3 was most pronounced in infants with no evidence of GMH-IVH at the start of treatment. No effects of rhIGF-1/rhIGFBP-3 replacement on WMI were observed. These results support further investigation of the potential beneficial effects of rhIGF-1/rhIGFBP-3 replacement in a larger cohort of extremely preterm infants.

DATA AVAILABILITY STATEMENT

The datasets, including the redacted study protocol, redacted statistical analysis plan, and individual participants data supporting the results reported in this article, will be available three months after the submission of a request, to researchers who provide a methodologically sound proposal. The data will be provided after its de-identification, in compliance with applicable privacy laws, data protection and requirements for consent and anonymization.

ETHICS STATEMENT

The studies involving human participants were reviewed and approved by EC/IRB and regulatory agency (as appropriate). Written informed consent to participate in this study was provided by the participants' legal guardian/next of kin.

AUTHOR CONTRIBUTIONS

SH, AP, BH, MM, IB-B, IH-P, MH, AM, NB, LR, AH, and DL made substantial contributions to conception and design, acquisition of data, or analysis and interpretation of data. All authors drafted the article or revised it critically for important intellectual content, approved the final manuscript as submitted, and agree to be accountable for all aspects of the work.

FUNDING

The authors declare that this study received funding from Shire, a Takeda company. The funder had the following involvement with the study: study design, data collection and analysis, decision to publish, and preparation of the manuscript.

ACKNOWLEDGMENTS

The authors thank Rui Tang and Yuna Wu, who provided assistance with additional statistical analysis funded by Takeda. Under direction of the authors, Rosalind Bonomally, MSc, of Excel Medical Affairs provided writing assistance for this publication. Editorial assistance in formatting, proofreading, and copyediting was provided by Excel Scientific Solutions. Shire, a Takeda company, provided funding to Excel Medical Affairs for support in writing and editing this manuscript.

REFERENCES

1. EXPRESS Group. One-year survival of extremely preterm infants after active perinatal care in Sweden. *JAMA*. (2009) 301:2225–33. doi: 10.1001/jama.2009.771
2. Costeloe KL, Hennessy EM, Haider S, Stacey F, Marlow N, Draper ES. Short term outcomes after extreme preterm birth in England: comparison of two birth cohorts in 1995 and 2006 (the EPICure studies). *BMJ*. (2012) 345:e7976. doi: 10.1136/bmj.e7976
3. Ancel PY, Goffinet F, Kuhn P, Langer B, Matis J, Hernandorena X, et al. EPIPAGE-2 Writing Group. Survival and morbidity of preterm children born at 22 through 34 weeks' gestation in France in 2011: results of the EPIPAGE-2 cohort study. *JAMA Pediatr*. (2015) 169:230–8. doi: 10.1001/jamapediatrics.2014.3351
4. Klebermass-Schrehof K, Czaba C, Olischar M, Fuiko R, Waldhoer T, Rona Z, et al. Impact of low-grade intraventricular hemorrhage on long-term neurodevelopmental outcome in preterm infants. *Childs Nerv Syst*. (2012) 28:2085–92. doi: 10.1007/s00381-012-1897-3
5. Maitre NL, Marshall DD, Price WA, Slaughter JC, O'Shea TM, Maxfield C, et al. Neurodevelopmental outcome of infants with unilateral or bilateral periventricular hemorrhagic infarction. *Pediatrics*. (2009) 124:e1153–60. doi: 10.1542/peds.2009-0953
6. Holwerda JC, Van Braeckel KNJA, Roze E, Hoving EW, Maathuis CGB, Brouwer OF, et al. Functional outcome at school age of neonatal post-hemorrhagic ventricular dilatation. *Early Hum Dev*. (2016) 96:15–20. doi: 10.1016/j.earlhumdev.2016.02.005
7. Hansen-Pupp I, Löfqvist C, Polberger S, Niklasson A, Fellman V, Hellström A, et al. Influence of insulin-like growth factor I and nutrition during phases of postnatal growth in very preterm infants. *Pediatr Res*. (2011) 69:448–53. doi: 10.1203/PDR.0b013e3182115000
8. Ye P, D'Ercole AJ. Insulin-like growth factor actions during development of neural stem cells and progenitors in the central nervous system. *J Neurosci Res*. (2006) 83:1–6. doi: 10.1002/jnr.20688
9. Ley D, Hallberg B, Hansen-Pupp I, Dani C, Ramenghi LA, Marlow N, et al. study team. rhIGF-1/rhIGFBP-3 in preterm infants: a phase 2 randomized controlled trial. *J Pediatr*. (2018) 206:56–65. doi: 10.1016/j.jpeds.2018.10.033
10. Papile LA, Burstein J, Burstein R, Koffler H. Incidence and evolution of subependymal and intraventricular hemorrhage: a study of infants with birth weights less than 1,500 gm. *J Pediatr*. (1978) 92:529–34. doi: 10.1016/S0022-3476(78)80282-0
11. Bowerman RA, Donn SM, Silver TM, Jaffe MH. Natural history of neonatal periventricular/intraventricular hemorrhage and its complications: sonographic observations. *AJR Am J Roentgenol*. (1984) 143:1041–52. doi: 10.2214/ajr.143.5.1041
12. Volpe J. *Neurology of the Newborn*. 5th ed. Philadelphia, PA: Saunders Elsevier (2008).
13. Dudink J, Lequin M, Weisglas-Kuperus N, Conneman N, van Goudoever JB, Govaert P. Venous subtypes of preterm periventricular haemorrhagic infarction. *Arch Dis Child Fetal Neonatal Ed*. (2008) 93:F201–6. doi: 10.1136/adc.2007.118067
14. Davies MW, Swaminathan M, Chuang SL, Betheras FR. Reference ranges for the linear dimensions of the intracranial ventricles in preterm neonates. *Arch Dis Child Fetal Neonatal Ed*. (2000) 82:F218–23. doi: 10.1136/fn.82.3.F218
15. Govaert P, de Vries L. *An Atlas of Neonatal Brain Sonography*. 2nd ed. London: Mac Keith Press (2010).
16. Bolisetty S, Dhawan A, Abdel-Latif M, Bajuk B, Stack J, Lui K. New South Wales and Australian Capital Territory Neonatal Intensive Care Units' Data Collection. Intraventricular hemorrhage and neurodevelopmental outcomes in extreme preterm infants. *Pediatrics*. (2014) 133:55–62. doi: 10.1542/peds.2013-0372
17. Mukerji A, Shah V, Shah PS. Periventricular/intraventricular hemorrhage and neurodevelopmental outcomes: a meta-analysis. *Pediatrics*. (2015) 136:1132–43. doi: 10.1542/peds.2015-0944
18. Gressens P, Richelme C, Kadhim HJ, Gadisseux JF, Evrard P. The germinative zone produces the most cortical astrocytes after neuronal migration in the developing mammalian brain. *Biol Neonate*. (1992) 61:4–24. doi: 10.1159/000243526
19. Vasileiadis GT, Gelman N, Han VK, Williams LA, Mann R, Bureau Y, et al. Uncomplicated intraventricular hemorrhage is followed by reduced cortical volume at near-term age. *Pediatrics*. (2004) 114:e367–72. doi: 10.1542/peds.2004-0500
20. Tortora D, Martinetti C, Severino M, Uccella S, Malova M, Parodi A, et al. The effects of mild germinal matrix-intraventricular haemorrhage on the developmental white matter microstructure of preterm neonates: a DTI study. *Eur Radiol*. (2018) 28:1157–66. doi: 10.1007/s00330-017-5060-0

21. Gram M, Sveinsdottir S, Ruscher K, Hansson SR, Cinthio M, Åkerström B, et al. Hemoglobin induces inflammation after preterm intraventricular hemorrhage by methemoglobin formation. *J Neuroinflammation.* (2013) 10:100. doi: 10.1186/1742-2094-10-100
22. Supramaniam V, Vontell R, Srinivasan L, Wyatt-Ashmead J, Hagberg H, Rutherford M. Microglia activation in the extremely preterm human brain. *Pediatr Res.* (2013) 73:301–9. doi: 10.1038/pr.2012.186
23. Chen Z, Gao C, Hua Y, Keep RF, Muraszko K, Xi G. Role of iron in brain injury after intraventricular hemorrhage. *Stroke.* (2011) 42:465–70. doi: 10.1161/STROKEAHA.110.602755
24. Ley D, Romantsik O, Vallius S, Sveinsdóttir K, Sveinsdóttir S, Agyemang AA, et al. High presence of extracellular hemoglobin in the periventricular white matter following preterm intraventricular hemorrhage. *Front Physiol.* (2016) 7:330. doi: 10.3389/fphys.2016.00330
25. Brouwer A, Groenendaal F, van Haastert IL, Rademaker K, Hanlo P, de Vries L. Neurodevelopmental outcome of preterm infants with severe intraventricular hemorrhage and therapy for post-hemorrhagic ventricular dilatation. *J Pediatr.* (2008) 152:648–54. doi: 10.1016/j.jpeds.2007.10.005
26. Whitelaw A, Jary S, Kmita G, Wroblewska J, Musialik-Swietlinska E, Mandera M, et al. Randomized trial of drainage, irrigation and fibrinolytic therapy for premature infants with posthemorrhagic ventricular dilatation: developmental outcome at 2 years. *Pediatrics.* (2010) 125:e852–8. doi: 10.1542/peds.2009-1960
27. Futagi Y, Suzuki Y, Toribe Y, Nakano H, Morimoto K. Neurodevelopmental outcome in children with posthemorrhagic hydrocephalus. *Pediatr Neurol.* (2005) 33:26–32. doi: 10.1016/j.pediatrneurol.2005.01.008
28. Volpe JJ. Brain injury in premature infants: a complex amalgam of destructive and developmental disturbances. *Lancet Neurol.* (2009) 8:110–24. doi: 10.1016/S1474-4422(08)70294-1
29. Back SA. White matter injury in the preterm infant: pathology and mechanisms. *Acta Neuropathol.* (2017) 134:331–49. doi: 10.1007/s00401-017-1718-6
30. Pierrat V, Duquennoy C, van Haastert IC, Ernst M, Guilley N, de Vries LS. Ultrasound diagnosis and neurodevelopmental outcome of localised and extensive cystic periventricular leucomalacia. *Arch Dis Child Fetal Neonatal Ed.* (2001) 84:F151–6. doi: 10.1136/fn.84.3.F151
31. de Vries LS, Eken P, Groenendaal F, van Haastert IC, Meiners LC. Correlation between the degree of periventricular leukomalacia diagnosed using cranial ultrasound and MRI later in infancy in children with cerebral palsy. *Neuropediatrics.* (1993) 24:263–8. doi: 10.1055/s-2008-1071554
32. Hamrick SEG, Miller SP, Leonard C, Glidden DV, Goldstein R, Ramaswamy V, et al. Trends in severe brain injury and neurodevelopmental outcome in premature newborn infants: the role of cystic periventricular leukomalacia. *J Pediatr.* (2004) 145:593–9. doi: 10.1016/j.jpeds.2004.05.042
33. Hintz SR, Newman JE, Vohr BR. Changing definitions of long-term follow-up: should "long term" be even longer? *Semin Perinatol.* (2016) 40:398–409. doi: 10.1053/j.semperi.2016.05.011
34. Edwards AD, Redshaw ME, Kennea N, Rivero-Arias O, Gonzales-Cinca N, Nongena P, et al. Effect of MRI on preterm infants and their families: a randomised trial with nested diagnostic and economic evaluation. *Arch Dis Child Fetal Neonatal Ed.* (2018) 103:F15–21. doi: 10.1136/archdischild-2017-313102
35. Ballabh P. Intraventricular hemorrhage in premature infants: mechanism of disease. *Pediatr Res.* (2010) 67:1–8. doi: 10.1203/PDR.0b013e3181c1b176
36. Tarantini S, Tucsek Z, Valcarcel-Ares MN, Toth P, Gautam T, Giles CB, et al. Circulating IGF-1 deficiency exacerbates hypertension-induced microvascular rarefaction in the mouse hippocampus and retrosplenial cortex: implications for cerebromicrovascular and brain aging. *Age.* (2016) 38:273–89. doi: 10.1007/s11357-016-9931-0
37. Fulop GA, Ramirez-Perez FI, Kiss T, Tarantini S, Valcarcel Ares MN, Toth P, et al. IGF-1 deficiency promotes pathological remodeling of cerebral arteries: a potential mechanism contributing to the pathogenesis of intracerebral hemorrhages in aging. *J Gerontol A Biol Sci Med Sci.* (2018) 74:446–54. doi: 10.1093/gerona/gly144
38. Toth P, Tucsek Z, Tarantini S, Sosnowska D, Gautam T, Mitschelen M, et al. IGF-1 deficiency impairs cerebral myogenic autoregulation in hypertensive mice. *J Cereb Blood Flow Metab.* (2014) 34:1887–97. doi: 10.1038/jcbfm.2014.156
39. Steggerda SJ, Leijser LM, Walther FJ, van Wezel-Meijler G. Neonatal cranial ultrasonography: how to optimize its performance. *Early Hum Dev.* (2009) 85:93–9. doi: 10.1016/j.earlhumdev.2008.11.008
40. Parodi A, Rossi A, Severino M, Morana G, Sannia A, Calevo MG, et al. Accuracy of ultrasound in assessing cerebellar haemorrhages in very low birthweight babies. *Arch Dis Child Fetal Neonatal Ed.* (2015) 100:F289–92. doi: 10.1136/archdischild-2014-307176

Conflict of Interest: SH, AP, MM, KB, MW, and LS have received consulting fees from Shire, a Takeda company; BH has received consulting fees from Premacure AB and Shire, a Takeda company; IH-P and DL hold stock/stock options in Premalux AB, and have received consulting fees from Shire, a Takeda company; NM has received consulting fees from Shire, a Takeda company, and partial funding from the Department of Health's National Institute for Health Research Biomedical Research Centre's funding scheme at University College London Hospitals/University College London; DD has received consulting fees from Shire, a Takeda company, and has received consulting fees from Ipsen regarding other indications for IGF-1 therapies; MH was employed by Shire, a Takeda company, at the time of the study and *post-hoc* analysis; AM and NB were employed by Shire, a Takeda company; LR has received consulting fees and research support from Shire, a Takeda company; AH holds stock/stock options in Premalux AB, and has received consulting fees from Shire, a Takeda company; IB-B declares that the research was conducted in the absence of any commercial or financial relationships that could be construed as a potential conflict of interest.

frontiers in Cellular Neuroscience

ORIGINAL RESEARCH
published: 03 December 2020
doi: 10.3389/fncel.2020.535320

A Model of Germinal Matrix Hemorrhage in Preterm Rat Pups

Masako Jinnai[1,2†], Gabriella Koning[1†], Gagandeep Singh-Mallah[1], Andrea Jonsdotter[1], Anna-Lena Leverin[1], Pernilla Svedin[1], Syam Nair[1], Satoru Takeda[2], Xiaoyang Wang[1,3], Carina Mallard[1], Carl Joakim Ek[1], Eridan Rocha-Ferreira[1†] and Henrik Hagberg[1†]*

[1] Department of Obstetrics and Gynecology, Centre of Perinatal Medicine, Health, Institute of Clinical Sciences, Institute of Neuroscience and Physiology, Sahlgrenska Academy, Gothenburg University, Gothenburg, Sweden, [2] Department of Obstetrics and Gynecology, Faculty of Medicine, Juntendo University, Tokyo, Japan, [3] Henan Key Laboratory of Child Brain Injury, Institute of Neuroscience, Third Affiliated Hospital of Zhengzhou University, Zhengzhou, China

Germinal matrix hemorrhage (GMH) is a serious complication in extremely preterm infants associated with neurological deficits and mortality. The purpose of the present study was to develop and characterize a grade III and IV GMH model in postnatal day 5 (P5) rats, the equivalent of preterm human brain maturation. P5 Wistar rats were exposed to unilateral GMH through intracranial injection into the striatum close to the germinal matrix with 0.1, 0.2, or 0.3 U of collagenase VII. During 10 days following GMH induction, motor functions and body weight were assessed and brain tissue collected at P16. Animals were tested for anxiety, motor coordination and motor asymmetry on P22–26 and P36–40. Using immunohistochemical staining and neuropathological scoring we found that a collagenase dose of 0.3 U induced GMH. Neuropathological assessment revealed that the brain injury in the collagenase group was characterized by dilation of the ipsilateral ventricle combined with mild to severe cellular necrosis as well as mild to moderate atrophy at the levels of striatum and subcortical white matter, and to a lesser extent, hippocampus and cortex. Within 0.5 h post-collagenase injection there was clear bleeding at the site of injury, with progressive increase in iron and infiltration of neutrophils in the first 24 h, together with focal microglia activation. By P16, blood was no longer observed, although significant gray and white matter brain infarction persisted. Astrogliosis was also detected at this time-point. Animals exposed to GMH performed worse than controls in the negative geotaxis test and also opened their eyes with latency compared to control animals. At P40, GMH rats spent more time in the center of open field box and moved at higher speed compared to the controls, and continued to show ipsilateral injury in striatum and subcortical white matter. We have established a P5 rat model of collagenase-induced GMH for the study of preterm brain injury. Our results show that P5 rat pups exposed to GMH develop moderate brain injury affecting both gray and white matter associated with delayed eye opening and abnormal motor functions. These animals develop hyperactivity and show reduced anxiety in the juvenile stage.

Keywords: preterm, brain, germinal matrix hemorrhage, intraventricular hemorrhage, neurodevelopment, neonatal brain

OPEN ACCESS

Edited by:
Ertugrul Kilic,
Istanbul Medipol University, Turkey

Reviewed by:
Catherine Gorrie,
University of Technology Sydney, Australia
Hemmen Sabir,
University Hospital Bonn, Germany

****Correspondence:***
Eridan Rocha-Ferreira
eridan.rocha.ferreira@gu.se

† These authors have contributed equally to this work

Specialty section:
This article was submitted to Cellular Neuropathology, a section of the journal Frontiers in Cellular Neuroscience

Received: *15 February 2020*
Accepted: *05 November 2020*
Published: *03 December 2020*

Citation:
Jinnai M, Koning G, Singh-Mallah G, Jonsdotter A, Leverin A-L, Svedin P, Nair S, Takeda S, Wang X, Mallard C, Ek CJ, Rocha-Ferreira E and Hagberg H (2020) A Model of Germinal Matrix Hemorrhage in Preterm Rat Pups. Front. Cell. Neurosci. 14:535320. doi: 10.3389/fncel.2020.535320

INTRODUCTION

Advances and improvement in health care have allowed continual increase in survival of preterm infants, including extremely preterm, i.e., born before gestational week 28. However, this increase in survival is not associated with a consistent reduction in morbidity (Lorenz et al., 1998; Kaiser et al., 2004; Bodeau-Livinec et al., 2008; Seri and Evans, 2008; Maršál et al., 2009; Hinojosa-Rodríguez et al., 2017). Most commonly, preterm infants weighing 500–1,500 g will suffer from neonatal and life-long complications such as respiratory bronchopulmonary dysplasia, a chronic respiratory disease, intestinal necrotizing enterocolitis and germinal matrix hemorrhage (GMH) resulting in intra- and periventricular hemorrhage (IVH/PVH) (Owens, 2005; Kenet et al., 2011).

GMH-IVH is a major cause of preterm brain injury. The germinal matrix (also termed the ganglionic eminence) is only present until gestational week 32 (Whitelaw, 2012). This is a highly vascularized brain area, which is central for development and a major source of neurons and glial cells. The germinal matrix vasculature is fragile, and the combination of reduced cerebral autoregulation and fluctuation of cerebral blood flow can result in vessel rupture within the germinal matrix (Kaiser et al., 2005). This rupture, known as GMH is particularly common in infants born extremely preterm (<28 weeks of gestation) (Kenet et al., 2011).

GMH is divided into four grades, with grades III and IV having the worst outcome (Brouwer et al., 2014). Grade IV cases have a prognosis of 90% mortality, with 80% of survivors suffering from cerebral palsy and cognitive difficulties (Stoll et al., 2004). In these severe cases, GMH results in blood clots which cause cell death as well as impairment in cerebrospinal fluid (CSF) circulation and drainage. There is an excess release of free iron with subsequent free radical production. This normally occurs within the first 72 h of life (Lekic et al., 2015). After resolution of hematoma, there is a secondary wave of tissue loss, as a result of CSF accumulation in the brain (hydrocephalus) causing tissue compression. Re-establishment of blood flow can result in ischemia-reperfusion injury, due to further generation of free radicals and continued oxidative injury, with further damage to various brain cells, particularly oligodendrocyte precursor cells. This induces a strong and prolonged inflammatory response, which further exacerbates white matter damage and results in poor neurological outcome (Brouwer et al., 2014). Around two thirds of severe GMH-IVH cases show significant impairment in both motor and cognitive function (Bassan et al., 2007).

The onset of GMH is difficult to prevent (Roland and Hill, 2003) and current treatment options consist of antenatal administration of corticosteroids and magnesium sulfate (Whitelaw, 2001; Hirtz et al., 2015; Crowther et al., 2017). Postnatally, around 25% of infants with severe GMH-IVH require the insertion of a shunt (Brouwer et al., 2014) and administration of indomethacin has shown a potential benefit (Fowlie and Davis, 2003). Unfortunately, in most cases only supportive care can be provided (Kenet et al., 2011). This has resulted in an urgent unmet need for development of novel treatment strategies. The characterization of standardized animal models for the study of GMH is therefore of great importance if the brain injury and neurological deficits following this condition are to be prevented and/or treated adequately (Ballabh et al., 2007; MacLellan et al., 2008; Chua et al., 2009).

Several animal species such as the mouse, rat, rabbit, sheep and piglet have been used for the study of GMH (Goddard et al., 1980; Balasubramaniam and Del Bigio, 2006; Aquilina et al., 2007; Chua et al., 2009). In these studies, GMH has been induced both via direct methods (blood injected into ventricle) and systemic alterations, including change of hemodynamic properties such as osmolality, oxygenation levels or blood pressure (Goddard et al., 1980; Balasubramaniam and Del Bigio, 2006; Georgiadis et al., 2008). The limitation of these models is that none of them sufficiently resembles the clinical cases. In a study from 2012, Lekic et al. (2011, 2012) reported that infusion of blood into the brain has little relation to a spontaneous bleed and that a hemodynamic property change will lead to secondary injury caused by hypoxia or hypertension. They also mention the lack of rodent models for the study of GMH mimicking the neurological consequences of premature newborns suffering from this condition (Lekic et al., 2011, 2012). In their study GMH is induced by injection of collagenase, a sterile collagen-degrading agent (Rosenberg et al., 1990) in the P7 rat. This causes a standardized, spontaneous rupture of vessels in the germinal matrix of the ganglionic eminence, and extravasation into the lateral ventricles (Lekic et al., 2012), enabling the study of features mimicking those of clinical GMH.

However, more recent studies have shown that P7 rats more closely resembles near-term human infants (Semple et al., 2013), where GMH is not one of the main risk factors for neonatal brain injury. Therefore, the aim of the present study was to develop and characterize a model of severe GMH, i.e., grades III and IV, using P5 rats—corresponding to brain maturation in preterm human infants and at an age when the germinal matrix is still present, and to further characterize the pathophysiology of this disease with the hope of assisting novel experimental therapy studies.

MATERIALS AND METHODS

Surgical Procedure

At P5, Wistar rat pups of either sex were randomly allocated into groups and injected into the medial striatum in proximity to the germinal matrix (**Figure 1A**) with collagenase VII (Sigma-Aldrich, cat# C2399) for induction of GMH or with an equivalent volume of saline as control. Additionally, naïve animals served as needle control. The animals were anaesthetized with isoflurane (5% induction, 1.5% maintenance), and the solution was injected free hand, using a guiding device, into the germinal matrix of the right hemisphere using a 27 G (0.4 mm) needle and a 1 ml Hamilton syringe connected to an infusion pump (CMA/100 microinjection pump). The correct position for needle insertion was located at 4 mm lateral of the midline and 1 mm rostral of bregma and the needle angled medially was inserted to a depth of 3.5 mm and the collagenase was injected with a steady infusion flow of 1 μl/min for 2 min. The needle remained in place for an additional minute following the injection in order to avoid

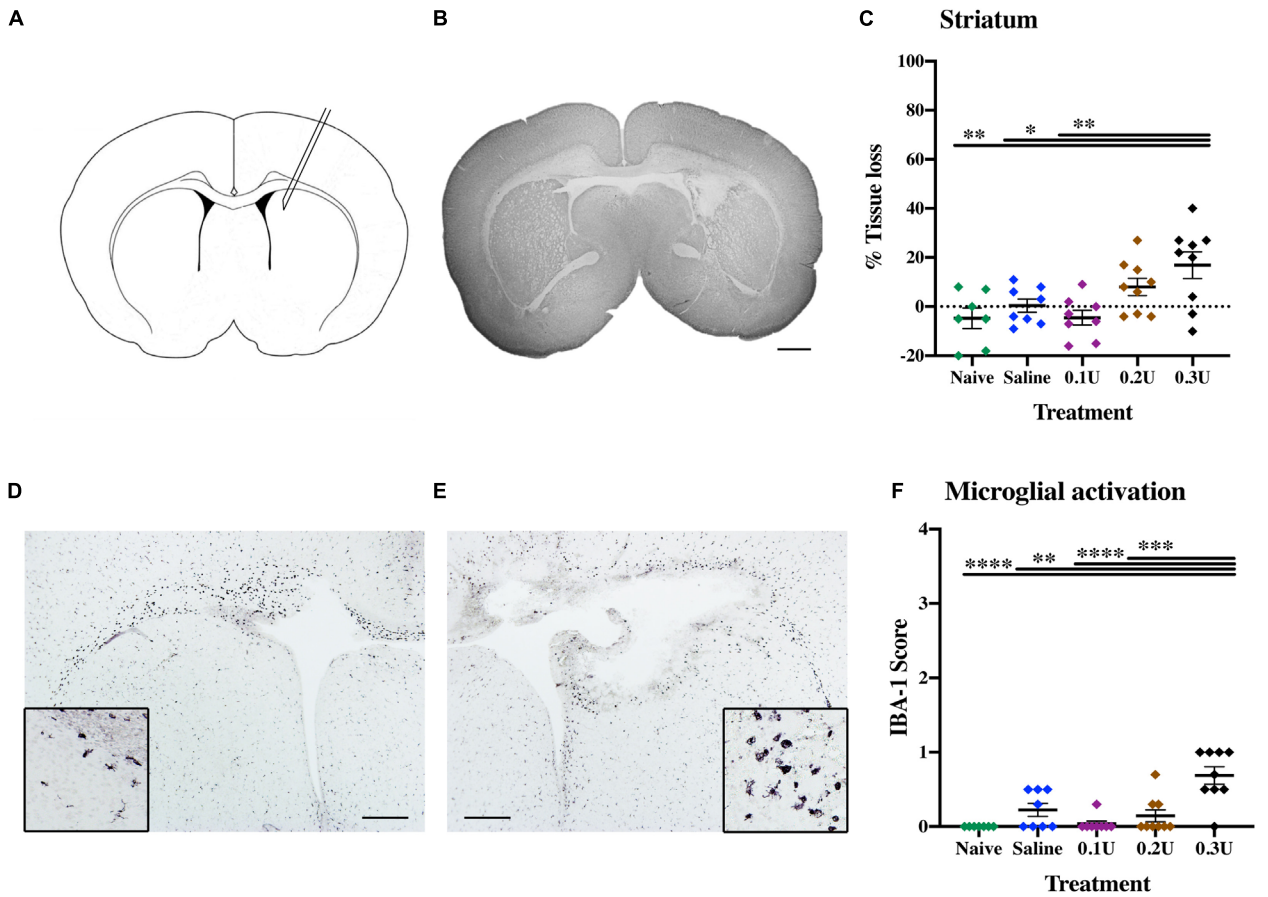

FIGURE 1 | Optimal collagenase dose to induce GMH. **(A)** Diagram of ICV injection site, with needle insertion located at 4 mm lateral of the midline and 1 mm rostral of bregma, with an insertion depth of 3.5 mm. **(B)** Representative MAP-2-stained whole brain micrograph of 0.3 U collagenase-mediated injury 24 h after injection. **(C)** Effect of different treatments—naïve (n = 8), saline (n = 8), 0.1 U (n = 8), 0.2 U (n = 9), and 0.3 U (n = 9) collagenase—on ipsilateral striatum tissue loss 24 h after injection. **(D)** Contralateral and **(E)** ipsilateral micrographs with magnification inserts (×20) showing IBA-1 microglia staining 24 h after injection. **(F)** Assessment of microglia activation (IBA-1) in the ipsilateral striatum 24 h after different collagenase dose administrations. Data represented as individual animals ± SEM and analyzed using one-way ANOVA followed by Tukey's multiple comparison test. *P < 0.05, **P < 0.01, ***P < 0.001, and ****P < 0.0001. Scale bar = 1 mm in **(B)**; 0.5 mm in **(D,E)**.

back-flow. After completing the procedure, the animals were allowed to rest on a heating pad set at 35°C and upon recovery from anesthesia all animals were returned to their dams. The duration of the procedure was <5 min/animal. No mortality was recorded in any of the different treatment groups. The animals that survived longer than 24 h were monitored daily for the first 10 days after GMH and no adverse effects were observed. Overall, combining all treatment groups and time-points, a total of 131 animals were used in this study (**Supplementary Figure 1**).

Dose Titration

Titration of the optimal collagenase concentration was performed to induce a hemorrhage contained in one hemisphere through infusion into the germinal matrix of the medial striatum (**Figure 1A**). Based on the study of Lekic et al. (2012), P5 pups were injected with 2 μl of 0.1 U (n = 8), 0.2 U (n = 9), or 0.3 U (n = 9) of collagenase VII (1,000–3,000 CDU/mg solid, C2399, Sigma-Aldrich, Saint Louis, United States) or saline as control (n = 8). Naïve animals (n = 8) served as needle control. Brains were collected 24 h after injection (P6) and evaluated immunohistochemically as described below.

Assessment of Early Motor Function

Following collagenase injection (0.3 U, n = 12), the development of a subgroup of the pups was blindly assessed over a period of 5 days. *Negative geotaxis* was used to test the amount of time required for a pup to rotate 180° after having been placed head down at a 20° downward slope. Latency of *eye opening* was noted for each eye in all pups. Both naïve (n = 10) and saline-injected animals (n = 10) were used as control groups.

Long-Term Sensorimotor and Behavior Tests

Naïve (n = 5), saline- (n = 12) and collagenase- (n = 19) injected animals were used for assessing long-term neurobehavior tests. All animals underwent these tests at two separate time-points,

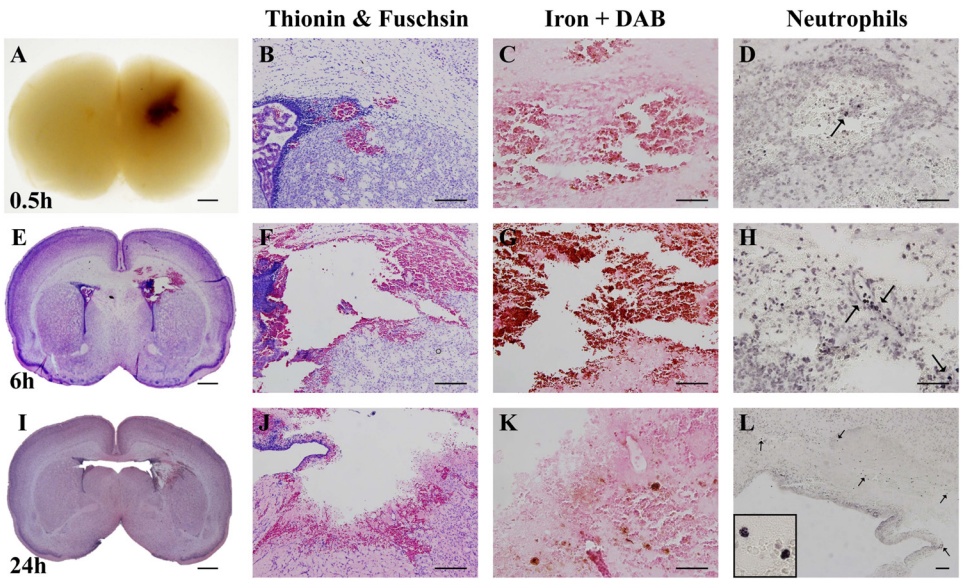

FIGURE 2 | Characterization of optimal collagenase dose. **(A)** Coronal view of paraffin-embedded rat brain collected 0.5 h after 0.3 U collagenase injection. Representative micrograph of **(B)** thionin and fuchsin, **(C)** DAB-enhanced iron and **(D)** Neutrophil (MPO) stainings showing ipsilateral striatum 0.5 h after 0.3 U collagenase injection (n = 7). **(E)** Whole brain (thionin and fuschisin) and ipsilateral striatum level representative micrographs of **(F)** thionin and fuchsin, **(G)** DAB-enhanced iron and **(H)** Neutrophil (MPO) 6 h after 0.3 U collagenase injection (n = 7). **(I)** Whole brain (thionin and fuchsin) and ipsilateral striatum level representative micrographs of **(J)** thionin and fuchsin, **(K)** DAB-enhanced iron, and **(L)** Neutrophil (MPO) 24 h after 0.3 U collagenase injection (n = 12). Scale bar = 1 mm in **(A,E,I)**; 100 μm in all other micrographs. MPO, myeloperoxidase.

2–3 weeks (P22–26) and 4–5 weeks (P36–40) after GMH. Brains were collected at P40 for immunohistochemistry.

Rotarod

Motor coordination and balance was analyzed using rotarod test on P22 and P36. The apparatus (Panlab, Harvard apparatus) consisted of a horizontal rod (25 cm diameter) with an inter-lane distance of 5 cm (P22) or 7.5 cm (P36). Rats were placed on the rod rotating at a constant speed of 4 rpm. The rotations were accelerated to 40 rpm over a period of 300 s, and the latency to fall was recorded. Each animal underwent three trials, with an inter-trial recovery time of 15–20 min spent in the home cage. The apparatus was cleaned using 70% ethanol between each trial.

Cylinder Rearing Test

Motor asymmetry analyzed using cylinder rearing test on P23 and P37. Rats were individually placed in a transparent glass cylinder (14 cm D × 21 cm H and 17 cm D × 28 cm H, for P23 and P37 rats, respectively) and video-recorded for 5 min to analyze forepaw preference during full rearing and lateral exploration as per the criteria suggested by Kadam et al. (2009). Two mirrors (30 × 30 cm) were placed behind the cylinder at an angle such that the forelimb movements could be observed when the rat turned away from the video camera. The forelimb asymmetry was measured by calculating the unimpaired forepaw initiation preference score (%) as follows: (unimpaired–impaired) / (unimpaired+impaired+both) × 100. Animals that made ≤10 full rears were excluded from the study (Schallert et al., 2000).

Open Field Test

General locomotor activity and anxiety-like behavior were tested on P23 and P37 using this stress-sensitive behavioral task. The test was conducted in dark for 30 min. To acclimatize the animals to the testing conditions, the animals were brought to the dark anteroom at least 30 min prior to the test. A dark-gray plexiglass square open-top box (100 cm × 100 cm × 40 cm) served as the testing arena. The box was mounted with an infrared-sensitive CCD camera on the ceiling, and two infrared lamps were used to illuminate the arena. The box was virtually divided into a central area (33 cm × 33 cm), corners (15 cm × 15 cm) and a peripheral area (remaining area) using the ANY-Maze tracking software (Stoelting Co.). Mean speed, mobile time and total time spent in each zone was recorded and analyzed using ANY-Maze. ANY-Maze tracked and used the center of animal's body for recording an entry into a zone. Data was split into 5 min time bins for statistical analysis. The box was cleaned off any feces and urine using 70% ethanol between each trial.

Tissue Collection and Processing

Brains were collected for histology at five different time-points following ICV injection. One subgroup of the animals was sacrificed 0.5 h (n = 7), and 6 h (n = 7) after ICV for descriptive assessment of injury progression. P5 naïve animals (n = 7) were used as control for both 0.5 and 6 h time-points. A second subgroup of animals were terminated on P6, P16, and P40 for immunohistochemistry and neurobehavioral (P40) measurements. The pups were deeply anesthetized with 0.1 ml of Pentocur and the brains dissected out and immersion fixed in

histofix (Histolab Products AB, Sweden). Brains were dehydrated and embedded in paraffin and cut with a microtome into 7 μm thick sections at the level of the striatum (equivalent to adult +0.2 mm from bregma) and hippocampus (equivalent to adult −3.3 mm from bregma) for immunohistochemical staining.

Histochemistry

Brains were collected at 0.5, 6, and 24 h after GMH surgery for histopathological assessment of injury and bleeding progression. Sections underwent deparaffination in xylene followed by rehydration in graded alcohol. For thionin and acid fuschsin staining, sections were incubated in thionin for 4 min, rinsed in water and then placed in acid fuschsin stain for 30 s. Iron staining was performed using the iron stain kit HT20 (Sigma-Aldrich) according to the manufacturer's instructions. Perl's blue staining was further enhanced using DAB peroxidase. All sections were dehydrated in increasing concentrations of alcohol, xylene and covered using Pertex.

Immunohistochemistry

Brain sections were prepared for immunohistochemical staining by deparaffination in xylene followed by rehydration in graded alcohol. Sections were boiled in 0.01 M citric acid buffer (pH 6.0) for antigen recovery and blocked for endogenous peroxidase (3 % H_2O_2) and nonspecific binding (horse and goat serum). Sections were incubated with the primary antibodies: Rabbit anti-glial fibrillary acidic protein (GFAP, Sigma-Aldrich; cat#G3893; 1:400), rabbit anti-ionized calcium binding adaptor molecule 1 (IBA-1, FUJIFILM Wako Chemicals, cat#019-19741; 1:2,000), mouse anti-microtubule-associated protein-2 (MAP-2, Sigma-Aldrich, cat#M4403; 1:1,000), mouse anti-myelin basic protein (MBP SMI-94, BioSite, cat#836504; 1:1,000), rabbit anti-myeloperoxidase (MPO, abcam, cat#AB9535; 1:100) overnight, washed and incubated with an appropriate secondary antibody. ABC elite was used for visualization of immunoreactivity and the sections were submerged into 0.5 mg/ml 3.3-diaminobenzidine (DAB) enhanced with nickel sulfate (15 mg/ml). Sections were dehydrated and mounted as described above.

Immunofluorescence

Paraffin embedded brains from 24 h survival post-GMH were sectioned at 7 μm, and paraffin removed by xylene, sections hydrated through decreasing concentrations of ethanol and washed in PBS with 0.05% tween20. Antigen retrieval was performed by boiling sections in 0.01 M citrate buffer (pH6.0) for 10 min followed by incubating in serum-free protein blocking solution (Agilent DAKO) for 30 min. Sections were then incubated in a mixture of rabbit anti-laminin antibodies (Novus Biologicals, cat#NB300-144; 1:200) and mouse anti-claudin5 antibodies (Thermo Fisher Scientific, cat#35-2500; 1:200) overnight in fridge. The next day, section were incubated in appropriate alexa-488 and -594 conjugated secondary antibodies for 2 h at room temperature. In between each step above sections were washed in PBS with 0.05% tween20. Finally, due to inherent autofluorescence around injury site, sections were treated using Vector TrueView autofluorescence quenching kit according to manufactures instructions, examined and photographed using an Olympus BX50 microscope fitted with a DP72 camera. All images were processed using Imaris v.9.1 (Bitplane AG).

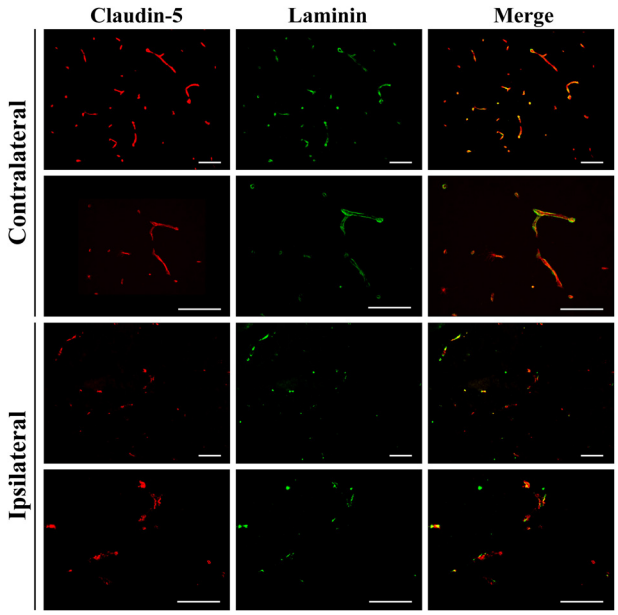

FIGURE 3 | Vascular damage 24 h after 0.3 U collagenase infusion. Immunofluorescence microscopy demonstrating representative claudin-5 and laminin expression in intact vessels of the contralateral striatum at ×20 (top row) and ×40 (second row) magnifications 24 h after 0.3 U collagenase ICV infusion. Conversely, within the ipsilateral striatum there is clear vessel rupture with loss of both claudin-5 and particularly of laminin, as seen at ×20 (third row) and ×40 (fourth row) magnifications (n = 12). Scale bar = 100 μm.

Data Analysis

Brain injury was quantified as the area loss of gray matter (MAP-2) and white matter (MBP) immunoreactivity at the levels of striatum and anterior hippocampus in P6 (MAP-2 only), P16 and P40 animals. Total area positive MAP-2 staining in each intact hemisphere and specific brain structures (striatum and hippocampus) and MBP positive staining of the subcortical white matter were outlined and measured using ImageJ (version 1.51, NIH). The percentage of tissue loss was calculated by subtracting the ipsilateral positive area from the corresponding contralateral regions. This method assumes that the contralateral hemisphere represents 100% intact area, however, there are sections, where due to potential symmetrical differences between contralateral and ipsilateral regions, the undamaged ipsilateral hemisphere might be larger, resulting in negative tissue loss. Microglial activation was determined using semi-quantitative score of IBA-1-positive cells, with a scale of 0—no activation, ramified microglia; 1—focal activation, ramified microglia; 2—mild diffusion activation with still predominant ramified microglia; 3—moderate widespread activation with cells showing retraction of the process and swollen cell body; to 4—widespread amoeboid microglia, as previously described (Rocha-Ferreira et al., 2015, 2016). GFAP immunoreactivity was assessed

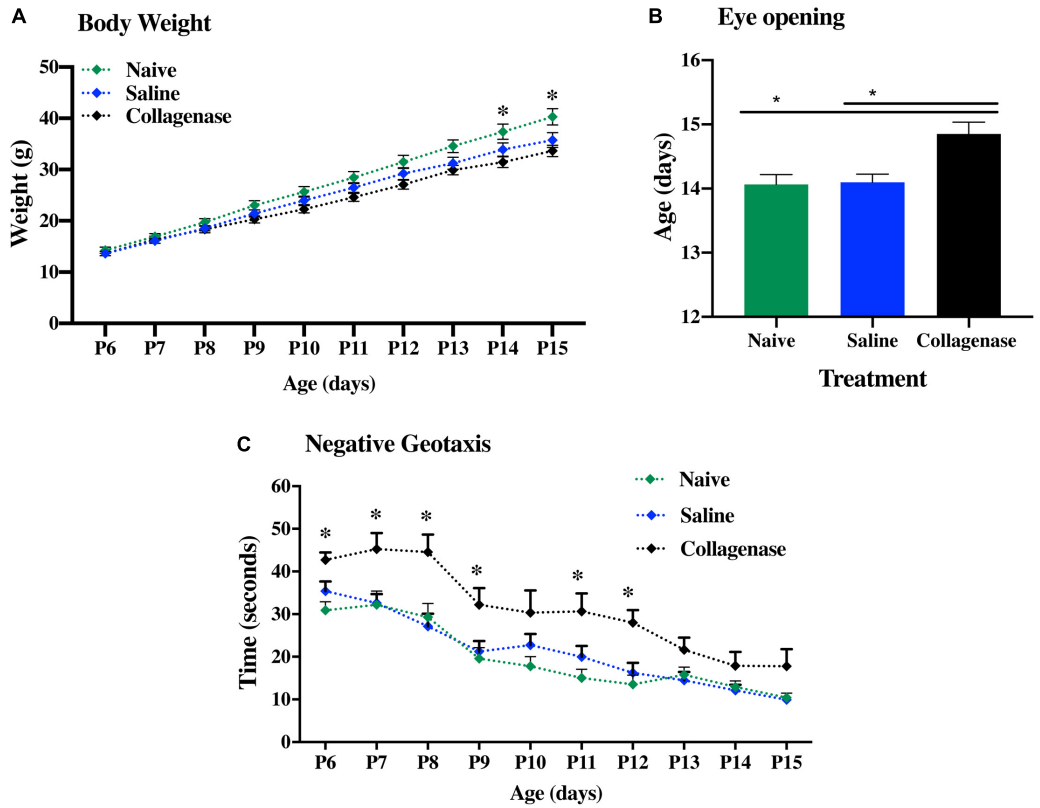

FIGURE 4 | Neurodevelopmental deficits following GMH. **(A)** Weight gain over time, **(B)** Latency in eye opening, and **(C)** negative geotaxis assessment of naïve (n = 10), saline (n = 10), and 0.3 U collagenase (n = 12) animals. Data represented as mean ± SEM and analyzed using Kruskal-Wallis Dunn's test. *P < 0.05–0.001.

using ImageJ threshold tool. In brief three non-overlapping RGB images from the striatum region were captured at x20 magnification, using an Olympus BX50 microscope fitted with a DP72 camera. Each image was duplicated and transformed into 8-bit grayscale images before the default red threshold setting was applied. The positive red threshold was calculated as percentage of entire image.

Statistical Analysis

Graph Pad Prism (version 8.3.0) and SPSS were used to perform all statistical analyses. The data was first checked for Gaussian distribution using D'Agostino and Pearson normality test. Kruskal-Wallis Dunn's test or ANOVA with Tukey's multiple comparisons test was used to determine statistical significance. The test used for each experiment is stated in the figure legends and P-values of < 0.05 were considered to be statistically significant and data is expressed as individual animals or mean ± SEM.

RESULTS

Dose Response

To establish the optimal collagenase dose for GMH induction via intracranial injection into the germinal matrix of medial striatum (**Figure 1A**), a dose response was performed through the injection of three different doses of collagenase (0.1, 0.2, and 0.3 U) or saline (control). Additionally, naïve animals were included as needle-control. At P6, gray matter injury evaluated using MAP-2 immunohistochemistry showed that saline injection did not result in brain injury when compared to naïve controls. GMH-mediated injury could be detected 24 h following ICV injection, with significant injury in the 0.3 U collagenase group (**Figure 1B**). MAP-2 analysis showed a significant tissue reduction specifically within the ipsilateral striatum brain region when compared to naïve (P = 0.0050), saline- (P = 0.0381), and 0.1 U-injected (P = 0.0038) rats (**Figure 1C**).

Microglia showed significant ipsilateral morphological changes, changing from resting to focal activation in the 0.3 U group (**Figures 1D,E**). This activation was significant when compared to all other groups: naïve (P = 0.0008), 0.1 U (P = 0.0019), and 0.2 U (P = 0.0236) (**Figure 1F**). No increased astroglial immunoreactivity was detected in any of the different injection groups (**Supplementary Figure 2A**).

Characterization of the Optimal Dose

Both macroscopic and microscopic descriptive assessments showed that the injury obtained in the 0.3 U collagenase-injected animals resulted in near-immediate bleeding. This bleeding was visible macroscopically at 0.5 h after injection

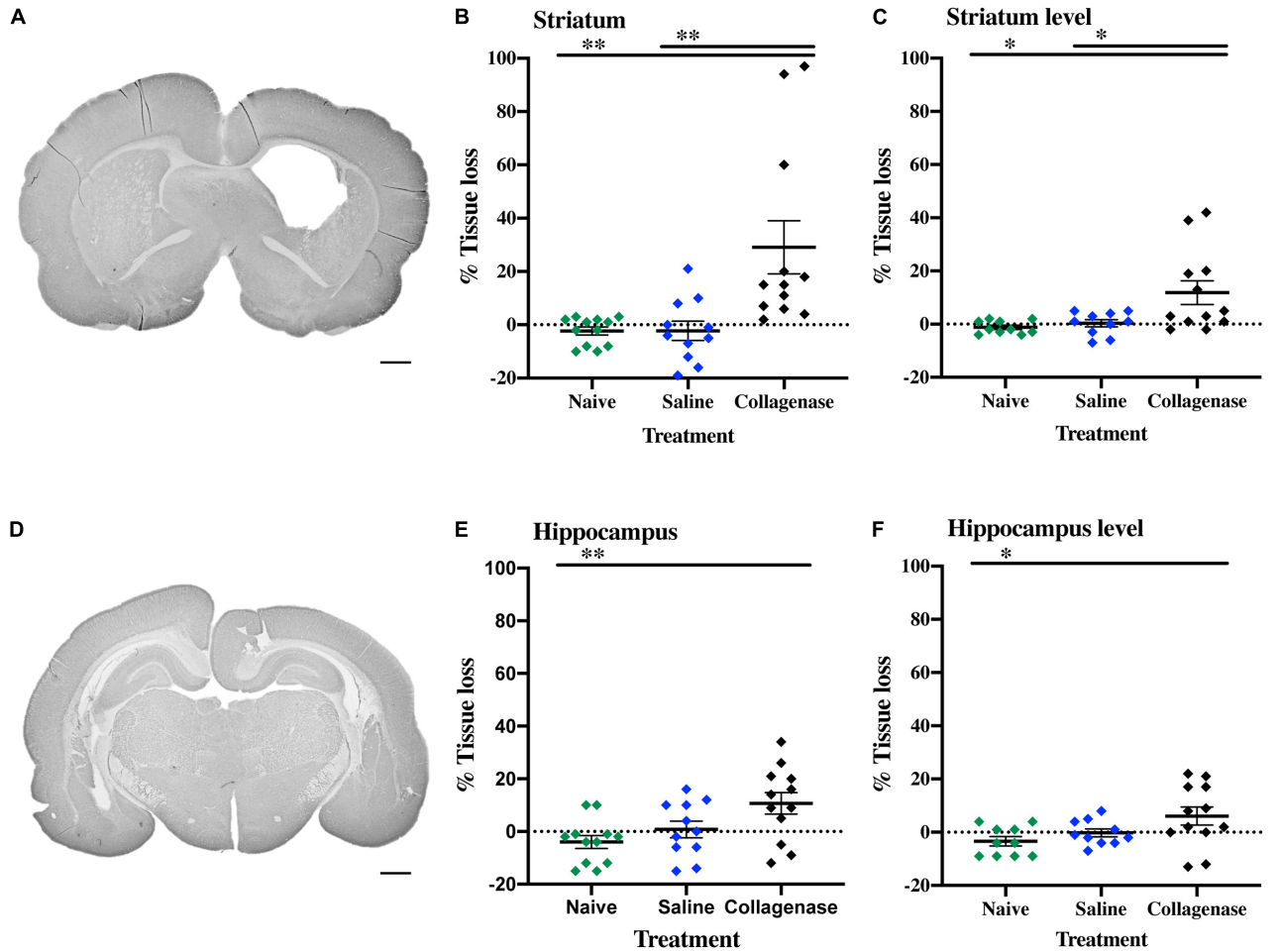

FIGURE 5 | Gray matter injury at P16. **(A)** Representative MAP-2-stained whole brain micrograph of 0.3 U collagenase-mediated striatal injury at P16. **(B)** Graph demonstrating striatum-specific tissue loss and **(C)** striatum level ipsilateral hemisphere loss in the collagenase group. **(D)** Representative MAP-2-stained whole brain micrograph of 0.3 U collagenase-mediated hippocampal injury at P16. **(E)** Graph demonstrating hippocampus-specific tissue loss and **(F)** hippocampus level ipsilateral hemisphere loss in the collagenase group (n = 12). Both naïve (n = 10) and saline-injected (n = 10) animals were used as control groups. Data represented as individual animals ± SEM and analyzed using one-way ANOVA followed by Tukey's multiple comparison test. *$P < 0.05$ and **$P < 0.01$. Scale bar = 1 mm.

(**Figure 2A**). Microscopic observation at this time-point demonstrated localized presence of erythrocytes, as observed in the thionin and fuschsin stain (**Figure 2B**). DAB-enhanced iron staining showed clear presence of iron (**Figure 2C**), however, there was minimal infiltration of MPO-positive neutrophils (**Figure 2D**). By 6 h after collagenase injection, thionin and fuchsin-stained coronal sections showed clear tissue loss surrounding the injection site (**Figure 2E**), as well as structural disorganization in the penumbra (**Figure 2F**). This was associated with substantial iron increase (**Figure 2G**) and a small increase in neutrophil numbers located within the injury site (**Figure 2H**). Both tissue loss and structural disorganization increase over time, as seen 24 h after insult (**Figure 2I**), together with the presence of cells with pyknotic nucleus within the site of injury (**Figure 2J**). Interestingly, at this time-point, i.e., at P6, there was almost a complete clearance of iron at the site of injury (**Figure 2K**), as well as clear infiltration of neutrophils also in the surrounding parenchyma (**Figure 2L**).

To investigate damage to the basal lamina and the blood-brain barrier of cerebral blood vessels immunofluorescence was carried out for laminin and claudin-5 on brain sections at 24 h after GMH (**Figure 3**). This showed extensive loss of laminin around blood vessels in the striatum of the injured/ipsilateral hemisphere. Key blood-brain barrier protein claudin-5 appeared fragmented in blood vessels at the injury site compared to the uninjured hemisphere. In general, claudin-5 immunoreactivity was more visible on blood vessels than laminin as some blood vessels with claudin-5 immunoreactivity were devoid of laminin.

Early Neurodevelopmental and Neuropathological Brain Injury Evaluation

Developmental assessment was performed in naïve (n = 10), saline- (n = 10), and collagenase-injected (n = 12) animals over a period of 10 continuous days, ranging between P6 and 15.

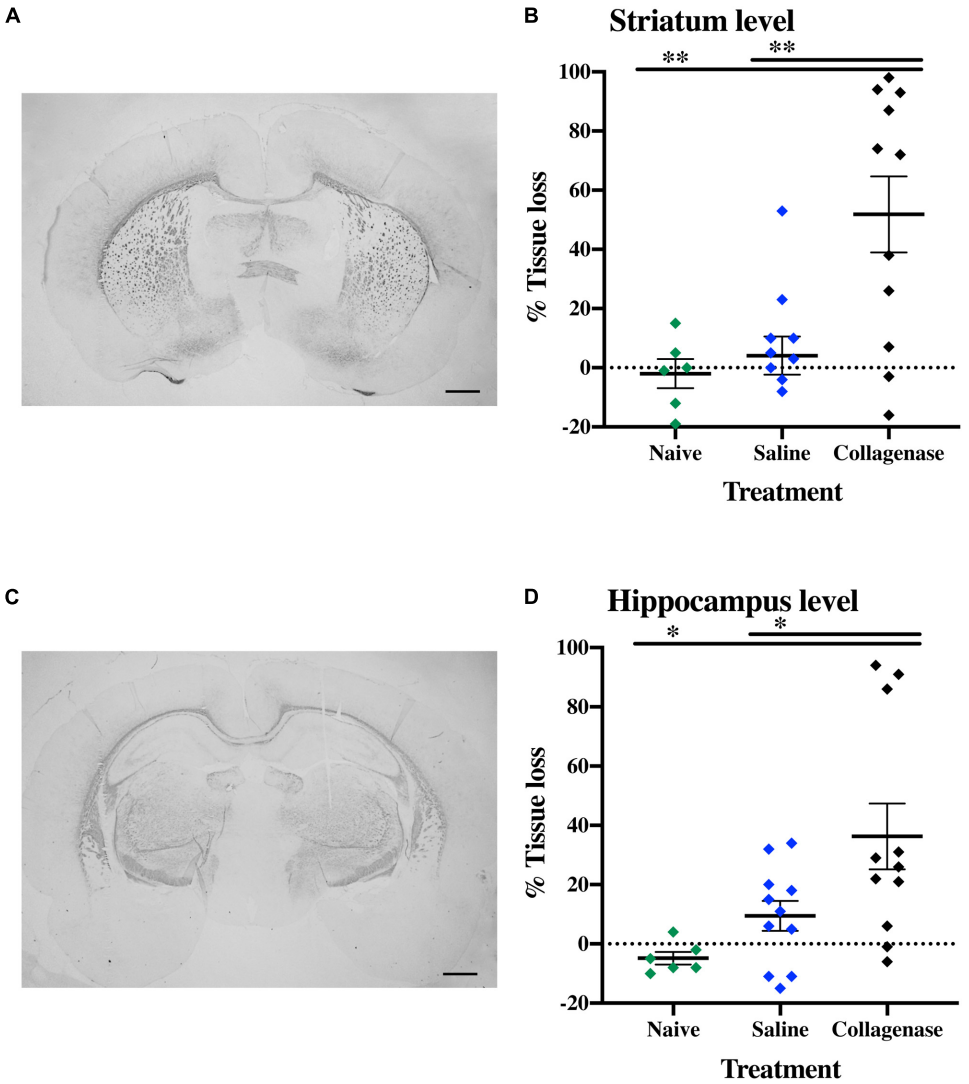

FIGURE 6 | White matter injury at P16. **(A)** Representative striatum level MBP-stained whole brain micrograph of 0.3 U collagenase-injected rats and **(B)** corresponding graph demonstrating collagenase-mediated reduction in subcortical white matter at P16. **(C)** Representative MBP-stained whole brain micrograph of 0.3 U collagenase-injected rats at the level of the hippocampus and **(D)** associated graph showing subcortical white matter in the collagenase group at P16 (n = 12). Both naïve (n = 10) and saline (n = 10) animals were used as control groups. Data represented as individual animals ± SEM and analyzed using one-way ANOVA followed by Tukey's multiple comparison test. *$P < 0.05$ and **$P < 0.01$. Scale bar = 1 mm.

The body weight of each pup was recorded daily. All three groups showed continued weight gain over time. However, at both P14 and P15, collagenase infused rats showed significantly less weight gain when compared to naïve animals (P = 0.0205 and P = 0.0277, respectively) (**Figure 4A**). By P14, around 80% of both naïve and saline-treated animals had opened their eyes, whereas in the collagenase group, only 45% had opened their eyes at this time point (P = 0.0205 and P = 0.0147, respectively). Furthermore, 33% of the pups in the collagenase group did not open their eyes until P16 whereas all animals in both naïve and saline groups had opened their eyes by P15 (**Figure 4B**). Negative geotaxis assessment demonstrated a significant impairment in the ability to rotate 180° upwards in the collagenase injected animals compared with both naïve and saline control groups at P6 (P = 0.0006 and P = 0.0325, respectively), P7 (P = 0.0706 and P = 0.0602, respectively), P8 (P = 0.0270 and P = 0.0602, respectively), naïve only at P9 (P = 0.0317) and P11 (P = 0.0317), and again both naïve and saline groups at P12 (P = 0.0024 and P = 0.0425, respectively) (**Figure 4C**).

At P16, the injury found in the collagenase group consisted of asymmetrical lateral ventricles with slight to severe ipsilateral dilation associated with shrinkage of the striatum, and occasionally, of the hippocampus. MAP-2 assessment showed significant reduction of gray matter in the striatum (**Figure 5A**) and hippocampus (**Figure 5D**) regions in the collagenase group: striatum naïve (P = 0.00031), striatum saline (P = 0.0039) (**Figure 5B**), and hippocampus naïve (P = 0.0090) (**Figure 5E**).

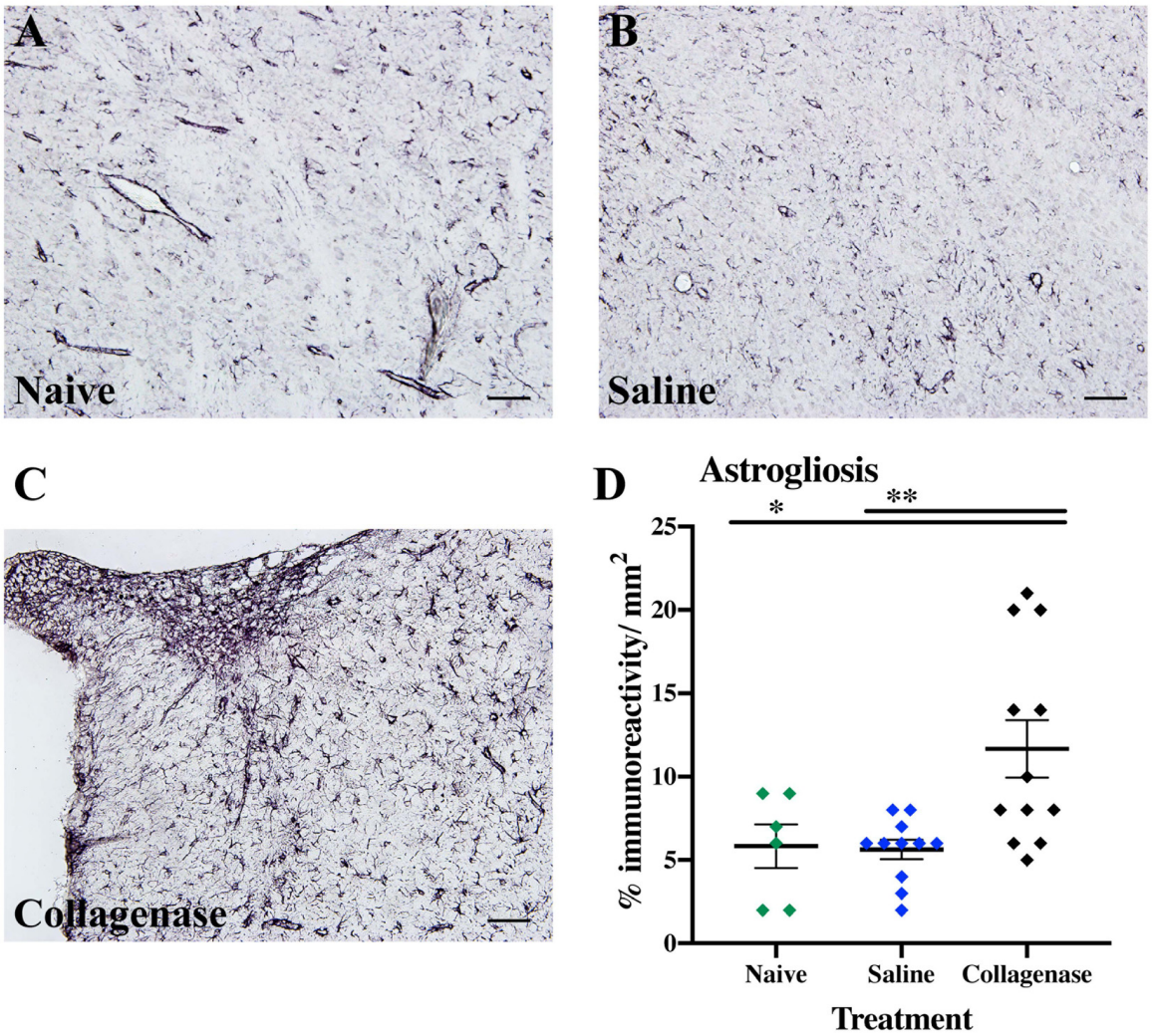

FIGURE 7 | GMH induces astrogliosis at P16. **(A)** Representative micrograph of GFAP staining in the ipsilateral striatum of naïve (n = 10), **(B)** saline (n = 10), and **(C)** collagenase (n = 12) groups at P16. **(D)** Corresponding graph showing increase in GFAP immunoreactivity in the collagenase-injected group at P16. Data represented as individual animals ± SEM and analyzed using one-way ANOVA followed by Tukey's multiple comparison test. *$P < 0.05$ and **$P < 0.01$. Scale bar = 100 μm.

By this time-point, there was a progression in injury extent, resulting in significant gray matter loss when assessing entire hemispheres, with a significant reduction in positive MAP-2 at the ipsilateral hemisphere at the striatum level when compared to naïve (P = 0.0118) and saline (P = 0.0275) controls (**Figure 5C**), and hippocampus level when compared to naïve animals (P = 0.0320) (**Figure 5F**).

MBP assessment showed a significant reduction in subcortical white matter in the collagenase group, both at the striatum (**Figure 6A**) and hippocampus (**Figure 6C**) levels when compared to naïve (P = 0.0054 and P = 0.0111, respectively) and saline controls (P = 0.0034 and P = 0.0542, respectively (**Figures 6B,D**).

IBA-1 measurements showed no microglia activation in the collagenase-injected animals at this time-point (**Supplementary Figure 2B**). However, astrogliosis was significantly present at the striatum level, when compared to both naïve (P = 0.0294) and saline-injected (P = 0.0063) animals (**Figures 7A–D**).

Effect of GMH on Long-Term Sensorimotor and Cognitive Functions

Sensorimotor and cognitive functions were assessed twice using a series of tests between P22–26 and P36–40. On P37, collagenase infused animals moved faster compared with the control animals in 5–10 min ($P < 0.001$) and 10–15 min ($P < 0.001$) (**Figure 8A**) time bins of the open field test. Collagenase-injected animals spent significantly longer time in the center of the open field compared with the control animals throughout the test ($P < 0.05$) (**Figure 8B**). There was no difference between the collagenase and control animals in all other behavior tests at either of the time points (**Supplementary Figure 3**). There was no difference

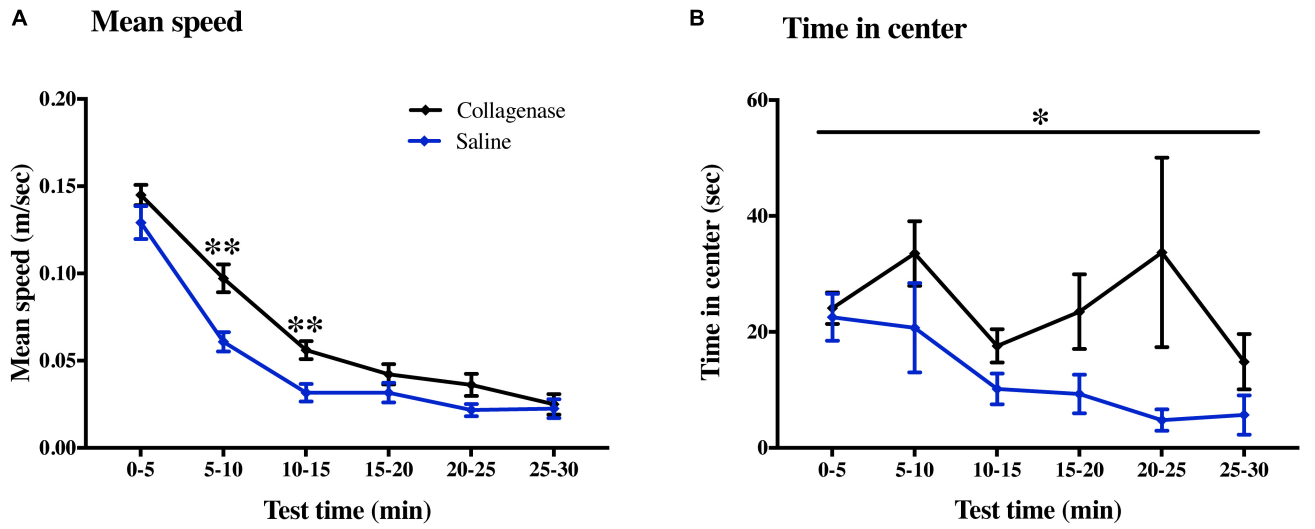

FIGURE 8 | Effect of GMH on long-term sensorimotor and cognitive functions. At P40, the open field test showed that **(A)** mean speed and **(B)** time spent in the center was affected by GMH (n = 19) when compared to saline controls (n = 12) . Data represented as mean ± SEM and analyzed using two-way mixed ANOVA. $^{*}P < 0.05$ and $^{**}P < 0.01$.

between the saline-injected and naïve animals in any of the behavior tests.

In brains from animals that had previously been assessed for behavior there was significant gray matter tissue loss within the striatum region (**Figure 9A**) of collagenase animals (n = 19) when compared to the naïve (n = 5) (P = 0.0189) and saline (n = 12) (P = 0.0053) groups (**Figure 9B**). Tissue loss was also significant in terms of total hemisphere loss (P = 0.0325 and P = 0.0420, respectively) (**Figure 9C**). There was no significant gray matter tissue loss at the hippocampus level (**Figures 9D–F**). MBP assessment at the striatum level (**Figure 10A**) showed significant reduction in subcortical white matter in the collagenase group when compared to naïve (P = 0.0452) and saline controls (P = 0.0273) (**Figure 10B**). At the hippocampus level, collagenase injection resulted in significant reduction in MBP (**Figure 10C**) when compared to naïve (P = 0.0482) and saline-injected animals (P = 0.0431) (**Figure 10D**). There was no significant astrogliosis or microglia activation in the collagenase group at this time-point (**Supplementary Figures 4A,B**).

DISCUSSION

In the current study we introduce a P5 rat model of GMH using intracranial striatal collagenase injections in proximity to the germinal matrix. Collagenase administration results in a standardized rupture of the vessels in the germinal matrix of the ganglionic eminence, associated with bleeding into the lateral ventricle of the injected hemisphere and reduction in white matter surrounding both the striatum and the affected ventricle.

Lekic et al. (2011, 2012) were the first group using unilateral 0.3 U collagenase VII injection into the germinal matrix of P7 rats mimicking pathological features present in clinical cases of GMH-IVH. However, in these studies, the collagenase infusion resulted in bilateral IVH (Lekic et al., 2011, 2012), which only occurs in a minority of cases at P5. A study by Maitre et al. (2009) has shown that unilateral GMH-IVH occurred in 75% of clinical cases, with bilateral cases consisting of only 15%. Furthermore, recent studies have suggested that in terms of brain maturation, P7 age in rats is closer to near-term human infants (Semple et al., 2013). A gestational age where the germinal matrix is no longer present and GMH is no longer considered to be one of the main risk factors for neonatal brain injury. Therefore, we sought to adapt this model to the P5 rat, which is comparable to that of a human fetus or newborn at 26–32 gestational weeks with respect to cortical developmental stages (Honig et al., 1996), presence of germinal matrix and maturation of white matter (Back et al., 2001).

Firstly, we sought to determine a collagenase infusion dose that would mimic the pathophysiology seen in clinical cases. Among the three different doses of collagenase VII (0.1, 0.2, and 0.3 U), only 0.3 U of collagenase resulted in ipsilateral striatal injury, as well as microglial activation surrounding the site of injury 24 h after injection. Clinically, microglia immune-response has been implicated in preterm brain injury, and have been shown to accumulate in the periventricular region in the first 48 h after IVH (Supramaniam et al., 2013; Mallard et al., 2014).

Further characterization of this dose showed a clear acute injury. Histological assessment 0.5 h after 0.3 U collagenase administration resulted in immediate bleeding within the injection site, as well as within the lateral ventricle and the appearance of iron. Within 6 h, there was a substantial increase in erythrocytes and deposits of loosely bound iron that also extended to the white matter surrounding the ipsilateral ventricle, together with focal infiltration of neutrophils. By 24 h there seemed to be an erythrocyte and iron clearance, whereas neutrophils appeared to migrate to the surrounding parenchyma. This neutrophil infiltration is in concordance with both clinical

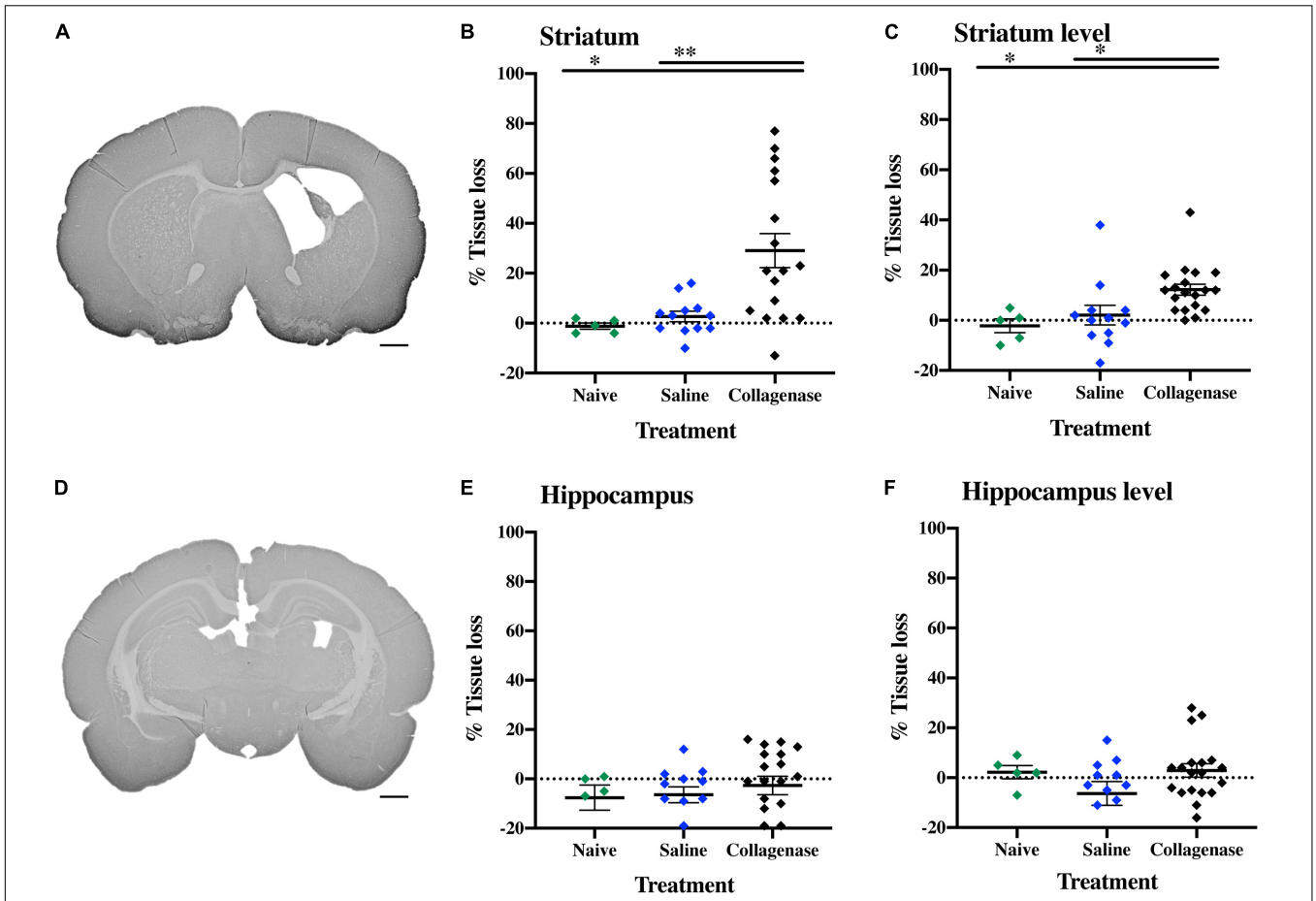

FIGURE 9 | Long term gray matter injury. **(A)** Representative MAP-2-stained whole brain micrograph of 0.3 U collagenase-mediated striatal injury at P40. **(B)** Graph demonstrating striatum-specific tissue loss and **(C)** striatum level ipsilateral hemisphere loss in the collagenase group. **(D)** Representative MAP-2-stained whole brain micrograph of 0.3 U collagenase-injected rat at the hippocampal level at P40. **(E)** Corresponding graph revealing non-significant hippocampus-specific tissue loss and **(F)** hippocampus level ipsilateral hemisphere measurement in the collagenase group (n = 19). Both naïve (n = 5) and saline-injected (n = 12) animals were used as control groups. Data represented as individual animals ± SEM and analyzed using one-way ANOVA followed by Tukey's multiple comparison test. $^{*}P < 0.05$ and $^{**}P < 0.01$. Scale bar = 1 mm.

and preclinical GMH studies. Paul et al. (2000) found that peripheral leukocytes and absolute neutrophils were increased in the first 72 h after birth in extremely preterm IVH cases. In a rabbit model of GMH-IVH, there was a greater number of microglia and neutrophils in the periventricular zone compared to control animals (Georgiadis et al., 2008).

In preterm infants, the site of origin of bleeding generally occurs in small blood vessels of the germinal matrix. GMH can result in disruption of the ependymal lining and extend the bleeding into the lateral ventricle. Germinal matrix vessels are fragile and have an endothelial layer with underdeveloped tight junctions, small pericyte numbers, and fibronectin deficiency in the immature basal lamina. Astrocyte end-feet have lower levels of glial fibrillary acidic protein expression. All these contribute to the rupture of germinal matrix blood vessels, and potential subsequent extravasation of blood into the lateral ventricle (Ballabh et al., 2004). We have shown extensive loss of laminin of blood vessels within the ipsilateral striatum 24 h after collagenase infusion, with some vessels devoid of laminin, indicating extensive damage to the basal lamina. Claudin-5, a key component of the blood-brain barrier also appeared fragmented in the vessels surrounding the site of injury.

Post hemorrhagic hydrocephalus is a clinical feature of GMH-IVH. It is thought that ventricular dilatation probably ensues soon after the hemorrhage in many preterm infants and is associated with poor prognosis (Brouwer et al., 2014). In the current study, the collagenase injection induced a periventricular/intraventricular hemorrhage best visualized 24 h after injection. The hemorrhage resulted in a progressive ipsilateral ventricular dilation at later time points, combined with continual loss of gray and white matter surrounding the site of injection.

Despite increase in survival of preterm infants, neurodevelopmental delay is a hallmark of GMH cases (Pierrat et al., 2017). We also found a quite marked initial deficit in motor coordination detected in the negative geotaxis test that persisted 1 week after collagenase admnistration. Interestingly, this developmental deficit lasted longer that observed by

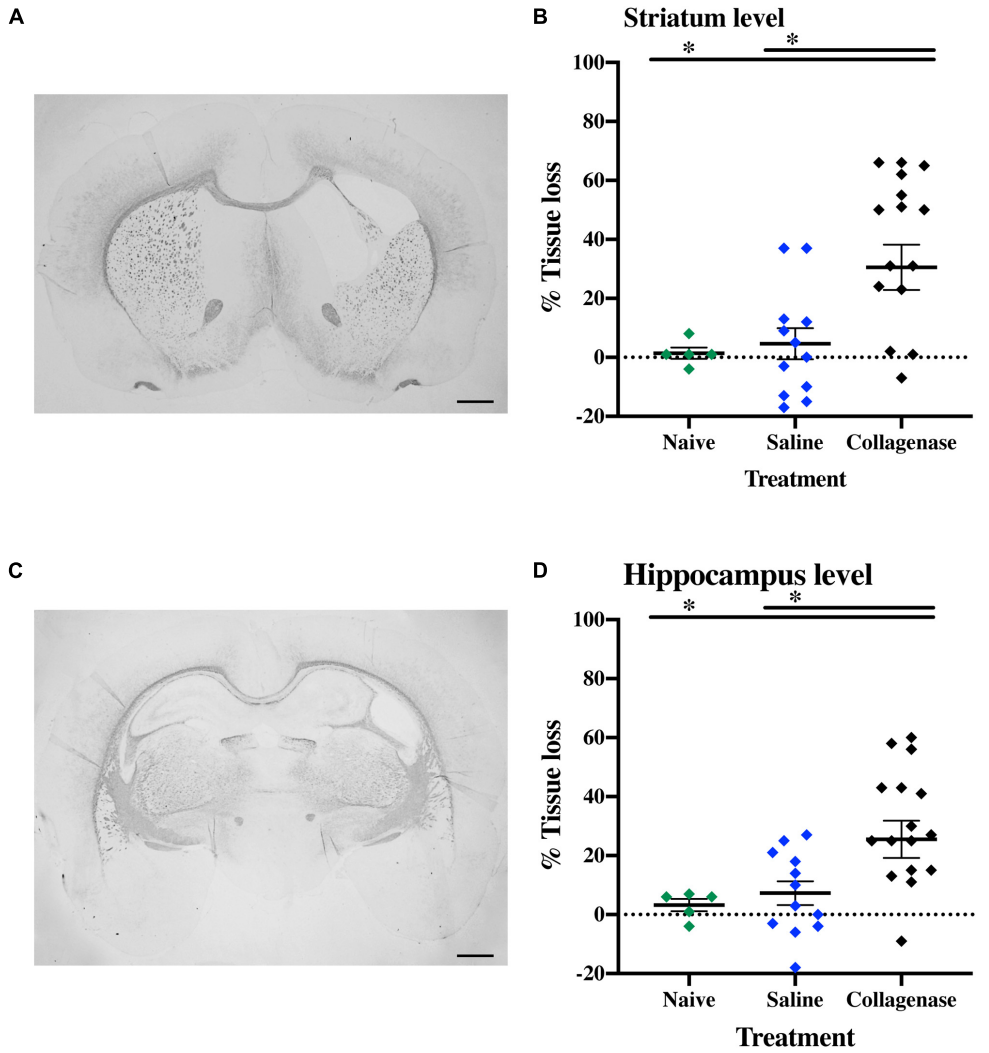

FIGURE 10 | Long term white matter injury at P40. **(A)** Representative MBP-stained whole brain micrograph of 0.3 U collagenase-injected rats at the level of the striatum and **(B)** corresponding graph demonstrating collagenase-mediated reduction in subcortical white matter at P40. **(C)** Representative MBP-stained whole brain micrograph of 0.3 U collagenase-injected rats at the level of the hippocampus and **(D)** associated graph showing subcortical white matter in the collagenase group (n = 19) at P40. Both naïve (n = 5) and saline (n = 12) animals were used as control groups. Data represented as individual animals ± SEM and analyzed using one-way ANOVA followed by Tukey's multiple comparison test. $^*P < 0.05$. Scale bar = 1 mm.

Lekic et al. (2012) which only saw significant differences in the first 48 h post-GMH (Alles et al., 2010). The successful completion of this task requires organized motor movement (Adams et al., 1985) and the initial abnormal outcome in this test indicates that the hemorrhage induced by intracranial striatal collagenase injection strongly affects development of the motor coordination during this period and seems to be a robust test for evaluation of early motor outcome in this model.

All animals were observed daily, and the body weight of each pup was recorded daily during this period. Despite a continual weight gain in all groups, by P14 collagenase infused rats had gained less weight than naïve animals. Coincidently, this is the age period (P14–15) when the day of eyelid opening occurs in rats (Bjerknes et al., 2015). This constitutes the starting point of the rats' exploratory behavior outside of the nest (Langston et al., 2010). We observed that animals exposed to GMH-IVH opened their eyes significantly later than naïve and saline-injected animals. These findings are in agreement with the results by Lekic et al. (2011, 2012) P7 study. Histological assessment of these animals revealed development of ventricular dilation, together with significant gray and white matter injury. Additionally, GFAP immunohistochemistry measurement showed significant astrogliosis within the ipsilateral striatum region.

Clinically, MRI is a tool commonly used to predict short- and long-term neurodevelopmental outcomes. The presence of white matter injury, in the form of delayed myelination, white matter loss, ventriculomegaly, among others have shown a strong correlation with cerebral palsy and other neuromotor deficits (Volpe, 2009; Anderson et al., 2015; van't Hooft et al., 2015;

Slaughter et al., 2016). We tested long-term sensorimotor and cognitive functions in a separate group of juvenile rats 2–3 weeks (P22–26) and 4–5 weeks (P36–40) after collagenase infusion. There was a significant increase in hyperactivity and a decrease in anxiety-like behavior in collagenase infused animals on P37 compared with the control group. However, motor coordination and motor asymmetry remained intact in the collagenase infused animals at both time points. Alles et al. (2010) reported similar findings in a P6 rat model of PVH/IVH using a much higher dose of collagenase (2.0 U), suggesting a compensatory neuroplasticity originating from the intact contralateral hemisphere. Subsequently, a bilateral infusion of collagenase caused significant impairments in both sensorimotor and cognitive functions that was apparent at the juvenile stage (Alles et al., 2010). Conversely, Lekic et al. reported a significant impairment in long-term sensorimotor and cognitive behavior in rats injected with the same dose of collagenase as used in the current study. However, unlike the current study, the authors observed a bilateral ventricular dilation and brain atrophy. Omizzolo et al. (2014) have reported that injury to the gray matter areas of the basal ganglia-thalamus of very preterm infants showed the strongest prediction for memory and learning outcome at 7 years of age. Infants with unilateral PVH infarction are found to have better sensorimotor/cognitive outcomes and are less likely to develop severe cerebral palsy compared to infants with bilateral PVH injury (Maitre et al., 2009). Gray matter histological assessment showed continued striatal injury with an almost unimpaired hippocampus in the ipsilateral hemisphere. The consistent pattern of injury in striatum suggests that in future studies should include striatum-dependent cognitive tasks, such as operant conditioning. MBP measurement of subcortical white matter thickness revealed a persistent long-term white matter injury around the fluid-filled ventricle.

Animal models are frequently used to study injury progression and pathophysiological mechanisms involved. In this study we have successfully shown that injection of collagenase VII into the medial striatum in proximity to the germinal matrix of the preterm equivalent P5 rat results in acute injury, leading to progressive ventricular dilation and secondary gray and white matter injury associated with impaired motor function during early development. Gray and white matter injury persisted into the juvenile period combined with hyperactivity and reduced anxiety. Overall, our model has relevance for mimicking GMH in preterm infant and has potential for assessment of therapeutic interventions.

DATA AVAILABILITY STATEMENT

The datasets generated for this study are available on request to the corresponding author.

ETHICS STATEMENT

The animal study was reviewed and approved by the Swedish Board of Agriculture and were approved by the Gothenburg Animal Ethics Committee (825-2017).

AUTHOR CONTRIBUTIONS

MJ and GK performed the animal experiments and developmental testing, and together with A-LL and PS carried out tissue preparation and processing. AJ and ER-F carried out the immunohistological analyses. CE carried out immunofluorescence analysis and SN assisted in the processing of all images and figures. GS-M and MJ performed behavioral testing and analysis. XW and CM participated in data interpretation. ST contributed to the funding and participated in the planning of the study. ER-F designed experiments, performed statistical analysis, interpreted data, and wrote the manuscript together with GK and HH. HH conceptualized and designed the study, assisted in data interpretation, and obtained funding. All authors reviewed and revised the manuscript and approved the final manuscript as submitted.

FUNDING

The authors gratefully acknowledge the funders and supporters of this work, the Department of Perinatal Imaging and Health, the Swedish Medical Research Council (VR (2019-01320), the Swedish Governmental Grant to Researchers at University Hospitals (ALFGBG-718591), the Action Medical Research, Hjärnfonden (Brain Foundation 2015-0004), ERA-NET (Contract: 0755101), Brain Foundation (2015-0004), and EU (Contract: 874721 Horizon 2020).

ACKNOWLEDGMENTS

We acknowledge the Centre for Cellular Imaging at the University of Gothenburg and the National Microscopy Infrastructure, NMI (VR-RFI 2016- 00968) for providing assistance in microscopy.

SUPPLEMENTARY MATERIAL

The Supplementary Material for this article can be found online at: https://www.frontiersin.org/articles/10.3389/fncel.2020.535320/full#supplementary-material

Supplementary Figure 1 | Schematic diagram of the different treatment groups, time-points, and assessments performed across the study.

Supplementary Figure 2 | (A) Assessment of astrogliosis (GFAP) in the ipsilateral striatum 24 h after different collagenase dose administrations, with groups consisting of: naïve (n = 8), saline (n = 8), 0.1 U (n = 8), 0.2 U (n = 9), and 0.3 U (n = 9) collagenase administration. **(B)** Assessment of microglia activation (IBA-1) in the ipsilateral striatum at P16 of naïve (n = 10), saline (n = 10), and 0.3 U collagenase (n = 12) animals. Data represented as individual animals ± SEM and analyzed using one-way ANOVA followed by Tukey's multiple comparison test.

Supplementary Figure 3 | Data from rotarod at **(A)** P26 and **(B)** P40, cylinder rearing test at **(C)** P26 and **(D)** P40 and P23 novel object recognition **(E)** mean speed and **(F)** time in the center. Collagenase injection (n = 19) did not affect behavioral function when compared to saline-injected (n = 12). Data represented as mean ± SEM and analyzed using two-way mixed ANOVA or unpaired t-test.

Supplementary Figure 4 | (A) Assessment of astrogliosis (GFAP) and **(B)** microglia activation (IBA-1) at P40 between naïve (n = 5), saline (n = 12), and collagenase (n = 19) groups. Data represented as individual animals ± SEM and analyzed using one-way ANOVA followed by Tukey's multiple comparison test.

REFERENCES

Adams, J., Buelke-Sam, J., Kimmel, C. A., Nelson, C. J., Reiter, L. W., Sobotka, T. J., et al. (1985). Collaborative behavioral teratology study: protocol design and testing procedures. *Neurobehav. Toxicol. Teratol.* 7, 579–586.

Alles, Y. C. J., Greggio, S., Alles, R. M., Azevedo, P. N., Xavier, L. L., and DaCosta, J. C. (2010). A novel preclinical rodent model of collagenase-induced germinal matrix/intraventricular hemorrhage. *Brain Res.* 1356, 130–138. doi: 10.1016/j.brainres.2010.07.106

Anderson, P. J., Cheong, J. L. Y., and Thompson, D. K. (2015). The predictive validity of neonatal MRI for neurodevelopmental outcome in very preterm children. *Semin. Perinatol.* 39, 147–158. doi: 10.1053/j.semperi.2015.01.008

Aquilina, K., Hobbs, C., Cherian, S., Tucker, A., Porter, H., Whitelaw, A., et al. (2007). A neonatal piglet model of intraventricular hemorrhage and posthemorrhagic ventricular dilation. *J. Neurosurg* 107(2 Suppl.), 126–136. doi: 10.3171/PED-07/08/126

Back, S. A., Luo, N. L., Borenstein, N. S., Levine, J. M., Volpe, J. J., and Kinney, H. C. (2001). Late oligodendrocyte progenitors coincide with the developmental window of vulnerability for human perinatal white matter injury. *J. Neurosci.* 21, 1302–1312. doi: 10.1523/jneurosci.21-04-01302.2001

Balasubramaniam, J., and Del Bigio, M. R. (2006). Animal models of germinal matrix hemorrhage. *J. Child Neurol.* 21, 365–371. doi: 10.2310/7010.2006.00074

Ballabh, P., Braun, A., and Nedergaard, M. (2004). Anatomic analysis of blood vessels in germinal matrix, cerebral cortex, and white matter in developing infants. *Pediatr. Res.* 56, 117–124. doi: 10.1203/01.PDR.0000130472.30874.FF

Ballabh, P., Xu, H., Hu, F., Braun, A., Smith, K., Rivera, A., et al. (2007). Angiogenic inhibition reduces germinal matrix hemorrhage. *Nat. Med.* 13, 477–485. doi: 10.1038/nm1558

Bassan, H., Limperopoulos, C., Visconti, K., Mayer, D. L., Feldman, H. A., Avery, L., et al. (2007). Neurodevelopmental outcome in survivors of periventricular hemorrhagic infarction. *Pediatrics* 120, 785–792. doi: 10.1542/peds.2007-0211

Bjerknes, T. L., Langston, R. F., Kruge, I. U., Moser, E. I., and Moser, M. B. (2015). Coherence among head direction cells before eye opening in rat pups. *Curr. Biol.* 25, 103-108. doi: 10.1016/j.cub.2014.11.009

Bodeau-Livinec, F., Marlow, N., Ancel, P. Y., Kurinczuk, J. J., Costeloe, K., and Kaminski, M. (2008). Impact of intensive care practices on short-term and long-term outcomes for extremely preterm infants: comparison between the british isles and france. *Pediatrics* 122, e1014–e1021. doi: 10.1542/peds.2007-2976

Brouwer, A. J., Groenendaal, F., Benders, M. J. N. L., and De Vries, L. S. (2014). Early and late complications of germinal matrix-intraventricular haemorrhage in the preterm infant: what is new? *Neonatology* 106, 296–303. doi: 10.1159/000365127

Chua, C. O., Chahboune, H., Braun, A., Dummula, K., Chua, C. E., Yu, J., et al. (2009). Consequences of intraventricular hemorrhage in a rabbit pup model. *Stroke* 40, 3369–3377. doi: 10.1161/STROKEAHA.109.549212

Crowther, C. A., Middleton, P. F., Voysey, M., Askie, L., Duley, L., Pryde, P. G., et al. (2017). Assessing the neuroprotective benefits for babies of antenatal magnesium sulphate: an individual participant data meta-analysis. *PLoS Med.* 14:e1002398. doi: 10.1371/journal.pmed.1002398

Fowlie, P. W., and Davis, P. G. (2003). Prophylactic indomethacin for preterm infants: a systematic review and meta-analysis. *Arch. Dis. Child. Fetal Neonatal Ed.* 88, F464–F466. doi: 10.1136/fn.88.6.f464

Georgiadis, P., Xu, H., Chua, C., Hu, F., Collins, L., Huynh, C., et al. (2008). Characterization of acute brain injuries and neurobehavioral profiles in a rabbit model of germinal matrix hemorrhage. *Stroke.* 39, 3378–3388. doi: 10.1161/STROKEAHA.107.510883

Goddard, J., Lewis, R. M., Armstrong, D. L., and Zeller, R. S. (1980). Moderate, rapidly induced hypertension as a cause of intraventricular hemorrhage in the newborn beagle model. *J. Pediatr.* 96, 1057-1060. doi: 10.1016/S0022-3476(80)80641-X

Hinojosa-Rodríguez, M., Harmony, T., Carrillo-Prado, C., Van Horn, J. D., Irimia, A., Torgerson, C., et al. (2017). Clinical neuroimaging in the preterm infant: diagnosis and prognosis. *NeuroImage Clin.* 16, 355–368. doi: 10.1016/j.nicl.2017.08.015

Hirtz, D. G., Weiner, S. J., Bulas, D., DiPietro, M., Seibert, J., Rouse, D. J., et al. (2015). Antenatal magnesium and cerebral palsy in preterm infants. *J. Pediatr.* 200, 595–609. doi: 10.1016/j.jpeds.2015.06.067

Honig, L. S., Herrmann, K., and Shatz, C. J. (1996). Developmental changes revealed by immunohistochemical markers in human cerebral cortex. *Cereb. Cortex.* 6, 794–806. doi: 10.1093/cercor/6.6.794

Kadam, S. D., Mulholland, J. D., Smith, D. R., Johnston, M. V., and Comi, A. M. (2009). Chronic brain injury and behavioral impairments in a mouse model of term neonatal strokes. *Behav. Brain Res.* 197, 77–83. doi: 10.1016/j.bbr.2008.08.003

Kaiser, J. R., Gauss, C. H., and Williams, D. K. (2005). The effects of hypercapnia on cerebral autoregulation in ventilated very low birth weight infants. *Pediatr. Res.* 58, 931–935. doi: 10.1203/01.pdr.0000182180.80645.0c

Kaiser, J. R., Tilford, J. M., Simpson, P. M., Salhab, W. A., and Rosenfeld, C. R. (2004). Hospital survival of very-low-birth-weight neonates from 1977 to 2000. *J. Perinatol.* 24, 343–350. doi: 10.1038/sj.jp.7211113

Kenet, G., Kuperman, A. A., Strauss, T., and Brenner, B. (2011). Neonatal IVH - Mechanisms and management. *Thromb. Res.* 127, S120-S122. doi: 10.1016/S0049-3848(11)70032-9

Langston, R. F., Ainge, J. A., Couey, J. J., Canto, C. B., Bjerknes, T. L., Witter, M. P., et al. (2010). Development of the spatial representation system in the rat. *Science* 328, 1576–1580. doi: 10.1126/science.1188210

Lekic, T., Klebe, D., Poblete, R., Krafft, P. R., Rolland, W. B., Tang, J., et al. (2015). Neonatal brain hemorrhage (NBH) of prematurity: translational mechanisms of the vascular-neural network. *Curr. Med. Chem.* 22, 1214–1238.

Lekic, T., Manaenko, A., Rolland, W., Krafft, P. R., Peters, R., Hartman, R. E., et al. (2012). Rodent neonatal germinal matrix hemorrhage mimics the human brain injury, neurological consequences, and post-hemorrhagic hydrocephalus. *Exp. Neurol.* 236, 69–78. doi: 10.1016/j.expneurol.2012.04.003

Lekic, T., Rolland, W., Hartman, R., Kamper, J., Suzuki, H., Tang, J., et al. (2011). Characterization of the brain injury, neurobehavioral profiles, and histopathology in a rat model of cerebellar hemorrhage. *Exp. Neurol.* 227, 96–103. doi: 10.1016/j.expneurol.2010.09.017

Lorenz, J. M., Wooliever, D. E., Jetton, J. R., and Paneth, N. (1998). A quantitative review of mortality and developmental disability in extremely premature newborns. *Arch. Pediatr. Adolesc. Med.* 152, 425–435. doi: 10.1001/archpedi.152.5.425

MacLellan, C. L., Silasi, G., Poon, C. C., Edmundson, C. L., Buist, R., Peeling, J., et al. (2008). Intracerebral hemorrhage models in rat: comparing collagenase to blood infusion. *J. Cereb. Blood Flow Metab.* 28, 516–525. doi: 10.1038/sj.jcbfm.9600548

Maitre, N. L., Marshall, D. D., Price, W. A., Slaughter, J. C., O'Shea, T. M., Maxfield, C., et al. (2009). Neurodevelopmental outcome of infants with unilateral or bilateral periventricular hemorrhagic infarction. *Pediatrics* 124, e1153–e1160. doi: 10.1542/peds.2009-0953

Mallard, C., Davidson, J. O., Tan, S., Green, C. R., Bennet, L., Robertson, N. J., et al. (2014). Astrocytes and microglia in acute cerebral injury underlying cerebral palsy associated with preterm birth. *Pediatr. Res.* 75, 234–240. doi: 10.1038/pr.2013.188

Maršál, K., Fellman, V., Hellström-Westas, L., Norman, M., Westgren, M., Källén, K., et al. (2009). One-year survival of extremely preterm infants after active perinatal care in Sweden. *J. Am. Med. Assoc.* 301, 2225–2233. doi: 10.1001/jama.2009.771

Omizzolo, C., Scratch, S. E., Stargatt, R., Kidokoro, H., Thompson, D. K., Lee, K. J., et al. (2014). Neonatal brain abnormalities and memory and learning outcomes at 7 years in children born very preterm. *Memory* 22, 605–615. doi: 10.1080/09658211.2013.809765

Owens, R. (2005). Intraventricular hemorrhage in the premature neonate. *Neonatal Netw.* 24, 55–71. doi: 10.1891/0730-0832.24.3.55

Paul, D. A., Leef, K. H., and Stefano, J. L. (2000). Increased leukocytes in infants with intraventricular hemorrhage. *Pediatr. Neurol.* 22, 194–199. doi: 10.1016/S0887-8994(99)00155-1

Pierrat, V., Marchand-Martin, L., Arnaud, C., Kaminski, M., Resche-Rigon, M., Lebeaux, C., et al. (2017). Neurodevelopmental outcome at 2 years for preterm

children born at 22 to 34 weeks' gestation in France in 2011: EPIPAGE-2 cohort study. *BMJ* 358:j3448. doi: 10.1136/bmj.j3448

Rocha-Ferreira, E., Phillips, E., Francesch-Domenech, E., Thei, L., Peebles, D. M., Raivich, G., et al. (2015). The role of different strain backgrounds in bacterial endotoxin-mediated sensitization to neonatal hypoxic–ischemic brain damage. *Neuroscience* 311, 292–307. doi: 10.1016/j.neuroscience.2015.10.035

Rocha-Ferreira, E., Rudge, B., Hughes, M. P., Rahim, A. A., Hristova, M., and Robertson, N. J. (2016). Immediate remote ischemic postconditioning reduces brain nitrotyrosine formation in a piglet asphyxia model. *Oxid. Med. Cell. Longev.* 2016:5763743. doi: 10.1155/2016/5763743

Roland, E. H., and Hill, A. (2003). Germinal matrix-intraventricular hemorrhage in the premature newborn: management and outcome. *Neurol. Clin.* 21, 833–851. doi: 10.1016/S0733-8619(03)00067-7

Rosenberg, G. A., Mun-Bryce, S., Wesley, M., and Komfeld, M. (1990). Collagenase-induced intracerebral hemorrhage in rats. *Stroke* 21, 801–817. doi: 10.1161/01.STR.21.5.801

Schallert, T., Fleming, S. M., Leasure, J. L., Tillerson, J. L., and Bland, S. T. (2000). CNS plasticity and assessment of forelimb sensorimotor outcome in unilateral rat models of stroke, cortical ablation, parkinsonism and spinal cord injury. *Neuropharmacology* 39, 777–787. doi: 10.1016/S0028-3908(00)00005-8

Semple, B. D., Blomgren, K., Gimlin, K., Ferriero, D. M., and Noble-Haeusslein, L. J. (2013). Brain development in rodents and humans: identifying benchmarks of maturation and vulnerability to injury across species. *Prog. Neurobiol.* 10, 1–16. doi: 10.1016/j.pneurobio.2013.04.001

Seri, I., and Evans, J. (2008). Limits of viability: definition of the gray zone. *J. Perinatol.* 28(Suppl. 1), S4–S8. doi: 10.1038/jp.2008.42

Slaughter, L. A., Bonfante-Mejia, E., Hintz, S. R., Dvorchik, I., and Parikh, N. A. (2016). Early conventional MRI for prediction of neurodevelopmental impairment in extremely-low-birth-weight infants. *Neonatology* 110, 47–54. doi: 10.1159/000444179

Stoll, B. J., Hansen, N. I., Adams-Chapman, I., Fanaroff, A. A., Hintz, S. R., Vohr, B., et al. (2004). Neurodevelopmental and growth impairment among extremely low-birth-weight infants with neonatal infection. *J. Am. Med. Assoc.* 292, 2357–2365. doi: 10.1001/jama.292.19.2357

Supramaniam, V., Vontell, R., Srinivasan, L., Wyatt-Ashmead, J., Hagberg, H., and Rutherford, M. (2013). Microglia activation in the extremely preterm human brain. *Pediatr. Res.* 73, 301–319. doi: 10.1038/pr.2012.186

van't Hooft, J., van der Lee, J. H., Opmeer, B. C., Aarnoudse-Moens, C. S. H., Leenders, A. G. E., Mol, B. W. J., et al. (2015). Predicting developmental outcomes in premature infants by term equivalent MRI: systematic review and meta-analysis. *Syst. Rev.* 7:71. doi: 10.1186/s13643-015-0058-7

Volpe, J. J. (2009). Brain injury in premature infants: a complex amalgam of destructive and developmental disturbances. *Lancet Neurol.* 8, 110–124. doi: 10.1016/S1474-4422(08)70294-1

Whitelaw, A. (2001). Intraventricular haemorrhage and posthaemorrhagic hydrocephalus: pathogenesis, prevention and future interventions. *Semin. Neonatol.* 6, 135–146. doi: 10.1053/siny.2001.0047

Whitelaw, A. (2012). Periventricular hemorrhage: a problem still today. *Early Hum. Dev.* 88, 965–969. doi: 10.1016/j.earlhumdev.2012.09.004

Conflict of Interest: The authors declare that the research was conducted in the absence of any commercial or financial relationships that could be construed as a potential conflict of interest.

Advantages of publishing in Frontiers

OPEN ACCESS
Articles are free to read for greatest visibility and readership

FAST PUBLICATION
Around 90 days from submission to decision

HIGH QUALITY PEER-REVIEW
Rigorous, collaborative, and constructive peer-review

TRANSPARENT PEER-REVIEW
Editors and reviewers acknowledged by name on published articles

Frontiers
Avenue du Tribunal-Fédéral 34
1005 Lausanne | Switzerland

Visit us: www.frontiersin.org
Contact us: frontiersin.org/about/contact

REPRODUCIBILITY OF RESEARCH
Support open data and methods to enhance research reproducibility

DIGITAL PUBLISHING
Articles designed for optimal readership across devices

FOLLOW US
@frontiersin

IMPACT METRICS
Advanced article metrics track visibility across digital media

EXTENSIVE PROMOTION
Marketing and promotion of impactful research

LOOP RESEARCH NETWORK
Our network increases your article's readership